

# **Genetic basis of susceptibility to invasive pneumococcal disease**



Thesis submitted for the degree of  
Doctor of Philosophy

by

**Vitor Silva Entrudo Fernandes**

Department of Infection, Immunity and Inflammation  
University of Leicester

2015

---

## Statement of originality

---



This thesis submitted for the degree of PhD entitled “*Genetic basis of susceptibility to invasive pneumococcal disease*” is based on the work accomplished by the author in the Department of Infection, Immunity and Inflammation at the University of Leicester (UK) during the period between January 2009 and July 2013.

To the best of my knowledge all the work recorded in this thesis is original, except where due reference or acknowledgement is made in the text.

None of the work has been accepted for the award of any other degree or diploma in any university or other tertiary institution.

Signed:  Date: 22/07/2015

Name: VITOR SILVA ENTRUDO FERNANDES

---

## **Preface**

---

The work described in this dissertation was carried out at the University of Leicester, Department of Infection, Immunity and Inflammation (UK), during the period January 2009 until July 2013, under the supervision of Professor Peter W. Andrew and Professor Aras Kadioglu. This thesis is the result of my own work and includes nothing that is the outcome of work done in collaboration unless specifically indicated in the text. Throughout this dissertation I have attempted to reference any theory or finding that is not my own. Finally, this dissertation does not exceed the limit of length prescribed by the Graduate School of the University of Leicester.

---

## Acknowledgements

---

My sincere gratitude goes to my supervisor Professor Peter Andrew for his support, advice and words of wisdom, friendship and for giving the opportunity to develop my skills in this challenging project, achieving extraordinary publications. Also, I would like to thank you for the incredible sliding tackles I've received on Thursday's football, which helped me understanding that passion and commitment are essential in our daily actions, either professionally or personally, helping to reach our goals (but not always reaching the ball). Nevertheless, it has been an honour to work with you. I am eternally thankful to you.

My sincere appreciation is extended to my co-supervisor Professor Aras Kadioglu for his continual support, sharing his knowledge with me, very grateful for choosing me to make part of remarkable researches that culminate in outstanding publications. Many thanks for his words of encouragement, friendship, and of course, for those poker nights with good music and where whiskey is part of the game.

Because there are bad things that happen for good...the best thing that happened to this project was the replacement of the Post Doctoral in this grant! I will be eternally grateful to Dr. Dan Neill for his invaluable support and guidance. *In vivo* work without your singing is not the same thing! With you, I have discovered not just *Spir1* candidate genes of susceptibility to pneumococcal infection, but also very good Ale beer in Britain - together we found the *GoodAle1* QTL in Oxfordshire. Dan, you are an excellent professional, a truly friend and I am very pleased that I have met you.

I would like to thank all my collaborators involved in this project: Paul Denny, Laura Wisby, Andrew Haynes, Anne Southwell, Debra Brooker, Michelle Simon, Saumya Kumar, Natalie Strickland and Lars Nitschke.

I would like to thank all members past/present of lab227 and 230, lab G28 and G43, who have helped me during this project, especially to Sandra, Mafalda, Marta, Rana, James, Hasan, Depesh, Ananth, Meenu, Wayne, Luke Andrew and Luke Richards. Many thanks to Alison J. Brown for reading my thesis and correcting my English. Thanks to the ladies in the media kitchen Elisabeth and Pam, and to Sushila for the quick ordering. Also, thanks to the members of the Division of Biomedical Services (past/present staff), in particular to Ken for his comprehension and amazing assistance, to Aimee, Anthony, Debbie, Paul, Linda, Pete, Helen, Amanda and Heather.

A big cheers to my football mate's past/present playing at the Moat College and for the 3I's Departmental football - best way for releasing stress!

Many thanks to Professor Leonor Faleiro (my teacher of Microbiology at the University of Algarve) for her help and support, and for "opening this door" to me, that was the University of Leicester, through her collaboration with Professor Peter Andrew.

Last, but not least, a big hug, to my friends and family. The following message to all of you in my mother language: um grande abraço à malta do "Bunho", da rua (Rui e Alex), da Universidade (Sobral, Luís, Rui, Marco, Maié, Joana e Tânia)...faltam muitos que não estão aqui, mas estão no meu coração! Um enorme abraço pelo apoio incondicional que me foi sempre dado: ao meu pai, à minha mãe, à minha maninha, sobrinha Lia e ao sobrinho James, aos meus sogrinhos Mário e Maria José, à minha cunhada e aos meus quasi-cunhados David e Carlos, à minha sobrinha Camila, à "avó adoptiva" Natália, aos meus tios José António e Georgina, José Maria e Noémia, à família Cardoso e Amália, e aos meus "irmãos" Filipe e Ruben. À memória dos meus avós, que não tive o prazer de conhecer: Victor e Quintina. Beijos muito muito grandes à minha esposa Sandra, ao meu filhote Gabriel e ao future rebento. Obrigado a todos!...E VIVA O BENFICA!

... e porque vocês merecem pelo menos  
uma página na minha Tese de Doutorado  
e muitas na minha vida, aqui fica uma  
lembrança...

Estou-vos eternamente grato e dedico-o a  
todos vós: ao meu pai, à minha mãe, à minha  
irmã, à minha querida esposa Sandra, ao meu  
filho Gabriel e ao futuro rebento.

Muito obrigado pelo vosso apoio,

Vitor Fernandes.

---

## Abstract

---

AUTHOR: VITOR SILVA ENTRUDO FERNANDES

TITLE: *GENETIC BASIS OF SUSCEPTIBILITY TO INVASIVE PNEUMOCOCCAL DISEASE*

*Streptococcus pneumoniae* (the pneumococcus) is a major cause of pneumonia, septicaemia and meningitis, particularly in high-risk groups such as children, the elderly and the immunocompromised. Host genetic factors play a significant role in susceptibility to pneumococcal disease. We have developed a mouse model of genetic susceptibility to invasive pneumococcal disease, with the purpose of identifying candidate disease genes.

A panel of nine inbred mouse strains were screened in response to pneumococcal pneumonia infection and two strains emerged showing different phenotypes to the disease, the resistant BALB/c and the susceptible CBA/Ca. On the F<sub>2</sub> intercrosses of the mentioned strains was mapped a major quantitative trait locus named *Streptococcus pneumoniae* infection resistance 1 (*Spir1*). The *Spir1* genetic interval found in chromosome 7, between *D7Mit341* and *D7Mit247*, in an interval with 13Mb and approximately 250 genes, containing several genes that encode molecules involved in inflammation or innate immunity.

Previous investigation on gene expression and protein levels in BALB/c and CBA/Ca lungs during an infection time course observed significant differences in transforming growth factor (*TGF*)- $\beta$ 1 and *Ikb $\beta$*  between strains in response to pneumococcal infection. Regarding the related host genetic differences, further research was done during my PhD, investigating host immune responses to pneumococcal infection and more intensely the contribution of TGF- $\beta$  and its downstream targets (including T regulatory cells). I have demonstrated that Foxp3<sup>+</sup> T regulatory cells have crucial protective functions during infection, as blocking their induction with an inhibitor of TGF- $\beta$  significantly alters the BALB/c resistance phenotype to infection and aids bacterial dissemination from lungs; and conversely, adoptive transfer of T regulatory cells to CBA/Ca mice, prior to infection, prolongs survival and decreases bacterial dissemination. This novel study provides key evidence for the importance of immunomodulation during pulmonary pneumococcal infection.

Within this genomic region located in chromosome 7, it was found in the pneumococcal-susceptible CBA/Ca strain a novel polymorphism in the *cd22* gene, predicted to prevent synthesis of the protein almost completely, whereas pneumococcal-resistant BALB/c mice have no impairment in the B-cell receptor CD22. Strikingly, CD22-deficient mice (C57BL/6J background) evidenced reduced survival and increased bacterial dissemination from lungs to blood and spleen, not observed in control mice. This study provides enthralling new indication for the contribution of B-cell receptor CD22 during invasive pneumococcal disease.

Together, these studies indicate that the *Spir1* region contains a cluster of genes contributing to susceptibility to pneumococcal disease.

---

## Publications from this work

---

The data in Chapter 5 and Chapter 7 (section 7.4) were published in the following article:

Daniel R. Neill, **Vitor E. Fernandes**, Laura Wisby, Andrew R. Haynes, Daniela M. Ferreira, Ameera Laher, Natalie Strickland, Stephen B. Gordon, Paul Denny, Aras Kadioglu, Peter W. Andrew. 2012. T Regulatory Cells Control Susceptibility to Invasive Pneumococcal Pneumonia in Mice. *Plos Pathogens* 8 (4): e1002660.

---

## Abbreviations

---

Nucleotides in DNA sequences were denoted according to standard IUPAC single letter base codes.

%	Percent
°C	Degrees Centigrade
$\alpha$	Alpha
$\beta$	Beta
$\gamma$	Gamma
$\delta$	Delta
$\mu\text{g}$	Micrograms
$\mu\text{l}$	Microlitres
$\mu\text{M}$	Micromolar
APC	Antigen presenting cell or Allophycocyanin, according to the context
bp	Base pairs
BAB	Blood Agar Base
BHI	Brain Hearth Infusion
CD	Cluster of Differentiation
CPS	Capsular Polysaccharide
CFU	Colony Forming Units
DC	Dendritic Cell
dH <sub>2</sub> O	Distilled water
DMSO	Dimethylsulfoxide
DNA	Deoxyribonucleic acid
dNTP	Deoxynucleotide triphosphate
ELISA	Enzyme-linked immunosorbent assay
FACS	Fluorescence Activated Cell Sorting
FBS	Fetal Bovine Serum
FC	Flow Cytometry
FCS	Fetal Calf Serum
FITC	Fluorescein isothiocyanate
g	Grams
<i>g</i>	<i>g</i> -force (RCF = Relative Centrifugal Force)

hr	Hours
IFN	Interferon
IL	Interleukin
Ig	Immunoglobulin
IN	Intranasal
IP	Intraperitoneal
IMS	Industrial Methylated Spirit
IV	Intravenous
IVC	Individually Ventilated Caging
IPD	Invasive Pneumococcal Disease
kb	Kilobases
l	Litres
LPS	Lipopolysaccharide
Mb	Megabases
mg	Milligram
MHC	Major Histocompatibility Complex
ml	Millilitre
mRNA	Messenger RNA
min	Minute
ng	nanogram
nH <sub>2</sub> O	Nanopure water
NACWO	Named Animal Care & Welfare Officer
NK	Natural Killer
OD	Optical Density
PBS	Phosphate Buffered Saline
PCR	Polymerase Chain Reaction
PE	Phycoerythrin
PE/Cy7	Phycoerythrin-Cy7 Tandem
PMN	Polymorphonuclear leukocyte
p.i.	Post-infection
QTL	Quantitative Trait Locus
rpm	Revolutions per minute
RPMI	Roswell Park Memorial Institute

RT	Room Temperature
SD	Standard Deviation
SEM	Standard Error of the Mean
TCR	T cell receptor
TGF	Transforming Growth Factor
T <sub>h</sub>	T helper
TLR	Toll-like Receptor
TNF	Tumour Necrosis Factor
Treg	T regulatory
UID	Unique Identifier
(v/v)	By volume
(w/v)	Weight by volume
WHO	World Health Organization

---

## Table of Contents

---

<b>STATEMENT OF ORIGINALITY</b>	<b>I</b>
<b>PREFACE</b>	<b>II</b>
<b>ACKNOWLEDGEMENTS</b>	<b>III</b>
<b>ABSTRACT</b>	<b>V</b>
<b>PUBLICATIONS FROM THIS WORK</b>	<b>VI</b>
<b>ABBREVIATIONS</b>	<b>VII</b>
<b>TABLE OF CONTENTS</b>	<b>X</b>
<b>LIST OF TABLES</b>	<b>XV</b>
<b>LIST OF FIGURES</b>	<b>XVI</b>
<b>CHAPTER 1. INTRODUCTION</b>	<b>1</b>
<b>1.1 STREPTOCOCCUS PNEUMONIAE</b>	<b>1</b>
1.1.1 HISTORY	2
1.1.2 GENERAL CHARACTERISTICS OF <i>S. PNEUMONIAE</i>	3
1.1.3 EPIDEMIOLOGY	4
1.1.4 ANTIMICROBIAL THERAPY AND VACCINATION	6
1.1.5 LIMITATION OF CURRENT THERAPIES	8
1.1.6 PATHOGENESIS OF PNEUMOCOCCAL DISEASE	10
1.1.7 VIRULENCE FACTORS	12
<b>1.2 HOST GENETIC CONTRIBUTION TO SUSCEPTIBILITY TO INFECTIOUS DISEASE</b>	<b>19</b>
1.2.1 POLYMORPHISMS IN HUMAN SUSCEPTIBILITY TO <i>S. PNEUMONIAE</i> INFECTION	20
1.2.2 MOUSE MODELS OF HUMAN DISEASES	22
1.2.3 MOUSE MODELS OF SUSCEPTIBILITY TO <i>S. PNEUMONIAE</i> INFECTION	23
1.2.4 MAPPING QTL RESPONSIBLE FOR MURINE SUSCEPTIBILITY TO INVASIVE PNEUMOCOCCAL DISEASE	28
<b>1.3 OVERVIEW OF THE IMMUNE SYSTEM</b>	<b>29</b>
1.3.1 INNATE IMMUNE SYSTEM	29
1.3.2 ROLE OF THE SPLEEN IN THE IMMUNE RESPONSE TO <i>S. PNEUMONIAE</i>	35
<b>1.4 AIMS OF THE THESIS</b>	<b>36</b>

<b>CHAPTER 2. MATERIALS AND METHODS</b>	<b>38</b>
<b>2.1 MATERIALS</b>	<b>38</b>
2.1.1 GENERAL	38
2.1.2 PEPTIDES	38
2.1.3 STANDARD STOCKS AND BUFFERS	38
2.1.4 BACTERIAL GROWTH MEDIA	39
<b>2.2 PNEUMOCOCCAL STRAIN</b>	<b>39</b>
2.2.1 PNEUMOCOCCAL STRAIN VALIDATION	39
2.2.2 QUELLUNG REACTION	41
2.2.3 VIABLE COUNTING	42
<b>2.3 PROCEDURES FOR <i>IN VIVO</i> EXPERIMENTS</b>	<b>42</b>
2.3.1 ANIMALS	42
2.3.2 MOUSE IDENTIFICATION	43
2.3.3 TAIL BIOPSY AND EAR NOTCHING OF MICE	43
2.3.4 PREPARATION OF <i>S. PNEUMONIAE</i> ANIMAL PASSAGED STOCKS	44
2.3.5 VIRULENCE TEST OF PASSAGED BACTERIA	45
2.3.6 INTRANASAL ADMINISTRATION TO MICE	46
2.3.7 INTRAPERITONEAL INJECTION OF MICE	46
2.3.8 INTRAVENOUS INJECTION OF MICE	47
2.3.9 SCORING OF ANIMAL SIGNS OF PNEUMOCOCCAL DISEASE	47
2.3.10 DETERMINATION OF VIABLE BACTERIA IN LUNG TISSUE	48
2.3.11 DETERMINATION OF VIABLE BACTERIA IN BLOOD	49
2.3.12 ADMINISTRATION OF PEPTIDE	49
2.3.13 BLOOD COLLECTION	49
2.3.14 BLOOD PLASMA COLLECTION	50
<b>2.4 GENERAL DNA MANIPULATION TECHNIQUES</b>	<b>50</b>
2.4.1 EXTRACTION OF GENOMIC DNA	50
2.4.2 PCR PRIMER DESIGN FOR PYROSEQUENCING	52
2.4.3 POLYMERASE CHAIN REACTION (PCR) METHOD FOR PYROSEQUENCING	52
<b>2.5 AGAROSE GEL ELECTROPHORESIS</b>	<b>54</b>
<b>2.6 PYROSEQUENCING</b>	<b>55</b>
2.6.1 ANALYSIS OF PYROSEQUENCING DATA	56
<b>2.7 FLOW CYTOMETRY</b>	<b>56</b>
2.7.1 LUNG CELL PREPARATION	56
2.7.2 PREPARATION OF CELLS FOR FLOW CYTOMETRIC STAINING	57
2.7.3 CELL CRYOPRESERVATION	57

2.7.4 SURFACE MARKER ANALYSIS	58
2.7.5 INTRACELLULAR STAINING	60
2.7.6 CALCULATION OF EVENTS PER MG OF TISSUE	61
<b>2.8 CYTOKINE ANALYSIS BY ENZYME-LINKED IMMUNOSORBENT ASSAY (ELISA)</b>	<b>62</b>
<b>2.9 HISTOLOGY</b>	<b>64</b>
2.9.1 PREPARATION OF FROZEN TISSUE	65
2.9.2 SECTIONING OF FROZEN LUNG TISSUE	65
2.9.3 HAEMATOXYLIN AND EOSIN (H&E) STAINING OF TISSUE SECTIONS	65
2.9.4 LUNG PARAFFIN WAX SECTIONS	66
2.9.5 TISSUE PATHOLOGY SEVERITY SCORE	66
2.9.6 CYTOCENTRIFUGATION OF LUNG CELLS	67
2.9.7 DIFFERENTIAL STAINING OF CELLS WITH GIEMSA STAIN	67
<b>2.10 STATISTICAL ANALYSIS</b>	<b>67</b>
<b><u>CHAPTER 3. INVESTIGATION OF HOST RESPONSES IN BALB/C AND CBA/CA MICE TO PNEUMOCOCCAL INFECTION</u></b>	<b>68</b>
<b>3.1 AIMS</b>	<b>68</b>
<b>3.2 RESULTS</b>	<b>68</b>
3.2.1 DIFFERENCES IN ACUTE RESPONSES BETWEEN BALB/C AND CBA/CA MICE ASSOCIATED WITH DIFFERENCES IN SUSCEPTIBILITY TO INVASIVE PNEUMOCOCCAL DISEASE	68
3.2.2 HOST IMMUNE RESPONSES TO PNEUMOCOCCAL LUNG INFECTION IN BALB/C AND CBA/CA MICE	76
3.2.3 PHENOTYPING OF THE CELLULAR RECRUITMENT IN BALB/C AND CBA/CA INBRED MICE IN RESPONSE TO INVASIVE PNEUMOCOCCAL INFECTION	76
3.2.4 BALB/C AND CBA/CA INBRED MICE CYTOKINE PROFILE IN RESPONSE TO PNEUMOCOCCAL INFECTION	105
<b><u>CHAPTER 4. GENERATION OF BALB/C AND CBA/CA CONGENIC MICE FOR INVESTIGATION OF THE <i>SP1</i> LOCUS</u></b>	<b>125</b>
<b>4.1 GENERATION AND CHARACTERISATION OF <i>SP1</i> CONGENIC MICE</b>	<b>125</b>
4.1.1 <i>SP1</i> CONGENIC-BREEDING STRATEGY	125
<b><u>CHAPTER 5. TGF-<math>\beta</math> AND T REGULATORY CELLS CONTROL SUSCEPTIBILITY TO INVASIVE PNEUMOCOCCAL INFECTION IN MICE</u></b>	<b>143</b>
<b>5.1 INTRODUCTION</b>	<b>143</b>
<b>5.2 AIMS</b>	<b>145</b>

<b>5.3 RESULTS</b>	<b>145</b>
5.3.1 TGF-B SIGNALLING IS REGULATED DIFFERENTIALLY IN BALB/C AND CBA/CA MICE DURING PNEUMOCOCCAL PNEUMONIA	145
5.3.2 BALB/C MICE DISPLAY A GREATER EXPANSION AND RECRUITMENT OF FOXP3 <sup>+</sup> CELLS TO THE LUNGS THAN CBA/CA MICE DURING PNEUMOCOCCAL INFECTION	149
5.3.3 LOWER T REGULATORY CELL NUMBERS CORRELATE WITH INCREASED LUNG CELL APOPTOSIS	161
5.3.4 INHIBITION OF TGF-B1 IMPAIRS BALB/C RESISTANCE TO <i>S. PNEUMONIAE</i> INFECTION	164
5.3.5 ADOPTIVE TRANSFER OF <i>IN VITRO</i> GENERATED T REGULATORY CELLS INCREASES CBA/CA MICE SURVIVAL	167
5.3.6 RESISTANCE TO INVASIVE PNEUMOCOCCAL PNEUMONIA IN OUTBRED MICE CORRELATES WITH STRONG T REGULATORY CELL RESPONSES	170
<b><u>CHAPTER 6. RESULTS: B-CELL RECEPTOR CD22 IS A MAJOR FACTOR OF HOST RESISTANCE TO <i>STREPTOCOCCUS PNEUMONIAE</i> INFECTION IN MICE</u></b>	<b>172</b>
<b>6.1 INTRODUCTION</b>	<b>172</b>
<b>6.2 AIMS</b>	<b>173</b>
<b>6.3 RESULTS</b>	<b>174</b>
6.3.1 A NEW POLYMORPHISM IN THE <i>Cd22</i> GENE IN THE CBA/CA BACKGROUND	174
6.3.2 DETECTION OF STOP CODON IN <i>CD22</i>	179
6.3.3 ANALYSIS OF CD22 <sup>+</sup> B CELL IN BALB/C AND CBA/CA MICE IN RESPONSE TO PNEUMOCOCCAL INFECTION	181
6.3.4 FUNCTIONAL ANALYSIS OF <i>CD22</i> FOLLOWING INFECTION WITH <i>S. PNEUMONIAE</i>	190
<b><u>CHAPTER 7. DISCUSSION</u></b>	<b>194</b>
<b>7.1 REPORTS ON BALB/C VS CBA/CA MICE IN RESPONSE TO DIFFERENT INFECTIONS</b>	<b>194</b>
<b>7.2 MAJOR PHENOTYPIC DIFFERENCES BETWEEN A RESISTANT AND A SUSCEPTIBLE HOST TO <i>S. PNEUMONIAE</i> INFECTION</b>	<b>194</b>
<b>7.3 OUTCOME OF THE <i>SP1</i> CONGENIC WORK</b>	<b>196</b>
<b>7.4 TGF-B AND T REGULATORY CELLS</b>	<b>198</b>
<b>7.5 <i>Cd22</i> ANOTHER CANDIDATE GENE CONTRIBUTING TO PNEUMOCOCCAL PNEUMONIA SUSCEPTIBILITY</b>	<b>203</b>
<b>7.6 OVERALL COMPONENTS OF MECHANISMS OF RESISTANCE AND SUSCEPTIBILITY TO <i>S. PNEUMONIAE</i> INFECTION</b>	<b>206</b>
<b>7.7 BENEFITS OF THIS RESEARCH PROJECT TO SOCIETY</b>	<b>210</b>
<b>7.8 FUTURE WORK</b>	<b>211</b>
<b><u>REFERENCES</u></b>	<b>213</b>

<b><u>APPENDIX 1: GENES IN THE <i>SP1</i> REGION</u></b>	<b>242</b>
<b><u>APPENDIX 2: PRIMER LIST</u></b>	<b>243</b>
<b><u>APPENDIX 3: PYROSEQUENCING - PYROGRAM OUTPUTS</u></b>	<b>244</b>
<b><u>APPENDIX 4: GENOTYPING AND PHENOTYPING DATA OF THE N<sub>10</sub> CONGENIC LINES</u></b>	<b>249</b>
<b><u>APPENDIX 5: LIST OF SNPS IN <i>TGFB1</i> GENE BETWEEN BALB/C AND CBA/CA MICE</u></b>	<b>255</b>
<b><u>APPENDIX 6: LIST OF SNPS IN <i>CD22</i> GENE BETWEEN BALB/C AND CBA/CA MICE</u></b>	<b>256</b>
<b><u>APPENDIX 7: REPRESENTATION OF THE DIFFERENT LEVEL OF CELLULAR INFILTRATION IN LUNG TISSUE SECTIONS.</u></b>	<b>263</b>
<b><u>APPENDIX 8: BALB/C AND CBA/CA LUNG AND SPLEEN WEIGHTS (QUANTIFICATION OF THE NUMBER OF CELLS PER MG OF LUNG TISSUE)</u></b>	<b>268</b>
<b><u>APPENDIX 9: AUTHOR'S PUBLICATIONS</u></b>	<b>271</b>

---

## List of Tables

---

Table 1.1- Pneumococcal virulence factors and their main role in colonisation and disease.	14
Table 1.2 - T <sub>helper</sub> cell subtypes classified by cytokine production (Borish & Steinke, 2003).	32
Table 2.1 - <i>Streptococcus pneumoniae</i> growth media.	39
Table 2.2 - Scoring the animal signs of disease (Morton & Griffiths, 1985).	48
Table 2.3 - Different components for the PCR mix (Wisby et al., 2013).	53
Table 2.4 - Standard conditions for PCR (Wisby et al., 2013).	54
Table 2.5 - Extracellular antibodies used in FACS analysis.	59
Table 2.6 - Intracellular antibodies used in flow cytometry analysis.	61
Table 2.7 - Collection speed multiplier.	62
Table 2.8 - Preparation of standards for each cytokine (eBioscience kits).	63
Table 2.9 - Preparation of detection antibodies for ELISA (eBioscience kits).	64
Table 2.10 - Numeric score for the level of cellular infiltration in lung tissue sections.	66
Table 3.1 - Statistical differences between BALB/c and CBA/Ca mice in the lung cellular recruitment at 24 hours post-infection.	101
Table 3.2 - Lung cytokine statistical differences between BALB/c and CBA/Ca mice.	124
Table 3.3 - Serum cytokine statistical differences between BALB/c and CBA/Ca mice.	124
Table 4.1 - Estimated percentage of recipient genome at each generation of the congenic-breeding development (Markel et al., 1997).	128
Table 4.2 - <i>Spir1</i> marker-assisted congenic fixed lines.	129
Table 4.3 - Tukey's multiple comparison tests of survival of <i>S. pneumoniae</i> -infected N <sub>10</sub> congenic lines.	132
Table 4.4 - Bonferroni's multiple comparison tests of bacteraemia at 24 hours <i>S. pneumoniae</i> -infected N <sub>10</sub> congenic lines.	133
Table 6.1 - Mutation found in CBA/Ca mice background introduced a stop codon in the <i>cd22</i> gene.	174
Table 6.2 - Analysis of pyrosequencing output (pyrogram) of the <i>cd22</i> SNP.	180

---

## List of Figures

---

Figure 1.1 - Electron micrograph of <i>Streptococcus pneumoniae</i> .	1
Figure 1.2 - Pneumococcal mortality rate.	4
Figure 1.3 - Causes of death in neonates and children under five in the world in 2004 (WHO, 2008).	5
Figure 1.4 - Proportion of invasive <i>Streptococcus pneumoniae</i> isolates with dual resistance to erythromycin and penicillin in 2006 (Gould, 2008).	8
Figure 1.5 - Routes of host infection by <i>S. pneumoniae</i> leading to invasive disease.	11
Figure 1.6 - <i>Streptococcus pneumoniae</i> virulence factors.	13
Figure 1.7 - Median survival times of the panel of inbred mouse strains tested against pneumococcal infection.	24
Figure 1.8 - Bacterial counts ( $\text{Log}_{10}$ CFU/ml) in blood from the panel of inbred mouse strains.	24
Figure 1.9 - Controlled bacterial growth in the lungs of BALB/c mice diminishes spreading into bloodstream.	25
Figure 1.10 - Rapid increase of neutrophil numbers in the lungs of BALB/c mice.	26
Figure 1.11 - Bacterial loads in the lung tissue of CBA/Ca mice increased during pneumococcal infection.	27
Figure 1.12 - The innate immune and the adaptive immune response (Dranoff, 2004).	29
Figure 1.13 - Summary of some aspects of the host immune response to pneumococcal infection during bronchopneumonia (Kadioglu & Andrew, 2004).	32
Figure 2.1 - Diagram representing identification and characterization methods of a <i>S. pneumoniae</i> isolate (Centers for Disease Control and Prevention, 2010).	40
Figure 2.2 - Pyrosequencing steps.	55
Figure 3.1 - Models of infection with BALB/c and CBA/Ca mice.	71
Figure 3.2 - Number of pneumococci in the blood of BALB/c and CBA/Ca mice after intranasal infection.	72
Figure 3.3 - Septicaemia model of infection with BALB/c and CBA/Ca mice.	75
Figure 3.4 - Numbers of CD45 <sup>+</sup> cells in the lungs of BALB/c and CBA/Ca mice post-infection with <i>S. pneumoniae</i> .	77
Figure 3.5 - Numbers of neutrophils in the lungs of BALB/c and CBA/Ca mice post-infection with <i>S. pneumoniae</i> .	79
Figure 3.6 - Numbers of macrophage in the lungs of BALB/c and CBA/Ca mice post-infection with <i>S. pneumoniae</i> .	81

Figure 3.7 - Numbers of T <sub>helper</sub> cells in the lungs of BALB/c and CBA/Ca mice post-infection with <i>S. pneumoniae</i> .	82
Figure 3.8 - Numbers of cytotoxic T cells in the lungs of BALB/c and CBA/Ca mice post-infection with <i>S. pneumoniae</i> .	84
Figure 3.9 - Numbers of B cells in the lungs of BALB/c and CBA/Ca mice post-infection with <i>S. pneumoniae</i> .	85
Figure 3.10 - Numbers of mast cells in the lungs of BALB/c and CBA/Ca mice post-infection with <i>S. pneumoniae</i> .	86
Figure 3.11 - Numbers of $\gamma\delta$ T cells in the lungs of BALB/c and CBA/Ca mice post-infection with <i>S. pneumoniae</i> .	88
Figure 3.12 - Numbers of IL-17 <sup>+</sup> $\gamma\delta$ T cells in the lungs of BALB/c and CBA/Ca mice post-infection with <i>S. pneumoniae</i> and mock infection with PBS.	89
Figure 3.13 - Numbers of IL-17 <sup>+</sup> cells in the lungs of BALB/c and CBA/Ca mice post-infection with <i>S. pneumoniae</i> and mock infection with PBS.	91
Figure 3.14 - Numbers of NK cells in the lungs of BALB/c and CBA/Ca mice post-infection with <i>S. pneumoniae</i> and mock infection with PBS.	93
Figure 3.15 - Numbers of IFN- $\gamma$ <sup>+</sup> NK cells in the lungs of BALB/c and CBA/Ca mice post-infection with <i>S. pneumoniae</i> and mock infection with PBS.	94
Figure 3.16 - Numbers of IFN- $\gamma$ <sup>+</sup> NK cells in the lungs of BALB/c and CBA/Ca mice post-infection with <i>S. pneumoniae</i> and mock infection with PBS.	96
Figure 3.17 - Numbers of T cells expressing IFN- $\gamma$ in the lungs of BALB/c and CBA/Ca mice post-infection with <i>S. pneumoniae</i> and mock infection with PBS.	97
Figure 3.18 - Numbers of IL-10 expressing cells in the lungs of BALB/c and CBA/Ca mice post-infection with <i>S. pneumoniae</i> and mock infection with PBS.	99
Figure 3.19 - Numbers of IL-10 <sup>+</sup> T regulatory cells in the lungs of BALB/c and CBA/Ca mice post-infection with <i>S. pneumoniae</i> and mock infection with PBS.	100
Figure 3.20 - Leukocyte recruitment in BALB/c and CBA/Ca lungs following pneumococcal-infection.	104
Figure 3.21 - Levels of cellular infiltration in the lung sections of BALB/c and CBA/Ca mice infected with <i>S. pneumoniae</i> .	105
Figure 3.22 - Levels of IL-1 $\beta$ cytokine in the lungs and serum of BALB/c and CBA/Ca mice.	107
Figure 3.23 - Levels of IL-6 cytokine in the lungs and serum of BALB/c and CBA/Ca mice.	109

Figure 3.24 - Levels of IL-10 cytokine in the lungs and serum of BALB/c and CBA/Ca mice.	111
Figure 3.25 - Levels of IL-17 cytokine in the lungs and serum of BALB/c and CBA/Ca mice.	113
Figure 3.26 - Levels of IFN- $\gamma$ cytokine in the lungs and serum of BALB/c and CBA/Ca mice.	115
Figure 3.27 - Levels of KC cytokine in the lungs and serum of BALB/c and CBA/Ca mice.	117
Figure 3.28 - Levels of MIP-2 cytokine in the lungs and serum of BALB/c and CBA/Ca mice.	119
Figure 3.29 - Levels of TNF- $\alpha$ cytokine in the lungs and serum of BALB/c and CBA/Ca mice.	121
Figure 3.30 - Levels of TGF- $\beta$ 1 cytokine in the lungs and serum of BALB/c and CBA/Ca mice.	123
Figure 4.1 - Chromosome 7 SNP markers used in the congenic-breeding program.	126
Figure 4.2 - Development of a congenic line.	127
Figure 4.3 - Correlation between mean 24 hours bacteraemia and mean survival time of each congenic line infected with <i>S. pneumoniae</i> .	130
Figure 4.4 - Survival of <i>S. pneumoniae</i> -infected N <sub>10</sub> congenic lines.	132
Figure 4.5 - Number of bacteria per ml blood assessed for each individual of the N <sub>10</sub> congenic lines at 24 hour post-infection.	133
Figure 4.6 - Illustration of linkage between survival, bacteraemia at 24 hours post-infection and the 7_09 marker.	134
Figure 4.7 - Additional SNP markers used to narrowing-down the QTL.	135
Figure 4.8 - Genotype of the congenic lines at each SNP tested.	136
Figure 4.9 - Survival of the phenotyped congenic lines at each tested SNP in chromosome 7.	138
Figure 4.10 - Survival curves and 24 hours bacteraemia analysed for all SNPs used in the congenic study.	139
Figure 4.11 - Correlation between mean 24 hours bacteraemia and mean survival time of each congenic line infected with <i>S. pneumoniae</i> .	141
Figure 5.1 - Microarray comparison of gene expression in the lung tissue indicated differential regulation of TGF- $\beta$ signalling pathway between BALB/c and CBA/Ca mice following pneumococcal infection.	146

Figure 5.2 - <i>tgfb1</i> expression and TGF- $\beta$ production is upregulated in BALB/c lungs in contrast to CBA/Ca lungs during pneumococcal infection. _____	148
Figure 5.3 - Foxp3 immunostaining (DAB staining) of lung sections taken from mice during pneumococcal infection. _____	150
Figure 5.4 - Increase in Foxp3 <sup>+</sup> T regulatory cells in BALB/c lungs over time post-infection. _____	150
Figure 5.5 - Increase in Foxp3 <sup>+</sup> T regulatory cells in BALB/c lungs at 24 hours post-infection. _____	152
Figure 5.6 - Number of Helios <sup>+/-</sup> Foxp3 <sup>+</sup> T regulatory cells in BALB/c and CBA/Ca lungs following pneumococcal infection. _____	153
Figure 5.7 - Number of Foxp3 <sup>+</sup> Helios <sup>+</sup> in the pneumococcal-infected BALB/c and CBA/Ca lungs following pneumococcal infection. _____	154
Figure 5.8 - Number of IL-10 <sup>+</sup> T regulatory cells in BALB/c lungs at 24 hours post-infection. _____	155
Figure 5.9 - Number of T regulatory cells expressing PD-L1 in BALB/c and CBA/Ca lungs following pneumococcal infection. _____	157
Figure 5.10 - Number of T regulatory cells expressing CTLA-4 in BALB/c and CBA/Ca lungs following pneumococcal infection. _____	158
Figure 5.11 - BALB/c mice display a greater percentage of Foxp3 <sup>+</sup> CTLA-4 <sup>+</sup> cells in their spleen by 24 hours post-infection. _____	159
Figure 5.12 - IL-17 <sup>+</sup> cell numbers in BALB/c or CBA/Ca lungs at 24 hours post-infection. _____	160
Figure 5.13 - CBA/Ca mice display uncontrolled lung inflammation and associated apoptosis following <i>S. pneumoniae</i> infection. _____	162
Figure 5.14 - Interferon- $\gamma$ producing cells in the lungs at 24 hours post-infection. ____	163
Figure 5.15 - Inhibition of TGF- $\beta$ activity impairs BALB/c resistance to pneumococcal infection. _____	166
Figure 5.16 - Adoptive transfer of in vitro generated Foxp3 <sup>+</sup> T regulatory cells improves CBA/Ca survival in pneumococcal infection. _____	169
Figure 5.17 - Disease resistance in outbred MF1 mice correlates with strong T regulatory cell responses in the lung. _____	171
Figure 6.1 - Diagram of <i>cd22</i> gene (top), highlighting exon 5/6 where the stop codon lies (bottom). _____	175
Figure 6.2 - Novel SNP found in the <i>cd22</i> gene of the CBA/Ca mice background. ____	177

Figure 6.3 - SNP in <i>cd22</i> gene identified on CBA/Ca background does not occur in 17 inbred mouse strains from Jackson Laboratories. _____	178
Figure 6.4 - Pyrosequencing output (pyrogram) of the <i>cd22</i> SNP observed in CBA/Ca background. _____	179
Figure 6.5 - Number of CD22 <sup>+</sup> B cell number in the lungs of BALB/c and CBA/Ca mice following <i>S. pneumoniae</i> infection. _____	182
Figure 6.6 - CD22 <sup>+</sup> and total B cell number in the lungs of BALB/c and CBA/Ca mice following <i>S. pneumoniae</i> infection. _____	183
Figure 6.7 - Numbers of IgM <sup>high</sup> B cells in the lungs of BALB/c and CBA/Ca mice post-infection with <i>S. pneumoniae</i> . _____	185
Figure 6.8 - IgM <sup>+</sup> and total B cell number in the lungs of BALB/c and CBA/Ca mice following <i>S. pneumoniae</i> infection. _____	186
Figure 6.9 - Number of CD22 <sup>+</sup> B cell number in the spleen of BALB/c and CBA/Ca mice following <i>S. pneumoniae</i> infection. _____	188
Figure 6.10 - Flow cytometric analysis of CD22 binding site tested with a different antibody clone Cy34.1 in lungs and spleen samples of BALB/c and CBA/Ca mice, prior and post- infection with <i>S. pneumoniae</i> . _____	189
Figure 6.11 - Comparison of outcome of pneumococcal infection of CD22-deficient and sufficient mice. _____	191
Figure 6.12 - Bacterial counts of <i>S. pneumoniae</i> in various organs following intranasal infection of CD22-deficient and sufficient mice. _____	193
Figure 7.1 - Components influencing resistance and susceptibility to pneumococcal pneumonia. _____	209

---

## CHAPTER 1. INTRODUCTION

---

### 1.1 *Streptococcus pneumoniae*

*Streptococcus pneumoniae* (Figure 1.1), also known as the pneumococcus, is an important respiratory pathogen responsible for substantial morbidity and mortality worldwide. The pneumococcus causes more deaths from invasive infections than any other bacterium and according to the World Health Organization is the leading infectious cause of death in children worldwide (WHO, 2014).

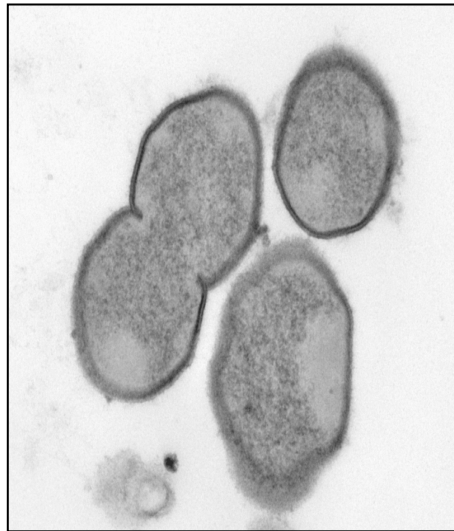


Figure 1.1 - Electron micrograph of *Streptococcus pneumoniae*. Figure showing encapsulated pneumococci.

The pneumococcus causes a wide variety of infections, from symptomless carriage or relatively benign mucosal infections such as otitis media, sinusitis and conjunctivitis, to invasive infections such as pneumonia. The bacterium may also invade the bloodstream to cause sepsis or septicaemia and spread to other secondary sites via the haematogeneous route to cause meningitis or other symptoms, collectively called invasive pneumococcal disease (IPD) (Kadioglu *et al.*, 2000; Mahdi *et al.*, 2008; Kayhty *et al.*, 2009). Invasive pneumococcal disease most frequently affects children less than 2 years old, adults over 65 years old and immunocompromised individuals (children or adults) (Lynch & Zhanel, 2010). The human nasopharynx is the major ecological niche and is the only reservoir of pneumococci, which are transmitted by droplet spread between individuals (Kayhty *et al.*, 2009; Lynch & Zhanel, 2010). The

pneumococcus produces a plethora of virulence factors that aid its spread from the nasopharynx to locations such as the lungs, blood and brain (Rose *et al.*, 2008; Chiavolini *et al.*, 2008; Gut *et al.*, 2008).

Antibiotics are the standard therapy for pneumococcal disease, however, in the last twenty years, resistance among pneumococci has become a threatening problem and is influenced by patterns of antibiotic use, population density, and spread of a few international clones (Lynch & Zhanel, 2010). On the other hand, vaccination can offer protection against a spectrum of pneumococcal serotypes, although there are various problems with current vaccination strategies, and horizontal gene transfer may further reduce the efficacy of both vaccines and antibiotics (Denny *et al.*, 2003; Kayhty *et al.*, 2009).

### **1.1.1 History**

*Streptococcus pneumoniae*, a major cause of human disease, was one of the first pathogens to be isolated and characterised (Austrian, 1981). The pneumococcus came to light in the golden era of microbiology that began in the last quarter of the 19<sup>th</sup> century (Siber *et al.*, 2008). Edwin Klebs, in 1875, was probably the first to recognize pneumococci in infected sputum and lung tissue, some years before they were isolated and identified. In 1881, *S. pneumoniae* was isolated by the chemist Louis Pasteur from the saliva of a patient with rabies (Siber *et al.*, 2008). At the same time, a physician, George Sternberg, discovered the pneumococcus, independently, by isolating and growing it in culture (Siber *et al.*, 2008).

In 1886, Albert Fraenkel found *S. pneumoniae* bacteria in the mouths and throats of patients with lobar pneumonia, and was able to distinguish them from other pneumonia causes using Gram stain, and gave the familiar name “pneumococcus” due to its role as a causative agent of pneumonia and being a lancet-shaped gram-positive diplococcus (Siber *et al.*, 2008). Fraental was also one of the first to recognize pneumococcal infections of other body sites in association with pneumonia. Within a few years, investigators documented other complications of pneumonia, either resulting from direct extension, like acute purulent tracheobronchitis and otitis media, or from hematogenous spread, for example abscess of the liver or spleen, meningitis and bacteraemia (Austrian, 1981; Watson *et al.*, 1993).

In the beginning of the 20<sup>th</sup> century the bacterium was termed *Diplococcus pneumoniae* due to its characteristic appearance, but it was renamed *Streptococcus pneumoniae* in 1974 due to its growth in chains in liquid medium. In 1902 Neufeld discovered the Quellung or capsular swelling test. However, only a few years later, Neufeld and L. Haedel developed these techniques to distinct serotypes (types I and II) of isolates using type-specific antiserum (Avery, 1915).

*Streptococcus pneumoniae* played a major role in scientific advances of the 20<sup>th</sup> century, where studies with this organism led to the recognition of DNA as the basic unit of genetic material. In the late 1920s, Griffith discovered the phenomenon of transformation when he observed that by injecting into a mouse lethal type II live organisms mixed inoculating with heat-killed encapsulated type III pneumococcus, the mice died, and live type III pneumococcus were recovered from their tissues. Avery, MacLeod and McCarty then demonstrated that the pneumococcus was capable of natural transformation, by incorporating exogenous DNA into the genome. These discoveries on genetic transformation marked the birth of molecular era of genetics (Lacks, 2003; Griffith, 1966).

Since *S. pneumoniae* was first isolated in the 19<sup>th</sup> century, many discoveries have been made in this field that have had an incredible impact on human life. Nevertheless, it is vital to remember that bacteria adapt extremely rapidly to environmental changes and so it is crucial that we continue to strive to a better understanding of bacterial pathogenesis, besides exploring why some humans show resistance to pneumococcal infections and use such attributes in benefit of humanity.

### **1.1.2 General characteristics of *S. pneumoniae***

The pneumococcus is a Gram-positive bacterium, “lancet-shaped” coccus approximately 0.5 to 1.25 micrometers in diameter (Todar, 2003). It is a fermentative aero-tolerant anaerobe, non-motile and does not form spores (Todar, 2003). It lacks catalase and ferments glucose to lactic acid. The colonies are usually seen as pairs (diplococci), but can also appear in long chains or single cells in culture (Todar, 2003). On blood agar, the bacteria grow as shiny colonies, approximately 1 mm in diameter, showing an incomplete green haemolysis ( $\alpha$ -haemolytic streptococci) around and a zone of inhibition ( $\geq 14$  mm) surrounding an optochin disc (optochin sensitive) (Todar,

2003). The bacterium can also be identified by the Quellung reaction (German word for "swelling"), in which a specific antibody binds to the polysaccharide antigen of the pneumococcal capsule or other bacterial strains appear to enlarge, becoming opaque (Todar, 2003).

### 1.1.3 Epidemiology

Annually, invasive pneumococcal diseases (IPD) cause an estimated 1.6 million deaths, including 1 million children less than 5 years old (Lynch & Zhanel, 2010). The highest incidence of IPD is at extremes of age and in individuals with comorbidities or defects in immunity (Tuomanen *et al.*, 2004). *S. pneumoniae* causes around 11% (8-12%) of all deaths in children aged 1-59 months (Figure 1.2).

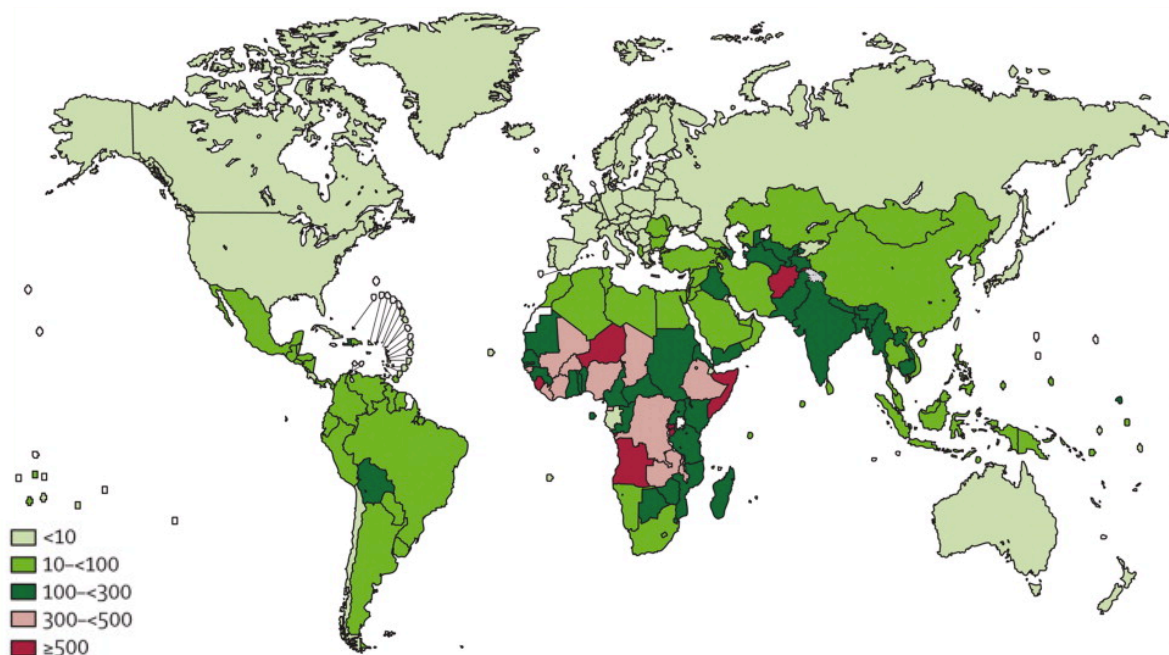


Figure 1.2 - Pneumococcal mortality rate. Pneumococcal deaths in children aged 1-59 months per 100,000 children younger than 5 years (HIV-negative pneumococcal deaths only) in 2000 (O'Brien *et al.*, 2009).

The available population-based surveillance reports show significant differences in the incidence and mortality rates of IPD worldwide, in particular between industrialised and developing countries. For example, a global surveillance study in children aged 1-59 months, in 2000, estimated the occurrence of approximately 14.5 million IPD episodes (O'Brien *et al.*, 2009). Approximately 826,000 deaths resulted, of which 91,000 occurred in HIV-positive and 735,000 in HIV-negative children. Of the deaths in

children without underlying medical conditions, over 61% occurred in ten African and Asian countries (Figure 1.2) (O'Brien *et al.*, 2009).

Pneumonia kills more children under five years of age than any other illness worldwide. In 2007, of the estimated 9 million child deaths, around 20% (or 1.8 million) were due to pneumonia (Figure 1.3).

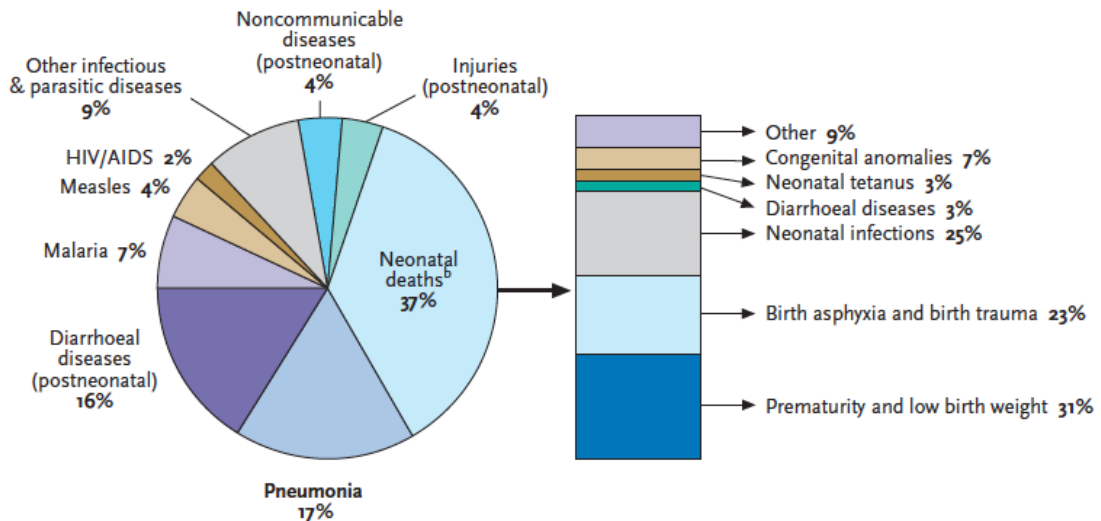


Figure 1.3 - Causes of death in neonates and children under five in the world in 2004 (WHO, 2008).

Interesting reports demonstrate that there are ethnic differences in susceptibility to invasive pneumococcal infection, and host genetics play a large part. One of the reports suggested that there was a much higher incidence of pneumococcal bacteremia in black populations in New York than white. The incidence rate for caucasians was 13.8 per 100,000 whereas it was 49.3 per 100,000 for African Americans (Bennett *et al.*, 1992). Environmental factors, more specifically the economic status, played a role in these cases, nonetheless they were not sufficient to explain the whole effect of ethnicity on incidence rates. Medical conditions that predispose people to pneumococcal infections showed no difference between races in this study. In 2001, the same conclusions were reached, namely that black individuals of all ages were at higher risk of invasive pneumococcal infections than white individuals (Robinson *et al.*, 2001).

Other studies with native and aborigine communities revealed high incidence rates of pneumococcal disease: in the Alaskan natives, from 1980 to 1986, the annual incidence

rates were 105 per 100,000 (Davidson *et al.*, 1989); in the White Mountain Apaches the incidence rate was 207 per 100,000 (Cortese *et al.*, 1992); and the highest incidence reported so far has been in Australian aboriginals, in which the overall incidence rates are 222.4 per 100,000 (Torzillo *et al.*, 1995). All these surveillance studies indicate incidence rates significantly higher than the reports for white populations in the United States (13.8 per 100,000) (Bennett *et al.*, 1992).

#### **1.1.4 Antimicrobial therapy and vaccination**

At present, healthcare providers when diagnosing pneumococcal pneumonia in patients, are most likely to prescribe antibiotics to treat this disease and other pneumococcal infections (NIAID, 2012).

Antibiotics are one class of antimicrobials (including anti-viral, anti-fungal, and anti-parasitic drugs), chemically produced by or derived from microorganisms, such as bacteria and fungi (eMed Expert, 2012). The antibiotic treatment depends on the infection site and patient age (Tuomanen *et al.*, 2004), where the drug effectiveness and allergic potential will determine a sole or combined administration of such prophylactic antibacterial agents (Internet FAQ Archives, 2012). Although, even when antimicrobial therapy shows effectiveness, pneumococcal diseases persist connected with significant morbidity and mortality. A few decades ago, Austrian and Gold compared data from the pre-antibiotic and post-antibiotic eras and demonstrated similar mortality rates during the first few days of the disease in patients with bacteremic pneumonia (Austrian & Gold, 1964). Such observation highlights the need for more effective alternative solutions, which may be an effective vaccine and/or effective new drugs against pneumococcal infection and disease.

Regarding vaccination, in 1977, Merck's 14-valent pneumococcal polysaccharide vaccine (PNEUMOVAX) was authorised for clinical use. Later, in 1983, this vaccine was reformulated after the emergence of additional data on the distribution of serotypes causing disease and immunologic properties of the capsular polysaccharide (Robbins *et al.*, 1983). Subsequently, a 23-valent pneumococcal polysaccharide vaccine (PPSV23) was introduced, which has been used to vaccinate adults and children over 2 years old, including individuals (aged 2-64 years) who have a chronic illness (e.g. cardiovascular or pulmonary disease, sickle cell disease, diabetes) or a weakened immune system due

to an illness (e.g. HIV infection, Hodgkin's disease, chronic renal failure) (Centers for Disease Control and Prevention, 2001; Schrag *et al.*, 2001).

At present, two types of pneumococcal vaccines, composed of purified *S. pneumoniae* capsular polysaccharides, are available on the market: the pneumococcal polysaccharide vaccine (PPSV23 from *Merck*) and the pneumococcal conjugated vaccines (PCV7, PCV13 from *Pfizer* and PCV10 from *GSK*). The limitations of PPV23 (see section 1.1.5) contributed to the development and subsequent introduction of the hepta-valent pneumococcal conjugated vaccine (PCV7, named *Prennar-7*), in 2000. The introduction of PCV7 radically reduced the IPD rates, otitis media and nasal carriage of the vaccine serotypes among all age groups, including the immunocompromised, older individuals and also reduced the racial disparities in pneumococcal disease (Flannery *et al.*, 2004). Besides it has proven to be a cost effective vaccine because of the disease it prevents in young children (Robinson *et al.*, 2001). These vaccine types were developed to induce the production of type-specific antibodies against pneumococcal capsular polysaccharides, that would activate and fix the complement, promoting bacterial opsonisation and phagocytosis, therefore, helping to prevent pneumococcal diseases (WHO, 2009). After the PCV7, in 2009 a 10-valent pneumococcal conjugate vaccine (PCV10, named *Synflorix*) was introduced, containing polysaccharides from PCV7 plus three extra serotypes that had increased the rates of IPD after PCV7 introduction, preventing IPD (but not pneumonia or otitis media) in children under 2 years old (Nordqvist, 2012). In 2010, the 13-valent pneumococcal conjugate vaccine (PCV13, named *Prennar-13*) for prevention of IPD and otitis media. PCV13 was approved for use among children aged 6 weeks to 71 months, with underlying medical conditions that increase their risk of pneumococcal disease or complications, gradually succeeding to PCV7 (Centers for Disease Control and Prevention, 2010). The companies commercialising the current vaccines (*Merck*, *Pfizer* and *GSK*) are developing a 3<sup>rd</sup> generation of pneumococcal-conjugated vaccines, that will cover a few more serotypes, but they are still at early clinical status phase (Siber, 2012).

Many pharmaceutical companies are committed to produce and commercialise more efficient vaccines to prevent pneumococcal infections. Encouragingly, the next generation of pneumococcal vaccines based on conserved pneumococcal proteins and whole-cell vaccines, are both being tested (Siber, 2012). The protein-based vaccines

induce functional antibody (by opsonising bacteria, preventing adhesion, inhibiting anti-toxin effects like from pneumolysin, inhibiting invasion and growth) and both (protein-based and whole-cell) stimulate T cell response (immunogenic), envisaged to replace or complement the current polysaccharide-based vaccines.

### 1.1.5 Limitation of current therapies

Antibiotic resistance among pneumococci and other bacterial species has become increasingly important in recent decades (Cunha, 2006). Pneumococcal drug resistance is the current problem, which is conferred throughout two primary genetic mechanisms: transformation (the uptake of free DNA from the environment) and conjugative transposons (the transfer of segments of genomic DNA during bacterial fusion) (WHO, 2001). Antibiotic-resistance is increasing in this microorganism, affecting the use of all classes of drugs, primarily the  $\beta$ -lactams and macrolides (Reinert, 2009), as observed in Figure 1.4.

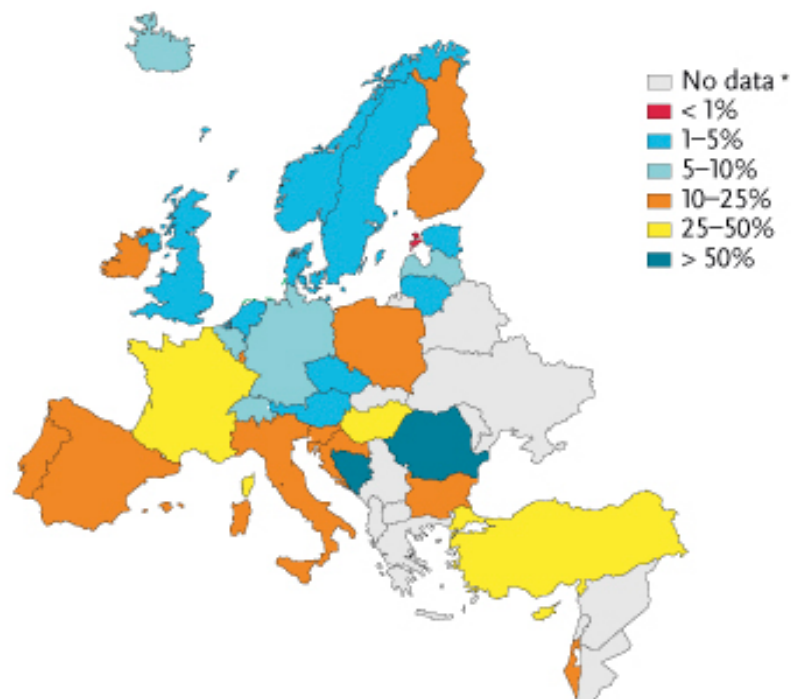


Figure 1.4 - Proportion of invasive *Streptococcus pneumoniae* isolates with dual resistance to erythromycin and penicillin in 2006 (Gould, 2008). (\*) These countries did not report any data or reported less than 10 isolates.

Multidrug resistance also is emerging (Feldman & Anderson, 2011). The resistance to antibiotics is escalating through overuse, misuse, improper dosing and the use of substandard or diluted medicines, all contributing to the rise of resistance (Hughes,

2011; Jenkins *et al.*, 2012). Surveillance data collected over recent decades has shown a trend of geographical variation in the prevalence of antimicrobial-resistant pneumococci. In the 1970s, penicillin-resistant pneumococci were most common in Israel, Papua New Guinea, Poland, South Africa and Spain, as well as some states in the United States (Appelbaum, 1992). At the beginning of the 21<sup>st</sup> century, resistant pneumococci have a worldwide distribution, although only limited surveillance data from a majority of African, Asian and South American countries are available (WHO, 2001), and specifically penicillin-resistance *S. pneumoniae* varies from 0% resistance in the Netherlands to 71.5% resistance in South Korea (Walsh & Amyes, 2004). Reports of consumption data between 1992 and 2000 show erythromycin resistance correlating to the consumption of total macrolides (Reinert *et al.*, 2002). In Turkey, antibiotic-resistance profiles from 2008, revealed a substantial increase in cumulative percentage of resistance to diverse antibiotics (penicillin 35%, trimethoprim-sulfamethoxazole 39%, tetracycline 19%, erythromycin 18%, azithromycin 18%, clarithromycin 10%, ofloxacin 13%), in invasive pneumococcal cases (Erdem, 2008). Because the pneumococcus is normally carried as a commensal bacterium in the nasopharynx and eradication of carriage is not a feasible outcome, prevention of invasive pneumococcal diseases may be part of the solution in the intervention process (WHO, 2001).

The existing polysaccharide vaccine (PPV23) remains one of the most controversial of the currently used vaccines because of its variable efficacy against all manifestations of pneumococcal infections. The vaccine is only about 60% effective in preventing invasive diseases and is less effective at preventing pneumococcal pneumonia and other localised respiratory tract infections (McDaniel & Swiatlo, 2004). Additionally, PPV23 is poorly immunogenic (being T cell independent antigens) (Gillespie, 1989; Siber *et al.*, 2008), particularly in children under two years of age (Laferriere, 2011), immunocompromised patients (Shapiro *et al.*, 1991; Niederman *et al.*, 2001) and the elderly with chronic illness (Huss *et al.*, 2009). Poor effectiveness of PPV23 against acute otitis media was also observed (Wadwa & Feigin, 1999). Polysaccharides are T-independent antigens and their effect is mediated by B cells without the involvement of T cells, resulting in diminished immunogenicity in children under two (Swiatlo & Ware, 2003). Also, this class of antigen induce poor memory immune responses, so boosting does not result in significantly higher antibody titres when compared to single

immunisation (Swiatlo & Ware, 2003). In addition, PPV23 delivers no protection against mucosal infections, and consequently are unable to reduce pneumococcal carriage in the nasopharynx (WHO, 2008).

Clinical trials with PCV7 demonstrated it to be highly efficacious against IPD (Black *et al.*, 2000), moderately efficacious against pneumonia (Black *et al.*, 2002), and effective in reducing otitis media episodes (Eskola *et al.*, 2001). The introduction of PCV7 provided high coverage of the serotypes associated with IPD among children (between 65% to 80% coverage), in industrialised countries. However, the geographical serotype variation has the consequence of a very low coverage provided in developing countries (WHO, 2007). Additionally, serotype replacement has been observed among populations of children, with an increase in cases of pneumococcal infections caused by non-vaccine serotypes (Eskola *et al.*, 2001; Jomaa *et al.*, 2005; O'Brien *et al.*, 2007). This also was recently observed in a surveillance study recently performed with Native America communities (Scott *et al.*, 2012). Another limiting factor is the high-cost of the vaccine, which restricts its use in developing countries (Lopalco, 2007). With PCV10 and later with PCV13 there was an increase in serotype coverage in Portugal, 55% and 83% respectively (Aguiar *et al.*, 2010). However, the critical aspect remains unchanged, namely vaccination results in selective pressure for replacement with non-vaccine *S. pneumoniae* serotypes (Black *et al.*, 2000).

#### **1.1.6 Pathogenesis of pneumococcal disease**

Figure 1.5 illustrates the main routes of *S. pneumoniae* infections and key host-microbe encounters that can lead to invasive diseases.

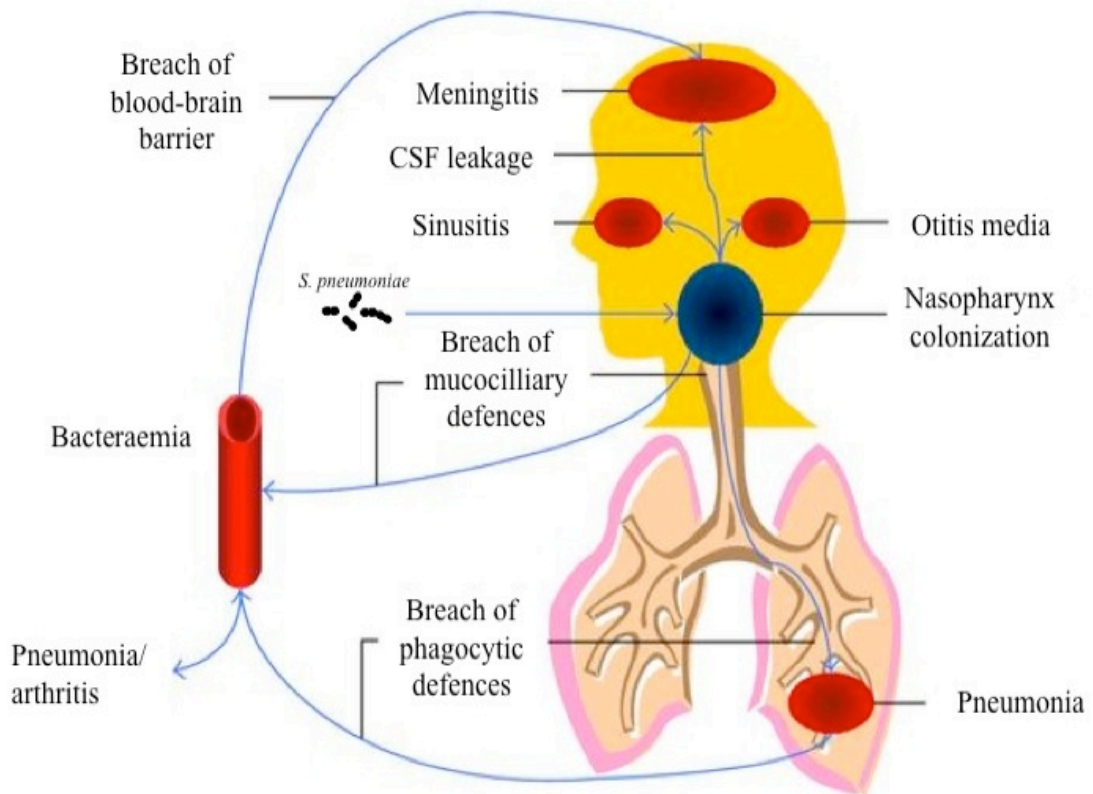


Figure 1.5 - Routes of host infection by *S. pneumoniae* leading to invasive disease. Pneumococci bind to mucosal epithelial cells colonising the nasopharynx, and can then spread to the sinuses or middle ear, or else can be aspirated into the lung, or invade the bloodstream. Progression to pneumonia or meningitis requires a susceptible host background, such as antecedent viral infections, lung injury, immunocompromised conditions. If the host physical barrier, humoral and cellular immune responses are ineffective in clearing the pneumococci, the bacteria can breach host barriers causing invasive diseases like pneumonia, meningitis and septicemia. Figure adapted from Goonetilleke *et al.* (2009).

The human nasopharynx is the only natural reservoir of *S. pneumoniae*, from which it can be transmitted via respiratory droplets from patients or healthy carriers to other individuals, by direct contact (Tuomanen *et al.*, 2004; WHO, 2009). Once established in the nasopharynx, pneumococci may be carried for long periods of time, asymptotically (especially in children), without causing disease (WHO, 2009). Nasopharyngeal colonisation may occur at early infancy, with most infants acquiring one or more pneumococcal serotypes, sequentially or simultaneously, and to declining with increasing age (Gillespie, 1989). In adults, pneumococcal carriage rate is directly associated to the frequency of direct contact with colonised-children (Gillespie, 1989), and also with cold temperature seasons when viral infections are more common (Gillespie, 1989; Dowell *et al.*, 2003; Klugman, 2011). Geographical area, genetic

background, and socio-economic conditions are also factors (Garcia-Rodriguez & Fresnadillo Martinez, 2002; Bogaert *et al.*, 2004). It has been reported that pneumococcal adherence to the epithelial cells of the upper respiratory tract can be augmented when preceded by influenza infections (Plotkowski *et al.*, 1986). An individual pneumococcal strain can be carried for weeks or months before its clearance (Lexau *et al.*, 2005), or the acquisition of a new serotype may trigger disease (Johnston, 1991).

The spread from the bacterial niche in the pharynx into host sterile sites is determined by the combination of the immunity status and the virulence of the colonising pneumococcal strain (AlonsoDeVelasco *et al.*, 1995; Bogaert *et al.*, 2004). It has been demonstrated that a rapid local immune response to a microorganism would prevent colonisation and limit its duration, whereas a poor immune response would result in more prolonged carriage (Faden *et al.*, 1995). A breach in the host defences of the upper respiratory tract, may facilitate transit of the microbe to the lower respiratory tract, nasal sinuses or the middle-ear space. The pneumococcus may also invade the bloodstream directly through the damage of mucosal epithelial cells (Boulnois, 1992; Musher, 1992).

When pneumococci invade the lungs, an inflammatory response is triggered by the host, and in the majority of cases, especially susceptible groups (e.g. immunocompromised, children and the elderly, smokers), but this reaction may not halt progression of the bacteria to the systemic circulation, causing septicaemia (Bogaert *et al.*, 2004). From the blood, *S. pneumoniae* may migrate to the meninges, cross the blood-brain barrier and transmigrate through brain microvascular endothelial cells, reaching the subarachnoid space, causing meningitis (Ring *et al.*, 1998; Zysk *et al.*, 2001).

### **1.1.7 Virulence factors**

*Streptococcus pneumoniae* has an armamentarium of virulence factors to colonise the upper respiratory tract, and consequently spread to sterile sites of the lower respiratory tract, causing pneumonia. The combination of the different virulence factor activities provides the microorganism with the ability to directly interact with the host structures or to evade the host innate and adaptive defence mechanisms, damaging host tissues. The majority of the virulence factors are localized on the pneumococcal cell surface,

whereas the rest are situated in the cytoplasm (Jedrzejewski, 2001; Kadioglu *et al.*, 2008). The major pneumococcal virulence factors are represented in Figure 1.6 and Table 1.1.

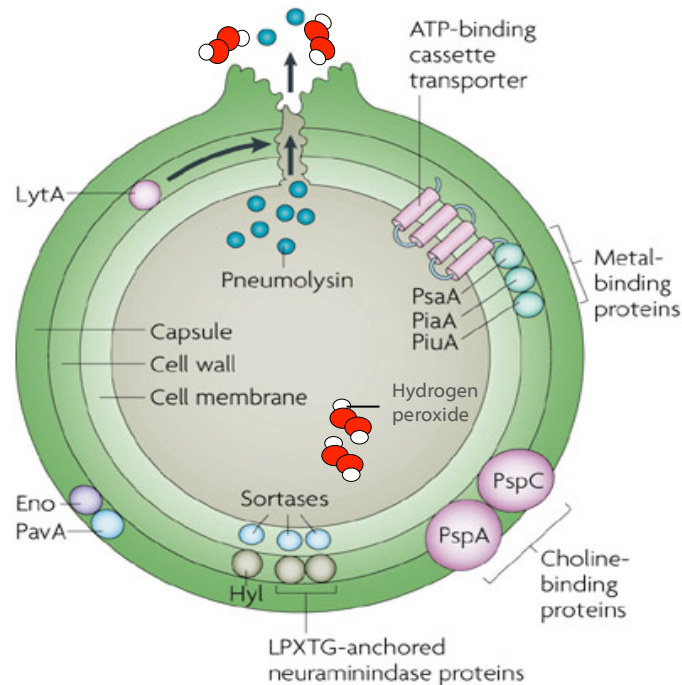


Figure 1.6 - *Streptococcus pneumoniae* virulence factors. Major virulence factors of the pneumococcus consist of: capsule (not in the figure), choline-binding proteins; pneumococcal surface proteins A and C (PspA and PspC); the LPXTG-anchored neuraminidase proteins (NanA, NanB and NanC); hyaluronate lyase (Hyl); pneumococcal adhesion and virulence A (PavA); enolase (Eno); pneumolysin (Ply); autolysin A (LytA); the metal-binding proteins pneumococcal surface antigen A (PsaA), pneumococcal iron acquisition A (PiaA) and pneumococcal iron uptake A (PiuA); and hydrogen peroxide (H<sub>2</sub>O<sub>2</sub>). Figure adapted from Kadioglu *et al.* (2008).

### 1.1.7.1 Virulence factors involved in pathogenesis of pneumococcal disease

Virulence and host-pathogen interactions are complex and contribute to the development and outcome of pneumococcal disease: colonisation and invasive disease. An overview of virulence factors is represented in Table 1.1.

	<b>Pneumococcal virulence factors and disease</b>	<b>Principal role</b>
Upper-airway colonisation	Capsule	Prevents entrapment in the nasal mucus, thereby allowing access to epithelial surfaces. Also inhibits effective opsonophagocytosis.
	Phosphorylcholine (ChoP)	Binds to rPAF on the epithelial surface of the human nasopharynx.
	Choline-binding protein A (CbpA or PspC)	Binds to human secretory component on a polymeric Ig receptor during the first stage of translocation across the epithelium (process of reverse transcytosis).
	$\beta$ -Galactosidase (BgaA) $\beta$ -N-Acetylglucosaminidase (StrH)	Act sequentially to cleave terminal sugars from human glycoconjugates, which might reveal receptors for adherence.
	Hyaluronidase (Hyl)	Breaks down hyaluronan-containing extracellular matrix components.
	Pneumococcal adhesion and virulence A (PavA)	Binds to fibronectin.
	Enolase (Eno)	Binds to plasminogen.
Respiratory-tract infection and pneumonia	Pneumolysin (Ply)	Cytolytic toxin that also activates complement. An important determinant of virulence in <i>in vivo</i> models of disease. Wide range of effects on host immune components at sub-lytic concentrations.
	Pneumococcal surface protein A (PspA)	Prevents binding of C3 onto pneumococcal surface. Also binds lactoferrin.
	Autolysin (LytA)	Digests the cell wall, which results in the release of Ply.
	Pneumococcal surface antigen A (PsaA)	Component of the ABC transport system, which is involved in resistance to oxidative stress.
	Pneumococcal iron acquisition A (PiaA) Pneumococcal iron uptake A (PiuA)	Component of the ABC transport system.
	Neuraminidases (NanA and NanB)	Aid colonisation by revealing receptors for adherence, modifying the surfaces of competing bacteria that are within the same niche and/or modifying the function of host clearance glycoproteins.
	IgA1 protease (IgAP)	Cleaves human IgA1.
	Superoxide dismutase A (SodA)	Detoxifies superoxide anion.

Table 1.1- Pneumococcal virulence factors and their main role in colonisation and disease. Adapted from Kadioglu *et al.* (2008).

### 1.1.7.2 Capsule

The pneumococcal capsule is a major virulence factor, which protects the bacterium from phagocytosis by polymorphonuclear leukocytes. The capsule is composed of polysaccharide (Bogaert *et al.*, 2004; Tuomanen *et al.*, 1995). The capsule

polysaccharides are highly heterogeneous and nearly 100 different capsular serotypes have been identified, which vary in the chemical composition (Selva *et al.*, 2012). There is a highly variable distribution of serotypes (Henriques Normark *et al.*, 2001). For instance, the serotype of invasive isolates varies according to country and time period (Henriques Normark *et al.*, 2001). The capsular polysaccharides have no contribution to host inflammatory response and do not appear to be involved in adherence to respiratory epithelium (Talbot *et al.*, 1996). In contrast, they contribute to inhibition of phagocytosis, by preventing complement C3b opsonisation of the bacterial cells (Todar, 2003). The negative charge of capsular polysaccharides seems to electrostatically repel pneumococci from phagocytic cells and evading of phagocytosis correlates with higher carriage prevalence (van Oss, 1978; Li *et al.*, 2013). Additionally, it is proposed that the capsule augments pneumococcal colonisation by electrostatically repulsion against highly negatively charged mucus (Nelson *et al.*, 2007). Different serotypes have differing propensities to be among invasive and carriage isolates. As the serotype is dependent on the capsular polysaccharide expressed, this is clearly an important virulence factor to the pneumococcus. Different serotypes are isolated at differing frequencies from different age groups (Sjostrom *et al.*, 2006). Pneumococcal strains belonging to serotypes and clones with differences in their invasive disease potential also differ in their capacity to evoke disease in mice (Sandgren *et al.*, 2005). Also, different pneumococcal clones of the same serotype were found to be different in virulence in murine models of pneumonia (Sandgren *et al.*, 2005).

### **1.1.7.3 Cell wall**

The cell wall is mainly composed of peptidoglycan, composed of disaccharides and peptides that surrounds the cell, conferring its shape and protects it from its internal osmotic pressure. In addition, the cell wall contains lipoteichoic acid attached to the membrane and teichoic acid linked to proteoglycan (Jennings *et al.*, 1980; Todar, 2003; Bogaert *et al.*, 2004). The cell wall also incorporates phospho-choline in the teichoic acids, which is used by a number of important virulence proteins for attachment to the cell surface (Tuomanen *et al.*, 1995; Bogaert *et al.*, 2004). The most immunogenic part of the cell wall is the presence of phosphorylcholine in the lipoteichoic acid, which plays a major role in the inflammatory process (Tuomanen *et al.*, 1995).

#### 1.1.7.4 Adhesins and surface proteins

The pneumococcal surface contains more than 500 surface proteins associated with specific interaction with host molecules. These bacterial proteins are considered as key players in the infection process. Pneumococcal attachment to eukaryotic cells is mediated by a diverse group of surface molecules, that can be distinguished by genome analysis, which include: lipoproteins: a family of proteins that recognizes the phosphorylcholine of the lipoteichoic and teichoic acids, which are the choline-binding proteins (CBPs); and also by non-classical surface proteins that lack a leader peptide and a membrane-anchor motif, designated as LPxTG (leucine, proline, x, threonine, and glycine, where “x” is any amino acid). These proteins are covalently anchored in the cell wall after cleavage of the LPxTG sequence by a transpeptidase, designated a sortase (Andersson *et al.*, 1983; Bergmann & Hammerschmidt, 2006).

The surface-exposed proteins pneumococcal surface protein A (PspA) and pneumococcal surface protein C (PspC) play important roles in the pathogenesis of invasive pneumococcal diseases (Cao *et al.*, 2010). The pneumococcal surface protein A (PspA) is a protein that was identified in all pneumococci, but is antigenically very variable (Crain *et al.*, 1990). Inactivation of PspA resulted in a significant reduction in full virulence of pneumococcus (McDaniel *et al.*, 1987). PspA is a lactoferrin-binding protein that can inhibit complement activation and this protein can also protect the bacteria from killing by apolactoferrin (Hammerschmidt *et al.*, 1999; Shaper *et al.*, 2004). Recent findings indicate that PspA also plays a role in secondary pneumococcal infection post influenza virus infection (King *et al.*, 2009). Moreover, it was demonstrated PspA or PspC immunization could give effective protection against invasive pneumococcal infections (Jounblat *et al.*, 2003; Orihuela *et al.*, 2004). PspC is associated with adherence of pneumococci to host tissues, which result in the protein's ability to bind glycoconjugates on the surface of host epithelial cells (Rosenow *et al.*, 1997). PspC also binds the polymeric immunoglobulin receptor, which plays a key role in the mucosal immunity by transporting the polymeric IgA across the mucosal epithelium and then the translocation of pneumococci across human nasopharyngeal epithelial cells (Zhang *et al.*, 2000).

The pneumococcal surface adhesion A (PsaA) is another pneumococcal surface protein (Sampson *et al.*, 1994). PsaA is a lipoprotein that belongs to the ABC-type transport

protein complex, which transports  $Mn^{2+}$ . It is also an adhesin that plays a major role in pneumococcal attachment to the host cell and virulence. This lipoprotein is immunogenic and natural nasopharyngeal colonisation of pneumococci elicits an increase in antibody towards PsaA (Rajam *et al.*, 2008).

#### **1.1.7.5 Pneumolysin**

Pneumolysin (PLY) is a cytoplasmic protein that plays important roles in the virulence of *S. pneumoniae* (Jonhson, 1977). Pneumolysin is a member of a family of structural and antigenically associated pore-forming toxins, denominated cholesterol-dependent cytolysins (CDCs) (Gilbert, 2002; Nollmann *et al.*, 2004; Tweten, 2005). Members of this family are produced by different species of Gram-positive bacteria (Tweten, 2005) and the majority of CDCs, including PLY, require the presence of membrane cholesterol for their cytolytic activity (Gilbert, 2002; Nollmann *et al.*, 2004; Tweten, 2005). A classical feature of these toxins is their ability to create transmembrane pores in cholesterol-containing membranes, causing cell lysis (Tweten, 2005).

Pneumolysin requires the presence of cholesterol for its cytolytic activity in the target cell membrane and the depletion of cholesterol from membranes decreases the extent of binding and affects the cytolytic activity of the toxin (Johnson *et al.*, 1980; Waheed *et al.*, 2001; Giddings *et al.*, 2003). In addition to anti-cellular activity this haemolytic toxin can activate the complement directly in the absence of specific antibody (Mitchell *et al.*, 1991). Also, it has been reported that apoptotic responses to pneumolysin are dependent on the cytolytic properties of the molecule, as shown by a study where a point mutant in the domain required for cytolytic activity of pneumolysin (W433F) failed to induce apoptosis, whereas a pneumolysin mutant defective for complement activation (D385N) induced apoptosis at the same extent as the wild-type pneumolysin (Braun *et al.*, 2002).

Pneumolysin is not actively secreted during pneumococcal growth (Walker *et al.*, 1987), but is found in the cytoplasm of the bacterial cells (Bogaert *et al.*, 2004), due to the lack of signal peptide at the N-terminus of the protein (Walker *et al.*, 1987). The toxin is released in the form of a soluble monomer (Tilley *et al.*, 2005), mediated by the action of the pneumococcal autolysin (AlonsoDeVelasco *et al.*, 1995; Canvin *et al.*, 1995). More recently, the presence of active pneumolysin at the cell wall of *S.*

*pneumoniae* was detected. This is interesting considering that pneumolysin lacks not only a signal peptide but also any of the cell wall anchoring motifs known in Gram-positive bacteria (Price & Camilli, 2009).

Pneumolysin has been investigated for many years to define its role in the pathogenesis of pneumococcal diseases. *In vivo* studies have shown evidence of the importance of this toxin on pneumococcal virulence. An early study with a pneumolysin-negative mutant, named as PLN-A, showed a reduction in the bacterial virulence after intranasal challenge of mice (Berry *et al.*, 1989). Additionally, when administered intravenously to mice, PLN-A bacteria showed significantly reduced survival than the wild-type strain (Berry *et al.*, 1989). Further reported studies with PLN-A strain revealed that mice challenged by intranasal route with this mutant showed reduced severity of the inflammatory response, as well as bacterial growth rate in the lungs and delayed bacterial invasion in the bloodstream (Canvin *et al.*, 1995). In another study, PLN-A infection induced a delayed and significantly less intense leukocyte recruitment into the lungs, whereas with wild-type pneumococci induced an early recruitment of neutrophils and bacterial dissemination in the lungs (Kadioglu *et al.*, 2000). A study with another pneumolysin deficient mutant, named as  $\Delta$ Ply, showed reduced virulence when compared to wild-type pneumococci, using a rat meningitis model (Hirst *et al.*, 2008).

#### **1.1.7.6 Autolysin A**

N-acetylmuramoyl-L-alanine amidase (Lyt A) or autolysin A is an enzyme localised on the pneumococcal cell envelope (Diaz *et al.*, 1989). This enzyme recognises the presence of choline in the cell wall, binding to choline (member of coline-binding protein family) moieties on lipoteichoid acid, which induces a significant stabilization and lytic activity by dimerisation through the C-terminal hairpin of the enzyme (Briese & Hakenbeck, 1985; Usobiaga *et al.*, 1996; Fernandez-Tornero *et al.*, 2001; Lopez & Garcia, 2004; Maestro & Sanz, 2005; Buey *et al.*, 2007). This enzyme is involved in pneumococci growth, allowing cell division by cleavage of the N-acetylmuramoyl-L-alanine bond of pneumococcal peptidoglycan. During the stationary phase, when levels of nutrients are low, daughter cell separation or after binding of penicillin, autolysin A is activated (Giudicelli & Tomasz, 1984; Dowson *et al.*, 1997). Also at this growth stage, enzyme activation is directly associated with pneumococcal release of the Forssman antigen, which is highly inhibitor of Lyt A (Horne & Tomasz, 1985;

AlonsoDeVelasco *et al.*, 1995). The result of the Forssman antigen release is an uncontrolled Lyt A activity, inducing bacterial lysis and an inflammatory boost through the release of the pneumococcal cytoplasm content and cell wall fragments, including hydrogen peroxide and pneumolysin (AlonsoDeVelasco *et al.*, 1995).

#### **1.1.7.7 Neuraminidases**

Neuraminidases, known as sialidases, are a family of enzymes that catalyse the cleavage of terminal sialic acid residues from mucin, glycolipids, glycoproteins and gangliosides, on the cell surface or in body fluids, helping to penetrate the mucin layer, and consequently, allowing the bacteria to colonise the lungs (Kelly *et al.*, 1967; Andersson *et al.*, 1983; Scanlon *et al.*, 1989; Schauer, 2000). Three types of pneumococcal neuraminidases have been identified: NanA and NanB produced by all pneumococcal strains and NanC produced by 51% of the pneumococcal strains (Pettigrew *et al.*, 2006). The activity of the neuraminidases may result in host cell surface receptor exposure, suggesting that can contribute to pneumococcal interaction, increased adhesion and other processes (Paton *et al.*, 1983; Manco *et al.*, 2006). In addition, it has been shown that sialic acid is a signalling molecule, which by itself can induce NanA and NanB expression, consequently enhancing the ability of pneumococci to adhere to host surfaces and/or survive within the biofilm environment (Trappetti *et al.*, 2009). The deletion of either *nanA* or *nanB* genes was shown to have significant effects on nasopharyngeal carriage and pneumonia (Orihuela *et al.*, 2004; Manco *et al.*, 2006; Trappetti *et al.*, 2009). Little is known with regard to NanC's biological role, however it is probable that it functions in coordination with NanA and NanB (Xu *et al.*, 2011).

#### **1.2 Host genetic contribution to susceptibility to infectious disease**

Host genetic factors significantly contribute to infection susceptibility. For example, a study in 1984 revealed that susceptibility to six different infectious diseases (measles, mumps, chickenpox, German measles, scarlet fever and whooping cough) was inherited in twins, observing very high heritability rates, which estimates range from 86% hereditary component in the case of measles to 100% environmental component in the case of scarlet fever (Gedda *et al.*, 1984). A few years later, a study by Sorensen investigating premature death in adopted children considered that susceptibility to infection had a strong genetic contribution (Sorensen *et al.*, 1988). More data on genetic predisposition to infection studied in twins has been reported, observing significant

input of host genetics in susceptibility to infections, including with Hepatitis B virus (Lin *et al.*, 1989), *Mycobacterium tuberculosis* (Sepulveda *et al.*, 1994), *Helicobacter pylori* (Malaty *et al.*, 1994), *Plasmodium falciparum* (Jepson *et al.*, 1995), human immunodeficiency virus (HIV) (Chang *et al.*, 1996).

The genetics associated with susceptibility to infectious diseases are complex. Genetic traits may not simply be the result of the Mendelian inheritance of a single gene variation (monogenic), but from variation in two or more genes controlling a characteristic (polygenic) and their interaction with behavioral and environmental factors (Lander & Schork, 1994; Gu *et al.*, 2009). Susceptibility to infection is modulated by the individual's environment, age and gender. These factors may affect the genetic trait when some individuals fail to express clinical symptoms, even though they carry the allele – known as incomplete penetrance (Lander & Schork, 1994). Other complications can interfere in genetic trait association with infection. For example, genetic heterogeneity, in which a mutation occurring in several genes result in the same disease phenotype (Lander & Schork, 1994), as was observed in mycobacterial infection (Doffinger *et al.*, 2000).

Until recently, the mapping of loci controlling continuous or linear traits (Quantitative Trait Loci or QTL) in naturally outbred populations, like humans, has been limited in its success and identifying candidate genes has largely been restricted to association studies in humans. These types of studies require a large numbers of cases and might not be successful in detecting weak associations (Hill, 1998; McPeck, 2000). Nevertheless, the recent advances in human genome wide studies have enabled the genetic mapping of several disease associated loci, for example heart disease, obesity, diabetes, and cancer (Hindorff *et al.*, 2009; Visscher & Montgomery, 2009; Ng *et al.*, 2014; Gao *et al.*, 2014).

### **1.2.1 Polymorphisms in human susceptibility to *S. pneumoniae* infection**

Human studies have identified polymorphisms in several genes, which are associated with increased susceptibility to *S. pneumoniae* infection. There was suggestive evidence, however, that homozygosity for certain codon variants of mannose binding lectin may influence susceptibility in humans for IPD (Roy *et al.*, 2002). Mutations in three codons in the *mbl* gene were identified in this study, and individuals homozygous

for a mutant genotype had very little or no serum MBL. Several polymorphisms have been reported in the gene encoding mannose-binding lectin (MBL) (Mombo *et al.*, 2003). Polymorphisms were identified in both coding sequences and in the promoter of *mbi*, which have shown to alter circulating levels of MBL in blood. A case control study was performed on polymorphisms in the *mbi* gene and its association with IPD (Roy *et al.*, 2002). Haplotype frequencies and therefore serum concentrations of MBL vary between Eskimo, Caucasian and African populations (Madsen *et al.*, 1995).

Increased mortality and morbidity due to IPD have also been associated with polymorphisms in the gene encoding C-reactive protein (CRP) (Roy *et al.*, 2002; Eklund *et al.*, 2006). 10-12% of patients were homozygous compared to 5% of controls. A micro-satellite polymorphism also was found in an intron of the C reactive protein gene in 65.6% of cases compared with 55.6% of controls (Roy *et al.*, 2002). In both studies from Roy and Eklund variations in the *crp* gene were identified that were associated with susceptibility to pneumococcal infection.

It also has been reported that polymorphisms in several genes involved in the TLR response are associated with susceptibility or resistance to pneumococcal infection in humans. These include *cd14* and *irak4*. A variation in the promoter of the gene encoding *cd14*, which results in increased expression of the protein, correlates with decreased risk of recurrent otitis media and an enhanced antibody response to the pneumococcal vaccine in young children (Wiertsema *et al.*, 2006). Further investigations using CD14<sup>-/-</sup> mice were however conflicting. Studies using CD14 knockout mice to investigate a model of pneumococcal infection in the central nervous system (CNS) reported that CD14<sup>-/-</sup> mice were more susceptible to meningitis when compared to wild-type mice (Echchannaoui *et al.*, 2005). Later, Dessing and his group reported that CD14<sup>-/-</sup> mice were resistant to intranasal pneumococcal infection (Dessing *et al.*, 2007). The dissimilarities in results between the two reports could be due to many factors, including the two distinct routes of infection used in these experimental models. Also, it has been suggested that *irak4* deficiency in humans may lead to recurrent pneumococcal infections in childhood (Ku *et al.*, 2007).

Two recent studies enhance this association between polymorphisms in human genes concomitant with immune mechanisms and susceptibility to pneumococcal infection:

one study showed polymorphisms on *tlr9* correlating with susceptibility to bacterial meningitis (Sanders *et al.*, 2011); and the second evidenced polymorphic variations on *nfkbi2* lead to susceptibility to IPD, in European and African populations (Chapman *et al.*, 2010). For instance, data have been published suggesting a strong association between genetic polymorphisms in 27 different immunity-related genes (such as IL-1 $\alpha$  and - $\beta$ , IFN- $\gamma$ , IL-6 and IL-10) and the risk of developing more severe sepsis and shock, with higher incidence in some types of infectious diseases common in intensive care units (Sapru & Quasney, 2011).

### **1.2.2 Mouse models of human diseases**

Animal models, in particular mouse models, provide an important tool for dissecting genetic linkage in disease and investigating the function of genetic elements. The advantage of using mice includes ease of control breeding, accessibility to inbred mice, generation times, litter size and high density of genetic markers (Malo & Skamene, 1994). By comparative mapping, a susceptible locus or loci identified in the mouse genome can be found in the human genome (DeBry & Seldin, 1996; Qureshi *et al.*, 1999; MacLeod & Hodges, 1945).

Breeding of the laboratory mouse and environment conditions can be controlled and using genetically identical inbred strains eliminates the genetic variability observed in humans. Mouse models have been utilised to identify QTL homologies in humans and this methodology has been efficacious in identifying infection susceptibility loci (Lavebratt *et al.*, 1999; Levison *et al.*, 2013; Wisby *et al.*, 2013). An example of published data for this approach is the mapping of two QTLs responsible for resistance to malaria in mice, located in chromosome 11 and 18, which were homologous to regions on human chromosome 5 (Hernandez-Valladares *et al.*, 2004). Another example is the successful studies on *Nramp1*, which was identified as a candidate gene for susceptibility to tuberculosis by genome-wide linkage studies in mice and by case control association studies in humans (Vidal *et al.*, 1993; Bellamy *et al.*, 1998). More recently a study showed the *Hectd2* candidate gene to be associated with susceptibility to prion disease. Initially thus was mapped in a mouse study and then confirmed in a human association study (Lloyd *et al.*, 2009).

### **1.2.3 Mouse models of susceptibility to *S. pneumoniae* infection**

A study performed by Gingles (Gingles *et al.*, 2001), investigated the susceptibility of a panel of nine inbred mouse strains (BALB/c, CBA/Ca, C3H/He, DBA/2, C57BL/6, AKR, NIH, FVB/n and SJL) to pneumococcal pneumonia. Mice were infected intranasally with *S. pneumoniae* wild-type D39, serotype 2, and each individual was assessed for survival time (Figure 1.7), 24 hours bacteraemia (Figure 1.8) and monitored for clinical signs of disease. The outcome of the study showed that BALB/c were resistant to infection (survived until end point of the experiment – 168 hours p.i.), and on the other hand, CBA/Ca and SJL showed susceptibility to pneumococcal infection, with median survival times of 27 and 28 hours p.i., respectively. The remaining murine strains exhibited intermediate susceptibility to *S. pneumoniae* infection. When observing the clinical pattern of disease, SJL showed different signs to CBA/Ca: SJL mice showed a rapid change from normal to lethargic during the course of infection, whereas CBA/Ca gradually change disease signs allowing a better understanding of disease progression. CBA/Ca was the susceptible strain selected for further investigation due to the short-term survival time and early high bacteraemia, but especially greater availability from supplier.

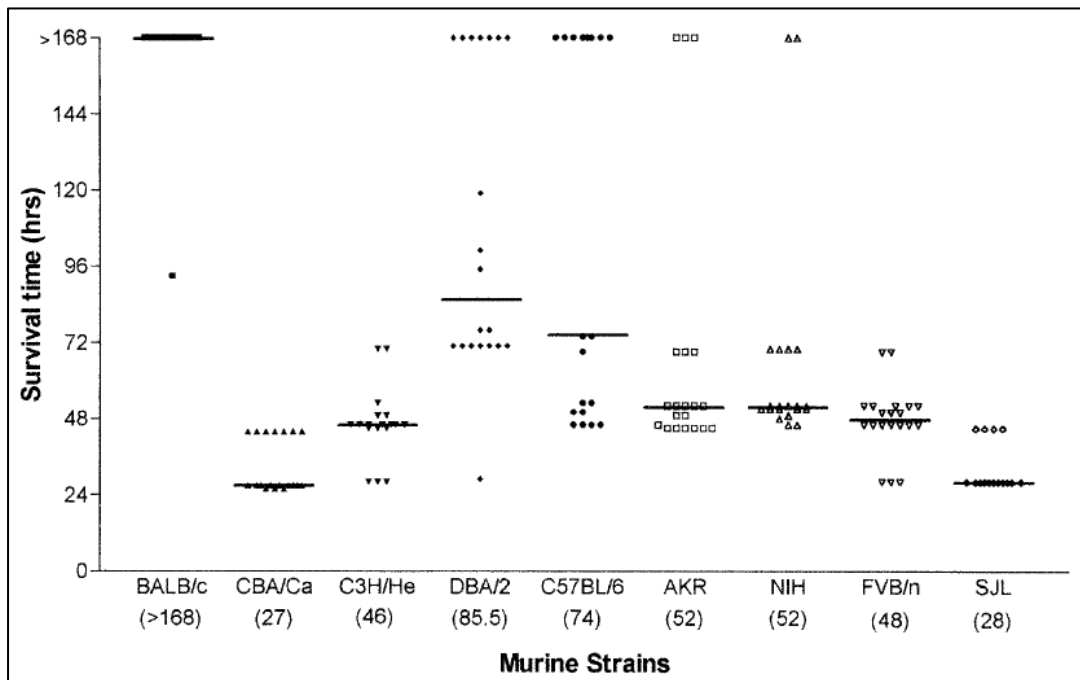


Figure 1.7 - Median survival times of the panel of inbred mouse strains tested against pneumococcal infection. Mice were intranasally infected with *S. pneumoniae* D39 and survival times observed. BALB/c mice were resistant, CBA/Ca and SJL were susceptible and remaining strains were intermediate in susceptibility to infection. Numbers in brackets represent the median survival time for each murine strain. Figure from Gingles *et al.* (2001).

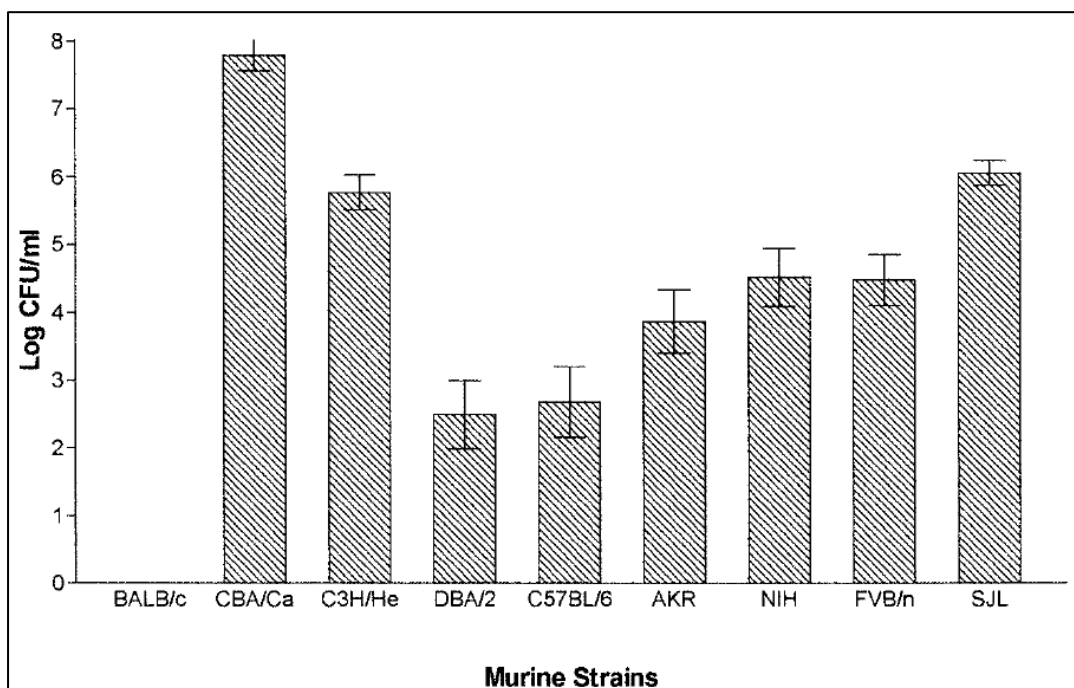


Figure 1.8 - Bacterial counts (Log<sub>10</sub> CFU/ml) in blood from the panel of inbred mouse strains. Mice were intranasally infected with *S. pneumoniae* D39 and blood collected at 24 hours post-infection. BALB/c mice showed no bacteraemia, but CBA/Ca mice had the highest numbers of bacteria in the blood (septicaemia). Figure from Gingles *et al.* (2001).

Focusing on the Gingles data from 2001 (Gingles *et al.*, 2001), pneumococcal numbers in the lungs of CBA/Ca mice rapidly increased over the first 24 hours of the infection, with dissemination into the bloodstream. CBA/Ca mice showed significantly higher bacterial numbers at 6, 12 and 24 hours. The BALB/c mice controlled the lung bacterial growth, although with a small increase from 12 to 24 hours p.i., but by 48 hours the lung CFU significantly dropped to numbers above the amount seen at the time of the intranasal challenge. In the blood of BALB/c mice, low bacterial levels were found, under  $\log_{10} 3$ , with less than 50% of mice showing bacteraemia by 48 hours p.i., and no bacteria detected by 168 hours (Figure 1.9).

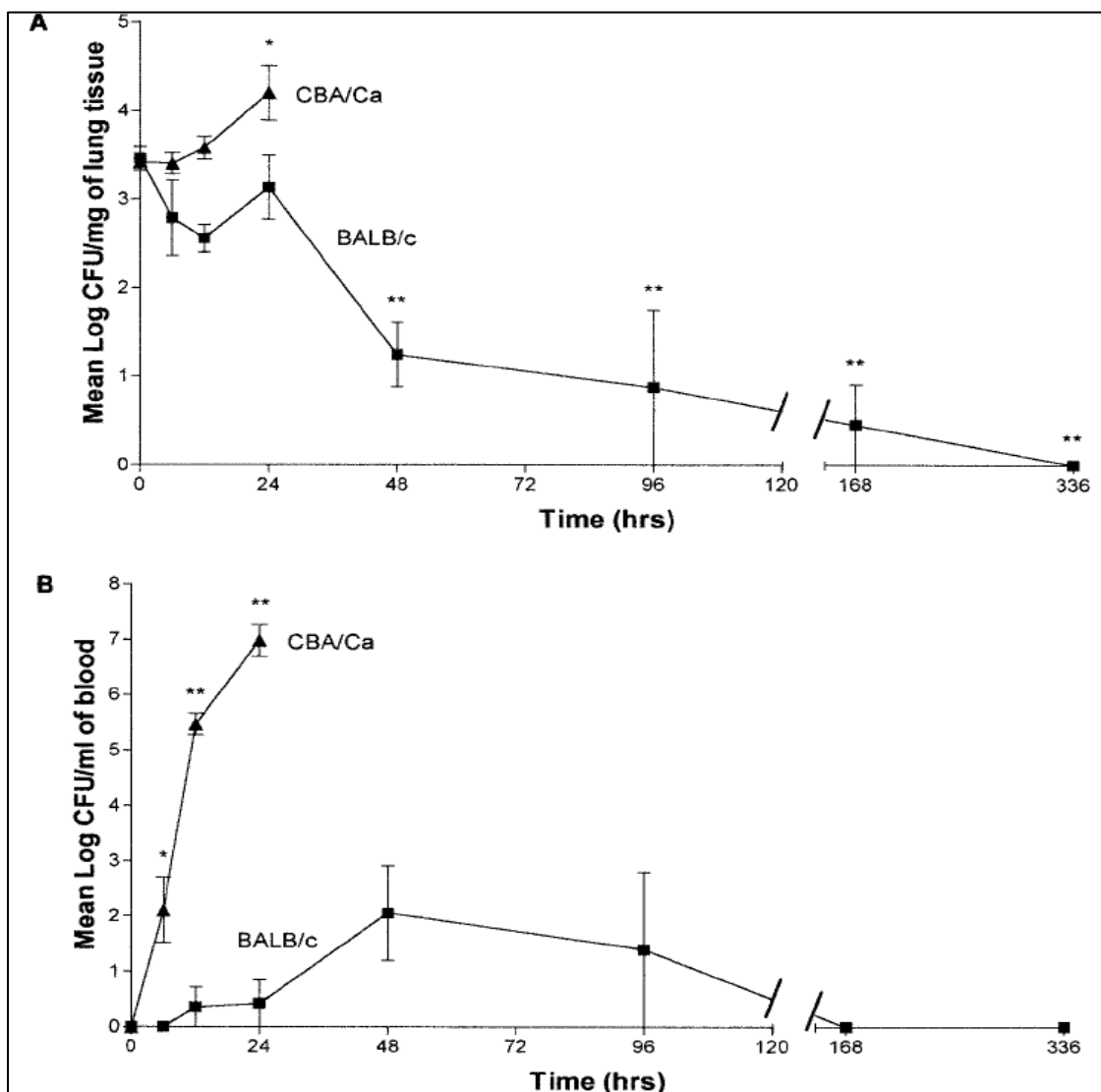


Figure 1.9 - Controlled bacterial growth in the lungs of BALB/c mice diminishes spreading into bloodstream. Figure from Gingles *et al.* (2001) represents the time course of *S. pneumoniae* numbers in the lungs (A) and in the blood (B) of BALB/c (■) and CBA/Ca mice (▲) intranasally infected with type 2 D39. \* indicates  $P < 0.05$  and \*\* indicates  $P < 0.001$  when compared with 0 hours.

A greater cellular infiltration was observed in the lungs of BALB/c mice when compared to CBA/Ca mice, which correlated with the larger inflammatory lesion observed in the BALB/c lung tissue, detected at an earlier time p.i. than in CBA/Ca. BALB/c exhibited higher amount of total leukocytes than CBA/Ca mice at all the examined time points post-challenge. In terms of differential counts, the neutrophil was the only cell type showing an increase in both strains, but significantly higher numbers in BALB/c than in CBA/Ca lungs, at 12 and 24 hours post-infection (Figure 1.10) (Gingles *et al.*, 2001).

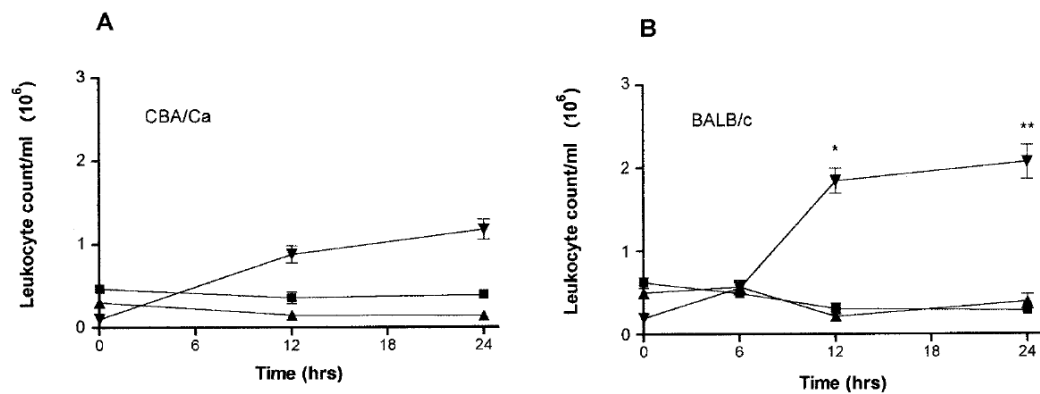


Figure 1.10 - Rapid increase of neutrophil numbers in the lungs of BALB/c mice. Figure from Gingles *et al.* (2001) illustrate the differential evaluation of macrophage (■), lymphocyte (▲) and neutrophil (▼) in digested lung samples from CBA/Ca (A) and BALB/c (B) mice after pneumococcal infection with D39. Data represent the mean (n = 5 mice per strain per time point) ± SEM. \*,  $P < 0.001$ ; \*\*,  $P < 0.01$  for BALB/c neutrophil levels as compared to CBA/Ca levels.

Kerr and colleagues (Kerr *et al.*, 2002) studied *S. pneumoniae* growth and host cytokine levels produced in response to pneumococcal infection in BALB/c and CBA/Ca lung tissue and airways (bronchoalveolar lavage). The bacterial loads in the lung tissue and airways quickly dropped between 12 and 36 hours p.i.. The CFUs in the airways of CBA/Ca mice also reduced in the airways of CBA/Ca mice, but in the lung tissue of CBA/Ca the bacterial growth was uncontrolled, the number of pneumococci increasing from the time of infection until the time of death.

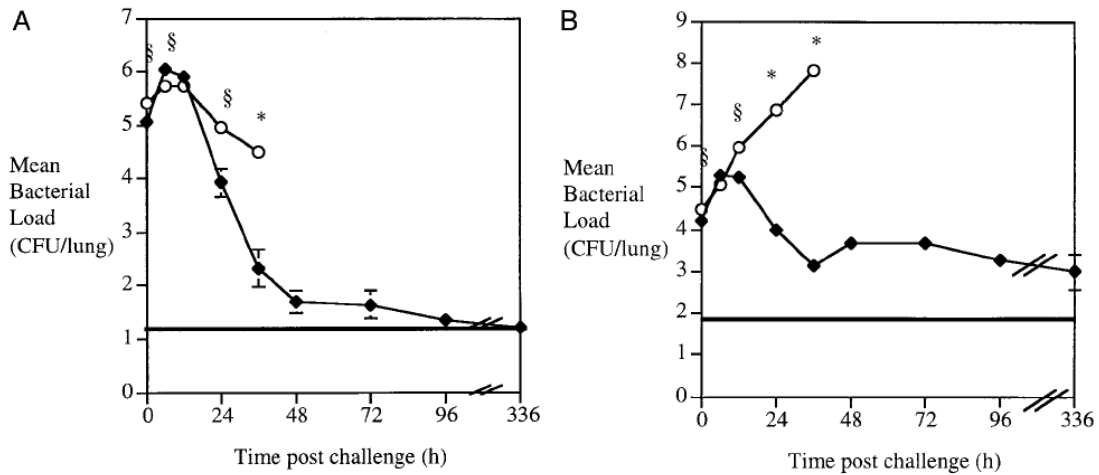


Figure 1.11 - Bacterial loads in the lung tissue of CBA/Ca mice increased during pneumococcal infection. Figure from Kerr *et al.* (2002) showing the numbers of bacteria present in the lung airways (A) and lung tissue (B) from BALB/c (◆) and CBA/Ca (○) mice intranasally infected with *S. pneumoniae* D39. \* indicates  $P < 0.01$  and § indicates  $P < 0.05$  for BALB/c compared to CBA/Ca.

Cytokine levels were also determined in Kerr's study, TNF- $\alpha$  activity was significantly higher in BALB/c airways when compared to CBA/Ca between 6 and 36 hours p.i.. Conversely, CBA/Ca mice showed significantly higher levels of TNF- $\alpha$  in the lung tissue when compared to BALB/c, between 24 and 36 hours. IL-1 $\beta$  and IL-6 levels had no significant difference in BALB/c and CBA/Ca lungs airways nor tissue, except for the levels of IL-6 in lung tissue between 12 and 36 hours (significantly higher in CBA/Ca than in BALB/c mice). Lastly, the levels of the anti-inflammatory cytokine IL-10 were significantly higher in BALB/c airways and lung tissue between 0 and 36 hours post-infection, when compared with CBA/Ca. Overall, Kerr's data suggested that the inflammatory response in BALB/c was more efficient than in CBA/Ca in the airways, while the inflammatory response in the lung tissue was delayed, excessive and uncontrolled in CBA/Ca mice contributing to the clinical course of the disease in this susceptible strain.

### 1.2.3.1 BALB/c and CBA/Ca inbred mouse strains

*BALB/cOlaHsd* (Harlan Laboratories, 2008)

In 1913, BALB/c inbred mouse strain (haplotype  $H-2^d$ ) were originally bred by H. Bagg from albino mice, subsequently named "Bagg albino" (Harlan Laboratories, 2008). Several people continued the breeding of the strain and in 1961 it was part of the NIH breeding colonies (Harlan Laboratories, 2008). The mouse strain was renamed as

BALB/c, and in 1994, was acquired by Harlan Laboratories (UK). Several BALB/c sub-strains, such as BALB/cJ, BALB/cByJ and BALB/cN mouse strains are currently available at different institutions (The Jackson Laboratory, US; NIH, US) and BALB/cOlaHsd mouse strain in Harlan (UK) since 1976 (Harlan Laboratories, 2008).

*CBA/CaOlaHsd* (Harlan Laboratories, 2008)

In 1920, the CBA/Ca inbred mouse strain (haplotype  $H-2^k$ ) was developed by L. C. Strong, from a cross between a Bagg albino and another inbred mouse strain designated DBA, exhibiting an agouti coat colouring. As it occurred with BALB/c mouse strain, many different suppliers have bred the CBA/Ca mouse strain, giving rise to different sub strains, such as CBA/CaOlaHsd mouse strain bred in Harlan (UK) since 1956 (Harlan Laboratories, 2008).

#### **1.2.4 Mapping QTL responsible for murine susceptibility to invasive pneumococcal disease**

Gingles and colleagues undertook the investigation of the BALB/c and CBA/Ca model of susceptibility to invasive pneumococcal disease (IPD) in a collaborative project with the MRC Harwell. This study will be discussed in detail in Chapter 4. In summary, a major QTL named *Spir1* (*Streptococcus pneumoniae* infection resistance 1) locus, contributing to susceptibility to IPD was mapped in the progeny of an F2 intercross, to the proximal end of chromosome 7 (Denny *et al.*, 2003). The *Spir1* locus spans a 7cM region, 12Mb in size (between 25Mb and 37Mb), and was estimated to account for around 15% of the phenotypic variance (genetic individual variance) (Denny *et al.*, 2003), suggesting susceptibility to pneumococcal disease is a complex trait with multiple genes involved. In the study in this thesis, a congenic breeding programme was performed to produce a mouse with a BALB/c background but with the QTL from the susceptible CBA/Ca, in order to study the impact of the *Spir1* locus on susceptibility to pneumococcal disease.

Overall, the genetic analysis of the host could reveal a number of novel elements of the innate immunity. The benefits of genetic exploration would be to investigate genes involved and their products, diagnosis targets, new therapeutics and vaccine development, as well as, detection of susceptible individuals as being at risk,

personalised medicine, and potential approaches to bypass genetic defects in the host's response to pathogens (Malo & Skamene, 1994; Doerr & Eng, 2012).

### 1.3 Overview of the immune system

Typically the immune system is divided into innate and adaptive response in the reaction to infection (Figure 1.12). First, a rapid innate response of pathogen recognition is mounted and, secondly, an adaptive response is generated that is built around antigen-driven selection and expansion of clonally restricted lymphocytes. This adaptive response also provides the basis for immunological memory.

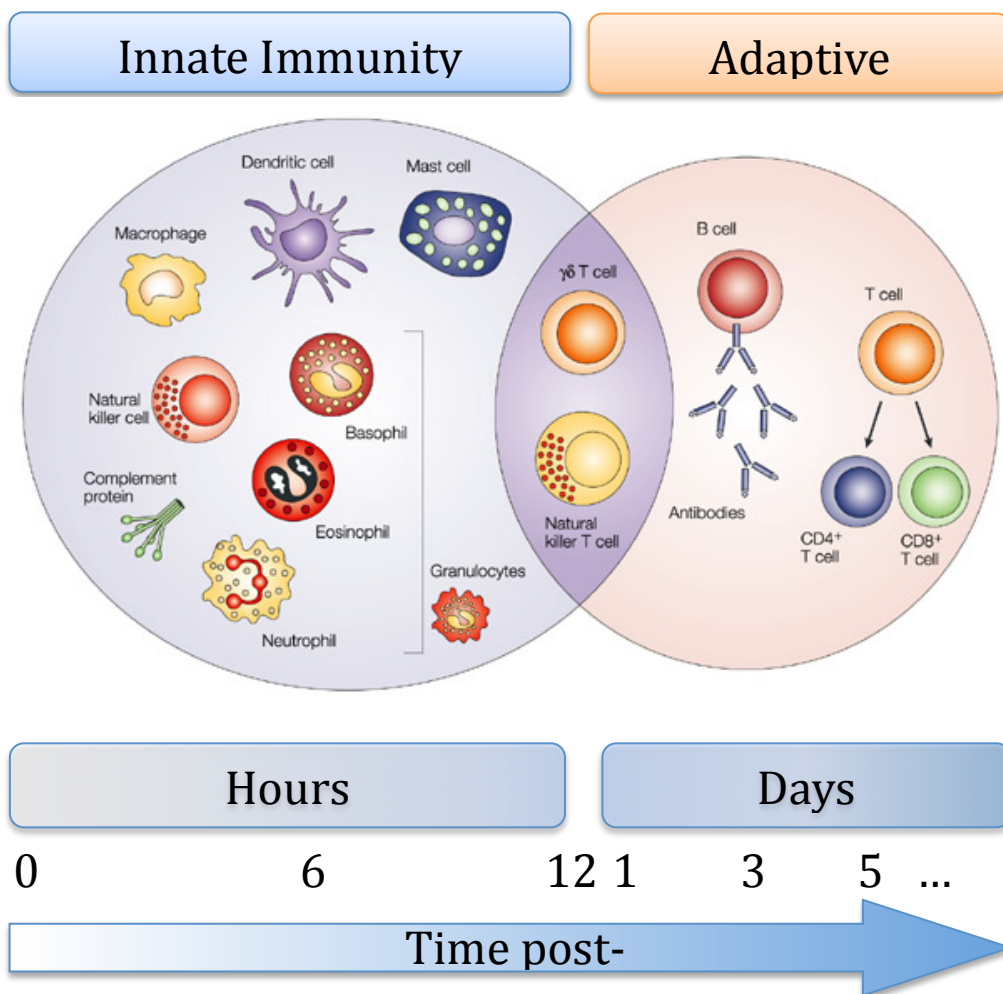


Figure 1.12 - The innate immune and the adaptive immune response (Dranoff, 2004).

#### 1.3.1 Innate immune system

The innate immune response is generated following the recognition of characteristic elements of pathogens or by serum components by receptors on a variety of cell types, including immune cells and epithelial cells. These microbial molecules, called pathogen-associated molecular patterns (PAMPs), can for example, be

lipopolysaccharides (LPS) on Gram-negative bacteria, lipoteichoic acid on Gram-positive bacteria, peptidoglycans, mannose, double-stranded and single-stranded RNA from viruses, bacterial RNA and DNA glucan, but they are generally molecular elements that are common components of infectious agents but are not part of the molecular make-up of the host. PAMP recognition is achieved through the pattern-recognition receptors (PRR's) capable of binding to conserved portions of the molecules, which include the toll-like receptors (TLR's) (Gay & Keith, 1991), the NOD-like receptors (NLR's) (Fritz *et al.*, 2006), the retinoic acid-inducible gene I protein (RIG-I) helicase receptors (Yoneyama & Fujita, 2004) and the C-type lectin receptors (CLR's), such as the mannose receptor (Stahl & Ezekowitz, 1998).

The recognition of PAMPs by PRRs typically results in the activation of innate effector cells and antimicrobial defences. Phagocytic cell activation, cytotoxic granulocyte activity and activation of the complement system are important to limit growth and spread of pathogens is limited early in infection (Mogensen, 2009). In most cases, this innate defence system is sufficient to contain and eradicate infection, however if these defences are breached, or infection persists, then an adaptive response tailored to the individual pathogen will be generated, ultimately resulting in resolution of infection but also may cause inflammatory diseases or autoimmunity (Mogensen, 2009).

Specific recognition of pathogens is rare in primary infections and it can take between 5 and 10 days, during which natural antibodies provide some cover for the selection and expansion of antigen-specific lymphocytes capable of fighting the infection (Briles *et al.*, 1982). This is why the innate immune system plays such a crucial role in defending the host from infection. Without it, pathogen replication would overwhelm the host before an adaptive response could be generated.

The innate and adaptive branches of the immune system are inextricably linked. Mediators released from innate cells shape the ensuing adaptive response and, likewise, the actions of adaptive immune cells feedback on the innate effectors to strengthen or dampen their functions. The two systems together form a highly effective barrier to infection but a balance is necessary to ensure that responses are limited to levels that will not do irreparable damage to the host and to prevent activation of effector cells to self or innocuous antigen (Thornton & Morgan, 2009; Hooper *et al.*, 2012). This is

achieved in part by negative feedback signalling via cell-cell interactions or the release of soluble mediators and also through the actions of a number of regulatory immune cells (Janeway *et al.*, 2001; Luster, 2002; Getz, 2005; Pasare & Medzhitov, 2005). When these feedback mechanisms fail it can lead to autoimmune diseases, due to an inappropriate response to self-antigen (Janeway *et al.*, 2001; Romagnani, 2004). Subsequently, specific subsets of antigen-specific lymphocytes are maintained as memory cells and will generate a rapid, enhanced response if re-infection occurs (Janeway *et al.*, 2001). This is called immunological memory and it is the scientific basis upon which vaccination strategies are normally developed.

#### **1.3.1.1 Cytokines and chemokines**

The quickness of the host-pneumococcal recognition, together with the capability of the innate immune system to boost a response, may determine the disease progression. Cytokines are involved in most aspects of immunity and inflammation, such as innate immunity, antigen presentation, bone marrow differentiation, cellular recruitment and activation, and adhesion molecule expression. Cytokines, produced in response to an immune insult, will determine whether it will trigger an immune response and subsequently the type of response, which could be cytotoxic, humoral, cell-mediated or allergic (Borish & Steinke, 2003). When a host is exposed to pneumococcal infection, cytokines are primarily derived from monocytes and mononuclear phagocytic cells and other antigen-presenting cells (APCs) that promote cellular infiltration and damage to resident tissue. APCs process and present proteinaceous pneumococcal antigens to T<sub>helper</sub> lymphocytes, providing a specific pathway for the cytokine production. Subclasses of T<sub>helper</sub> lymphocytes can be identified on the basis of their repertoire of cytokines, as arranged on Table 1.2.

T helper lymphocyte family	Cytokines
T <sub>h</sub> 0	IL-2
T <sub>h</sub> 1	IFN- $\gamma$ , TNF- $\beta$ TNF- $\alpha$ , GM-CSF, IL-2, IL-3, IL-10, IL-13
T <sub>h</sub> 2	IL-4, IL-5, IL-9, IL-25 TNF- $\alpha$ , GM-CSF, IL-2, IL-3, IL-10, IL-13
T <sub>r</sub> 1 (T <sub>h</sub> 3)	TGF- $\beta$ , IL-10

Table 1.2 - T<sub>helper</sub> cell subtypes classified by cytokine production (Borish & Steinke, 2003).

### 1.3.1.2 Neutrophils and macrophages

The host immune response to pneumococcal lung infection is commonly characterised by an intense inflammatory response, firstly involving resident alveolar macrophages, followed by an enhanced neutrophil recruitment into infected lungs (Figure 1.13).

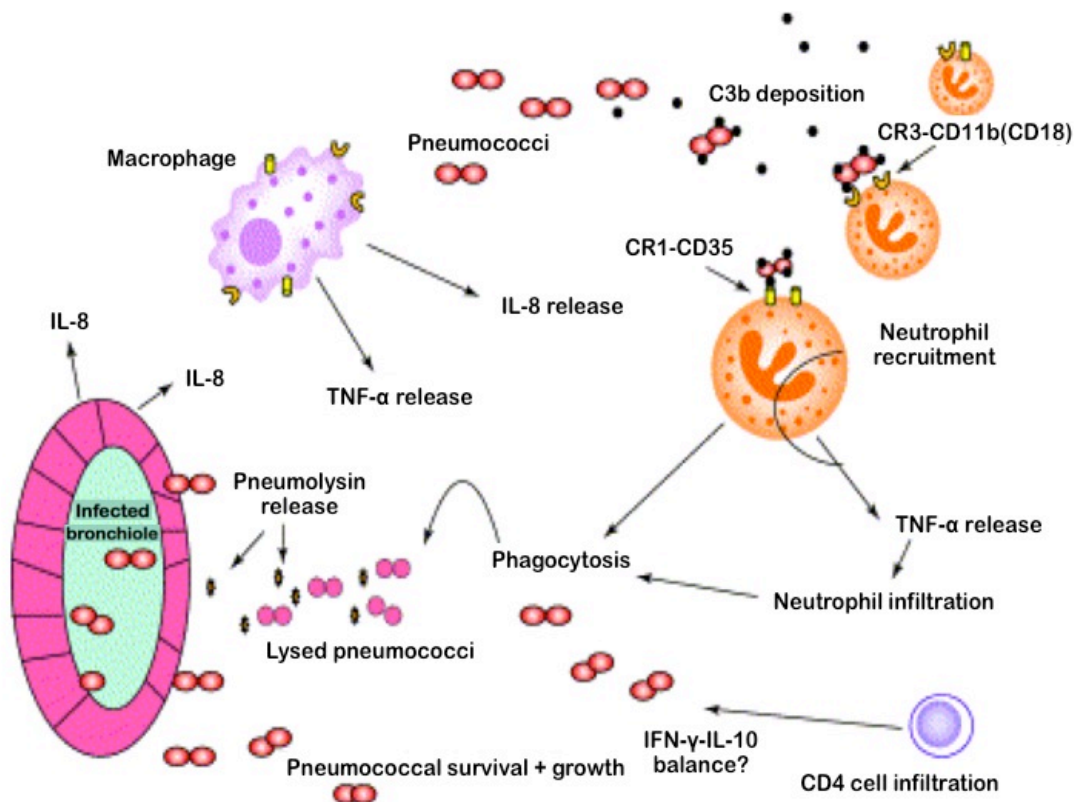


Figure 1.13 - Summary of some aspects of the host immune response to pneumococcal infection during bronchopneumonia (Kadioglu & Andrew, 2004).

Neutrophils are phagocytic cells, which have a short life span and are promptly recruited to sites of infection. These polymorphonuclear (PMN) leukocyte cells engulf and degrade microorganisms using an array of oxidative and non-oxidative mechanisms that include reactive oxygen species (ROS), antimicrobial peptides, and proteases such as cathepsin G, elastase and proteinase 3 (Pham, 2006). Neutrophils have granules in their cytoplasm, which contain antimicrobial molecules that can be released to kill invading microorganisms (Witko-Sarsat *et al.*, 2000). Once inside the neutrophils, pneumococci are sequestered in a compartment called the phagosome. The process of phagocytosis activates the membrane-bound NADPH oxidase system, generating large quantities of ROS that are released into the phagosome, constituting the oxidative arm of the microbicidal action of neutrophils (Witko-Sarsat *et al.*, 2000). The phagocytosis process is accompanied by the fusion of neutrophil granules with the phagosome and the release of antimicrobial peptides and proteases from the granules into the phagosome, constituting the non-oxidative arm of the microbicidal action of neutrophils (Faurischou & Borregaard, 2003). Hence, neutrophils contain an array of cytotoxic agents prepared for mobilisation in response to invading microorganisms. Nevertheless, as a result of a strong inflammatory response to infection, neutrophils also produce excessive antimicrobial reactive oxygen species which can contribute to host tissue damage (Standish & Weiser, 2009). Although neutrophils play an important role in the immune response to *S. pneumoniae*, prolonged neutrophil activity can be detrimental to the host (Bass *et al.*, 1986; Chollet-Martin *et al.*, 1992).

Pulmonary macrophages play a key role in defence against respiratory infection with phagocytic activity, antigen presentation and immunomodulatory functions (Gordon & Read, 2002). Macrophages are a heterogeneous group of cells with an important role in both innate and acquired immunity in the respiratory tract, and have a role in lung defence against viruses, bacteria and fungi (Gordon & Read, 2002). Interactions of pathogens with lung macrophages are mediated by soluble immune components including complement, collectins and immunoglobulins (Gordon & Read, 2002). Macrophages play an important part in an effective immune response to *S. pneumoniae* infection. Studies *in vivo* showed that CCL2-deficient mice (lacking the monocyte/macrophage chemotactic cytokine) are more susceptible to *S. pneumoniae* septicaemia due in part to a reduced influx of macrophages into the lungs when compared to wild-type mice (Winter *et al.*, 2009). Furthermore, alveolar macrophages

are also essential for the transport of pneumococcal antigens from the lung to draining lymph nodes (Kirby *et al.*, 2009). Macrophage function can also be modulated by cytokines, environmental exposures, recent and chronic infection including HIV infection, drug therapy and gene transfer (Gordon & Read, 2002).

### 1.3.1.3 Lymphocytes

Lymphocytes are complex cells that are responsible for immune responses. There are two main types of lymphocytes: T cells and B cells. T lymphocytes are differentiated in the bone marrow from pluripotent hematopoietic stem cells, and then migrate into the thymus gland where they mature. B lymphocytes mature in the bone marrow. After maturation, the lymphocytes enter the circulation and peripheral lymphoid organs (such as the spleen and lymph nodes) where they survey for invading pathogens and/or tumour cells (Janeway *et al.*, 2001).

T cells can be subdivided into various groups including CD8<sup>+</sup> cytotoxic T cells (T<sub>c</sub>) (recognise antigen displayed on MHC I molecules) and CD4<sup>+</sup> T cells (recognise antigen displayed on MHC II molecules), which include T helper cells (T<sub>h</sub>), regulatory T cells (T<sub>reg</sub>), gamma-delta T cells ( $\gamma\delta$  T cells), natural killer T cells (NK T cells) and memory T cells (Janeway *et al.*, 2001). CD4<sup>+</sup> T cells, after being activated and differentiated into distinct effector subtypes, play a major role in mediating immune response through the secretion of specific cytokines. The CD4<sup>+</sup> T cells carry out multiple functions, ranging from activation of the cells of the innate immune system, as well as non-immune cells, besides playing key role in the suppression of immune reactions (Mogensen, 2009). Other subsets of CD4<sup>+</sup> cells have been recently discovered besides the classical T-helper 1 (T<sub>h</sub>1) and T-helper 2 (T<sub>h</sub>2) cells, these include T-helper 17 (T<sub>h</sub>17), follicular helper T cell (T<sub>fh</sub>), induced T-regulatory cells (iT<sub>reg</sub>), and the regulatory type 1 cells (T<sub>r</sub>1) as well as the potentially distinct T-helper 9 (T<sub>h</sub>9) (Luckheeram *et al.*, 2012). The differentiation of the different lineages depends on the complex network of specific cytokine signalling (Luckheeram *et al.*, 2012).

Early recruitment of T cells to inflammatory sites in the lung is observed during *S. pneumoniae* infection, which is in part as a response to the toxin pneumolysin (Kadioglu *et al.*, 2000; Kadioglu *et al.*, 2004). MHC II<sup>-/-</sup> mice are deficient in CD4<sup>+</sup> T cells and are more susceptible to pneumococcal infection, evidencing reduced clearance

of pneumococci from the lung and increased bacteraemia when compared to wild-type mice (Kadioglu *et al.*, 2004). It has also been reported that CD4<sup>+</sup> T cells play an important role in the clearance of colonising pneumococci from the nasopharynx (van Rossum *et al.*, 2005). Similar to the observations with CD4<sup>+</sup> T cells, it was reported that CD8<sup>-/-</sup> mice exhibited significantly more bacterial dissemination and lung inflammation and a significantly more lethal phenotype than wild-type mice to intranasal infection with *S. pneumoniae* (Weber *et al.*, 2011).

B lymphocytes are involved in the humoral immune response with an important role in immunity to pneumococcal infection. Patients with complement deficiencies and asplenia are very susceptible to recurrent infections by *S. pneumoniae* (Ram *et al.*, 2010). A report in 2003 evidenced that the spleen was required for the generation of IgM memory B cells, which are required for protection against pneumococcal infection (Kruetzmann *et al.*, 2003). Mice over expressing CD19 predominantly develop B-1a B cells, which are important in the innate immune response to pneumococcal polysaccharide, due to the production of natural antibodies. CD19-deficient mice predominately develop B-1b B cells and are more susceptible to *S. pneumoniae* infection pre-vaccination than wild-type mice, and than those over expressing CD19 due to the lack B-1a B cell natural antibody. However, CD19-deficient mice do develop acquired long-lived immunity to pneumococcal infection (Haas *et al.*, 2005).

### **1.3.2 Role of the spleen in the immune response to *S. pneumoniae***

The spleen has an important role in the host defence in septicaemia such as that caused by pneumococcal infection, primarily acting as a blood filter. Reported data suggests that splenic weight is directly correlated with the phagocytic function of the spleen (Malangoni *et al.*, 1985) and has reported that surgical conservation of spleen with intact blood supply maintains more efficient reticuloendothelial activity than splenic autotransplants (Malangoni *et al.*, 1985). Splenectomy impairs survival after pneumococcal challenge in rats, and human splenectomy patients have higher rates of pneumococcal disease (Ram *et al.*, 2010) correlating with the observation that preservation of sufficient splenic tissue can be protective (Malangoni *et al.*, 1985).

In pneumococcal bacteraemia, the splenic clearance is a determinant factor for the outcome of the disease, which hepatic clearance cannot counterbalance (Brown *et al.*,

1981). The complement system and the spleen interact during innate immune response, specialised cells in the marginal zone (MZ) of the spleen play a predominant role in this particular challenge. The MZ contains MZ macrophages, B cells, dendritic cells and metallophilic macrophages (found in rodents but not in humans) (Steiniger *et al.*, 2006). Marginal zone B cells are distinct from follicular B cells (of the germinal centers) and function as rapidly responding innate cells. Briefly, encapsulated pneumococci are captured by a layer of macrophages in the MZ of the spleen, promoting clearance of the bacteria (Koppel *et al.*, 2008). MZ macrophages stimulate MZ B cells in a T cell independent manner to produce IgM (Koppel *et al.*, 2008), essential for control of disease in the early stages and later significantly prompting the adaptive immune response via cell-cell interaction (Hosea, 1983; Salehen & Stover, 2008). As well as activation through macrophages, multivalent antigens (e.g. capsular polysaccharide) that can cross-link the BCR directly activate B cells and promote antibody secretion (Clutterbuck *et al.*, 2012).

The polysaccharides present in the capsule of pneumococci are poorly immunogenic, due to the predominance of the negative charge of the capsule, inhibiting phagocytosis which, antibody and complement mediated opsonisation are able to antagonise (Lee *et al.*, 2001). The MZ is underdeveloped in children under two years of age, requiring conjugation of polysaccharide antigens to protein, stimulating a T cell dependent pathway (Klein Klouwenberg & Bont, 2008). Additionally it has been shown that systematic disease may originate from a single cell bottle knock “escape mutant” in the spleen, rather than an over powering of clearance mechanisms (Gerlini *et al.*, 2014).

#### **1.4 Aims of the thesis**

In this project the susceptibility and resistance to *S. pneumoniae* in mice was investigated. Mouse studies were performed in collaboration with the MRC, Mammalian Genetics Unit in Harwell Oxfordshire (UK) to attempt to confirm the contribution of the chromosome 7 QTL (*Spir1*) locus previously identified as a basis of variation in resistance and susceptibility to invasive pneumococcal disease (Denny *et al.*, 2003). Further studies were assessed to narrow the mapped region, identify candidate gene(s) influencing the pathology of pneumonia and develop new hypotheses on mechanisms of innate resistance to pneumococcal disease. As the project developed, data suggested a role for two *Spir1* genes, *cd22* and *tgfb1* (including its downstream

targets – TGF- $\beta$ , T regulatory cells and IL-10), and the investigation of these genes became an additional aim.

As discussed in sections 1.2.2 and 1.2.3, the mouse provides an important model to study and search for genes associated with the susceptibility and resistance to diseases. In this context, this project used a mouse model to study the genetics involved in pneumococcal infection susceptibility, in order to identify and investigate further, the locus responsible for the difference in susceptibility to invasive pneumococcal infection in the BALB/c and CBA/Ca mouse model. In this project the contribution of the chromosome 7 QTL (*Spir1*) was examined in several ways:

- Phenotyping of cellular recruitment into the lungs and cytokine protein levels in the lungs and plasma during the infection time course were investigated in BALB/c and CBA/Ca. This work is reported in Chapter 3.
- The genetic contribution of the *Spir1* locus was assessed in congenic mice. A 10-generation backcross using a marker-assisted strategy for mapping the QTL, was used to construct a congenic strain with introgressed CBA/Ca genome on a BALB/c background. The susceptibility of these incipient congenics to pneumococcal infection was investigated in order to confirm the contribution of the location of the mapped QTL, obtained with the analysis of the F2 crosses, and to aid the investigation of candidate genes. This work is reported in Chapter 4.
- Genes located in the *Spir1* region that showed preliminary evidence of a major role during *S. pneumoniae* infection were also investigated: *tgfb1* and *cd22* genes. The gene *tgfb1* (located at 25Mb in chromosome 7), TGF- $\beta$  protein, T regulatory cells (a source and a target of TGF- $\beta$ ) and IL-10 were studied in order to understand the role of these components and how they can control susceptibility to pneumococcal pneumonia. This work is reported in Chapter 5.
- The gene *cd22* (located at 31Mb in chromosome 7) and the B cell transmembrane protein CD22 were studied with the purpose of understanding how changes to the functional structure of CD22 may interfere with the outcome of pneumococcal infection. This work is reported in Chapter 6.

Discussion of all the work completed in this thesis is presented in Chapter 7.

---

## CHAPTER 2. MATERIALS AND METHODS

---

### 2.1 Materials

#### 2.1.1 General

Unless stated in the text, the following companies supplied chemicals and consumables: general chemicals were purchased by BDH Supplies (distributed through VWR International, UK), Fisher Scientific Ltd. (UK) and Sigma-Aldrich (UK); all bacteriological growth media were supplied by Oxoid (UK); tissue culture media and solutions were supplied by Gibco (UK) and Invitrogen (UK); tissue culture plasticware was obtained by BD Biosciences (UK), Sigma-Aldrich (UK) and Sarstedt (Germany); DNA ladders were supplied by New England Biolabs Ltd. (UK); DNA primers were manufactured by MWG (Germany); enzymes were supplied by Roche Diagnostics (UK); all antibodies were from BioLegend (UK) and BD Biosciences (UK).

#### 2.1.2 Peptides

The peptide P17 was a generous gift from Dr. Javier Dotor de las Herrerías, University of Navarra, Spain.

#### 2.1.3 Standard Stocks and Buffers

All solutions were prepared with dH<sub>2</sub>O.

*PBS* (per litre): 10 phosphate buffered saline tablets (Oxoid) were added to 1 litre dH<sub>2</sub>O. Alternatively PBS was prepared according to the following recipe: 7.35 g NaCl; 2.35 g Na<sub>2</sub>HPO<sub>4</sub>; 1.3 g NaH<sub>2</sub>PO<sub>4</sub>·2H<sub>2</sub>O in 1L of solution; adjusted to pH 7.1. This solution was autoclaved at 121°C, 15 psi for 20 minutes.

*TAE buffer* (per litre of solution) (50x): 242 g tris base; 57.1 ml glacial acetic acid; 37.2 g Na<sub>2</sub>EDTA·2H<sub>2</sub>O; adjusted to pH 8.5.

*ELISA wash buffer* (per litre of solution): 1 x PBS; 500 µl of 0.05% (v/v) Tween-20.

*ELISA stop solution* (per litre of solution): 1M H<sub>3</sub>PO<sub>4</sub>.

### 2.1.4 Bacterial Growth Media

Blood Agar Base (BAB) medium containing 5% (v/v) defibrinated horse blood and Brain Heart Infusion (BHI) broth was used for the growth of *S. pneumoniae*. Media were autoclaved at 121°C, 15 psi for 20 minutes. To prepare blood agar plates, medium was cooled to around 50°C and defibrinated horse blood was added to 5% (v/v), gently mixed and poured into Petri dishes. The compositions of the media are described in Table 2.1.

Medium	Composition	Source
Blood Agar Base	<ul style="list-style-type: none"><li>- 16 g BAB powder</li><li>- 400 ml distilled H<sub>2</sub>O</li></ul>	Oxoid
Brain Heart Infusion	<ul style="list-style-type: none"><li>- 14.8 g BHI powder</li><li>- 400 ml distilled H<sub>2</sub>O</li></ul>	Oxoid

Table 2.1 - *Streptococcus pneumoniae* growth media. Blood Agar Base was used to culture and isolate the bacterium on a Petri dish and Brain Heart Infusion was the broth used to grow in liquid.

## 2.2 Pneumococcal strain

The *S. pneumoniae* strain D39, serotype 2, was used in the study. This pneumococcal strain was obtained from the collection of Professor Peter W. Andrew, Department of Infection, Immunity and Inflammation, University of Leicester (UK).

### 2.2.1 Pneumococcal strain validation

Prior to experimental, bacteria were identified as pneumococci by Gram stain (section 2.2.1.1), catalase test (section 2.2.1.2), observation of alpha-haemolysis on blood agar plates (section 2.2.1.3) and confirmation of optochin sensitivity (section 2.2.1.4), as described on Figure 2.1, except for the bile solubility testing, which was not done.

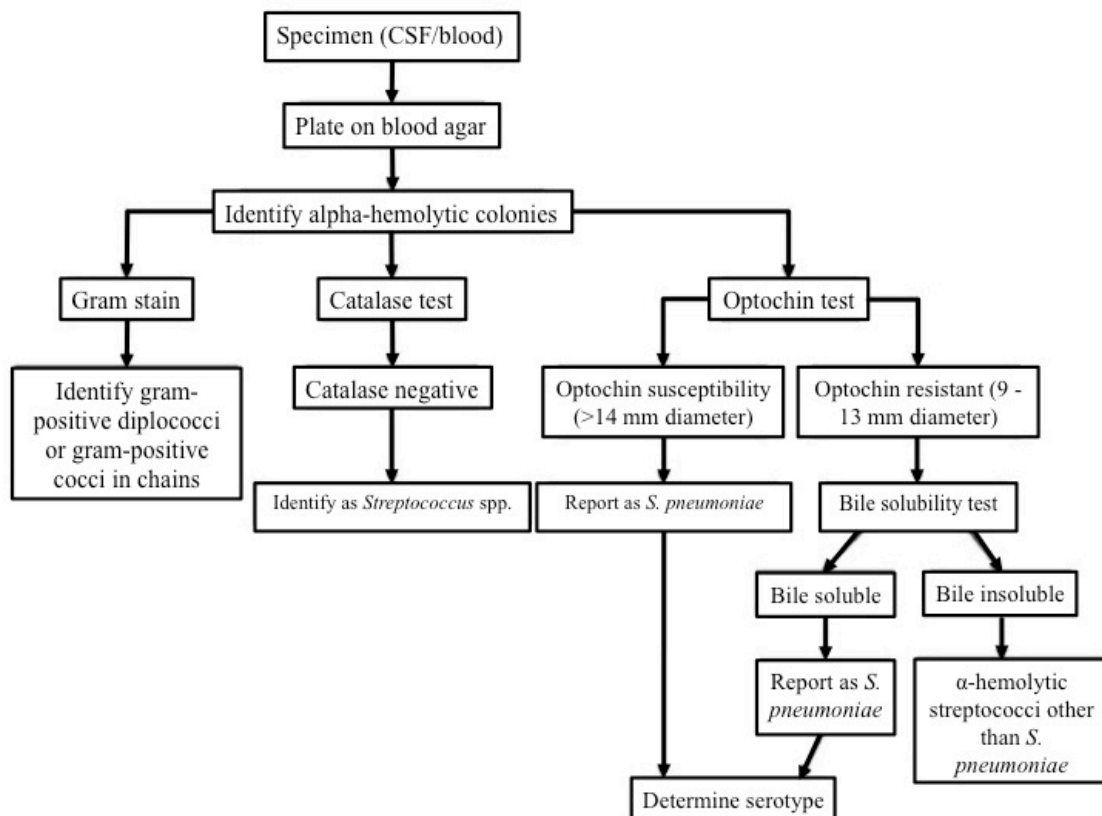


Figure 2.1 - Diagram representing identification and characterization methods of a *S. pneumoniae* isolate (Centers for Disease Control and Prevention, 2010).

### 2.2.1.1 Gram staining

First a bacterial smear was fixed to a microscope slide, by passing the slide through a hot Bunsen flame. The slide was flooded with crystal violet (or methylene blue) for 1 to 2 minutes, and then with iodine for 1 to 2 minutes. The slide was washed with acetone for 2 to 3 seconds and then washed with water. The slide was then flooded with safranin counterstain for 2 minutes, washed with water and dried over the Bunsen flame. Finally, the slide was examined under a light microscope for bacterial group classification (Cann, 2012).

### 2.2.1.2 Catalase test

The catalase test was done by a method previously described (Clarke & Cowan, 1952). A drop of hydrogen peroxide was placed onto a slide and mixed with the colony being tested. Release of bubbles (positive reaction), within 10 seconds, indicates a catalase-positive organism (was used *Staphylococci* as a positive control); *S. pneumoniae* is catalase-negative.

### **2.2.1.3 Determination of haemolysis**

The bacterium tested was streaked to single colonies on blood agar and the plate was incubated overnight at 37°C, in an inverted position in a candle jar with 5% CO<sub>2</sub>. On the blood agar plate, the presence of α-haemolytic colonies was characterised by greenish discoloration around the colonies (*S. pneumoniae* is alpha-haemolytic bacterium); β-haemolytic, by a clear zone meaning haemolysis; or γ-haemolytic, when no haemolysis was observed. *S. pneumoniae* is alpha-hemolytic bacterium (Lorian & Markovits, 1973).

### **2.2.1.4 Optochin sensitivity test**

Optochin (ethylhydrocupreine hydrochloride) is used for identification, by causing a selective lysis of *S. pneumoniae* (Kellogg *et al.*, 2001). A streak of the microorganism to be tested was made on a blood agar plate. A sterile disk impregnated with optochin (Oxoid) was placed on the first sector of an isolation plate before incubation. The plate was incubated in an inverted position in a candle jar, overnight, at 37°C. After incubation, plates were inspected for the presence of a zone of inhibition (area with no growth) of 14 mm or more around the disc, with at least 5 mm clear from the edge of the disc, if the organism *S. pneumoniae*.

### **2.2.2 Quellung reaction**

The quellung reaction was used to check the presence of type-specific polysaccharide capsule (Perlino, 1984). A loop of overnight broth culture was smeared onto a slide and left to dry in air. On a coverslip, 10 µl of type-specific capsular antiserum (Statens Serum Institut) was added and this was mixed with 10 µl of 1% (w/v) methylene blue in water, before being placed, fluid side down, onto the smear. The slide was examined under x 1000 oil immersion and compared to a control slide prepared with non-immune serum (heat inactivated foetal bovine serum). If the capsule was seen distinctly outlined around the cells, which stain blue, then the bacteria were counted as positive. If the capsule was not immediately obvious, the slide was re-examined after leaving in a humid environment (e.g. in a Petri dish on a damp tissue) for 1 hour.

### 2.2.3 Viable counting

Viable counting was performed by the technique described by Miles and Misra (1938). Serial dilutions of 20 µl of sample – bacterial stock, blood or lung homogenate – was performed in sterile 96 well microtitre plates (Nunc) containing 180 µl sterile phosphate buffered saline (PBS) per well. By drawing the well contents into a pipette tip and back to the well several times, homogenous mixing was achieved. Serial dilutions were made up to 10<sup>-6</sup>, changing the tip after each dilution. Blood plates were marked into six sectors and 3 x 20 µl aliquots from each dilution were plated onto one sector. This procedure was repeated in duplicate. Spots were allowed to dry into the agar and when completely dried, plates were placed in an inverted position into a candle jar with 5% (v/v) CO<sub>2</sub> for overnight incubation at 37°C. Colonies were counted in the sector containing approximately 100 to 200 colonies. To calculate the number of colony forming units (CFU) from each sample the following equation was used:

$$CFU \text{ per ml} = \frac{\text{Number of colonies in sector}}{60\mu\text{l (Volume per sector)}} \times \text{Dilution} \times 1000 \text{ (Conversion factor)}$$

## 2.3 Procedures for *in vivo* experiments

### 2.3.1 Animals

All animal experiments described in this project were performed under the authority of a project licence issued under the Animal Scientific Procedures Act 1986 of the United Kingdom and with local ethical approval.

Inbred C57BL/6J and CD22-deficient (C57BL/6-Cd22<sup>tm1Lam</sup>/J) mice (Nitschke *et al.*, 1997) were kindly sent by Professor Lars Nitschke from Germany (University of Erlangen), as part of collaborative work. CD22 knockout (abbreviated to CD22 KO) mouse details can be found in the Jackson Laboratories (US) website (<http://jaxmice.jax.org/strain/006940.html>). The CD22-deficient strain has decreased mature B cell and marginal zone B cells numbers. Mice were obtained with an age range of 12 to 18 weeks. After arrival, mice were kept for a minimum of two weeks in the Division of Biomedical Services in quarantine and to acclimatise, prior to use in experimental procedures.

Outbred MF1 OlaHsd (abbreviated to MF1) mice and inbred BALB/cOlaHsd (abbreviated to BALB/c) and CBA/CaOlaHsd (=CBA/Ca) mice were obtained from Harlan Olac (UK). MF1 mice also were obtained from Charles River (UK), as a secondary source of MF1 mice. BALB/c and CBA/Ca mouse strains show a distinct immune profile: BALB/c show a good splenic PFC immune response to pneumococcal polysaccharide, whereas CBA/Ca strain has a poor splenic response (Amsbaugh *et al.*, 1972). Congenic lines derived from BALB/c and CBA/Ca were bred in the Division of Biomedical Services, Leicester University (section 4.1.1). Mice were obtained from Harlan Olac (UK), at approximately 8 weeks old, in between 9 and 18 weeks of age. Mice were kept for a minimum of one week in the Division of Biomedical Services to acclimatise, prior to use in experiments. All animals were kept under standard conditions, with free access to food and water, and were housed in individually ventilated cages (IVC).

### **2.3.2 Mouse identification**

A unique identifier (UID) number was assigned to every mouse in the congenic-breeding programme, due to genetic differences between individuals, so that each mouse was traceable. The code was a 4-digit code, starting with the number 3000.

### **2.3.3 Tail biopsy and ear notching of mice**

In accordance with legislation at the time of study, tail biopsies not exceeding 0.5 cm long, were taken from BALB/c, CBA/Ca and congenic mice, after the mice had been weaned (> 3-4 weeks old). The mouse was gently scruffed and the tail was positioned between the ring and little finger. The tail tip was then placed over an inverted plastic Petri dish (90 mm or smaller). A drop or two of ethyl chloride was released over the tail tip. Within seconds, the tail tip was frozen (the area of application of local anaesthesia changed to a white colour when frozen). The frozen tail tip was placed on a fresh Petri dish and a piece of the tip  $\leq 0.5$  cm was removed using a fresh scalpel blade and a cauteriser (Vet Tech Solutions) was gently run over the frozen tail tip (Jones *et al.*, 2012). To ensure that it was sealed, the tail surface was inspected for signs of bleeding. The mice were re-examined 24 hours later to ensure that the tail tip was healed and that there were no signs of infection and/or inflammation. If not healed, an animal technician or a Named Animal Care & Welfare Officer (NACWO) was assigned for monitoring and to provide animal health care assistance. After biopsy, mice were

transferred into a fresh cage. The tail biopsy specimens were placed in an appropriately labelled cryotube (Nunc). The tube was immediately placed in dry ice or liquid nitrogen and then stored at -80°C until required.

Alternatively, mice were ear notched by the Division of Biomedical Services staff and tissue samples stored at -80°C. Tail biopsies and ear notched tissues were then used for preparation of genomic DNA as described in section 2.4.1.

### **2.3.4 Preparation of *S. pneumoniae* animal passaged stocks**

The procedure to prepare animal passaged stocks of *S. pneumoniae* was adapted from (Kadioglu *et al.*, 2000). Pneumococci were passaged through MF1 mice in order to obtain a consistent level of virulence (defined as the ability to transfer across epithelium and cause septicaemia).

A laboratory bead, impregnated with pure culture of bacteria, or a frozen aliquot from previous frozen stock preparation was thawed in hand, and then was streaked to single colonies on blood agar. The plate was incubated overnight at 37°C in a candle jar with 5% (v/v) CO<sub>2</sub>. From the streak plates, a sweep of colonies was inoculated into BHI broth and incubated overnight statically at 37°C. Next day, the culture was centrifuged at 1734 g (Allegra X-22 centrifuge) for 15 min and the pellet was resuspended in 5 ml of sterile phosphate buffered saline (PBS) to give an optical density (OD<sub>500</sub>) of 1.4-1.6, which corresponds to 2x10<sup>7</sup> CFU/ml. This was confirmed by viable counting (section 2.2.3), after the dose had been administered to the mice. The cell suspension was kept at room temperature and used within 20 minutes of preparation.

Using a 0.5 ml insulin syringe (BD), 100 µl of cell suspension was injected intraperitoneally (section 2.3.7) into each of two MF1 mice. After infection with *S. pneumoniae*, mice were housed in a fresh IVC and closely monitored for visual development of the signs of disease (section 2.3.9) over the duration of the experimental period. After 22-28 hours, blood was collected by cardiac puncture. For this, animals were anaesthetised with 2.5% (v/v) isoflurane (Isocare) over oxygen (1.6-1.8 L O<sub>2</sub>/min), in an anaesthetic box. Subsequently for each mouse anaesthetic was delivered via a facemask. Absence of reflex reaction was confirmed by pinching of the joints to determine that effective anaesthesia has been reached. Mice were exsanguinated by

cardiac puncture, as described in section 2.3.13.1. After collecting the required volume of blood, the mouse was immediately culled by cervical dislocation.

The collected samples were individually processed by inoculating 50 µl of blood from each mouse into separate universal tubes containing 10 ml of BHI broth and incubated for 16 to 20 hours, statically at 37°C. The next day, supernatant was removed without disturbing the loose sediment of red cells. The supernatant was centrifuged at 1734 g (Allegra X-22 centrifuge) for 15 min and the pellet was resuspended in 1 ml serum broth (800 µl brain heart infusion plus 200 µl heat inactivated foetal bovine serum) and 700 µl of this suspension was added to 10 ml serum broth, to give an optical density (OD<sub>500</sub>) of approximately 0.7. Cultures were incubated statically at 37°C for 5 hours and samples with an OD<sub>500</sub> of 1.6 were removed from the incubator. Cultures with an OD below 1.6 were left until this value was reached. If after 8 hours incubation the OD<sub>500</sub> of 1.6 was not reached, the samples were discarded. The suspension culture was vortexed, before 500 µl aliquots were pipetted into sterile cryotubes (Sarstedt), frozen and stored at -80°C, with the appropriate label.

After 24 hours at -80°C, the viability was determined, and checked monthly, by determining the colony forming units (CFU) of the prepared stocks and confirming optochin sensitivity (section 2.2.1.4). For this procedure, animal passaged samples were thawed in hand and the aliquots were centrifuged at 15115 g for 2 min in a benchtop microfuge. Supernatant was removed with a pipette and resuspended in 400 µl of sterile phosphate buffered saline (PBS). Viable count was determined as described in section 2.2.3. The stock aliquots were used within 6 months of preparation.

### **2.3.5 Virulence test of passaged bacteria**

Before using new stocks of passaged bacteria, the vials were tested to measure the pneumococcal stock virulence, as previously described in (Kadioglu *et al.*, 2000). Five female MF1 mice were used for this test. The testing of dose stocks and the intranasal infection was performed as described in section 2.3.6. After completion of infections, the viable count of the inoculum was determined to confirm the dose. Mice were housed in a fresh IVC and closely monitored for visual development of the signs of disease (section 2.3.9) for 72 hours or until they became lethargic. The time that the animals

became lethargic was recorded and the animals were then culled by dislocation of the neck, confirming death by the absence of eye and joint reflexes. The stock was considered virulent when the intranasally challenged MF1 mice became severely lethargic and the median survival time was within 24 and 72 hours. If these premises (reaching lethargy and survival timeframe) were not achieved, the pneumococcal stock was discarded.

### **2.3.6 Intranasal administration to mice**

All the *in vivo* studies were performed using a model, pneumonia following intranasal infection (Kadioglu *et al.*, 2000), unless stated otherwise in the text.

Frozen animal passaged bacteria were thawed in hand and then pelleted at 15115 g for 2 min in a benchtop microfuge. Supernatant was removed with a Gilson pipette and the pellet resuspended in 400 µl sterile PBS. From the viable counting data of the animal passaged stock (section 2.2.3), the number of CFU per ml was known. Pneumococci were diluted in PBS to give  $2 \times 10^7$  CFU/ml. The prepared dose was placed on ice and used within 2 hours. Animals were anaesthetised with 2.5% (v/v) isoflurane (Isocare) over oxygen (1.6-1.8 L O<sub>2</sub>/min). Pinching joints and observing no reflex reaction from the animal confirmed had reached effective anaesthesia. This step was done in a fume hood with scrubber. The animals were scruffed to hold the nose upright and the pneumococci inoculated intranasally by placing the 50 µl suspension into the nostrils. After inoculation, the animal was placed on its back until recovery.

After completion of infection, the viable count of the inoculum was determined to confirm the dose. Mice were housed in a fresh IVC and closely monitored for visual development of the signs of disease (section 2.3.9) over the duration of the experimental period or until they became lethargic. The time that the animals became lethargic (section 2.3.9 contains the detailed animal signs of disease) was recorded and the animals were then culled by dislocation of the neck, confirming death by the absence of eye and joint reflexes.

### **2.3.7 Intraperitoneal injection of mice**

For this route of infection, described on (Canvin *et al.*, 1995), each mouse was scruffed, using the thumb and the index finger. The tail was held with the fourth and the fifth

fingers of the same hand against the palm, in order to stretch the mouse gently. The hand was turned to show the ventral side of the mouse and dropped forward, so that the head of the animal was at a lower level than the tail. This was done to slightly displace the organs forward to avoid their puncture. Then a 100 µl dose was injected with an insulin syringe by penetration of the needle into the lower right quadrant of the abdominal cavity, at an approximating 45° angle.

### **2.3.8 Intravenous injection of mice**

The intravenous route was used to inoculate  $5 \times 10^5$  pneumococci in 100 µl of PBS, or substances for immune modulation into mice (section 5.3.5). This procedure was adapted from a reported method (Kerr *et al.*, 2004).

Mice were placed in a thermocage or in a cage inside an incubator at 37°C, for 20 minutes, to dilate their tail veins. After incubation, the cage was removed and the mice were kept warm under an infra-red lamp. A mouse was then placed inside a restrainer, leaving the tail of the animal exposed. The tail was disinfected with 70% (v/v) hibitane (5% (w/v) chlorhexidine gluconate from Regent Medical Ltd.; UK) in ethanol. Then, a 0.5 ml insulin syringe, containing 100 µl of bacterial dose, of immune cells (T cells, T<sub>regs</sub>) or sterile PBS, was carefully inserted into one of the lateral tail veins and the plunger slowly pulled back to confirm the presence blood from the vein and then the dose was gently injected into the vein.

### **2.3.9 Scoring of animal signs of pneumococcal disease**

The characteristic signs of pneumococcal disease were regularly assessed and scored, as represented on Table 2.2, based on Morton's scheme (Morton & Griffiths, 1985). Any animal that became lethargic (numeric code = 6 on Table 2.2) was considered to have reached the end point and was then culled by cervical dislocation. The time to the end point was recorded as the "survival time".

<b>Disease sign</b>	<b>Description</b>	<b>Numeric Score</b>
Normal	Healthy appearance, smooth coat, active behaviour	1
+ Hunched	Slight convex curvature of the back	2
+ Starey coat (piloerection)	Slight piloerection of the coat	
+ Hunched / + Starey	Slight curvature of the back and piloerection of the coat	3
+ Hunched / ++ Starey	Slight curvature of the back and pronounced piloerection of the coat	4
++ Hunched / + Starey	Pronounced curvature of the back and slight piloerection of the coat	
++ Hunched / ++ Starey	Pronounced curvature of the back and piloerection of the coat	5
+ Lethargic	Pronounced hunching and piloerection accompany by a considerable reduction of activity	6
++ Lethargic	Pronounced hunching and piloerection accompany by a severe reduction of activity	

Table 2.2 - Scoring the animal signs of disease (Morton & Griffiths, 1985). Each mouse was monitored regularly and the frequency of animal checking increased proportionally according to the severity signs of disease.

### **2.3.10 Determination of viable bacteria in lung tissue**

After the required period post-infection, mice were culled by dislocation of the neck, confirming death by the absence of eye and joint reflexes. Then, the fur was drenched with ethanol, and sterile scissors and forceps were used to carefully open the chest and abdomen, avoiding penetration of the internal organs. An incision was made in the rib cage and the lungs were aseptically dissected from the chest cavity and placed into a pre-weighed universal tube containing 10 ml of ice cold PBS, and kept on ice. The tubes containing the lungs were weighed again to determine the weight of the tissue. The lungs were homogenized with an Ultra-Turrax T8 tissue homogenizer (IKA-Werke) and then kept on ice. Between samples, the homogenizer was cleaned, using forceps to remove tissue debris in the blender, washed with PBS and finally

sterilised with industrial methylated spirit (IMS). Following homogenisation of the lung tissue, the number of CFU/mg of tissue was determined as described in section 2.2.3.

### **2.3.11 Determination of viable bacteria in blood**

The blood was collected as described in section 2.3.13. The nature of the experiment decided the collection route: cardiac puncture (section 2.3.13.1), when organ collection was required or at the experimental ending; or tail bleed (section 2.3.13.2), when the experiment had to continue (time point or survival experiment) and only a small amount of blood was required. Following blood collection, the number of CFU/ml of blood was determined as described in section 2.2.3.

### **2.3.12 Administration of peptide**

When required, 500 µg P17 peptide (Gil-Guerrero *et al.*, 2008; Dotor *et al.*, 2007) in 100 µl PBS was administered by intraperitoneal injection 1 hour before and 6 hours after intranasal challenge with wild-type D39 *S. pneumoniae*.

### **2.3.13 Blood collection**

#### **2.3.13.1 Cardiac puncture of mice**

This technique was used to obtain a large sample of blood. It was done under terminal anaesthesia. The mice were deeply anaesthetised with 2.5% (v/v) isoflurane (Isocare) over oxygen (1.6-1.8 L O<sub>2</sub>/min) inside an anaesthetic box. After the mouse was unconscious it was placed on its back, making sure it had a constant anaesthetic supply and also confirming it had reached effective anaesthesia by pinching joints and observing no reflex reaction. The base of the ribcage was compressed slightly on each side with the thumb and forefingers, lifting it slightly. A 21G x 5/8" needle attached to a 2 ml syringe (BD) was inserted parallel to the sternum through the diaphragm line, approximately 4 mm below the sternum and 5-10 mm towards the chin from below the ribs, penetrating the heart. By this method, it was possible to obtain 0.5 to 1 ml of blood, according to the mouse weight. The mouse was immediately culled by cervical dislocation, after blood collection. 5 µl of heparin sodium (5 units/µl) in PBS was added as an anticoagulant to each tube.

### **2.3.13.2 Tail bleed of mice**

The tail bleeding technique allowed for continuing animal monitoring and experimentation. The volume of blood withdrawn from each mouse did not exceed 10% of its blood volume in a 24-hour period. For this procedure, mice were placed in an incubator for 20 minutes, at 37°C, to promote vasodilatation. Once the mouse was removed from the incubator, it was placed inside a plastic cylinder and the lid was then closed, leaving the tail exposed. For aseptic blood collection, the tail was cleaned before puncture with 70% (v/v) hibitane (5% (w/v) chlorhexidine gluconate; Regent Medical, UK) in ethanol. The needle of a 0.5 ml insulin syringe was placed parallel to the tail vein and introduced with the sharp side down and at a slight angle. The syringe plunger was gently pulled to withdraw the blood. After collecting the blood, the punctured tail area was cleaned with 70% (v/v) hibitane in ethanol and it was confirmed that the bleeding had stopped before returning the mouse to its cage. 1 µl of heparin sodium (5 units/µl) in PBS was added as an anticoagulant to each tube.

### **2.3.14 Blood plasma collection**

Blood from mice was collected by cardiac puncture (2.3.13.1) or tail bleeding (2.3.13.2). Immediately after blood collection the viable numbers of bacteria in the blood was determined (section 2.2.3) and the remaining blood was centrifuged at 8,000 g for 3 minutes. The supernatant (blood serum) was carefully collected, aliquoted at a volume up to 100 µl per tube and stored at -20°C for cytokine quantification by ELISA (section 3.2.4).

## **2.4 General DNA manipulation techniques**

### **2.4.1 Extraction of genomic DNA**

Mouse-tail tips and ear notches were collected for preparation of genomic DNA (section 2.3.3).

#### **2.4.1.1 Method I - for sequencing**

These methods of preparation of genomic DNA from murine tissue were used for sequencing purposes. When pyrosequencing assays were required, genomic DNA was extracted according to section 2.4.1.2. The high yield extraction of genomic DNA method was also to extract high quality genomic DNA of BALB/c and CBA/Ca inbred

mouse strains, for further sequencing of mouse strains whole genome, at The Wellcome Trust Centre for Human Genetics (University of Oxford, UK). It was prepared a gDNA Library and a single lane of paired end data (100nt), with approximately 8 to 10 reads per lane.

#### *Extraction of 'normal' yields of genomic DNA*

For recovery of 10-25 µg DNA from the mouse tail tissue (0.5-1.2 cm in length) and ear notches two Qiagen (UK) kits were used: DNeasy Blood & Tissue Kit (spin-column protocol) for small-scale number of samples and the DNeasy 96 Blood & Tissue Kit (DNeasy 96-well protocol) for large scale number of samples. All buffers and purification columns/plates were provided with the kits. All centrifugation steps in the spin-column protocol were carried out in a SciQuip 1-15 benchtop microfuge (Sigma) or in a Sigma laboratory centrifuge 4K15C for the 96-well protocol (Sigma).

#### *Extraction of high yields of genomic DNA*

When the recovery of 40-100 µg of highly intact DNA was required, DNA was extracted from mouse-tail tissue (0.5-1.2 cm in length) and ear notch, using a Nucleon kit (Gen-probe, UK). Buffer and resin were provided with the kit. All centrifugation steps were carried out in a SciQuip 1-15 benchtop microfuge (Sigma).

All DNA samples were quantified by absorbance at 260 nm measured in a NanoDrop spectrophotometer (Thermo Scientific) and were kept at 4 °C for use within a week and at -20°C or -80°C for up to 6 months.

#### **2.4.1.2 Method II - for pyrosequencing (Wisby *et al.*, 2013)**

Mouse-tail biopsy samples (0.5 to 1 cm in length) or ear notches were added to 200 µl DirectPCR Lysis Reagent (Bioquote Limited) containing 0.2-0.4 mg/ml proteinase K (Sigma or Qiagen) in individual Eppendorf tubes. Digestion of the tissue samples was done overnight at 55°C, rotating the tubes at ~200 rpm. Two to three hours after digestion started, each sample tube was quickly inverted a few times to complete lysis of tissue not in contact with the solution. The rotation was performed to improve the tissue lysis. After the digestion step, the crude lysates were incubated at 85°C for 45 min on a water bath, to inactivate the proteinase K in order to protect the Taq

polymerase from this enzyme. DNA samples were quantified by absorbance at 260 nm measured in a NanoDrop spectrophotometer (Thermo Scientific). Crude lysates were used as PCR template and then stored at -20°C for up to 6 months (or at 4°C for 1 week).

#### **2.4.2 PCR primer design for pyrosequencing**

Single Nucleotide Polymorphisms (SNPs) were selected using the Mouse Phenome Database (<http://phenome.jax.org/pub-cgi/phenome/mpdcgi?rtn=docs/home>) and the SNP sequences were exported from the NCBI Entrez SNP database (<http://www.ncbi.nlm.nih.gov/sites/entrez>).

Primers for pyrosequencing were designed using the PSQ Assay Design software from Biotage AB, performed by the collaborators Anne Southwell and Debra Brooker (MRC Harwell, Oxfordshire).

Primer sets of 3 primers for each SNP were designed: one pair of primers for the PCR (one of which was biotinylated); and a sequencing primer for the pyrosequencing reaction. The minimum and maximum  $T_m$  for the PCR primers were 64 and 66°C. The sequencing primers were designed with a maximum distance of 3 bases from the SNP. Primers were manufactured by MWG-Biotech (Germany).

The list of primers used in the pyrosequencing assays and respective sequences are listed in Appendix 2.

#### **2.4.3 Polymerase Chain Reaction (PCR) method for pyrosequencing**

The PCR mix for reaction in 10  $\mu$ l, was set up on ice, and contained the reagents described in Table 2.3 (Wisby *et al.*, 2013).

Reagents	Stock concentration	Volume ( $\mu\text{l}$ )
Qiagen nuclease-free water	—	2.6
Qiagen <i>Taq</i> PCR Master mix (Cat. Number 201443; includes <i>Taq</i> DNA polymerase, Qiagen PCR Buffer, dNTPs and $\text{MgCl}_2$ )	250 Units	5
Primer (forward)	10 $\mu\text{M}$	0.2
Primer (reverse)	10 $\mu\text{M}$	0.2
DNA template	5 $\mu\text{g}/\mu\text{l}$	2
Total		10

Table 2.3 - Different components for the PCR mix (Wisby *et al.*, 2013).

PCR reactions in 10  $\mu\text{l}$  were set up on ice using 5  $\mu\text{l}$  *Taq* PCR master mix (Qiagen), 0.2  $\mu\text{l}$  forward primer and 0.2  $\mu\text{l}$  reverse primer (at 10 pmol/ $\mu\text{l}$ ), 2.6  $\mu\text{l}$  nuclease-free water and 2  $\mu\text{l}$  DNA ( $\sim 5$  ng/ $\mu\text{l}$ ). PCR reactions were done according to the programme described in Table 2.4.

Step	Temperature (°C)	Duration	No. of cycles
Initial denaturation	95	5 min	1
Denaturation	95	15 sec	44
Annealing	60	30 sec	
Extension	72	15 sec	
Final extension	72	5 min	1
Final hold	4	∞	

Table 2.4 - Standard conditions for PCR (Wisby *et al.*, 2013).

The PCR products were analysed by agarose gel electrophoresis (section 2.5).

### 2.5 Agarose gel electrophoresis

The agarose gel consisted of 1 to 2% (w/v) agarose (Bioline) and 1x TAE buffer (prepared as described in section 2.1.3). After melting the agarose mixture until a clear liquid had formed, ethidium bromide at a concentration of 1 µg/ml was added. The gel was poured into a sealed tray with a well-forming comb. Once set, the comb was removed gently, without distorting the shape of the wells, and the lab gel was submerged in an electrophoresis tank containing 1x TAE buffer. One well of the gel was loaded with DNA marker solution, either a 100 bp or 1 Kb DNA ladder (New England Biolabs), to enable assessment of the size of the DNA fragments of interest. All samples, including the DNA ladder, contained 1:5 loading dye (New England Biolabs). Electrophoresis was done in 1x TAE buffer at 80 to 120 volts, for approximately 20 to 30 minutes, then visualized under UV-light and photographed using ImageQuant 100 (GE Healthcare) imaging system with the IQuant Capture 100 software (GE Healthcare).

The pyrosequencing step was performed at the MRC Harwell (Harwell Science & Innovation Campus, Oxford, UK), as described on section 2.6.

## 2.6 Pyrosequencing

Pyrosequencing is a method of DNA sequencing by synthesis (Wisby *et al.*, 2013). It involves synthesizing its complementary strand enzymatically from a single strand of DNA. The DNA sequence is determined by light emitted upon incorporation of each new complementary nucleotide, detected by a photomultiplier (Figure 2.2).

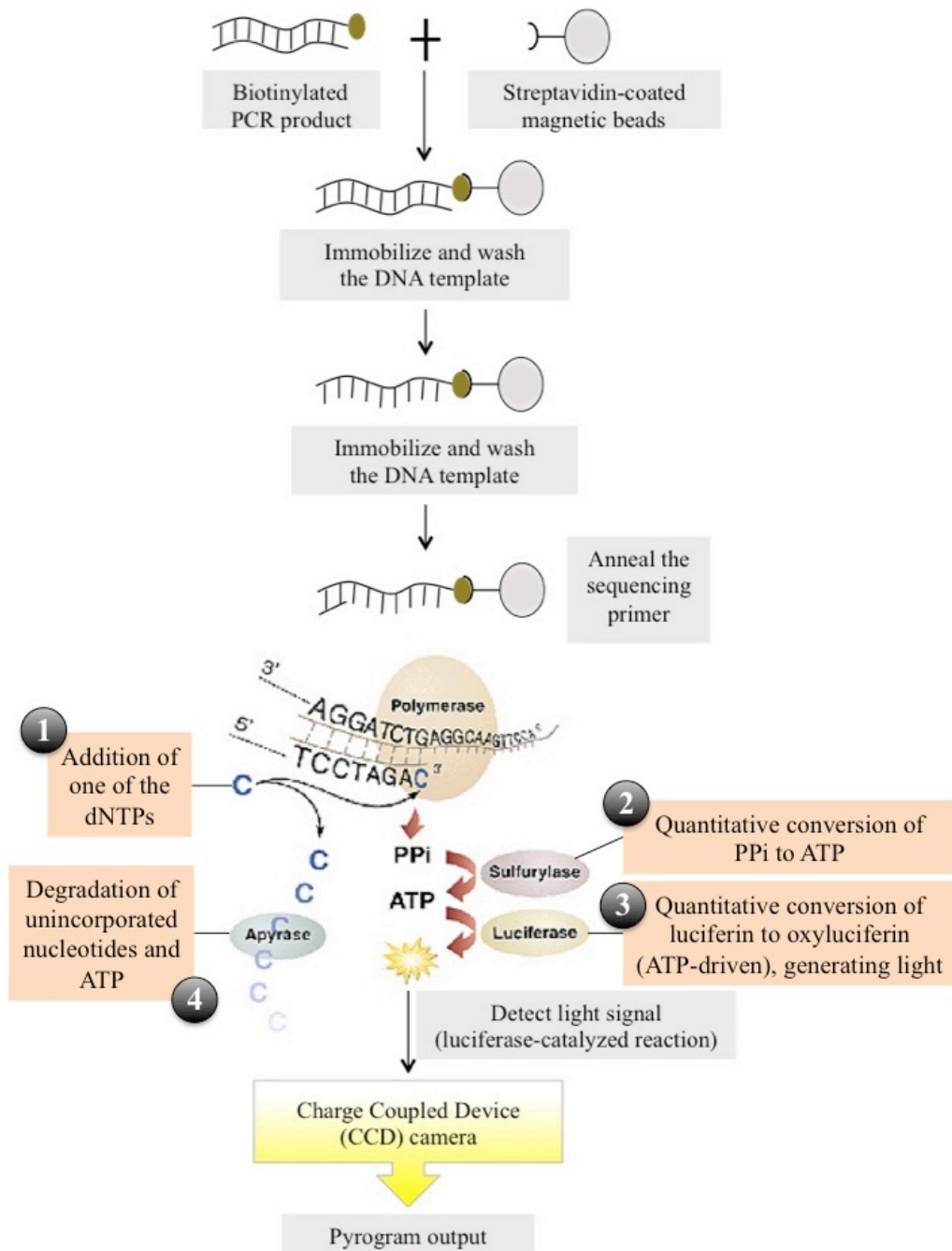


Figure 2.2 - Pyrosequencing steps. Adapted from (Pyrosequencing AB, 2012).

10 µl PCR product, 2 µl streptavidin-sepharose beads (GE Healthcare), 38 µl binding buffer (Biotage AB) and 30 µl ddH<sub>2</sub>O were combined in wells of a 96-well plate and mixed vigorously on a plate shaker for 5 min, so that the biotin-labelled PCR product bound to the streptavidin-coated beads. The PCR products were then prepared using a vacuum prep work table (Biotage AB). The biotinylated PCR products, attached to the filter probes of the vacuum tool, were immersed in 70% (v/v) ethanol for 5 seconds, denatured in PyroMark Denaturation solution (Biotage AB) for 5 sec (allowing only the biotin labelled strand of the PCR product to stay magnetically attached to the filter probes) before immersion in 1X PyroMark Wash buffer (Biotage AB) for 5 sec. The single-stranded PCR products were then re-suspended in a PSQ HS 96-well plate containing 0.5 µl sequencing primer (at 10 pmol/µl) and 11.5 µl annealing buffer (Biotage AB) per well.

The plate was incubated at 80°C for 2 min to allow the sequencing primer to anneal to the single-stranded PCR product. The PSQ 96-well plate and a PSQ HS 96 capillary dispensing tip holder (Biotage AB) containing enzyme, substrate and dNTPs (PyroGold reagent kit, Biotage AB) were placed into the PSQ HS 96 Pyrosequencer (Biotage AB) and the assays were performed (Figure 2.2).

### **2.6.1 Analysis of pyrosequencing data**

The pyrosequencing data were analysed using the SNP software (Biotage AB). Pyrogram examples for each of the analysed SNPs on chromosome 7 can be found in Appendix 2.

## **2.7 Flow cytometry**

### **2.7.1 Lung cell preparation**

After the lung tissue was collected, it was placed into a clean Petri dish and then cut into fine pieces using two clean disposable scalpel blades. Tissue then was transferred into a 1.5 ml Eppendorf tube containing 500 µl PBS, supplemented with 10 mg/ml collagenase D, incubating for 30 minutes at 37°C, to digest connective tissue and to release the haematopoietic cells (Neill *et al.*, 2012). Following incubation, the lung tissue was then prepared as described in section 2.7.2.

### **2.7.2 Preparation of cells for flow cytometric staining**

In the *in vivo* studies, lungs, spleen, cervical lymph nodes and mediastinal lymph nodes were collected post-necropsy and were prepared for flow cytometric analysis. Tissue weight was checked in order to quantificate the number of positive cells per mg of tissue (section 2.7.6). For the following steps, all tissues were treated in the same way as lung tissue, except no erythrocyte lysis solution was added (Neill *et al.*, 2012).

To remove cell debris, each sample was pushed through a 40 µm cell strainer (BD) using a plunger from a disposable 2 ml or 5 ml syringe. The remaining cells in the cell strainer were flushed into a Falcon tube (Corning) with 10 ml 1x PBS 3% (v/v) FCS. The cells were pelleted by centrifugation at 300 x g for 5 minutes, at 4°C. After centrifugation, without disturbing the pellet, the lung supernatant was collected, aliquoted and stored at -20°C for further cytokine quantification by ELISA (section 3.2.4). The pelleted cells were then resuspended in 5 ml erythrocyte lysis solution of 1:10 ammonium chloride lysis solution (BD Biosciences) in nanopure water and then incubated at room temperature for 5 minutes to lyse red blood cells. Prior to centrifugation at 300 g for 5 minutes at 4°C, 5 ml RPMI medium was added to prevent any further action of the erythrocyte lysis solution on the cells. Following centrifugation, cells were resuspended in 1x PBS 3% (v/v) FCS, to a concentration no more than  $1 \times 10^7$  /ml. The volume of 1x PBS 3% (v/v) FCS added to the cell suspension was done either defined by using a hemocytometer or using an approximation guide according to the tissue sample: lung cells in 750 µl; spleen cells in 5 ml; cervical lymph nodes cells in 750 µl; and mediastinal lymph nodes cells in 500 µl. Cells were then stained as described in section 2.7.4 or cryopreserved for further analysis (section 2.7.3).

### **2.7.3 Cell cryopreservation**

The cold-preserved tissue samples were resuspended in a cryoprotectant solution, minimizing the ice formation that could cause loss of cellular viability. After the preparation of cells, as described in section 2.7.2, instead of resuspending cells in the final buffer (1x PBS 3% (v/v) FCS), the cell pellet was resuspended in 1 ml of storing solution (10% (v/v) DMSO, 15% (v/v) FBS and 75% (v/v) RPMI), the vials were labelled and subjected to a -1°C/min cooling in a polycarbonate cryogenic container (Nalgene) and stored at -80°C.

#### **2.7.4 Surface marker analysis**

Extracellular antibody staining was performed to immunophenotype different mouse strains to pneumococcal infection (Neill *et al.*, 2012). FACS buffer (1x PBS supplemented with 3% (v/v) FCS) was used throughout for cell suspension, as a wash buffer and for the dilution of the antibodies. Cell suspensions from mouse tissues were stained for cell surface markers using a combination of FITC-, PE-, PE-Cy7-, APC-conjugated monoclonal antibodies (Table 2.5). In each experiment the appropriate isotype control monoclonal antibodies were also included. Between  $5 \times 10^5$  and  $1 \times 10^6$  cells from each sample were stained with purified anti-Fc receptor blocking antibody (anti-CD16/CD32 from eBioscience) at a 1 in 200 dilution, at 50  $\mu$ l/well and for 30 minutes on ice. This was to prevent fluorescently-conjugated antibodies binding via their Fc domain, which would give a high fluorescent background. Cells were washed and then stained with the appropriate antibody or antibodies (Table 2.5), at 50  $\mu$ l/well, for 30 minutes on ice and covered with aluminium foil. Finally, cells were washed and resuspended in a total volume of 300  $\mu$ l 1x PBS 3% (v/v) FCS. Samples were analysed with a FACSCalibur (BD), using the manufacturer's standard protocols. Before running samples involved in a study, the flow cytometry machine was set up by adjusting compensation and fluorescence intensity for each tissue and then gating the cell populations for analysis. Flow cytometry data acquisition was done using CellQuest software (BD), analysed using FlowJo software (version 8.8.3, Tree Star) and further statistical analysis with Prism GraphPad software (version 5.0).

<b>Antibody</b>	<b>Fluorochoime</b>	<b>Target Cell</b>
Anti-mouse CD4 (clone GK1.5)	FITC, PE and PE/Cy7	T helper cell
Anti-mouse CD8 (clone 53-6.7)	FITC and PE/Cy7	Cytotoxic T cell
Anti-mouse CD19 (clone 6D5)	FITC and PE/Cy7	B cell
Anti-mouse CD22 (clones OX-97 and Cy34.1)	FITC and PE	B cell
Anti-mouse CD25 (clone PC61)	PE/Cy7 and APC	Activated lymphocyte
Anti-mouse CD45 (clone 30-F11)	FITC, PE and APC	Hematopoietic cells
Anti-mouse CD79a (clone F11-172)	APC	B cell
Anti-mouse FcεRIα (clone MAR-1)	PE	Mast cell and basophil
Anti-mouse F4/80 (clone BM8)	APC	Murine macrophage
Anti-mouse IgM (clone RMM-1)	APC	B cell
Anti-mouse Ly-6G/Ly-6C (Gr-1) (clone RB6-8C5)	FITC and PE/Cy7	Neutrophil, granulocytes and macrophages
Anti-mouse TCR γ/δ (clone GL3)	FITC	γ/δ T cells
Anti-mouse NKp46 (clone 29A1.4)	FITC	NK cells
Rat IgG2a (clones eBR2a and RTK2758)	FITC, PE, PE/Cy7 and APC	Isotype control
Rat IgG2b (clone RTK4530)	FITC, PE, PE/Cy7 and APC	Isotype control
Anti-mouse CD16/CD32 (clone 2.4G2)	-	Blocks non-antigen-specific binding of Igs to FcγIII/FcγII receptor (Fc block)
Anti-mouse CD152 (clone UC10-4B9)	APC	T helper cell

Table 2.5 - Extracellular antibodies used in FACS analysis. All antibodies were used for flow cytometry following manufacturer's instructions (eBioscience).

### **2.7.5 Intracellular staining**

Intracellular antibody staining was performed to quantify cytokines in the cellular matrix (Neill *et al.*, 2012). For intracellular cytokine staining, cells were cultured for four hours at  $5 \times 10^5$  cells per well in round-bottomed 96-well plate in RPMI medium supplemented with GolgiPlug (BD Biosciences), according to manufacturer's instructions, to block cellular secretion of cytokines. The medium was further supplemented with 500 ng/ml ionomycin and 50 ng/ml phorbol 12-myristate 13-acetate (PMA), and cells were cultured for a minimum of 4 hours at 37°C. Following culture, wells were washed and stained with antibodies against extracellular markers (Table 2.5), as described in section 2.7.4. Cells were then incubated with 100 µl Fix/Perm solution (1 part of concentrate and 3 parts of diluent) (BD Biosciences) for 20 minutes before washing with 100 µl Perm/Wash buffer (1:10 diluted in nanopure water) (BD Biosciences). Staining with antibodies against intracellular cytokines (listed in Table 2.6) was performed with antibodies diluted in Perm/Wash buffer. After staining, cells were washed and resuspended in a total volume of 300 µl 1x PBS 3% (v/v) FCS. Samples were analysed with a FACSCalibur (BD), using the manufacturer's standard protocol. Before testing samples involved in the study, the flow cytometer was set up by adjusting the compensation and fluorescence intensity for each tissue and then gating cell populations for analysis. Flow cytometry data acquisition was done using CellQuest software (BD), analysed using FlowJo software (version 8.8.3, Tree Star) and further statistical analysis with Prism GraphPad software (version 5.0).

<b>Antibody</b>	<b>Fluorochrome</b>	<b>Target Cell</b>
Anti-mouse IFN- $\gamma$ (clone XMG1.2)	APC	IFN- $\gamma$ cytokine (IFN- $\gamma$ producing cells)
Anti-mouse IL-10 (clone JES5-16E3)	APC	IL-10 cytokine (IL-10 producing cells)
Anti-mouse IL-17a (clone TC11-18H10.1)	APC	IL-17 cytokine (IL-17 producing cells)
Anti-mouse Foxp3 (clone FJK-16s)	PE	Transcriptor factor (T regulatory cells)
Anti-mouse Helios (clone 22F6)	APC	DNA binding protein (T regulatory cells)

Table 2.6 - Intracellular antibodies used in flow cytometry analysis. All antibodies were used for flow cytometry following manufacturer's instructions (eBioscience).

### 2.7.6 Calculation of events per mg of tissue

The flow cytometric data were standardised by converting to events per mg of tissue using the following equation:

$$\text{Cells per mg of tissue} = \left[ \frac{\text{No. of events}}{\text{Collection time}} \times \frac{\text{Final volume for FC}}{\text{Collection speed multiplier (Table 2.7)}} \right] \times \left( \frac{\text{Total resuspension volume}}{\text{Volume per stain}} \right) \div \text{Tissue weight (mg)}$$

The speed of sample collection by the FACSCalibur (collection speed multiplier) was determined according to Table 2.7.

		Collection speed multiplier
FACSCalibur speed	Time to collect 300 $\mu$ l	Volume per sec
Low	300 sec	1
Medium	240 sec	1.25
High	180 sec	1.67

Table 2.7 - Collection speed multiplier. Ratio of the time in which the FACSCalibur collected data from 300  $\mu$ l of sample, according to the speed at which the machine was set up.

## 2.8 Cytokine analysis by enzyme-linked immunosorbent assay (ELISA)

Cytokine quantification was performed by ELISA, using the following kits: Ready-set-go kit (eBioscience) to quantify IL-1 $\beta$ , IL-6, IL-10, IL-17, IFN- $\gamma$ , TNF- $\alpha$  and TGF- $\beta$ ; except for pre-coated 96-well plates (Biorbyt) to quantify KC and MIP-2. The cytokine profiles were assessed for lung homogenate (section 2.7.1) and blood plasma (section 2.3.14). Assays were done according to manufacturer's instructions.

### *Ready-set-go kit (eBioscience)*

In brief, 96-well plates were coated with 100  $\mu$ l of the 1:10 coating antibody per well, then sealed with tape polyolefin film and incubated overnight at 4°C. Next day, the plates were emptied by quickly inverting and then were washed five times with washing buffer (see section 2.1.3), quickly inverted between washes to empty the wells. The plates then were blotted onto paper towels. The wells were blocked with 200  $\mu$ l assay diluent and incubated at room temperature for 1 hour. Plates were quickly inverted and then were washed five times with washing buffer before blotting onto paper towels. Standards were prepared according to Table 2.8:

<b>Cytokine</b>	<b>Concentration (pg/ml)</b>	<b>Standard stock</b>	<b>1x Assay diluent</b>
IL-1 $\beta$	2,000	20 $\mu$ l	10 ml
IL-6	2,000	20 $\mu$ l	10 ml
IL-10	8,000	20 $\mu$ l	2.5 ml
IL-17	2,000	20 $\mu$ l	10 ml
IFN- $\gamma$	2,000	20 $\mu$ l	10 ml
TGF- $\beta$	8,000	20 $\mu$ l	2.5 ml
TNF- $\alpha$	2,000	20 $\mu$ l	10 ml

Table 2.8 - Preparation of standards for each cytokine (eBioscience kits).

The standard sample was added to the first well of the microtitre plate, pipetted up and down, and then transferred to the next well. Serial dilution of standards were done up to the 8<sup>th</sup> well (for plates with lung samples) and up to the 16<sup>th</sup> well (for plates with blood samples), prepared in duplicate.

Lung homogenates and blood plasma were diluted 1:10 of 1 x PBS and 100  $\mu$ l added to each well. Control wells contained 100  $\mu$ l of 1 x PBS. Plates were sealed with tape polyolefin film and incubated overnight at 4°C. The next day, plates were quickly inverted and then washed five times with washing buffer, quickly inverting between washes to empty the wells. Finally plates were blotted onto paper towels (or another absorbent material). Detection antibodies were prepared according to Table 2.9:

<b>Cytokine</b>	<b>Detection antibody stock</b>	<b>1x Assay diluent</b>
IL-1 $\beta$	48 $\mu$ l	12 ml
IL-6	48 $\mu$ l	12 ml
IL-10	12 $\mu$ l	12 ml
IL-17	48 $\mu$ l	12 ml
IFN- $\gamma$	48 $\mu$ l	12 ml
TGF- $\beta$	48 $\mu$ l	12 ml
TNF- $\alpha$	12 $\mu$ l	12 ml

Table 2.9 - Preparation of detection antibodies for ELISA (eBioscience kits).

100  $\mu$ l of detection antibody, prepared as shown in Table 2.9 was added to each well. Plates were sealed with tape polyolefin film and incubated for 1 hour at RT. Plates were quickly inverted and then were washed five times with washing buffer, quickly inverting between washes to empty the wells and then plates were blotted onto paper towels. 100  $\mu$ l of Avidin-HRP (72 ml of 1x assay diluent and 288  $\mu$ l of 250x horseradish peroxidase enzyme solution) were added to each well, and then the plates were sealed with tape polyolefin film and incubated for 30 minutes at RT, in the dark. Plates were quickly inverted and then were washed ten times with washing buffer as before. 100  $\mu$ l of substrate solution was added to each well, and then plates were sealed with tape polyolefin film and incubated for 15 minutes at RT, in the dark. Finally, 50  $\mu$ l of stop solution (see section 2.1.3) was added to each well and absorbance determined at 450 and 570 nm in a Multiskan GO plate reader (Thermo Scientific). Data were collected with SkanIt Software (Thermo Scientific), version 3.2, and exported to Excel and analysed using Prism GraphPad, version 5.0.

## 2.9 Histology

Following infection, at pre-selected periods, mice were culled and whole lungs surgically removed. Tissue samples were examined for pathological signs and to study

the progression of the disease in different hosts, using either classical staining (Haematoxylin & Eosin staining - H&E) or immunostaining (antibody-based method).

### **2.9.1 Preparation of frozen tissue**

For histopathological examination, mice were culled and whole lungs were excised, at selected time points post-infection. OCT embedding matrix (CellPath) compound was placed into aluminium foil containers, made by moulding the foil around 7 ml bijou tubes. The embedding compound was placed to cover the bottom of the foil container (approximately 0.5 cm) and the tissue was added and then completely immersed in embedding compound. The tissue was immersed in a tube, within a beaker containing iso-pentane (BDH) to prevent snap freezing and tissue damage, into liquid nitrogen (Manco *et al.*, 2006). When completely frozen, the samples were stored at -80°C until required (Manco *et al.*, 2006).

### **2.9.2 Sectioning of frozen lung tissue**

After one day at -20°C, the tissue was fixed onto a cryostat mount with OCT embedding matrix and allowed to equilibrate to between -18 and -24°C, the working temperature of the cryostat (Bright). Sections were cut to between 10 to 20 microns thickness, using a microtome blade (Bright). The sections were allowed to dry at room temperature for 30 minutes. Once dried, sections were either wrapped in aluminium foil at -20°C for further use or stained with H&E stain (section 2.9.3) (Manco *et al.*, 2006).

### **2.9.3 Haematoxylin and Eosin (H&E) staining of tissue sections**

Slides containing tissue sections were placed in 90% (v/v) ethanol for 5 minutes and then immersed in haematoxylin (BDH). After 30 seconds in the solution, slides were rinsed under tap water. To differentiate and destain, slides were placed in acidic alcohol (70% (v/v) ethanol/1% (v/v) hydrochloric acid) for a few seconds, until the sections appeared red. Slides were then rinsed briefly in tap water to remove the acid alcohol. Once washed, slides were placed in eosin stain (BDH) for 30 seconds and then excess stain removed under tap water. Slides were dehydrated through a series of alcohol washes: 70% (v/v), 90% (v/v) and 100% (v/v) solutions. After 30 seconds in each solution, slides were placed into xylene for 1 minute. Finally, sections were left to dry

briefly, mounted in DPX solution (BDH) and covered with a coverslip. If bubbles were present, they were removed by gently pressing on the coverslip. Slides were left to dry overnight (Manco *et al.*, 2006). Lung tissue slides were scored according to the severity of the inflammatory processes (section 2.9.5) and pictures were taken.

#### 2.9.4 Lung paraffin wax sections

When collected, whole-lung samples were immersed in neutral buffered formaldehyde 10% (v/v) in distilled water and sent for conventional processing and embedding in paraffin wax. Assessment of haematoxylin and eosin (H&E) staining was done by Janine Moreton (Department of Histology, University of Leicester). Histopathological assessment was performed on tissue sections, as described in section 2.9.5. Immunohistochemical staining was done by Andy Haynes (Medical Research Council, Harwell) for lung Foxp3<sup>+</sup> cells or by Natalie Strickland (Liverpool School of Tropical Medicine) for lung apoptotic cells, as described on (Neill *et al.*, 2012).

#### 2.9.5 Tissue pathology severity score

Lung pathology was scored based on the level of inflammatory cellular infiltration in the peribronchial and perivascular areas, and alveolar spaces. The tissue scoring of each section was performed and translated to a numeric scale of severity, as described in Table 2.10 (Gingles *et al.*, 2001). Each tissue section was scored and the sections from the same animal strain and time point post-infection were then averaged.

<b>Numeric Score</b>	<b>Level of the tissue inflammation</b>
0	Normal
1	Light
2	Mild
3	Moderate
4	Substantial

Table 2.10 - Numeric score for the level of cellular infiltration in lung tissue sections. Example images characterising each level of tissue inflammation are illustrated in the appendix (Appendix 7).

### **2.9.6 Cytocentrifugation of lung cells**

Prior to cytocentrifuge of the samples, the number of cells was enumerated with a haemocytometer to determine the cell concentration in the sample. It then was diluted in RPMI to give a total of  $5 \times 10^5$  to  $1 \times 10^6$  cells per ml. The cells were centrifuged onto labelled cytopsin slides (Shandon), using a cytocentrifuge (Cytospin 2, Shandon) at 108 g for 3 minutes. Following centrifugation, the slides were left overnight to air-dry (Gingles *et al.*, 2001).

### **2.9.7 Differential staining of cells with Giemsa stain**

Dried cytopsin slides (described in section 2.9.6) were placed in a rack and fixed with 100% acetone for 15 minutes. Differential staining was performed by flooding the slides with 1 in 20 Giemsa's stain (BDH) in distilled water for 20 minutes, before rinsing with tap water. For permanent mounting, a coverslip was gently lowered onto the section covered with a drop of DPX resin (BDH). The slide was then turned over to allow the DPX to spread between the section and coverslip. Excess resin was removed and the absence of air bubbles in the tissue area confirmed by gently pressing the coverslip. Slides then were then left to dry. Slides were examined using a light microscope at 400x and differential leukocyte counting was performed (Gingles *et al.*, 2001). At least 10 different areas were counted, using an ocular graticule.

### **2.10 Statistical Analysis**

The computer software program Graph Pad Prism was used to calculate the Standard Deviation (SD) between experimental samples, when each experimental group contained an equal number of data sets. In the case where different numbers of data sets existed in each experimental group, the Standard Error of the Mean (SEM) was used. When data could be assumed to be normally distributed and when two independent variables were being analysed, 2-way ANOVA followed by Bonferroni post-test was performed. Statistical differences between groups were calculated using Mann-Whitney test and Student's *t* test. Statistical significance was assumed at  $P < 0.05$ .

---

## CHAPTER 3. INVESTIGATION OF HOST RESPONSES IN BALB/C AND CBA/CA MICE TO PNEUMOCOCCAL INFECTION

---

### 3.1 Aims

In this study, the phenotypic basis for determining differences in susceptibility and resistance to *S. pneumoniae* infection was investigated (using BALB/c and CBA/Ca mice). The innate immune profile of the two inbred mouse strains was examined and compared to understand what underlies the distinct susceptibility pattern in response to pneumococcal infection. This investigation focused on the timing of cellular infiltration into lungs, the nature and type of host immune cells involved in these processes, and the progress of the lung pathology during the infection. Overall, the data contribute to a clear view of host immunological properties and responses, helping to classify a resistant and susceptible pneumococcal-infected host.

### 3.2 Results

#### 3.2.1 Differences in acute responses between BALB/c and CBA/Ca mice associated with differences in susceptibility to invasive pneumococcal disease

The strains used in this project, BALB/c and CBA/Ca inbred mice, were phenotyped to compare their survival, animal pain score, and viable bacteria in the lungs and blood post-infection. These results were consistent with the results obtained previously by Gingles (Gingles *et al.*, 2001).

Firstly, *in vivo* studies with the two host strains were performed to investigate the bacterial dissemination following acute intranasal infection with *Streptococcus pneumoniae* D39 (Figure 3.1).

Intranasal infection was performed and mice were assessed for 7 days, to monitor physical condition and signs of disease (Figure 3.1-B). During this study, all BALB/c survived until the end point – 168 hours post-infection (Figure 3.1-A) and none of them showed signs of disease (Figure 3.1-B), providing evidence for resistance against pneumococcal disease. Conversely, CBA/Ca mice survived no longer than 36 hours post-infection and with mean survival of 28 hours (Figure 3.1-A). Mean survival was significantly different to that of BALB/c mice ( $P < 0.0001$ ). As represented in Figure

3.1-B, the susceptible CBA/Ca mice developed signs of illness as early as 18 hours after challenge and the difference in animal pain score was significantly different to BALB/c mice 24 hours post-infection ( $P < 0.0001$ ). By 24 hours p.i., the first CBA/Ca mice reached the lethargic state (experimental end-point), and during the next 11 hours (24 to 35 hours p.i.) all CBA/Ca mice showed such pronounced disease signs, whereas BALB/c mice were normal during the 7 days of challenging. When the CBA/Ca mice were lethargic, laboured breathing tremor was observed.

In time point experiments (0, 6, 12 and 24 hours p.i.), BALB/c and CBA/Ca mice were infected intranasally, assessing the CFU numbers in the lungs (per mg) and blood (per ml) (Figure 3.1-C and -D, respectively). In the lungs (Figure 3.1-C), in the first 6 hours after infection, the bacteria doubled in both strains. Pneumococcal numbers stayed unchanged at a concentration around  $10^3$  CFU per mg of lung tissue of BALB/c and CBA/Ca between 6 and 12 hours p.i., then by 12 to 24 hours, significant differences were observed amongst the two host strains ( $P < 0.01$  at 24 hrs p.i.). In the lungs of CBA/Ca mice the bacterial numbers had an increase of 10 times (from  $\sim 10^3$  to  $\sim 10^4$  Log<sub>10</sub> CFU per mg of lung tissue), whereas in BALB/c mice the pneumococci sharply dropped close to the limit of detection (under  $10^1$  Log<sub>10</sub> CFU per mg lung tissue). In the blood of CBA/Ca mice bacteria growing exponentially during the time course of the experiment (0, 6, 12 and 24 hours p.i.) were detected, reaching approximately  $10^8$  Log<sub>10</sub> CFU per ml of blood. BALB/c mice showed no bacteraemia at any experimental time point.

Overall, this study evidenced the two extremes of susceptible phenotyping to invasive pneumococcal disease. BALB/c mice survived the infection, showing no signs of disease, and when the lung and blood CFUs were determined, it was clear that this resistant host could contain and weaken the pneumococcal numbers in the lungs within 24 hours, avoiding dissemination into the blood (no septicaemia). On the other hand, CBA/Ca mice failed to survive the *S. pneumoniae*-infection (up to 36 hours p.i.), showing severe signs of disease (from 18 hours p.i. onwards). When analysing the lung CFUs, CBA/Ca mice clearly could not limit the lung bacterial growth (peak of  $10^4$  Log<sub>10</sub> CFU per mg lung tissue at 24 hours p.i.), resulting in early bacterial spreading into the blood. Once in the blood of CBA/Ca mice, the pneumococcal numbers

increased sharply (peak of  $10^8$  Log<sub>10</sub> CFU per ml of blood at 24 hours p.i.), causing blood poisoning (septicaemia).

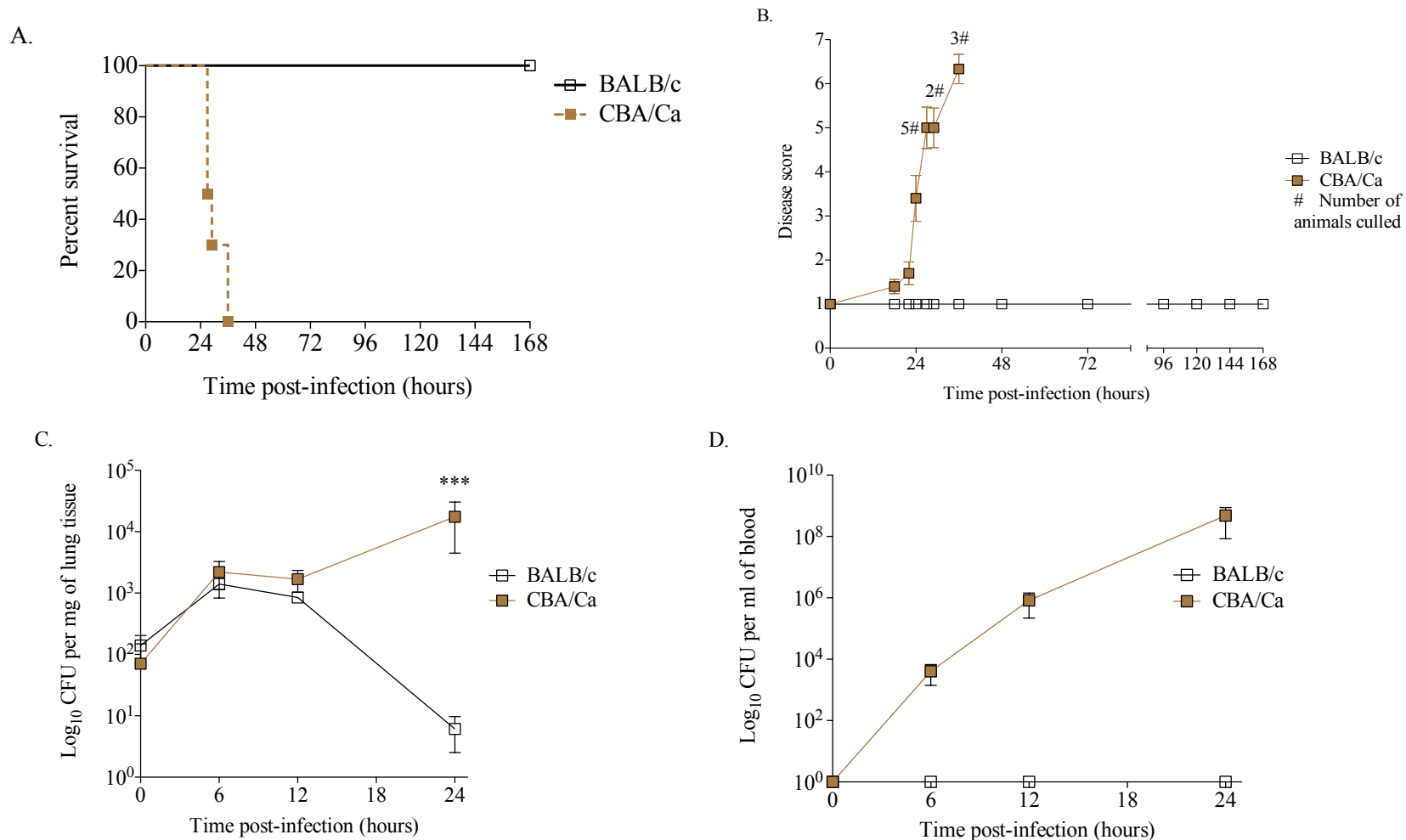


Figure 3.1 - Models of infection with BALB/c and CBA/Ca mice. All results in (A–D) are from intranasal infection of BALB/c (□) and CBA/Ca mice (■) with wild-type D39 *S. pneumoniae*. (A) Survival of *S. pneumoniae*-infected mice was monitored for 7 days. Median survival time of >168 hours for BALB/c mouse strain and 28 hours for CBA/Ca mouse strain (n = 10 mice per strain) and (B) animal disease scored (see Table 2.2 in section 2.3.9). (C) Number of bacteria per mg of lung tissue and (D) per ml of blood collected at 0, 6, 12 and 24 hours post-infection. For all graphs data represent mean values ± SEM (graph B) and ± SD (graphs C and D). The p-value (\*\*\*,  $P < 0.0001$ ) in graph (A) was calculated by means of the log-rank (Mantel-Cox) test. The p-value in graph (B) (\*\*\*,  $P < 0.001$  from 24 hours p.i. until end of the experiment), graph (C) (\*\*,  $P < 0.01$  at 24 hrs p.i.) and graph (D) (\*\*,  $P < 0.01$  at 6 hours p.i.; \*\*\*,  $P < 0.001$  at 12 and 24 hours p.i.) were obtained with two-way ANOVA followed by Bonferroni post-test. Results in (C and D) are representative of 2 independent experiments with  $\geq 4$  mice per strain and time point.

After this result, in which CBA/Ca mice succumb rapidly to pneumococcal disease, it was relevant to assess how quickly the bacteria disseminate into the bloodstream in a susceptible host. It is important to assess the bacterial growth in host blood, considering that wild type D39 bacterium in BHI broth has a duplication time of approximately 30 minutes at exponential phase. Both animal strains were once again tested for invasive pneumonia and blood was collected from their tail vein at the following time points post-infection: 0, 0.5, 2, 4, 6, 8, 12 and 24 hours. As illustrated in Figure 3.2, pneumococci were detected in the blood of CBA/Ca mice 2 hours post-challenge ( $3.32 \times 10^2$  mean CFU/ml). In the following hours, bacteraemia levels increased rapidly in CBA/Ca mice, showing a significant increase along the time course of the infection ( $P < 0.05$ , between 0 and 24 hours, 30 min and 24 hours; 2 and 24 hours; and 4 and 24 hours p.i.), and from 2 hours post-infection onwards became statistically significant ( $P < 0.001$ ) when compared to BALB/c mice. At 24 hours post-infection, this susceptible inbred strain showed extremely high septicaemia (mean  $10^9$  CFU/ml) and a 4 Log<sub>10</sub> rise in the last 12 hours time points (12 to 24 hours).

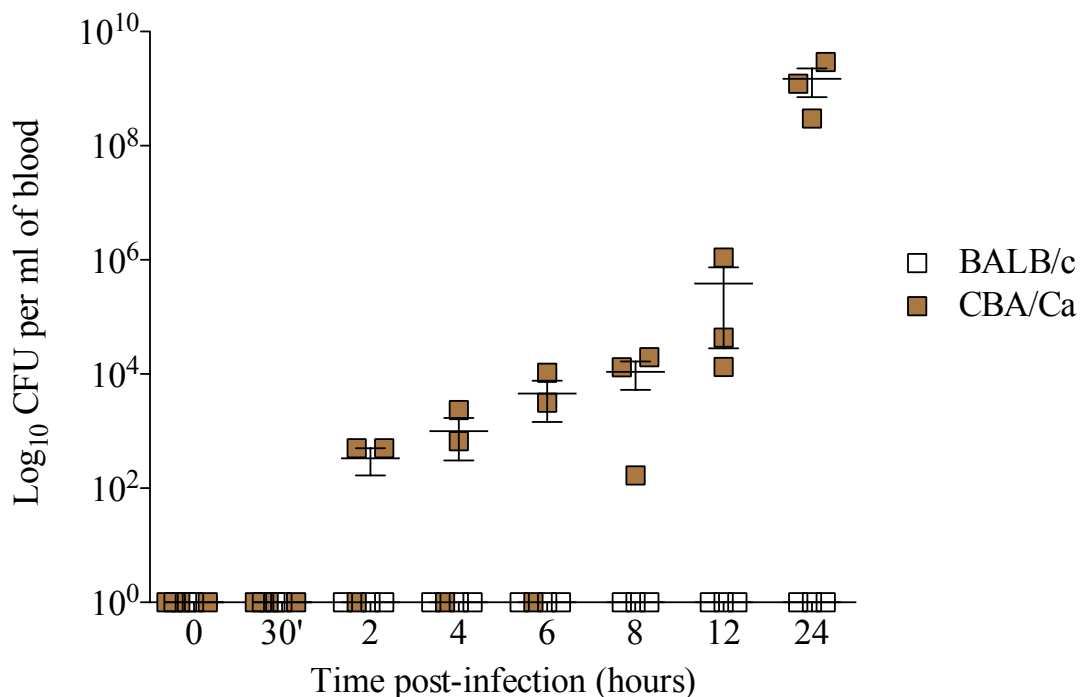


Figure 3.2 - Number of pneumococci in the blood of BALB/c and CBA/Ca mice after intranasal infection. Mice were intranasally challenged with  $10^6$  CFU of passaged *S. pneumoniae* D39. Blood of BALB/c and CBA/Ca mice was collected from tail vein at 0, 30 min, 2, 4, 6, 8, 12 and 24 hours post-infection and assessed for CFU counting. In the figure, each dot ( $\square$  for BALB/c mice and  $\blacksquare$  for CBA/Ca mice) represents the CFU count from an individual mouse and the horizontal lines represent mean of CFU values  $\pm$  SD. The p-value (\*\*\*,  $P < 0.001$  at 8, 12 and 24 hours post-infection) was obtained with two-way ANOVA followed by Bonferroni post-test. Data are representative of 2 experiments with 3 mice per strain and time point.

BALB/c contained the bacteria in the lungs and survived, whilst, in contrast, CBA/Ca in the bloodstream is rapidly invaded by pneumococci and the mice consequently succumb.

### *Bacteraemia Model*

To answer the question whether the observed resistant phenotype in BALB/c mice (Figure 3.1) of retaining and reducing the number of bacteria in lungs and limiting dissemination is a consequence of key features in the lungs, BALB/c and CBA/Ca mice were challenged intravenously.

A susceptible phenotype was observed in the BALB/c mice, although, their survival was better than that for infected CBA/Ca mice (Figure 3.3). Sham-infected BALB/c and CBA/Ca mice ( $n = 3$  per mouse strain) with PBS administered intravenously were used as a control in this study, with all mice surviving the 7 days challenge and showing no signs of disease and no bacteria in the blood at any experimental time point (data not shown). In the pneumococcal-infected groups ( $n = 6$  per mouse strain), the survival period of CBA/Ca mice was very short (average survival of 24 hours p.i.) compared to BALB/c mice (average survival of 100 hours p.i.), showing a significantly different survival rate ( $P < 0.001$ ) (Figure 3.3-A). The first BALB/c mice to be culled (2 mice out of 6) occurred after 48 hours post-infection, and only two more mice from this strain were culled, each one on of them succumb on the two following days (one mouse at 72 hrs and the other mouse at 96 hrs p.i.). Overall, 2/6 of BALB/c mice survived, but no CBA/Ca mice survived the bacteraemia challenge. Mice were monitored for signs of disease (Figure 3.3-B), with CBA/Ca mice showing the first signs of disease at 8 hours post-infection. By 12 hours p.i., CBA/Ca mice evidenced more pronounced signs of disease, significantly different ( $P < 0.001$ ) to BALB/c mice, which at this time point still had no visible signs of pneumococcal infection. At 24 hours post-infection, CBA/Ca mice were all lethargic (experimental end-point), but at this time point the BALB/c mice were only starting to show the first signs of disease (2 out of 6 BALB/c mice were hunched and the 4 remaining animals were still normal) significantly different when compared with the signs observed in CBA/Ca mice ( $P < 0.001$ ). The examination of the bacteraemia levels (Figure 3.3-C) evidenced similar CFU numbers in BALB/c and CBA/Ca mice, in the first 8 hours of the intravenous infection. Only after 12 hours post-infection, the pneumococcal numbers significantly increased in

CBA/Ca mice when compared to BALB/c mice ( $P < 0.001$ ), which had similar bacterial numbers to previous time points. By 24 hours post-infection, the bacteraemia differences between mouse strains were augmented, with CBA/Ca mice reaching nearly  $\log_{10} 10$  CFU/ml while BALB/c maintained bacteraemia levels to previous time points. Although the BALB/c mice showed poor protection when infected intravenously, the number of bacteria in the blood had no significant change during the course of the infection, whereas CBA/Ca mice were more susceptible and evidenced a significant increase of CFUs in blood ( $P < 0.001$ ). Of the 4 BALB/c mice with higher CFU numbers at 24 hours post-infection, 2 of them rapidly developed signs of disease and one day later were lethargic. The same observation was seen with the other 2 BALB/c mice, one culled at 72 hours and the other at 96 hours post-infection.

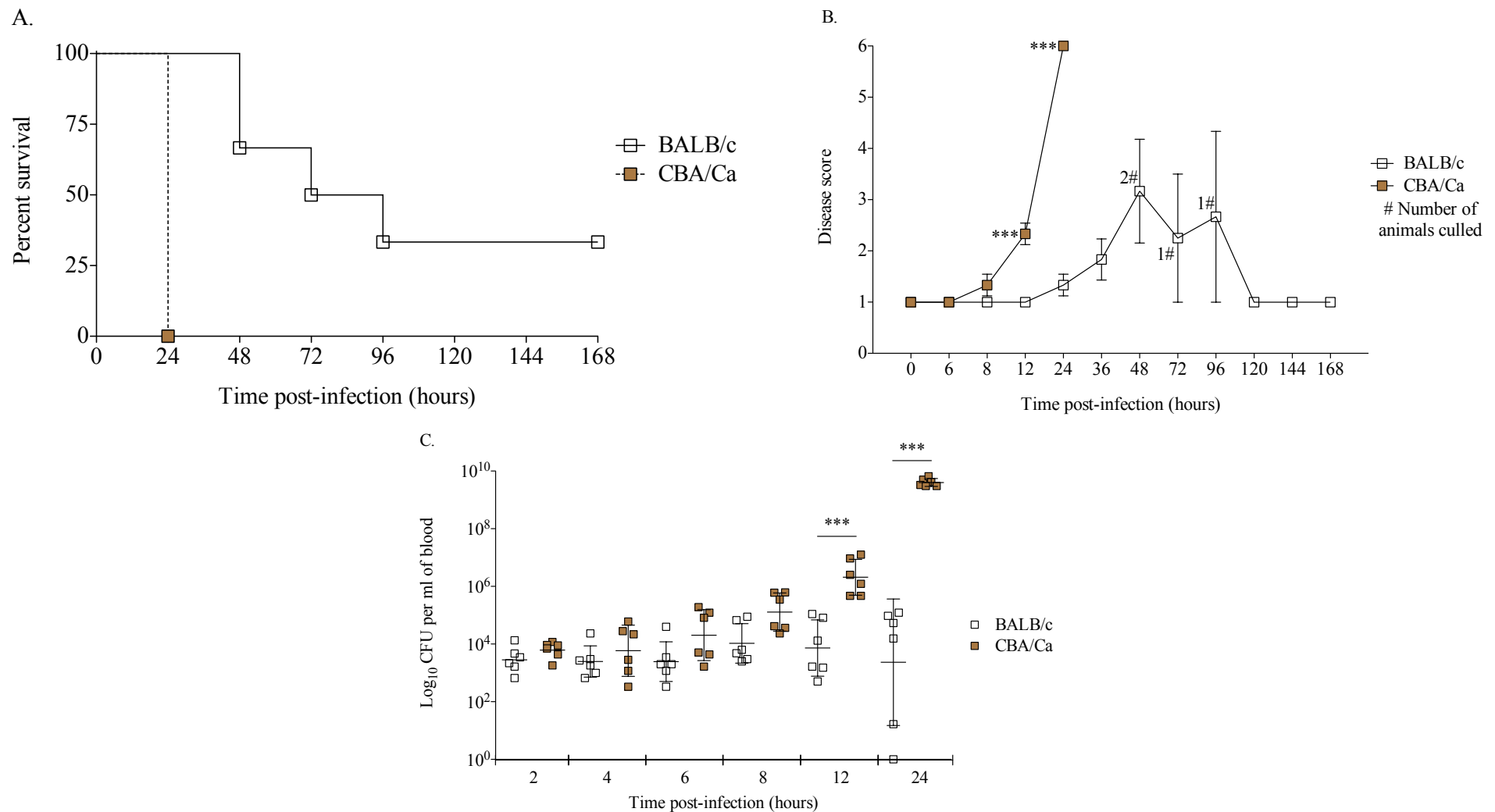


Figure 3.3 - Septicaemia model of infection with BALB/c and CBA/Ca mice. All results in (A–C) are from intravenous-infection of BALB/c (□) and CBA/Ca (■) mice (n = 6 mice per strain) with wild-type D39 *S. pneumoniae*. Sham-infected BALB/c and CBA/Ca mice (n = 2 mice per strain) were intravenously challenged with PBS (data not plotted). (A) Survival of *S. pneumoniae*-infected mice was monitored for 7 days. (B) Animal disease scored (see Table 2.2 in section 2.3.9). (C) Number of bacteria per ml of blood collected at 2, 4, 6, 8, 12 and 24 hours post-infection. For all graphs data represent mean values ± SEM. The p-value (\*\*\*,  $P < 0.0001$ ) in graph (A) was calculated by means of the log-rank (Mantel-Cox) test. The p-value in graph (B) (\*\*\*,  $P < 0.001$  at 12 and 24 hours p.i.), graph (C) (\*\*\*,  $P < 0.001$  at 12 and 24 hrs p.i.) was obtained with one-way ANOVA.

BALB/c and CBA/Ca mouse strains showed different levels of susceptibility in the intravenous (bacteraemia) model and a complete divergence in susceptibility to the acute infection (pneumonia) model. Such differences in the host ability to contain the infection in the lung, suggest that the lung innate responses, could be crucial to determining survival. Therefore, further analysis was assessed regarding host immune responses and its correlation with susceptibility to invasive pneumococcal disease (section 3.2.2).

### **3.2.2 Host immune responses to pneumococcal lung infection in BALB/c and CBA/Ca mice**

This investigation was done to characterise the immunological responses of BALB/c and CBA/Ca mice, understand how a resistant and a susceptible host respond differently in terms of cellular recruitment to pneumococcal infection, mechanisms behind the host responses, and finally, to identify the correlation between the host phenotype and the genetic make-up, conferring susceptibility to *S. pneumoniae* infection (using a congenic mouse strain – see Chapter 4).

### **3.2.3 Phenotyping of the cellular recruitment in BALB/c and CBA/Ca inbred mice in response to invasive pneumococcal infection**

To study the overall cellular recruitment in the lungs of BALB/c and CBA/Ca inbred mice, differential analysis of leukocytes was done in a time course experiment, with four animals per group per time point post-infection. The quantification of immune cells was performed by flow cytometry. The raw data of the lung weight used to quantify all cell subsets presented in this chapter and to further calculate the number of immune cells per mg of lung tissue was added to the appendix (Appendix 8).

Firstly, CD45<sup>+</sup> hematopoietic cell numbers were evaluated in the lungs of BALB/c and CBA/Ca mice (Figure 3.4). These showed a significant increase over time in both strains following pneumococcal infection ( $P < 0.001$ ). However, in the BALB/c lungs leukocyte recruitment steadily increased to the last time point of cellular evaluation (24 hrs p.i.), whereas in the CBA/Ca mice the increase occurred within the first 6 hours post-infection. Additionally, at 24 hours post-challenge, BALB/c lungs evidenced significantly more leukocytes when compared to CBA/Ca lungs ( $P < 0.001$ ). During the time course of infection the total number of leukocytes showed a significant increase in

BALB/c mice ( $P < 0.001$ ), whereas in CBA/Ca mice the increase overtime was smoother but still significant between 0 and 24 hours post-infection ( $P < 0.05$ ).

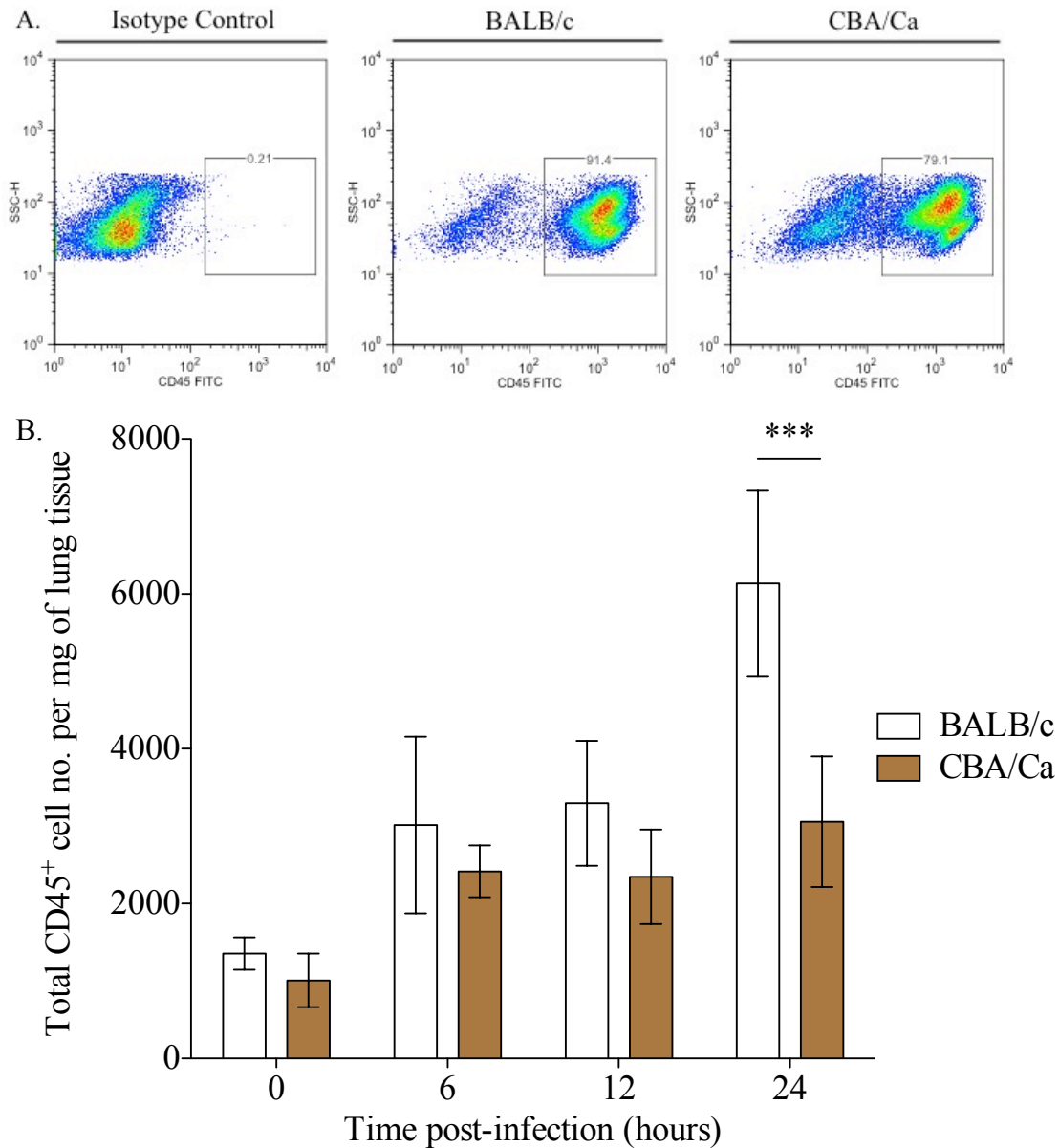


Figure 3.4 - Numbers of CD45<sup>+</sup> cells in the lungs of BALB/c and CBA/Ca mice post-infection with *S. pneumoniae*. Mice were intranasally infected with 10<sup>6</sup> CFU and lungs were collected at 0, 6, 12 and 24 hours post-infection. (A) Flow cytometric analysis of leukocyte cells was determined by gating for CD45<sup>+</sup> events (example of a BALB/c and CBA/Ca 24 hour time point sample). (B) Number of leukocytes per mg of lung tissue, at the various time points, analysed by flow cytometry. Data represent the mean of positive events  $\pm$  SD. The p-value (\*\*\*,  $P < 0.001$ ) was obtained by two-way ANOVA followed by Bonferroni post-test. Data are representative of two independent experiments with  $> 4$  mice per group in each experiment.

The results obtained from the neutrophil analysis of the lungs of BALB/c and CBA/Ca mice (Figure 3.5), followed the prediction of published data on this cell subset (Gingles

*et al.*, 2001). These cells were the leading population recruited into pneumococcal-infected lungs of both animal strains. Looking at Figure 3.5, both BALB/c and CBA/Ca revealed a significant neutrophil expansion following *S. pneumoniae* infection ( $P < 0.0001$ ) and interestingly the observed pattern was similar between animal strains with the neutrophil peak at 12 hours post-infection. The differences found in the analysis of the two strains was essentially the neutrophil increase from 6 to 12 hours post-infection, significantly greater in BALB/c ( $P < 0.01$  between 6 and 12 hrs p.i.) than CBA/Ca ( $P < 0.05$  between 6 and 12 hrs p.i.). The differences in neutrophil numbers persisted at 24 hours post-infection, at which time the lungs of BALB/c mice exhibited significantly higher numbers of cells than lungs of CBA/Ca mice ( $P < 0.05$ ). When comparing to 0 hours post-infection, a significant increase was observed in the lungs of both strains ( $P < 0.001$ ). Overall, neutrophils represented the main cell subset population (nearly half of the leukocyte cells per mg of lung tissue) recruited into the infection site.

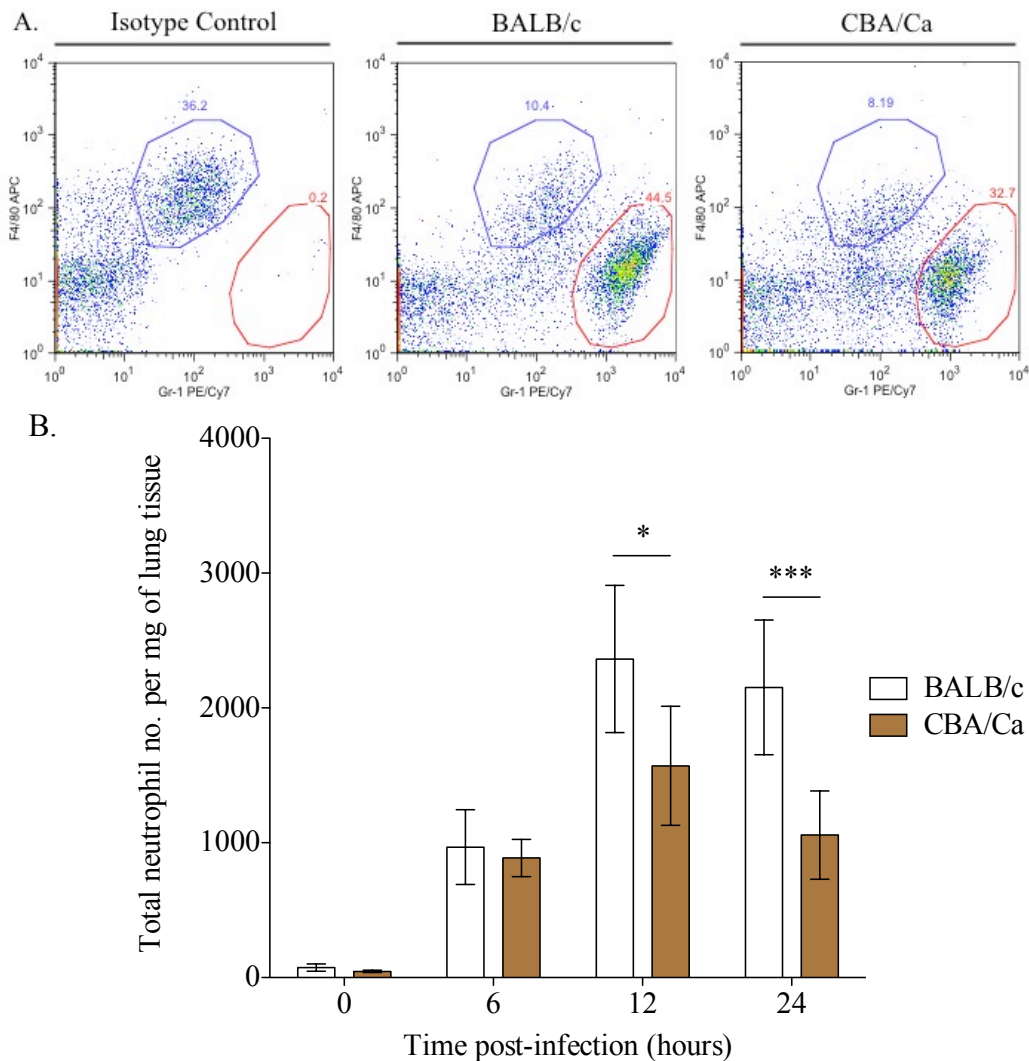


Figure 3.5 - Numbers of neutrophils in the lungs of BALB/c and CBA/Ca mice post-infection with *S. pneumoniae*. Mice were intranasally infected with  $10^6$  CFU and lungs were collected at 0, 6, 12 and 24 hours post-infection. (A) Flow cytometric analysis of neutrophils was determined by gating for  $CD45^+$ ,  $Fc\epsilon R1^+$ ,  $F4/80^{lo}$  and  $Gr-1^+$  events (example of a BALB/c and CBA/Ca 24 hour time point sample). (B) Number of neutrophil per mg of lung tissue, at the various time points, analysed by flow cytometry. Data represent the mean of positive events  $\pm$  SD. The p-value (\*,  $P < 0.05$ ; \*\*\*,  $P < 0.001$ ) was obtained by two-way ANOVA followed by Bonferroni post-test. Data are representative of two independent experiments with  $> 4$  mice per group in each experiment.

Quantification of macrophages in the lungs of BALB/c and CBA/Ca mice (Figure 3.6) indicated different host responses in this cell subset during disease progression. In the BALB/c mice, the number of macrophages significantly increased within the first 12 hours post-infection ( $P < 0.05$  between 0 and 12 hrs p.i.), when the peak in macrophage cells infiltrating into the lungs was reached. On the other hand, it was revealed that the pneumococcal infection induced no significant changes in macrophage numbers in the

lungs of CBA/Ca mice ( $P > 0.05$ ). During the course of infection, the number of macrophages showed a significant increase when compared to 0 hours ( $P < 0.05$ ), but in CBA/Ca lungs no significant changes in macrophage recruitment were observed ( $P > 0.05$ ). Between the two mouse strains, differences in the macrophage numbers were significant at 24 hours post-infection ( $P < 0.05$ , BALB/c compared to CBA/Ca) (Figure 3.6-B).

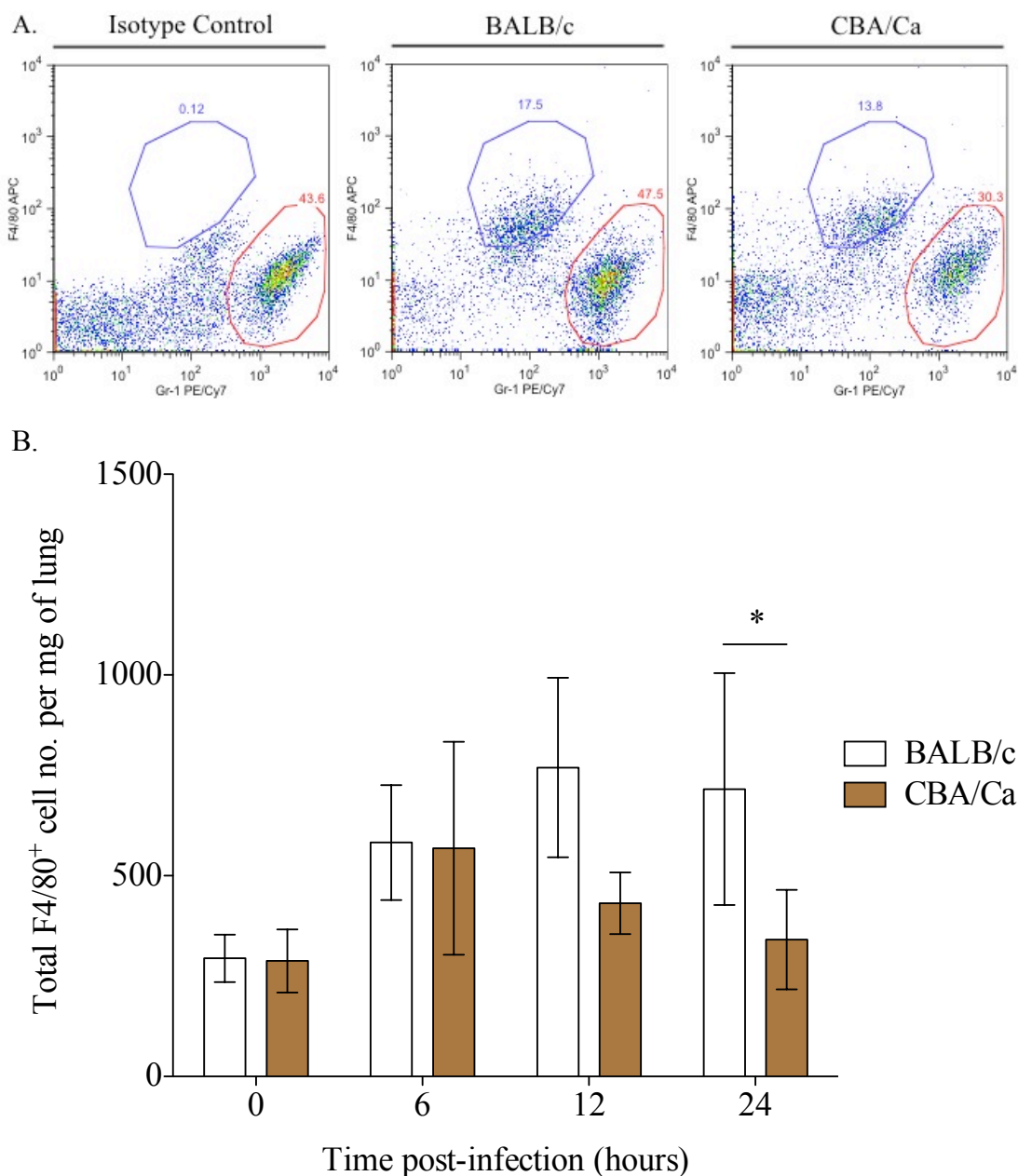


Figure 3.6 - Numbers of macrophage in the lungs of BALB/c and CBA/Ca mice post-infection with *S. pneumoniae*. Mice were intranasally infected with  $10^6$  CFU and lungs were collected at 0, 6, 12 and 24 hours post-infection. (A) Flow cytometric analysis of macrophage cells was determined by gating for  $CD45^+$ ,  $Fc\epsilon RI^-$ ,  $Gr-1^-$  and  $F4/80^+$  events (example of a BALB/c and CBA/Ca 24 hour time point sample). (B) Number of macrophage per mg of lung tissue, at the various time points, analysed by flow cytometry. Data represent the mean of positive events  $\pm$  SD. The p-value (\*,  $P < 0.05$ ) was obtained by two-way ANOVA followed by Bonferroni post-test. Data are representative of two independent experiments with  $> 4$  mice per group in each experiment.

The analysis made of  $T_{\text{helper}}$  cells showed a distinctive phenotype between the two inbred mouse strains during IPD (Figure 3.7). The BALB/c displayed an enhancement of  $CD4^+$  T cell recruitment to the lungs over time following infection, revealing a

significant cellular increase at 24 hours ( $P < 0.001$  compared to 0 hrs p.i.) post-infection (Figure 3.7-B). By contrast, there was no significant increase in CD4<sup>+</sup> T cells in the lungs of CBA/Ca mice over the course of the infection ( $P > 0.05$ ). When comparing the CD4<sup>+</sup> T cell numbers between mouse strains, by 24 hours post-infection the lungs of BALB/c mice showed approximately two times the amount of CD4<sup>+</sup> T lymphocytes observed in the CBA/Ca mice, which resulted in a great significant difference in CD4<sup>+</sup> T cell recruitment between pneumococcal-infected host strains ( $P < 0.001$ ).

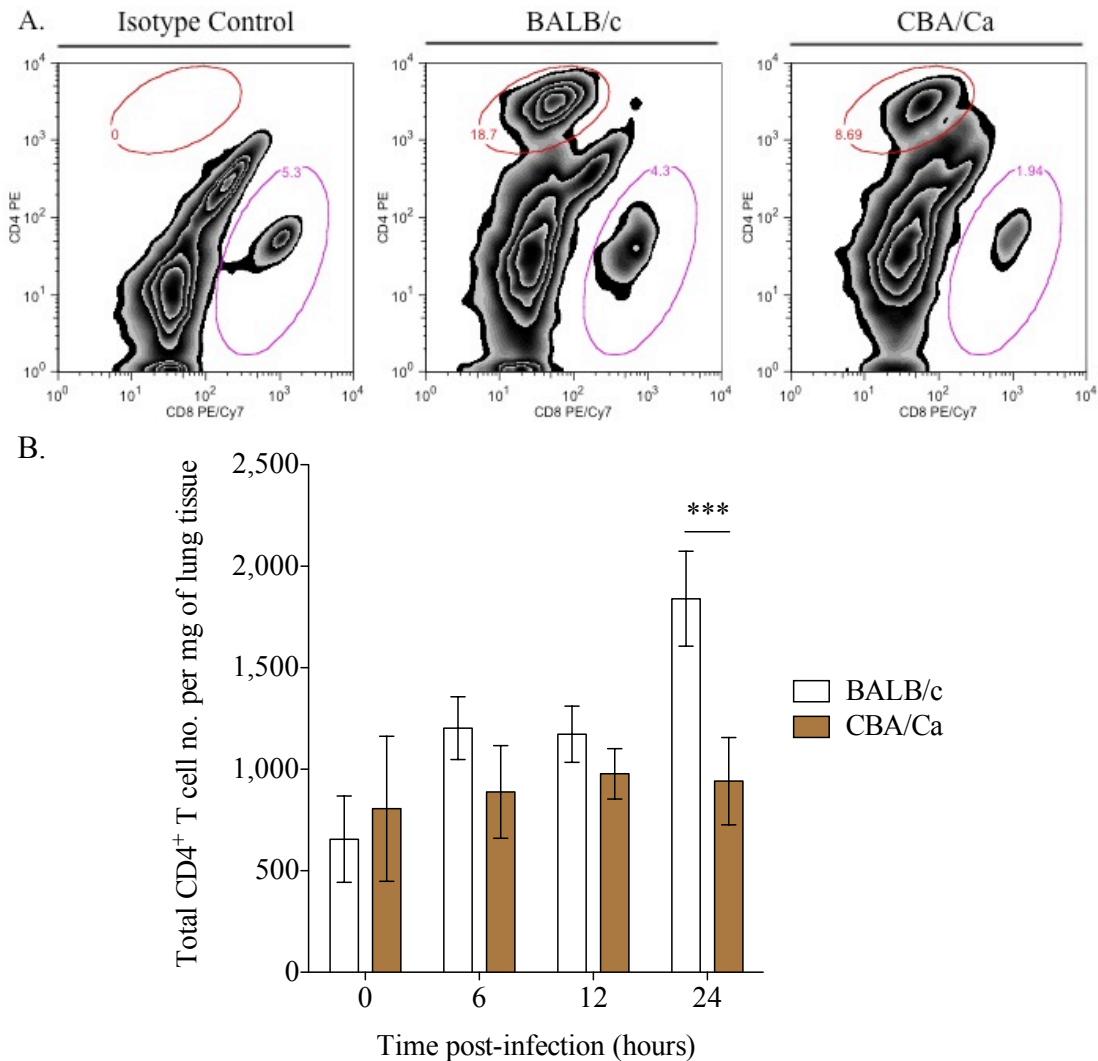


Figure 3.7 - Numbers of T<sub>helper</sub> cells in the lungs of BALB/c and CBA/Ca mice post-infection with *S. pneumoniae*. Mice were intranasally infected with 10<sup>6</sup> CFU and lungs were collected at 0, 6, 12 and 24 hours post-infection. (A) Flow cytometric analysis of CD4 T cells was determined by gating for CD45<sup>+</sup>, CD4<sup>+</sup> and CD8<sup>-</sup> events (example of a BALB/c and CBA/Ca 24 hour time point sample). (B) Number of T<sub>helper</sub> cells per mg of lung tissue, at the various time points, analysed by flow cytometry. Data represent the mean of positive events  $\pm$  SD. The p-value (\*\*\*,  $P < 0.001$ ) was obtained by two-way ANOVA followed by Bonferroni post-test. Data are representative of two independent experiments with  $> 4$  mice per group in each experiment.

The determination of influx of T lymphocytes into pneumococcal-infected lungs of BALB/c and CBA/Ca was extended to the CD8<sup>+</sup> T cells subset (Figure 3.8). The number of CD8<sup>+</sup> T lymphocytes showed a significant increase in the lungs of both host strains, however with a greater rise in BALB/c ( $P < 0.001$ ) than in CBA/Ca mice ( $P < 0.05$ ) during the time course of the experiment (Figure 3.8-B). In the first 6 hours after infection the proportion of cytotoxic T cells in the lungs significantly rose and nearly doubled in the BALB/c mice ( $P < 0.01$  between 0 and 6 hrs p.i.) and with a substantial increase in CBA/Ca mice ( $P < 0.05$  between 0 and 6 hrs p.i.). In the CBA/Ca lungs, the number of CD8<sup>+</sup> T cells reached a plateau at 6 hours post-infection. However, changes in cell number were observed in BALB/c mice at 24 hours that were statistically different to CBA/Ca ( $P < 0.05$ ). When looking at changes during the course of the infection within each mouse strain, a highly significant increase ( $P < 0.001$ ) in the lungs of BALB/c mice and also a significant increase ( $P < 0.05$ ) in the number of cytotoxic T cells in the lungs of CBA/Ca mice. Intriguingly, this cell subset is well known for inducing apoptosis in cells infected by viruses or transformed in tumours, nevertheless, these results suggest a proactive role of the cytotoxic T lymphocytes during invasive bacterial infections. A role for concomitant exhausted T cells is not known (Williams & Bevan, 2006).

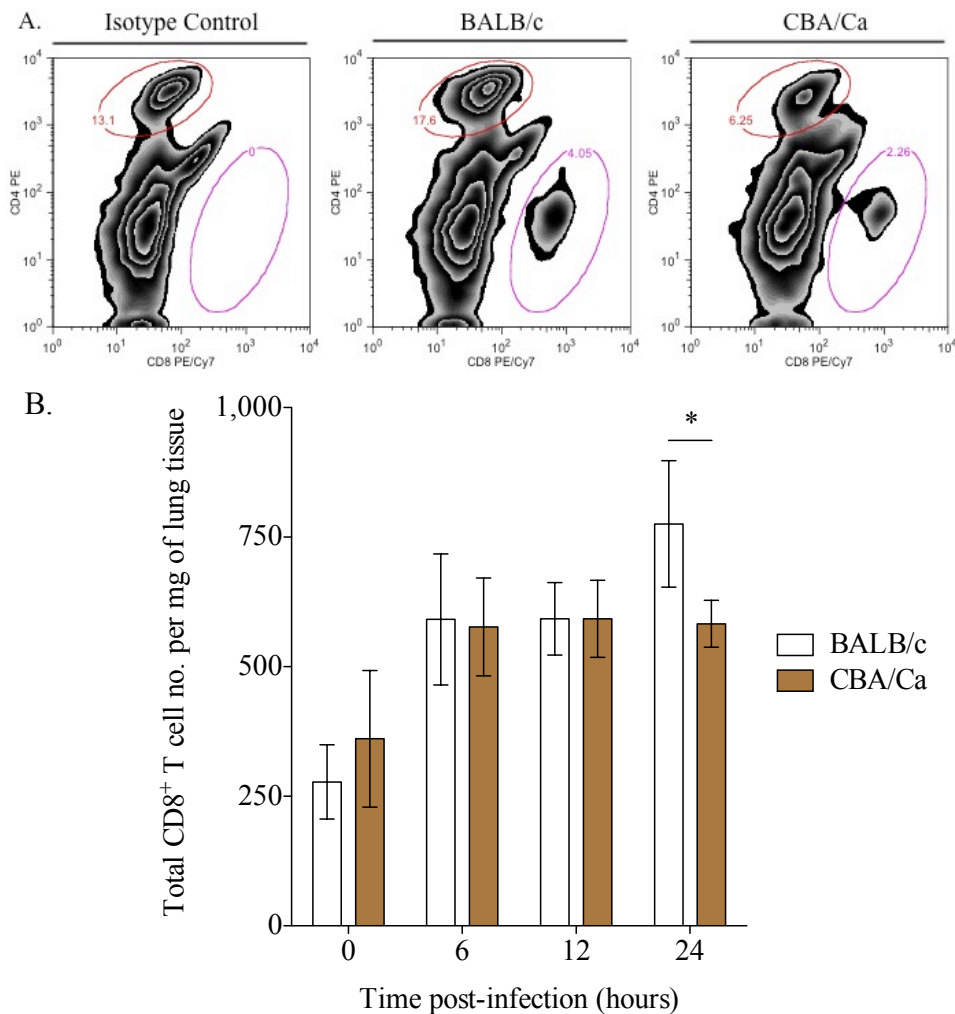


Figure 3.8 - Numbers of cytotoxic T cells in the lungs of BALB/c and CBA/Ca mice post-infection with *S. pneumoniae*. Mice were intranasally infected with 10<sup>6</sup> CFU and lungs were collected at 0, 6, 12 and 24 hours post-infection. (A) Flow cytometric analysis of CD8 T cells was determined by gating for CD45<sup>+</sup>, CD8<sup>+</sup> and CD4<sup>-</sup> events (example of a BALB/c and CBA/Ca 24 hour time point sample). (B) Number of cytotoxic T cells per mg of lung tissue, at the various time points, analysed by flow cytometry. Data represent the mean of positive events  $\pm$  SD. The p-value (\*,  $P < 0.05$ ) was obtained by two-way ANOVA followed by Bonferroni post-test. Data are representative of two independent experiments with  $> 4$  mice per group in each experiment.

An assessment of B lymphocyte cells in BALB/c and CBA/Ca lungs following pneumococcal pneumonia infection was performed (Figure 3.9). A significant influx of CD19<sup>+</sup> cells into the lungs of BALB/c ( $P < 0.001$  was observed during the time course of infection) but no significant changes in B cells influx into the lungs of CBA/Ca mice were observed ( $P > 0.05$  during the time course of infection) (Figure 3.9-B). By 24 hours post-infection, BALB/c mice showed a significant rise in B cell recruitment when compared to CBA/Ca ( $P < 0.001$ ).

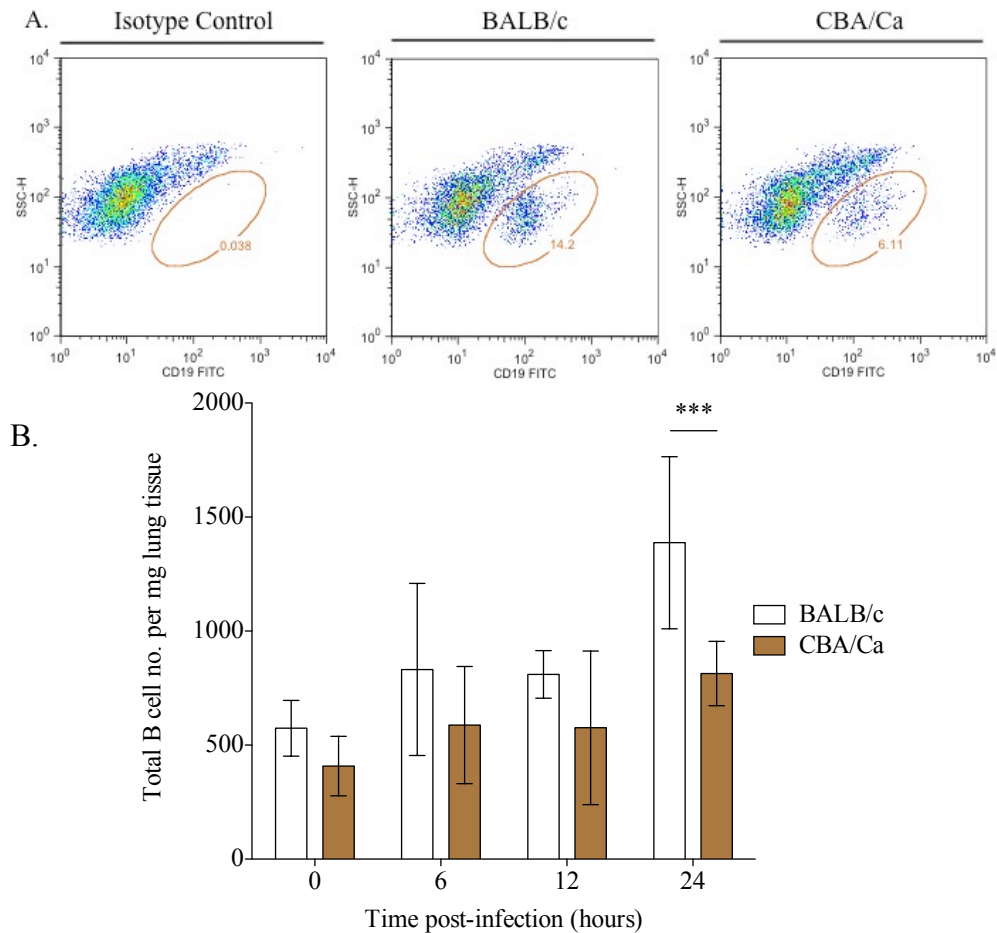


Figure 3.9 - Numbers of B cells in the lungs of BALB/c and CBA/Ca mice post-infection with *S. pneumoniae*. Mice were intranasally infected with 10<sup>6</sup> CFU and lungs were collected at 0, 6, 12 and 24 hours post-infection. (A) Flow cytometric analysis of B cells was determined by gating for CD45<sup>+</sup> and CD19<sup>+</sup> events (example of a BALB/c and CBA/Ca 24 hour time point sample). (B) Number of B cells per mg of lung tissue, at the various time points, analysed by flow cytometry. Data represent the mean of positive events  $\pm$  SD. The p-value (\*\*\*,  $P < 0.001$ ) was obtained by two-way ANOVA followed by Bonferroni post-test. Data are representative of two independent experiments with  $> 4$  mice per group in each experiment.

The numbers of mast cells in the lungs of BALB/c and CBA/Ca (Figure 3.10) were quantified, but as expected these cells were found in very low magnitude. The primary role of mast cells is to initiate an appropriate programme of inflammation and repair in response to tissue damage initiated against bacterial infection (Moiseeva & Bradding, 2011). It was observed that there was a low, but significant, presence in the BALB/c lungs occurred over the time course of infection ( $P < 0.05$ ), whereas the CBA/Ca mice no significant changes were observed during the period of experimentation ( $P > 0.05$ )

(Figure 3.10-B). There was a significant difference in numbers of mast cells between BALB/c and CBA/Ca at 24 hours post-infection ( $P < 0.05$ ).

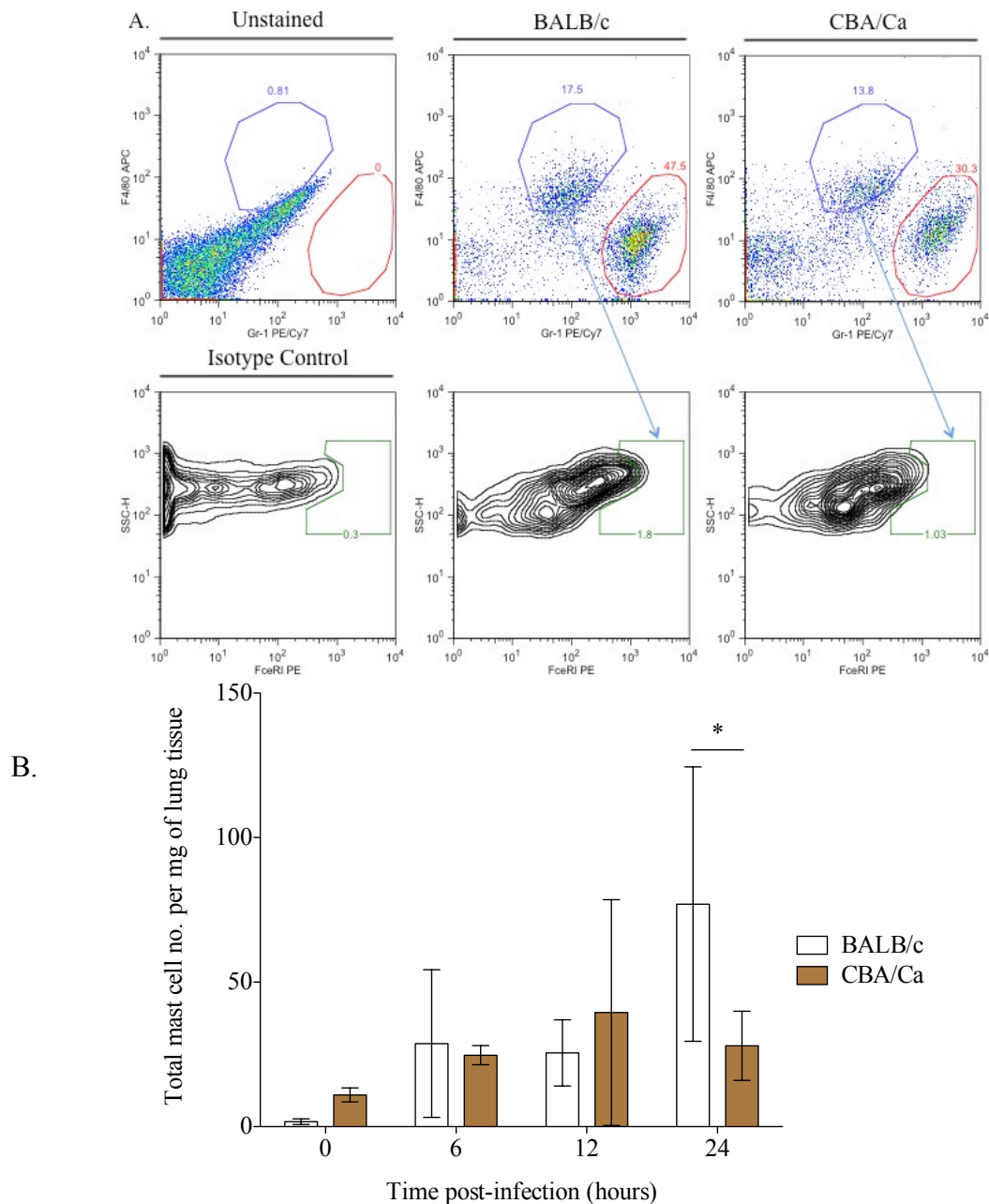


Figure 3.10 - Numbers of mast cells in the lungs of BALB/c and CBA/Ca mice post-infection with *S. pneumoniae*. Mice were intranasally infected with  $10^6$  CFU and lungs were collected at 0, 6, 12 and 24 hours post-infection. (A) Flow cytometric analysis of mast cells was determined by gating for CD45<sup>+</sup>, F4/80<sup>-</sup> and finally FcεRI<sup>+</sup> events (example of a BALB/c and CBA/Ca 24 hour time point sample). (B) Number of mast cells per mg of lung tissue, at the various time points, analysed by flow cytometry. Data represent the mean of positive events  $\pm$  SD. The p-value (\*,  $P < 0.05$ ) was obtained by two-way ANOVA followed by Bonferroni post-test. Data are representative of two independent experiments with  $> 4$  mice per group in each experiment.

Gamma delta T cells ( $\gamma\delta$  T cells), a T lymphocyte subset with a role in innate immunity (Born *et al.*, 2000), were analysed to assess for potential differences between a resistant and a susceptible host and to assess if the  $\gamma\delta$  T cells play a role during invasive pneumococcal disease (Figure 3.11). These cells are a source of IL-17 and IL17<sup>+</sup>  $\gamma\delta$  T cells and have been reported to have pathological and protective roles in inflammatory diseases (Sutton *et al.*, 2012). Therefore the phenotype of  $\gamma\delta$  T cells producing IL-17 cytokine was evaluated, following *S. pneumoniae* infection (Figure 3.12).

The analysis of  $\gamma\delta$  T cells was performed in lung tissue of BALB/c and CBA/Ca mice at 0 and 24 hours post-infection (Figure 3.11-B), showed differing cell numbers between strains at 24 hours post-infection. In the resistant strain a significant increase over time ( $P < 0.01$ ) was seen and, in contrast, the susceptible strain showed a significant decrease between the time points ( $P < 0.05$ ). By 24 hours post-challenge, a significantly higher number of  $\gamma\delta$  T cells in the lungs of BALB/c than in the CBA/Ca mice ( $P < 0.01$ ) was observed.

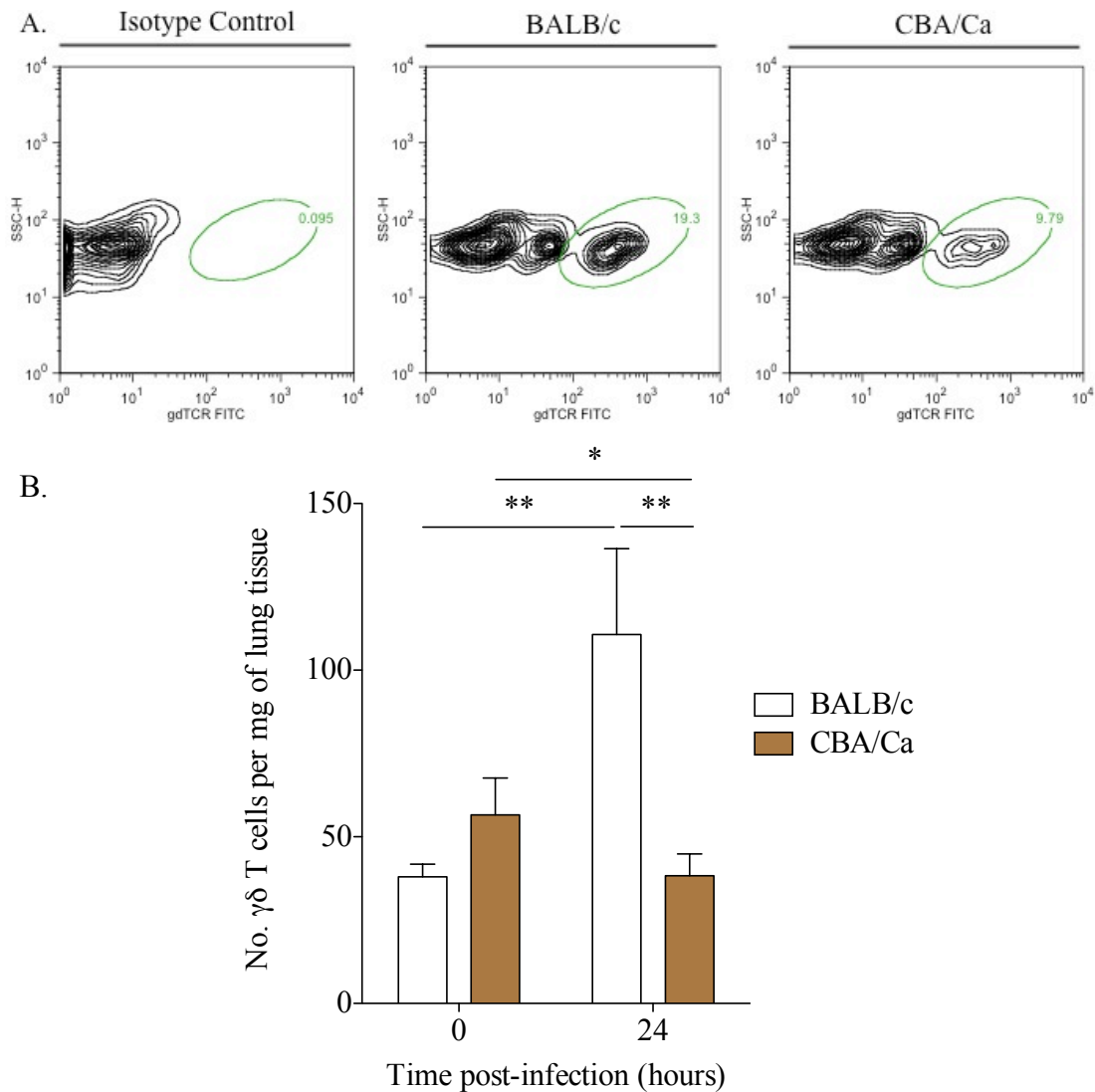


Figure 3.11 - Numbers of  $\gamma\delta$  T cells in the lungs of BALB/c and CBA/Ca mice post-infection with *S. pneumoniae*. Mice were intranasally infected with  $10^6$  CFU and lungs were collected at 0 and 24 hours post-infection. (A) Flow cytometric analysis of  $\gamma\delta$  T cells was determined by gating for  $CD45^+$  and finally  $\gamma\delta$  TCR $^+$  events (example of a BALB/c and CBA/Ca 24 hour time point sample). (B) Number of  $\gamma\delta$  T cells per mg of lung tissue was assessed, at 0 and 24 hours post-infection, and analysed by flow cytometry. Data represent the mean of positive events  $\pm$  SD. The p-values (\*,  $P < 0.05$  and \*\*,  $P < 0.01$ ) were obtained by one-way ANOVA. Data are representative of 2 experiments with 5 mice per strain and time point.

The numbers of  $\gamma\delta$  T cells producing IL-17 were quantified in the lungs of the two host strains during the course of infection (Figure 3.12-B). It was found that there were no significant changes in IL-17 $^+$   $\gamma\delta$  T cells in CBA/Ca lungs at 24 hours post-infection ( $P > 0.05$ ) compared to PBS sham-infected. However, in the BALB/c host there was a significant increase of IL-17-producing  $\gamma\delta$  T cells compared to PBS sham-infected ( $P < 0.01$ ) and to CBA/Ca at 24 hours after infection ( $P < 0.05$ ).

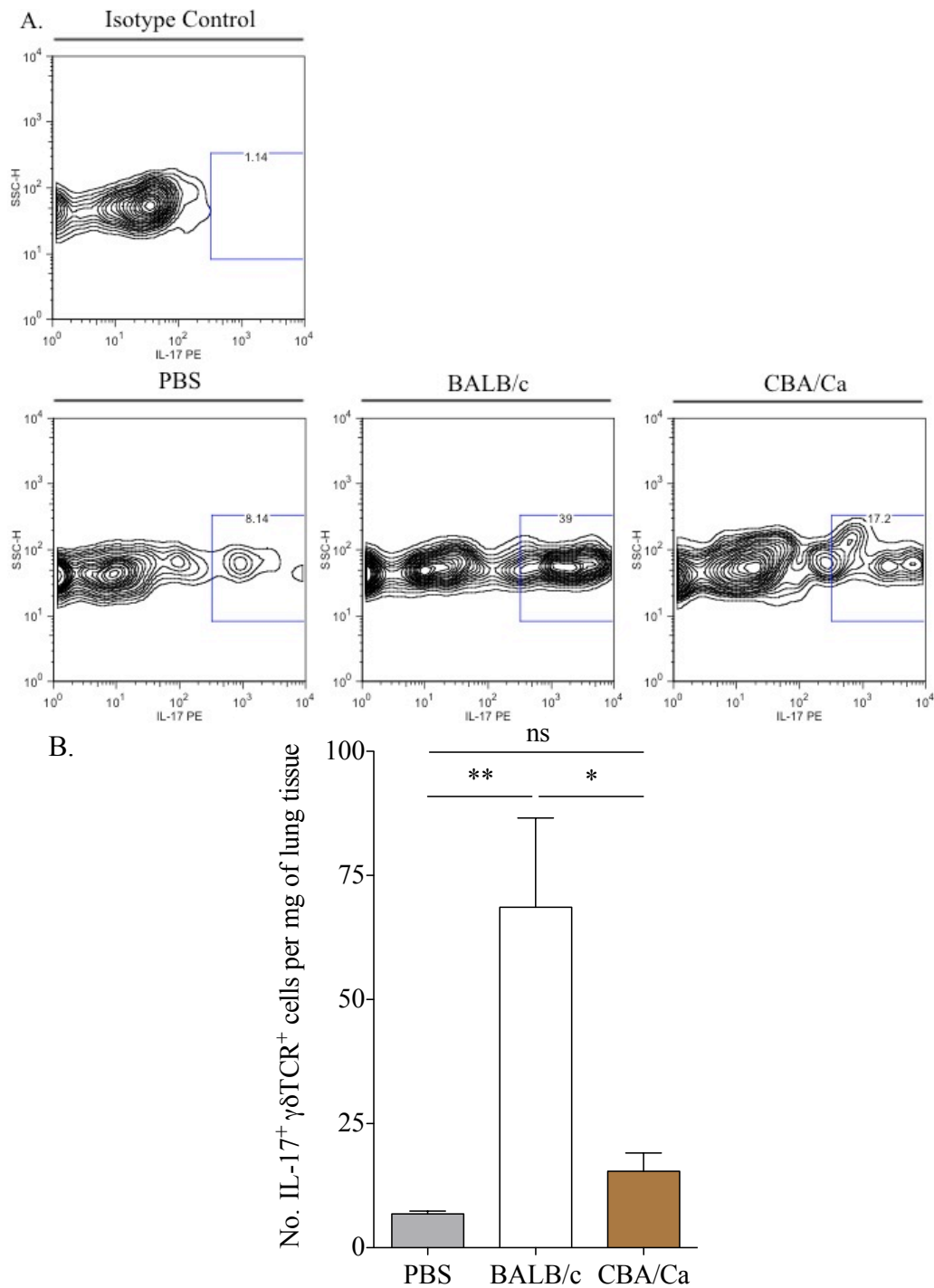


Figure 3.12 - Numbers of IL-17<sup>+</sup>  $\gamma\delta$  T cells in the lungs of BALB/c and CBA/Ca mice post-infection with *S. pneumoniae* and mock infection with PBS. Mice were intranasally infected with 10<sup>6</sup> CFU and lungs were collected at 0 and 24 hours post-infection. (A) Flow cytometric analysis of  $\gamma\delta$  T cells was determined by gating for CD45<sup>+</sup>,  $\gamma\delta$  TCR<sup>+</sup> and finally IL-17<sup>+</sup> events (example of a BALB/c and CBA/Ca 24 hour time point sample). (B) Number of IL-17<sup>+</sup>  $\gamma\delta$  T cells per mg of lung tissue was assessed, at 0 and 24 hours post-infection, and analysed by flow cytometry. Data represent the mean of positive events  $\pm$  SD. The p-values (\*,  $P < 0.05$  and \*\*,  $P < 0.01$ ) were obtained by one-way ANOVA. Data are representative of 2 experiments with 5 mice per strain and time point.

In Figure 3.13, described in more detail in section 5.3.2 (Figure 5.12), it was interestingly observed that in infected-BALB/c mice most of the IL-17 was produced by  $\gamma\delta$  T cells (~80%), but not in the infected-CBA/Ca mice (~20%) (Figure 3.12). At 24 hours post-infection, from the IL-17 produced in the CBA/Ca lungs only approximately a quarter of the total of this cytokine came from  $\gamma\delta$  T cells (~15 cell out of ~70 IL-17-producing cells per mg lung tissue), indicating that  $T_h17$  cells might produce the remaining cytokine (~55 IL-17-producing cells per mg lung tissue). Overall, the amount of IL-17-producing cells was little (very low number when compared to the number of IL-10-producing cells per mg of lung tissue, represented in Figure 3.18) and showed no significant differences between pneumococcal-infected BALB/c and CBA/Ca mice ( $P > 0.05$ ) (Figure 3.14-B).

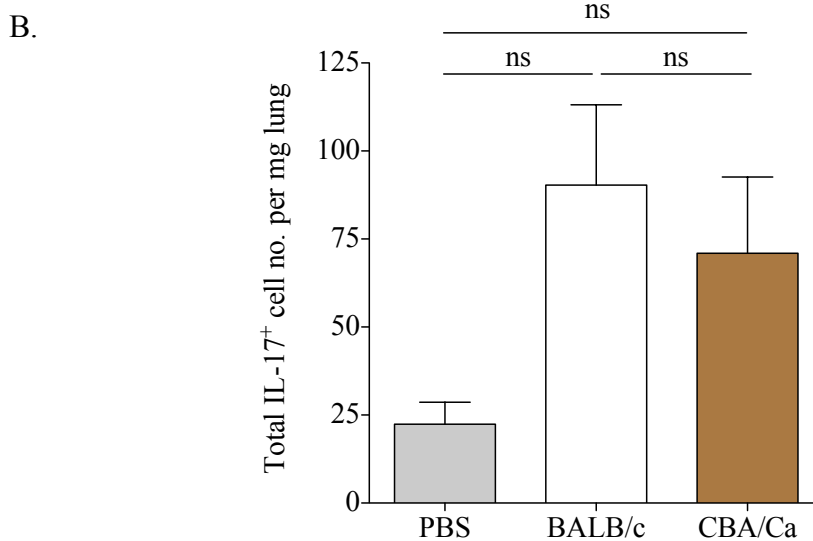
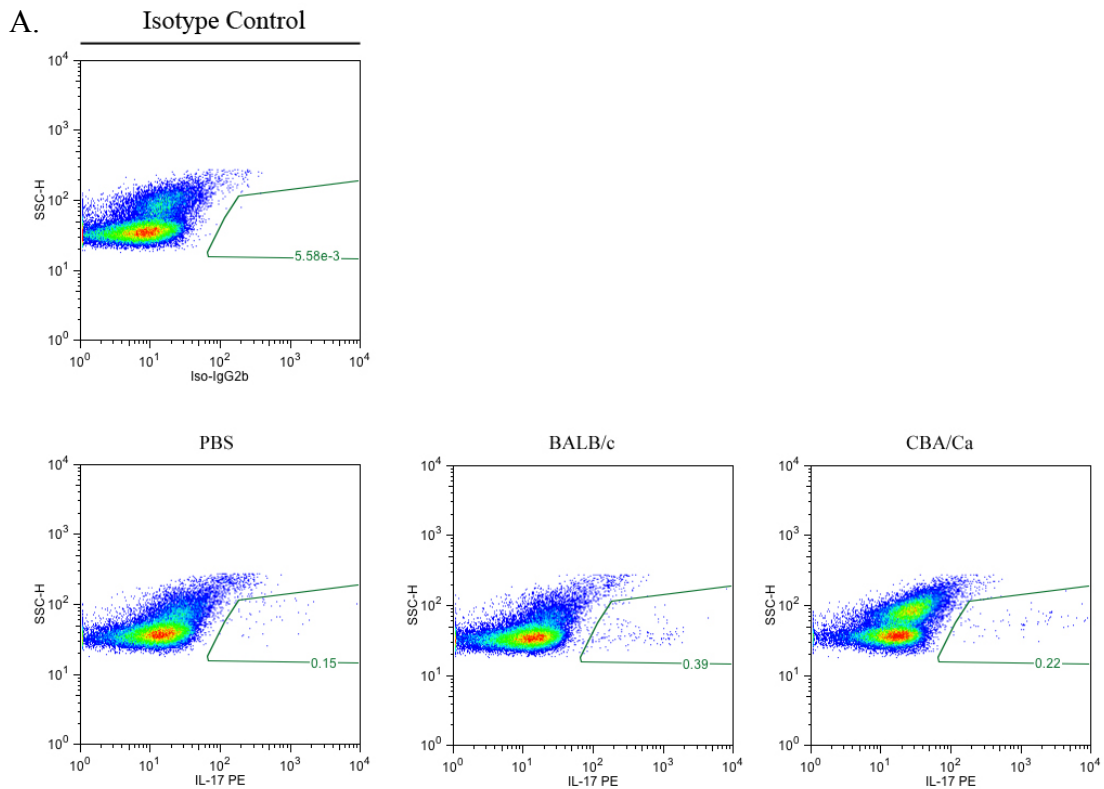


Figure 3.13 - Numbers of IL-17<sup>+</sup> cells in the lungs of BALB/c and CBA/Ca mice post-infection with *S. pneumoniae* and mock infection with PBS. BALB/c and CBA/Ca mice were intranasally-infected with wild-type D39 or PBS as a control. PBS group contains BALB/c and CBA/Ca animals. (A) Flow cytometric analysis of IL-17<sup>+</sup> cells was determined by gating for CD45<sup>+</sup>, IL-17<sup>+</sup> events (example of a BALB/c and CBA/Ca 24 hour time point sample). (B) Number of IL-17<sup>+</sup> cells per mg of lung tissue, at the various time points, analysed by flow cytometry. Data represent the mean of positive events  $\pm$  SD and the data was analysed by one-way ANOVA. Data are representative of two independent experiments with > 4 mice per group in each experiment.

Natural killer (NK) cells play important roles in the innate immune system, by recognizing a variety of “stressed cells” in the absence or in the presence of antibodies, resulting in a quick immune reaction (Vivier *et al.*, 2011). During the inflammation process, this cytotoxic lymphocyte is biased to produce IFN- $\gamma$ , and subsequently induces cell apoptosis (Ross & Caligiuri, 1997). As part of the phenotyping of innate immune responses to pneumococcal pneumonia in a resistant (BALB/c) and a susceptible host (CBA/Ca), NK cell numbers were evaluated (Figure 3.14), as well as leukocyte-producing interferon-gamma (Figure 3.15) and IFN- $\gamma^+$  NK cells (Figure 3.16). Additionally, the number of IFN- $\gamma^+$  T cells was assessed (Figure 3.17), remaining to determine the amount of NK T cells and cytotoxic T cells producing IFN- $\gamma$ . In this study a significant boost of NK cells in the lungs of BALB/c mice was observed ( $P < 0.01$ , when compared to PBS sham-infected), which was more pronounced in the CBA/Ca mice ( $P < 0.001$ ) (Figure 3.14-B). At 24 hours post-infection, the numbers of NK cells between host strains were not significantly different ( $P > 0.05$ ).

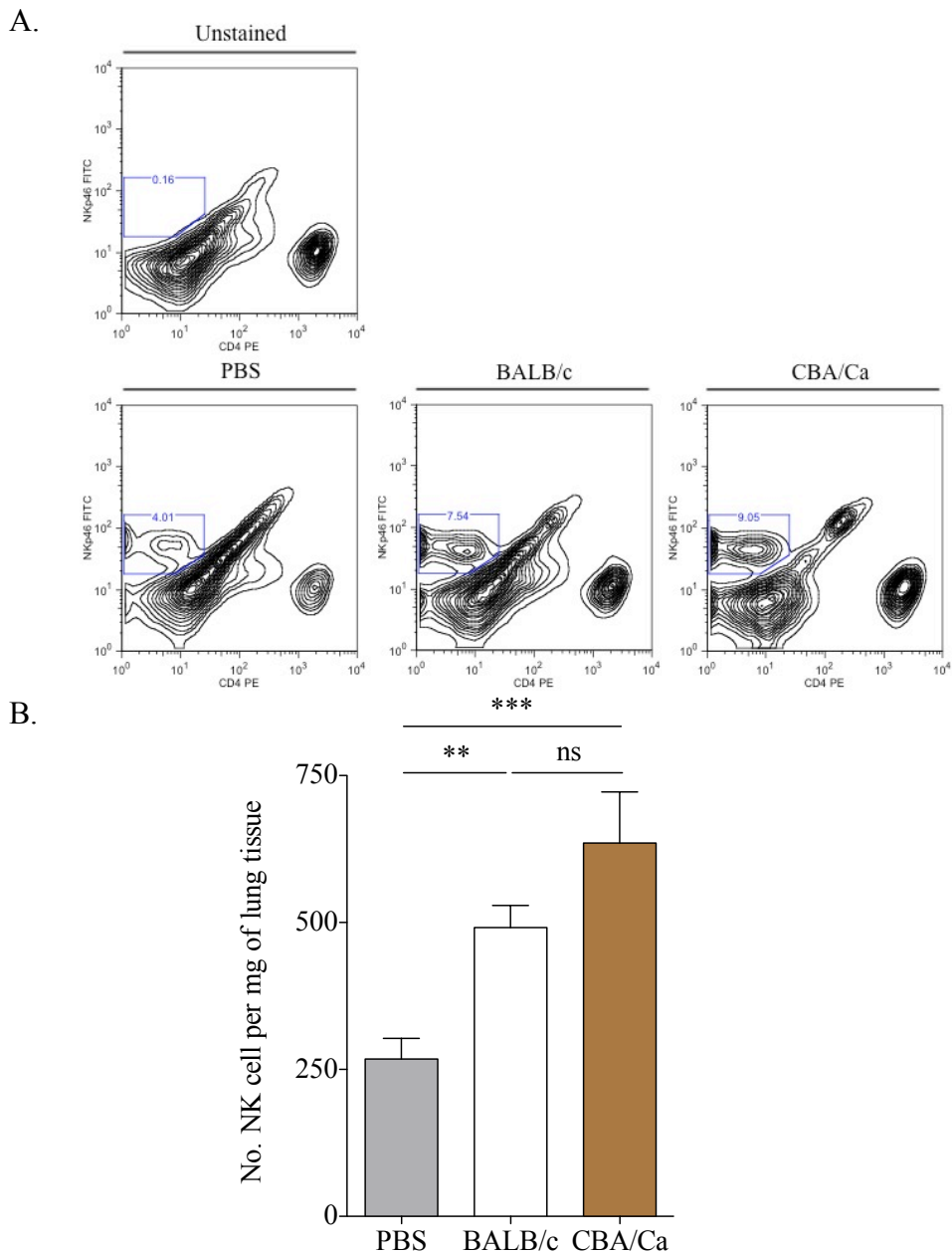


Figure 3.14 - Numbers of NK cells in the lungs of BALB/c and CBA/Ca mice post-infection with *S. pneumoniae* and mock infection with PBS. (A) Flow cytometric analysis of NK cells was determined by gating for CD45<sup>+</sup> NKp46<sup>hi</sup> CD4<sup>lo</sup> events (example of a BALB/c and CBA/Ca 24 hour time point sample). (B) Number of NK cells per mg of lung tissue was assessed, at 0 and 24 hours post-infection, and analysed by flow cytometry. Data represent the mean of positive events  $\pm$  SD. The p-values (\*\*,  $P < 0.01$  and \*\*\*,  $P < 0.001$ ) were obtained by one-way ANOVA. Data are representative of 2 experiments with 5 mice per strain and time point.

When examining the total leukocytes producing IFN- $\gamma$  in the lungs of the two mouse strains (Figure 3.15-B), a slight but significant increase in the number of IFN- $\gamma$ <sup>+</sup> CD45<sup>+</sup> cells in BALB/c host was found ( $P < 0.05$ , between PBS sham-infected and 24 hrs p.i. BALB/c). This also was the case in infected-CBA/Ca mice ( $P < 0.001$ , between PBS sham-infected and 24 hrs p.i. CBA/Ca). When comparing BALB/c and CBA/Ca mice at

24 hours p.i., it was evident that CBA/Ca lungs had significantly more IFN- $\gamma^+$  leukocyte cells than BALB/c mice ( $P < 0.001$  at 24 hrs p.i.).

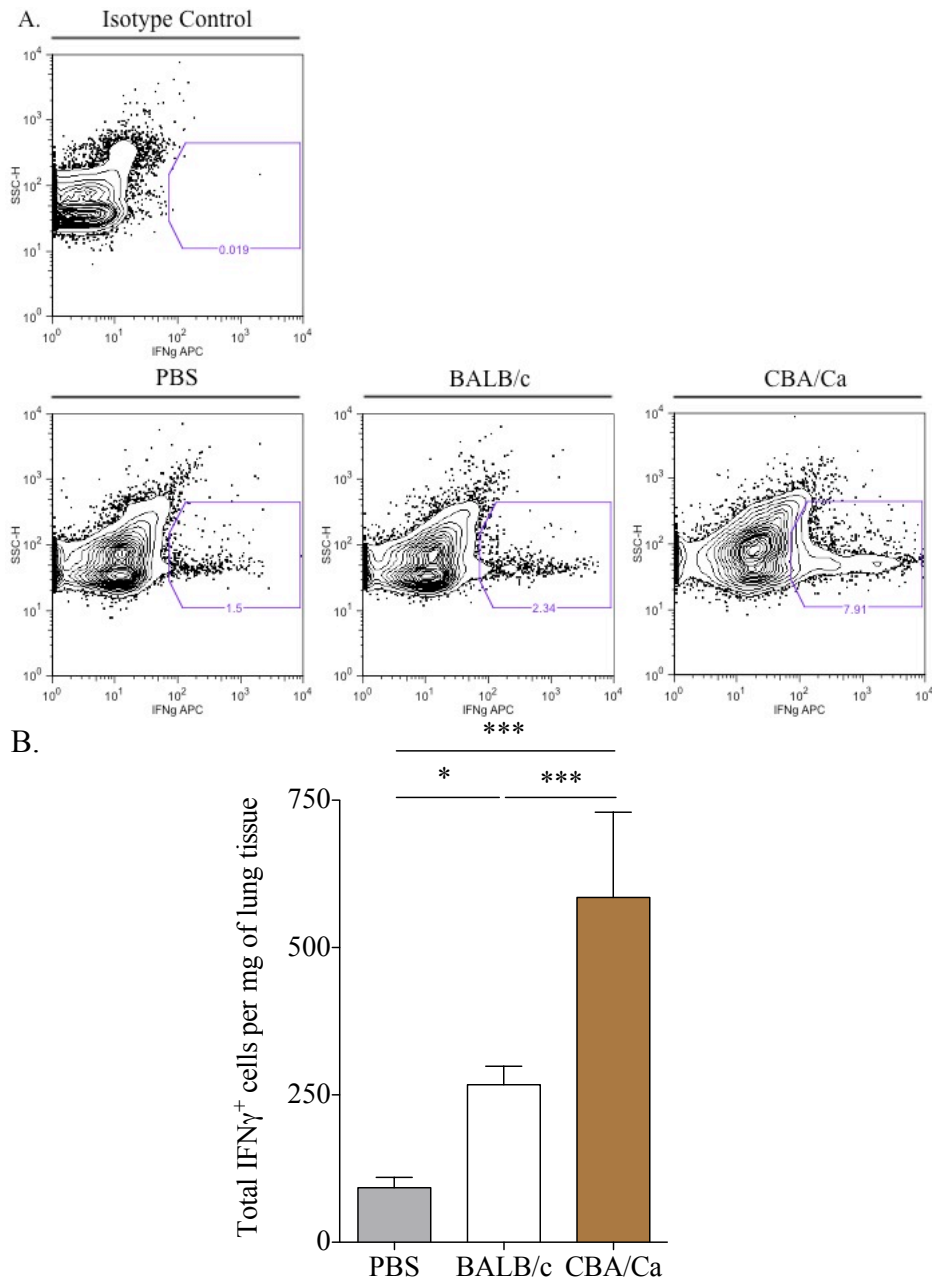


Figure 3.15 - Numbers of IFN- $\gamma^+$  NK cells in the lungs of BALB/c and CBA/Ca mice post-infection with *S. pneumoniae* and mock infection with PBS. Mice were intranasally infected with  $10^6$  CFU and lungs were collected at 24 hours post-infection. The PBS group contained BALB/c mice sham infected with PBS. (A) Flow cytometric analysis of IFN- $\gamma^+$  NK cells was determined by gating CD45 $^+$  NKp46 $^{\text{hi}}$  CD4 $^{\text{lo}}$  and finally IFN- $\gamma^+$  events (example of a BALB/c and CBA/Ca 24 hour time point sample). (B) Numbers of IFN- $\gamma^+$  NK cells per mg of lung tissue, at 24 hours post-infection, analysed by flow cytometry. Data represent the mean of positive events  $\pm$  SD. The p-values (\*,  $P < 0.05$  and \*\*\*,  $P < 0.001$ ) were obtained by one-way ANOVA. Data are representative of 2 experiments with 5 mice per strain and time point.

The data in Figure 3.16 have been described in more detail in section 5.3.3 (Figure 5.13-A and Figure 5.13-B), but are highlighted here to show the contribution of the different cell subsets in the production and release of IFN- $\gamma$  during pneumococcal infection. In fact, it was observed that the majority of this cytokine production, approximately 50-60% of the IFN- $\gamma$ -producing cells (Figure 3.15-B), was performed by NK cells (Figure 3.16-B); another 10% was produced by T cells (Figure 3.17-B) and the remaining 30-40% of IFN- $\gamma$ -producing cells could not be determined, but could be NK T cells and/or cytotoxic T cells (Schoenborn & Wilson, 2007).

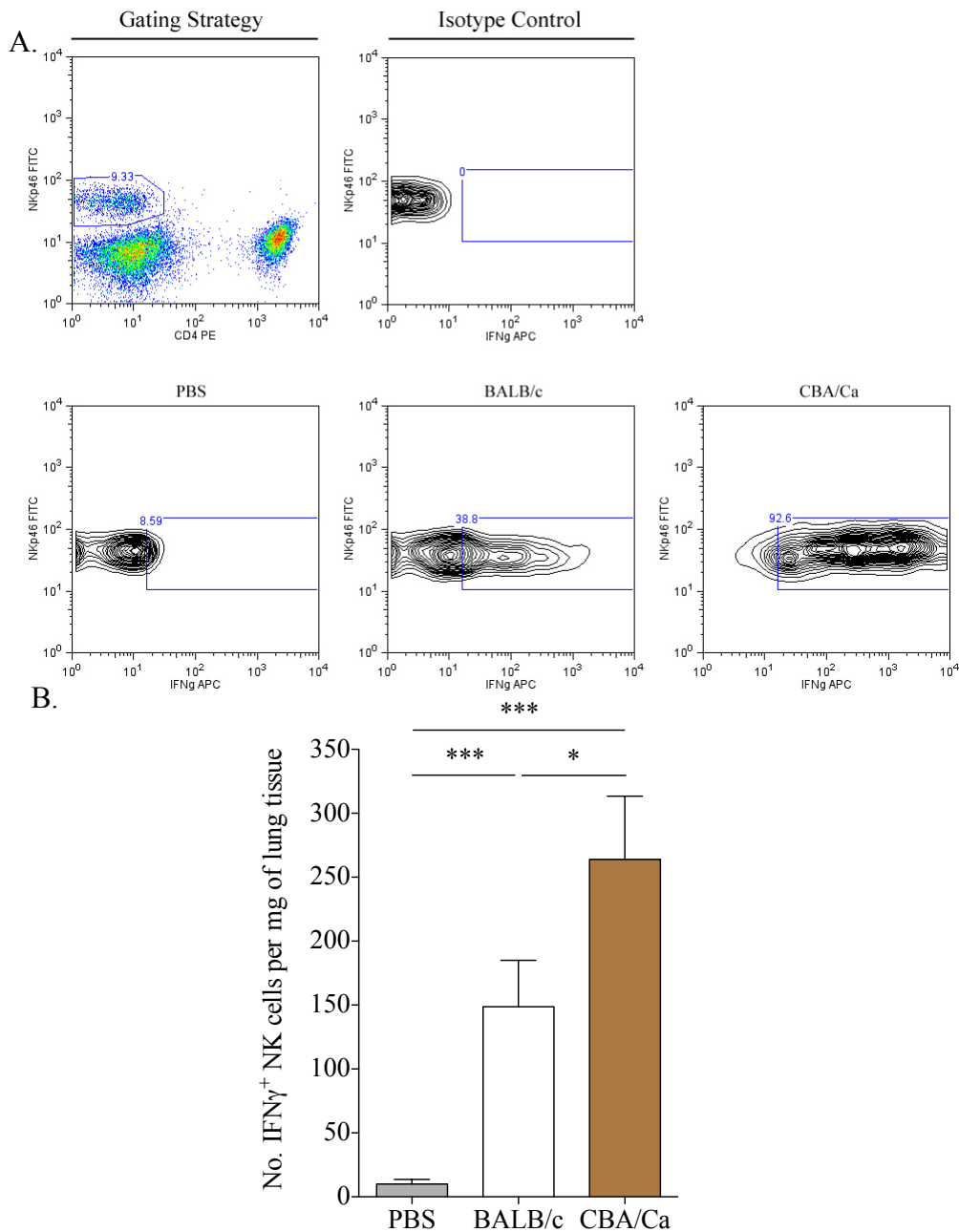


Figure 3.16 - Numbers of IFN- $\gamma$ <sup>+</sup> NK cells in the lungs of BALB/c and CBA/Ca mice post-infection with *S. pneumoniae* and mock infection with PBS. Mice were intranasally infected with 10<sup>6</sup> CFU and lungs were collected at 24 hours post-infection. The PBS group contained BALB/c mice sham infected with PBS. (A) Flow cytometric analysis of IFN- $\gamma$ <sup>+</sup> NK cells was determined by gating CD45<sup>+</sup> NKp46<sup>hi</sup> CD4<sup>lo</sup> and finally IFN- $\gamma$ <sup>+</sup> events (example of a BALB/c and CBA/Ca 24 hour time point sample) (data shown in Figure 5.13-A). (B) Numbers of IFN- $\gamma$ <sup>+</sup> NK cells per mg of lung tissue, at 24 hours post-infection, analysed by flow cytometry (data shown in Figure 5.13-B). Data represent the mean of positive events  $\pm$  SD. The p-values (\*,  $P < 0.05$  and \*\*\*,  $P < 0.001$ ) were obtained by one-way ANOVA. Data are representative of 2 experiments with 5 mice per strain and time point.

The number of T cells producing IFN- $\gamma$  in the lungs of BALB/c and CBA/Ca mice was very low (Figure 3.17). After pneumococcal infection a significant increase in the number of CD4<sup>+</sup> T cells producing IFN- $\gamma$  in both strains ( $P < 0.05$  between PBS

sham-infected and BALB/c at 24 hrs p.i.;  $P < 0.01$  between PBS sham-infected and CBA/Ca at 24 hrs p.i.) was observed. By 24 hours post-infection, the number of IFN- $\gamma$ -producing T cells was not significantly different between host strains ( $P > 0.05$ ).

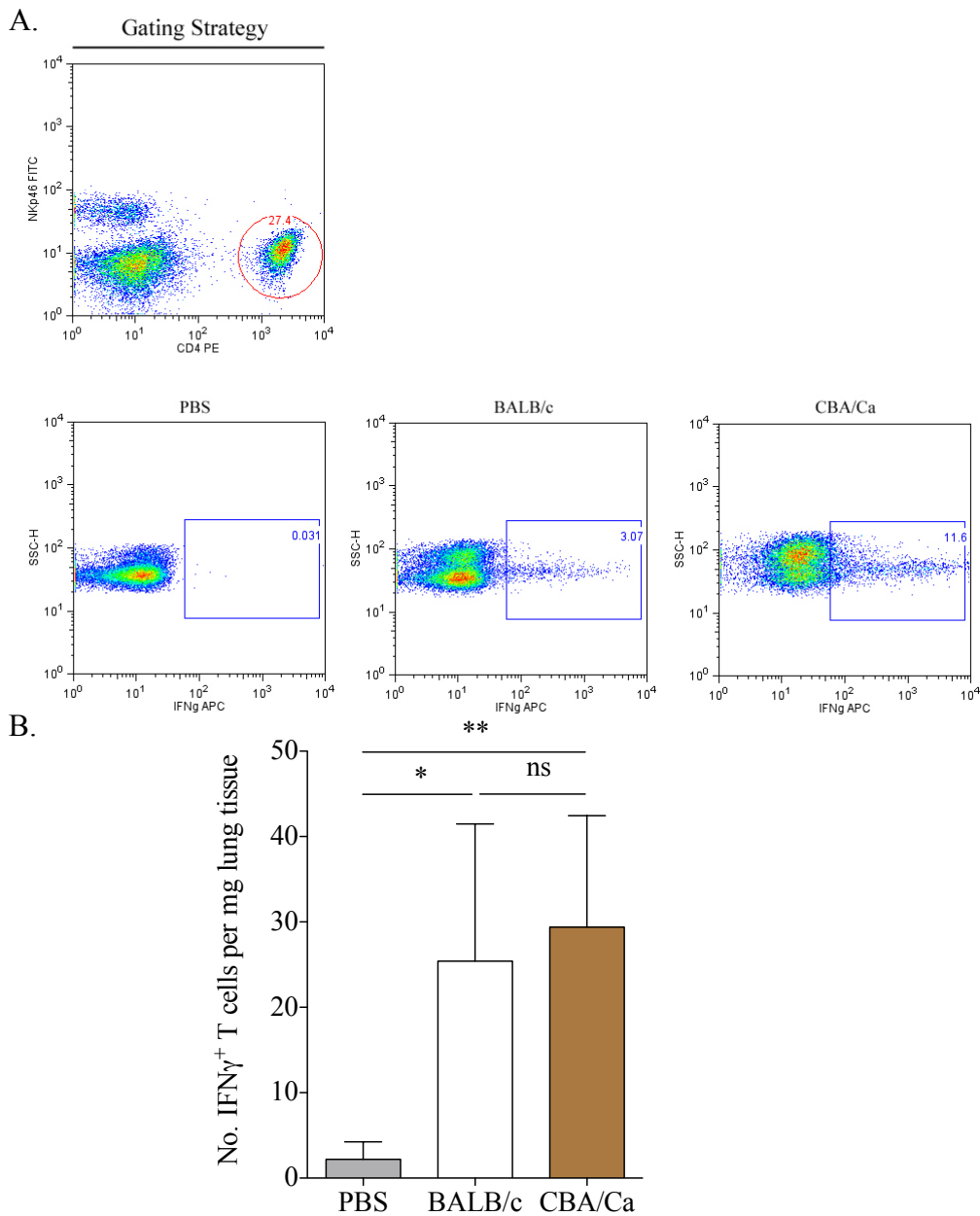


Figure 3.17 - Numbers of T cells expressing IFN- $\gamma$  in the lungs of BALB/c and CBA/Ca mice post-infection with *S. pneumoniae* and mock infection with PBS. Mice were intranasally infected with  $10^6$  CFU and lungs were collected at 24 hours post-infection. The PBS group contained BALB/c mice sham infected with PBS. (A) Flow cytometric analysis of IFN- $\gamma^+$  T cells was determined by gating CD45 $^+$  CD4 $^+$  and finally IFN- $\gamma^+$  events (example of a BALB/c and CBA/Ca 24 hour time point sample). (B) Number of IFN- $\gamma^+$  cells per mg of lung tissue, at 24 hours post-infection, analysed by flow cytometry. Data represent the mean of positive events  $\pm$  SD. The p-values (\*,  $P < 0.05$  and \*\*,  $P < 0.01$ ) were obtained by one-way ANOVA. Data are representative of 2 experiments with 5 mice per strain and time point.

As part of the immunophenotyping of BALB/c and CBA/Ca lungs during pneumococcal pneumonia, IL-10-producing cells were analysed (Figure 3.18). The number of IL-10<sup>+</sup> leukocyte cells significantly increased both in BALB/c ( $P < 0.001$  between PBS sham-infected and BALB/c at 24 hrs p.i.) and CBA/Ca lungs ( $P < 0.05$  between PBS sham-infected and CBA/Ca at 24 hrs p.i.) following *S. pneumoniae* infection. Remarkably, at 24 hours post-infection, the number of IL-10-producing cells expanded to a significantly greater extent in the BALB/c lungs than in the CBA/Ca lungs ( $P < 0.001$ ).

Studies of T regulatory cells (T<sub>regs</sub>) and their immunosuppressive role associated with IL-10 cytokine production are described in more detail in Chapter 5. Nevertheless, now the T<sub>regs</sub> were emphasised as a component of the innate immune response of BALB/c and CBA/Ca mice to IPD. T<sub>regs</sub> express the protein Foxp3 (transcription factor) during the development and functioning of this immunoregulatory cell subset (Mellor & Munn, 2011), which was used to quantify T<sub>regs</sub> cells by flow cytometry. T<sub>regs</sub> cells were shown to produce IL-10 cytokine during the inflammatory process, as evidenced in Figure 3.19. Following pneumococcal infection, the number of IL-10<sup>+</sup> T<sub>regs</sub> showed a significantly higher increase in BALB/c ( $P < 0.01$  between PBS sham-infected and BALB/c at 24 hrs p.i.) when compared to CBA/Ca lungs ( $P < 0.05$  between PBS sham-infected and CBA/Ca at 24 hrs p.i.). Significant differences in the number of IL-10<sup>+</sup> Foxp3<sup>+</sup> T cells (also known as IL-10 producing T<sub>regs</sub> cells) between infected mouse strains were observed, with the resistant host showing greater number of T<sub>regs</sub> producing IL-10 when compared with the susceptible host ( $P < 0.05$  between BALB/c and CBA/Ca at 24 hrs p.i.). Finally, approximately 75% of the IL-10-producing cells in infected-BALB/c lungs were T regulatory cells (Figure 3.21-B), which was a clear sign that a regulative response triggered in the resistant host strain to acute pneumonia.

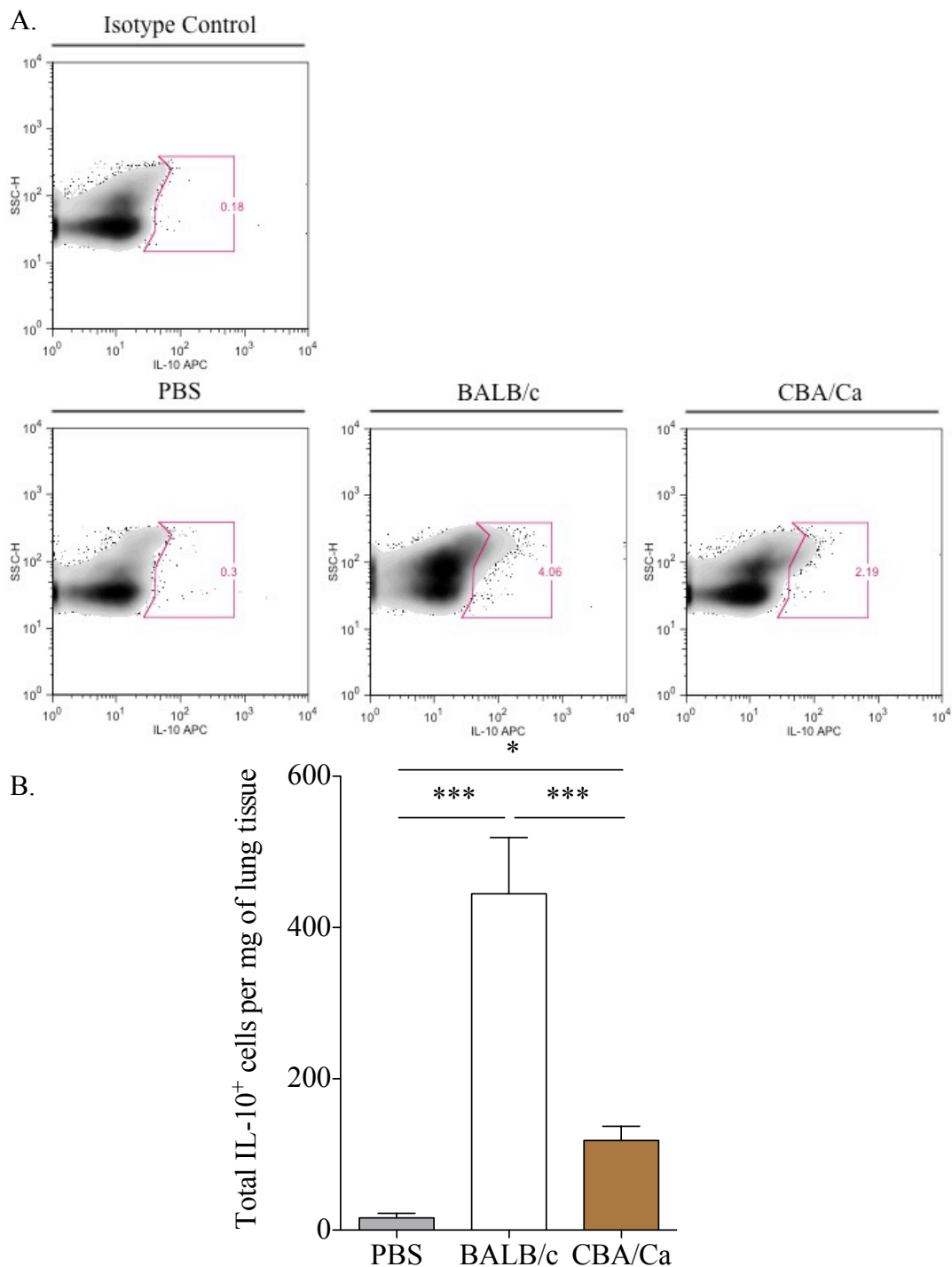


Figure 3.18 - Numbers of IL-10 expressing cells in the lungs of BALB/c and CBA/Ca mice post-infection with *S. pneumoniae* and mock infection with PBS. Mice were intranasally infected with  $10^6$  CFU and lungs were collected at 24 hours post-infection. The PBS group contained BALB/c mice sham infected with PBS. (A) Flow cytometric analysis of IL-10<sup>+</sup> cells was determined by gating CD45<sup>+</sup> and IL-10<sup>hi</sup> events (example of a BALB/c and CBA/Ca 24 hour time point sample). (B) Numbers of IL-10<sup>+</sup> cells per mg of lung tissue, at 24 hours post-infection, analysed by flow cytometry. Data represent the mean of positive events  $\pm$  SD. The p-value (\*,  $P < 0.05$  and \*\*\*,  $P < 0.001$ ) was obtained by one-way ANOVA. Data are representative of 2 experiments with 5 mice per strain and time point.

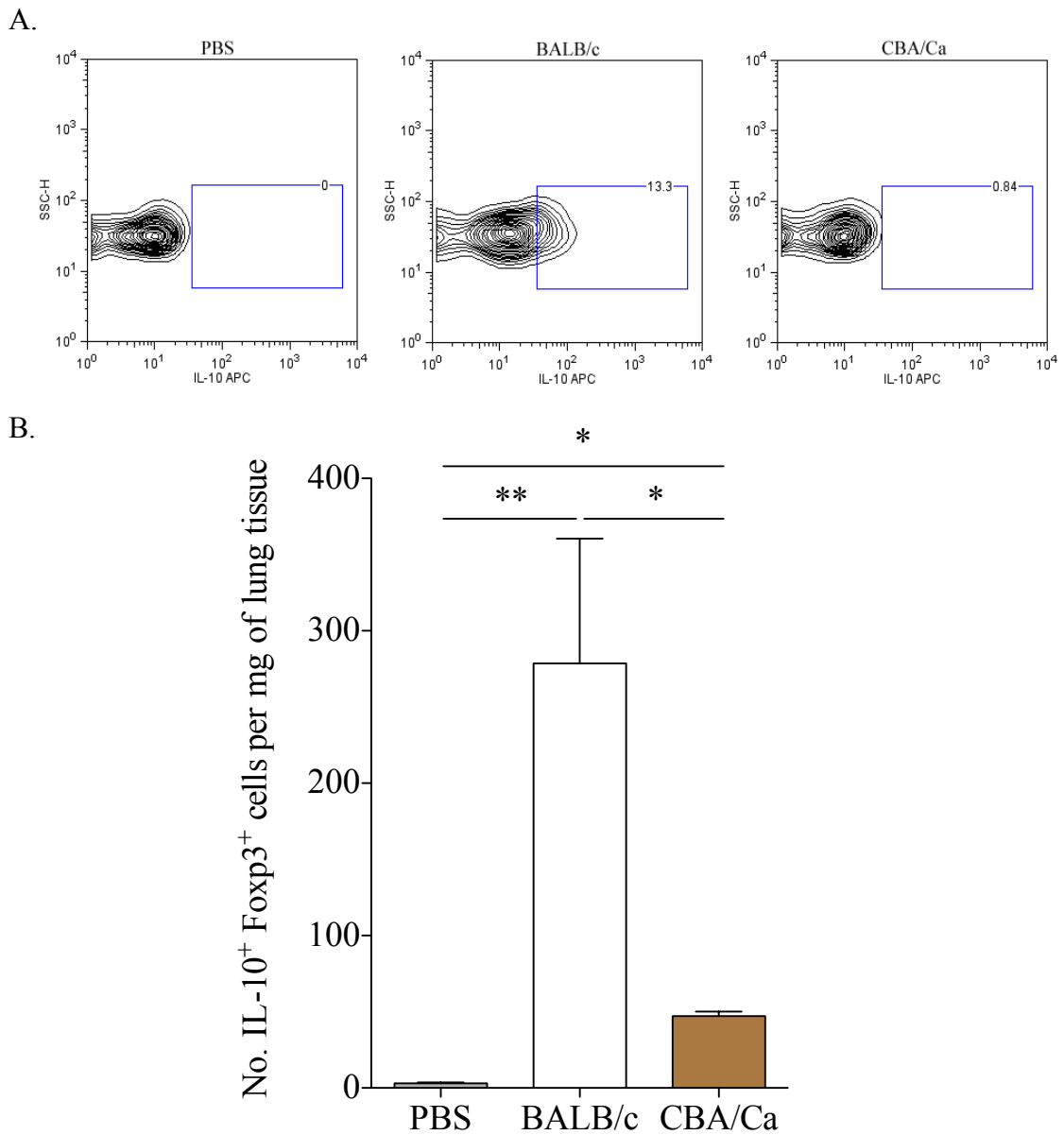


Figure 3.19 - Numbers of IL-10<sup>+</sup> T regulatory cells in the lungs of BALB/c and CBA/Ca mice post-infection with *S. pneumoniae* and mock infection with PBS. Mice were intranasally infected with 10<sup>6</sup> CFU and lungs were collected at 24 hours post-infection. The PBS group contained BALB/c mice sham infected with PBS. (A) Flow cytometric analysis of IL-10<sup>+</sup> Foxp3<sup>+</sup> cells was determined by gating CD45<sup>+</sup>, CD4<sup>+</sup>, Foxp3<sup>+</sup> and finally IL-10<sup>+</sup> events (example of a BALB/c and CBA/Ca 24 hour time point sample) (data shown in Figure 5.8-A). (B) Number of IL-10<sup>+</sup> Foxp3<sup>+</sup> cells per mg of lung tissue, at 24 hours post-infection, analysed by flow cytometry (data shown in Figure 5.8-B). Data represent the mean of positive events  $\pm$  SEM. The p-values (\*,  $P < 0.05$ ; \*\*,  $P < 0.01$ ) were obtained by two-way ANOVA followed by Bonferroni post-test. Data are representative of 2 experiments with  $\geq 4$  mice per strain and time point.

Marker and cell target	24 hr p.i.
CD45 <sup>+</sup> cells (hematopoietic cells)	B > C ( <i>P</i> < 0.001)
Gr-1 <sup>+</sup> cells (neutrophil cells)	B > C ( <i>P</i> < 0.001)
F4/80 <sup>+</sup> cells (macrophage cells)	B > C ( <i>P</i> < 0.05)
CD4 <sup>+</sup> cells (T <sub>helper</sub> cells)	B > C ( <i>P</i> < 0.001)
CD8 <sup>+</sup> cells (cytotoxic T cells)	B > C ( <i>P</i> < 0.05)
CD19 <sup>+</sup> cells (B cells)	B > C ( <i>P</i> < 0.001)
FcεRI <sup>+</sup> cells (mast cells)	B > C ( <i>P</i> < 0.05)
γδ TCR <sup>+</sup> cells (γδ T cells)	B > C ( <i>P</i> < 0.01)
NKp46 <sup>+</sup> cells (NK cells)	-

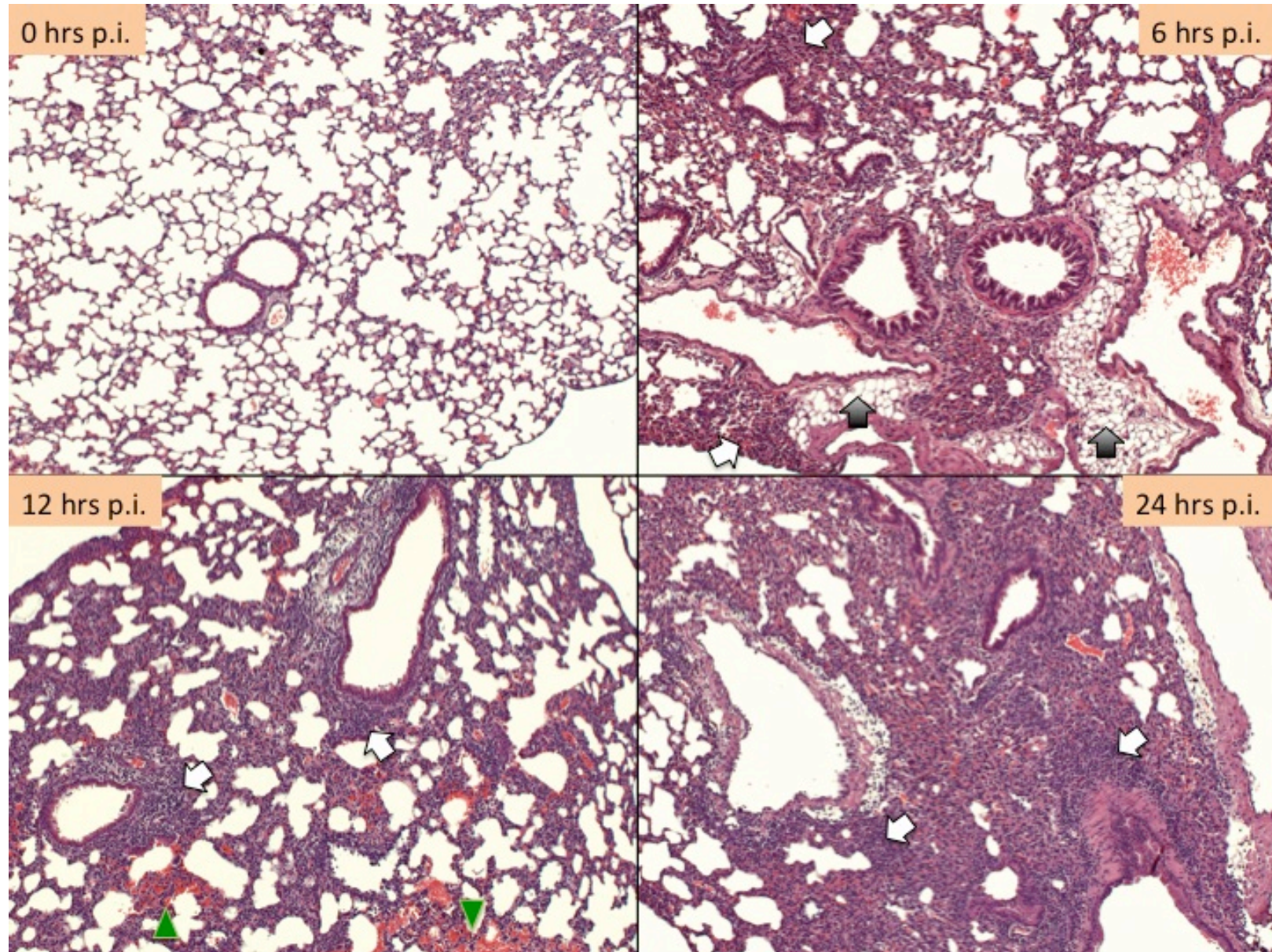
Table 3.1 - Statistical differences between BALB/c and CBA/Ca mice in the lung cellular recruitment at 24 hours post-infection. P-values result from two-way ANOVA analysis followed by Bonferroni post-test. “B” for BALB/c, “C” for CBA/Ca and “-” for no significant differences between strains at the time point.

Following the lung immunophenotyping of BALB/c and CBA/Ca mice during the progression of pneumococcal infection, lung paraffin sections, were scored the level of cellular infiltration and histopathological manifestations of pulmonary pneumococcal infection were examined (Figure 3.20). Histological analysis of lung tissue sections from BALB/c and CBA/Ca mice infected with wild-type pneumococci (Figure 3.20), showed comparable cellular infiltration between strains, but distinct signs of inflammation. The analysis of the lung sections from both host strains indicated a significant leukocyte increase (cells stained in purple with hematoxylin and eosin staining) and hyperplasia (observed the increase of lung size and weight) over the course of infection in both strains (Figure 3.20). The levels of cellular recruitment (Figure 3.21) also were scored and they showed a significant increment of leukocyte cells in the lungs of BALB/c (*P* < 0.001) and CBA/Ca (*P* < 0.001) over the time points post-infection. A quicker cellular recruitment in BALB/c lungs was observed (Figure 3.20-A), with a significant increase evident at 6 hours post-infection (*P* < 0.05 between 0 and 6 hrs p.i. in the BALB/c mice). This was not observed in the CBA/Ca mice at this time point (*P* < 0.01 between BALB/c and CBA/Ca at 6 hrs p.i.) (Figure 3.20-B). At 12 hours post-infection, both strains had increased levels of cellular infiltration (*P* < 0.001 between 0 and 12 hrs p.i.), but BALB/c showed significantly greater leukocyte recruitment than CBA/Ca (*P* < 0.01), reaching a cellular infiltration peak, and maintaining these leukocyte levels throughout the following time period (24 hrs p.i.).

By 24 hours post-infection, the levels of leukocytes in CBA/Ca lungs (Figure 3.20-B) reached a peak and attained the levels found in BALB/c lungs (Figure 3.20-A). At this time there were no significant differences in recruitment levels between the two strains ( $P > 0.05$ ).

The examination of the lung sections showed remarkable observations that characterise the two strains. At 24 hours post-infection, all the inspected sections from the susceptible CBA/Ca mice evidenced signs of inflammation (Figure 3.20-B), rarely seen in the resistant BALB/c lung sections (Figure 3.20-A). In Figure 3.20-B (24 hrs sample picture from CBA/Ca lungs), signs of inflammation and tissue injuries can be observed around the bronchioles and perivascular areas. Inflammation presented itself as extensive deposition of cells around the bronchioles, as well as intensive peribronchial and intraalveolar fluid. Interestingly, in the susceptible strain, a substantial swelling of the bronchioles wall thickness and a severe narrowing of their diameter was observed (Figure 3.20-B), correlating with the shortness of breath observed when the animals were lethargic.

A.



B.

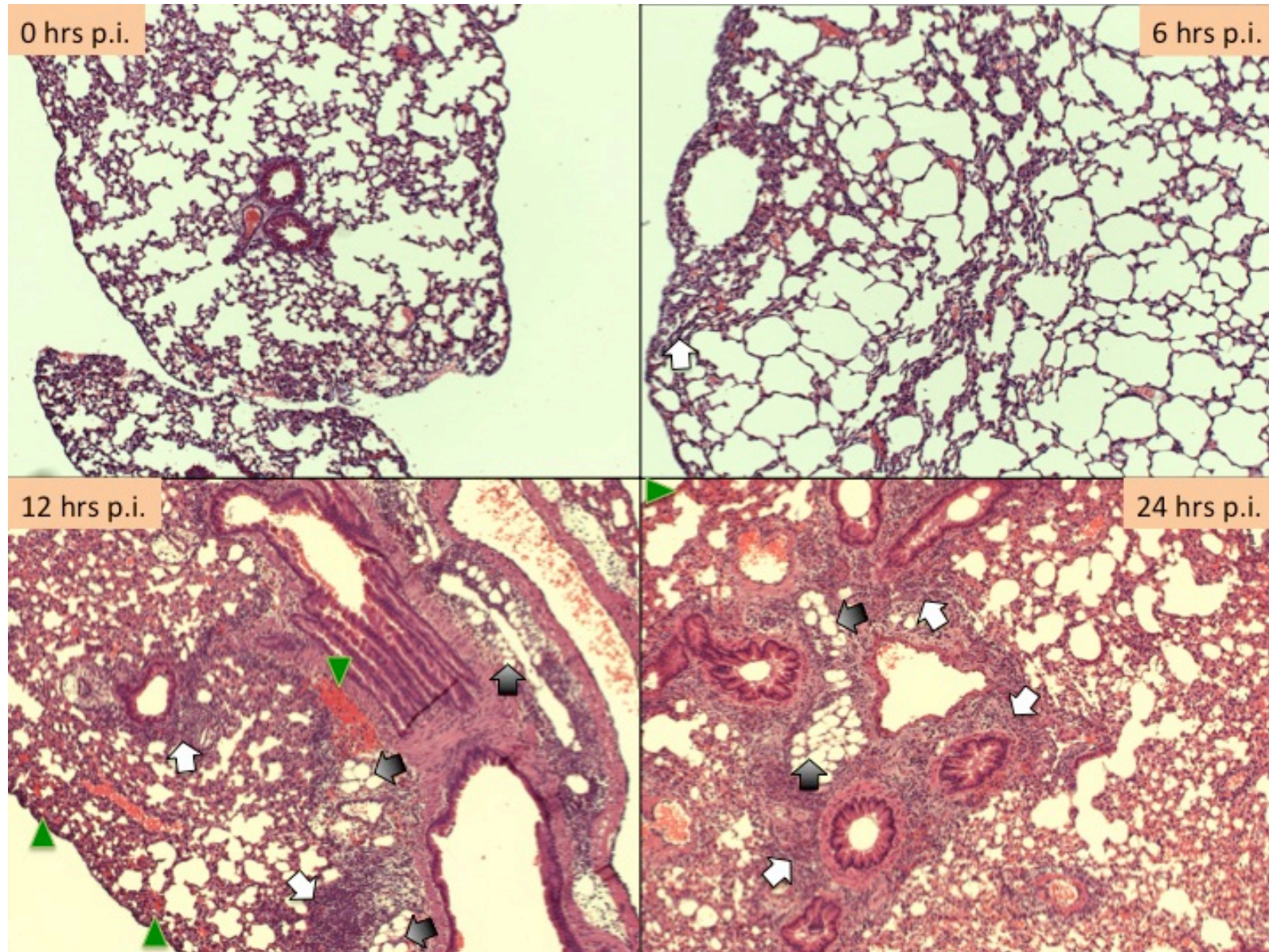


Figure 3.20 - Leukocyte recruitment in BALB/c and CBA/Ca lungs following pneumococcal-infection. Hematoxylin-and-eosin-stained paraffin wax cut lung tissue sections from (A) BALB/c and (B) CBA/Ca mice (n = 2 for each time point: 0, 6, 12 and 24 hours) following intranasal infection with  $10^6$  CFU of *S. pneumoniae* D39. While intact alveoli were seen at 0 hrs, infiltration (↑) and haemorrhage feature (▲) were prominently as of 12 hrs. Septae was thickened and intraalveolar fluid (↑) was observed.

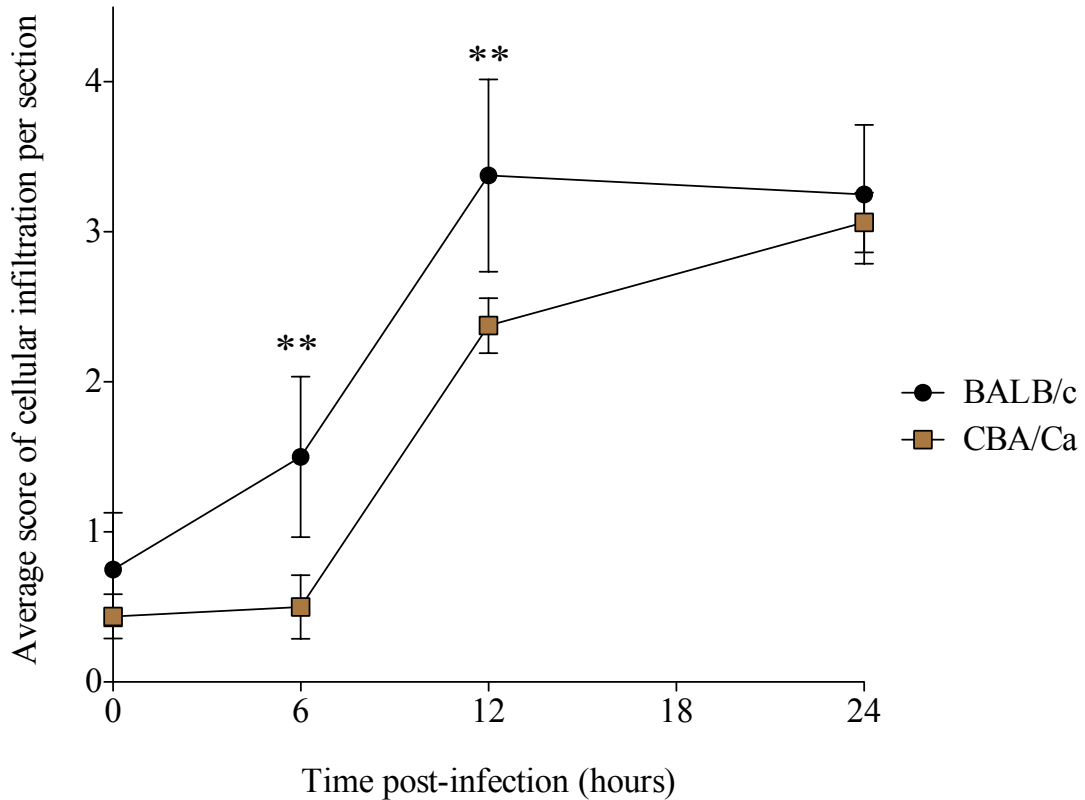


Figure 3.21 - Levels of cellular infiltration in the lung sections of BALB/c and CBA/Ca mice infected with *S. pneumoniae*. Mice were intranasally infected with  $10^6$  CFU, lungs were collected at 0, 6, 12 and 24 hours post-infection and then temporarily stored in 10% (v/v) neutral buffered formaldehyde. BALB/c and CBA/Ca lung paraffin sections were prepared and scored (based on Table 2.10 and exemplified on Appendix 7) independently by two operators and performed blind. Values represent average of the two individual scores generated from evaluating cellular infiltration criteria for a total of two sections per mouse at each time point ( $n = 4$  scores per time point per strain), with error bars showing the standard deviation. The p-values (\*\*,  $P < 0.01$ ) at 6 and 12 hours post-infection were obtained with two-way ANOVA followed by Bonferroni post-test. Data is representative of 1 experiment with 2 mice per strain and time point.

### 3.2.4 BALB/c and CBA/Ca inbred mice cytokine profile in response to pneumococcal infection

In this study, several cytokines and chemokines (IL-1 $\beta$ , IL-6, IL-10, IL-17, IFN- $\gamma$ , KC, MIP-2, TNF- $\alpha$  and TGF- $\beta$ ) were assessed in the lungs and blood of BALB/c and CBA/Ca mice. Together with the cellular responses profile (section 3.2.3), this investigation may contribute to understanding of mechanisms occurring in a resistant host (BALB/c strain) or a susceptible host (CBA/Ca strain). Furthermore, the cytokine profile was performed to identify potential biomarkers of pneumococcal pneumonia that could lead to a more targeted treatment and increasing the chances of disease recovery. Ideally in the future, potential pneumococcal patients could be screened on arrival at

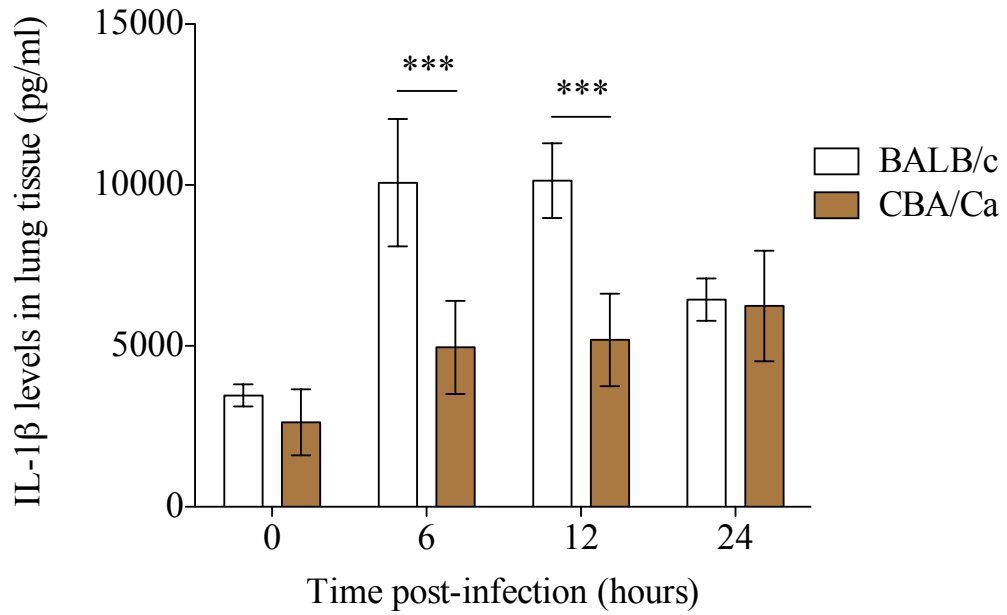
hospital from a quick and easy sample collection (blood sample) that could indicate the severity prognosis and aid in initial stratification.

*Interleukin 1-beta (IL-1 $\beta$ )*

The results have shown that the concentration of IL-1 $\beta$  rapidly increases in the lungs of BALB/c with time ( $P < 0.001$ ), but there was only very slow increase in CBA/Ca mice ( $P < 0.05$ , between sham and 24 hrs p.i.) (Figure 3.22-A). When comparing the two strains, the differences between them were observed at 6 and 12 hours post-infection, with BALB/c mice showing a significant increase in lung IL-1 $\beta$  when compared to CBA/Ca mice ( $P < 0.001$ ).

When assessing the serum for IL-1 $\beta$  (Figure 3.22-B), whereas, in the BALB/c this cytokine was barely detected, in the serum of CBA/Ca mice a tremendous increase was observed at 24 hours post-infection ( $P < 0.001$ ), when this strain is already at the lethargic stage.

A.



B.

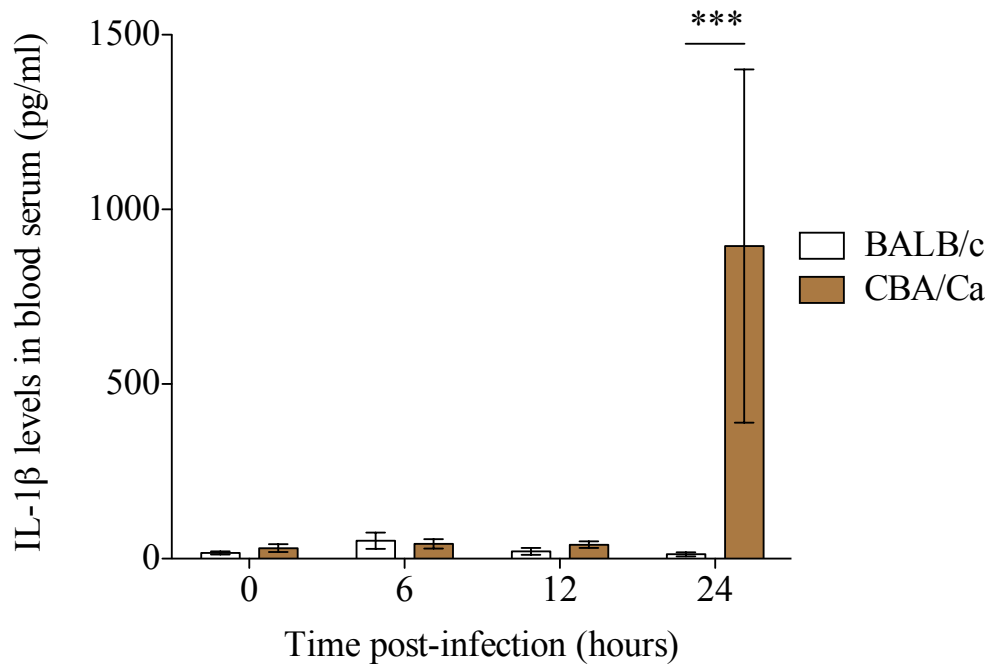


Figure 3.22 - Levels of IL-1 $\beta$  cytokine in the lungs and serum of BALB/c and CBA/Ca mice. Mice were intranasally infected with  $10^6$  CFU of *S. pneumoniae*, except for the time 0 hours p.i. (sham-infected mice that received PBS intranasally). IL-1 $\beta$  levels were assessed by ELISA in (A) lung supernatant and in (B) blood serum of BALB/c and CBA/Ca mice, in PBS sham-infected mice and in pneumococcal-infected mice at 6, 12 and 24 hours post-challenge. Data represent the mean of cytokine level  $\pm$  SD. The p-values (\*\*\*,  $P < 0.001$ ) were obtained by two-way ANOVA followed by Bonferroni post-test with Bonferroni post-test. Data are representative of an experiment with 4 mice per strain and time point.

### *Interleukin 6 (IL-6)*

The quantification of IL-6 in the lungs of BALB/c mice (Figure 3.23-A) showed a significant increase in the first 12 hours after infection ( $P < 0.001$  when compared to sham-infected) and then at 24 hours post-infection it dropped to uninfected levels ( $P > 0.05$  when compared to sham-infected). In the CBA/Ca lungs, the amount of IL-6 in infected-lungs was double that detected in the BALB/c lungs, ( $P < 0.001$  at 6, 12 and 24 hours p.i. between strains).

Interestingly when looking at the levels of IL-6 in serum (Figure 3.23-B), the changes in BALB/c mice during the infection were small but significant ( $P < 0.05$  between sham-infected and 12 hours p.i.), whereas, the amount of IL-6 in the serum of CBA/Ca mice showed a very significant increase during the course of the infection ( $P < 0.001$ ). By 12 hours after infection, the rise of IL-6 in the serum of CBA/Ca mice was significant when compared to sham-infected ( $P < 0.01$ ) and when compared to BALB/c ( $P < 0.01$ ). Twelve hours later, by 24 hours post-infection, the IL-6 levels reached high levels in CBA/Ca serum, very significantly different when compared to sham-infected ( $P < 0.001$ ) and to BALB/c at the same time point ( $P < 0.001$ ).

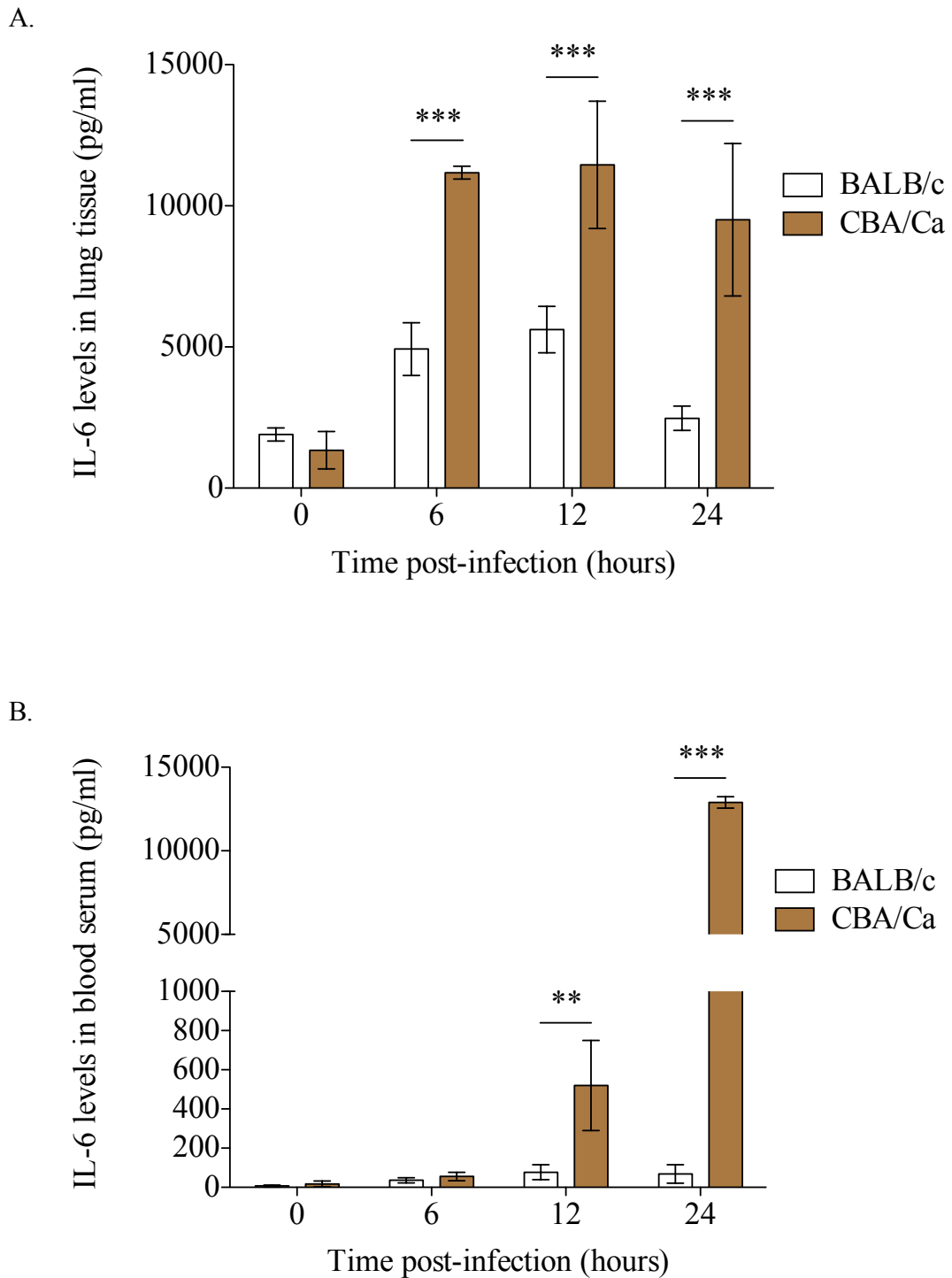


Figure 3.23 - Levels of IL-6 cytokine in the lungs and serum of BALB/c and CBA/Ca mice. Mice were intranasally infected with  $10^6$  CFU of *S. pneumoniae*, except for the time 0 hours p.i. (sham-infected mice that received PBS intranasally). IL-6 levels were assessed by ELISA in (A) lung supernatant and in (B) blood serum of BALB/c and CBA/Ca mice, in PBS sham-infected mice and in pneumococcal-infected mice at 6, 12 and 24 hours post-challenge. Data represent the mean of cytokine level  $\pm$  SD. The p-values (\*,  $P < 0.05$ ; \*\*\*,  $P < 0.001$ ) were obtained by two-way ANOVA followed by Bonferroni post-test. Data are representative of an experiment with 4 mice per strain and time point.

### *Interleukin 10 (IL-10)*

A different pattern of IL-10 cytokine production during pneumococcal infection was observed in the lungs of BALB/c and CBA/Ca mice (Figure 3.24-A). BALB/c mice had a peak of IL-10 production at 6 hours post-infection ( $P < 0.001$  when compared to sham-infected BALB/c) that was significantly different to CBA/Ca mice at this time point ( $P < 0.001$ ). IL-10 production in the lungs of CBA/Ca mice did not change during the course of infection ( $P > 0.05$ ).

The quantification of IL-10 in serum (Figure 3.24-B) of BALB/c mice showed no differences in the cytokine levels at any time point ( $P > 0.05$ ). In contrast, at 24 hours post-infection, CBA/Ca mice had a massive increase of IL-10, not observed in the serum of BALB/c mice ( $P < 0.001$  compared to sham-infected CBA/Ca mice and to BALB/c at 24 hrs p.i.).

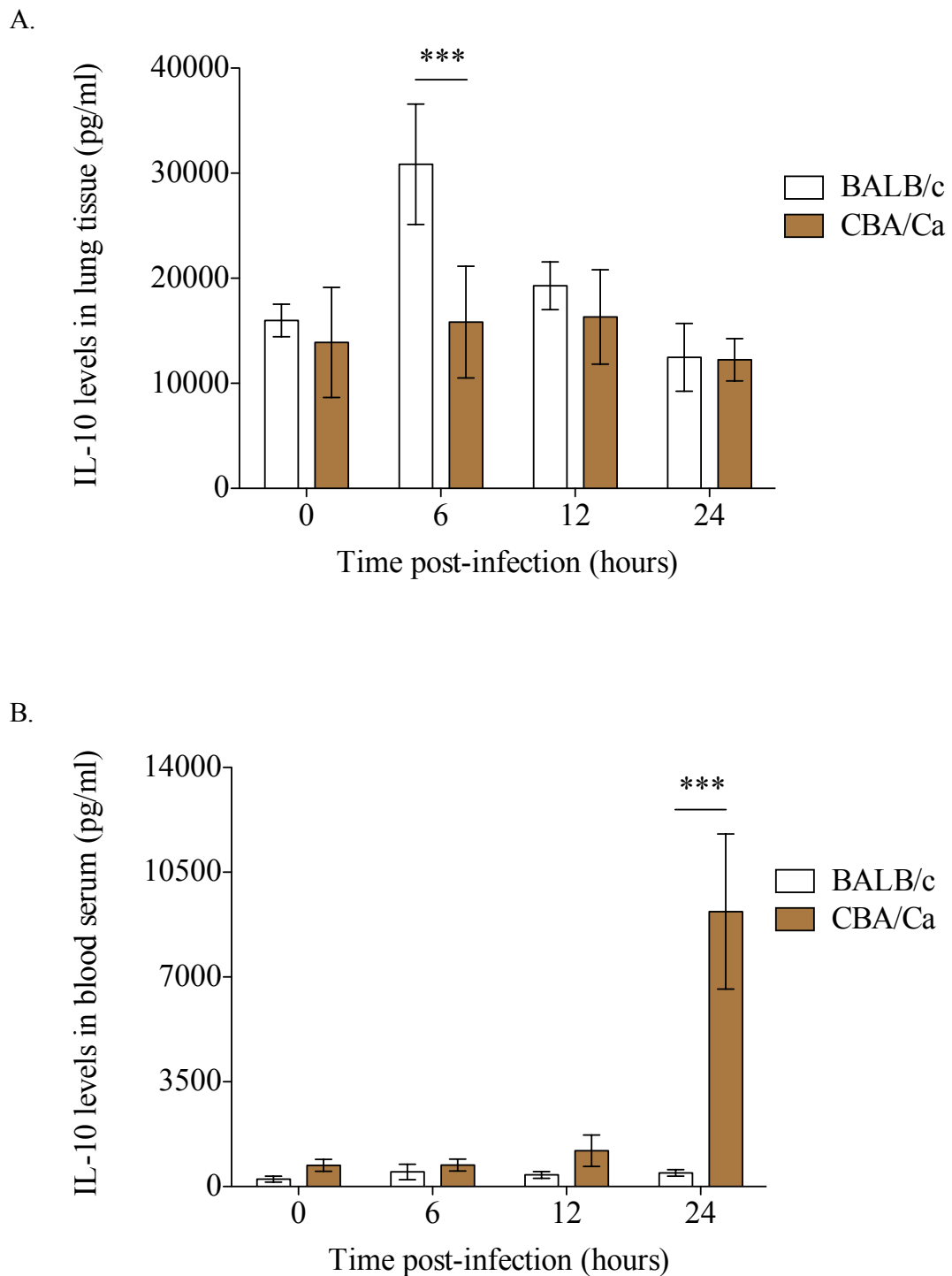


Figure 3.24 - Levels of IL-10 cytokine in the lungs and serum of BALB/c and CBA/Ca mice. Mice were intranasally infected with  $10^6$  CFU of *S. pneumoniae*, except for the time 0 hours p.i. (sham-infected mice that received PBS intranasally). IL-10 levels were assessed by ELISA in (A) lung supernatant and in (B) blood serum of BALB/c and CBA/Ca mice, in PBS sham-infected mice and in pneumococcal-infected mice at 6, 12 and 24 hours post-challenge. Data represent the mean of cytokine level  $\pm$  SD. The p-values (\*\*\*,  $P < 0.001$ ) were obtained by two-way ANOVA followed by Bonferroni post-test. Data are representative of an experiment with 4 mice per strain and time point.

### *Interleukin 17 (IL-17)*

IL-17 measured in the lungs (Figure 3.25-A) of BALB/c mice had significant peak at 6 hours post-infection with *S. pneumoniae*, when comparing to sham-infected ( $P < 0.001$ ) BALB/c, and to CBA/Ca at the same time point ( $P < 0.001$ ). Levels then dropped to those of the uninfected. No changes in IL-17 levels were seen in the lungs of CBA/Ca mice at any of the assessed time points ( $P > 0.05$ ).

When assessing the serum for quantification of IL-17 (Figure 3.25-B), no significant differences were found in BALB/c mice during the time course ( $P > 0.05$ ), whereas, in the serum of CBA/Ca mice a significant increase of IL-17 at 24 hours post-infection was observed, when compared to sham-infected ( $P < 0.05$ ) and also to BALB/c mice at the same time point ( $P < 0.001$ ).

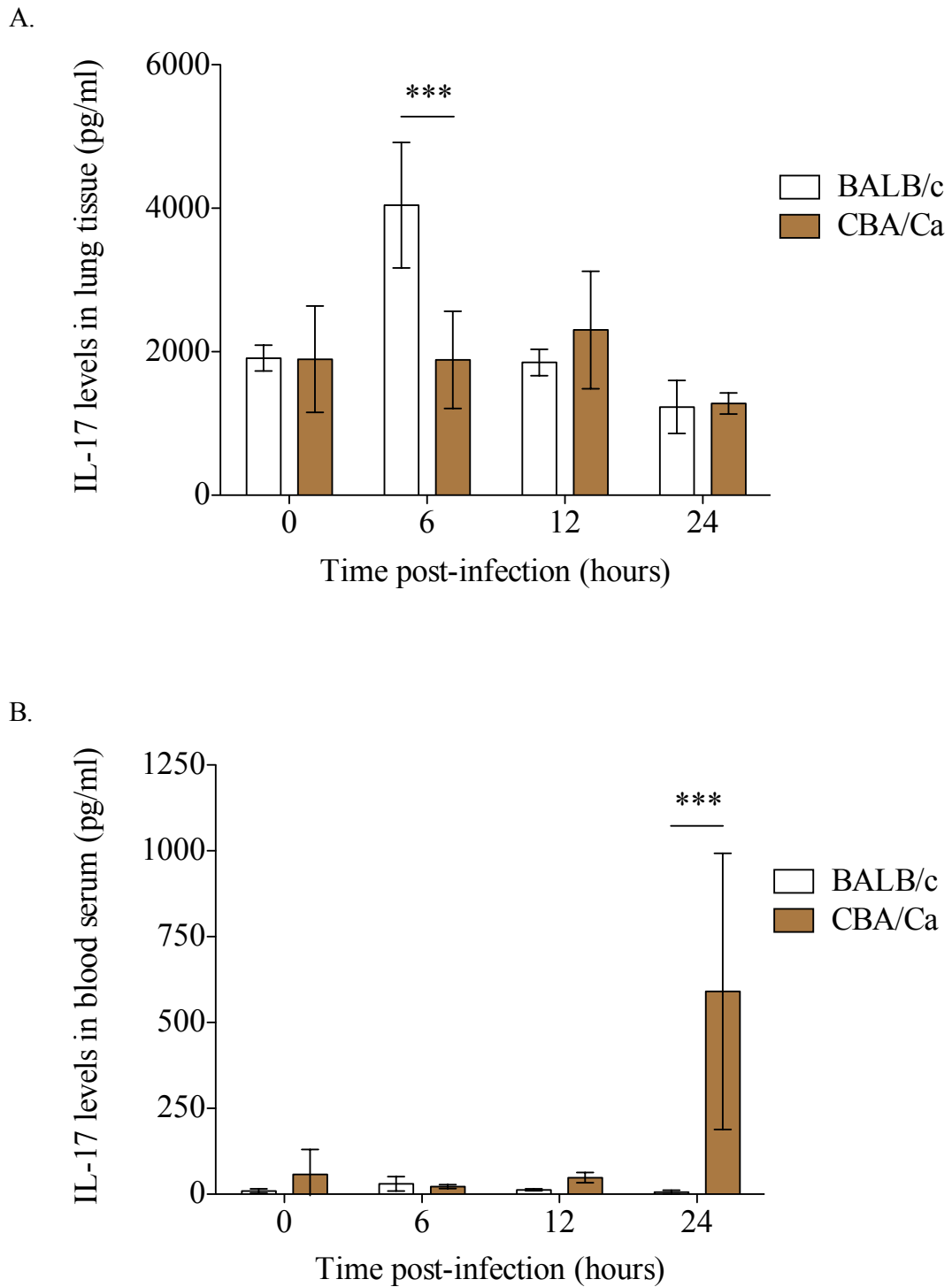


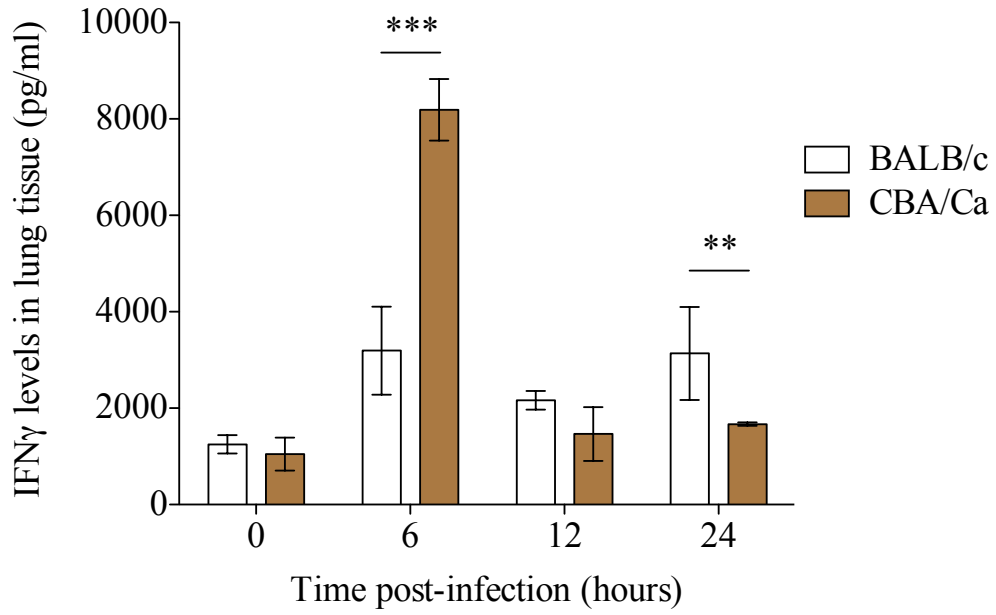
Figure 3.25 - Levels of IL-17 cytokine in the lungs and serum of BALB/c and CBA/Ca mice. Mice were intranasally infected with  $10^6$  CFU of *S. pneumoniae*, except for the time 0 hours p.i. (sham-infected mice that received PBS intranasally). IL-17 levels were assessed by ELISA in (A) lung supernatant and in (B) blood serum of BALB/c and CBA/Ca mice, in PBS sham-infected mice and in pneumococcal-infected mice at 6, 12 and 24 hours post-challenge. Data represent the mean of cytokine level  $\pm$  SD. The p-values (\*\*\*,  $P < 0.001$ ) were obtained by two-way ANOVA followed by Bonferroni post-test. Data are representative of an experiment with 4 mice per strain and time point.

### *Interferon-gamma (IFN- $\gamma$ )*

From analysis of the results obtained for IFN- $\gamma$  quantification in the lungs of BALB/c and CBA/Ca mice (Figure 3.26-A), the two strains showed a significant increase during the time course ( $P < 0.01$  in BALB/c and  $P < 0.001$  in CBA/Ca), but with a completely different pattern of IFN- $\gamma$  response to pneumococcal infection. BALB/c lungs had a slight significant increase of IFN- $\gamma$  at 6 hours post-infection ( $P < 0.01$  when compared to 0 hours) and then maintained the cytokine levels of approximately 3,000 pg/ml of lung supernatant during the remaining time points. On the other hand, the susceptible strain showed a very high increase of cytokine in the lungs at 6 hours post-infection, significantly different to BALB/c mice and to the sham-infected CBA/Ca ( $P < 0.001$ ). At 12 hours post-infection, the cytokine levels in the CBA/Ca lungs dropped to uninfected levels and maintained at 24 hours post-infection ( $P > 0.05$  between 0 and 12 hours and between 0 and 24 hours). At 24 hours, BALB/c mice showed significantly higher levels of IFN- $\gamma$  comparing to CBA/Ca ( $P < 0.01$ ), but no significant changes within BALB/c strain from 6 hours to 24 hours post-infection ( $P > 0.05$ ).

The levels of IFN- $\gamma$  in the serum (Figure 3.26-B) of BALB/c mice significantly increased from 12 hours to 24 hours post-challenge ( $P < 0.01$ ). This also occurred in CBA/Ca mice but the increase was much greater than in BALB/c ( $P < 0.001$  at 24 hours).

A.



B.

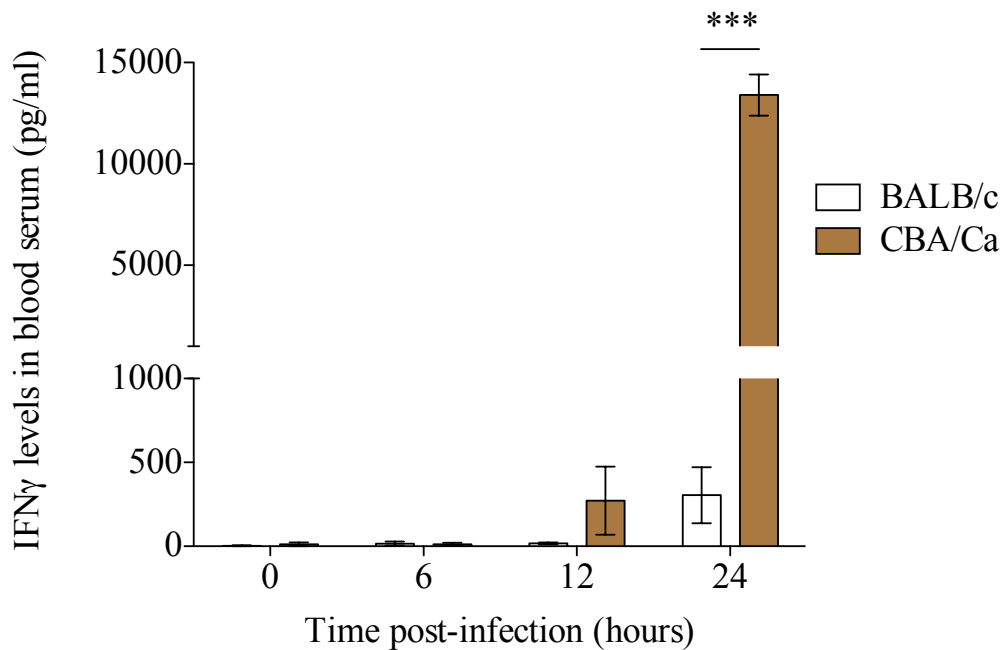


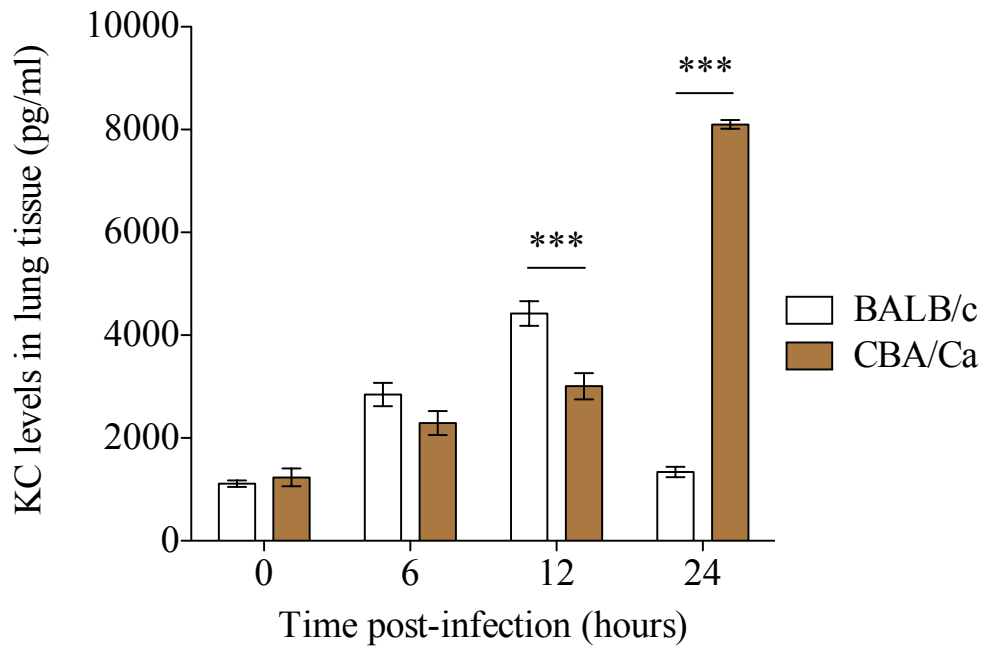
Figure 3.26 - Levels of IFN- $\gamma$  cytokine in the lungs and serum of BALB/c and CBA/Ca mice. Mice were intranasally infected with  $10^6$  CFU of *S. pneumoniae*, except for the time 0 hours p.i. (sham-infected mice that received PBS intranasally). IFN- $\gamma$  levels were assessed by ELISA in (A) lung supernatant and in (B) blood serum of BALB/c and CBA/Ca mice, in PBS sham-infected mice and in pneumococcal-infected mice at 6, 12 and 24 hours post-challenge. Data represent the mean of cytokine level  $\pm$  SD. The p-values (\*\*,  $P < 0.01$ ; \*\*\*,  $P < 0.001$ ) were obtained by two-way ANOVA followed by Bonferroni post-test. Data are representative of an experiment with 4 mice per strain and time point.

### *Keratinocyte-derived Cytokine (KC)*

Examining the results of assay of KC production in the lungs of BALB/c and CBA/Ca mice (Figure 3.27-A), it was found that there was a significant increase over time in both host strains ( $P < 0.0001$ ), but strikingly, BALB/c had a 12 hours peak of KC, coinciding with the climax of lung neutrophil recruitment (Figure 3.5). The KC levels dropped back to normal by 24 hours post-infection ( $P > 0.05$  between 0 and 24 hrs p.i.). At the 12 hour time point, significantly higher chemokine values were observed in BALB/c compared to CBA/Ca lungs ( $P < 0.001$ ), but at 24 hours two different patterns were observed: in the pneumococcal-susceptible lungs (CBA/Ca mice) the KC levels showed a very high increase ( $P < 0.001$  from 12 to 24 hrs p.i.), though, in the pneumococcal-resistant lungs (BALB/c mice) the production of chemokine dropped to baseline levels ( $P < 0.001$  from 12 to 24 hrs p.i.).

The KC levels in the serum of BALB/c and CBA/Ca mice (Figure 3.27-B) showed no changes between sham and pneumococcal-infected BALB/c mice at any time point after challenge ( $P > 0.05$ ). The CBA/Ca serum had a drastic increase of KC levels at 24 hours post-infection ( $P < 0.0001$  compared to BALB/c at 24 hours and to 0 hours). Comparing the chemokine levels between strains, a significant difference was observed at the 12 hour time point ( $P < 0.001$ ). The level in the BALB/c did not change with time post-infection whereas in the CBA/Ca the cytokine levels had a significant and abrupt rise from 12 to 24 hours post-challenge ( $P < 0.001$ ).

A.



B.

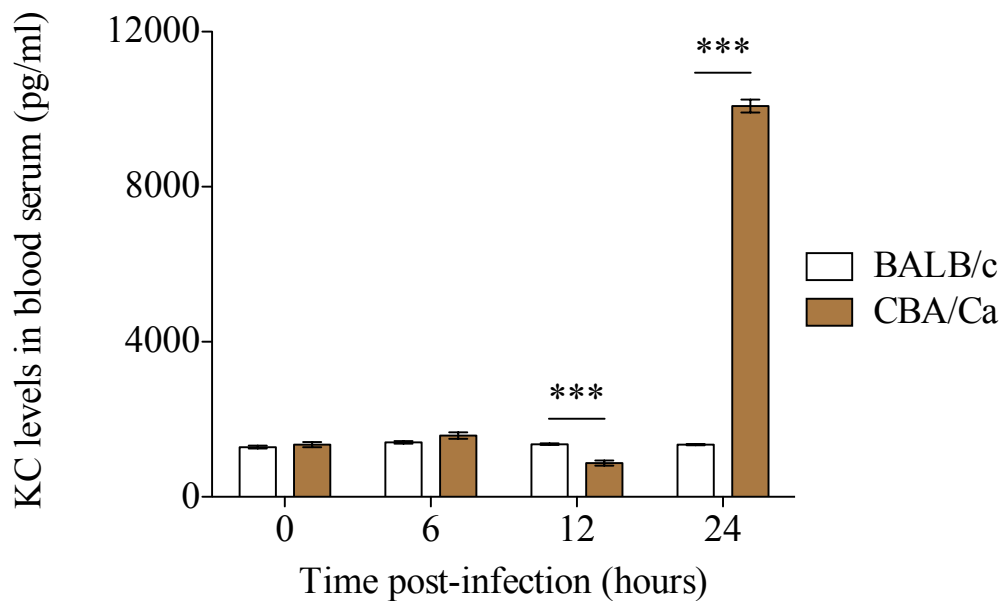


Figure 3.27 - Levels of KC cytokine in the lungs and serum of BALB/c and CBA/Ca mice. Mice were intranasally infected with  $10^6$  CFU of *S. pneumoniae*, except for the time 0 hours p.i. (sham-infected mice that received PBS intranasally). KC levels were assessed by ELISA in (A) lung supernatant and in (B) blood serum of BALB/c and CBA/Ca mice, in PBS sham-infected mice and in pneumococcal-infected mice at 6, 12 and 24 hours post-challenge. Data represent the mean of cytokine level  $\pm$  SD. The p-values (\*\*\*,  $P < 0.001$ ) were obtained by two-way ANOVA followed by Bonferroni post-test. Data are representative of an experiment with 4 mice per strain and time point.

### *Macrophage inflammatory protein 2 (MIP-2)*

The ELISA results of MIP-2 in the lungs of BALB/c and CBA/Ca mice (Figure 3.28-A) showed an increase of cytokine production after pneumococcal infection. During the first 12 hours of the infection, MIP-2 levels in BALB/c lungs had a significant and progressive rise ( $P < 0.0001$  compared to 0 hours). This was a similar pattern to that observed for KC in BALB/c lungs, namely a peak at 12 hours post-infection and a drop at 24 hours post-infection, but still significantly higher levels than the sham-infected animals ( $P < 0.01$ ). In the lungs of CBA/Ca mice, the picture was similar except that KC levels were unchanged between 12 and 24 hours ( $P > 0.05$ ). At 12 hours post-infection, MIP-2 in BALB/c lungs exceeded the levels observed in the CBA/Ca lungs ( $P < 0.05$ ), but, at 24 hours post-infection the situation was reversed: in the CBA/Ca host reached the chemokine plateau and in the BALB/c a drop was observed to significantly different values ( $P < 0.001$ ).

Assessment of MIP-2 levels in the serum of both inbred mouse strains (Figure 3.28-B), showed a quicker rise of the chemokine in BALB/c with significant difference ( $P < 0.001$  compared to CBA/Ca at 12 hrs post-infection and to BALB/c sham-infected). By 24 hours post-infection MIP-2 levels had not changed in BALB/c serum ( $P > 0.05$ ). In contrast at 24 hours, a high concentration of MIP-2 was seen in the serum of CBA/Ca mice ( $P < 0.001$  compared to BALB/c at 24 hrs p.i. and to CBA/Ca sham-infected).

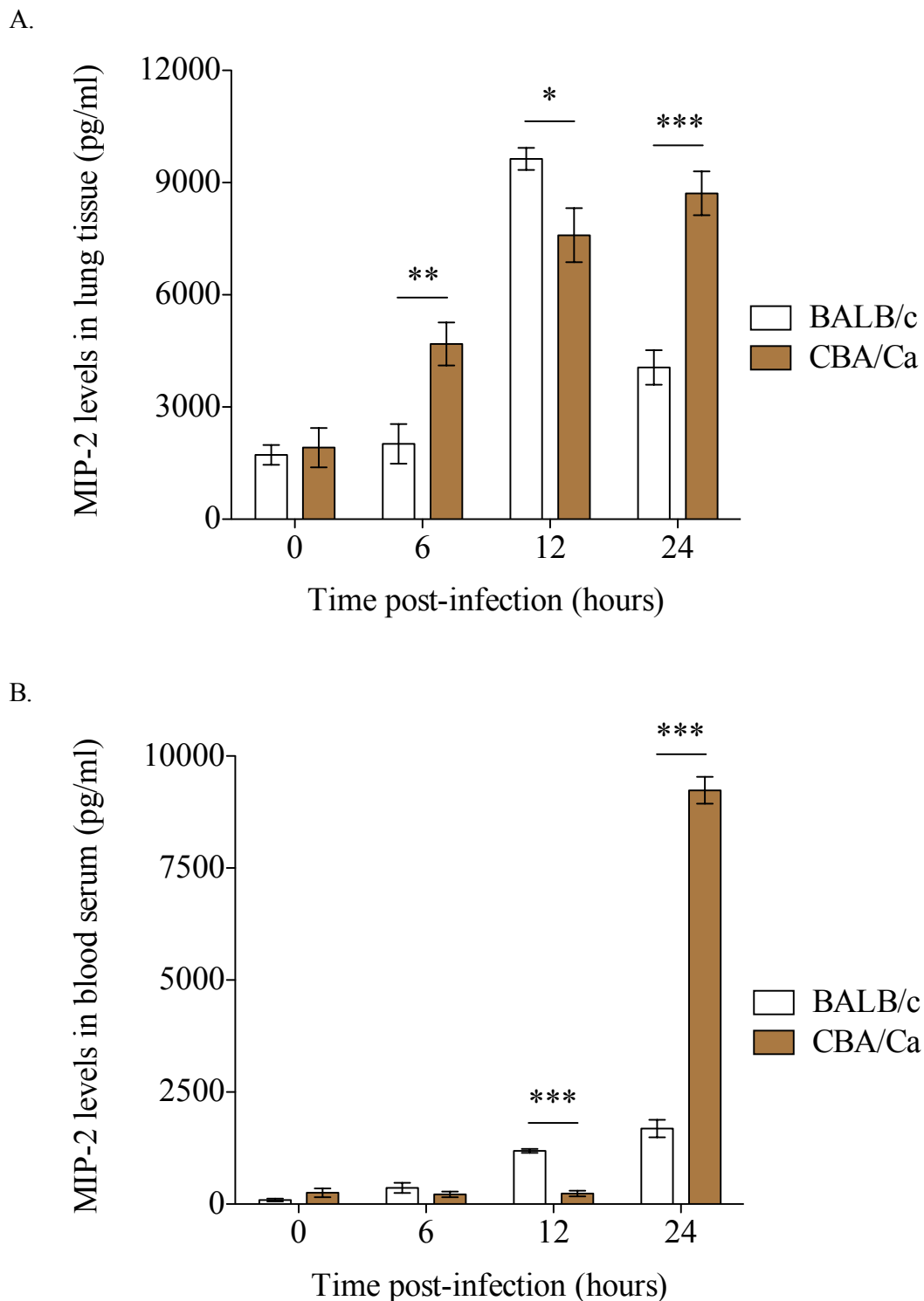


Figure 3.28 - Levels of MIP-2 cytokine in the lungs and serum of BALB/c and CBA/Ca mice. Mice were intranasally infected with  $10^6$  CFU of *S. pneumoniae*, except for the time 0 hours p.i. (sham-infected mice that received PBS intranasally). MIP-2 levels were assessed by ELISA in (A) lung supernatant and in (B) blood serum of BALB/c and CBA/Ca mice, in PBS sham-infected mice and in pneumococcal-infected mice at 6, 12 and 24 hours post-challenge. Data represent the mean of cytokine level  $\pm$  SD. The p-values (\*,  $P < 0.05$ ; \*\*,  $P < 0.01$ ; \*\*\*,  $P < 0.001$ ) were obtained by two-way ANOVA followed by Bonferroni post-test. Data are representative of an experiment with 4 mice per strain and time point.

### *Tumour necrosis factor alpha (TNF- $\alpha$ )*

In Figure 3.29-A the results of the quantification of TNF- $\alpha$  levels in the lungs of BALB/c and CBA/Ca mice during infection are shown. They reveal a significant increase of TNF- $\alpha$  in BALB/c ( $P < 0.0001$ ) and in CBA/Ca mice ( $P < 0.05$ ) post pneumococcal challenge. The production of TNF- $\alpha$  in the lungs of BALB/c mice had a significant boost at 6 hours post-infection ( $P < 0.001$  compared to sham-infected) that was sustained for six more hours (until 12 hrs p.i.) and declined by 24 hours ( $P < 0.05$  compared to sham-infected). In the CBA/Ca lungs, TNF- $\alpha$  levels also had a significant increase at 6 hours post-infection ( $P < 0.05$  compared to sham-infected), but there were significantly lower values than in BALB/c at 6 and 12 hours post-challenge ( $P < 0.001$ ). 24 hours after pneumococcal infection, the TNF- $\alpha$  levels dropped to uninfected levels ( $P > 0.05$  when compared to 0 hours and to BALB/c at 24 hours).

Levels of TNF- $\alpha$  in the serum of these two strains of mice were also analysed (Figure 3.29-B). However, the only significant changes observed were at 24 hours post-infection in the CBA/Ca host. At this time point, the levels of cytokine in the blood increased abruptly to values significantly different to BALB/c mice and to the CBA/Ca sham-infected with PBS ( $P < 0.001$ ).

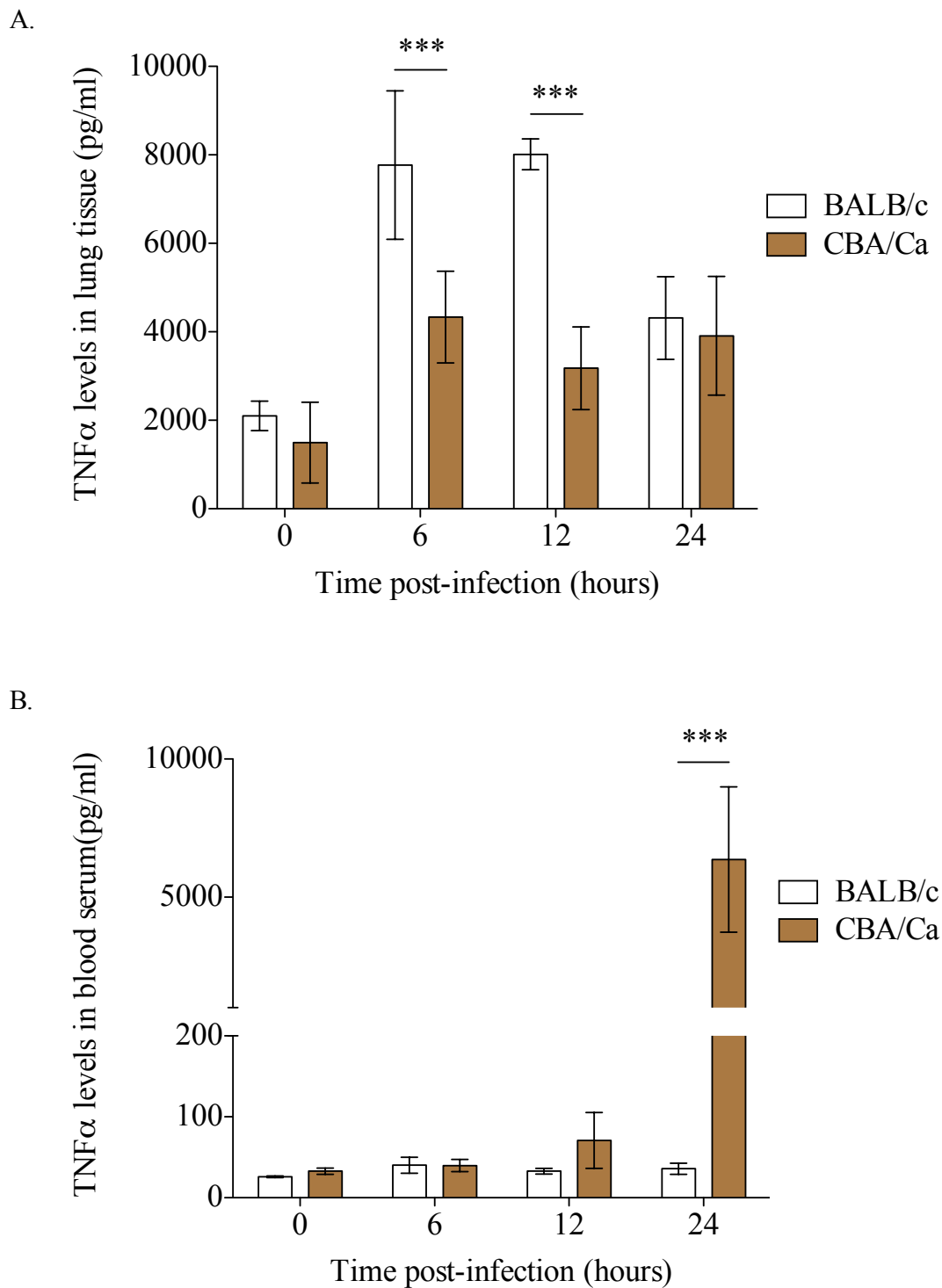


Figure 3.29 - Levels of TNF- $\alpha$  cytokine in the lungs and serum of BALB/c and CBA/Ca mice. Mice were intranasally infected with  $10^6$  CFU of *S. pneumoniae*, except for the time 0 hours p.i. (sham-infected mice that received PBS intranasally). TNF- $\alpha$  levels were assessed by ELISA in (A) lung supernatant and in (B) blood serum of BALB/c and CBA/Ca mice, in PBS sham-infected mice and in pneumococcal-infected mice at 6, 12 and 24 hours post-challenge. Data represent the mean of cytokine level  $\pm$  SD. The p-values (\*\*\*,  $P < 0.001$ ) were obtained by two-way ANOVA followed by Bonferroni post-test. Data are representative of an experiment with 4 mice per strain and time point.

### *Transforming growth factor beta (TGF- $\beta$ )*

From analysis of the results obtained from ELISA of TGF- $\beta$ 1 in the lungs of BALB/c and CBA/Ca (Figure 3.30-A), a significant increase in BALB/c lung over time post-infection ( $P < 0.0001$ ) was observed, whereas the susceptible CBA/Ca mice had no significant changes of this cytokine in the lungs at any time point post-pneumococcal infection ( $P > 0.05$ ). Interestingly, in the BALB/c lungs, a strong boost of TGF- $\beta$ 1 cytokine from baseline (PBS sham-infected BALB/c mice) was detected at 6 hours post-infection ( $P < 0.001$ ). The TGF- $\beta$ 1 levels also were significantly different when compared to CBA/Ca ( $P < 0.001$ ). At 12 post-infection, the lung TGF- $\beta$ 1 level in BALB/c mice had a slight drop but was still significantly higher than the observed levels of cytokine in CBA/Ca lungs ( $P < 0.05$ ). By 24 hours post-infection, the TGF- $\beta$ 1 level in BALB/c was restored to uninfected levels, showing no significant results ( $P > 0.05$  compared to CBA/Ca and to 0 hours).

Evaluating the amount of TGF- $\beta$ 1 in the serum of BALB/c and CBA/Ca (Figure 3.30-B), the levels were very low in both strain at the various time points and no significant changes were detected ( $P > 0.05$ ).

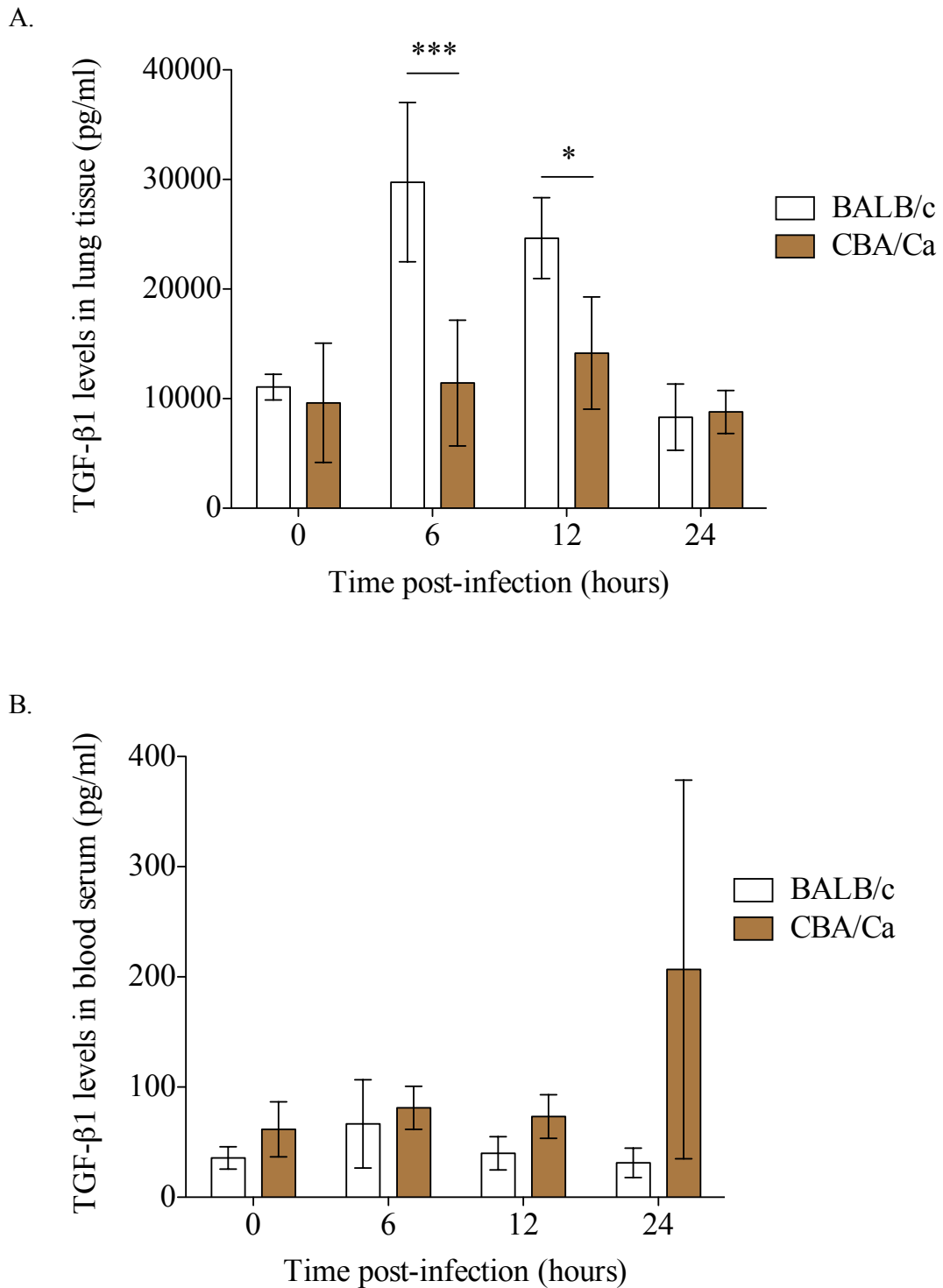


Figure 3.30 - Levels of TGF- $\beta$ 1 cytokine in the lungs and serum of BALB/c and CBA/Ca mice. Mice were intranasally infected with  $10^6$  CFU of *S. pneumoniae*, except for the time 0 hours p.i. (sham-infected mice that received PBS intranasally). TGF- $\beta$ 1 levels were assessed by ELISA in (A) lung supernatant and in (B) blood serum of BALB/c and CBA/Ca mice, in PBS sham-infected mice and in pneumococcal-infected mice at 6, 12 and 24 hours post-challenge. Data represent the mean of cytokine level  $\pm$  SD. The p-values (\*,  $P < 0.05$ , \*\*\*,  $P < 0.001$ ) were obtained by two-way ANOVA followed by Bonferroni post-test. Data are representative of an experiment with 4 mice per strain and time point.

Overall, the cytokines analysis showed a different profile in the resistant BALB/c and the susceptible CBA/Ca in response to pneumococcal pneumonia (Table 3.2).

Cytokine	Sham-PBS	6 hr p.i.	12 hr p.i.	24 hr p.i.
IL-1 $\beta$	-	B > C ( $P < 0.001$ )	B > C ( $P < 0.001$ )	-
IL-6	-	C > B ( $P < 0.001$ )	C > B ( $P < 0.001$ )	C > B ( $P < 0.001$ )
IL-10	-	B > C ( $P < 0.001$ )	-	-
IL-17	-	B > C ( $P < 0.001$ )	-	-
IFN- $\gamma$	-	C > B ( $P < 0.001$ )	-	B > C ( $P < 0.01$ )
KC	-	-	B > C ( $P < 0.001$ )	C > B ( $P < 0.001$ )
MIP-2	-	C > B ( $P < 0.01$ )	B > C ( $P < 0.05$ )	C > B ( $P < 0.001$ )
TNF- $\alpha$	-	B > C ( $P < 0.001$ )	B > C ( $P < 0.001$ )	-
TGF- $\beta$ 1	-	B > C ( $P < 0.001$ )	B > C ( $P < 0.05$ )	-

Table 3.2 - Lung cytokine statistical differences between BALB/c and CBA/Ca mice. P-values result from two-way ANOVA analysis followed by Bonferroni post-test. “B” for BALB/c, “C” for CBA/Ca and “-” for no significant differences between strains at the time point.

Cytokine	Sham-PBS	6 hr p.i.	12 hr p.i.	24 hr p.i.
IL-1 $\beta$	-	-	-	C > B ( $P < 0.001$ )
IL-6	-	-	C > B ( $P < 0.01$ )	C > B ( $P < 0.001$ )
IL-10	-	-	-	C > B ( $P < 0.001$ )
IL-17	-	-	-	C > B ( $P < 0.001$ )
IFN- $\gamma$	-	-	-	C > B ( $P < 0.001$ )
KC	-	-	B > C ( $P < 0.001$ )	C > B ( $P < 0.001$ )
MIP-2	-	-	B > C ( $P < 0.001$ )	C > B ( $P < 0.001$ )
TNF- $\alpha$	-	-	-	C > B ( $P < 0.001$ )
TGF- $\beta$ 1	-	-	-	-

Table 3.3 - Serum cytokine statistical differences between BALB/c and CBA/Ca mice. P-values result from two-way ANOVA analysis followed by Bonferroni post-test. “B” for BALB/c, “C” for CBA/Ca and “-” for no significant differences between strains at the time point.

---

## CHAPTER 4. Generation of BALB/c and CBA/Ca congenic mice for investigation of the *Spir1* locus

---

### 4.1 Generation and Characterisation of *Spir1* congenic mice

Congenic mice were generated to follow the inheritance of susceptibility to intranasal pneumococcal infection.

#### 4.1.1 *Spir1* congenic-breeding strategy

Congenic lines were produced by targeting a genomic region from one genetic background (CBA/Ca inbred mice) and transferring this genomic region into another inbred strain (BALB/c) through repeated backcrossing. The production of *Spir1* congenic mice was a marker-assisted process, using three polymorphic markers between BALB/c and CBA/Ca strains, equally spaced within proximal chromosome 7. The three SNP markers (coded as 7\_09, 7\_54 and 7\_123) were used for genotyping the N<sub>1</sub> to N<sub>10</sub> *Spir1* congenic progenies (section 4.1.1) for chromosome 7 QTL mapping were selected based on Denny et al., (2003). The positions of these chromosome 7 polymorphic markers were: 7\_09 (7:11029385), 7\_54 (7:73234304) and 7\_123 (7:141852931), as shown in Figure 4.1. The *Spir1* region is located between 24Mb and 37Mb (7:25,147,108 – 7:37,927,961), containing at least 250 genes (Supplementary Figure 1) and is flanked by these three SNP markers (7\_09 downstream and 7\_54 and 7\_123 upstream).

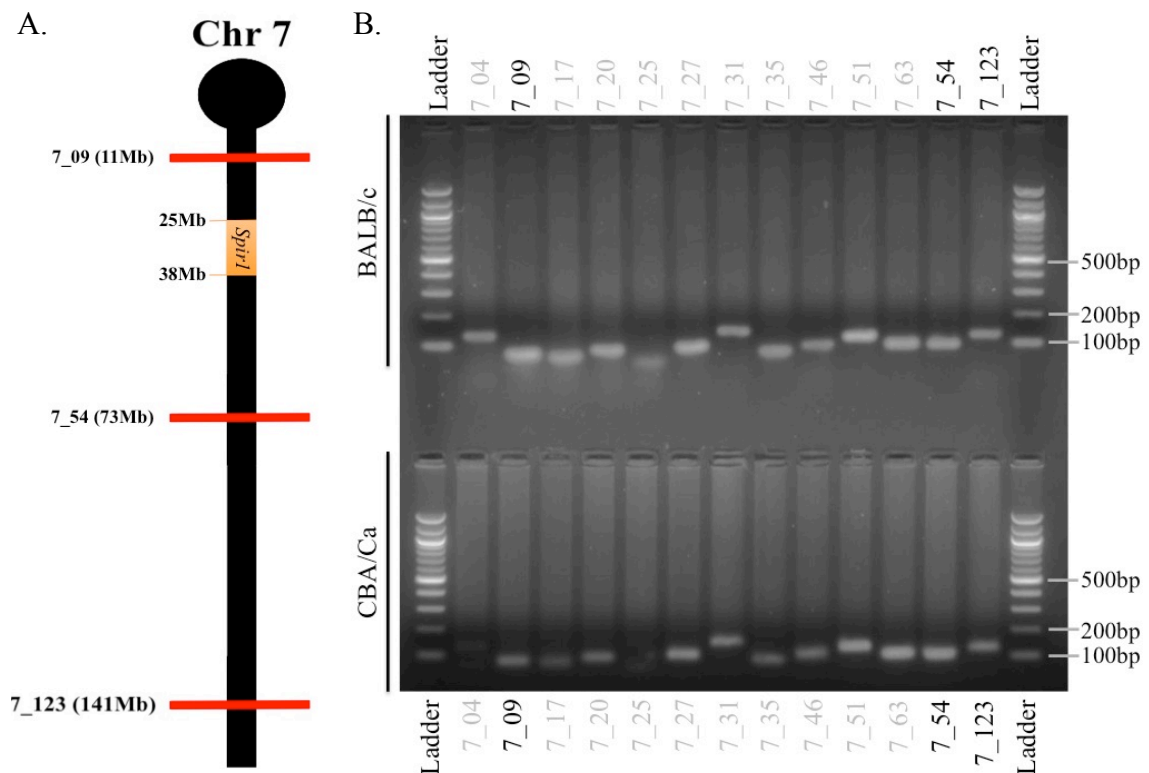


Figure 4.1 - Chromosome 7 SNP markers used in the congenic-breeding program. (A) SNP markers used for genotyping the *Spir1* congenic progeny for QTL mapping and their distribution across chromosome 7 (red bars represent each SNP location). The orange box indicates the *Spir1* region (between 24 and 37Mb). (B) Example of agarose gel electrophoresis, treated with Ethidium bromide, used to testing each of the SNP markers (7\_09, 7\_54 and 7\_123) on BALB/c and CBA/Ca DNA template, prior to pyrosequencing of PCR products. The tainted SNP markers in the figure (7\_04, 7\_17, 7\_20, 7\_25, 7\_27, 7\_31, 7\_35, 7\_46, 7\_51 and 7\_63) were used to narrow down the *Spir1* QTL (Figure 4.7) and described with more detail further on in this chapter. Picture was taken under UV light conditions and shows PCR products for all markers. PCR products size was compared to the 100bp DNA ladder (molecular marker). All PCR products in the figure were amplified as described in section 2.4.1.2.

Initially, male CBA/Ca mice were crossed with female BALB/c mice. From the offspring of those crosses (“N<sub>1</sub>” generation, notation for the 1<sup>st</sup> generation), males presenting one copy of CBA/Ca DNA (heterozygous) at the various polymorphic marker positions, were picked to mate with female BALB/c mice to give the 1<sup>st</sup> backcross. Their male offspring (N<sub>2</sub> males), also containing heterozygous DNA at all three polymorphic markers, were then selected for backcrossing with female BALB/c mice, producing N<sub>3</sub> mice. This strategy for selection of male breeders, applying the same criteria for selection of male breeders (one copy of CBA/Ca DNA at the three polymorphic markers: 7\_09, 7\_54 and 7\_123), and then backcrossing with female BALB/c mice was performed 9 times to give the N<sub>10</sub> generation. A strain is considered fully congenic after ten generations: one intercross and nine subsequent backcrosses

(Markel *et al.*, 1997). Overall, the congenic strategy consisted in incorporating the region of DNA in chromosome 7 associated with susceptibility to pneumococcal disease (*Spir1* QTL) from the CBA/Ca strain (the donor line) into the pneumococcal-resistant BALB/c strain (the recipient line), as illustrated in Figure 4.2.

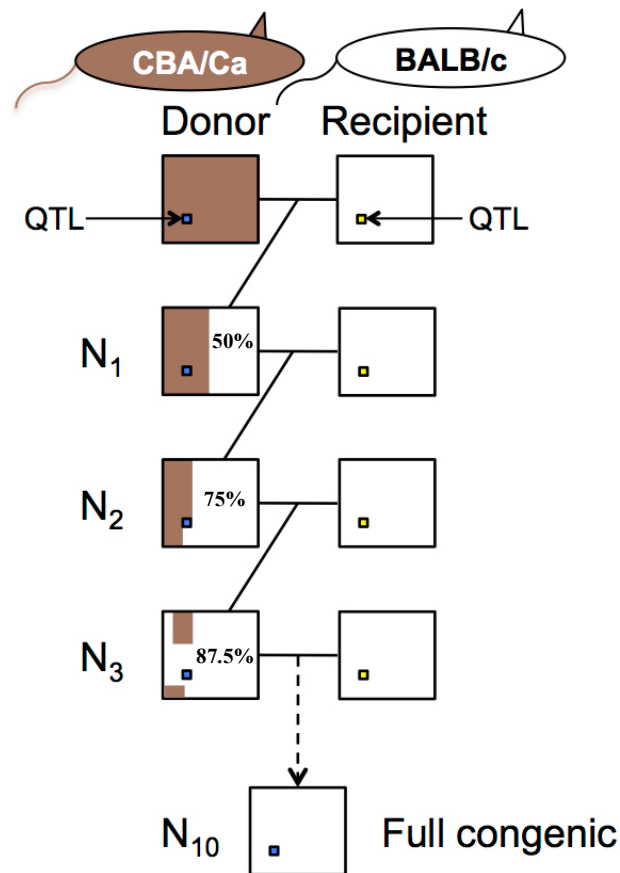


Figure 4.2 - Development of a congenic line. Figure represents a congenic line in which a quantitative trait locus (QTL) from the donor line (CBA/Ca mouse strain) is being bred into the recipient line (BALB/c mouse strain). The brown and white areas represent genetic material inherited from the two progenitors. The N<sub>1</sub> offspring of a cross between donor and recipient carries approximately 50 percent of the genetic material from each parent, as according to Mendel's laws. By repeatedly breeding the N<sub>1</sub> animals and their offspring with the recipient line, the proportion of genetic material from the donor line becomes progressively less, as represented on Table 4.1 (estimated percentages at each generation), until only the *Spir1* SNP marker positions contain DNA from the donor line. Adapted from (Dick & Foroud, 2002).

At the 10<sup>th</sup> generation (N<sub>10</sub>), the congenic mice were carrying an introgressed region of interest (region heterozygous) and it is predicted homozygous BALB/c outside region covered by the SNP markers, in approximately 99.90% recipient genome (see Table 4.1).

<b>Generation</b>	<b>% Recipient genome</b>
N <sub>1</sub>	50.00
N <sub>2</sub>	75.00
N <sub>3</sub>	87.50
N <sub>4</sub>	93.75
N <sub>5</sub>	96.88
N <sub>6</sub>	98.44
N <sub>7</sub>	99.22
N <sub>8</sub>	99.61
N <sub>9</sub>	99.81
N <sub>10</sub>	99.90

Table 4.1 - Estimated percentage of recipient genome at each generation of the congenic-breeding development (Markel *et al.*, 1997). The percentage of recipient genome at generations N<sub>1</sub>, N<sub>2</sub>, N<sub>3</sub> and N<sub>10</sub> were introduced in the white area of each square in Figure 4.2.

Finally, brother and sister mating of N<sub>10</sub> mice, presenting heterozygous DNA at the QTL, were intercrossed to generate congenic mice with homozygous DNA at the various polymorphic marker positions (7\_09, 7\_54 and 7\_123). In order to confirm the trait of susceptibility to invasive pneumococcal disease associated with the *Spir1* locus, six different congenic lines were set up (Table 4.2).

Line Code	Chromosome 7 SNP markers			No. of mice phenotyped per N <sub>10</sub> line (Resistant mice / Susceptible phenotype)
	7_09	7_54	7_123	
CCC	CBA/Ca	CBA/Ca	CBA/Ca	61 mice (18/43)
CCB	CBA/Ca	CBA/Ca	BALB/c	52 mice (23/29)
CBB	CBA/Ca	BALB/c	BALB/c	51 mice (23/28)
BCC	BALB/c	CBA/Ca	CBA/Ca	48 mice (38/10)
BBC	BALB/c	BALB/c	CBA/Ca	63 mice (54/9)
BBB	BALB/c	BALB/c	BALB/c	54 mice (45/9)

Table 4.2 - *Spir1* marker-assisted congenic fixed lines. Each row represents a fixed line and each mouse of the different lines has homozygous DNA in every single polymorphic marker, which can be either BALB/c or CBA/Ca (for instance, a mouse from line CBB, highlighted in red, has a CBA/Ca SNP at the position 7\_09, and BALB/c SNPs at the positions 7\_54 and 7\_123).

Each of the six *Spir1* congenic lines, brothers and sisters with the same genotype were intercrossed and their offspring were then phenotyped (minimum of 40 mice per fixed line). The phenotype was determined by infecting the mice intranasally with a dose of  $1 \times 10^6$  CFU/ml of wild-type D39 and then assessing survival time (Figure 4.4), up to 1-week post-infection, and detection of viable bacteria in the blood at 24 hours post-infection (Figure 4.5). The survival data (Figure 4.4) showed two different patterns within the congenic lines: three resistant lines (BBB, BBC and BCC) had a resistant phenotype; and a second group composed of three lines (CCC, CCB and CBB) had a susceptible phenotype. No statistical difference was observed in the survival between the resistant congenic lines ( $P > 0.05$ ), nor between the three susceptible congenic strains ( $P > 0.05$ ). The data on bacteraemia at 24 hours post-infection (Figure 4.5) showed the same two patterns with the congenic lines: the group of resistant lines had a low number of bacteria in the blood, under  $2 \log_{10}$  CFU per ml, whereas the group of susceptible lines showed a high number of bacteria in the blood, over  $2 \log_{10}$  CFU per ml. Within the susceptible strains, the CCC line revealed the highest number of bacteraemia at 24 hours post-infection, when compared to the CCB line ( $P < 0.05$ ) and

to the CBB line ( $P < 0.01$ ). In addition, a correlation was observed (Figure 4.3) between both survival time (Figure 4.4) and bacteraemia at 24 hours post-infection (Figure 4.5) and the N<sub>10</sub> congenic lines genotype: the three resistant congenic lines had greater percentage survival and the lowest bacteraemia levels at 24 hours post-infection. On the other hand, the three susceptible congenic lines had reduced percentage survival and the highest bacteraemia levels at 24 hours post-infection (Figure 4.6).

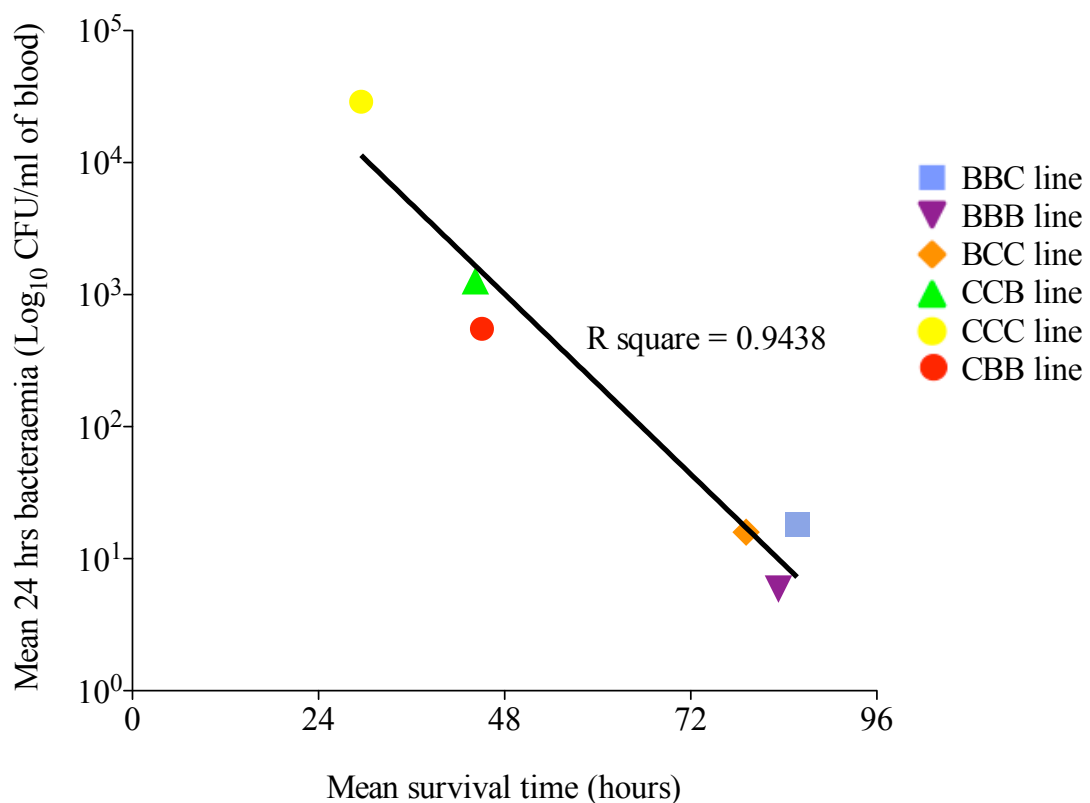


Figure 4.3 - Correlation between mean 24 hours bacteraemia and mean survival time of each congenic line infected with *S. pneumoniae*. Each dot represents the mean of 24 hours bacteraemia and mean of survival time per congenic line (BBB, BBC, BCC, CCC, CCB and CBB). The p-value (\*\*,  $P < 0.01$ ) and the  $R^2 = 0.9438$  were obtained by the analysis for correlation with Pearson test, two-tailed with 95% confidence interval.

The phenotyping data of the congenic lines (Figure 4.4, Figure 4.5 and Figure 4.6) were analysed one-by-one. A resistant phenotype was observed in the BBB line, with 83% survival ( $n = 54$  mice challenged) and evidencing the lowest average number of CFUs in the blood at 24 hours post-infection (under 1 log<sub>10</sub> CFU per ml of blood). The animals from the BBC congenic line ( $n = 63$  mice challenged) showed the highest survival rate (85% survival), besides a low amount of bacteria in the blood at 24 hours post-infection (approximately 1 log<sub>10</sub> CFU per ml of blood) and no statistical differences were found between BBB and BBC lines in survival rate ( $P > 0.05$ ) or

bacteraemia at 24 hours post-infection ( $P > 0.05$ ). In fact, having CBA/Ca DNA at the third marker (marker 7\_123) did not reduce survival nor increase the bacteraemia levels at 24 hours post-infection in the BBC mice, indicating that the 7\_123 region is not directly linked to susceptibility to *S. pneumoniae* infection. The BCC line ( $n = 48$  mice challenged) have also exhibited a resistant phenotype to pneumococcal infection, in which 79% of the animals from this line survived and these mice presented low bacteraemia levels at 24 hours post-infection, having a concentration similar to that found in BBC mice (roughly  $1 \log_{10}$  CFU per ml of blood). The phenotype of the BCC congenic line indicated that the first marker (7\_09 SNP, upstream the *Spir1* region) containing BALB/c DNA showed linkage to resistance to IPD. On the other hand, the CBB congenic line ( $n = 51$  mice challenged) that contained CBA/Ca DNA in the first marker (7\_09 SNP) and BALB/c DNA in the other two markers (7\_54 and 7\_123, downstream the *Spir1* region) evidenced susceptibility to infection. These observations support the results obtained by Denny *et al.* (Denny *et al.*, 2003) with the F<sub>2</sub> mice crosses (BALB/c x CBA/Ca) – chromosome 7 QTL association to susceptibility to IPD. The CBB line had 45% survival and 24 hours bacteraemia higher than  $2 \log_{10}$  ( $2.7 \log_{10}$  CFU per ml of blood) and the phenotype was significantly different to the BCC line in terms of survival rate ( $P < 0.01$ ) and bacteraemia at 24 hours post-infection ( $P < 0.05$ ). As mentioned in the text before, the CBB line belongs to a group of three congenic lines with a susceptible phenotype when infected with pneumococcal pneumonia. The CCB line ( $n = 52$  mice challenged) is part of this group that displayed a susceptible pattern, in fact very similar to the CBB line ( $P > 0.05$ , for survival and bacteraemia at 24 hours p.i.), showing 44% survival and  $3.1 \log_{10}$  CFU per ml of blood at 24 hours post-challenge. Finally, the CCC congenic line showed the lowest survival rate (30%) and the highest CFU in the blood at 24 hours post-infection ( $4.4 \log_{10}$  CFU per ml of blood). The number of bacteria in the blood at 24 hours post-infection in the CCC line was significantly different to the CCB line ( $P < 0.05$ ) and CBB line ( $P < 0.01$ ), although no significant differences were found in survival rate between these susceptible congenic strains ( $P > 0.05$ ).

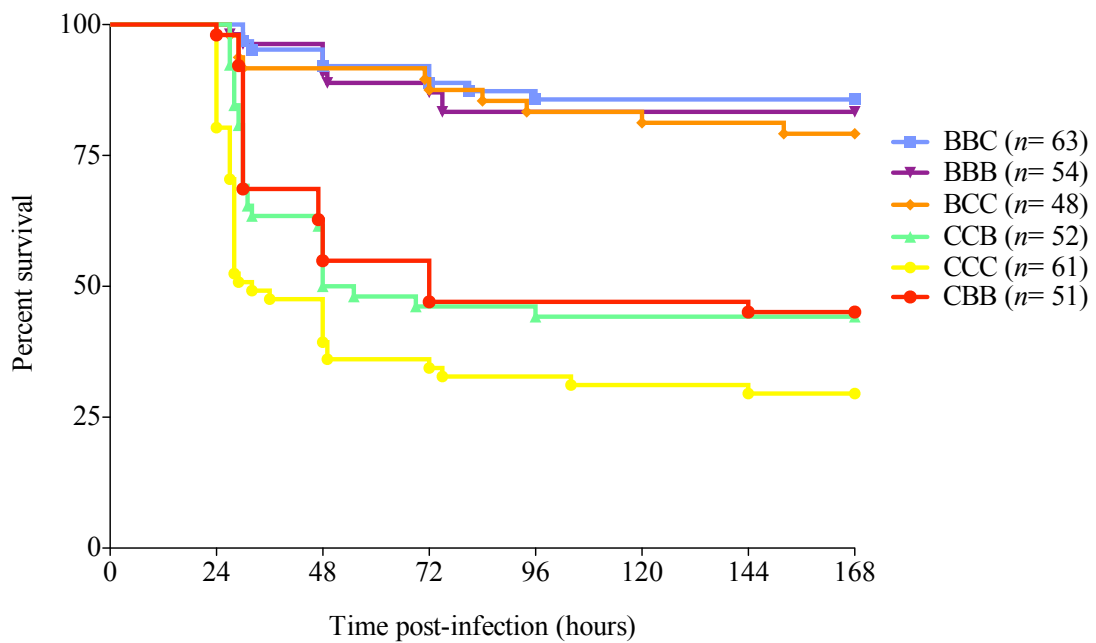


Figure 4.4 - Survival of *S. pneumoniae*-infected N<sub>10</sub> congenic lines. Each line represents a distinct N<sub>10</sub> congenic line. Mice from each congenic line (BBB, BBC, BCC, CCB, CBB and CCC) were intranasally infected with 10<sup>6</sup> CFU and monitored for up to 168 hours (7 days) post-infection. Each line represents the percentage of survival of a congenic line. The p-values were calculated by one-way ANOVA followed by Tukey's multiple comparison tests (Table 4.3).

Tukey's Multiple Comparison Test	Mean Diff.	q	Significant? P < 0.05?	Summary
BBB (54) vs BBC (63)	0.02381	0.4169	No	ns
BBB (54) vs BCC (48)	-0.04167	0.682	No	ns
BBB (54) vs CCC (61)	-0.5383	9.354	Yes	***
BBB (54) vs CCB (52)	-0.391	6.535	Yes	***
BBB (54) vs CBB (51)	-0.3824	6.358	Yes	***
BBC (63) vs BCC (48)	-0.06548	1.11	No	ns
BBC (63) vs CCC (61)	-0.5621	10.16	Yes	***
BBC (63) vs CCB (52)	-0.4148	7.189	Yes	***
BBC (63) vs CBB (51)	-0.4062	7.001	Yes	***
BCC (48) vs CCC (61)	-0.4966	8.357	Yes	***
BCC (48) vs CCB (52)	-0.3494	5.667	Yes	**
BCC (48) vs CBB (51)	-0.3407	5.501	Yes	**
CCC (61) vs CCB (52)	0.1472	2.533	No	ns
CCC (61) vs CBB (51)	0.1559	2.668	No	ns
CCB (52) vs CBB (51)	0.008673	0.1429	No	ns

Table 4.3 - Tukey's multiple comparison tests of survival of *S. pneumoniae*-infected N<sub>10</sub> congenic lines. The p-values (ns, not significant; \*\*, P < 0.01; \*\*\*, P < 0.001) were calculated with Tukey's multiple comparison test between all the combinations of congenic lines.

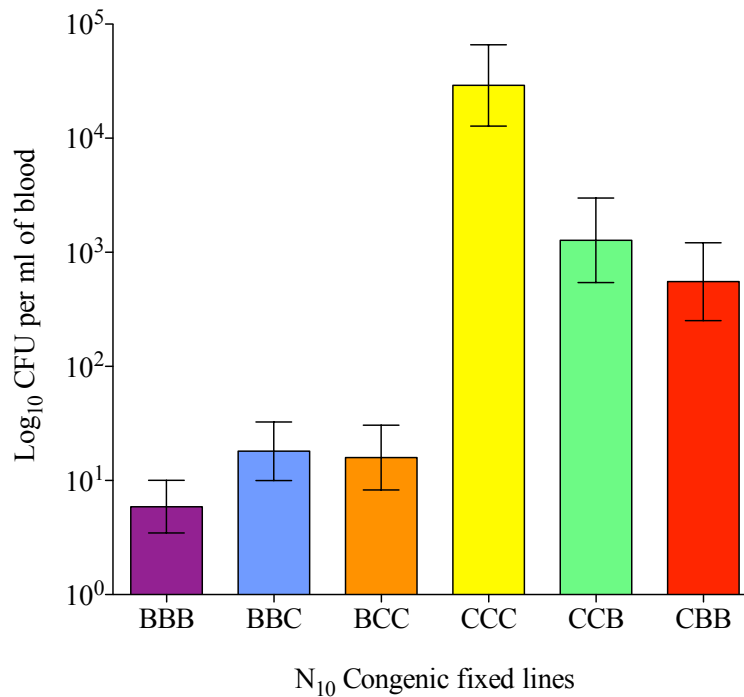


Figure 4.5 - Number of bacteria per ml blood assessed for each individual of the N<sub>10</sub> congenic lines at 24 hour post-infection. Mice from each congenic line (BBB, BBC, BCC, CCB, CBB and CCC) were intranasally infected with 10<sup>6</sup> CFU and blood was collected by tail-vein at 24 hours post-infection for determination of bacterial counts. Each bar represent the mean ± SEM of log<sub>10</sub> CFU per ml of blood of a congenic line. The p-values were calculated by one-way ANOVA followed by Bonferroni's multiple comparison tests (Table 4.4).

Bonferroni's Multiple Comparison Test	Mean Diff.	<i>t</i>	Significant? P < 0.05?	Summary
BBB vs BBC	-0.4863	1.137	No	ns
BBB vs BCC	-0.4314	0.9427	No	ns
BBB vs CCC	-3.693	8.566	Yes	***
BBB vs CCB	-2.336	5.211	Yes	***
BBB vs CBB	-1.971	4.375	Yes	***
BBC vs BCC	0.05489	0.1242	No	ns
BBC vs CCC	-3.206	7.737	Yes	***
BBC vs CCB	-1.849	4.278	Yes	***
BBC vs CBB	-1.485	3.416	Yes	*
BCC vs CCC	-3.261	7.326	Yes	***
BCC vs CCB	-1.904	4.124	Yes	***
BCC vs CBB	-1.54	3.318	Yes	*
CCC vs CCB	1.357	3.116	Yes	*
CCC vs CBB	1.721	3.933	Yes	**
CCB vs CBB	0.3646	0.8019	No	ns

Table 4.4 - Bonferroni's multiple comparison tests of bacteraemia at 24 hours *S. pneumoniae*-infected N<sub>10</sub> congenic lines. The p-values (ns, not significant; \*, *P* < 0.05; \*\*, *P* < 0.01; \*\*\*, *P* < 0.001) were calculated with Bonferroni's multiple comparison test between all the combinations of congenic lines.

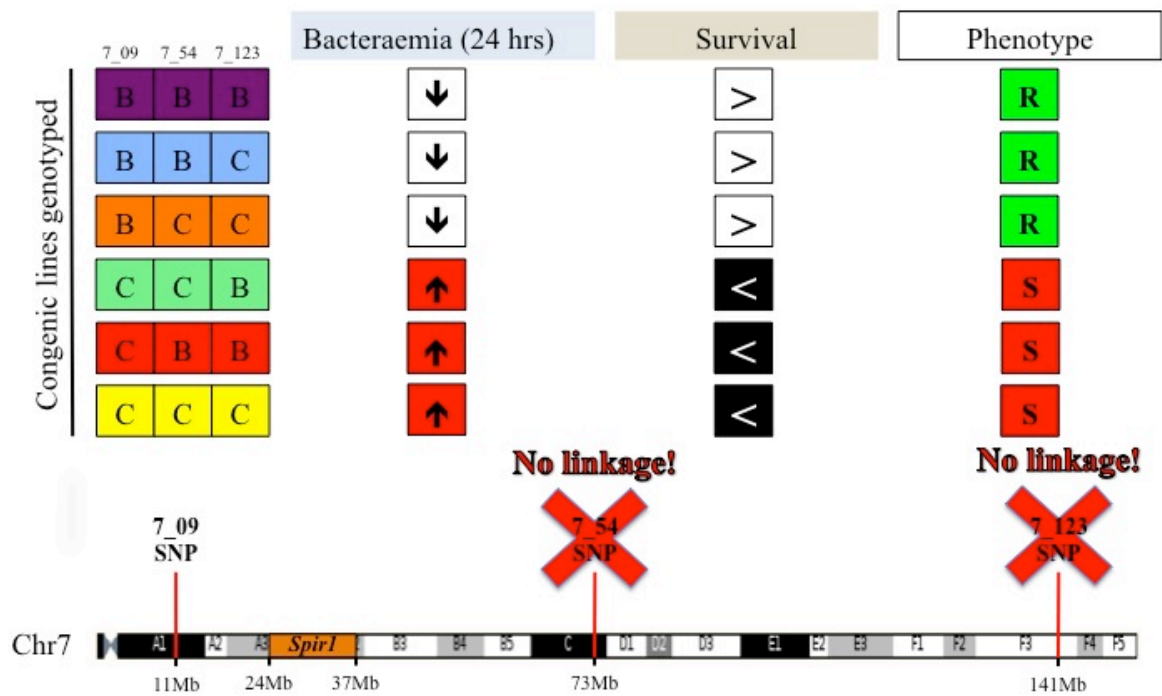


Figure 4.6 - Illustration of linkage between survival, bacteraemia at 24 hours post-infection and the 7\_09 marker. Mice from each congenic line (BBB, BBC, BCC, CCB, CBB and CCC) were intranasally infected with  $10^6$  CFU and blood was collected by tail-vein at 24 hours post-infection for determination of bacterial counts. In the top of the figure, a table with all the congenic lines and the description of the phenotype observed: bacteraemia at 24 hours post-infection was measured as low (↓) or high (↑), percent survival was considered as short (≡) or long (>) term, and the congenic line phenotyping was a combination of the survival rate and bacteraemia at 24 hours post-infection – resistant (R) or susceptible (S) phenotype. In the bottom of the figure, a scheme of the chromosome 7 arm, containing the three SNP markers (7\_09, 7\_54 and 7\_123) used to mapping the susceptibility QTL, and the *Spir1* region (orange box between 24 and 37 Mb), associated with the highest peak of correlation between phenotype and genotype (Denny *et al.*, 2003).

To narrow down the QTL and subsequently reduce the number of candidate genes contributing to resistance or susceptibility to invasive pneumococcal disease, an additional number of single nucleotide polymorphisms (SNPs) between BALB/c and CBA/Ca were tested. An additional set of SNP markers between BALB/c and CBA/Ca mouse strains was used to narrow areas of suggestive linkage in chromosome 7.  $N_{10}$  congenic fixed lines were re-typed at 10 additional SNP positions, using the pyrosequencer. Therefore, 10 additional SNPs between BALB/c and CBA/Ca were investigated on the congenic lines phenotyped (BBB, BBC, BCC, CCB, CBB and CCC line), as shown in Figure 4.7.

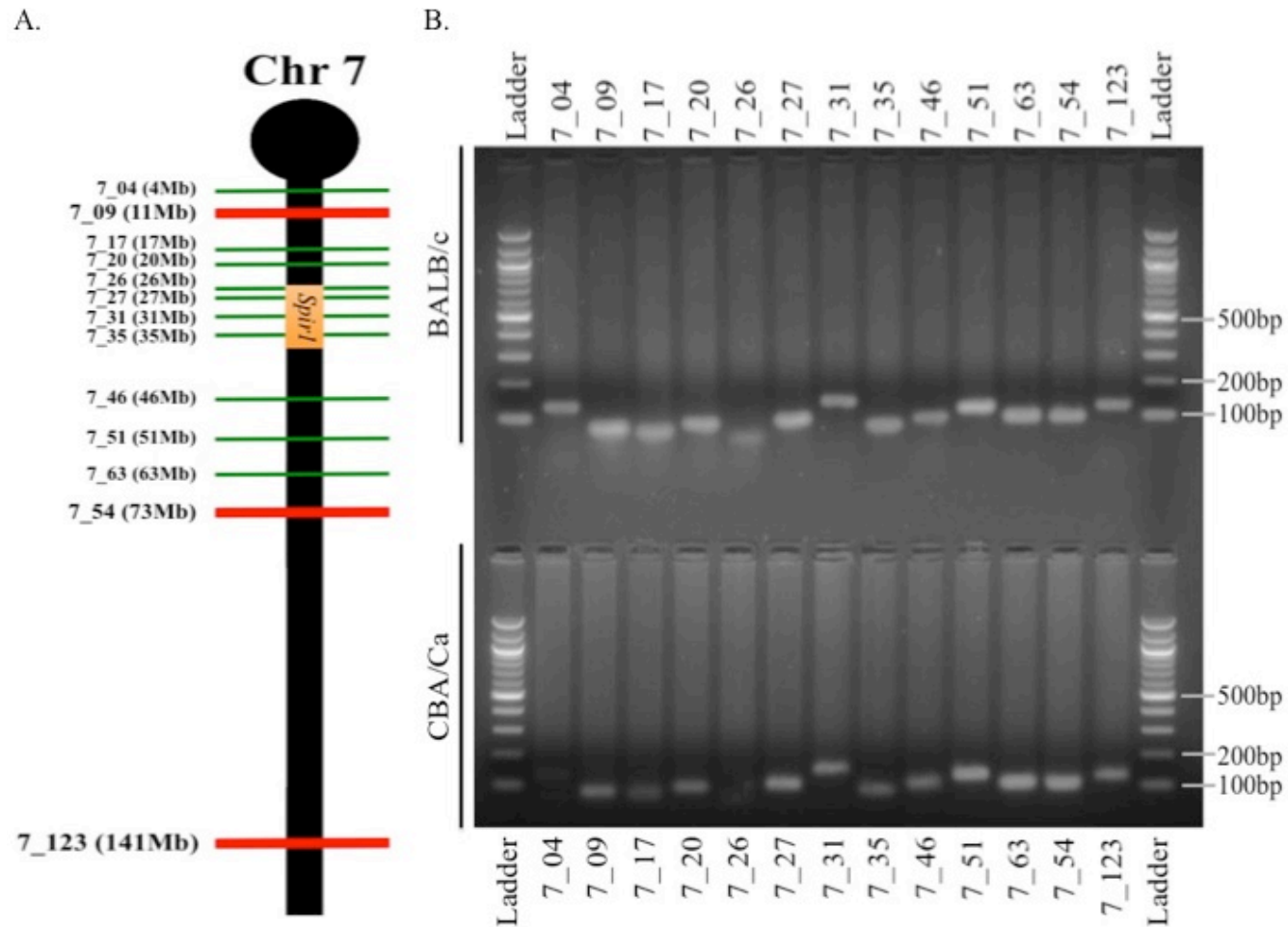


Figure 4.7 - Additional SNP markers used to narrowing-down the QTL. (A) SNP markers used for genotyping the *Spir1* congenic progeny for QTL mapping and their distribution across chromosome 7 (red bars represent each SNP location). The orange box indicates the *Spir1* region (between 24 and 37Mb). (B) Example of agarose gel electrophoresis, treated with Ethidium bromide, used to testing each of the SNP markers (7\_09, 7\_54 and 7\_123) on BALB/c and CBA/Ca DNA template, prior to pyrosequencing of PCR products (also represented in Figure 4.1). The additional SNP markers in the figure (7\_04, 7\_17, 7\_20, 7\_25, 7\_27, 7\_31, 7\_35, 7\_46, 7\_51 and 7\_63) were used to narrow down the *Spir1* QTL (Figure 4.7) and described with more detail further on in this chapter. Picture was taken under UV light conditions and shows PCR products for all markers. PCR products size was compared to the 100bp DNA ladder (molecular marker). All PCR products in the figure were amplified as described in section 2.4.1.2.

An interesting observation was the fact that the two complementary congenic lines (BCC and CBB), showed the highest number of regions of recombination, as illustrated in Figure 4.8 (relevant data in Appendix 4). The BCC line had a region of recombination downstream of the *Spir1* region, at the markers 7\_46, 7\_51 and 7\_63, and the CBB line had the highest level of recombination at the SNPs located within the *Spir1* region, at the markers 7\_27, 7\_31 and 7\_35 (Figure 4.8). The absence of detected recombination events in the majority of the congenic strains (BBB, BBC, CCC and CCB lines) reduced the chances of narrowing the QTL of susceptibility to IPD. The two complementary congenic strains – BCC and CBB lines – had long regions of recombination (Figure 4.8), in the BCC line the region of recombination is downstream the *Spir1* region (7\_46, 7\_51 and 7\_63 SNPs) and in the CBB line the region of recombination is within the *Spir1* locus (7\_27, 7\_31 and 7\_35 SNPs).

Chromosome 7 SNP markers														
Congenic Line	7_04	7_09	7_17	7_20	7_26	7_27	7_31	7_35	7_46	7_51	7_63	7_54	7_123	No. of mice phenotyped
BBB	B	B	B	B	B	B	B	B	B	B	B	B	B	54
BBC	B	B	B	B	B	B	B	B	B	B	B	B	C	63
BCC	B	B	B	B	B	B	B	B	B HET C	B HET C	B HET C	C	C	48
CCC	C	C	C	C	C	C	C	C	C	C	HET C	C	C	61
CCB	B	C	C	C	C	C	C	C	C	C	HET C	C	B	52
CBB	HET C	C	C	C	C	B HET C	B HET C	B HET C	B C	B C	B	B	B	51
						<i>Spir1</i> region								

Figure 4.8 - Genotype of the congenic lines at each SNP tested. DNA samples from each of the phenotyped congenic mice were retyped at 10 additional SNPs (7\_04, 7\_17, 7\_20, 7\_26, 7\_27, 7\_31, 7\_35, 7\_46, 7\_51 and 7\_63 marker). The labels “HET C” (found in the SNP 7\_04 of CBB congenic lines), “HET C” (found in the SNP 7\_63 of CCC and CCB congenic lines), “B C” (mice showing predominantly CBA/Ca DNA at the SNP) and “B C” (mice showing predominantly BALB/c DNA at the SNP) (found in the SNP 7\_46 and 7\_51 of CBB congenic line), “B HET C” (found in the SNPs 7\_27, 7\_31, 7\_35 of BCC congenic line and 7\_46, 7\_51 and 7\_63 CBB congenic lines) indicate the number of copies from a background: “B” homozygous BALB/c, “C” homozygous CBA/Ca and “HET” one copy from BALB/c and one copy from CBA/Ca (heterozygous). The *Spir1* region (orange box) covers 4 of the SNPs (7\_26, 7\_27, 7\_31, 7\_35 markers). Supporting data in Appendix 4.

The results obtained on the re-typing of the congenic lines with these additional markers (see Appendix 4) showed that two of the ten SNP markers used, 7\_04 and 7\_26 SNPs, failed in most of the samples pyrosequenced and were excluded from the analysis. Further analysis was done with the additional SNPs used. It was investigated whether having BALB/c or CBA/Ca at a particular SNP would determine resistance or susceptibility to pneumococcal infection in terms of survival (Figure 4.9 and Figure 4.10-A) and 24 hours bacteraemia (Figure 4.10-B) of the congenic mice.

In Figure 4.9 a very significantly different survival curve ( $P < 0.001$ ) can be observed between BALB/c and CBA/Ca at SNPs 7\_09, 7\_17, 7\_20, 7\_25, 7\_27, 7\_31, 7\_35, 7\_46 and 7\_51 and also a significantly different survival curve ( $P < 0.01$ ) at SNPs 7\_63 and 7\_54. Differences were not significant ( $P > 0.05$ ) at SNP 7\_123. The subsequent figure (Figure 4.10-A) represents all survival curves of the tested SNPs in one plot. A variation of the survival curves was observed that depends on the presence of BALB/c or CBA/Ca at a particular SNP. Strikingly, the curves showing lower percentages of survival were composed of congenic mice more susceptible (survival curves highlighted in Figure 4.10-A with a “S” for susceptible) having CBA/Ca DNA at SNP positions 7\_09, 7\_17, 7\_27, 7\_31, 7\_35 and 7\_46. This correlation between a CBA/Ca SNP at these positions and a susceptible phenotype was also supported by the data in Figure 4.11. The N<sub>10</sub> congenic mice were also analysed for association between 24 hours bacteraemia and all the SNP markers tested (Figure 4.10-B), except for 7\_04 and 7\_26 SNPs. Figure 4.10-B showed that congenic animals with CBA/Ca observed SNP at the positions tested had significantly higher bacteraemia ( $P < 0.001$ ) than mice with BALB/c SNP at the same position (SNPs 7\_09, 7\_17, 7\_20, 7\_27, 7\_31, 7\_35, 7\_46, 7\_51, 7\_63 and 7\_54), except for SNP 7\_123 where no significant difference was observed ( $P > 0.05$ ).

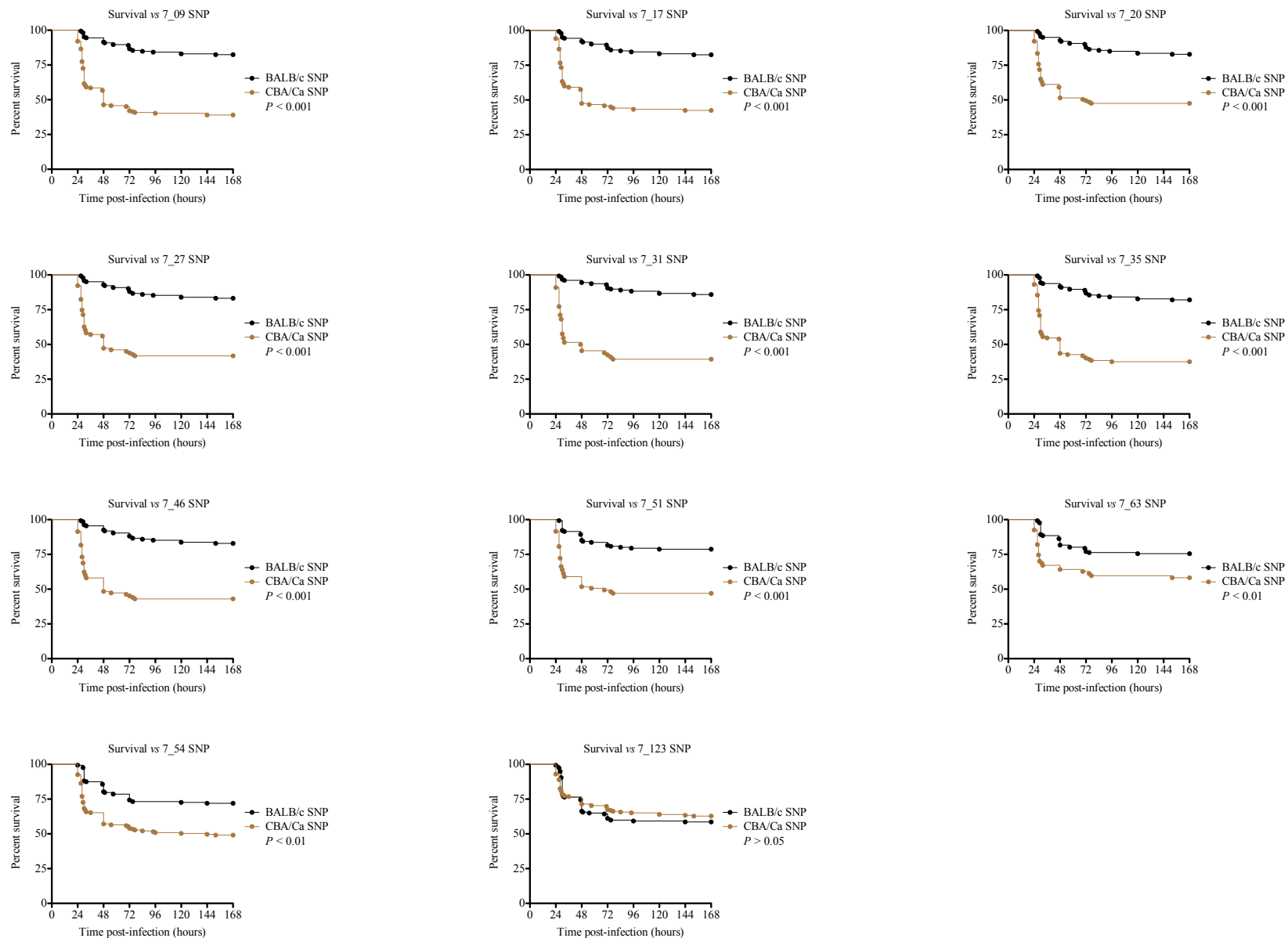
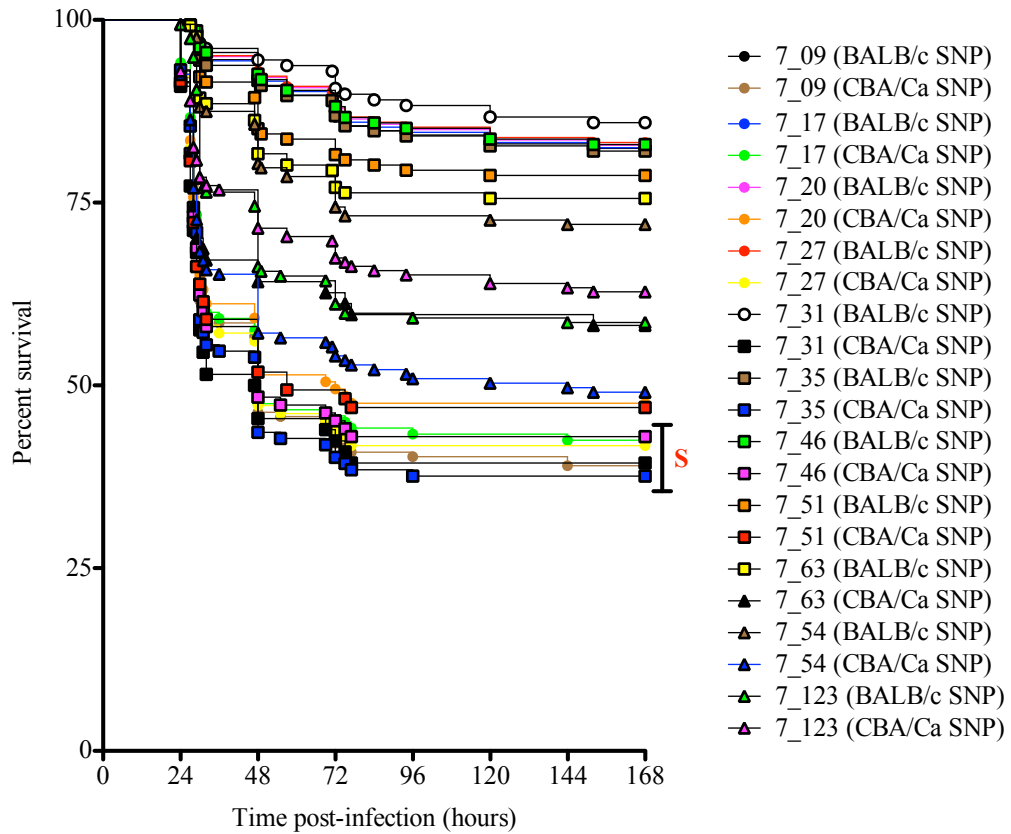


Figure 4.9 - Survival of the phenotyped congenic lines at each tested SNP in chromosome 7. N<sub>10</sub> congenic mice from each congenic line (BBB, BBC, BCC, CCB, CBB and CCC) were intranasally infected with 10<sup>6</sup> CFU and monitored for up to 168 hours (7 days) post-infection. Each graph in the figure represents the percentage of survival for each SNP marker genotyped (7\_09, 7\_17, 7\_20, 7\_27, 7\_31, 7\_35, 7\_46, 7\_51, 7\_63, 7\_54 and 7\_123). The p-values were calculated by means of the log-rank (Mantel-Cox) test.

A.



B.

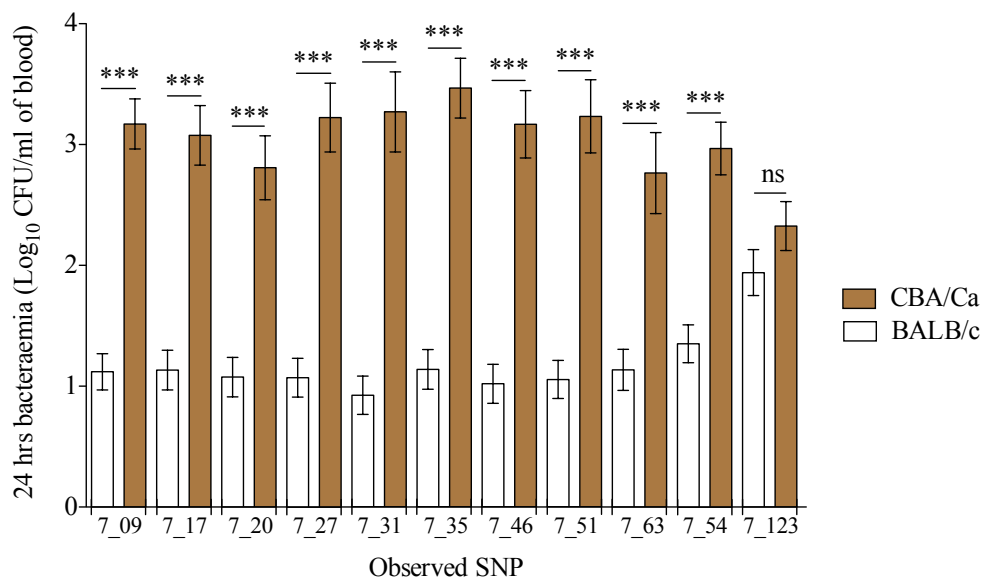


Figure 4.10 - Survival curves and 24 hours bacteraemia analysed for all SNPs used in the congenic study. N<sub>10</sub> congenic mice from each congenic line (BBB, BBC, BCC, CCB, CBB and CCC) were intranasally infected with 10<sup>6</sup> CFU of *S. pneumoniae* and monitored for up to 168 hours (7 days) post-infection. (A) Each curve in the figure represents the percentage of survival for each SNP marker genotyped (7\_09, 7\_17, 7\_20, 7\_27, 7\_31, 7\_35, 7\_46, 7\_51, 7\_63, 7\_54 and 7\_123). The survival curves in the area coded as “S” were considered susceptible. (B) Mean number of bacteria at 24 hours post-infection analysed for all SNP markers (between BALB/c and CBA/Ca) of the congenic mice. The p-values on graph (B) (\*\*\*, *P* < 0.001) were obtained by one-way ANOVA followed by Bonferroni post-test.

The data plotted on Figure 4.9 and Figure 4.10 were then analysed to look for a correlation between both survival time and 24 hours bacteraemia of the phenotyped N<sub>10</sub> congenic mice and a specific or multiple SNPs (Figure 4.11). Interestingly, a correlation between genotype and phenotype during pneumococcal pneumonia was observed. Three distinct groups were found in this correlation (Figure 4.11-A): a cluster of resistant mice (coded in the figure as “R”), where the animals shared the same SNP variation (BALB/c) and had long term survival and low bacteraemia at 24 hours post-infection (approximately 1 Log<sub>10</sub> CFU/ml of blood); a cluster of susceptible mice (coded in the figure as “S”), where the animals shared the same SNP variation (CBA/Ca) and had short term survival and high bacteraemia at 24 hours post-infection (higher than 3 Log<sub>10</sub> CFU/ml of blood); and also a dispersed group, where the animals have intermediate resistance. Further analysis by removing the group of intermediate resistance mice (Figure 4.11-B), showed an increase on the correlation (from R<sup>2</sup>= 0.9299 observed in Figure 4.11-A to R<sup>2</sup>= 0.9950 observed in Figure 4.11-B). As the aim of this investigation was to study and identify genes in this chromosome 7 region contributing to susceptibility (not resistance), therefore, the SNPs in the susceptible cluster, which exhibited the CBA/Ca variation SNPs (7\_09, 7\_17, 7\_27, 7\_31, 7\_35, 7\_46, 7\_51 gated in the “S” coded area) represented a very positive result and are a target for further studies.

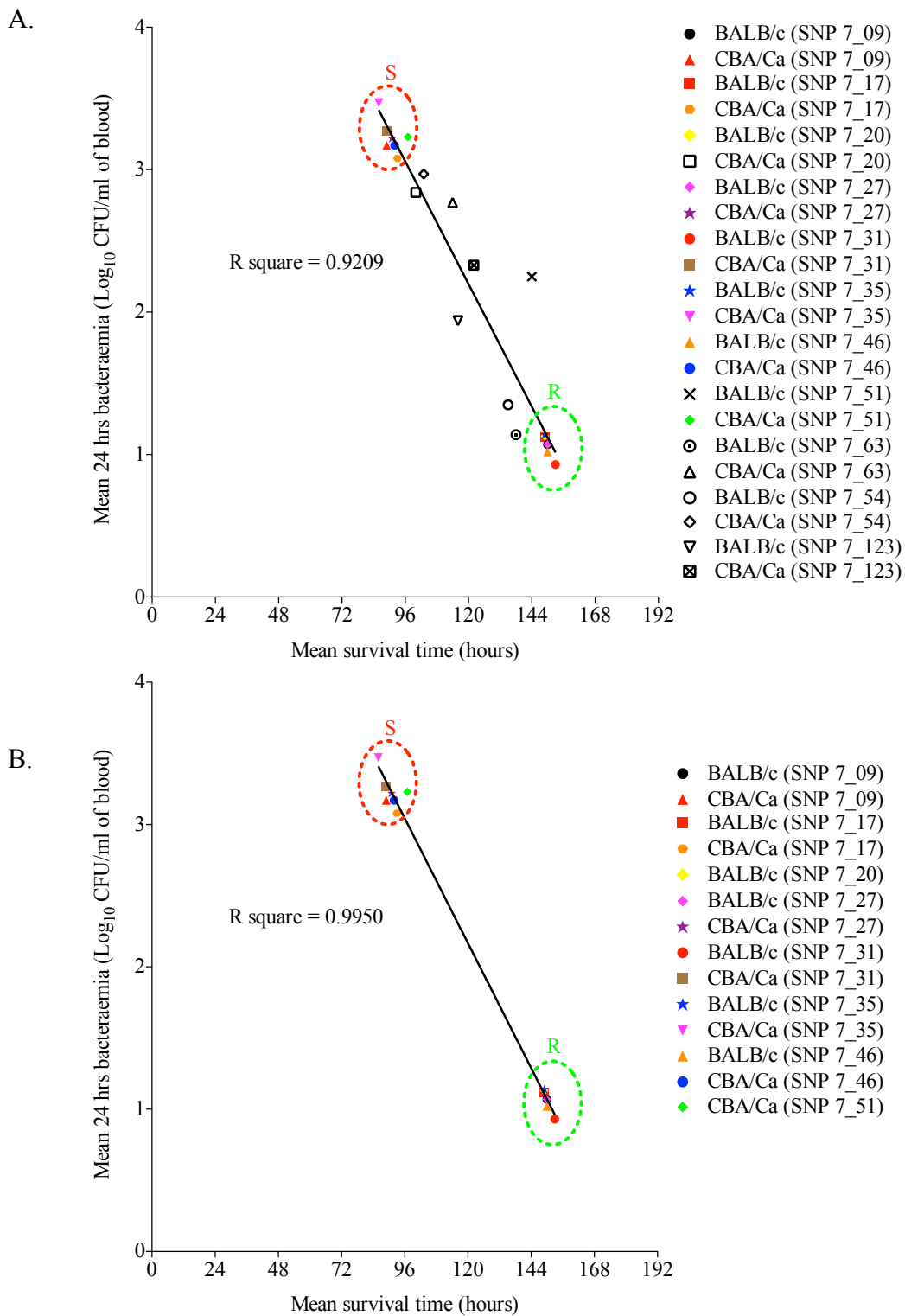


Figure 4.11 - Correlation between mean 24 hours bacteraemia and mean survival time of each congenic line infected with *S. pneumoniae*. Each dot represent the mean of 24 hours bacteraemia and mean of survival time per congenic line at the SNP markers tested (SNPs 7\_09, 7\_17, 7\_20, 7\_27, 7\_31, 7\_35, 7\_46, 7\_51, 7\_63, 7\_54 and 7\_123). The dashed areas were gating SNP markers linked to susceptibility (coded as “S”) and resistant (coded as “R”). Figure (A) includes outliers in the analysis ( $R^2= 0.9299$ ) and figure (B) outliers were removed from the analysis ( $R^2= 0.9950$ ). The p-value (\*\*\*,  $P < 0.001$  for graphs A and B) was obtained by linear regression.

Generating the congenic strain (N<sub>10</sub> mice) and fixing each of the congenic lines (CCC, CCB, CBB, BBB, BBC and BCC lines) took approximately 4 years to conclude. In the meantime, each of the parental inbred mouse strains involved in the congenic programme (BALB/c and CBA/Ca strains) were immunophenotyped to investigate their immunological responses to *S. pneumoniae* infection and how those differences might explain the outcome of the infection. Furthermore, two genes located in the *Spir1* region, *tgfb1* (Chapter 5) and *cd22* (Chapter 6), were studied more closely to analyse the function of each of the gene during pneumococcal pneumonia infection.

---

## CHAPTER 5. TGF- $\beta$ and T regulatory cells control susceptibility to invasive pneumococcal infection in mice

---

### 5.1 Introduction

Determination of host protective immune responses to pneumococcal infection is highly desirable, not least because an improved understanding of the cellular and molecular interactions of host and pathogen might enable the design of specific, targeted therapies that are able to overcome the limitations of current treatment and prevention strategies.

Neutrophils are one of the primary mediators of early defence against pulmonary pneumococcal infection (Paterson & Orihuela, 2010; Buttery & Moxon, 2002; Kaplanski *et al.*, 2003) but more recently an additional key role for T cells against the pneumococcus has emerged. It has been noted that T cells infiltrate the lungs of intranasally-infected mice at an early time post-infection and that the peak of infiltration coincides with a cessation in pneumococcal growth in the lungs (Kadioglu *et al.*, 2000). Furthermore, it has been demonstrated that CD4<sup>+</sup> T cells contribute to protective immunity to invasive pneumococcal pneumonia, as MHC-II-deficient mice, which have severely reduced numbers of CD4<sup>+</sup> T cells, are highly susceptible to infection (Kadioglu *et al.*, 2004). However, whilst there is an expanding body of work outlining the roles of inflammatory T cell subsets (Haraguchi *et al.*, 1998; Groneck *et al.*, 2009; Wang *et al.*, 2010; McNeela *et al.*, 2010), little has been made of regulatory and anti-inflammatory T cells and their influence on the outcome of pneumococcal pneumonia. This is an important gap in the understanding of the immunology of pneumococcal disease.

Several immune cell types, including tolerogenic DCs (Fu *et al.*, 2009), myeloid suppressor cells (Nagaraj *et al.*, 2009), IL-10-producing CD4<sup>+</sup> T cells (Fujio *et al.*, 2010), B cells (Noh *et al.*, 2010) and Foxp3<sup>+</sup> T regulatory cells (Sakaguchi *et al.*, 2010), have confirmed roles in the modulation and inhibition of inflammation in the context of infection. Of these immunomodulatory cells, Foxp3<sup>+</sup> T regulatory cells are probably the best characterised. These cells have emerged as essential components of the mammalian immune system and play crucial roles in immune homeostasis as well as limiting infection-associated inflammation and facilitating resolution of tissue damage post-infection (Barnes & Powrie, 2009; Mills, 2004). Indeed, for West Nile Virus, a link

has been made between T regulatory cell activities and symptomatic versus asymptomatic infection (Lanteri *et al.*, 2009).

Little is known about the actions of immunomodulatory cytokines and T regulatory cells during infection with *S. pneumoniae*, but recent data suggest an importance of immunomodulation in anti-pneumococcal responses. Intraperitoneal administration of *S. pneumoniae* serotype 1 capsular polysaccharide induces CD8<sup>+</sup>CD28<sup>-</sup> T-cells with a regulatory phenotype that synthesise both IL-10 and TGF- $\beta$  and are immunosuppressive for CD4<sup>+</sup> T cells *in vivo* and *in vitro* (Mertens *et al.*, 2009). However, whether regulatory cells play protective roles during infection with invasive *S. pneumoniae* strains remained to be elucidated. Although it has previously been observed that CD25<sup>+</sup> T cells are induced during pneumococcal pneumonia (Kadioglu *et al.*, 2004) and that the administration of heat-killed *S. pneumoniae* to mice can suppress allergic airway disease by the induction of T regulatory cell expansion (Preston *et al.*, 2011), the studies here reported now provide new evidence for the important protective role performed by T regulatory cells in an *in vivo* model of invasive pneumococcal pneumonia.

The need to address the role of immunomodulatory cells and cytokines in pneumococcal infection is pressing, not least because it is unclear at present whether their actions are protective or detrimental to the outcome of infection. For example, IL-10 is a cytokine produced by T regulatory cells that plays key protective roles in limiting inflammation in a number of diseases (such as influenza) through its inhibitory effects on immune cells, but it has also been shown to impair defense mechanisms in pneumococcal pneumonia (albeit post-influenza infection) (van der Sluijs *et al.*, 2004). In a recent study, adenoidal cells from children testing positive for pneumococcal carriage were found to contain higher numbers of Foxp3<sup>+</sup> T regulatory cells than those taken from children without pneumococcal carriage suggesting an immunosuppressive role for these cells (Zhang *et al.*, 2011). Furthermore, *in vitro*, pneumococcal whole cell antigen induced T regulatory cell proliferation and production of IL-10 by adenoidal mononuclear cells from children (Zhang *et al.*, 2011). In this work, the role of T regulatory cells *in vivo* during invasive pneumococcal pneumonia was addressed.

To determine the involvement of T regulatory cells and immunomodulatory cytokines in resistance to pneumococcal infection, BALB/c and CBA/Ca inbred mouse strains that

have strikingly different susceptibility to pneumococcal pneumonia (Gingles *et al.*, 2001; Denny *et al.*, 2003; and this work) were utilised in these studies. As previously stated in this thesis, BALB/c mice are highly resistant to respiratory infection against a wide range of invasive pneumococci and confine their infection to the lung (without developing sepsis) and then eliminate it within 7 days. By contrast, CBA/Ca mice succumb quickly to respiratory infection, developing septicaemia and dying within 24 hours of infection (Gingles *et al.*, 2001). These significantly different phenotypes logically imply qualitatively distinct immune responses. To quantify the contribution of likely candidates, the influence of the cytokines IL-10 and TGF- $\beta$ , as well as the importance of T regulatory cell population will be investigated next.

## 5.2 Aims

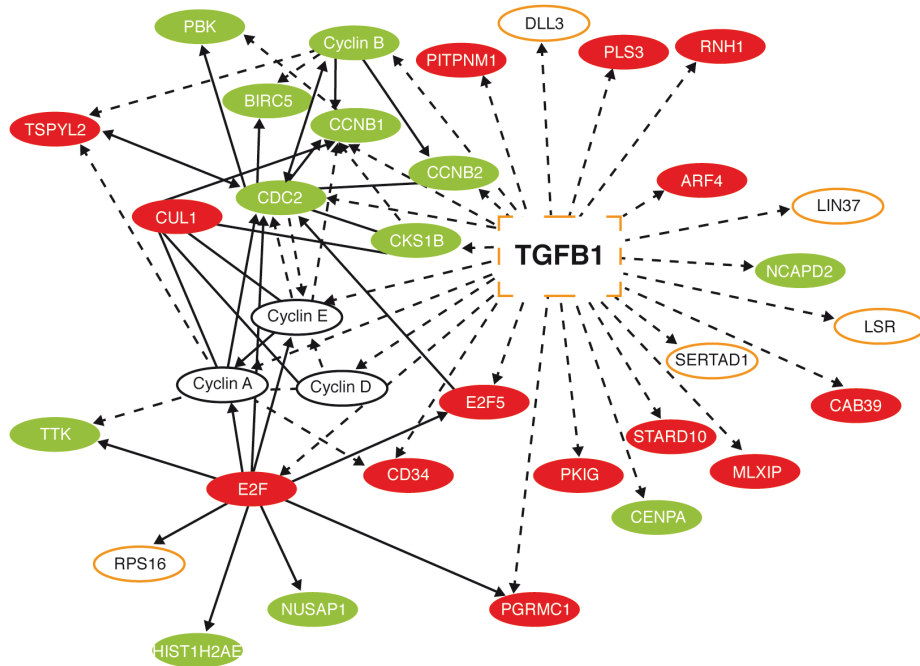
The gene *tgfb1* is located on chromosome 7 (~25Mb), within the *Spir1* locus, located between 7\_20 and 7\_27 SNPs used in the N<sub>10</sub> congenic mice phenotyping. This prompted investigation of the contribution of TGF- $\beta$  and its downstream target, namely T regulatory cells to the differing susceptibilities of BALB/c and CBA/Ca mice to pneumococcal disease. The data presented in this chapter (Chapter 5) were published in *Plos Pathogens* (Neill *et al.*, 2012).

## 5.3 Results

### 5.3.1 TGF- $\beta$ signalling is regulated differentially in BALB/c and CBA/Ca mice during pneumococcal pneumonia

In a preliminary study, involving gene expression profiling, signaling pathways analysis, quantitative real-time PCR (qRT-PCR) and immunohistochemical analysis of BALB/c and CBA/Ca lung tissue, were performed by a collaborator Laura Wisby (MRC Harwell, Oxfordshire). Microarray comparison of gene expression in lung tissue from BALB/c or CBA/Ca mice, following intranasal infection with *S. pneumoniae*, indicated significant differential regulation of the TGF- $\beta$  signalling pathway between the two strains (Figure 5.1 - performed by a collaborator, Laura Wisby). At 6 hours post-infection many of the interaction partners of *tgfb1* showed opposing regulation in BALB/c and CBA/Ca mice (for example *e2f* and *e2f5* were upregulated and *cks1b* and *hist1h2ae* downregulated in BALB/c).

A.



B.

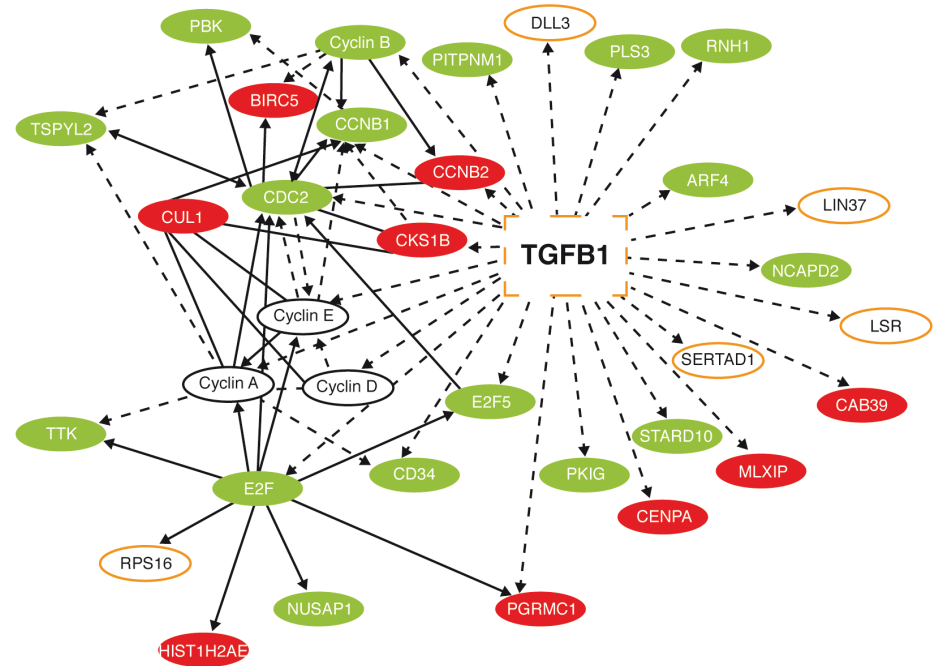


Figure 5.1 - Microarray comparison of gene expression in the lung tissue indicated differential regulation of TGF- $\beta$  signalling pathway between BALB/c and CBA/Ca mice following pneumococcal infection. High scoring network of interactions involving genes differentially expressed at 6 hours post-infection. Solid lines indicate direct interactions, dashed lines indicate indirect interactions. Genes outlined in orange are located in the *Spir1* locus. (A) Genes shaded in red are up regulated in BALB/c and those in green were down regulated in BALB/c in response to infection. (B) Genes shaded in red are up regulated in CBA/Ca and those in green were down regulated in CBA/Ca in response to infection.

Because TGF- $\beta$  and five of its interaction partners (*dll3*, *lin37*, *lsr*, *sertad1* and *rps16*) are found within the *Spir1* susceptibility locus (Figure 5.1) (Denny *et al.*, 2003), *tgfb1* was selected for further analysis. qRT-PCR analysis was performed on lung tissue from intranasally-infected BALB/c and CBA/Ca mice to determine *tgfb1* expression over the course of pneumococcal pneumonia. Importantly, expression of *tgfb1* was significantly higher in BALB/c than in CBA/Ca mice both before infection and at 6 hours p.i. (Figure 5.2-A and -B - performed by a collaborator, Laura Wisby).

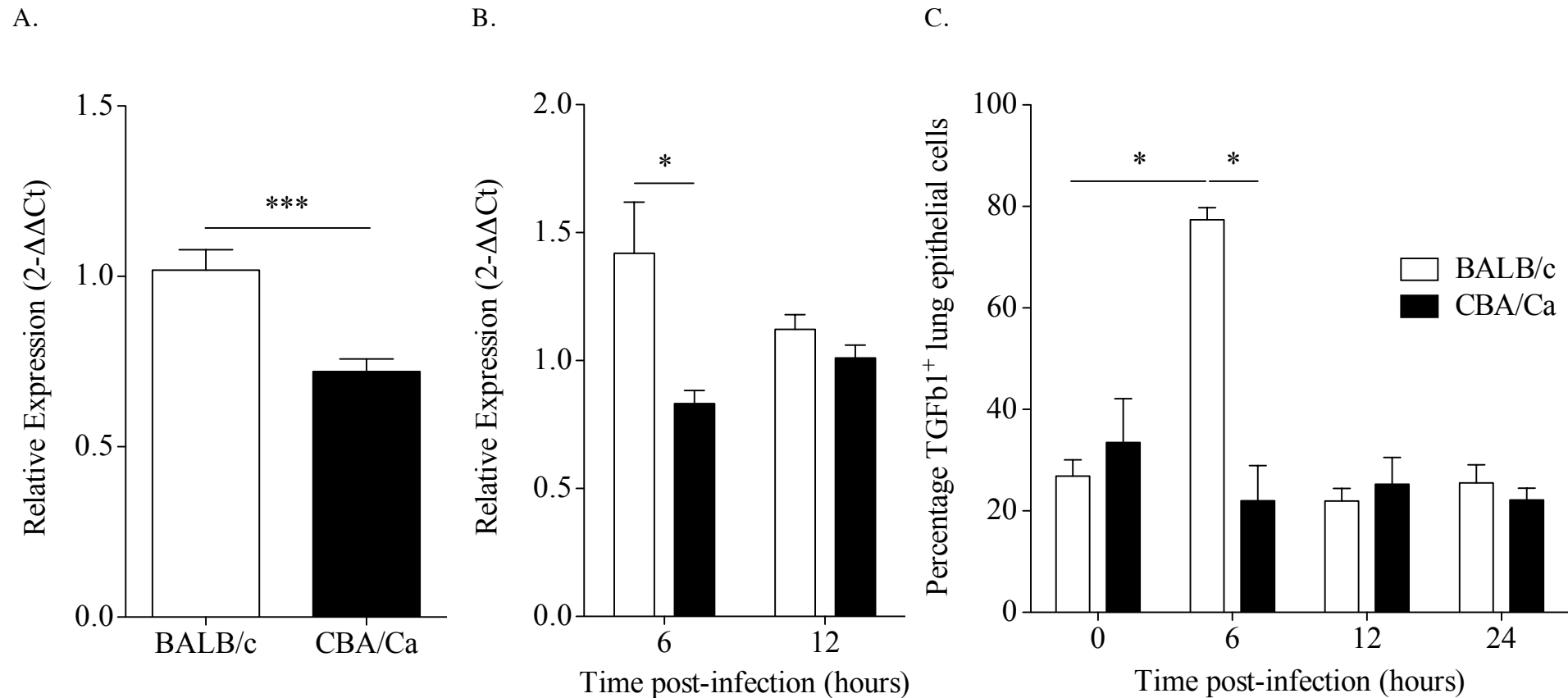


Figure 5.2 - *tgfb1* expression and TGF- $\beta$  production is upregulated in BALB/c lungs in contrast to CBA/Ca lungs during pneumococcal infection. Relative gene expression of *tgfb1* in lungs of BALB/c and CBA/Ca mice before (A) and during (B) pneumococcal infection. Data were normalised against a housekeeping gene (*hprt1*) and are presented using BALB/c results as a calibrator (A) or else using BALB/c or CBA/Ca sham-infection data from the appropriate time-point as calibrators (B). For 6 and 12 hours p.i. data for each strain was calibrated against sham-infection data for that strain at the same time-point. i.e. BALB/c to BALB/c sham and CBA/Ca to CBA/Ca sham. (C) Antibody staining of TGF- $\beta$  in airway epithelial cells from BALB/c and CBA/Ca mice during pneumococcal infection. The p-values (\*,  $P < 0.05$ ; \*\*\*,  $P < 0.005$ ) were obtained with unpaired two-tailed Student *t* test (A) *t* test (B) and two-way ANOVA followed by Bonferroni post-test (C). For all figures data represent mean  $\pm$  SEM. Data are representative of two independent experiments with 5 mice per time-point per strain and per treatment group.

To investigate whether the observed differences in *tgfb1* gene expression were reflected in changes in TGF- $\beta$ 1 protein in the lungs, immunohistochemical analysis was performed on lung sections (Figure 5.2-C). A significant increase in the percentage of epithelial cells staining TGF- $\beta$ 1<sup>+</sup> in the lungs of BALB/c mice, but not CBA/Ca mice was observed between 0 and 6 hours p.i. Interestingly, the percentage of TGF- $\beta$ 1<sup>+</sup> epithelial cells in BALB/c lungs returned to pre-infection levels by 12 hours p.i., perhaps as the result of cleavage of active TGF- $\beta$  protein from the surface of the cells. These data indicate a rapid and robust increase in TGF- $\beta$ 1 synthesis and export by BALB/c airway epithelial cells in response to infection, which is absent in CBA/Ca mice.

### **5.3.2 BALB/c mice display a greater expansion and recruitment of Foxp3<sup>+</sup> cells to the lungs than CBA/Ca mice during pneumococcal infection**

T regulatory cells are both a source and a target of TGF- $\beta$ , so the numbers and function of these cells were investigated in the lungs of BALB/c and CBA/Ca mice before and during pneumococcal infection. Staining of lung tissue sections for Foxp3 (Figure 5.3), performed by a collaborator, Andrew Haynes (MRC Harwell, Oxfordshire), revealed no differences in the numbers of Foxp3<sup>+</sup> cells in the lungs of uninfected CBA/Ca and BALB/c mice but substantially increased numbers in BALB/c at both 12 and 24 hours p.i. ( $P < 0.05$ ), with no significant changes ( $P > 0.05$ ) apparent in the CBA/Ca strain (Figure 5.4).

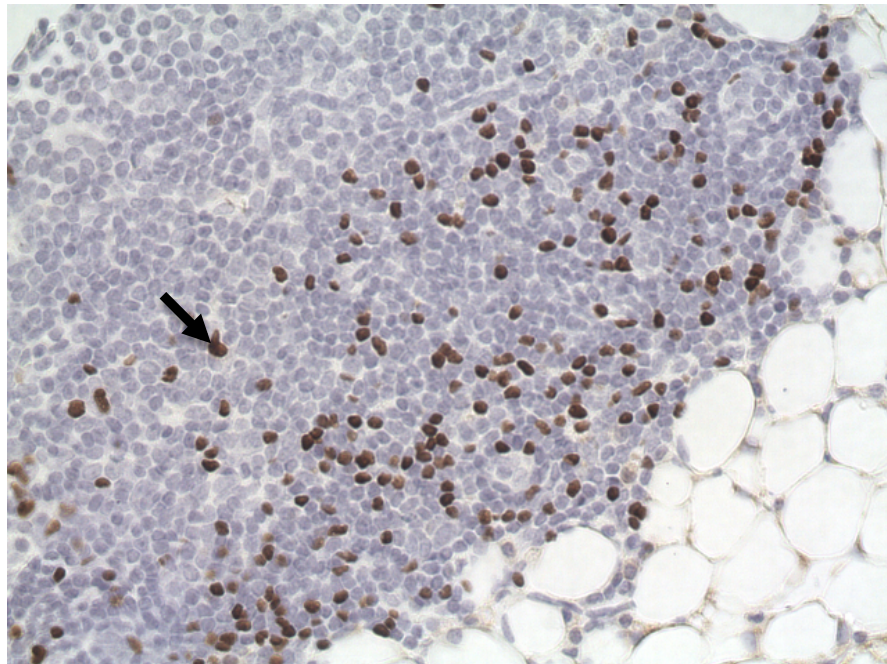


Figure 5.3 - Foxp3 immunostaining (DAB staining) of lung sections taken from mice during pneumococcal infection. Inset shows example staining from 12 hour BALB/c mouse. Foxp3<sup>+</sup> cells stain brown (arrow indicate a positive cell).

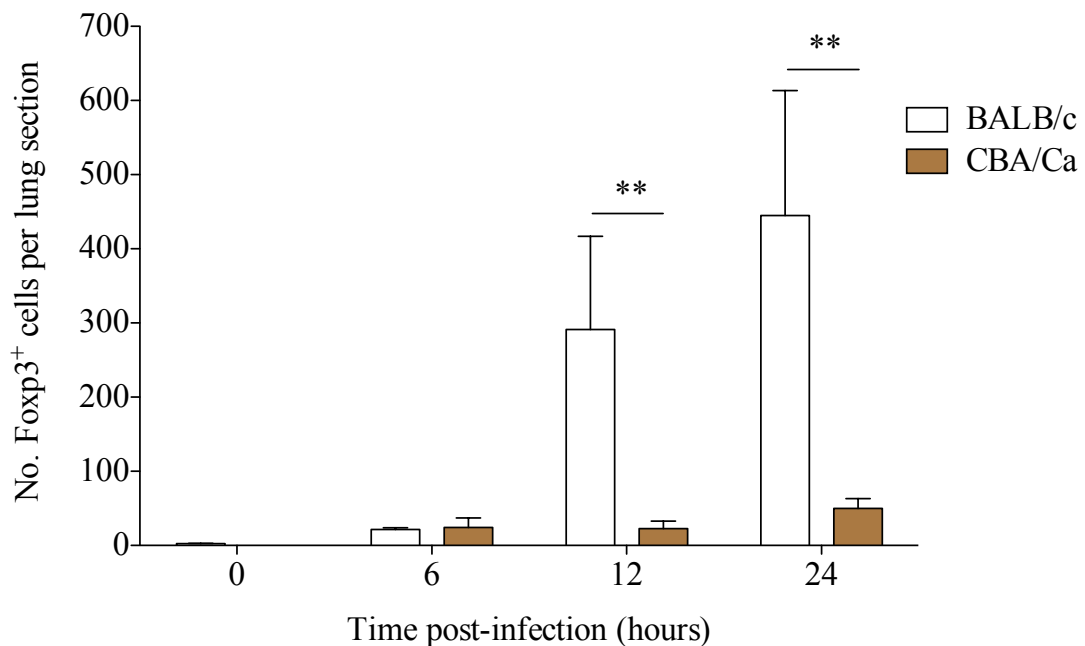


Figure 5.4 - Increase in Foxp3<sup>+</sup> T regulatory cells in BALB/c lungs over time post-infection. Mice were intranasally infected with 10<sup>6</sup> CFU and lungs were collected at 0, 6, 12 and 24 hours post-infection. Foxp3<sup>+</sup> T regulatory cells were counted from lung sections (3 slides per time point per strain, as shown in Figure 5.3) taken from BALB/c and CBA/Ca mice during pneumococcal infection. Data represent the mean of Foxp3<sup>+</sup> cells counted  $\pm$  SEM. The p-value (\*\*,  $P < 0.01$ ) was obtained with two-way ANOVA followed by Bonferroni post-test. Data are representative of two independent experiments with  $\geq 4$  mice per group.

The correlation between T regulatory cell numbers and the effectiveness of the immune response in the lung is readily apparent as bacterial CFUs in the lungs of BALB/c mice fell rapidly between 0 and 24 hours p.i., while bacterial numbers in CBA/Ca lungs increased over the same time period (Figure 3.1-C).

To further characterise Foxp3<sup>+</sup> cells identified in the lungs during pneumococcal infection, flow cytometry was performed on lung cells from infected mice. Intracellular staining for Foxp3 confirmed the immunohistochemistry finding that whilst there was no apparent difference in the number of T regulatory cells in the lungs of uninfected BALB/c and CBA/Ca mice (Figure 5.5), by 24 hours p.i. T regulatory cell numbers in the lungs had risen approximately 2.5-fold in BALB/c mice ( $P < 0.01$ ) but remained unchanged in CBA/Ca mice ( $P > 0.05$ ) (Figure 5.5).

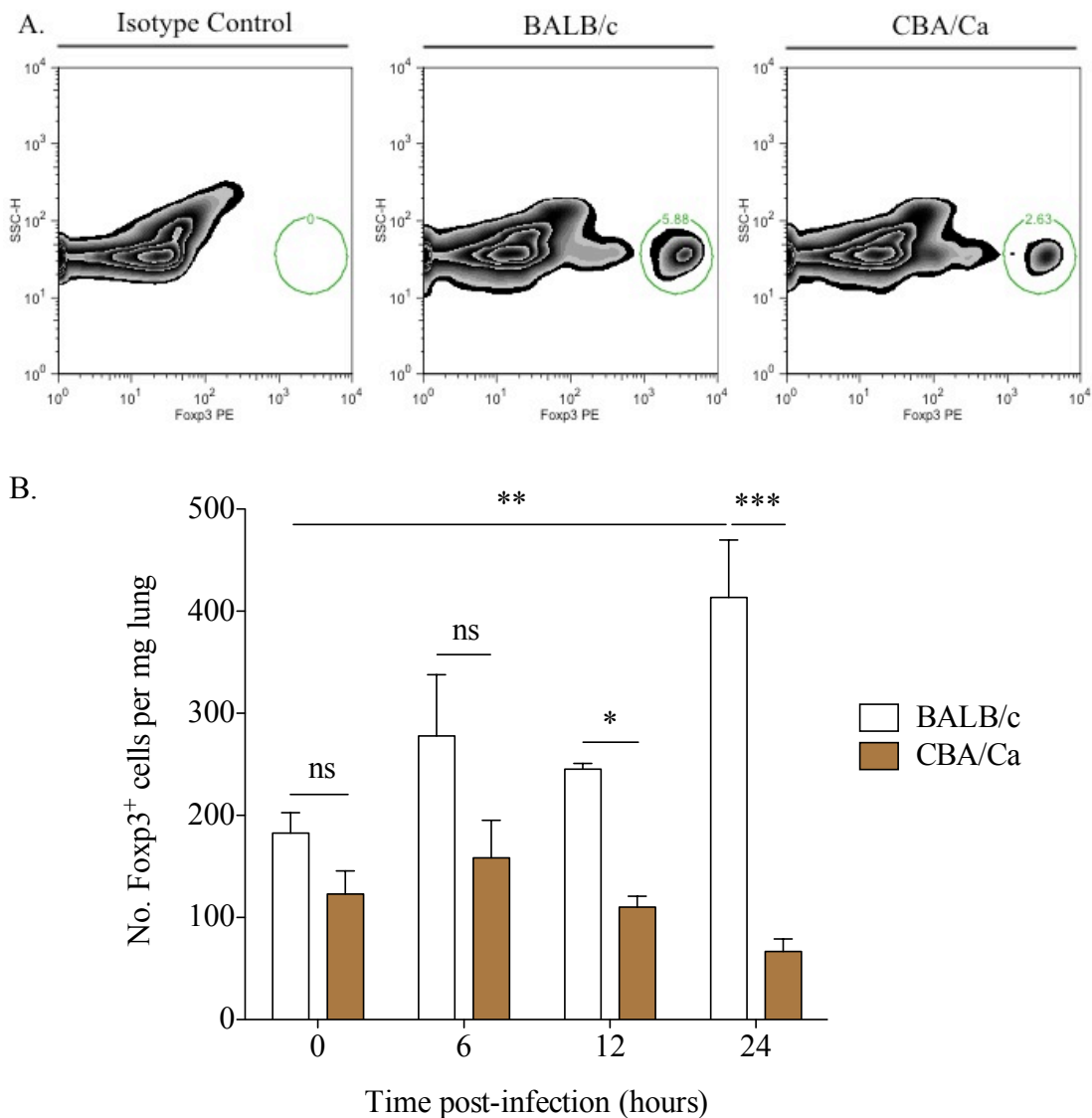


Figure 5.5 - Increase in Foxp3<sup>+</sup> T regulatory cells in BALB/c lungs at 24 hours post-infection. Mice were intranasally infected with 10<sup>6</sup> CFU and lungs were collected at 0, 6, 12 and 24 hours post-infection. (A) Flow cytometric analysis of T regulatory cells was determined by gating for CD45<sup>+</sup> CD4<sup>+</sup> Foxp3<sup>+</sup> events. (B) Number of T regulatory cells per mg of lung tissue, at the various time points, analysed by flow cytometry. Data represent the mean of positive events ± SEM. The p-values (\*,  $P < 0.05$ ; \*\*,  $P < 0.01$ ; \*\*\*,  $P < 0.001$ ) were obtained with two-way ANOVA followed by Bonferroni post-test. Data are representative of two independent experiments with ≥ 4 mice per group.

Regulatory T cells can develop in the thymus or from CD4<sup>+</sup> T cells in the periphery (Sakaguchi, 2003). The thymus-derived cells are commonly referred to as natural T regulatory cells (nT<sub>regs</sub>) and they can be distinguished from the cells developing in the periphery (induced T regulatory cells; iT<sub>regs</sub>) by their expression of the Ikaros family transcription factor Helios (Thornton *et al.*, 2010). Analysis of Helios expression in T

cells revealed that the increase in T regulatory cells in BALB/c lungs following *S. pneumoniae* infection was due to increased nTreg numbers (Figure 5.7). Foxp3<sup>+</sup> Helios<sup>+</sup> cells increased approximately 3-fold over the first 24 hours p.i. in BALB/c mice ( $P < 0.001$ ), but not CBA/Ca mice ( $P > 0.05$ ). By contrast, there was no significant increase ( $P > 0.05$ ) in Foxp3<sup>+</sup> Helios<sup>-</sup> cells in the lungs of either BALB/c or CBA/Ca mice (Figure 5.6).

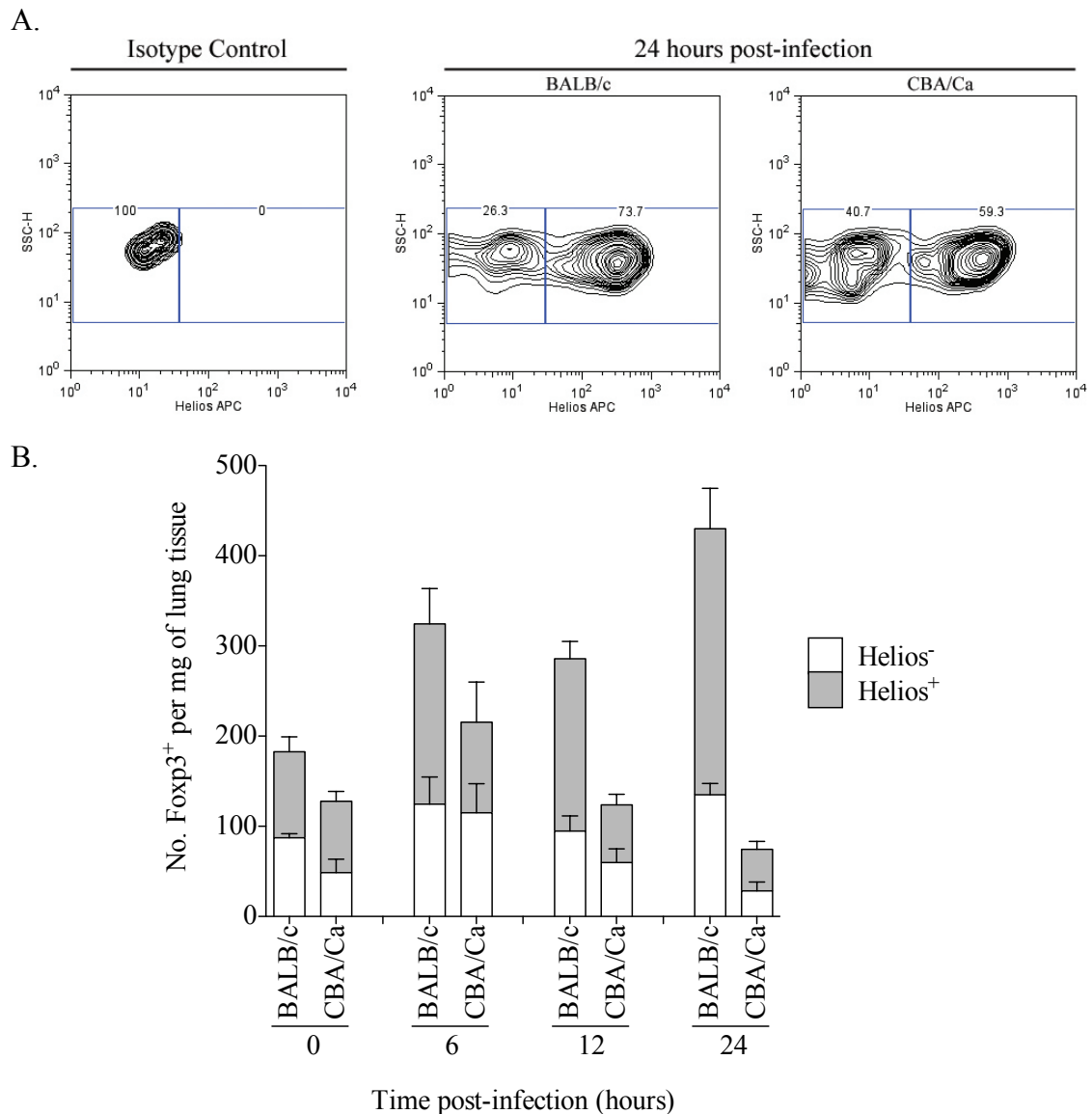


Figure 5.6 - Number of Helios<sup>+/-</sup> Foxp3<sup>+</sup> T regulatory cells in BALB/c and CBA/Ca lungs following pneumococcal infection. Mice were intranasally infected with 10<sup>6</sup> CFU and lungs were collected at 0, 6, 12 and 24 hours post-infection. (A) Flow cytometric analysis of Helios<sup>-</sup> (left gate) and Helios<sup>+</sup> (right gate) foxp3<sup>+</sup> T regulatory cells was determined by gating for CD45<sup>+</sup>, Foxp3<sup>+</sup> and finally Helios<sup>-</sup> and Helios<sup>+</sup> events. (B) Number of Helios<sup>-</sup> (grey area of bars) and Helios<sup>+</sup> (white area of bars) T regulatory cells per mg of lung tissue, at the various time points, analysed by flow cytometry. Data represent the mean of positive events  $\pm$  SEM. Data are representative of two independent experiments with  $\geq 4$  mice per group.

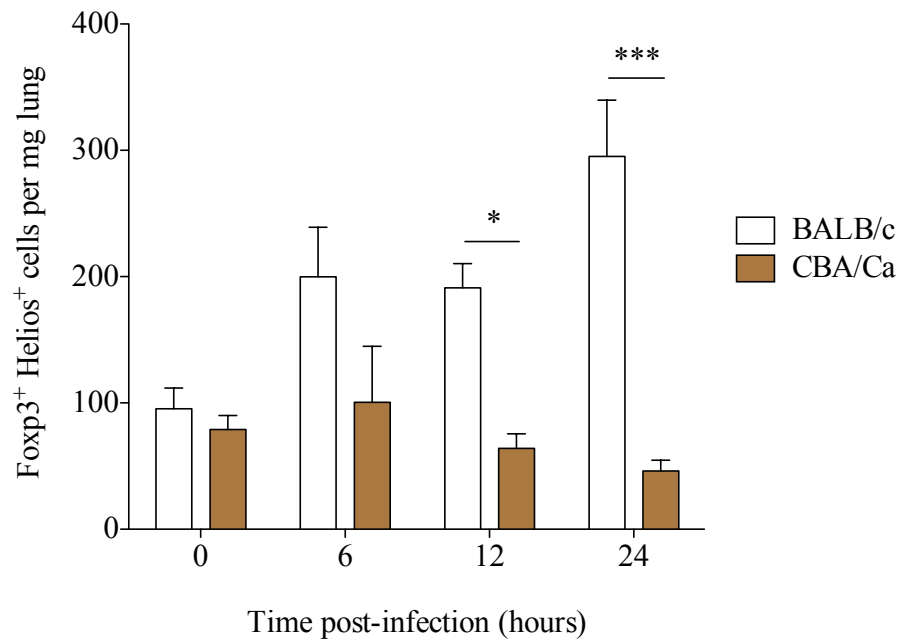


Figure 5.7 - Number of Foxp3<sup>+</sup> Helios<sup>+</sup> in the pneumococcal-infected BALB/c and CBA/Ca lungs following pneumococcal infection. Mice were intranasally infected with 10<sup>6</sup> CFU and lungs were collected at 0, 6, 12 and 24 hours post-infection. Number of Helios<sup>+</sup> T regulatory cells per mg of lung tissue, at the various time points, analysed by flow cytometry. Data represent the mean of positive events ± SEM. The p-values (\*,  $P < 0.05$ ; \*\*\*,  $P < 0.001$ ) were obtained with two-way ANOVA followed by Bonferroni post-test. Data are representative of two independent experiments with ≥ 4 mice per group.

To assess whether lung T regulatory cells actively secreted immunomodulatory cytokines during pneumococcal infection, the number of IL-10<sup>+</sup> T regulatory cells was assessed (Figure 5.8). T regulatory cell-derived IL-10 has an important role in determining resistance or susceptibility to infection against a range of pathogens (Belkaid *et al.*, 2002; Rowe *et al.*, 2011) and has been shown to influence susceptibility to disease in pneumococcal pneumonia (Jeong *et al.*, 2011). In this study, a significant increase in IL-10<sup>+</sup> T regulatory cells was readily apparent in both BALB/c ( $P < 0.01$ ) and CBA/Ca ( $P < 0.05$ ) mice, compared to PBS inoculated controls, at 24 hours p.i. Furthermore, the number of IL-10<sup>+</sup> T regulatory cells in BALB/c mice was significantly higher than in CBA/Ca mice ( $P < 0.05$ ).

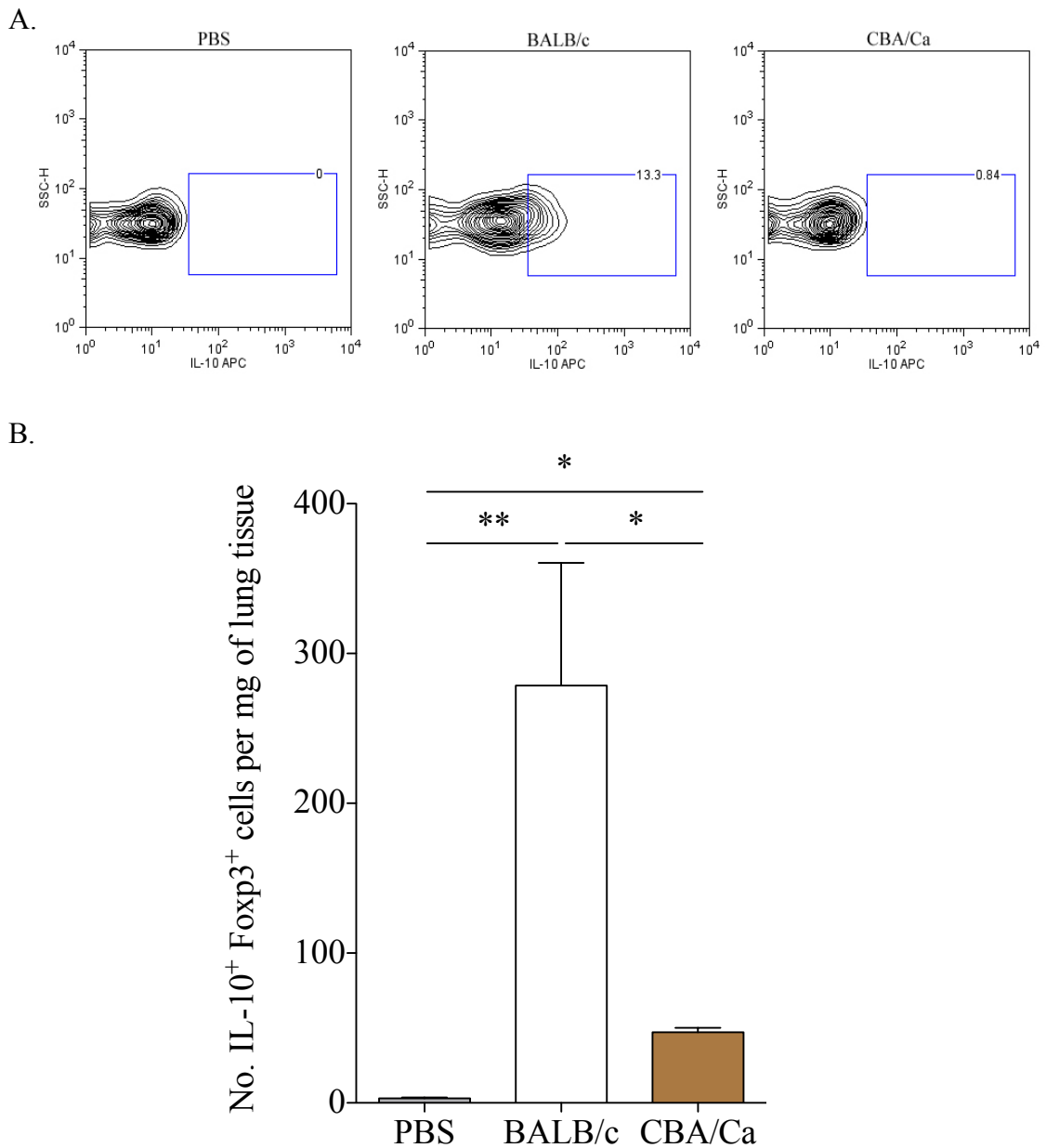


Figure 5.8 - Number of IL-10<sup>+</sup> T regulatory cells in BALB/c lungs at 24 hours post-infection. Mice were intranasally infected with 10<sup>6</sup> CFU and lungs were collected at 24 hours post-infection. The PBS group contained BALB/c mice sham infected with PBS. (A) Flow cytometric analysis of IL-10<sup>+</sup> Foxp3<sup>+</sup> cells was determined by gating CD45<sup>+</sup>, CD4<sup>+</sup>, Foxp3<sup>+</sup> and finally IL-10<sup>+</sup> events (example of a BALB/c and CBA/Ca 24 hour time point sample). (B) Number of IL-10<sup>+</sup> Foxp3<sup>+</sup> cells per mg of lung tissue, at 24 hours post-infection, analysed by flow cytometry. Data represent the mean of positive events  $\pm$  SEM. The p-values (\*,  $P < 0.05$ ; \*\*,  $P < 0.01$ ) were obtained with two-way ANOVA followed by Bonferroni post-test. Data are representative of 2 experiments with  $\geq 4$  mice per strain and time point.

In addition to IL-10, several other markers, including PD-L1 (Lohr *et al.*, 2006) and CTLA-4 (Wing *et al.*, 2008), have been suggested to play a role in T regulatory cell immunosuppressive functions. The expression of PD-L1 and CTLA-4 by T regulatory cells in the lungs of BALB/c and CBA/Ca mice was assessed. It was seen that there was barely detectable expression of PD-L1 on T regulatory cells from either BALB/c or CBA/Ca mice (Figure 5.9) and low-level expression of CTLA-4 on the majority of T regulatory cells from both strains (Figure 5.10). However, a population of CTLA-4<sup>high</sup> T regulatory cells was also observed in both strains of mice (Figure 5.10). There was a significant difference in CTLA-4<sup>high</sup> T regulatory cell numbers in BALB/c compared to 0 hours and to CBA/Ca mice at 24 hours p.i. ( $P < 0.001$ ), with BALB/c lungs containing substantially more CTLA-4<sup>high</sup> cells (Figure 5.10).

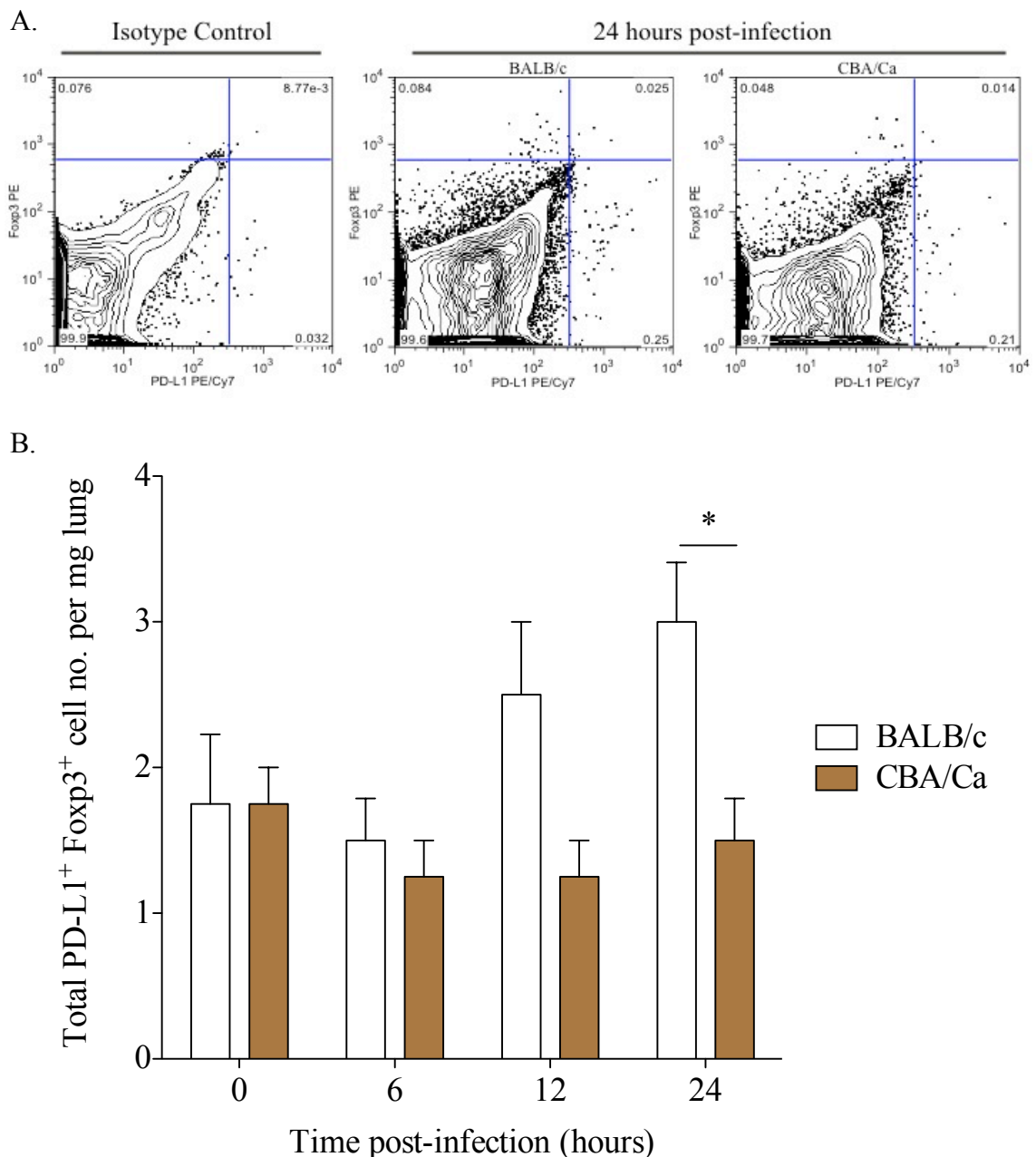


Figure 5.9 - Number of T regulatory cells expressing PD-L1 in BALB/c and CBA/Ca lungs following pneumococcal infection. Mice were intranasally infected with  $10^6$  CFU and lungs were collected at 0, 6, 12 and 24 hours post-infection. (A) Flow cytometric analysis of T regulatory cells expressing PD-L1 was determined by gating for  $CD45^+$ ,  $Foxp3^+$  and  $PD-L1^+$  events (example of a BALB/c and CBA/Ca 24 hour time point sample). (B) Number of  $Foxp3^+$   $PD-L1^+$  cells per mg of lung tissue, at the various time points, analysed by flow cytometry. Data represent the mean of positive events  $\pm$  SD. The p-value (\*,  $P < 0.05$ ) was obtained with two-way ANOVA followed by Bonferroni post-test. Data are representative of two independent experiments with 4 mice per group.

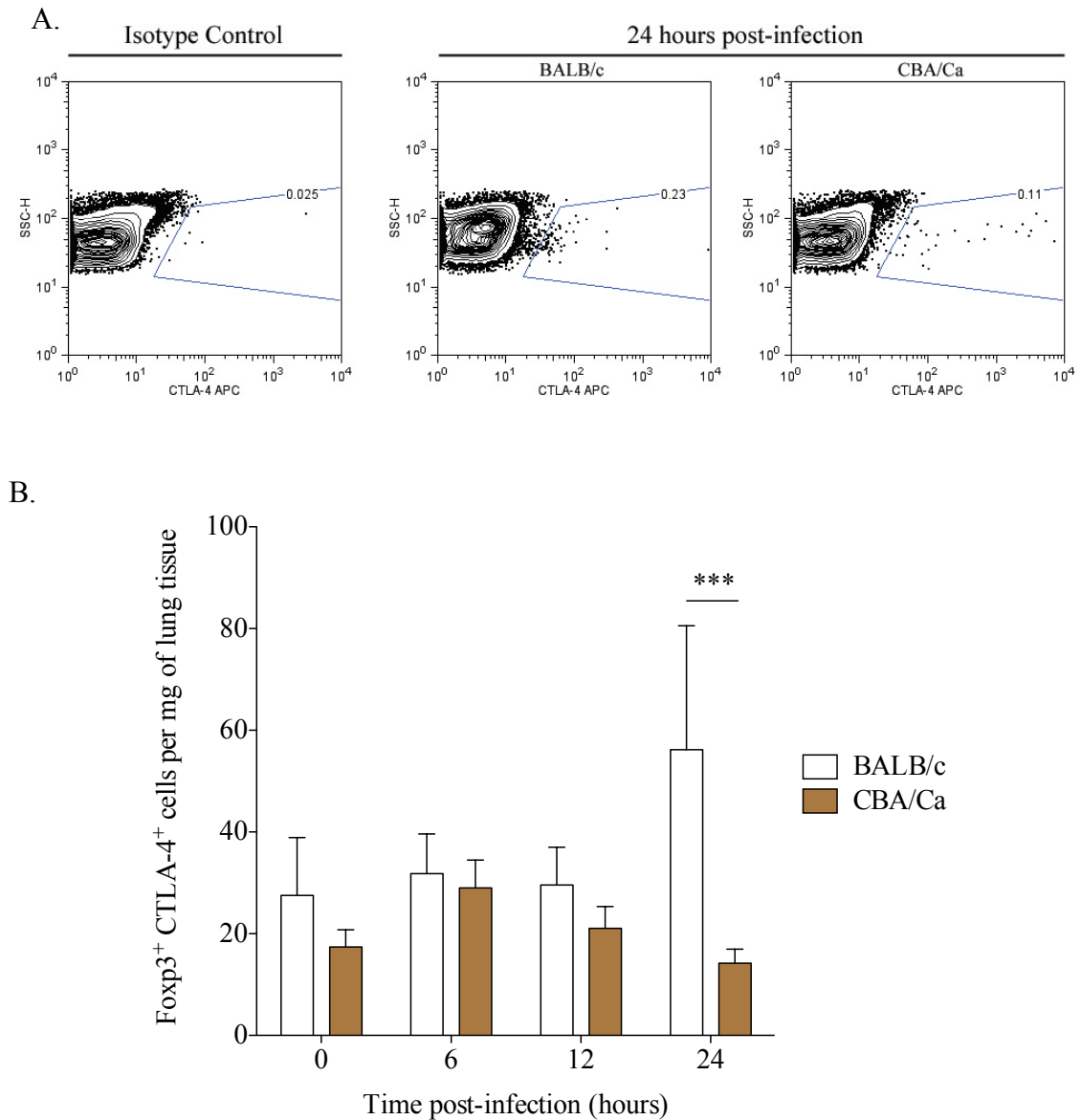


Figure 5.10 - Number of T regulatory cells expressing CTLA-4 in BALB/c and CBA/Ca lungs following pneumococcal infection. Mice were intranasally infected with  $10^6$  CFU and lungs were collected at 0, 6, 12 and 24 hours post-infection. (A) Flow cytometric analysis of T regulatory cells expressing CTLA-4 was determined by gating for  $CD45^+$ ,  $Foxp3^+$  and finally  $CTLA-4^+$  events (example of a BALB/c and CBA/Ca 24 hour time point sample). (B) Number of  $Foxp3^+$   $CTLA-4^+$  cells per mg of lung tissue, at the various time points, analysed by flow cytometry. Data represent the mean of positive events  $\pm$  SD. The p-value (\*\*\*,  $P < 0.001$ ) was obtained with two-way ANOVA followed by Bonferroni post-test. Data are representative of two independent experiments with 4 mice per group.

This increase in  $CTLA-4^+$  T regulatory cells in BALB/c mice could also be observed in the spleen at 24 hours p.i. (Figure 5.11), suggesting the presence of a circulating population of suppressive T cells. This result further highlights the strong regulatory environment generated in BALB/c mice following infection.

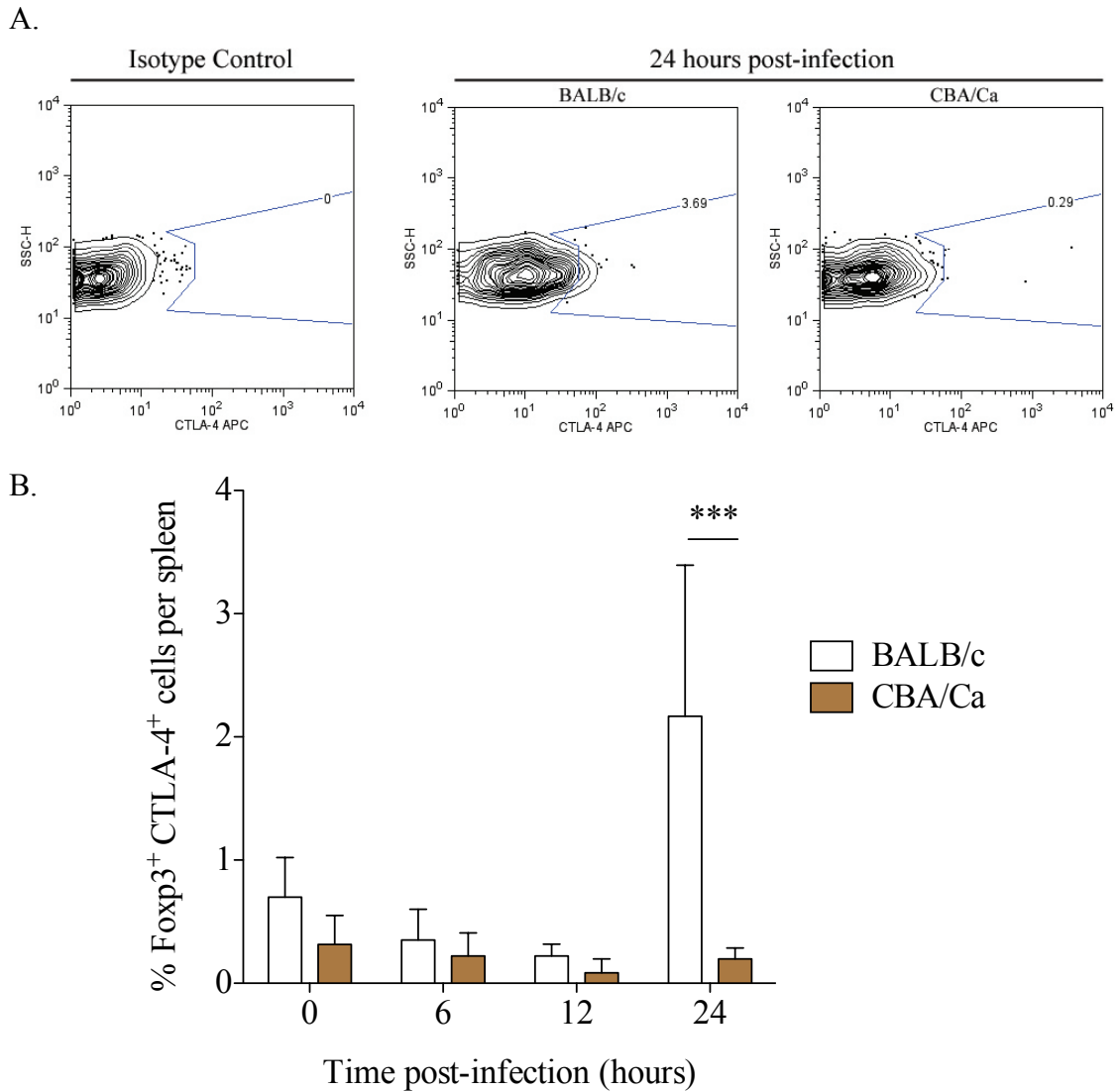


Figure 5.11 - BALB/c mice display a greater percentage of Fcpx3<sup>+</sup> CTLA-4<sup>+</sup> cells in their spleen by 24 hours post-infection. Mice were intranasally infected with 10<sup>6</sup> CFU and spleens were collected at 0, 6, 12 and 24 hours post-infection. (A) Flow cytometric analysis of T regulatory cells expressing CTLA-4 was determined by gating for CD45<sup>+</sup>, Fcpx3<sup>+</sup> and finally CTLA-4<sup>+</sup> events (example of a BALB/c and CBA/Ca 24 hour time point sample). (B) Percentage of Fcpx3<sup>+</sup> CTLA<sup>+</sup> cells per spleen, at the various time points, analysed by flow cytometry. Data represent the mean of positive events  $\pm$  SD. The p-value (\*\*\*,  $P < 0.001$ ) was obtained with two-way ANOVA followed by Bonferroni post-test. Data are representative of two independent experiments with 4 mice per group.

To rule out the possibility that the differences in TGF- $\beta$  signaling between BALB/c and CBA/Ca mice were affecting disease-resistance through modulation of T<sub>h</sub>17 responses, the production of IL-17 was assessed in the lungs of BALB/c and CBA/Ca mice at 24 hours p.i. (Figure 5.12). Only a small population of IL-17<sup>+</sup> cells was observed in either mouse strain and no significant difference in CD4<sup>+</sup>IL-17<sup>+</sup> cells was observed ( $P > 0.05$ ).

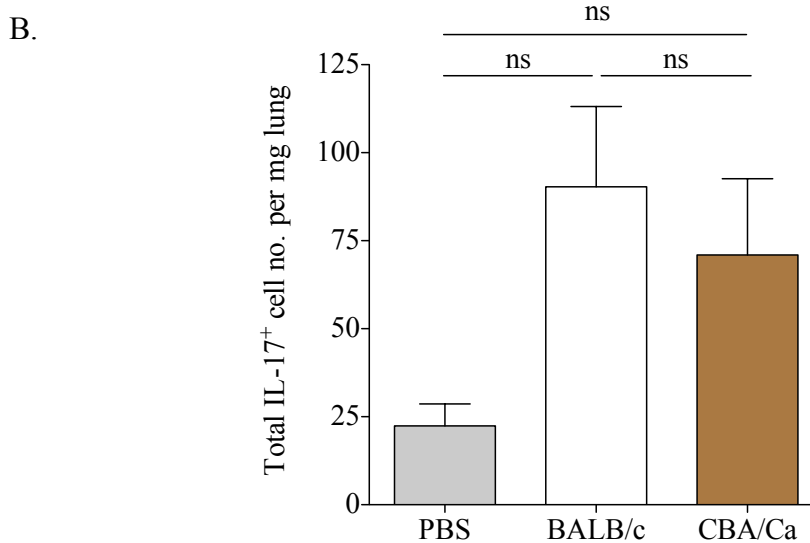
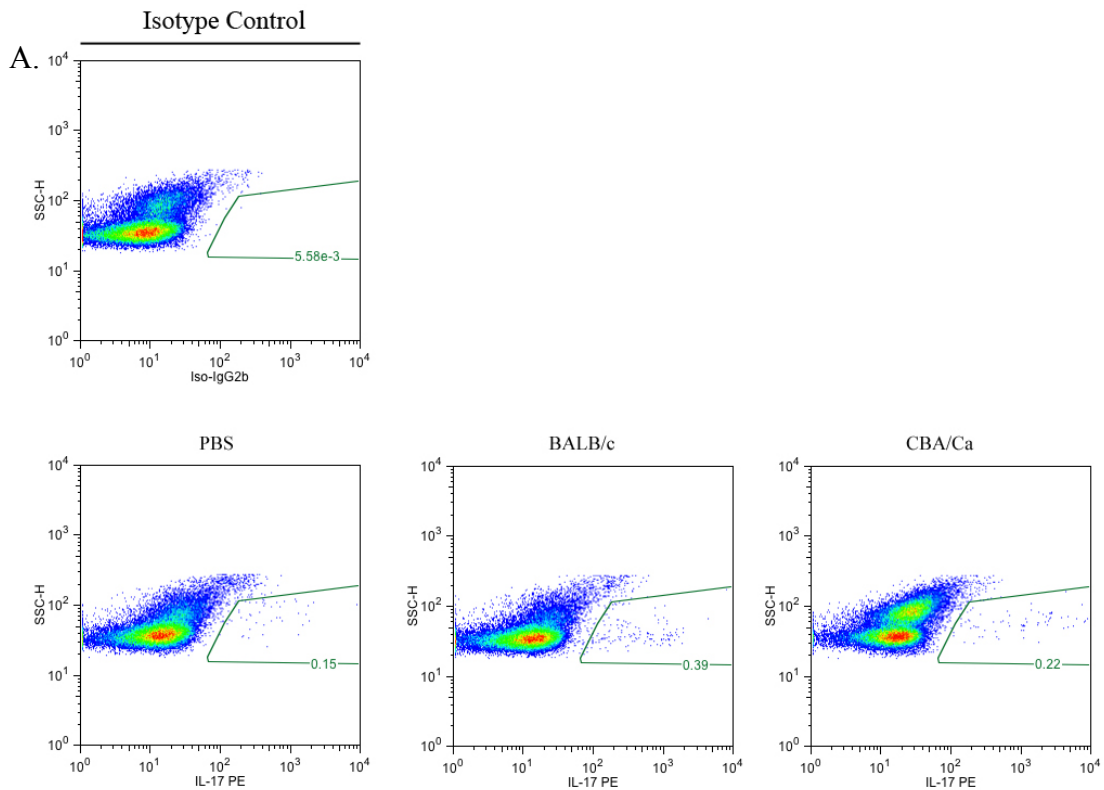


Figure 5.12 - IL-17<sup>+</sup> cell numbers in BALB/c or CBA/Ca lungs at 24 hours post-infection. BALB/c and CBA/Ca mice were intranasally-infected with wild-type D39 or PBS as a control. PBS group contains BALB/c and CBA/Ca animals. (A) Flow cytometric analysis of IL-17<sup>+</sup> cells was determined by gating for CD45<sup>+</sup>, IL-17<sup>+</sup> events (example of a BALB/c and CBA/Ca 24 hour time point sample). (B) Number of IL-17<sup>+</sup> cells per mg of lung tissue, at the various time points, analysed by flow cytometry. Data are representative of two independent experiments with > 4 mice per group (ns =  $P > 0.05$ ).

### 5.3.3 Lower T regulatory cell numbers correlate with increased lung cell apoptosis

The strong immunomodulatory environment generated in BALB/c lungs during pneumococcal pneumonia likely accounts for the lower levels of proinflammatory cytokine seen in these mice p.i. than compared to CBA/Ca (Figure 5.13). Production of interferon (IFN)- $\gamma$  in CBA/Ca lungs at 24 hours p.i. was significantly higher than in BALB/c lungs ( $P < 0.05$ ) (Figure 5.13-B), and over 90% of NKp46<sup>+</sup> NK cells were found to be IFN- $\gamma$ <sup>+</sup>, as compared to 30-50% in BALB/c mice (Figure 5.13-A). NK cells accounted for over 80% of IFN- $\gamma$ -producing cells in both BALB/c and CBA/Ca mice, with the remaining 20% coming from an unidentified CD45<sup>+</sup>CD4<sup>-</sup>CD8<sup>-</sup>NKp46<sup>-</sup> cell type (Figure 5.14). The higher levels of IFN- $\gamma$  production in CBA/Ca mice suggest mechanisms limiting proinflammatory cytokine production are more effective in BALB/c than in CBA/Ca lungs during pneumococcal pneumonia. IFN- $\gamma$  is known to induce apoptosis in a range of cell types, including lung epithelial cells (Coulter *et al.*, 2002; Wen *et al.*, 1997), and so it is possible that modulation of IFN- $\gamma$  production is one mechanism by which T regulatory cells may help maintain epithelial barrier integrity.

Intriguingly, the immunomodulation occurring in BALB/c lungs at early time-points following infection appears to be a specific process rather than a general dampening of immune responses because BALB/c mice generate strong neutrophil responses in the lung following intranasal infection (Figure 3.5) that are thought to be critical in clearance of *S. pneumoniae* (Gingles *et al.*, 2001). Little influx of neutrophils was observed in CBA/Ca mice over the first 24 hours p.i. (Figure 3.5) and so this response must be absent or else occurring after bacteria have already disseminated to the bloodstream (Figure 3.1-D and Figure 3.2).

To determine whether reduced T regulatory cell numbers and increased proinflammatory cytokine production correlated with inflammation and tissue damage in CBA/Ca mice, apoptosis was assessed in the inflammatory loci within the lungs of *S. pneumoniae*-infected mice (Figure 5.13-C and D), performed by collaborator Natalie Strickland (Liverpool School of Tropical Medicine, Liverpool). At 24 hours p.i., a timepoint at which BALB/c lungs contain more T regulatory cells and less IFN- $\gamma$  than CBA/Ca mice (Figure 5.4, Figure 5.5 and Figure 5.13-B), a significantly higher proportion of cells in the inflamed tissue had undergone apoptosis in the lungs of CBA/Ca than in BALB/c mice ( $P < 0.05$ ) (Figure 5.13).

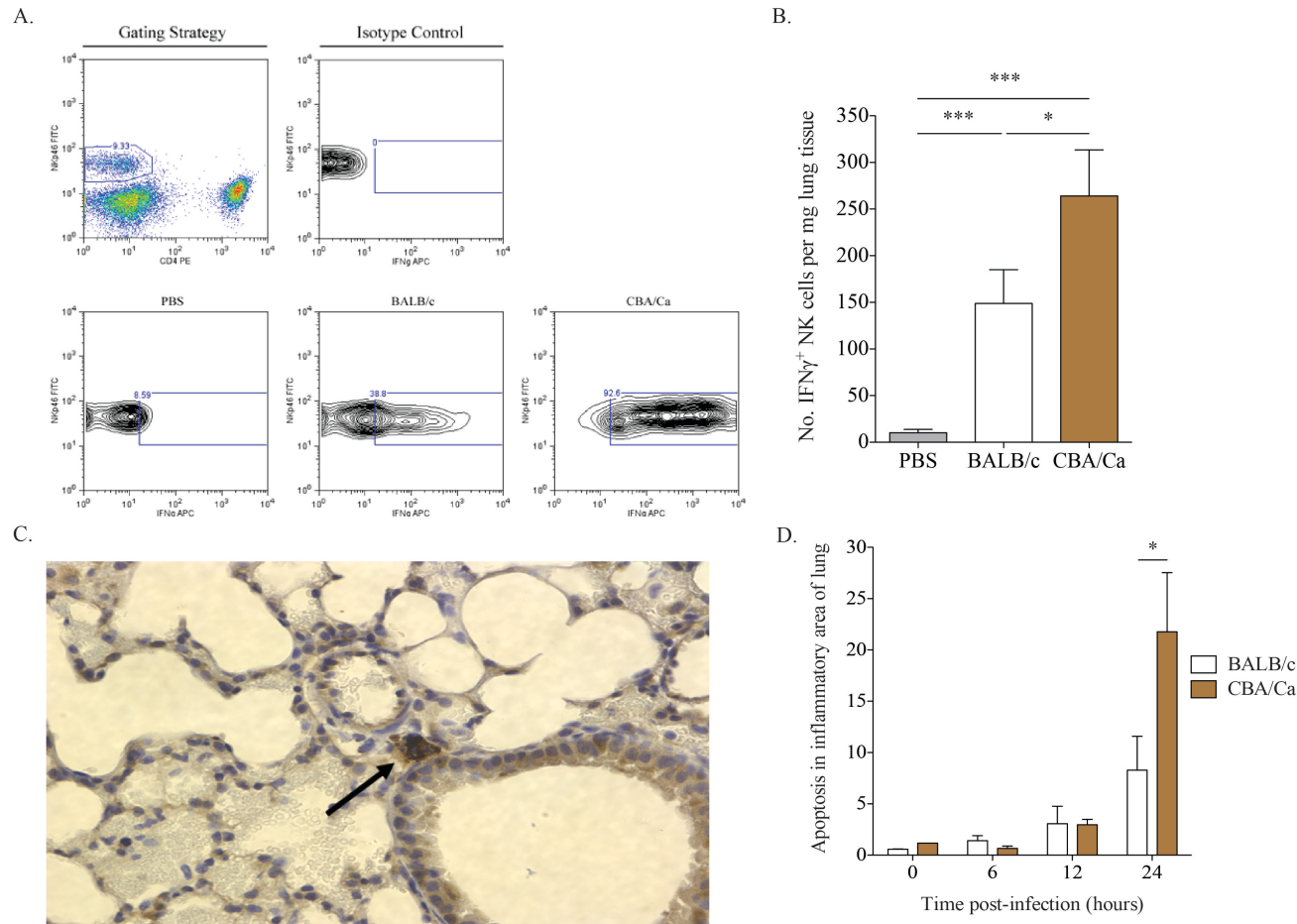


Figure 5.13 - CBA/Ca mice display uncontrolled lung inflammation and associated apoptosis following *S. pneumoniae* infection. All results were from intranasal infection of mice with *S. pneumoniae* D39. Lungs were collected from PBS-treated or *S. pneumoniae*-infected BALB/c and CBA/Ca mice at 24 hours p.i. (A) Flow cytometric analysis of IFN- $\gamma^+$  cells was determined by gating IFN- $\gamma^+$ , Nkp46 $^+$ , CD4 $^-$  events. (B) Numbers of IFN- $\gamma^+$  NK cells per mg of lung tissue, at 24 hours post-infection, analysed by flow cytometry. Data represent the mean of positive events  $\pm$  SEM. The p-values (\*,  $P < 0.05$  and \*\*\*,  $P < 0.001$ ) were obtained with two-way ANOVA followed by Bonferroni post-test. Data are representative of 3 independent experiments with  $> 4$  mice per group. (C) Illustration of apoptotic cells in areas of inflammation within lungs of *S. pneumoniae*-infected BALB/c and CBA/Ca mice. Inset shows apoptotic cell (arrow) within area of inflammation as defined by presence of inflammatory infiltrate. The number of brown-staining apoptotic cells (marked with anti-active caspase polyclonal antibody) were expressed as a percentage of total cells as assessed by number of blue-staining nuclei. (D) Proportion of apoptotic cells in areas of inflammation within pneumococcal-infected lungs. Data represent mean  $\pm$  SEM. The p-value (\*,  $P < 0.05$ ) was obtained with two-way ANOVA followed by Bonferroni post-test.

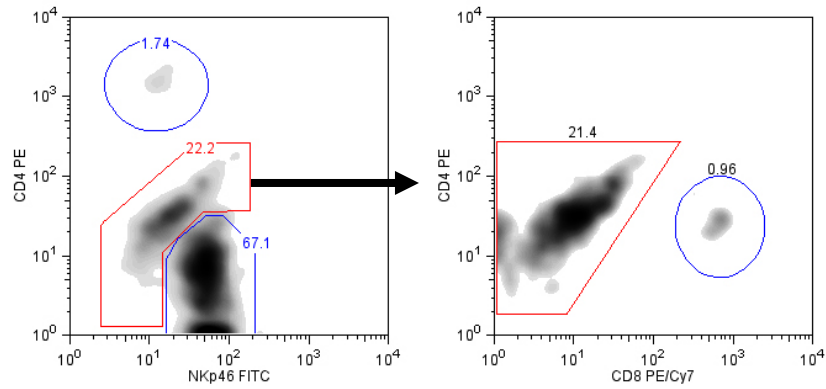


Figure 5.14 - Interferon- $\gamma$  producing cells in the lungs at 24 hours post-infection. Flow cytometric analysis of IFN- $\gamma$  producing cell gating on CD45<sup>+</sup> CD4<sup>-</sup> CD8<sup>-</sup> Nkp46<sup>-</sup> events.

The higher levels of apoptosis in CBA/Ca lungs correlated with bacterial dissemination into the bloodstream, with CBA/Ca mice, but not BALB/c mice, having significant septicaemia at 6, 12 and 24 hours p.i. ( $P < 0.01$  at 6 hours p.i.;  $P < 0.001$  at 12 and 24 hours p.i.) (Figure 3.1-D). In addition, BALB/c mice were able to control and reduce the CFU in the lungs 3-fold (Figure 3.1-C).

#### **5.3.4 Inhibition of TGF- $\beta$ 1 impairs BALB/c resistance to *S. pneumoniae* infection**

Having demonstrated differences in TGF- $\beta$  production and T regulatory cell activity over the course of infection in BALB/c and CBA/Ca mice, next to be investigated was the potential to influence the resistant phenotype in BALB/c mice to pneumococcal pulmonary infection by TGF- $\beta$ 1-inhibition. A short synthetic peptide (P17) was utilized to inhibit TGF- $\beta$  activity in BALB/c animals. The ability of P17 to effectively inhibit TGF- $\beta$ 1 and TGF- $\beta$ 2 activity is well documented (Gil-Guerrero *et al.*, 2008; Dotor *et al.*, 2007) and this dose was followed. P17, or PBS as a control, was administered to BALB/c mice 1 hour prior to intranasal challenge with *S. pneumoniae* and then again at 6 hours p.i..

Mice treated with the P17 peptide developed visible signs of disease earlier than PBS-treated control animals, and by 48 hours p.i. all P17-treated animals, but only one mouse from the control group, displayed visible signs of disease (Figure 5.15-A). Furthermore, 50% of P17-treated mice had to be culled due to illness, while 100% of the control group survived. Although mice from both treatment groups showed similar lung CFUs by 24 and 48 hours p.i., (Figure 5.15-B), the significantly higher CFUs in their blood demonstrated the increased susceptibility P17-treated BALB/c mice (Figure 5.15-C). Whilst none of the PBS-treated BALB/c mice developed bacteraemia over the 48-hour experiment, 50% of the P17-treated animals had substantial levels of bacteria in the blood by 48 hours p.i., indicating that systemic inhibition of TGF- $\beta$  promotes bacterial seeding from lungs to blood. This is a key finding, as BALB/c mice intranasally infected with *S. pneumoniae* do not develop septicaemia. Therefore, in the absence of an effective T regulatory cell and TGF- $\beta$  response, resistant mice become susceptible to pneumococcal pneumonia, developing sepsis (which control mice do not) and substantially increased mortality.

While TGF- $\beta$  has a role to play in mucosal immunity, it is also thought to be required for T regulatory cell development, it was decided to investigate whether P17 treatment had had any effect on T regulatory cell numbers in the lungs of infected BALB/c mice. Analysis of Foxp3-stained lung sections (Figure 5.15-D), performed by a collaborator Andrew Haynes (MRC Mouse Genome Centre, Oxford), from *S. pneumoniae*-infected PBS-treated and P17-treated mice confirmed that P17 treatment substantially reduced

numbers of Foxp3<sup>+</sup> cells in the lungs of infected BALB/c mice at both 24 and 48 hours p.i., which correlated with development of sepsis in these mice (Figure 5.15-E).

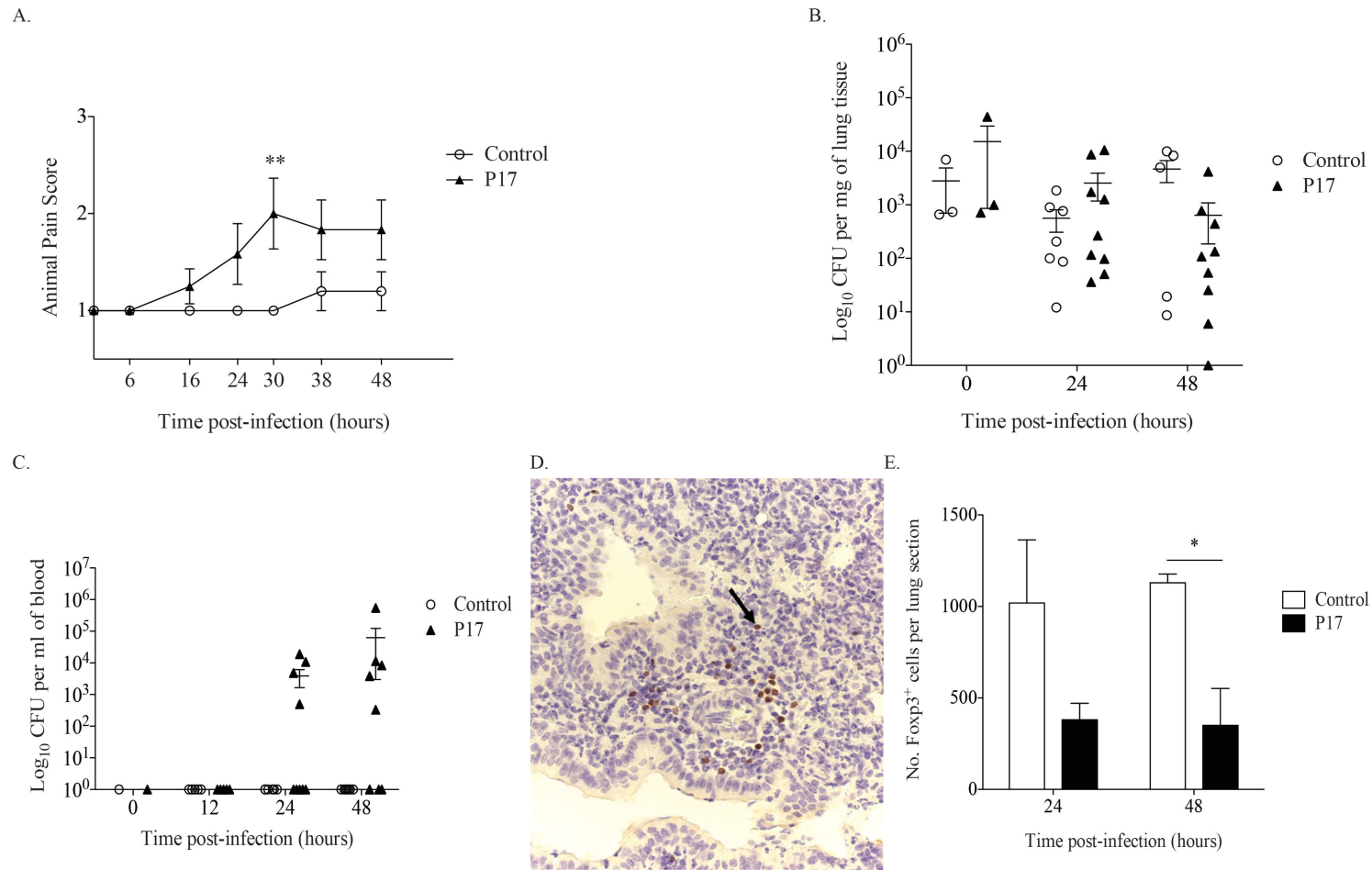


Figure 5.15 - Inhibition of TGF- $\beta$  activity impairs BALB/c resistance to pneumococcal infection. All results are from intranasal infection of mice with wild-type *S. pneumoniae* D39. The peptide P17 (500  $\mu$ g) in 100  $\mu$ l PBS was administered by intraperitoneal (i.p.) injection 1 hour before and 6 hours after intranasal challenge with wild-type D39 *S. pneumoniae*. Control animals received i.p. injections of PBS as a control. (A) Mean animal pain score (based on Table 2.2) in *S. pneumoniae*-infected PBS-treated or P17-treated BALB/c mice over a 48-hour time course. (B) Number of bacteria per mg lung tissue and (C) per ml blood in P17- or PBS-treated mice. (D) Illustration of Foxp3<sup>+</sup> cell (arrow) in BALB/c lung at 48 hours post-infection. The lung tissue was sectioned after paraffin embedded, dewaxed followed by immunostaining method: Foxp3 primary antibody (eBiosciences - clone FJK-16s, Insight Biotech), used as a marker of Foxp3<sup>+</sup> cells, counterstained with hematoxylin. (E) Quantification of Foxp3<sup>+</sup> immunostaining in antibody-stained lung sections from P17- or PBS-treated *S. pneumoniae*-infected mice. The numbers of brown-staining Foxp3<sup>+</sup> cells were counted double-blind (2 slides per mouse per time point). For all graphs data represent mean  $\pm$  SEM. The p-values (\*,  $P < 0.05$ ; \*\*,  $P < 0.01$ ) were obtained with two-way ANOVA. Results are representative of 2 independent experiments with  $\geq 5$  mice per group.

### 5.3.5 Adoptive transfer of *in vitro* generated T regulatory cells increases CBA/Ca mice survival

Next to be investigated was whether increased numbers of T regulatory cells in CBA/Ca mice might boost resistance to pneumococcal pneumonia. To generate sufficient numbers of cells for adoptive transfer experiments, inducible T regulatory cells from CD4<sup>+</sup>, CD25<sup>negative</sup> T cells were differentiated *in vitro*, by culture with TGF- $\beta$  in the presence of anti-CD3 and anti-CD28 stimulation. Whilst these cells lack Helios expression and have differentiation requirements more similar to iT<sub>regs</sub> than nT<sub>regs</sub>, they share similar immunosuppressive qualities with nT<sub>regs</sub>, such as IL-10 production and CTLA-4 expression (Fantini *et al.*, 2007). The differentiation protocol yielded approximately 90% CD4<sup>+</sup> Foxp3<sup>+</sup> T regulatory cells, with a few contaminating CD4<sup>+</sup> Foxp3<sup>negative</sup> T cells (Figure 5.16-A).

Adoptive transfer of *in vitro* generated CBA/Ca Foxp3<sup>+</sup> T regulatory cells, via the tail vein, 2 hours prior to intranasal infection with *S. pneumoniae* led to a significant increase in mean survival in CBA/Ca mice ( $P < 0.01$ ) (Figure 5.16-B). By contrast, CD4<sup>+</sup> Foxp3<sup>negative</sup> T cells generated in the same culture conditions, but without TGF- $\beta$ , and transferred into a separate group of mice to control for contaminating T cells in the T regulatory cell population, failed to increase survival (Figure 5.16-B). At 24 hours p.i., a significant increase ( $P < 0.01$ ) in total T regulatory cells (Figure 5.16-C) and IL-10<sup>+</sup> T regulatory cells (Figure 5.16-D) was observable in the lungs of mice that had received i.v. administration of T regulatory cells, in contrast to mice that had received PBS or CD4<sup>+</sup> Foxp3<sup>negative</sup> T cells i.v.. This finding suggested an ability of the *in vitro* generated T regulatory cells to influence immune responses leading to increased host survival following transfer into the tail vein. Crucially, the bacterial load in the blood at 24 hours p.i. was significantly lower in mice that had received T regulatory cells than either of the other two treatment groups ( $P < 0.001$ ) (Figure 5.16-E). This suggests reduced translocation of pneumococci from lungs to blood during pneumonia as a result of T regulatory cell activity. This is a significant result because the CBA/Ca strain is highly susceptible to invasive pneumococcal pneumonia, and yet transfer of T regulatory cells alone was sufficient to double survival time. Furthermore, the increased survival and decreased seeding of bacteria to the blood in CBA/Ca mice that had received T regulatory cells correlated with a decrease in the number of IFN- $\gamma$ <sup>+</sup> cells in the lungs, suggesting an improved generation of an immunomodulatory environment in

these mice (Figure 5.16-F). The decreased levels of pro-apoptotic IFN- $\gamma$  in these mice may contribute to the decreased seeding of bacteria from the lungs to the blood (Figure 5.16-E).

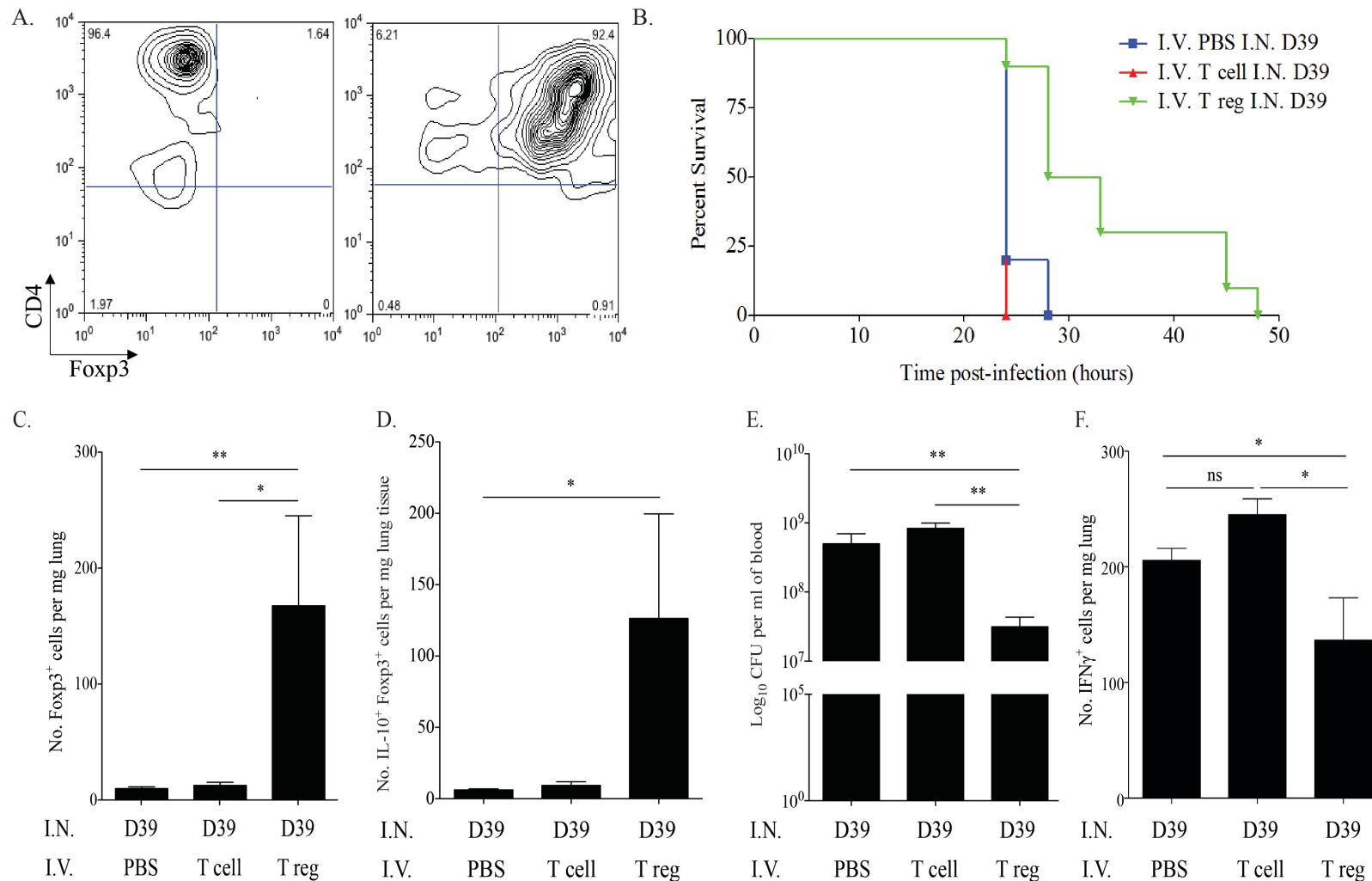


Figure 5.16 - Adoptive transfer of *in vitro* generated Foxp3<sup>+</sup> T regulatory cells improves CBA/Ca survival in pneumococcal infection. (A) CD4 and Foxp3 FACS staining of isolated CBA/Ca CD4<sup>+</sup>, CD25<sup>-</sup> splenocytes before (left column) and after (right column) 5 days culture with anti-CD3, anti-CD28 and TGF-β. 5 day cultured cells were used for adoptive transfer. All results in (B-D) are from intranasal infection of mice with wild-type D39 *S. pneumoniae*. (B) Survival of *S. pneumoniae*-infected CBA/Ca mice that had received PBS (■), CD4<sup>+</sup> T cells (▲), or T regulatory cells (▼) i.v. prior to intranasal infection with *S. pneumoniae*. Survival of T regulatory cell treatment group is significantly different to both CD4<sup>+</sup> T cell treatment group ( $p < 0.01$ ) and PBS treatment group ( $P < 0.01$ ) (C) Number of Foxp3<sup>+</sup> cells and (D) Number of IL-10<sup>+</sup> Foxp3<sup>+</sup> cells per mg lung at 24 hours p.i. (E) Number of bacteria per ml blood at 24 hour post-infection. (F) Number of IFN-γ<sup>+</sup> cells per mg lung at 24 hours p.i.. Results in (A) are representative of 5 independent experiments and results in (B-F) are representative of two independent experiments with > 6 mice per group.

### **5.3.6 Resistance to invasive pneumococcal pneumonia in outbred mice correlates with strong T regulatory cell responses**

To test the hypothesis that strong T regulatory cell responses correlate with resistance to pneumococcal pneumonia in other mouse strains, outbred MF1 mice were infected and the progression of disease assessed in relation to T regulatory cell activity (Figure 5.17). At 48 hours p.i., mice showing visible signs of disease were considered to have invasive pneumonia (Figure 5.17-A). The remaining mice, which showed no disease signs, were deemed to have “controlled infection” or non-invasive pneumonia. This was confirmed by analysis of bacteraemia at 48 hours p.i., as all mice which showed visible signs of disease had bacteria in their blood compared with no bacteraemia in mice in the non-invasive pneumonia group (Figure 5.17-B). Strikingly, the resistant phenotype correlated with significantly higher numbers of T regulatory cells in the lungs of mice from the non-invasive pneumonia group as compared to the invasive pneumonia group at 48 hours p.i. ( $P < 0.05$ ) (Figure 5.17-C). Intriguingly, neutrophil numbers in the lungs of the invasive pneumonia group were significantly higher than in the non-invasive pneumonia group at the same time point ( $P < 0.05$ ) (Figure 5.17-D), suggesting that neutrophil influx alone is insufficient to mediate resistance to infection in the absence of protective T regulatory cell responses.

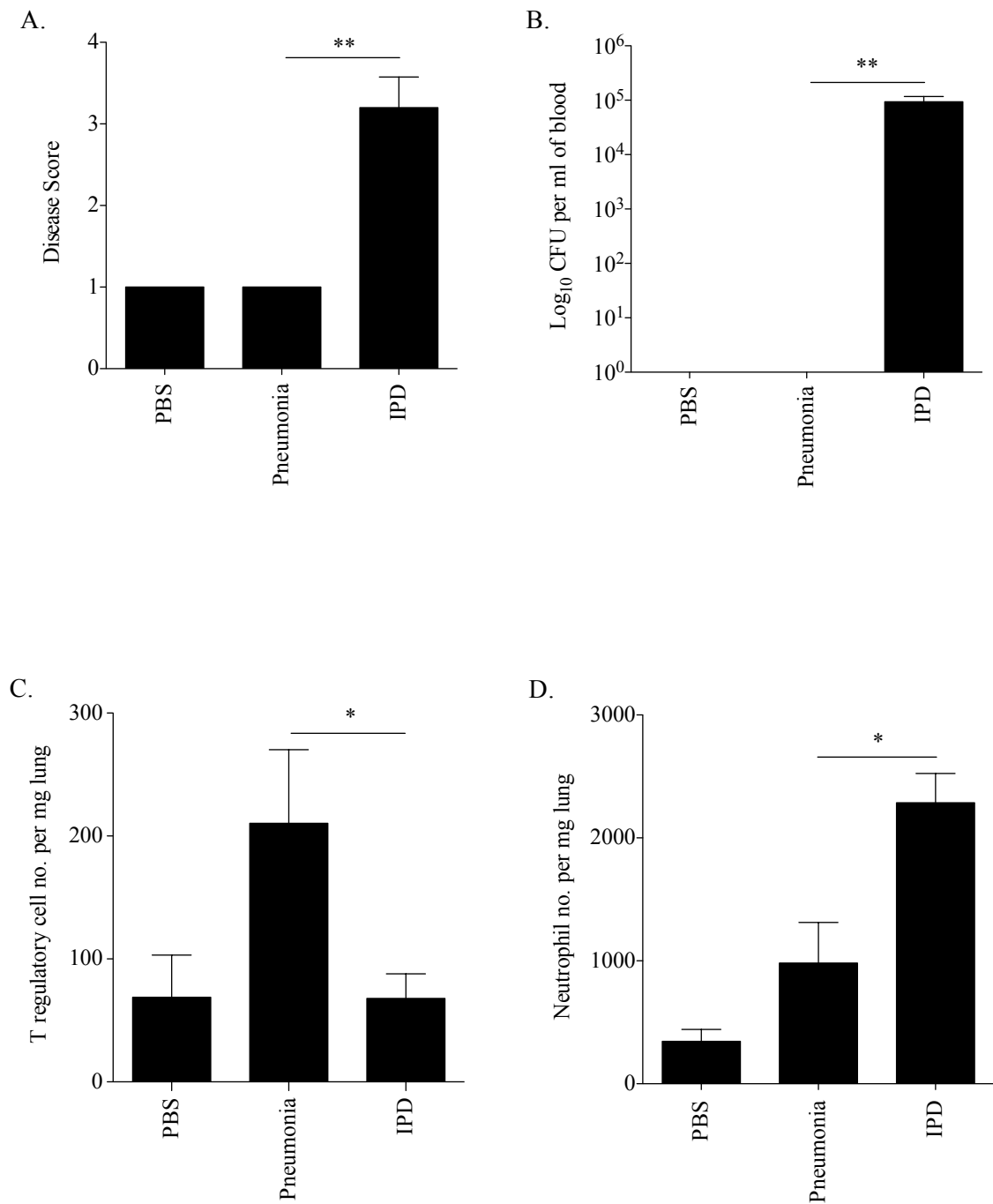


Figure 5.17 - Disease resistance in outbred MF1 mice correlates with strong T regulatory cell responses in the lung. All results were from intranasal infection of outbred MF1 mice with wild-type *S. pneumoniae* D39. (A) Animal disease score at 48 hours p.i. A score of 1 is a normal mouse. Any infected mouse scoring 1 (normal) at 48 hours p.i. was considered to have a controlled infection. (B) Number of bacteria per ml blood at 48 hours p.i.. Number of Foxp3<sup>+</sup> T regulatory cells (C) and Gr-1<sup>hi</sup> F4/80<sup>lo</sup> neutrophils (D) per mg lung in PBS-treated or *S. pneumoniae*-infected MF1 mice at 48 hours p.i., as identified in flow cytometry. P-values (\*,  $P < 0.05$  and \*\*,  $P < 0.01$ ) indicate significant difference and were obtained with t-test statistical analysis. For all graphs data represent mean  $\pm$  SEM. Results are representative of 2 independent experiments, each with 3 PBS-treated and >10 infected mice.

---

## CHAPTER 6. RESULTS: B-cell receptor CD22 is a major factor of host resistance to *Streptococcus pneumoniae* infection in mice

---

### 6.1 Introduction

The *cd22* gene encodes for a B-lymphocyte adhesion molecule, which belongs to the sialic acid binding Ig-like lectin (SIGLEC-2) family of lectins (Crocker *et al.*, 1998) and is a member of the immunoglobulin superfamily (Hatta *et al.*, 1999). CD22 (Siglec-2) is a type I membrane protein expressed on B cells and regulates B cell receptor signaling, cell survival, proliferation and antibody production (Walker & Smith, 2008; Ma *et al.*, 2013). It is a B-cell transmembrane glycoprotein found on the surface of mature B cells and in some immature B cells that binds to sialic acid, it is involved in adhesion and activation and acts as an accessory-signaling component of the B-cell antigen receptor (BCR) (Hatta *et al.*, 1999).

The extracellular portion of CD22 is composed by seven immunoglobulin domains, the most distal of which is a V-set immunoglobulin domain that is responsible for binding  $\alpha 2,6$ Sia ligands (Engel *et al.*, 1995; Law *et al.*, 1995; Nath *et al.*, 1995). Within this domain, two arginine residues (R130 and R137 in the mouse) are required for  $\alpha 2,6$ Sia-binding, and mutation of the residues abolishes this interaction (van der Merwe *et al.*, 1996). The intracellular portion contains six tyrosine residues, three of which (Y762, Y822 and Y842) are part of the ITIM motifs (Fujimoto *et al.*, 2006). Upon cross-linking of the BCR by antigen, the CD22 that is associated with it, is quickly phosphorylated (Leprince *et al.*, 1993).

CD22 is one of the molecules involved in a mechanism of shutting-off the signalling process of the B cell activation. In this regulatory process, CD22 acts as a safety valve of sorts, preventing the accidental or aberrant activation of B cells. The lack of this protein in mice indicates a hyperactive immune system and may result in development of spontaneous autoimmune disease (Han *et al.*, 2005).

In 1997, an investigation performed by Tedder *et al.*, inspected the phenotype of CD22-deficient mice and suggested that CD22 is primarily involved in the generation of mature B cells within the bone marrow, blood, and marginal zones of lymphoid tissues (Tedder *et al.*, 1997). Remarkably, the CD22-deficient mice showed a significant

diminution of surface Ig levels in the B cell population, which suggests that CD22 functions *in vivo* to adjust the signaling threshold of cell surface antigen receptors (Tedder *et al.*, 1997). Little is known about the actions of CD22 protein during infection. Published data on bacterial infection studies evidenced a reduction of the marginal zone B cell compartment in the spleen tissue of CD22-deficient mice (Gjertsson *et al.*, 2004).

In viral infection studies, CD22 have been shown to play an essential role in controlling West Nile Virus (WNV) infection by governing cell migration and CD8<sup>+</sup> T cell responses, and it was found that CD22-deficient mice had decreased WNV-specific CD8<sup>+</sup> T cell responses compared to wild-type mice, associated with decreased lymphocyte migration into the draining lymph nodes of infected CD22<sup>-/-</sup> mice, that induce a reduced cytotoxic activity or increased cell death (Ma *et al.*, 2013). Further reported evidence indicates that this regulatory molecule prevents the overactivation of the immune system and the development of autoimmune diseases, that may occur due to genetic variation of *cd22* and by the development of auto-antibodies that may generate dysfunction of the BCR-associated lipid rafts of B cells in autoimmune states (Hatta *et al.*, 1999; Renaudineau *et al.*, 2004). In terms of published studies in pneumococcal infection, it has been shown that IL-10 induces B-1 cell migration, which differentiate into IgM-secreting cells in lymphoid or mucosal tissues, enhancing the effectiveness of the secreted antibodies in neutralizing pathogens (Baumgarth, 2011). B-1 cells spontaneously produce natural antibodies important for early protection (Haas *et al.*, 2005). Interestingly, CD22 it is also found on primary T cells and has a role in setting TCR signaling thresholds (Sathish *et al.*, 2004).

## 6.2 Aims

The gene *cd22* is located on chromosome 7, within the *Spir1* locus. The 7\_31 SNP used (see Appendix 2) in the N<sub>10</sub> congenic phenotyping (see section 4.1.1) is located in the *cd22* gene. Further understanding of CD22 function is required and could reveal roles for CD22 in disease susceptibility. The potential function of this molecule during *S. pneumoniae* infections is still unknown. To determine the involvement of CD22 in defense mechanisms during pneumococcal pneumonia, mouse strains deficient in CD22<sup>+</sup> B cells were utilised.

## 6.3 Results

### 6.3.1 A new polymorphism in the *Cd22* gene in the CBA/Ca background

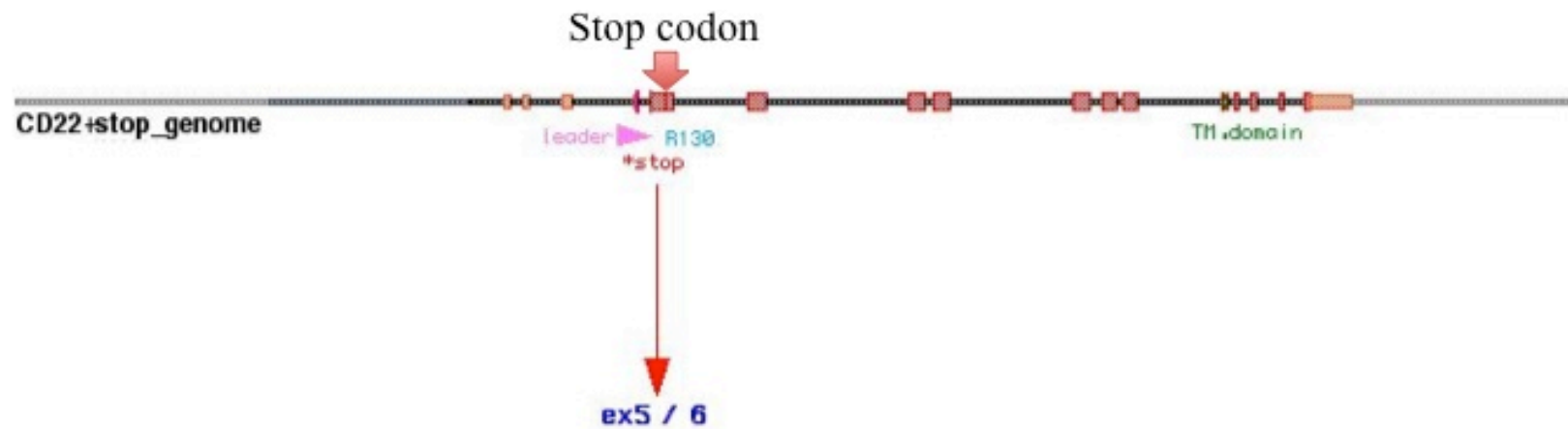
The *Cd22* gene, also known as *Sialic acid-binding immunoglobulin-type lectin 2* (SIGLEC-2) is located in proximal chromosome 7, circa 31Mb (7:31,650,421-31,665,361 location, obtained from Ensembl, release 67), with a length of 14,940 bp.

The *cd22* sequence was uploaded to Variant Effect Predictor (VEP), a tool provided by the *Ensembl* website ([www.ensembl.org](http://www.ensembl.org)) to predict functional consequences of variants between strains. This tool enabled analysis of variants and it determines the consequence of the variants on the protein sequence (McLaren *et al.*, 2010). When analysing preliminary sequencing data, 40 SNPs were observed within the *cd22* gene between BALB/c and CBA/Ca backgrounds (Appendix 3), of these three were 3 synonymous mutations, 5 were non-synonymous mutations and more interestingly, a mutation in CBA/Ca background that introduced a stop codon TAA (Table 6.1).

Uploaded Variation	Location	CBA/Ca Allele	BALB/c Allele	Feature type	Consequence	Position in cDNA	Position in CDS	Position in protein	Amino acid change	Codon change
7_31662605_G/A	7:31662605	A	G	Transcript	STOP_GAINED	658	295	99	Q/*	Caa/Taa

Table 6.1 - Mutation found in CBA/Ca mice background introduced a stop codon in the *cd22* gene. The table shows the polymorphism details and the consequence of this variant between the two strains (see Appendix 6). Data analysis extracted from the Ensembl VEP tool. The mutation introduced in CBA/Ca a stop codon “TAA” whereas BALB/c showed the codon “CAA”.

The polymorphism was initially detected by the alignment of BALB/c and CBA/Ca sequences (Figure 6.2). BALB/c share the same nucleotide as the reference C57BL/6J strain i.e. guanine, whereas CBA/Ca differed from them at this nucleotide (CBA/Ca allele is adenine). The mutation in the *cd22* gene of CBA/Ca background resulted in the introduction of the stop codon TAA (Figure 6.1). This polymorphism is located in exon 5/6 (exon 5 if ignoring the splicing region or exon 6 if counting the splicing region), which encodes for the first Ig-like domain of CD22 that is the ligand-binding one site. The mutation sits in front of this at aminoacid 99 (Q) and consequently was predicted to prevent synthesis of the protein almost completely (personal communication with collaborator Lars Nitschke, University of Erlangen, Germany).



```

GA CAC GTG GCT TCG GCT CGG TAC AGC TCA GCA AAT GAT TGG ACC GTT GAC CAT CCC CAA ACC CTC TTT GCC TGG GAG GGA GCC TGC ATC AGG ATT CCT TGC
CT GTG CAC CGA AGC CGA GCC ATG TCG AGT CGT TTA CTA ACC TGG CAA CTG GTA GGG GTT TGG GAG AAA CGG ACC CTC CCT CGG ACG TAG TCC TAA GGA ACG

▶ H V A S A R Y S S A N D V T V D H P Q T L F A W E G A C I R I P C

RAG TAC AAA ACT CCA CTA CCC AAG GCA CGT CTG GAC AAC ATC CTC CTT TTT CAG AAC TAT GAG TTT GAC AAG GCC ACC AAG AAA TTC ACA GGA ACT GTC CTG
TTC ATG TTT TGA GGT GAT GGG TTC CGT GCA GAC CTG TTG TAG GAG GAA AAA GTC TTG ATA CTC AAA CTG TTC CGG TGG TTC TTT AAG TGT CCT TGA CAG GAC

K Y K T P L P K A R L D N I L L F Q N Y E F D K A T K K F T G T V L

TAC AAC GCC ACA AAG ACT GAG AAG GAC CCA GAG TCT GAG CTG TAC CTT TCT AAG TAA GGG AGA GTA ACA TTT CTG GGG AAC AGA ATA GAC AAT TGT ACC CTG
ATG TTG CGG TGT TTC TGA CTC TTC CTG GGT CTC AGA CTC GAC ATG GAA AGA TTC ATT CCC TCT CAT TGT AAA GAC CCC TTG TCT TAT CTG TTA ACA TGG GAC

Y N A T K T E K D P E S E L Y L S K • G R V T F L G N R I D N C T L

AAA ATC CAC CCG ATA CGT GCC AAT GAC AGT GGG AAT CTG GGG TTG AAG ATG ACC GCA GGG ACT GAA CGA TGG ATG GAG CCC ATT CAC CTC AAT GTC TCG G
TTT TAG GTG GGC TAT GCA CGG TTA CTG TCA CCC TTA GAC CCC AAC TCC TAC TGG CGT CCC TGA CTT GCT ACC TAC CTC GGG TAA GTG GAG TTA CAG ACG C
K I H P I R A N D S G N L G L R M T A G T E R V M E P I H L N V S

```

Figure 6.1 - Diagram of *cd22* gene (top), highlighting exon 5/6 where the stop codon lies (bottom). This exon codes for the first Ig-like domain of *cd22* (ligand-binding one). The mutation is located at aminoacid Q99 (red underline and font colour). Underlined in blue is the sialic acid binding site (aminoacid R130). *Cd22* gene encodes for seven Ig-like domains. This sketch was produced by collaborator Lars Nitschke (University of Erlangen, Germany).

Notably, the identified polymorphism in *cd22* gene of the CBA/Ca mouse strain (Figure 6.2) has not been identified before in online databases (Figure 6.3). The gene locus (within the *Spir1* region), the novelty and predicted consequence of the gene mutation contributed to the decision to investigate the gene, the encoded protein and whether it contributes to susceptibility to pneumococcal pneumonia in the CBA/Ca strain.

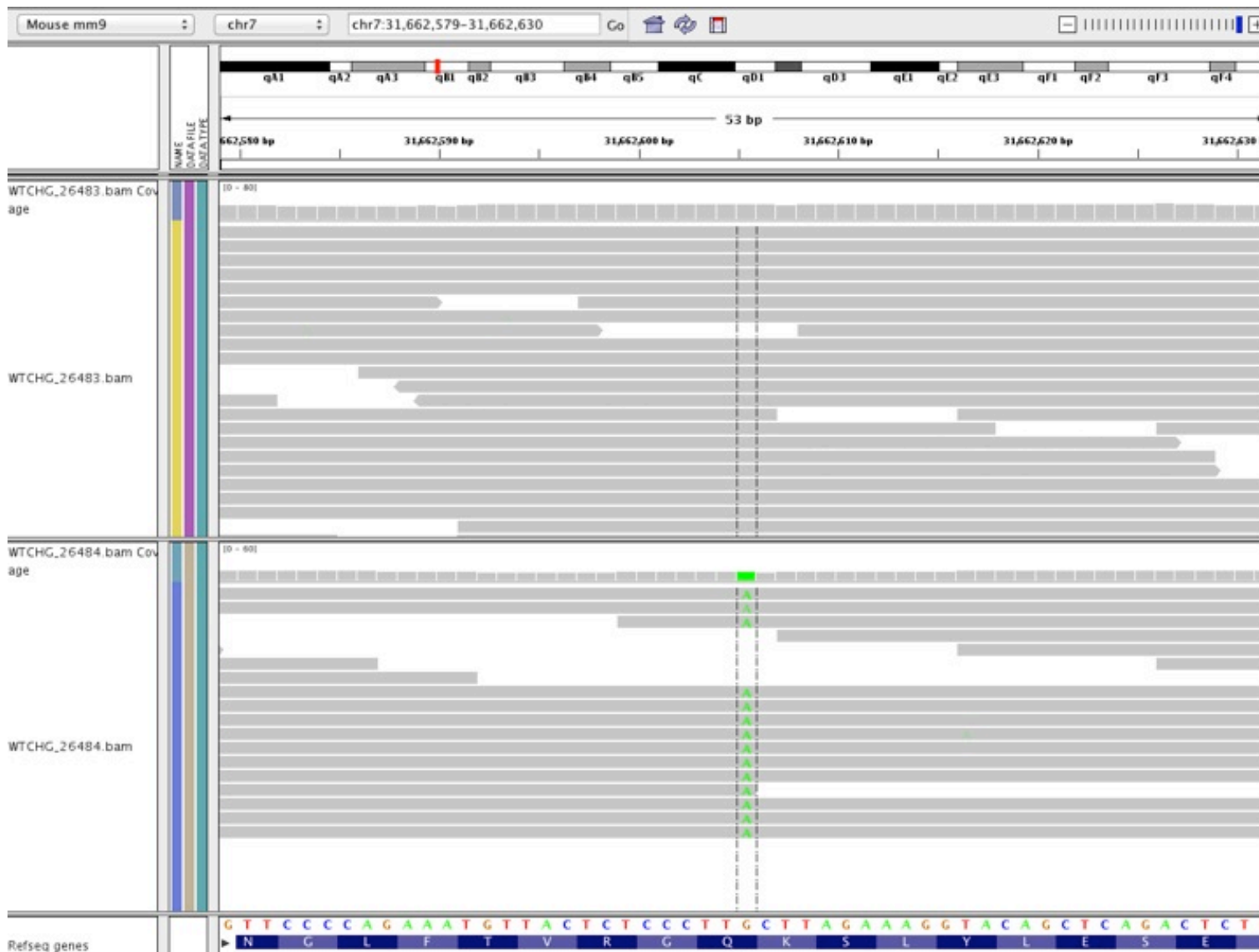


Figure 6.2 - Novel SNP found in the *cd22* gene of the CBA/Ca mice background. The figure shows a snapshot of BALB/c (coded as WTCHG\_26483.bam) and CBA/Ca (coded as WTCHG\_26484.bam) sequences alignment on the *cd22* gene, using IGV software (version 2.1). The CBA/Ca sequence has highlighted between dashed lines includes the polymorphism that introduces the stop codon, namely “A” nucleotide. BALB/c has the same nucleotide as the reference strain, *Mus musculus* C57BL/6J inbred strain, “G” nucleotide. The SNP located in chromosome 7 (*Spir1* locus) at position 7:31,662,605.

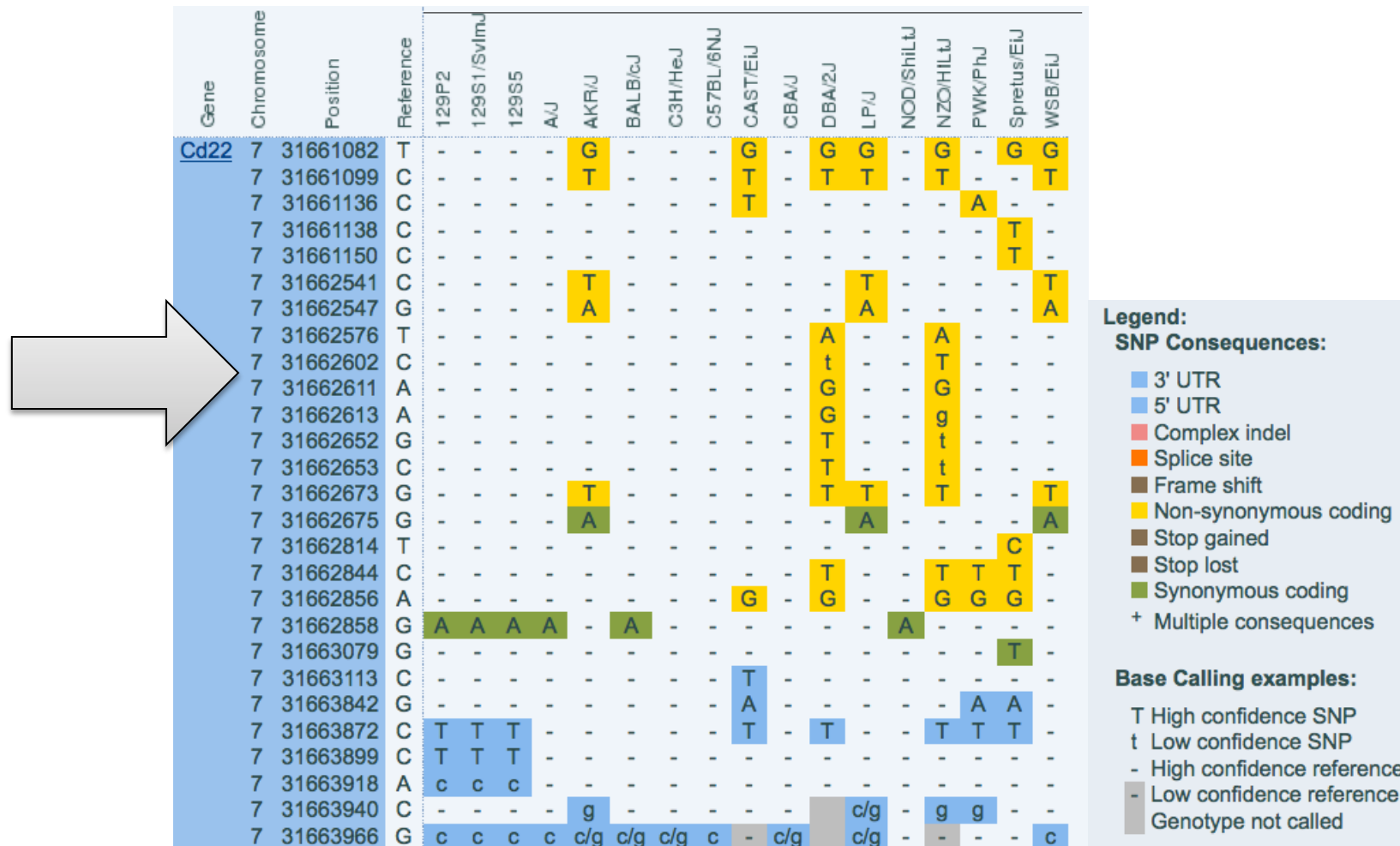


Figure 6.3 - SNP in *cd22* gene identified on CBA/Ca background does not occur in 17 inbred mouse strains from Jackson Laboratories. Snapshot of *cd22* annotated SNPs from whole-genome sequencing data of 17 inbred mouse strains from Jackson Laboratories (US). The novel SNP found in the *cd22* gene in the CBA/Ca inbred strain is located at the position 7:31,662,605, but absent in the sequenced strains is pointed in the figure by the grey arrow. Snapshot legend (right side of the SNPs list) describes the SNPs consequence. Data were collected from the Mouse Genomes Project available on the Wellcome Trust Sanger's Institute website (<http://www.sanger.ac.uk>).

### 6.3.2 Detection of stop codon in *cd22*

To confirm that the novel *cd22* SNP (coded as 7\_31, see Appendix 2), detected in the sequencing data of BALB/c and CBA/Ca was genuine, tissue samples from both strains were assessed by pyrosequencing (Figure 6.4), described in section 2.6. Figure 6.4 displays pyrosequencing outputs, highlighting the *cd22* SNP position (yellow highlight) of a BALB/c sample (Figure 6.4-A) and a CBA/Ca sample (Figure 6.4-B). The result confirmed the published sequencing data because the BALB/c strain exhibited “C” (for cytosine) nucleotide and CBA/Ca exhibit “T” (for thymine), as shown in Table 6.2.

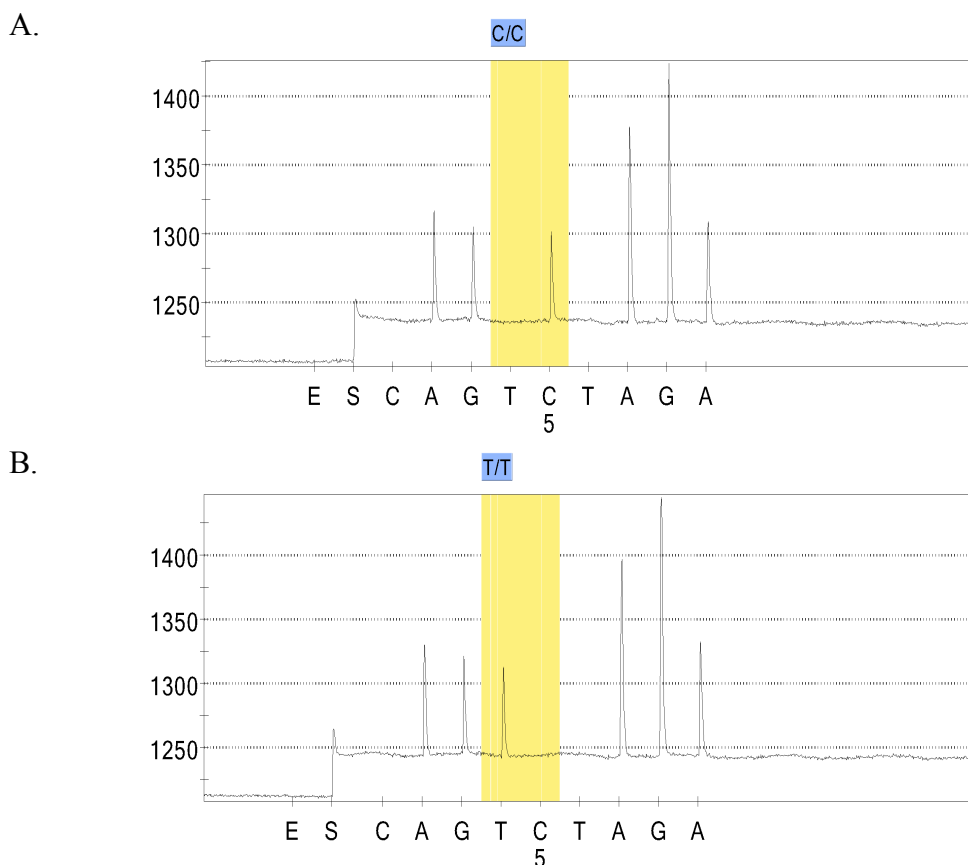


Figure 6.4 - Pyrosequencing output (pyrogram) of the *cd22* SNP observed in CBA/Ca background. The figure shows pyrograms of the *cd22* novel SNP (coded as 7\_31) in (A) BALB/c inbred mice pyrogram, which revealed a peak for nucleotide “C” (shown in the yellow background) and in (B) CBA/Ca inbred mice pyrogram, which revealed a peak for nucleotide “T” (shown in the yellow background). The *cd22* SNP testing by pyrosequencing was done in 5 animals per strain, with (A) representing one of the five BALB/c and (B) one of the five CBA/Ca pyrogram results. Primers details are described in Appendix 2.

Mouse Strain	Mouse ID	Observed nucleotides
BALB/cOlaHsd	BALB/c1	C/C
	BALB/c2	C/C
	BALB/c3	C/C
	BALB/c4	C/C
	BALB/c5	C/C
CBA/CaOlaHsd	CBA1	T/T
	CBA2	T/T
	CBA3	T/T
	CBA4	T/T
	CBA5	T/T

Table 6.2 - Analysis of pyrosequencing output (pyrogram) of the *cd22* SNP. PCR products amplified for 7\_31 SNP in BALB/c and CBA/Ca mice (n= 5 mice per strain). Primers for this SNP were designed for the complementary strands of the aligned sequences shown in Figure 6.2.

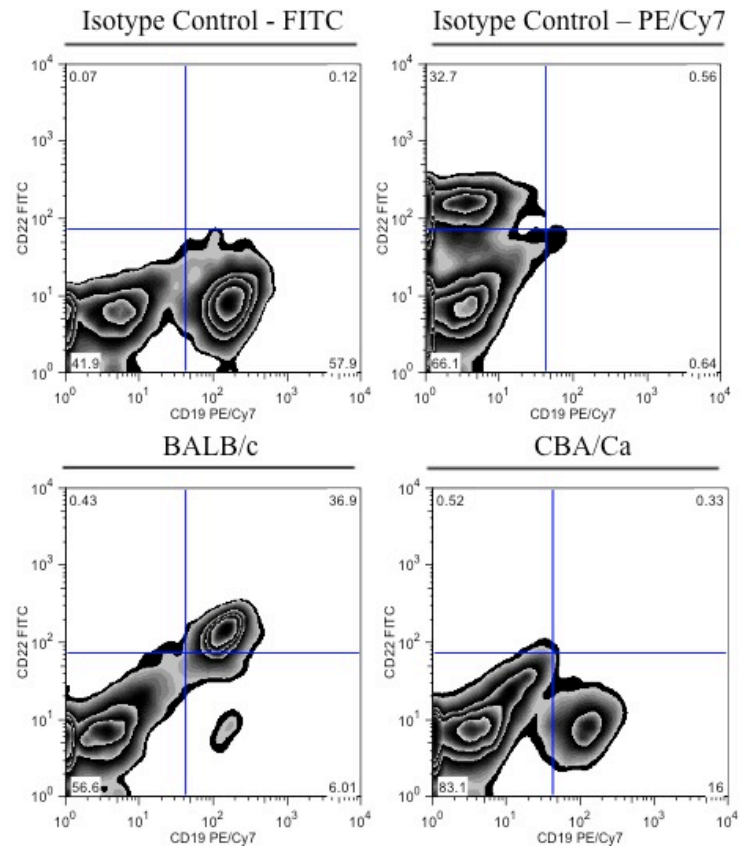
After confirming the *cd22* SNP between BALB/c and CBA/Ca inbred strains, the next step was to assess B cells expressing CD22 protein in the lungs and spleen of BALB/c mice and CBA/Ca mice, before and after pneumococcal infection (section 6.3.3). The aim of this *in vivo* study was to investigate immunophenotypical changes in BALB/c mice and to compare with CBA/Ca mice during pneumococcal infection, analysing the impact of the stop codon on the CD22 protein.

### 6.3.3 Analysis of CD22<sup>+</sup> B cell in BALB/c and CBA/Ca mice in response to pneumococcal infection

In order to investigate whether or not the observed differences in the *cd22* sequences in the two host strains were reflected in changes in CD22<sup>+</sup> B cells, flow cytometric analysis of the cell subset was performed using lung and spleen tissue from BALB/c and CBA/Ca mice.

Initially, to quantify the CD22<sup>+</sup> B cell subset in the lungs and spleen the monoclonal antibody anti-mouse CD22 (clone OX-97, rat IgG1 isotype) that recognizes the 2<sup>nd</sup> domain of the CD22 was used. As expected from analysis of the primary structure, from the flow cytometric analysis of lung samples from CBA/Ca mice (Figure 6.5), it was observed that this mouse strain did not express the CD22 protein on the B cell surface. The results showed that all the B cells from the CBA/Ca inbred mice were CD22<sup>negative</sup> (Figure 6.5-A). In contrast, 80 to 98% of B cells from the BALB/c lungs were CD22<sup>+</sup>. Also interesting was the fact that the number of CD22<sup>+</sup> CD19<sup>+</sup> cells significantly increased in the BALB/c lungs during the time course of pneumococcal challenge (\*\*,  $P < 0.01$  between 0 and 6 hrs p.i.; \*,  $P < 0.05$  between 12 and 24 hrs p.i.) (Figure 6.5-B). Figure 6.6 illustrates the proportion of B cells that express the CD22 protein (white area of the bars) and the total B cell number that include CD22<sup>+</sup> cells in the lungs (grey plus white area of the bars).

A.



B.

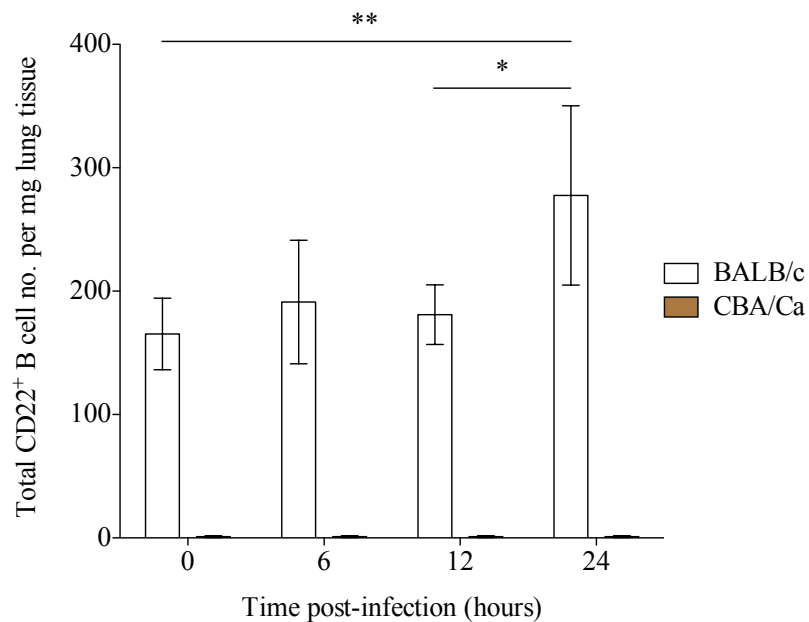


Figure 6.5 - Number of CD22<sup>+</sup> B cell number in the lungs of BALB/c and CBA/Ca mice following *S. pneumoniae* infection. Mice were intranasally infected with 10<sup>6</sup> CFU of *S. pneumoniae* and lungs were collected at 0, 6, 12 and 24 hours post-infection. (A) Flow cytometric analysis of CD22<sup>+</sup> B cells (CD22, clone OX-97 bind to domain 2 of mouse CD22) was determined by gating for CD45<sup>+</sup>, CD19<sup>+</sup> and finally CD22<sup>+</sup> events (example of a BALB/c and CBA/Ca 24 hour time point sample). (B) Number of CD22<sup>+</sup> B cells per mg of lung tissue, at the various time points, analysed by flow cytometry. Data represent the mean of positive events  $\pm$  SD. The p-value (\*\*\*,  $P < 0.001$ ) was obtained with two-way ANOVA followed by Bonferroni post-test and the p-values (\*,  $P < 0.05$ , \*\*  $P < 0.01$ ) with one-way ANOVA. Data are representative of two independent experiments with 8 mice per strain per time point.

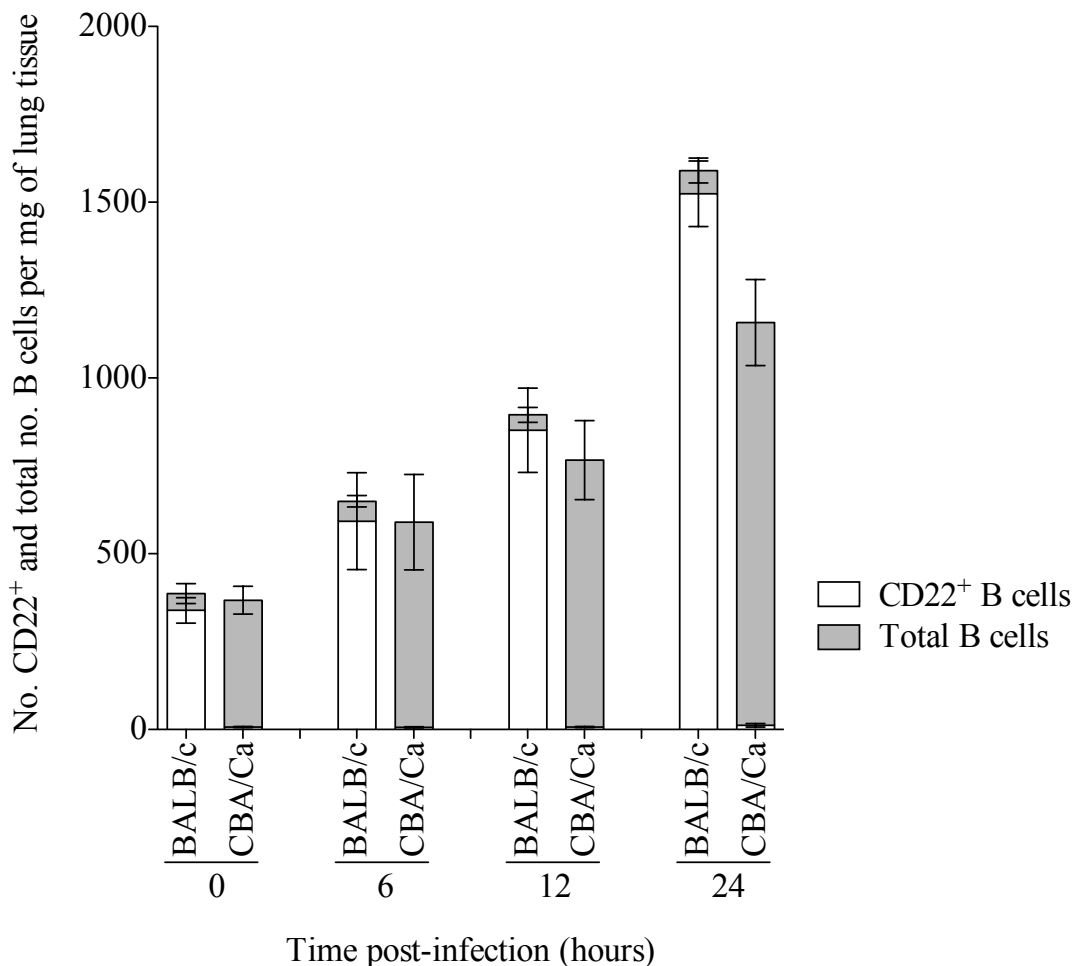
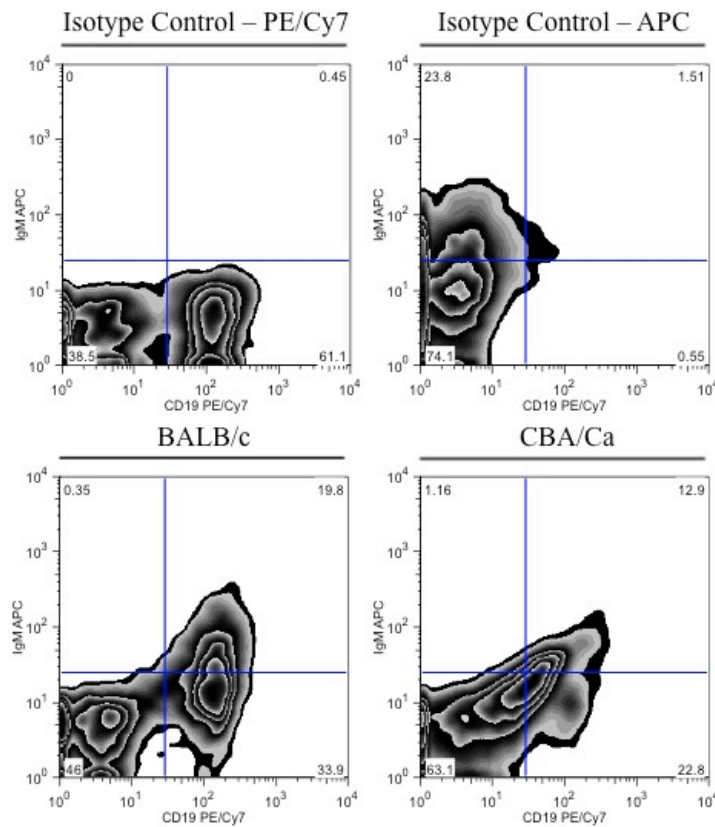


Figure 6.6 - CD22<sup>+</sup> and total B cell number in the lungs of BALB/c and CBA/Ca mice following *S. pneumoniae* infection. Mice were intranasally infected with 10<sup>6</sup> CFU and lungs were collected at 0, 6, 12 and 24 hours post-infection. Number of CD22<sup>+</sup> CD19<sup>+</sup> cells (white area of bars) and total number of B cells (grey plus white area of bars) per mg of lung tissue (clone OX-97, binds to domain 2 of mouse CD22), at the various time points, analysed by flow cytometry. Data represent the mean of positive events  $\pm$  SD. The p-values for CD22<sup>+</sup> B cells are given on Figure 6.5 and for total B cells on Figure 3.9. Data are representative of two independent experiments with 8 mice per group.

B cells were also assessed for the expression of IgM (Figure 6.7). A subpopulation of IgM<sup>high</sup> CD19<sup>high</sup> cells, reported in the literature as B-1 cells (Baumgarth, 2011), was identified. In this study (Figure 6.7), a significant increase in the number of IgM<sup>+</sup> B cells in the BALB/c was observed ( $P < 0.01$  between BALB/c and CBA/Ca at 6 and 12 hrs p.i.;  $P < 0.05$  between BALB/c and CBA/Ca at 24 hrs p.i.). The increase of IgM<sup>+</sup> B cells in the lungs of BALB/c mice was significant along the time course of pneumococcal infection ( $P < 0.05$  between 0 and 6 hrs p.i. and between 0 and 24 hrs p.i. in BALB/c mice). However, the number of IgM<sup>+</sup> B cells in the CBA/Ca lungs showed no significant changes during the infection ( $P > 0.05$ ). As elucidated in Figure 6.8, the total number of B cells increased during the time course in the lungs of both host

strains, but the phenotype of these cells was different between the strains: in the pneumococcal-infected BALB/c mice the recruitment of IgM<sup>+</sup> B cells was observed, whereas in pneumococcal-infected CBA/Ca mice only the recruitment of IgM<sup>-</sup> B cells was observed.

A.



B.

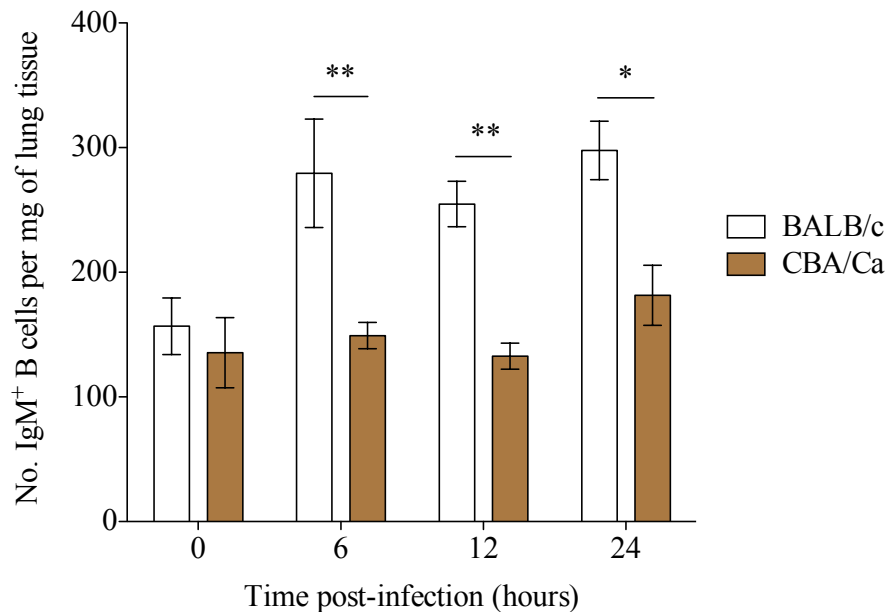


Figure 6.7 - Numbers of IgM<sup>high</sup> B cells in the lungs of BALB/c and CBA/Ca mice post-infection with *S. pneumoniae*. Mice were intranasally infected with 10<sup>6</sup> CFU of *S. pneumoniae* and lungs were collected at 0, 6, 12 and 24 hours post-infection. (A) Flow cytometric analysis of IgM<sup>+</sup> B cells was determined by gating for CD45<sup>+</sup>, CD19<sup>+</sup> and finally IgM<sup>+</sup> events (example of a BALB/c and CBA/Ca 6 hour time point sample). (B) Number of IgM<sup>+</sup> B cells (B-1 cells subset) per mg of lung tissue, at the various time points, analysed by flow cytometry. Data represent the mean of positive events  $\pm$  SD. The p-values (\*,  $P < 0.05$ ; \*\*,  $P < 0.01$ ) were obtained with two-way ANOVA followed by Bonferroni post-test. Data are representative of two independent experiments with 4 mice per group.

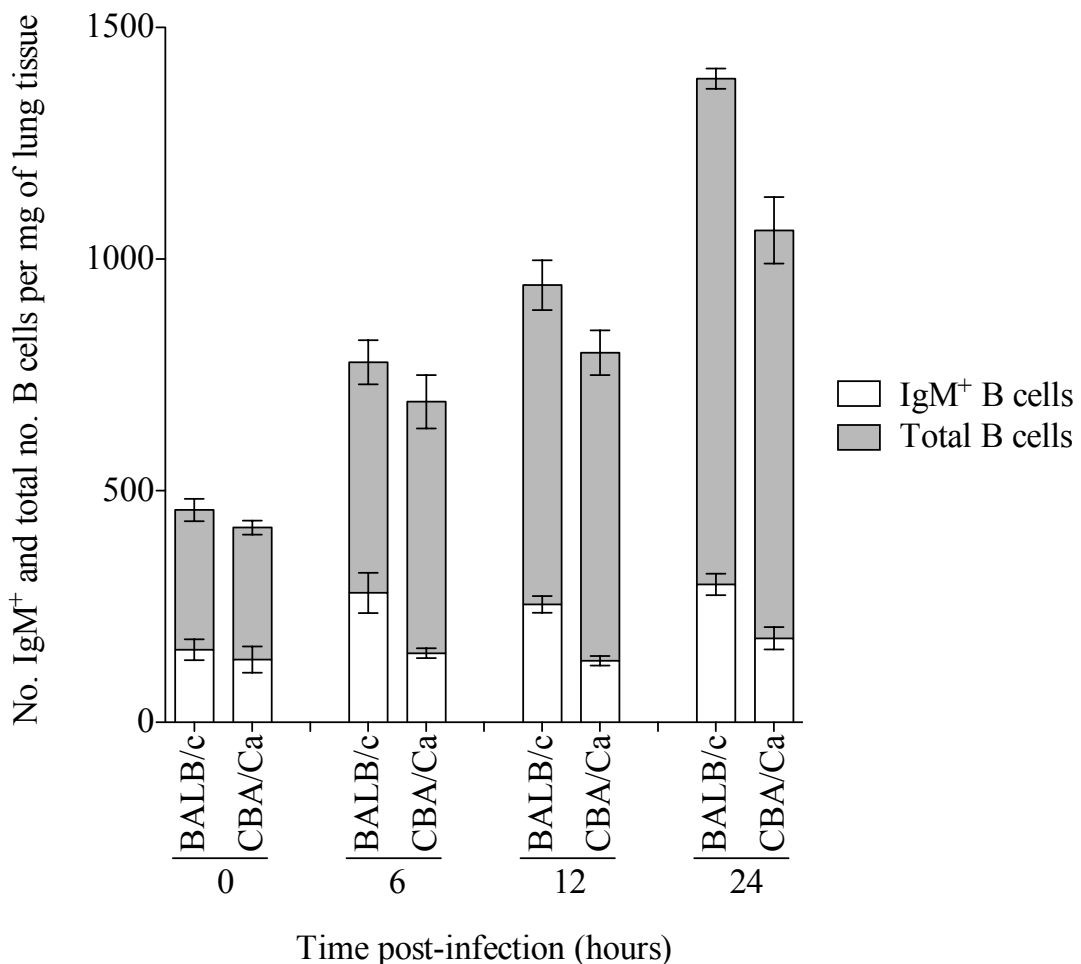


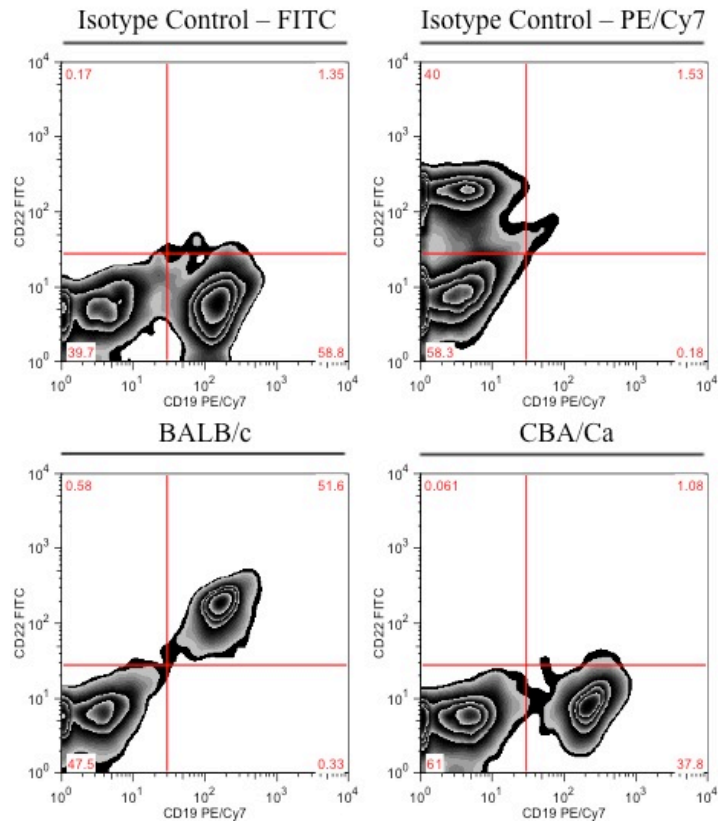
Figure 6.8 - IgM<sup>+</sup> and total B cell number in the lungs of BALB/c and CBA/Ca mice following *S. pneumoniae* infection. Mice were intranasally infected with 10<sup>6</sup> CFU and lungs were collected at 0, 6, 12 and 24 hours post-infection. Number of IgM<sup>+</sup> CD19<sup>+</sup> cells (white area of bars) and total number of B cells (grey plus white area of bars) per mg of lung tissue, at the various time points, analysed by flow cytometry. Data represent the mean of positive events ± SD. The p-values for IgM<sup>+</sup> B cells are given on Figure 6.7 and for total B cells on Figure 3.9. Data are representative of two independent experiments with 4 mice per group.

The results of the CD22<sup>+/−</sup> B cells observed in the splenocytes from these strains (Figure 6.9) was similar to those seen in lungs of BALB/c and CBA/Ca mice, in other words no CD22<sup>+</sup> CD19<sup>+</sup> cells in CBA/Ca mice. The main difference was that in the BALB/c spleens, 100% of the cells were double-positive CD22 and CD19. In addition, the CBA/Ca spleen showed significantly higher number of B cells at 0 hours ( $P < 0.001$ ) and at 24 hours ( $P < 0.001$ ) post-infection than BALB/c. The total B cell number in the spleens of both strains, as well as the CD22<sup>+</sup> CD19<sup>+</sup> cells in BALB/c significantly decreased from 0 to 24 hours post-infection ( $P < 0.05$ ).

To confirm the absence of the CD22 protein on the B cell surface in CBA/Ca mice, a different antibody clone (Cy34.1) was used. This monoclonal antibody binds to the 2<sup>nd</sup> IgG-like domain of CD22. B cells from BALB/c and CBA/Ca lungs and spleen tissue (using the same tissue samples used for clone OX-97) were assessed for CD22 positivity, as shown in Figure 6.10. The results with lung (Figure 6.10-A) and spleen (Figure 6.10-B) samples from BALB/c and CBA/Ca mice were essentially identical to those observed with anti-CD22 monoclonal antibody OX-97 (lung data in Figure 6.5 and spleen data on Figure 6.9). Basically, Figure 6.10 shows the flow cytometric analysis of B cells expressing CD22 (CD22<sup>+</sup> CD19<sup>+</sup> cells), using the monoclonal antibody Cy34.1, which in the lungs of BALB/c mice (Figure 6.10-A) represent 48% and 0% in the lungs of CBA/Ca mice of the acquired events. With the spleens (Figure 6.10-B) the observations were similar, with these cells representing 49% in BALB/c mice and 0% in CBA/Ca mice of the acquired events. Both antibody clones (OX-97 and Cy34.1) indicated the absence of CD22 expression on B cells surface in CBA/Ca mouse tissue.

The subsequent step was to investigate whether any role of the CD22 protein during *S. pneumoniae* infection could be determined. The results of a pilot experiment are described in section 6.3.4.

A.



B.

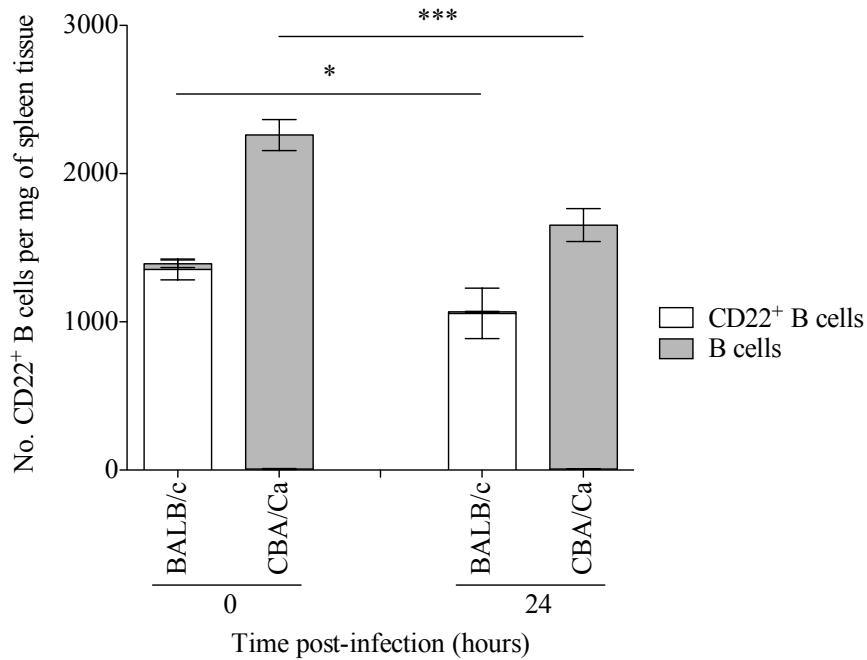
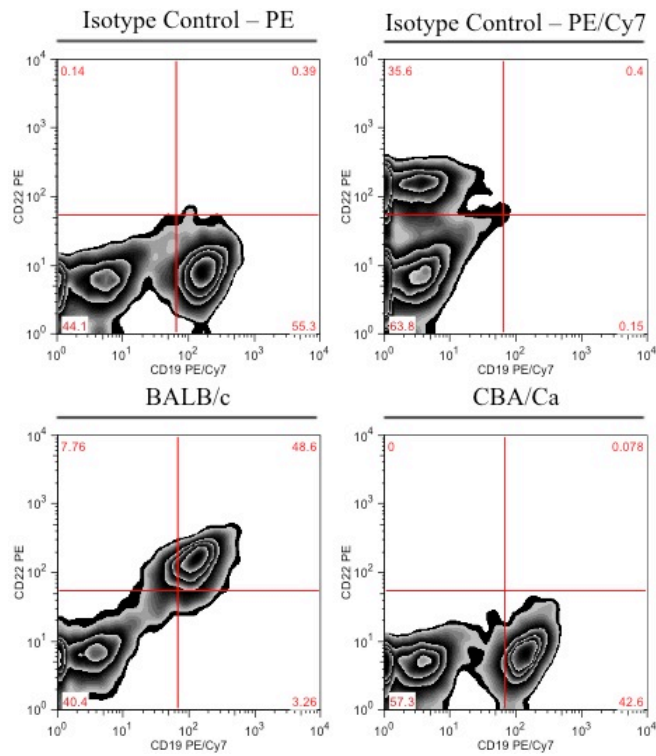


Figure 6.9 - Number of CD22<sup>+</sup> B cell number in the spleen of BALB/c and CBA/Ca mice following *S. pneumoniae* infection. Mice were intranasally infected with 10<sup>6</sup> CFU of *S. pneumoniae* and spleen tissue was collected at 0 and 24 hours post-infection. Number of CD22<sup>-</sup> CD19<sup>+</sup> (grey area of bars) and CD22<sup>+</sup> CD19<sup>+</sup> (white area of bars) cells per mg of spleen tissue (clone OX-97, bind to domain 2 of mouse CD22), at the various time points, analysed by flow cytometry. Data represent the mean of positive events  $\pm$  SD. The p-values (\*,  $P < 0.05$ ; \*\*\*,  $P < 0.001$ ) were calculated for total B cells, obtained with two-way ANOVA analysis. Data are representative of one independent experiment with 4 mice per group.

A.



B.

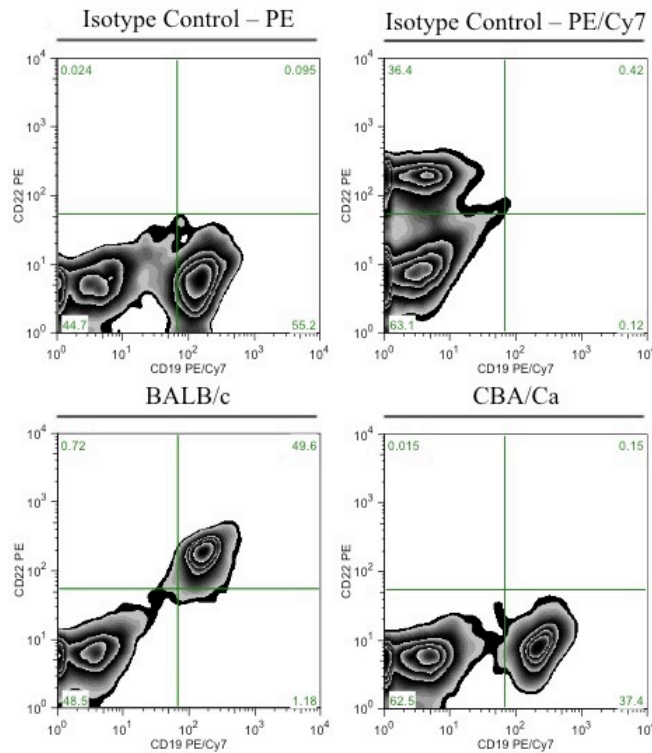


Figure 6.10 - Flow cytometric analysis of CD22 binding site tested with a different antibody clone Cy34.1 in lungs and spleen samples of BALB/c and CBA/Ca mice, prior and post- infection with *S. pneumoniae*. Mice were intranasally infected with  $10^6$  CFU of *S. pneumoniae* and the lungs and spleen were collected at 0 and 24 hours post-infection. Tissue samples from same mice as used to assess the number of CD22<sup>+</sup> CD19<sup>+</sup> cells (A) in the lung and (B) in the spleen of BALB/c and CBA/Ca mice, using the anti-mouse CD22 antibody (clone Cy34.1, bind to 2<sup>nd</sup> Ig-like domain of CD22). Example of a representative sample of BALB/c and CBA/Ca mice, (A) lung and (B) spleen tissue, collected at 24 hours time point.

#### 6.3.4 Functional analysis of *cd22* following infection with *S. pneumoniae*

To determine the contribution of the *cd22* gene and the encoded protein during IPD an *in vivo* experiment was performed with CD22-deficient mice and control mice (C57BL/6J mice – the background of the CD22<sup>-/-</sup> mice). C57BL/6J mouse strain has intermediate resistance to wild-type D39 serotype 2, therefore, prior to study of the role of *cd22* gene during pneumococcal pneumonia, dose titration (adjusting volume and bacterial concentration) was performed on C57BL/6J mice, in order to achieve a percentage of survival in the control group of between 50 and 100%, making it easier to detect any dissimilarity with the test group (CD22-deficient mice). Subsequently, control and CD22-deficient mice were infected intranasally with 3-4x10<sup>5</sup> CFU of *S. pneumoniae* in 25 µl PBS and monitored for 7 days, assessing survival time, disease signs and the number of bacteria in the blood at 24 and 48 hours post-infection (Figure 6.11).

Strikingly, the survival rate of C57BL/6J mice was significantly higher than CD22-deficient mice after pneumococcal infection ( $P < 0.001$ ), as shown in Figure 6.11-A. During the 7 days of the experiment, all CD22-deficient mice ( $n = 10$ ) succumbed to pneumococcal pneumonia (0% survival and median survival of 44 hours p.i.), whereas 5 out of 9 wild-type mice reached the experimental end point (55% survival and median survival of 123 hours p.i.). Following infection, the CD22<sup>-/-</sup> group started showing visible signs of disease after 24 hours post-infection, although the control mice were nearly 1 day later (42 hours p.i.) than the knockout mice (Figure 6.11-B), exhibiting significant difference from 35 hours until the end of the experiment ( $P < 0.01$ ). Interestingly, mice that lack CD22 protein displayed significantly higher numbers of bacteria in the blood at 24 ( $P < 0.001$ ) and 48 hours ( $P < 0.01$ ) post-infection (Figure 6.11-C and Figure 6.11-D, respectively), when compared to control mice.

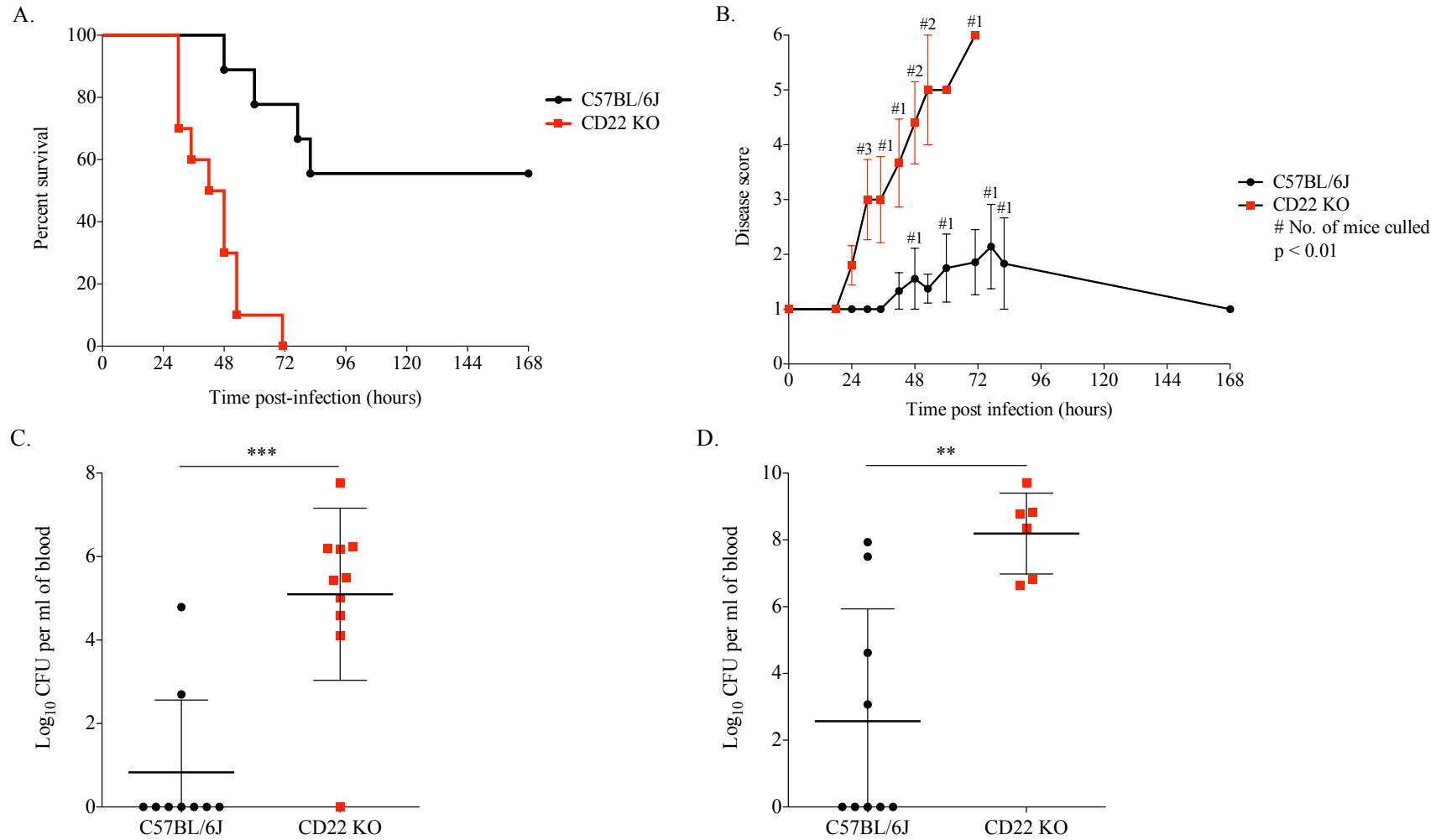


Figure 6.11 - Comparison of outcome of pneumococcal infection of CD22-deficient and sufficient mice. All results in (A–D) are from intranasal infection of C57BL/6J (●) and CD22 KO mice (■) with wild-type D39 *S. pneumoniae*. (A) Survival of pneumococcal-infected mice was monitored for 7 days and (B) assessment of animal disease score (see Table 2.2 in section 2.3.9). Number of bacteria per per ml of blood collected (C) at 24 hours p.i. and (D) at 48 hours p.i.. For all graphs data represent mean values  $\pm$  SEM. The p-values in graph (A) and (C) (\*\*\*,  $P < 0.001$ ); in graph (B) (\*\*,  $P < 0.01$ ) showing significance from 35 hours p.i. until end of the experiment; in graph (D) (\*\*,  $P < 0.01$ ) were obtained with two-tailed *t* test, except for graph (A) that the analysis was done by Log-rank test. Results are from one experiment with 9 C57BL/6J mice and 10 CD22 KO mice.

Next, the progress of pneumococcal disease in CD22<sup>-/-</sup> mice was investigated, in a time point experiment (Figure 6.12), analysing in detail the bacterial dissemination: lung CFUs (Figure 6.12-A), blood CFUs (Figure 6.12-B) and spleen CFUs (Figure 6.12-C) at 0, 6, 12, 24 and 48 hours post-infection.

The results showed no significant differences in the number of bacteria in the lungs (Figure 6.12-A) of the control group during the time course of the infection ( $P > 0.05$  when compared to 0 hours). Also in the lungs of CD22-deficient mice the number of bacteria had no significant changes during the time points ( $P > 0.05$  when compared to 0 hours). When comparing the lung CFUs between the control group with CD22-deficient mice, no significant differences at any time point ( $P > 0.05$ ) were observed.

The detection of bacteria in the blood (Figure 6.12-B) showed two different patterns. The CD22-deficient mice started to develop bacteraemia at 12 hours, which increased at 24 and 48 hours post-infection, showing a significant increase over the time points ( $P < 0.01$ ), whereas in the blood of control mice no significant changes were observed ( $P > 0.05$ ). Between the control and the test group, significant differences were shown at 24 ( $P < 0.01$ ) and 48 hours ( $P < 0.001$ ) post-infection, with the CD22-deficient mice displaying higher bacteraemia than the control group at both time points.

The spleen tissue was also assessed for bacteria (Figure 6.12-C) and followed the pattern observed in the blood. The control group had no bacteria in the tissue at any time point, but all the CD22-deficient mice had bacteraemia, except for one mouse (with lower CFU in the blood at 12 hours post-infection), which also had bacteria in the spleen tissue. The CD22-deficient mice showed a significant increase of bacteria in the spleen during the time points ( $P < 0.0001$ ) and when compared to control mice at 24 ( $P < 0.01$ ) and 48 hours ( $P < 0.001$ ) post-infection.

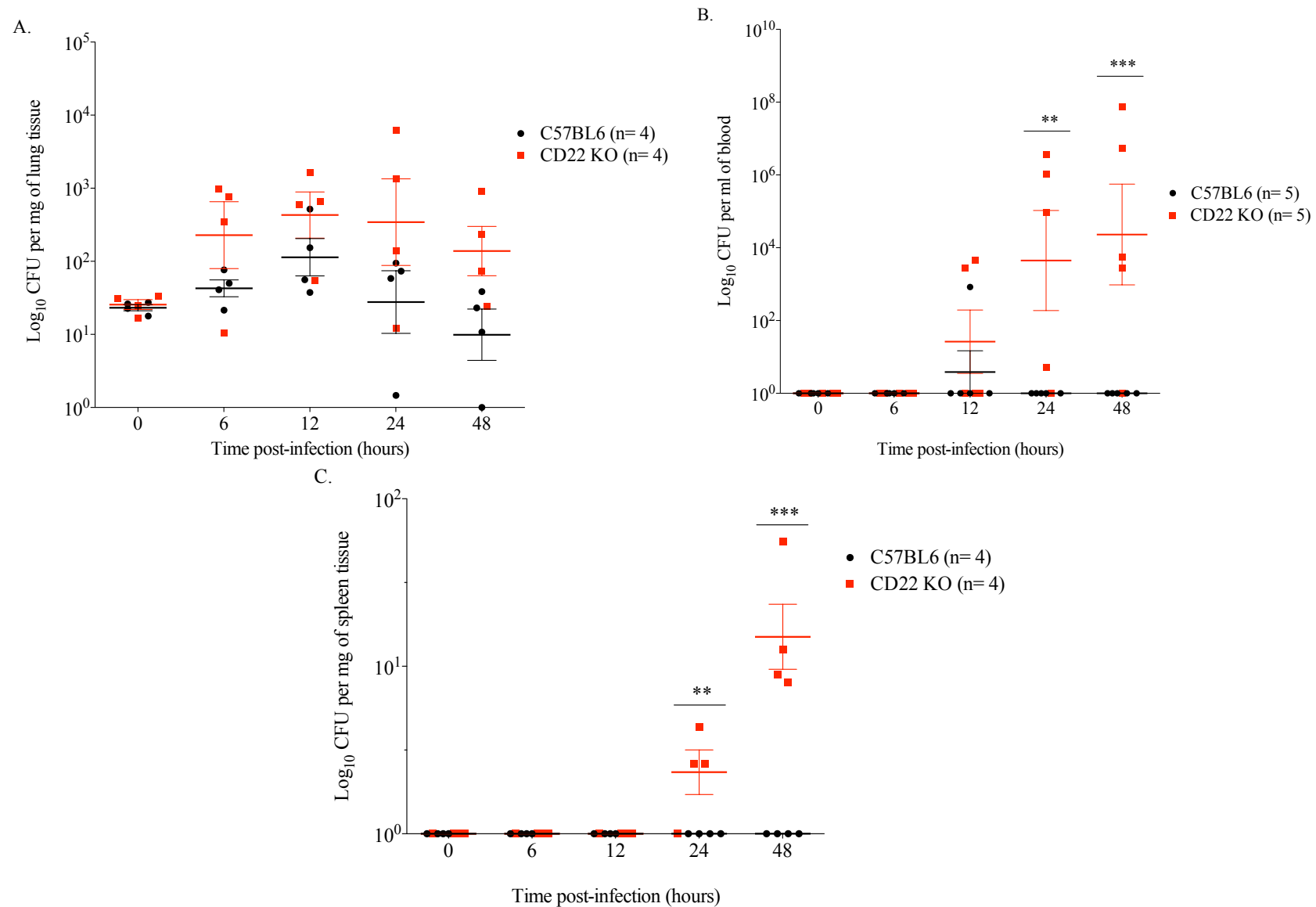


Figure 6.12 - Bacterial counts of *S. pneumoniae* in various organs following intranasal infection of CD22-deficient and sufficient mice. All results in (A–C) are from intranasal infection of C57BL/6J (●) and CD22 KO mice (■) with wild-type D39 *S. pneumoniae*. Number of bacteria (A) per mg of lung tissue and (B) per ml of blood and (C) per mg of spleen tissue at 0, 6, 12, 24 and 48 hours post-infection. For all graphs data represent mean values  $\pm$  SEM. The p-values in graph (B) and (C) (\*\*,  $P < 0.01$ , \*\*\*,  $P < 0.001$ ) were obtained with two-way ANOVA followed by Bonferroni post-test. Results are from one experiment with 5 mice per group per time point, except for 0 hours p.i. ( $n = 4$  per group).

---

## CHAPTER 7. DISCUSSION

---

The work described in this thesis has investigated the BALB/c and CBA/Ca mouse models of susceptibility to pneumococcal infection, in order to identify the impact of chromosome 7 *Spir1* locus to the phenotypic differences observed in these two inbred mouse strains. The production of the congenic mouse was performed to identify candidate genes that are the basis for variation in susceptibility to invasive pneumococcal disease and how it influences the pathology of pneumonia. Besides the congenic study, immune cellular and cytokine responses to pneumococcal infection were inspected in BALB/c and CBA/Ca mouse strains to identify which are the critical features determining resistance and susceptibility.

### **7.1 Reports on BALB/c vs CBA/Ca mice in response to different infections**

Others have shown that BALB/c and CBA/Ca mouse strains display distinct phenotype in response to different infections. For instance, BALB/c mice are susceptible and CBA resistant to infection with *Salmonella typhimurium* (Plant & Glynn, 1976), *Leishmania donovani* infection (Bradley & Kirkley, 1977) and *Mycobacterium leprae murium* (Brown *et al.*, 1982). Host susceptibility in response to these intracellular pathogens suggested an association with chromosome 1 locus. Data have also been reported that show host response to other infections with reverse phenotypes: BALB/c mice are resistant and CBA/Ca susceptible to encephalitis due to *Toxoplasma gondii* (Suzuki *et al.*, 1993) and to intravenous infection by *Streptococcus pyogenes* (Goldmann *et al.*, 2003; Goldmann *et al.*, 2004).

### **7.2 Major phenotypic differences between a resistant and a susceptible host to *S. pneumoniae* infection**

To improve this knowledge and comprehend the host defence mechanisms against pneumococcal infection, a resistant and a susceptible host to *S. pneumoniae* was examined, namely BALB/c and the CBA/Ca (Gingles *et al.*, 2001), respectively. Major differences between the two host strains may help to determine critical elements of the immune response that failed or delayed to respond during the disease progression.

In order to understand whether pneumococcal infection was confined in the lungs of the resistant BALB/c mouse strain, mice were infected intravenously (bacteraemia model). Comparing the BALB/c and CBA/Ca susceptible phenotypes, it was obvious that the pneumococcal bacteria rapidly grew in the bloodstream of CBA/Ca mice, very quickly reaching intolerable numbers to the host's homeostasis. On the other hand, the resistant phenotype of the BALB/c was significantly different to the CBA/Ca, showing longer survival time, later disease signs but with prompt development to lethargy and lower numbers in the blood. The results obtained with BALB/c mice showed that immune cells were recruited into the lungs during infection. The data suggests that the cells mediating the infection may have been recruited from peripheral tissues, such as lymph nodes and the spleen, holding bacterial proliferation. In addition, the longer survival and lower bacteraemia in the first 24 hours post-infection observed in BALB/c mice, together with the exponential pneumococcal growth registered in the CBA/Ca, indicate that the immune response of CBA/Ca mice was qualitatively different with impaired efficiency affecting a timely response and adequate cellular recruitment.

Obviously, it is important to understand why CBA/Ca mice succumb to pneumococcal pneumonia displaying bacteraemia so rapidly, and on the other hand, how BALB/c mice control bacterial proliferation within the lungs. The data collected in this study suggest that the protective elements that confer a resistant phenotype to BALB/c mice are present in the lungs, because when BALB/c mice were infected by intravenous route, they also showed a susceptible phenotype. Overall, the pulmonary cellular recruitment in pneumococcal-infected BALB/c mice is more robust and balanced than CBA/Ca mice. Basically, the resistant host strain evidenced a prompt and greater infiltration into infected lungs, essentially by neutrophils and macrophages, together with the support of thymus and bone marrow matured lymphocyte subsets (T helper, cytotoxic, gamma-delta, regulatory and B cells).

As important as a robust cellular recruitment is the regulation of the innate immune response, balancing the bacterial clearance with tissue damaging caused by excessive inflammation. Predominantly cytokines, as well as oxygen free radicals and coagulation factors, characterise these inflammatory mechanisms. Interestingly, the number of CD4<sup>+</sup> T cells in the lungs of BALB/c mice (Figure 3.7-B) exhibited a significant increase within 24 hours of infection ( $P < 0.001$ ), whereas the number of these cells in CBA/Ca

lungs had no significant change ( $P > 0.05$ ) during the time points of the experiment. The displayed differences in  $T_{\text{helper}}$  cells was reflected in the contrasts found in lung cytokine production between resistant and susceptible host (section 3.2.4). A recent publication showed a novel function in regulation of the immune system, by restraining the excessive inflammatory responses (Mauri & Bosma, 2012), through IL-10 production (observed cytokine production in the lungs – higher in BALB/c mice – Figure 3.24-A), which may explain the input of B cell during IPD. Remarkably, two different cytokine profiles were observed in the lungs of the two host strains: BALB/c mice exhibited a proinflammatory cytokine production, with high levels of IL-1 $\beta$  and TNF- $\alpha$ , balanced with immunosuppressive response, with the production of IL-10 and TGF- $\beta$ ; CBA/Ca mice showed proinflammatory response, with high levels of IL-6 and IFN- $\gamma$ . These observations may be relevant to understand and uncover new therapy targets, as modulating the cytokine producing-cells will reflect in the outcome of the immune response.

### 7.3 Outcome of the *Spir1* congenic work

Mouse models provide a vital tool for interrogating genetic elements in human disease and for investigating their functions *in vivo* (DeBry & Seldin, 1996). The QTL located on chromosome 7 (see Appendix 1), the previously reported *Spir1* locus (Denny *et al.*, 2003) was mapped in progeny from an F<sub>2</sub> intercross. This mouse chromosome 7 *Spir1* region has even more relevance because it shows complete conservation of synteny with human chromosome 19 (chr 19q13.1-q13.3 region) (Denny *et al.*, 2003). The breeding of congenic mice for this QTL and the infection phenotype analysis of incipient congenic mice have significantly strengthened the evidence for the contribution of the chromosome 7 QTL to *S. pneumoniae* susceptibility, previously observed in the F<sub>2</sub> mapping results (Denny *et al.*, 2003). Thanks to phenotyping a large cohort of congenic mice, a major correlation between the 7\_09 SNP marker (upstream the *Spir1* region) and survival and bacteraemia of congenic mice was observed, confirming the hypothesis that a major QTL resides in this region. Strikingly, mice with a BALB/c background, which were homozygous for the chromosome 7 *Spir1* locus from CBA/Ca were significantly more at risk from death due to the pneumococcal pneumonia, and this correlated with significantly higher levels of bacteraemia at 24 hours, than mice homozygous for BALB/c at the *Spir1* locus. The QTL region downstream the *Spir1* locus (markers 7\_54 and 7\_123) did not correlate with the *S. pneumoniae* reduced

disease phenotype. Overall, prior to this project, a significant correlation of this locus with IPD was only determined by statistical analysis (Denny *et al.*, 2003), whereas this congenic study provided concrete biological evidence of the *Spir1* region impact on pneumococcal susceptibility. Moreover, in a separate study with 26 inbred mouse strains (from Jackson Laboratory), a genome wide association study (GWAS) approach was used to map genetic loci associated with IPD (Jonczyk *et al.*, 2014). Importantly, this study also identified a QTL on chromosome 7, precisely within the *Spir1* region (Jonczyk *et al.*, 2014). It provides a strong support on mapping pneumococcal susceptibility, and with the use of such large number of mouse strains, it also demonstrates that the *Spir1* region is not a genetic element generated by specifically crossing the resistant BALB/c strain with the susceptible CBA/Ca strain.

Narrowing down the QTL region by adding additional SNP markers showed significant linkage between 7\_09, 7\_17, 7\_27, 7\_31, 7\_35, 7\_46 and 7\_51 and the mouse phenotype (survival and 24 hr bacteraemia). The aim of this investigation was to study and identify genes in this chromosome 7 QTL contributing to susceptibility (not resistance). Strikingly, the correlation observed was between SNPs in the susceptible background (mouse strain donor of the QTL in the congenic breeding programme) that exhibited the CBA/Ca variation SNPs. These observations were encouraging for the project, providing to this locus a prospective target for further investigation. Following this investigation on the *Spir1* locus, showing that a cluster of genetic SNP markers was linked to a susceptible phenotype to pneumococcal pneumonia, it suggests that a combination of genes could modulate the outcome of the pneumococcal disease.

Parallel to the congenic programme, an investigation on genes in the *Spir1* locus, whose role is known to be involved in immune mechanisms, was developed. These genes were screened before and after pneumococcal infection in BALB/c and CBA/Ca mice. Preliminary data from gene expression, protein expression and cytokine profiling in the lung tissue have identified the gene *tgfb1* (section 7.4), and the sequencing data together with the lung tissue immunophenotyping of BALB/c and CBA/Ca mice identified the gene *cd22* (section 7.5), both suitable candidate genes in the chromosome 7 *Spir1* QTL. Further studies on these and other possible candidates should be considered (sections 7.5 and 7.8), including sequencing of the *Spir1* region from CBB and BCC congenic mice (considering the strong linkage found between 7\_09 SNP and the infection

phenotype), to identify polymorphic genes between BALB/c and CBA/Ca and correlation with survival and bacteraemia, and therefore contributing to the difference in pneumococcal susceptibility between these two strains.

Collectively, the biological evidence acquired with the *Spir1* congenic strain has opened up new avenues for future research. It would be relevant to investigate the impact of other microbial diseases in the congenic strain, as the genes in the *Spir1* region may be involved in common features of the immune response to other bacterial infections. Moreover, an improved understanding of the role of candidate genes studies in this thesis (*tgfb1* and *cd22*) could be determined by mapping the genetic inheritance in the congenic strain (presence of BALB/c or CBA/Ca allele variants), correlating with the disease phenotype.

Due to the strong correlation found between the 7\_09 SNP from the CBB line and susceptibility to pneumococcal disease, this line was sent for genome sequencing (by Source Bioscience) for further narrowing of the QTL region, as an alternative to pyrosequencing analysis of SNPs. Currently, the data is being analysed by collaborators in bioinformatics (MRC Harwell).

#### **7.4 TGF- $\beta$ and T regulatory cells**

The fact that *tgfb1* gene is located within the *Spir1* region encouraged investigation of the contribution of TGF- $\beta$  and its downstream targets (T regulatory cells and IL-10) to the differing susceptibilities of BALB/c and CBA/Ca mice to IPD. In a pilot study, microarray comparison of gene expression in lung tissue from BALB/c or CBA/Ca mice following pneumococcal infection showed significant differential regulation of the TGF- $\beta$  signalling pathway between strains. Furthermore, qRT-PCR analysis on pneumococcal-infected lung tissue from BALB/c and CBA/Ca mice showed expression of *tgfb1* significantly higher in BALB/c than in CBA/Ca mice, both pre- and post-infection. The *tgfb1* gene sequences from BALB/c and CBA/Ca were also recently compared and two SNPs were identified (one intronic and one downstream) (Appendix 5). These findings were key to proceeding with further investigation.

Collectively, the data demonstrate an important role for T regulatory cell activity in mediating resistance to pneumococcal pneumonia. Thus, the differing susceptibilities of

BALB/c and CBA/Ca mice can be attributed, at least in part, to differences in the coordination and regulation of TGF- $\beta$  signaling pathways in these mice. Evidence from other diseases suggests that CD4<sup>+</sup> Foxp3<sup>+</sup> T regulatory cells play prominent roles in immune regulation (Morampudi *et al.*, 2011). Indeed, in infectious diseases such as Lyme arthritis, down-regulation of T regulatory cells by pathogens is a feature of infection that correlates with poor prognosis (Shen *et al.*, 2010). It is well known that infection with *S. pneumoniae* results in a rapid and vigorous immune response in the lungs, characterised by early infiltration of neutrophils and increased macrophage numbers (Haslett, 1999) followed by an influx of lymphocytes (Kadioglu & Andrew, 2004), but an uncontrolled and sustained influx of proinflammatory leukocytes to the lung could be highly detrimental to the host. Excessive inflammatory infiltrate can lead to substantial tissue damage through the actions of degradative enzymes and other soluble mediators released from the infiltrating cells and such tissue damage could compromise the integrity of the epithelial cell barrier of the lung and aid bacterial dissemination to the bloodstream. Pneumococcal pneumolysin can also be toxic through its proinflammatory activity and not just its cell damaging. Therefore, appropriately regulated immune responses in the lung during pneumococcal infection are essential, and help to contain the bacteria within the lungs and eventually clear them. T regulatory cells in such an environment might limit the inflammatory reaction thus preventing tissue damage and preserving epithelial barrier integrity. In CBA/Ca mice, with fewer T regulatory cells, less TGF- $\beta$  and no immunosuppression, this process is inefficient and may lead to compromise of the lung architecture. This is supported by the substantially increased levels of apoptosis seen within the lungs of CBA/Ca mice, and increased levels of bacterial seeding into blood. Nevertheless, not only direct damage (necrosis) could be the cause for bacterial dissemination and death. An uncontrolled cytokine signal can cause an exaggerated response with too many immune cells in a single site (cytokine storm) (Osterholm, 2005), and if occurring in the lungs, fluids and immune cells can block the airways resulting in death (Ibelgaufts, 2013). Besides, a physiological disruption (such as septic shock, blood pressure, heart rate, respiratory rate, body temperature) could be the cause of death (Kumar *et al.*, 2007; Martin, 2012). In CBA/Ca mice, one of the disease signs observed was a significant drop in respiratory rate when mice reached lethargic.

The correlation between strong T regulatory cell responses and decreased IFN- $\gamma$  production has been reported previously in patients with severe trauma (MacConmara *et al.*, 2006). A recent study described a correlation between increased Foxp3<sup>+</sup> T regulatory cells in Malawian adults with asymptomatic HIV infection and an associated skewing of T cell cytokine production away from IFN- $\gamma$  (Glennie *et al.*, 2011). In the study in this thesis, the T cell contribution to IFN- $\gamma$  production was minimal but reduced NK cell-derived IFN- $\gamma$  was observed in BALB/c mice, which have strong T regulatory cell responses.

The finding that pneumococcal pneumonia induces IL-10 production in the lung is a significant one. T regulatory cell-derived IL-10 has a well-documented role in immune homeostasis in the lung during allergy (Taams *et al.*, 2002; Bellinghausen *et al.*, 2003; Jutel *et al.*, 2003; Ling *et al.*, 2004). For example, mice in which IL-10 was specifically ablated in T regulatory cells, by insertional mutagenesis of the *foxp3* gene locus, displayed perivasculitis and mononuclear cell infiltration around the large airways of the lung (Rubtsov *et al.*, 2008). The same mice also displayed exacerbated disease signs in an ovalbumin-driven model of allergic airways inflammation (Rubtsov *et al.*, 2008). Thus, it appears that T regulatory cell-derived IL-10 plays an important role in the suppression of immunological reactivity in the lung in both allergic inflammation and infection, where it may help limit infection-related tissue damage.

In addition to IL-10 production, the T regulatory cells induced in response to pneumococcal infection might mediate immune regulation and the suppression of pathological inflammatory responses through a direct cell-cell contact mechanism. The finding that CTLA-4 is highly expressed on a subset of T regulatory cells in resistant BALB/c, but not susceptible CBA/Ca mice following pneumococcal infection supports this assertion. Moreover, the observed increase in T regulatory cells in BALB/c lungs following infection is rapid (Figure 5.6), supporting a greater role for nT<sub>regs</sub> than for iT<sub>regs</sub>, which can take several days to differentiate in the periphery in response to TGF- $\beta$  and low doses of antigen. The main difference between these T<sub>regs</sub> subsets (natural and induced) is that nT<sub>regs</sub> develop in the thymus, whereas iT<sub>regs</sub> develop from mature CD4<sup>+</sup> T cells outside of the thymus (mucosal-associated lymphoid tissue) (Curotto de Lafaille & Lafaille, 2009). nT<sub>regs</sub> present in tissues can become activated upon Ag stimulation

immediately, while  $iT_{reg}$  populations are generated in the periphery and recruited to the site of infection (Curotto de Lafaille & Lafaille, 2009).

Interestingly, the studies in outbred MF1 mice provided complementary evidence for a link between resistance to invasive disease and a high number of regulatory T cells in lungs, but also suggested that uncontrolled lung neutrophil influx in susceptible mice might contribute to lung tissue damage that may promote bacterial dissemination. A similar destructive role for neutrophils has been suggested previously after it was demonstrated that depletion of neutrophils with monoclonal antibodies could prolong survival in mice given a lethal intranasal dose of serotype 8 pneumococci (Marks *et al.*, 2007). Furthermore, the detrimental effects of excessive neutrophil recruitment have been documented recently in a study investigating sex-based differences in susceptibility to pneumococcal disease (Kadioglu *et al.*, 2011). The greater susceptibility of male mice to invasive pneumococcal disease was attributed, in part, to the uncontrolled presence of proinflammatory cytokines (highly elevated levels of cytokines such as TNF- $\alpha$ , IL-1 and IL-6) and greater neutrophil infiltration into lungs following intranasal pneumococcal infection as compared to reduced proinflammatory cytokines and lower neutrophil infiltration in lungs of female mice. However, these data must be balanced against the proven role for neutrophils in bacterial clearance (Craig *et al.*, 2009). It is likely that it is the timing of the neutrophil influx that is crucial (Denny *et al.*, 2003; Buttery & Moxon, 2002; Kaplanski *et al.*, 2003; Paterson & Orihuela, 2010). If recruitment can occur whilst the bacteria are still confined to the lung then disease resolution may occur, but if the influx occurs later, the neutrophils may fail to clear the infection and may aid bacterial dissemination via contribution to lung damage. The earlier influx of neutrophils to the lungs in BALB/c versus CBA/Ca mice certainly correlates with bacterial clearance.

Collectively, these novel findings impact on our perception of host immune responses to pneumococcal infection, emphasizing the importance of balancing proinflammatory responses in the lung with controlled anti-inflammatory and immunomodulatory activity. Furthermore, it is clear that achieving this balance is fundamental to containment and clearance of pneumococcal infection in lungs. The finding that the correlation between strong regulatory cell responses and invasive disease resistance is not restricted to BALB/c and CBA/Ca mice but were also observed in a group of MF1

mice in which individual animals varied in resistance. These genetically variable populations mimic more closely the spectrum of disease resistant phenotypes seen in human populations. In this thesis it has been shown how differences in the regulation and balance of host immune responses can dramatically alter the development and outcome of infection by either leading to containment and clearance of the pathogen from lungs or the development of severe invasive pneumonia and lethal septicaemia. It follows that genetic differences or polymorphisms in components of immunomodulatory pathways may predispose individuals to the development of septicaemia following acute pneumonia.

These studies have unearthed an important but hitherto unappreciated role for T regulatory cells in limiting immune-mediated damage in the lungs during pneumococcal infection. This is a novel study, identifying protective roles for T regulatory cells in anti-pneumococcal responses and it is to be hoped that the findings herein may facilitate the design of pneumococcal therapies aiming to improve T regulatory cell responses in susceptible or infected individuals.

In this thesis the role of TGF- $\beta$  through an effect on T regulatory cells was explored. Nevertheless, TGF- $\beta$  has a multifunctional role during the inflammatory response. TGF- $\beta$  is involved in the regulation of a vast range of cellular responses (Akhurst & Hata, 2012), with particular focus to its role in the regulation of fibroblast differentiation in IPD (Jonczyk *et al.*, 2014). The data collected in this thesis together with the new findings on pulmonary gene expression analysis suggest that TGF- $\beta$  may also have impact in lung vasculature through fibroblasts, contributing to host survival modulation of vessel functioning (Jonczyk *et al.*, 2014). Combining the two sets of data, it was also observed that the gene *lsr* (Lipolysis-stimulated lipoprotein), which is a *Spir1* QTL gene involved in TGF- $\beta$  signalling (Figure 5.1) was likewise differentially expressed between BALB/c and CBA/Ca controls in the pulmonary gene data (Jonczyk *et al.*, 2014). The protein encoded by the *slr* gene is a cell surface receptor involved in binding, internalisation and degradation of lipoproteins (Herbsleb *et al.*, 2008) and tricellular tight junction formation (Furuse *et al.*, 2012). Besides the interesting role of the SLR protein, the consistency on these observations from two different sources suggests further investigation is warranted.

### **7.5 *Cd22* another candidate gene contributing to pneumococcal pneumonia susceptibility**

Among the 250 genes within the *Spir1* region, the *cd22* gene was selected as a candidate gene contributing to susceptibility to pneumococcal infection. The interest in this gene arose after the analysis of BALB/c and CBA/Ca genome sequences and SNPs between the two mouse strains. Out of the 12,626 SNPs between BALB/c and CBA/Ca found in the *Spir1* QTL, three SNPs introduced a stop codon function: one in *sptbn4* (spectrin beta 4) gene with a stop codon at amino acid 2,222 within a 2,559 protein full-length; a second one in *prodh2* (proline dehydrogenase oxidase 2) gene with a stop at amino acid 137 within a 536 protein full-length; and a third one in the *cd22* (cluster of differentiation 22) gene with a codon at amino acid 99 within a 847 protein full-length. The *cd22* gene was chosen for study because it was the only one in which the smallest portion (if any) of the protein may be produced.

In this study, 40 SNPs were identified in the *cd22* gene (including 3 synonymous and 5 non-synonymous mutations), in which a novel SNP between BALB/c and CBA/Ca mouse strains was revealed (Appendix 6). The variant found in CBA/CA's exon 5/6 of the first Ig-like domain of *cd22* (ligand-binding one) introduced a stop codon. The absence of this protein was determined by testing two different anti-CD22 antibodies (clones OX-97 and Cy34.1), binding to different sites of the 2<sup>nd</sup> IgG-like domain (out of seven binding sites), and the results confirmed the lack of the CD22 protein on the B cell surface in CBA/Ca mice and confirmed its presence in BALB/c mice.

To address the role of the transmembrane protein CD22 in response to pneumococcal infection, CD22<sup>+</sup> B cells flux in spleen and lung tissue (prior to and during infection) was assessed (section 6.3.3). These studies have demonstrated that during pneumococcal infection B cell numbers in the spleen significantly drop in both strains (BALB/c and CBA/Ca), whereas in the lungs a significant increase was observed, also in both strains, but significantly more in BALB/c than CBA/Ca (at 24 hours p.i.). This observation suggests that a translocation of B cells to the lungs from the spleen occurs. Thus the spleen may function as a reservoir of mature B cells that were mobilised as a response to the infection. Evidence of similar behaviour in response to influenza virus infection has been reported (Baumgarth *et al.*, 1999). Another interesting morphological observation was that the spleen from BALB/c mice was, in every case, nearly two times

the size of the spleen from CBA/Ca mice, which correlated with their average weight: the BALB/c spleen was approximately 120 mg and CBA/Ca spleen approximately 70 mg.

Following, a pilot experiment involving intranasal challenge with CD22-deficient mice and C57BL/6J control mice *S. pneumoniae* was performed to assess the functional activity of CD22. Strikingly, when challenging CD22-deficient and control mice, significant differences were observed between groups in survival (0% compared to 55% survival, respectively) and signs of disease (more pronounced in CD22-deficient mice). Although there were no significant differences in the number of bacteria in the lungs between wild-type and CD22-deficient mice, the control group contained the bacteria in the lungs and the study group developed septicemia, inclusively affecting secondary tissue (spleen). Furthermore, BALB/c mice showed a significant increase in natural IgM produced by CD22<sup>+</sup> B cells compared to CBA/Ca mice.

B cells produce antibodies as cell-surface receptors (role as antigen receptor) and as secreted molecules (upon B cell activation). IgM is the first class of antibody made by a developing B cell and it is a naturally circulating serum antibody, which appear early in the course of an infection, with active role in maintenance of immune homeostasis (Gronwall *et al.*, 2012). CD22 acts as a receptor to antigen and soluble IgM that negatively regulates signalling via B cell receptor (BCR) (Adachi *et al.*, 2012). IgM molecules can be found on the surface of B cells (monomeric) and also secreted by B cells (soluble as a pentamer) (Adachi *et al.*, 2012). When soluble, IgM is effective at complement activation thus contributing to bacterial opsonisation and macrophage phagocytosis (Wellek *et al.*, 1976). Collected data in Figure 6.7 showed IgM-secreting B cells (B-1 cells) with significant increase on IgM production by CD22<sup>+</sup> cells in BALB/c mice, whereas the susceptible CBA/Ca mice (that lack the CD22 protein) had no significant change in IgM production by CD22<sup>-</sup> B cells. Further investigation to provide a clearer view of CD22 role during pneumococcal infection is required. Nevertheless, the data suggest that upon antigen activation, B cells are recruited into the lungs, releasing IgM which may activate the complement, opsonise bacteria and induce a phagocytic response. It seems that in the infection site (lungs) is where CD22 may have an active role by negatively regulating B cells, via BCR signalling, controlling excessive activation of B cells (Lajaunias *et al.*, 2002). In the susceptible CBA/Ca mice,

the lack of CD22 may result in a deregulation of B cells and consequent impaired release of IgM can contribute to increase susceptibility to infection (Etzioni & Ochs, 2004).

Overall, this study evidenced an important role of CD22 during pneumococcal infection. Various lectins are expressed on immune cells, suggesting that glycans play crucial roles in the regulation of immune responses (Demetriou *et al.*, 2001; Rabinovich *et al.*, 2002; Crocker *et al.*, 2007; Gleeson, 2008). These data suggest that natural IgM-secreting B cells (B-1 cells) provide an effective early frontline defense against *S. pneumoniae* invading the lungs, preventing the dissemination into other sites (such as blood and spleen tissue) and eliminating the bacteria, as supported by published data (Weber *et al.*, 2014). B1 cells are major producers of natural IgM antibodies that protect the host by opsonising pathogens and promoting complement receptor-mediated phagocytosis (Weber *et al.*, 2014). The levels of natural antibodies in CBA/Ca are currently under investigation.

Another hypothesis may be considered regarding IL-10-producing B cells. The results obtained in the flow cytometric analysis on IL-10 showed that T<sub>regs</sub> produced 75% of IL-10 produced (approximately 300 T<sub>reg</sub> cells per mg of lung tissue) (Figure 3.19) and were found around 400 IL-10-producing cells per mg of lung tissue (Figure 3.18) in BALB/c mice. It was not determined which cell type was involved in the production of the remainder (approximately 25%). Recently it has been reported that a subset of B cells producing IL-10 may have substantial anti-inflammatory and immunosuppressive functions that regulate innate immune responses (Stanic *et al.*, 2014). It would be of interest to further compare the phenotype of the B cells between lungs of BALB/c and CBA/Ca mice to better understand their role and impact in the protective immune mechanisms.

In conclusion, it is speculated that once B cells are activated through BCR, immediately after an exposure to pneumococcal disease, they migrate into the lungs and then stimulate the secretion of IgM, inducing opsonisation of the bacteria and a phagocytic response, via activation of the complement system. The CD22 seems to help preventing excessive B cell activation and autoantibody production (Lajaunias *et al.*, 2002). It should be kept in mind that B cells may also produce IL-10, and therefore can have immunoregulatory capacity, helping to prevent excessive inflammation. Moreover, it

still not clear how CD22 activate B-1 cells, and the limited published data available indicate no correlation between CD22 expression and the inflammatory response during bacterial infection (Gjertsson *et al.*, 2004), which enhances the novelty of this study. The success of current results leads to a further dissection of the mechanisms involving *cd22* gene and its downstream targets that may play a role during pneumococcal infection.

### **7.6 Overall components of mechanisms of resistance and susceptibility to *S. pneumoniae* infection**

The collected lung cytokine data showed interesting results that clearly help in understanding the host immune mechanisms and to distinguish an immune pattern associated with a resistant phenotype and a different immune pattern associated with a susceptible phenotype to pneumococcal infection.

Looking at Table 3.2 (section 3.2.4), it is evident that the earlier (in time p.i.) the cytokine assessment was done, the greater the differences found between host strains. Notably, the resistant BALB/c evidenced a more rapid cytokine response than the susceptible CBA/Ca. The cytokine production in BALB/c was significantly higher than in CBA/Ca lungs. For instance, at 6 hrs p.i. BALB/c showed significantly higher levels in 5 cytokines and CBA/Ca only 3 cytokines, but the opposite was observed at the latest time point. Analysing the results of the chemoattractant cytokines for neutrophils, KC and MIP-2, significantly higher production of both chemokines at 12 hours post-infection was observed in the BALB/c lungs, which correlates with the greater increase of neutrophils (Figure 3.5) and macrophages (Figure 3.6) cells in the lungs of BALB/c compared to CBA/Ca mice. These are cell types that contribute to bacterial clearance by recognition, phagocytosis and killing in innate immunity (Soehnlein *et al.*, 2008).

Also evident in this cytokine's profile was a more rapid increase (at 6 hrs p.i.) of a potent inflammatory mediator – interleukin 17 – that acts synergistically with IL-1 $\beta$  and TNF- $\alpha$  (Miossec *et al.*, 2009; Chiricozzi *et al.*, 2011), both found at significantly higher levels at 6 and 12 hours post-infection in the BALB/c lungs compared to CBA/Ca. On the other hand, in the CBA/Ca lungs was observed a significant increase on the levels of IFN- $\gamma$  and IL-6, working in synergy in the recruitment and clearance of neutrophils

during acute infection (McLoughlin *et al.*, 2003). This data suggests that in CBA/Ca mice the exacerbated IFN- $\gamma$  cytokine levels may not provide an effective host defense, and this interplay with high levels of IL-6 may induce apoptosis of neutrophils, in addition to epithelial cells damaging (Wen *et al.*, 1997; McLoughlin *et al.*, 2003), contributing to bacterial dissemination into the bloodstream.

Around 6 to 12 hours after pneumococcal infection, when neutrophils provide phagocytic activity, and granulocytes release inflammatory mediators and attract more immune cells to the infection site, it is crucial that the bacterial growth is controlled and the level of inflammation caused by the intense influx of leukocyte cell into the lungs and mediators release are also sustained. This control role is established by TGF- $\beta$ , which can reduce inflammation and re-establish homeostasis. In the cytokine profile, it was observed that the levels of TGF- $\beta$ 1 significantly increased in the lungs of the resistant strain at 6 and 12 hours post-infection ( $P < 0.001$  and  $P < 0.05$ , respectively), whereas no significant changes were observed in CBA/Ca lungs, at any time point.

The differences in susceptibility to pneumococcal infection observed in BALB/c and CBA/Ca mice showed an interesting association with cytokines production. Strikingly, these two inbred strains are also characterised by a dissimilar T<sub>helper</sub> differentiation, suggesting different host mechanisms in response to pneumococcal infection, resulting in a distinct cytokine production profiles. The susceptible CBA/Ca inbred strain evidenced a T<sub>h</sub>1 response to pneumococcal infection, producing a strong proinflammatory response mediated by IFN- $\gamma$  cytokine (Figure 3.26-A), stimulating cell-mediated responses (those involving cytotoxic T cells and macrophages), which induces the killing of intracellular bacteria (Jin *et al.*, 2004). However, an unbalanced or uncontrolled proinflammatory response may lead to tissue injury that contributes to pathogenesis (Herbst *et al.*, 2011). Such a mechanism to counterpoise this reaction was not observed in the CBA/Ca immunoprofile. Interestingly, the resistant BALB/c inbred strain seem to have the contribution of a suppressor T cell population, suppressing immune responses via cell-cell interactions and/or the production of IL-10 (Figure 3.24-A) and TGF- $\beta$ 1 (Figure 3.30-A). It has been reported  $\gamma\delta$  T cells function as Treg cells and their implication in the down regulation of immune responses, by releasing the immunosuppressive T<sub>r</sub>1- and T<sub>h</sub>3-type cytokines IL-10 and TGF- $\beta$ 1, playing a role in the inhibition of immune responses to tumours and in various inflammatory disorders

and may acquire immunoregulatory properties at mucosal sites, such as in autoimmune diabetes (Hanninen & Harrison, 2000; Groux, 2001). There are other suppressive mechanisms operating, such as the mechanism through CTLA-4 expression. Foxp3 controls the expression of CTLA-4 in  $T_{\text{regs}}$ , and deficiency on CTLA-4 impairs *in vivo* and *in vitro* suppressive function of  $T_{\text{regs}}$ , besides it was observed that CTLA-4 knockout mice succumb prematurely from multiorgan inflammation (Wing *et al.*, 2008).

From the analysis of the results obtained on blood cytokines, it was clear that by the time that CBA/Ca mice reached lethargy (at 24 hrs p.i.), the cytokine levels were all extremely high, showing a sign of an unregulated and uncontrolled response to pneumococcal infection. At the earlier time points, the IL-6 cytokine in the blood of CBA/Ca mice (Figure 3.23-B). At 12 hours post-infection, the levels of IL-6 had a significant increase in the CBA/Ca mice ( $P < 0.01$  compared to BALB/c at 12 hrs p.i. and to CBA/Ca sham-infected). Curiously, the level of IL-6 in the lungs of CBA/Ca mice reflects on the observed increase of cytokine in the blood (Figure 3.23). Reported data support the contribution of this cytokine as an inflammatory marker (Rincon, 2012).

In summary, in the data collected in the model of infection used, the resistant BALB/c strain has shown an immunologically distinct reaction from the susceptible CBA/Ca strain. The data generated by this work led to the production of Figure 7.1. This data suggests that rapidly after infection the resistant host recognizes pneumococcal molecules (possibly through TLRs and NLRP3 inflammasome), promoting the maturation of inflammatory cytokines (such as IL-1 $\beta$  and TNF- $\alpha$ ). The acute phase initiates a cascade of cytokines, these cytokines increase vascular permeability, likewise inducing proliferation and recruitment of macrophage and neutrophils (including through KC affinity – the neutrophil chemoattractant) to the site of infection (the lungs) (Janeway *et al.*, 2001). Neutrophils are specialised to engulf and destroy the pneumococci and its molecules. At this stage of the innate response, to avoid an exacerbated inflammatory response, the homeostatic balance is established by an enhanced immunosuppressive response. This reaction is led by the T regulatory cells, which during *S. pneumoniae* infection in the resistant host actively secreted the immunomodulatory cytokine TGF- $\beta$  and the major immunoregulatory cytokine IL-10.

Together they inhibit the activity of lymphocytes, monocytes and macrophages (Letterio & Roberts, 1998; Couper *et al.*, 2008). This active and balanced innate response is important to protect the host against pneumococcal infection. In the susceptible host, data suggest a different innate immune response to pneumococcal infection. The pulmonary leukocyte recruitment is delayed and occurs to a lesser extent. Neutrophils and macrophages also increased in numbers during disease progression, although the cellular response was late to control the increase in lung bacterial loads during the infection. In addition to that, an impaired proinflammatory response through the synthesis and release of cytokines IFN- $\gamma$  and IL-6 may be inducing apoptosis of neutrophils (McLoughlin *et al.*, 2003) and epithelial cells damaging (Wen *et al.*, 1997), aggravating the lung pathology. Reported data have shown that an exacerbated expression of IFN- $\gamma$  and IL-6 may increase lung inflammation and accelerate mortality in mice (Moreira *et al.*, 2002). Although TGF- $\beta$  regulates T<sub>regs</sub>, IL-6 can suppress Foxp3 expression, required for T<sub>regs</sub> differentiation, inhibiting TGF- $\beta$ -dependent Foxp3<sup>+</sup> Treg cell induction that results in enhanced Th1 differentiation (Bettelli *et al.*, 2006; Yang *et al.*, 2008), as observed in CBA/Ca mice. This lung cytokine storm induces apoptosis and tissue damage (Khajanchi *et al.*, 2011), resulting in bacterial dissemination into the blood causing lethal septicaemia in the susceptible host.

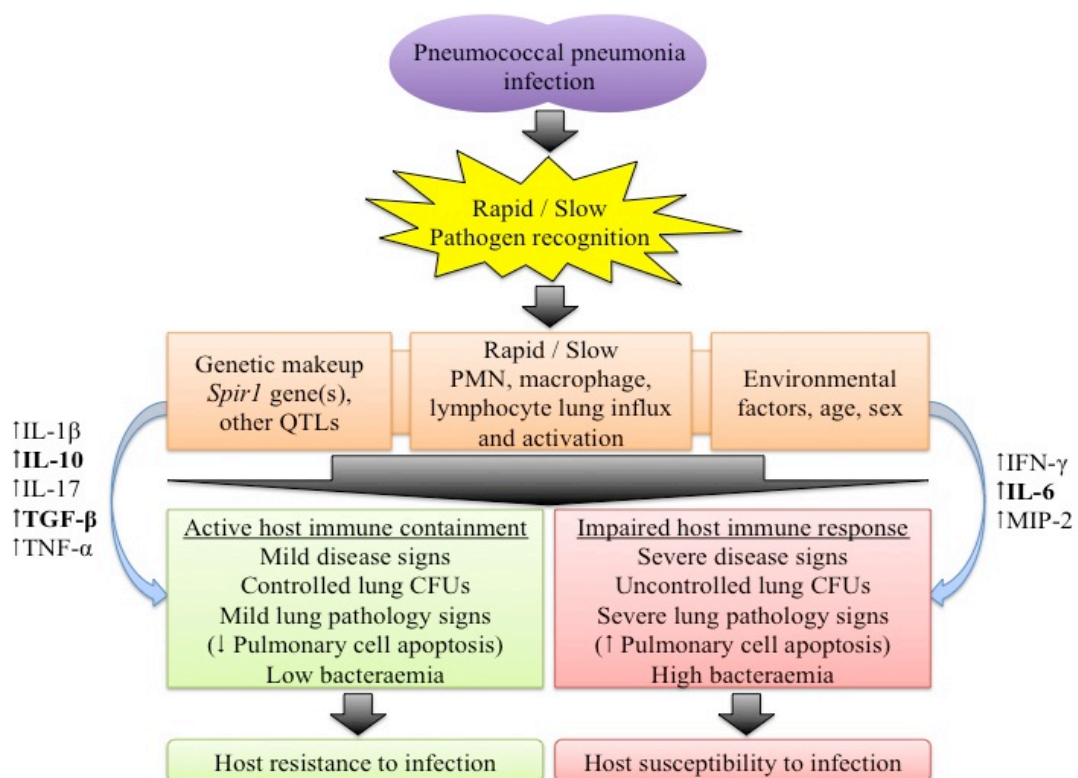


Figure 7.1 - Components influencing resistance and susceptibility to pneumococcal pneumonia.

## **7.7 Benefits of this research project to society**

An ideal outcome of this work would be to add to the current knowledge of this field of scientific study and to translate this into a clinical setting, with a view to identifying genes associated with pneumococcal infection susceptibility in humans, as a means of providing personalised medical treatment to patients and aid the development of future drug targets and vaccines.

The map of the human genome project provides a DNA library that may transform medicine in the 21<sup>st</sup> century. Diagnosis, prognosis, treatment and, most importantly, prevention may be tailored to individuals' genetic and phenotypic information. Investments in molecular biology, bioinformatics, disease management and the unravelling of the human genome are all beginning to bear fruit (Rochman, 2012). Several crucial things need to materialise in order for us to make major headway, however. Extremely well-integrated multidisciplinary teams are required to establish methods to understand the large amounts of molecular and genetic information available and to develop robust scientific hypotheses to test in a clinical setting so that individualised medicine can become a reality (Rochman, 2012). The collection, processing, and storing of molecular information will become a new and important driver of demand for technological information. It is acknowledged that publicity will help to encourage investment and engage the public's interest. However, it is the fundamental science behind individualised medicine that will eventually allow attainment of our proposed goal (Rochman, 2012). Besides, economic success for pharmaceutical and diagnostic industries is predicted, as well as for research funding in the academic sector. The existing synergy between the academic sector and hospitals in the United Kingdom may help to implement personalised medicine strategies, in order to: diagnose a patient's genetic predisposition by targeting crucial mutations linked to diseases (e.g. pneumococcal disease) and phenotypic information; correct gene faults; host defence strategies to boost or suppress; identify those at risk so that they have tailored prophylactics. A care action plan for individual patients may provide both efficient medical treatment and economically efficient, with benefit to patients lifestyle.

This work may contribute to an improved understanding of the mechanisms operating in the lungs and the role that regulatory cells, *cd22* and encoding protein and cytokines, such as IL-6 and TGF- $\beta$  play in these processes, which may allow prediction of

outcomes of *S. pneumoniae* infection and tailor treatments accordingly. It will also certainly be of interest to develop novel pneumococcal vaccines that can induce protective IgM-secreting CD22<sup>+</sup> B-1 cell and/or T regulatory cell responses. Another contribution of this study in this field could be by assessing the patients for genetic mutations in the *Spir1* region that contribute to susceptibility to pneumococcal disease.

### 7.8 Future work

Two candidate genes were studied in this thesis, however there are good reasons to study other genes located in the *Spir1* QTL. Genome sequencing of congenic mice (CBB line – susceptible line showing recombination in the QTL), focusing on the *Spir1* region, and further bioinformatic analysis (in process in collaboration with MRC Harwell) would help to confirm, identify and prioritise genes for further investigation. The analysis of the sequencing data obtained from congenic mice samples may provide crucial evidence on the success of the congenic mapping. This means that the amount of genetic contamination with fragments DNA from the QTL donor (CBA/Ca strain) along the recipient genome, apart from *Spir1* region can be determined. In addition to that, the sequencing analysis may provide great enough resolution to, not only to narrowing QTL, but furthermore to identify new candidate genes contributing to susceptibility to pneumococcal disease.

Moreover, sequencing data from BALB/c and CBA/Ca mouse strains have identified two more genes in the *Spir1* region containing stopping codons in the CBA/Ca background: *spectrin beta non-erythrocytic 4* (SPTBN4), located at 28Mb, which encodes a protein localised to the nuclear matrix, PML nuclear bodies, and cytoplasmic vesicles, and functions in the determination of cell shape, arrangement of transmembrane proteins, and organization of organelles (Tse *et al.*, 2001), and *proline dehydrogenase (oxidase) 2* (PRODH2), located at 31Mb, which encodes a protein related to apoptosis after *Trichinella spiralis* infection (Wu *et al.*, 2008). Interestingly the *lsr* gene (Lipolysis-stimulated lipoprotein), which encodes protein shown to be required for full barrier function of epithelial cells (Furuse *et al.*, 2012), may be a candidate gene for further examination. *Lsr* gene is a *Spir1* QTL gene located at 30Mb, present in both, TGF- $\beta$  signalling pathway analysis (Figure 5.1) and in the differentiated pulmonary gene expression data between BALB/c and CBA/Ca (Jonczyk *et al.*, 2014). Furthermore, one more gene containing a stop codon located downstream the *Spir1*

region – the *coiled-coil domain containing 114* (CCDC114), located at 53Mb. Interestingly it was reported that mutations in this gene cause primary ciliary dyskinesia (Knowles *et al.*, 2013).

There are knockout mice available for most of the candidate genes selected in this thesis, although only CD22-deficient mice have been tested for their susceptibility to pneumococcal infection. It would be interesting to breed these knockouts onto the appropriate genetic backgrounds and investigate their infection susceptibilities. Ideally, an allele swap of candidate genes may indicate the contribution of each mutation to pneumococcal disease phenotype.

---

## References

---

- Adachi, T., Harumiya, S., Takematsu, H., Kozutsumi, Y., Wabl, M., Fujimoto, M., Tedder, T.F., 2012. CD22 serves as a receptor for soluble IgM. *European Journal of Immunology*. **42**, 241-247.
- Aguiar, S.I., Brito, M.J., Goncalo-Marques, J., Melo-Cristino, J., Ramirez, M., 2010. Serotypes 1, 7F and 19A became the leading causes of pediatric invasive pneumococcal infections in Portugal after 7 years of heptavalent conjugate vaccine use. *Vaccine*. **28**, 5167-5173.
- Akhurst, R.J. & Hata, A., 2012. Targeting the TGFbeta signalling pathway in disease. *Nature Reviews.Drug Discovery*. **11**, 790-811.
- AlonsoDeVelasco, E., Verheul, A.F., Verhoef, J., Snippe, H., 1995. Streptococcus pneumoniae: virulence factors, pathogenesis, and vaccines. *Microbiological Reviews*. **59**, 591-603.
- Amsbaugh, D.F., Hansen, C.T., Prescott, B., Stashak, P.W., Barthold, D.R., Baker, P.J., 1972. Genetic control of the antibody response to type 3 pneumococcal polysaccharide in mice. I. Evidence that an X-linked gene plays a decisive role in determining responsiveness. *The Journal of Experimental Medicine*. **136**, 931-949.
- Andersson, B., Dahmen, J., Frejd, T., Leffler, H., Magnusson, G., Noori, G., Eden, C.S., 1983. Identification of an active disaccharide unit of a glycoconjugate receptor for pneumococci attaching to human pharyngeal epithelial cells. *The Journal of Experimental Medicine*. **158**, 559-570.
- Appelbaum, P.C., 1992. Antimicrobial resistance in Streptococcus pneumoniae: an overview. *Clinical Infectious Diseases : An Official Publication of the Infectious Diseases Society of America*. **15**, 77-83.
- Austrian, R., 1981. Pneumococcus: the first one hundred years. *Reviews of Infectious Diseases*. **3**, 183-189.
- Austrian, R. & Gold, J., 1964. Pneumococcal bacteremia with especial reference to bacteremic pneumococcal pneumonia. *Annals of Internal Medicine*. **60**, 759-776.
- Avery, O.T., 1915. A further study on the biologic classification of pneumococci. *The Journal of Experimental Medicine*. **22**, 804-819.
- Barnes, M.J. & Powrie, F., 2009. Regulatory T cells reinforce intestinal homeostasis. *Immunity*. **31**, 401-411.
- Bass, D.A., Olbrantz, P., Szejda, P., Seeds, M.C., McCall, C.E., 1986. Subpopulations of neutrophils with increased oxidative product formation in blood of patients with infection. *Journal of Immunology (Baltimore, Md.: 1950)*. **136**, 860-866.
- Baumgarth, N., 2011. The double life of a B-1 cell: self-reactivity selects for protective effector functions. *Nature Reviews.Immunology*. **11**, 34-46.

- Baumgarth, N., Herman, O.C., Jager, G.C., Brown, L., Herzenberg, L.A., Herzenberg, L.A., 1999. Innate and acquired humoral immunities to influenza virus are mediated by distinct arms of the immune system. *Proceedings of the National Academy of Sciences of the United States of America*. **96**, 2250-2255.
- Belkaid, Y., Piccirillo, C.A., Mendez, S., Shevach, E.M., Sacks, D.L., 2002. CD4+CD25+ regulatory T cells control *Leishmania* major persistence and immunity. *Nature*. **420**, 502-507.
- Bellamy, R., Ruwende, C., Corrah, T., McAdam, K.P., Whittle, H.C., Hill, A.V., 1998. Variations in the NRAMP1 gene and susceptibility to tuberculosis in West Africans. *The New England Journal of Medicine*. **338**, 640-644.
- Bellinghausen, I., Klostermann, B., Knop, J., Saloga, J., 2003. Human CD4+CD25+ T cells derived from the majority of atopic donors are able to suppress TH1 and TH2 cytokine production. *The Journal of Allergy and Clinical Immunology*. **111**, 862-868.
- Bennett, N.M., Buffington, J., LaForce, F.M., 1992. Pneumococcal bacteremia in Monroe County, New York. *American Journal of Public Health*. **82**, 1513-1516.
- Bergmann, S. & Hammerschmidt, S., 2006. Versatility of pneumococcal surface proteins. *Microbiology (Reading, England)*. **152**, 295-303.
- Berry, A.M., Yother, J., Briles, D.E., Hansman, D., Paton, J.C., 1989. Reduced virulence of a defined pneumolysin-negative mutant of *Streptococcus pneumoniae*. *Infection and Immunity*. **57**, 2037-2042.
- Bettelli, E., Carrier, Y., Gao, W., Korn, T., Strom, T.B., Oukka, M., Weiner, H.L., Kuchroo, V.K., 2006. Reciprocal developmental pathways for the generation of pathogenic effector TH17 and regulatory T cells. *Nature*. **441**, 235-238.
- Black, S., Shinefield, H., Fireman, B., Lewis, E., Ray, P., Hansen, J.R., Elvin, L., Ensor, K.M., Hackell, J., Siber, G., Malinoski, F., Madore, D., Chang, I., Kohberger, R., Watson, W., Austrian, R., Edwards, K., 2000. Efficacy, safety and immunogenicity of heptavalent pneumococcal conjugate vaccine in children. Northern California Kaiser Permanente Vaccine Study Center Group. *The Pediatric Infectious Disease Journal*. **19**, 187-195.
- Black, S.B., Shinefield, H.R., Ling, S., Hansen, J., Fireman, B., Spring, D., Noyes, J., Lewis, E., Ray, P., Lee, J., Hackell, J., 2002. Effectiveness of heptavalent pneumococcal conjugate vaccine in children younger than five years of age for prevention of pneumonia. *The Pediatric Infectious Disease Journal*. **21**, 810-815.
- Bogaert, D., De Groot, R., Hermans, P.W., 2004. *Streptococcus pneumoniae* colonisation: the key to pneumococcal disease. *The Lancet Infectious Diseases*. 154.
- Bogaert, D., Hermans, P.W., Adrian, P.V., Rumke, H.C., de Groot, R., 2004. Pneumococcal vaccines: an update on current strategies. *Vaccine*. **22**, 2209-2220.

Borish, L.C. & Steinke, J.W., 2003. 2. Cytokines and chemokines. *The Journal of Allergy and Clinical Immunology*. **111**, S460-75.

Born, W.K., Lahn, M., Takeda, K., Kanehiro, A., O'Brien, R.L., Gelfand, E.W., 2000. Role of gammadelta T cells in protecting normal airway function. *Respiratory Research*. **1**, 151-158.

Boulnois, G.J., 1992. Pneumococcal proteins and the pathogenesis of disease caused by *Streptococcus pneumoniae*. *Journal of General Microbiology*. **138**, 249-259.

Bradley, D.J. & Kirkley, J., 1977. Regulation of *Leishmania* populations within the host. I. the variable course of *Leishmania donovani* infections in mice. *Clinical and Experimental Immunology*. **30**, 119-129.

Braun, J.S., Sublett, J.E., Freyer, D., Mitchell, T.J., Cleveland, J.L., Tuomanen, E.I., Weber, J.R., 2002. Pneumococcal pneumolysin and H<sub>2</sub>O<sub>2</sub> mediate brain cell apoptosis during meningitis. *The Journal of Clinical Investigation*. **109**, 19-27.

Briese, T. & Hakenbeck, R., 1985. Interaction of the pneumococcal amidase with lipoteichoic acid and choline. *European Journal of Biochemistry / FEBS*. **146**, 417-427.

Briles, D.E., Forman, C., Hudak, S., Claflin, J.L., 1982. Anti-phosphorylcholine antibodies of the T15 idiotype are optimally protective against *Streptococcus pneumoniae*. *The Journal of Experimental Medicine*. **156**, 1177-1185.

Brown, E.J., Hosea, S.W., Frank, M.M., 1981. The role of the spleen in experimental pneumococcal bacteremia. *The Journal of Clinical Investigation*. **67**, 975-982.

Brown, I.N., Glynn, A.A., Plant, J., 1982. Inbred mouse strain resistance to *Mycobacterium lepraemurium* follows the Ity/Lsh pattern. *Immunology*. **47**, 149-156.

Buttery, J. & Moxon, E.R., 2002. Capsulate bacteria and the lung. *British Medical Bulletin*. **61**, 63-80.

Cann, A.J., 2012. *Microbiology Bytes*. [online]. Available at: <http://www.microbiologybytes.com/>.

Canvin, J.R., Marvin, A.P., Sivakumaran, M., Paton, J.C., Boulnois, G.J., Andrew, P.W., Mitchell, T.J., 1995. The role of pneumolysin and autolysin in the pathology of pneumonia and septicemia in mice infected with a type 2 pneumococcus. *The Journal of Infectious Diseases*. **172**, 119-123.

Cao, J., Gong, Y., Yin, Y., Wang, L., Ying, B., Chen, T., Zhang, X., 2010. Pneumococcal proteins PspA and PspC induce CXCL8 production in human neutrophils: implications in pneumococcal infections. *Microbes and Infection / Institut Pasteur*. **12**, 1051-1060.

Centers for Disease Control and Prevention, 2010. *Morbidity and Mortality Weekly Report (MMWR)*. [online]. Available at: <http://www.cdc.gov/mmwr/preview/mmwrhtml/mm5909a2.htm2012>].

Centers for Disease Control and Prevention, 2001. *Recommendations of the Advisory Committee on Immunization Practices (ACIP): Use of Vaccines and Immune Globulins in Persons with Altered Immunocompetence*. [online]. Available at: <http://www.cdc.gov/mmwr/preview/mmwrhtml/00023141.htm>2012].

Chang, J., Naif, H.M., Li, S., Sullivan, J.S., Randle, C.M., Cunningham, A.L., 1996. Twin studies demonstrate a host cell genetic effect on productive human immunodeficiency virus infection of human monocytes and macrophages in vitro. *Journal of Virology*. **70**, 7792-7803.

Chapman, S.J., Khor, C.C., Vannberg, F.O., Rautanen, A., Walley, A., Segal, S., Moore, C.E., Davies, R.J., Day, N.P., Peshu, N., Crook, D.W., Berkley, J.A., Williams, T.N., Scott, J.A., Hill, A.V., 2010. Common NFKBIL2 polymorphisms and susceptibility to pneumococcal disease: a genetic association study. *Critical Care (London, England)*. **14**, R227.

Chiavolini, D., Pozzi, G., Ricci, S., 2008. Animal models of Streptococcus pneumoniae disease. *Clinical Microbiology Reviews*. **21**, 666-685.

Chiricozzi, A., Guttman-Yassky, E., Suarez-Farinas, M., Nograles, K.E., Tian, S., Cardinale, I., Chimenti, S., Krueger, J.G., 2011. Integrative responses to IL-17 and TNF-alpha in human keratinocytes account for key inflammatory pathogenic circuits in psoriasis. *The Journal of Investigative Dermatology*. **131**, 677-687.

Chollet-Martin, S., Montravers, P., Gibert, C., Elbim, C., Desmots, J.M., Fagon, J.Y., Gougerot-Pocidallo, M.A., 1992. Subpopulation of hyperresponsive polymorphonuclear neutrophils in patients with adult respiratory distress syndrome. Role of cytokine production. *The American Review of Respiratory Disease*. **146**, 990-996.

Clarke, P.H. & Cowan, S.T., 1952. Biochemical methods for bacteriology. *Journal of General Microbiology*. **6**, 187-197.

Clutterbuck, E.A., Lazarus, R., Yu, L.M., Bowman, J., Bateman, E.A., Diggle, L., Angus, B., Peto, T.E., Beverley, P.C., Mant, D., Pollard, A.J., 2012. Pneumococcal conjugate and plain polysaccharide vaccines have divergent effects on antigen-specific B cells. *The Journal of Infectious Diseases*. **205**, 1408-1416.

Cortese, M.M., Wolff, M., Almeida-Hill, J., Reid, R., Ketcham, J., Santosham, M., 1992. High incidence rates of invasive pneumococcal disease in the White Mountain Apache population. *Archives of Internal Medicine*. **152**, 2277-2282.

Coulter, K.R., Doseff, A., Sweeney, P., Wang, Y., Marsh, C.B., Wewers, M.D., Knoell, D.L., 2002. Opposing effect by cytokines on Fas-mediated apoptosis in A549 lung epithelial cells. *American Journal of Respiratory Cell and Molecular Biology*. **26**, 58-66.

Couper, K.N., Blount, D.G., Riley, E.M., 2008. IL-10: the master regulator of immunity to infection. *Journal of Immunology (Baltimore, Md.: 1950)*. **180**, 5771-5777.

- Craig, A., Mai, J., Cai, S., Jeyaseelan, S., 2009. Neutrophil recruitment to the lungs during bacterial pneumonia. *Infection and Immunity*. **77**, 568-575.
- Crain, M.J., Waltman, W.D., 2nd, Turner, J.S., Yother, J., Talkington, D.F., McDaniel, L.S., Gray, B.M., Briles, D.E., 1990. Pneumococcal surface protein A (PspA) is serologically highly variable and is expressed by all clinically important capsular serotypes of *Streptococcus pneumoniae*. *Infection and Immunity*. **58**, 3293-3299.
- Crocker, P.R., Clark, E.A., Filbin, M., Gordon, S., Jones, Y., Kehrl, J.H., Kelm, S., Le Douarin, N., Powell, L., Roder, J., Schnaar, R.L., Sgroi, D.C., Stamenkovic, K., Schauer, R., Schachner, M., van den Berg, T.K., van der Merwe, P.A., Watt, S.M., Varki, A., 1998. Siglecs: a family of sialic-acid binding lectins. *Glycobiology*. **8**, v.
- Crocker, P.R., Paulson, J.C., Varki, A., 2007. Siglecs and their roles in the immune system. *Nature Reviews.Immunology*. **7**, 255-266.
- Cunha, B.A., 2006. Antimicrobial therapy of multidrug-resistant *Streptococcus pneumoniae*, vancomycin-resistant enterococci, and methicillin-resistant *Staphylococcus aureus*. *The Medical Clinics of North America*. **90**, 1165-1182.
- Curotto de Lafaille, M.A. & Lafaille, J.J., 2009. Natural and adaptive foxp3+ regulatory T cells: more of the same or a division of labor? *Immunity*. **30**, 626-635.
- Davidson, M., Schraer, C.D., Parkinson, A.J., Campbell, J.F., Facklam, R.R., Wainwright, R.B., Lanier, A.P., Heyward, W.L., 1989. Invasive pneumococcal disease in an Alaska native population, 1980 through 1986. *JAMA : The Journal of the American Medical Association*. **261**, 715-718.
- DeBry, R.W. & Seldin, M.F., 1996. Human/mouse homology relationships. *Genomics*. **33**, 337-351.
- Demetriou, M., Granovsky, M., Quaggin, S., Dennis, J.W., 2001. Negative regulation of T-cell activation and autoimmunity by Mgat5 N-glycosylation. *Nature*. **409**, 733-739.
- Denny, P., Hopes, E., Gingles, N., Broman, K.W., McPheat, W., Morten, J., Alexander, J., Andrew, P.W., Brown, S.D., 2003. A major locus conferring susceptibility to infection by *Streptococcus pneumoniae* in mice. *Mammalian Genome : Official Journal of the International Mammalian Genome Society*. **14**, 448-453.
- Dessing, M.C., Knapp, S., Florquin, S., de Vos, A.F., van der Poll, T., 2007. CD14 facilitates invasive respiratory tract infection by *Streptococcus pneumoniae*. *American Journal of Respiratory and Critical Care Medicine*. **175**, 604-611.
- Diaz, E., Garcia, E., Ascaso, C., Mendez, E., Lopez, R., Garcia, J.L., 1989. Subcellular localization of the major pneumococcal autolysin: a peculiar mechanism of secretion in *Escherichia coli*. *The Journal of Biological Chemistry*. **264**, 1238-1244.
- Dick, D.M. & Foroud, T., 2002. Genetic strategies to detect genes involved in alcoholism and alcohol-related traits. *Alcohol Research & Health : The Journal of the National Institute on Alcohol Abuse and Alcoholism*. **26**, 172-180.

- Doerr, M. & Eng, C., 2012. Personalised care and the genome. *BMJ (Clinical Research Ed.)*. **344**, e3174.
- Doffinger, R., Altare, F., Casanova, J.L., 2000. Genetic heterogeneity of Mendelian susceptibility to mycobacterial infection. *Microbes and Infection / Institut Pasteur*. **2**, 1553-1557.
- Dotor, J., Lopez-Vazquez, A.B., Lasarte, J.J., Sarobe, P., Garcia-Granero, M., Riezu-Boj, J.I., Martinez, A., Feijoo, E., Lopez-Sagaseta, J., Hermida, J., Prieto, J., Borrascueta, F., 2007. Identification of peptide inhibitors of transforming growth factor beta 1 using a phage-displayed peptide library. *Cytokine*. **39**, 106-115.
- Dowell, S.F., Whitney, C.G., Wright, C., Rose, C.E., Jr, Schuchat, A., 2003. Seasonal patterns of invasive pneumococcal disease. *Emerging Infectious Diseases*. **9**, 573-579.
- Dowson, C.G., Barcus, V., King, S., Pickerill, P., Whatmore, A., Yeo, M., 1997. Horizontal gene transfer and the evolution of resistance and virulence determinants in *Streptococcus*. *Society for Applied Bacteriology Symposium Series*. **26**, 42S-51S.
- Dranoff, G., 2004. Cytokines in cancer pathogenesis and cancer therapy. *Nature Reviews.Cancer*. **4**, 11-22.
- Eklund, C., Huttunen, R., Syrjanen, J., Laine, J., Vuoto, R., Hurme, M., 2006. Polymorphism of the C-reactive protein gene is associated with mortality in bacteraemia. *Scandinavian Journal of Infectious Diseases*. **38**, 1069-1073.
- eMed Expert, 2012. *Antibiotics*. [online]. Available at: <http://www.emedexpert.com/classes/antibiotics.shtml2012>].
- Engel, P., Wagner, N., Miller, A.S., Tedder, T.F., 1995. Identification of the ligand-binding domains of CD22, a member of the immunoglobulin superfamily that uniquely binds a sialic acid-dependent ligand. *The Journal of Experimental Medicine*. **181**, 1581-1586.
- Erdem, H., 2008. An update on invasive pneumococcal antibiotic resistance in Turkey, 2008. *Journal of Chemotherapy (Florence, Italy)*. **20**, 697-701.
- Eskola, J., Kilpi, T., Palmu, A., Jokinen, J., Haapakoski, J., Herva, E., Takala, A., Kayhty, H., Karma, P., Kohberger, R., Siber, G., Makela, P.H., Finnish Otitis Media Study Group, 2001. Efficacy of a pneumococcal conjugate vaccine against acute otitis media. *The New England Journal of Medicine*. **344**, 403-409.
- Etzioni, A. & Ochs, H.D., 2004. The hyper IgM syndrome--an evolving story. *Pediatric Research*. **56**, 519-525.
- Faden, H., Duffy, L., Williams, A., Krystofik, D.A., Wolf, J., 1995. Epidemiology of nasopharyngeal colonization with nontypeable *Haemophilus influenzae* in the first 2 years of life. *The Journal of Infectious Diseases*. **172**, 132-135.

- Fantini, M.C., Dominitzki, S., Rizzo, A., Neurath, M.F., Becker, C., 2007. In vitro generation of CD4<sup>+</sup> CD25<sup>+</sup> regulatory cells from murine naive T cells. *Nature Protocols*. **2**, 1789-1794.
- Faurschou, M. & Borregaard, N., 2003. Neutrophil granules and secretory vesicles in inflammation. *Microbes and Infection / Institut Pasteur*. **5**, 1317-1327.
- Feldman, C. & Anderson, R., 2011. Bacteraemic pneumococcal pneumonia: current therapeutic options. *Drugs*. **71**, 131-153.
- Flannery, B., Schrag, S., Bennett, N.M., Lynfield, R., Harrison, L.H., Reingold, A., Cieslak, P.R., Hadler, J., Farley, M.M., Facklam, R.R., Zell, E.R., Whitney, C.G., Active Bacterial Core Surveillance/Emerging Infections Program Network, 2004. Impact of childhood vaccination on racial disparities in invasive Streptococcus pneumoniae infections. *Jama*. **291**, 2197-2203.
- Fritz, J.H., Ferrero, R.L., Philpott, D.J., Girardin, S.E., 2006. Nod-like proteins in immunity, inflammation and disease. *Nature Immunology*. **7**, 1250-1257.
- Fu, B.M., He, X.S., Yu, S., Hu, A.B., Ma, Y., Wu, L.W., Tam, N.L., Huang, J.F., 2009. Tolerogenic semimature dendritic cells induce effector T-cell hyporesponsiveness by the activation of antigen-specific CD4<sup>+</sup> CD25<sup>+</sup> T-regulatory cells. *Experimental and Clinical Transplantation : Official Journal of the Middle East Society for Organ Transplantation*. **7**, 149-156.
- Fujimoto, M., Kuwano, Y., Watanabe, R., Asashima, N., Nakashima, H., Yoshitake, S., Okochi, H., Tamaki, K., Poe, J.C., Tedder, T.F., Sato, S., 2006. B cell antigen receptor and CD40 differentially regulate CD22 tyrosine phosphorylation. *Journal of Immunology (Baltimore, Md.: 1950)*. **176**, 873-879.
- Fujio, K., Okamura, T., Yamamoto, K., 2010. The Family of IL-10-secreting CD4<sup>+</sup> T cells. *Advances in Immunology*. **105**, 99-130.
- Furuse, M., Oda, Y., Higashi, T., Iwamoto, N., Masuda, S., 2012. Lipolysis-stimulated lipoprotein receptor: a novel membrane protein of tricellular tight junctions. *Annals of the New York Academy of Sciences*. **1257**, 54-58.
- Gao, H., Li, L., Rao, S., Shen, G., Xi, Q., Chen, S., Zhang, Z., Wang, K., Ellis, S.G., Chen, Q., Topol, E.J., Wang, Q.K., 2014. Genome-Wide Linkage Scan Identifies Two Novel Genetic Loci for Coronary Artery Disease: In GeneQuest Families. *PloS One*. **9**, e113935.
- Garcia-Rodriguez, J.A. & Fresnadillo Martinez, M.J., 2002. Dynamics of nasopharyngeal colonization by potential respiratory pathogens. *The Journal of Antimicrobial Chemotherapy*. **50 Suppl S2**, 59-73.
- Gay, N.J. & Keith, F.J., 1991. Drosophila Toll and IL-1 receptor. *Nature*. **351**, 355-356.

- Gedda, L., Rajani, G., Brenci, G., Lun, M.T., Talone, C., Oddi, G., 1984. Heredity and infectious diseases: a twin study. *Acta Geneticae Medicae Et Gemellologiae*. **33**, 497-500.
- Gerlini, A., Colomba, L., Furi, L., Braccini, T., Manso, A.S., Pammolli, A., Wang, B., Vivi, A., Tassini, M., van Rooijen, N., Pozzi, G., Ricci, S., Andrew, P.W., Koedel, U., Moxon, E.R., Oggioni, M.R., 2014. The role of host and microbial factors in the pathogenesis of pneumococcal bacteraemia arising from a single bacterial cell bottleneck. *PLoS Pathogens*. **10**, e1004026.
- Giddings, K.S., Johnson, A.E., Tweten, R.K., 2003. Redefining cholesterol's role in the mechanism of the cholesterol-dependent cytolysins. *Proceedings of the National Academy of Sciences of the United States of America*. **100**, 11315-11320.
- Gilbert, R.J., 2002. Pore-forming toxins. *Cellular and Molecular Life Sciences : CMLS*. **59**, 832-844.
- Gil-Guerrero, L., Dotor, J., Huibregtse, I.L., Casares, N., Lopez-Vazquez, A.B., Rudilla, F., Riezu-Boj, J.I., Lopez-Sagaseta, J., Hermida, J., Van Deventer, S., Bezunartea, J., Llopiz, D., Sarobe, P., Prieto, J., Borrás-Cuesta, F., Lasarte, J.J., 2008. In vitro and in vivo down-regulation of regulatory T cell activity with a peptide inhibitor of TGF-beta1. *Journal of Immunology (Baltimore, Md.: 1950)*. **181**, 126-135.
- Gillespie, S.H., 1989. Aspects of pneumococcal infection including bacterial virulence, host response and vaccination. *Journal of Medical Microbiology*. **28**, 237-248.
- Gingles, N.A., Alexander, J.E., Kadioglu, A., Andrew, P.W., Kerr, A., Mitchell, T.J., Hopes, E., Denny, P., Brown, S., Jones, H.B., Little, S., Booth, G.C., McPheat, W.L., 2001. Role of genetic resistance in invasive pneumococcal infection: identification and study of susceptibility and resistance in inbred mouse strains. *Infection and Immunity*. **69**, 426-434.
- Giudicelli, S. & Tomasz, A., 1984. Attachment of pneumococcal autolysin to wall teichoic acids, an essential step in enzymatic wall degradation. *Journal of Bacteriology*. **158**, 1188-1190.
- Gjertsson, I., Nitschke, L., Tarkowski, A., 2004. The role of B cell CD22 expression in Staphylococcus aureus arthritis and sepsis. *Microbes and Infection / Institut Pasteur*. **6**, 377-382.
- Gleeson, P.A., 2008. The sweet side of immunology: glycobiology of the immune system. *Immunology and Cell Biology*. **86**, 562-563.
- Glennie, S.J., Sepako, E., Mzinza, D., Harawa, V., Miles, D.J., Jambo, K.C., Gordon, S.B., Williams, N.A., Heyderman, R.S., 2011. Impaired CD4 T cell memory response to Streptococcus pneumoniae precedes CD4 T cell depletion in HIV-infected Malawian adults. *PLoS One*. **6**, e25610.

- Goldmann, O., Chhatwal, G.S., Medina, E., 2004. Role of host genetic factors in susceptibility to group A streptococcal infections. *The Indian Journal of Medical Research*. **119 Suppl**, 141-143.
- Goldmann, O., Chhatwal, G.S., Medina, E., 2003. Immune mechanisms underlying host susceptibility to infection with group A streptococci. *The Journal of Infectious Diseases*. **187**, 854-861.
- Goonetilleke, U.R., Ward, S.A., Gordon, S.B., 2009. Could proteomic research deliver the next generation of treatments for pneumococcal meningitis? *Interdisciplinary Perspectives on Infectious Diseases*. **2009**, 214216.
- Gordon, S.B. & Read, R.C., 2002. Macrophage defences against respiratory tract infections. *British Medical Bulletin*. **61**, 45-61.
- Gould, I.M., 2008. The epidemiology of antibiotic resistance. *International Journal of Antimicrobial Agents*. **32 Suppl 1**, S2-9.
- Griffith, F., 1966. The significance of pneumococcal types. *The Journal of Hygiene*. **64**, 129-144.
- Groneck, L., Schrama, D., Fabri, M., Stephen, T.L., Harms, F., Meemboor, S., Hafke, H., Bessler, M., Becker, J.C., Kalka-Moll, W.M., 2009. Oligoclonal CD4+ T cells promote host memory immune responses to Zwitterionic polysaccharide of *Streptococcus pneumoniae*. *Infection and Immunity*. **77**, 3705-3712.
- Gronwall, C., Vas, J., Silverman, G.J., 2012. Protective Roles of Natural IgM Antibodies. *Frontiers in Immunology*. **3**, 66.
- Groux, H., 2001. An overview of regulatory T cells. *Microbes and Infection / Institut Pasteur*. **3**, 883-889.
- Gu, Y., Harley, I.T., Henderson, L.B., Aronow, B.J., Vietor, I., Huber, L.A., Harley, J.B., Kilpatrick, J.R., Langefeld, C.D., Williams, A.H., Jegga, A.G., Chen, J., Wills-Karp, M., Arshad, S.H., Ewart, S.L., Thio, C.L., Flick, L.M., Filippi, M.D., Grimes, H.L., Drumm, M.L., Cutting, G.R., Knowles, M.R., Karp, C.L., 2009. Identification of IFRD1 as a modifier gene for cystic fibrosis lung disease. *Nature*. **458**, 1039-1042.
- Gut, H., King, S.J., Walsh, M.A., 2008. Structural and functional studies of *Streptococcus pneumoniae* neuraminidase B: An intramolecular trans-sialidase. *FEBS Letters*. **582**, 3348-3352.
- Haas, K.M., Poe, J.C., Steeber, D.A., Tedder, T.F., 2005. B-1a and B-1b cells exhibit distinct developmental requirements and have unique functional roles in innate and adaptive immunity to *S. pneumoniae*. *Immunity*. **23**, 7-18.
- Hammerschmidt, S., Bethe, G., Remane, P.H., Chhatwal, G.S., 1999. Identification of pneumococcal surface protein A as a lactoferrin-binding protein of *Streptococcus pneumoniae*. *Infection and Immunity*. **67**, 1683-1687.

- Han, S., Collins, B.E., Bengtson, P., Paulson, J.C., 2005. Homomultimeric complexes of CD22 in B cells revealed by protein-glycan cross-linking. *Nature Chemical Biology*. **1**, 93-97.
- Hanninen, A. & Harrison, L.C., 2000. Gamma delta T cells as mediators of mucosal tolerance: the autoimmune diabetes model. *Immunological Reviews*. **173**, 109-119.
- Haraguchi, S., Day, N.K., Nelson, R.P., Jr, Emmanuel, P., Duplantier, J.E., Christodoulou, C.S., Good, R.A., 1998. Interleukin 12 deficiency associated with recurrent infections. *Proceedings of the National Academy of Sciences of the United States of America*. **95**, 13125-13129.
- Harlan Laboratories, 2008. *BALB/cOlaHsd*.
- Harlan Laboratories, 2008. *CBA/CaOlaHsd*.
- Haslett, C., 1999. Granulocyte apoptosis and its role in the resolution and control of lung inflammation. *American Journal of Respiratory and Critical Care Medicine*. **160**, S5-11.
- Hatta, Y., Tsuchiya, N., Matsushita, M., Shiota, M., Hagiwara, K., Tokunaga, K., 1999. Identification of the gene variations in human CD22. *Immunogenetics*. **49**, 280-286.
- Henriques Normark, B., Kalin, M., Ortqvist, A., Akerlund, T., Liljequist, B.O., Hedlund, J., Svenson, S.B., Zhou, J., Spratt, B.G., Normark, S., Kallenius, G., 2001. Dynamics of penicillin-susceptible clones in invasive pneumococcal disease. *The Journal of Infectious Diseases*. **184**, 861-869.
- Herbst, S., Schaible, U.E., Schneider, B.E., 2011. Interferon gamma activated macrophages kill mycobacteria by nitric oxide induced apoptosis. *PLoS One*. **6**, e19105.
- Hernandez-Valladares, M., Naessens, J., Nagda, S., Musoke, A.J., Rihet, P., Ole-Moiyoi, O.K., Iraqi, F.A., 2004. Comparison of pathology in susceptible A/J and resistant C57BL/6J mice after infection with different sub-strains of *Plasmodium chabaudi*. *Experimental Parasitology*. **108**, 134-141.
- Hill, A.V., 1998. Host genetics of infectious diseases: old and new approaches converge. *Emerging Infectious Diseases*. **4**, 695-697.
- Hindorff, L.A., Sethupathy, P., Junkins, H.A., Ramos, E.M., Mehta, J.P., Collins, F.S., Manolio, T.A., 2009. Potential etiologic and functional implications of genome-wide association loci for human diseases and traits. *Proceedings of the National Academy of Sciences of the United States of America*. **106**, 9362-9367.
- Hirst, R.A., Gosai, B., Rutman, A., Guerin, C.J., Nicotera, P., Andrew, P.W., O'Callaghan, C., 2008. *Streptococcus pneumoniae* deficient in pneumolysin or autolysin has reduced virulence in meningitis. *The Journal of Infectious Diseases*. **197**, 744-751.
- Hooper, L.V., Littman, D.R., Macpherson, A.J., 2012. Interactions between the microbiota and the immune system. *Science (New York, N.Y.)*. **336**, 1268-1273.

- Horne, D. & Tomasz, A., 1985. Pneumococcal Forssman antigen: enrichment in mesosomal membranes and specific binding to the autolytic enzyme of *Streptococcus pneumoniae*. *Journal of Bacteriology*. **161**, 18-24.
- Hosea, S.W., 1983. Role of the spleen in pneumococcal infection. *Lymphology*. **16**, 115-120.
- Hughes, J.M., 2011. Preserving the lifesaving power of antimicrobial agents. *JAMA : The Journal of the American Medical Association*. **305**, 1027-1028.
- Huss, A., Scott, P., Stuck, A.E., Trotter, C., Egger, M., 2009. Efficacy of pneumococcal vaccination in adults: a meta-analysis. *CMAJ : Canadian Medical Association Journal = Journal De L'Association Medicale Canadienne*. **180**, 48-58.
- Ibelgaufts, H., 2013. *COPE article about systemic inflammatory response*. [online]. Available at: <http://www.copewithcytokines.de/cope.cgi?key=Systemic%20inflammatory%20response%20syndrome2015>].
- Internet FAQ Archives, 2012. *Antianxiety drugs to Bacteremia: antibiotics*. [online]. Available at: <http://www.faqs.org/health/topics/59/Antibiotics.html>2012].
- Janeway, C.A.J., Travers, P. and Walport, M., 2001. The components of the immune system. 5th edition ed. New York: Garland Science.
- Janeway, C.A.J., Travers, P. and Walport, M., 2001. Principles of innate and adaptive immunity. *Immunobiology: The Immune System in Health and Disease*. 5th edition ed. New York: Garland Science.
- Jedrzejewski, M., 2001. Pneumococcal virulence factors: Structure and function. *Microbiology and Molecular Biology Reviews*. **65**, 187-207.
- Jenkins, T.C., Sakai, J., Knepper, B.C., Swartwood, C.J., Haukoos, J.S., Long, J.A., Price, C.S., Burman, W.J., 2012. Risk Factors for Drug-resistant *Streptococcus pneumoniae* and Antibiotic Prescribing Practices in Outpatient Community-acquired Pneumonia. *Academic Emergency Medicine : Official Journal of the Society for Academic Emergency Medicine*. **19**, 703-706.
- Jennings, H.J., Lugowski, C., Young, N.M., 1980. Structure of the complex polysaccharide C-substance from *Streptococcus pneumoniae* type 1. *Biochemistry*. **19**, 4712-4719.
- Jeong, D.G., Jeong, E.S., Seo, J.H., Heo, S.H., Choi, Y.K., 2011. Difference in Resistance to *Streptococcus pneumoniae* Infection in Mice. *Laboratory Animal Research*. **27**, 91-98.
- Jepson, A.P., Banya, W.A., Sisay-Joof, F., Hassan-King, M., Bennett, S., Whittle, H.C., 1995. Genetic regulation of fever in *Plasmodium falciparum* malaria in Gambian twin children. *The Journal of Infectious Diseases*. **172**, 316-319.

- Jin, Y., Lundkvist, G., Dons, L., Kristensson, K., Rottenberg, M.E., 2004. Interferon-gamma mediates neuronal killing of intracellular bacteria. *Scandinavian Journal of Immunology*. **60**, 437-448.
- Johnson, M.K., Geoffroy, C., Alouf, J.E., 1980. Binding of cholesterol by sulfhydryl-activated cytolysins. *Infection and Immunity*. **27**, 97-101.
- Johnston, R.B., Jr, 1991. Pathogenesis of pneumococcal pneumonia. *Reviews of Infectious Diseases*. **13 Suppl 6**, S509-17.
- Jomaa, M., Kyd, J.M., Cripps, A.W., 2005. Mucosal immunisation with novel *Streptococcus pneumoniae* protein antigens enhances bacterial clearance in an acute mouse lung infection model. *FEMS Immunology and Medical Microbiology*. **44**, 59-67.
- Jonczyk, M.S., Simon, M., Kumar, S., Fernandes, V.E., Sylvius, N., Mallon, A.M., Denny, P., Andrew, P.W., 2014. Genetic factors regulating lung vasculature and immune cell functions associate with resistance to pneumococcal infection. *PLoS One*. **9**, e89831.
- Jones, C.P., Carver, S., Kendall, L.V., 2012. Evaluation of common anesthetic and analgesic techniques for tail biopsy in mice. *Journal of the American Association for Laboratory Animal Science : JAALAS*. **51**, 808-814.
- Jonhson, M.K., 1977. Cellular location of pneumolysin. *FEMS Microbiology Letters*. **2**, 243-245.
- Jounblat, R., Kadioglu, A., Mitchell, T.J., Andrew, P.W., 2003. Pneumococcal behavior and host responses during bronchopneumonia are affected differently by the cytolytic and complement-activating activities of pneumolysin. *Infection and Immunity*. **71**, 1813-1819.
- Jutel, M., Akdis, M., Budak, F., Aebischer-Casaulta, C., Wrzyszczyk, M., Blaser, K., Akdis, C.A., 2003. IL-10 and TGF-beta cooperate in the regulatory T cell response to mucosal allergens in normal immunity and specific immunotherapy. *European Journal of Immunology*. **33**, 1205-1214.
- Kadioglu, A. & Andrew, P.W., 2004. The innate immune response to pneumococcal lung infection: the untold story. *Trends in Immunology*. **25**, 143-149.
- Kadioglu, A., Coward, W., Colston, M.J., Hewitt, C.R., Andrew, P.W., 2004. CD4-T-lymphocyte interactions with pneumolysin and pneumococci suggest a crucial protective role in the host response to pneumococcal infection. *Infection and Immunity*. **72**, 2689-2697.
- Kadioglu, A., Cuppone, A.M., Trappetti, C., List, T., Spreafico, A., Pozzi, G., Andrew, P.W., Oggioni, M.R., 2011. Sex-based differences in susceptibility to respiratory and systemic pneumococcal disease in mice. *The Journal of Infectious Diseases*. **204**, 1971-1979.

- Kadioglu, A., Gingles, N.A., Grattan, K., Kerr, A., Mitchell, T.J., Andrew, P.W., 2000. Host cellular immune response to pneumococcal lung infection in mice. *Infection and Immunity*. **68**, 492-501.
- Kadioglu, A., Weiser, J.N., Paton, J.C., Andrew, P.W., 2008. The role of *Streptococcus pneumoniae* virulence factors in host respiratory colonization and disease. *Nature Reviews.Microbiology*. **6**, 288-301.
- Kaplanski, G., Marin, V., Montero-Julian, F., Mantovani, A., Farnarier, C., 2003. IL-6: a regulator of the transition from neutrophil to monocyte recruitment during inflammation. *Trends in Immunology*. **24**, 25-29.
- Kayhty, H., Nurkka, A., Soininen, A., Vakevainen, M., 2009. The Immunological Basis for Immunization Series (Module 12: pneumococcal vaccines). *World Health Organization*. **12**.
- Kellogg, J.A., Bankert, D.A., Elder, C.J., Gibbs, J.L., Smith, M.C., 2001. Identification of *Streptococcus pneumoniae* revisited. *Journal of Clinical Microbiology*. **39**, 3373-3375.
- Kelly, R.T., Farmer, S., Greiff, D., 1967. Neuraminidase activities of clinical isolates of *Diplococcus pneumoniae*. *Journal of Bacteriology*. **94**, 272-273.
- Kerr, A.R., Irvine, J.J., Search, J.J., Gingles, N.A., Kadioglu, A., Andrew, P.W., McPheat, W.L., Booth, C.G., Mitchell, T.J., 2002. Role of inflammatory mediators in resistance and susceptibility to pneumococcal infection. *Infection and Immunity*. **70**, 1547-1557.
- Kerr, A.R., Wei, X.Q., Andrew, P.W., Mitchell, T.J., 2004. Nitric oxide exerts distinct effects in local and systemic infections with *Streptococcus pneumoniae*. *Microbial Pathogenesis*. **36**, 303-310.
- Khajanchi, B.K., Kirtley, M.L., Brackman, S.M., Chopra, A.K., 2011. Immunomodulatory and protective roles of quorum-sensing signaling molecules N-acyl homoserine lactones during infection of mice with *Aeromonas hydrophila*. *Infection and Immunity*. **79**, 2646-2657.
- King, Q.O., Lei, B., Harmsen, A.G., 2009. Pneumococcal surface protein A contributes to secondary *Streptococcus pneumoniae* infection after influenza virus infection. *The Journal of Infectious Diseases*. **200**, 537-545.
- King, S.J., Whatmore, A.M., Dowson, C.G., 2005. NanA, a neuraminidase from *Streptococcus pneumoniae*, shows high levels of sequence diversity, at least in part through recombination with *Streptococcus oralis*. *Journal of Bacteriology*. **187**, 5376-5386.
- Kirby, A.C., Coles, M.C., Kaye, P.M., 2009. Alveolar macrophages transport pathogens to lung draining lymph nodes. *Journal of Immunology (Baltimore, Md.: 1950)*. **183**, 1983-1989.

Klein Klouwenberg, P. & Bont, L., 2008. Neonatal and infantile immune responses to encapsulated bacteria and conjugate vaccines. *Clinical & Developmental Immunology*. **2008**, 628963.

Klugman, K.P., 2011. Contribution of vaccines to our understanding of pneumococcal disease. *Philosophical Transactions of the Royal Society of London. Series B, Biological Sciences*. **366**, 2790-2798.

Knowles, M.R., Leigh, M.W., Ostrowski, L.E., Huang, L., Carson, J.L., Hazucha, M.J., Yin, W., Berg, J.S., Davis, S.D., Dell, S.D., Ferkol, T.W., Rosenfeld, M., Sagel, S.D., Milla, C.E., Olivier, K.N., Turner, E.H., Lewis, A.P., Bamshad, M.J., Nickerson, D.A., Shendure, J., Zariwala, M.A., Genetic Disorders of Mucociliary Clearance Consortium, 2013. Exome sequencing identifies mutations in CCDC114 as a cause of primary ciliary dyskinesia. *American Journal of Human Genetics*. **92**, 99-106.

Koppel, E.A., Litjens, M., van den Berg, V.C., van Kooyk, Y., Geijtenbeek, T.B., 2008. Interaction of SIGNR1 expressed by marginal zone macrophages with marginal zone B cells is essential to early IgM responses against *Streptococcus pneumoniae*. *Molecular Immunology*. **45**, 2881-2887.

Kruetzmann, S., Rosado, M.M., Weber, H., Germing, U., Tournilhac, O., Peter, H.H., Berner, R., Peters, A., Boehm, T., Plebani, A., Quinti, I., Carsetti, R., 2003. Human immunoglobulin M memory B cells controlling *Streptococcus pneumoniae* infections are generated in the spleen. *The Journal of Experimental Medicine*. **197**, 939-945.

Ku, C.L., von Bernuth, H., Picard, C., Zhang, S.Y., Chang, H.H., Yang, K., Chrabieh, M., Issekutz, A.C., Cunningham, C.K., Gallin, J., Holland, S.M., Roifman, C., Ehl, S., Smart, J., Tang, M., Barrat, F.J., Levy, O., McDonald, D., Day-Good, N.K., Miller, R., Takada, H., Hara, T., Al-Hajjar, S., Al-Ghonaïm, A., Speert, D., Sanlaville, D., Li, X., Geissmann, F., Vivier, E., Marodi, L., Garty, B.Z., Chapel, H., Rodriguez-Gallego, C., Bossuyt, X., Abel, L., Puel, A., Casanova, J.L., 2007. Selective predisposition to bacterial infections in IRAK-4-deficient children: IRAK-4-dependent TLRs are otherwise redundant in protective immunity. *The Journal of Experimental Medicine*. **204**, 2407-2422.

Kumar, V., Abbas, A.K. and Fausto, N.e.a., eds., eds, 2007. *Robbins Basic Pathology*. 8th ed. Saunders, Elsevier.

Lacks, S.A., 2003. Rambling and scrambling in bacterial transformation—a historical and personal memoir.

Laferriere, C., 2011. The immunogenicity of pneumococcal polysaccharides in infants and children: a meta-regression. *Vaccine*. **29**, 6838-6847.

Lajaunias, F., Nitschke, L., Moll, T., Martinez-Soria, E., Semac, I., Chicheportiche, Y., Parkhouse, R.M., Izui, S., 2002. Differentially regulated expression and function of CD22 in activated B-1 and B-2 lymphocytes. *Journal of Immunology (Baltimore, Md.: 1950)*. **168**, 6078-6083.

- Lander, E.S. & Schork, N.J., 1994. Genetic dissection of complex traits. *Science (New York, N.Y.)*. **265**, 2037-2048.
- Lanteri, M.C., O'Brien, K.M., Purtha, W.E., Cameron, M.J., Lund, J.M., Owen, R.E., Heitman, J.W., Custer, B., Hirschhorn, D.F., Tobler, L.H., Kiely, N., Prince, H.E., Ndhlovu, L.C., Nixon, D.F., Kamel, H.T., Kelvin, D.J., Busch, M.P., Rudensky, A.Y., Diamond, M.S., Norris, P.J., 2009. Tregs control the development of symptomatic West Nile virus infection in humans and mice. *The Journal of Clinical Investigation*. **119**, 3266-3277.
- Lavebratt, C., Apt, A.S., Nikonenko, B.V., Schalling, M., Schurr, E., 1999. Severity of tuberculosis in mice is linked to distal chromosome 3 and proximal chromosome 9. *The Journal of Infectious Diseases*. **180**, 150-155.
- Law, C.L., Aruffo, A., Chandran, K.A., Doty, R.T., Clark, E.A., 1995. Ig domains 1 and 2 of murine CD22 constitute the ligand-binding domain and bind multiple sialylated ligands expressed on B and T cells. *Journal of Immunology (Baltimore, Md.: 1950)*. **155**, 3368-3376.
- Lee, C.J., Lee, L.H., Lu, C.S., Wu, A., 2001. Bacterial polysaccharides as vaccines--immunity and chemical characterization. *Advances in Experimental Medicine and Biology*. **491**, 453-471.
- Leprince, C., Draves, K.E., Geahlen, R.L., Ledbetter, J.A., Clark, E.A., 1993. CD22 associates with the human surface IgM-B-cell antigen receptor complex. *Proceedings of the National Academy of Sciences of the United States of America*. **90**, 3236-3240.
- Letterio, J.J. & Roberts, A.B., 1998. Regulation of immune responses by TGF-beta. *Annual Review of Immunology*. **16**, 137-161.
- Levison, S.E., Fisher, P., Hankinson, J., Zeef, L., Eyre, S., Ollier, W.E., McLaughlin, J.T., Brass, A., Grecis, R.K., Pennock, J.L., 2013. Genetic analysis of the *Trichuris muris*-induced model of colitis reveals QTL overlap and a novel gene cluster for establishing colonic inflammation. *BMC Genomics*. **14**, 127-2164-14-127.
- Lexau, C.A., Lynfield, R., Danila, R., Pilishvili, T., Facklam, R., Farley, M.M., Harrison, L.H., Schaffner, W., Reingold, A., Bennett, N.M., Hadler, J., Cieslak, P.R., Whitney, C.G., Active Bacterial Core Surveillance Team, 2005. Changing epidemiology of invasive pneumococcal disease among older adults in the era of pediatric pneumococcal conjugate vaccine. *JAMA : The Journal of the American Medical Association*. **294**, 2043-2051.
- Li, Y., Weinberger, D.M., Thompson, C.M., Trzcinski, K., Lipsitch, M., 2013. Surface charge of *Streptococcus pneumoniae* predicts serotype distribution. *Infection and Immunity*. **81**, 4519-4524.
- Lin, T.M., Chen, C.J., Wu, M.M., Yang, C.S., Chen, J.S., Lin, C.C., Kwang, T.Y., Hsu, S.T., Lin, S.Y., Hsu, L.C., 1989. Hepatitis B virus markers in Chinese twins. *Anticancer Research*. **9**, 737-741.

- Ling, E.M., Smith, T., Nguyen, X.D., Pridgeon, C., Dallman, M., Arbery, J., Carr, V.A., Robinson, D.S., 2004. Relation of CD4+CD25+ regulatory T-cell suppression of allergen-driven T-cell activation to atopic status and expression of allergic disease. *Lancet*. **363**, 608-615.
- Lloyd, S.E., Maytham, E.G., Pota, H., Grizenkova, J., Molou, E., Uphill, J., Hummerich, H., Whitfield, J., Alpers, M.P., Mead, S., Collinge, J., 2009. HECTD2 is associated with susceptibility to mouse and human prion disease. *PLoS Genetics*. **5**, e1000383.
- Lohr, J., Knoechel, B., Abbas, A.K., 2006. Regulatory T cells in the periphery. *Immunological Reviews*. **212**, 149-162.
- Lopalco, P.L., 2007. Measuring the impact of PCV7 in the European Union: why it is a priority. *Euro Surveillance : Bulletin Europeen Sur Les Maladies Transmissibles = European Communicable Disease Bulletin*. **12**, E070614.6.
- Lorian, V. & Markovits, G., 1973. Disk test for the differentiation of pneumococci from other alpha-hemolytic streptococci. *Applied Microbiology*. **26**, 116-117.
- Luckheeram, R.V., Zhou, R., Verma, A.D., Xia, B., 2012. CD4(+)T cells: differentiation and functions. *Clinical & Developmental Immunology*. **2012**, 925135.
- Lynch, J.P., 3rd & Zhanel, G.G., 2010. Streptococcus pneumoniae: epidemiology and risk factors, evolution of antimicrobial resistance, and impact of vaccines. *Current Opinion in Pulmonary Medicine*. **16**, 217-225.
- Ma, D.Y., Suthar, M.S., Kasahara, S., Gale, M., Jr, Clark, E.A., 2013. CD22 is required for protection against West Nile Virus infection. *Journal of Virology*.
- MacConmara, M.P., Maung, A.A., Fujimi, S., McKenna, A.M., Delisle, A., Lapchak, P.H., Rogers, S., Lederer, J.A., Mannick, J.A., 2006. Increased CD4+ CD25+ T regulatory cell activity in trauma patients depresses protective Th1 immunity. *Annals of Surgery*. **244**, 514-523.
- MacLeod, C.M. & Hodges, R.G., 1945. Prevention of pneumococcal pneumonia by immunization with specific capsular polysaccharides. *The Journal of Experimental Medicine*. **82**, 445-465.
- Madsen, H.O., Garred, P., Thiel, S., Kurtzhals, J.A., Lamm, L.U., Ryder, L.P., Svejgaard, A., 1995. Interplay between promoter and structural gene variants control basal serum level of mannan-binding protein. *Journal of Immunology (Baltimore, Md.: 1950)*. **155**, 3013-3020.
- Mahdi, L.K., Ogunniyi, A.D., LeMessurier, K.S., Paton, J.C., 2008. Pneumococcal virulence gene expression and host cytokine profiles during pathogenesis of invasive disease. *Infection and Immunity*. **76**, 646-657.

- Malangoni, M.A., Dawes, L.G., Droege, E.A., Almagro, U.A., 1985. The influence of splenic weight and function on survival after experimental pneumococcal infection. *Annals of Surgery*. **202**, 323-328.
- Malangoni, M.A., Dawes, L.G., Droege, E.A., Rao, S.A., Collier, B.D., Almagro, U.A., 1985. Splenic phagocytic function after partial splenectomy and splenic autotransplantation. *Archives of Surgery (Chicago, Ill.: 1960)*. **120**, 275-278.
- Malaty, H.M., Engstrand, L., Pedersen, N.L., Graham, D.Y., 1994. Helicobacter pylori infection: genetic and environmental influences. A study of twins. *Annals of Internal Medicine*. **120**, 982-986.
- Malo, D. & Skamene, E., 1994. Genetic control of host resistance to infection. *Trends in Genetics : TIG*. **10**, 365-371.
- Manco, S., Hernon, F., Yesilkaya, H., Paton, J.C., Andrew, P.W., Kadioglu, A., 2006. Pneumococcal neuraminidases A and B both have essential roles during infection of the respiratory tract and sepsis. *Infection and Immunity*. **74**, 4014-4020.
- Markel, P., Shu, P., Ebeling, C., Carlson, G.A., Nagle, D.L., Smutko, J.S., Moore, K.J., 1997. Theoretical and empirical issues for marker-assisted breeding of congenic mouse strains. *Nature Genetics*. **17**, 280-284.
- Marks, M., Burns, T., Abadi, M., Seyoum, B., Thornton, J., Tuomanen, E., Pirofski, L.A., 2007. Influence of neutropenia on the course of serotype 8 pneumococcal pneumonia in mice. *Infection and Immunity*. **75**, 1586-1597.
- Martin, G.S., 2012. Sepsis, severe sepsis and septic shock: changes in incidence, pathogens and outcomes. *Expert Review of Anti-Infective Therapy*. **10**, 701-706.
- Mauri, C. & Bosma, A., 2012. Immune regulatory function of B cells. *Annual Review of Immunology*. **30**, 221-241.
- McDaniel, L.S. & Swiatlo, E., 2004. Pneumococcal disease: pathogenesis, treatment, and prevention. *Infectious Diseases in Clinical Practice*. **12**, 93-98.
- McDaniel, L.S., Yother, J., Vijayakumar, M., McGarry, L., Guild, W.R., Briles, D.E., 1987. Use of insertional inactivation to facilitate studies of biological properties of pneumococcal surface protein A (PspA). *The Journal of Experimental Medicine*. **165**, 381-394.
- McLaren, W., Pritchard, B., Rios, D., Chen, Y., Flicek, P., Cunningham, F., 2010. Deriving the consequences of genomic variants with the Ensembl API and SNP Effect Predictor. *Bioinformatics (Oxford, England)*. **26**, 2069-2070.
- McLoughlin, R.M., Witowski, J., Robson, R.L., Wilkinson, T.S., Hurst, S.M., Williams, A.S., Williams, J.D., Rose-John, S., Jones, S.A., Topley, N., 2003. Interplay between IFN-gamma and IL-6 signaling governs neutrophil trafficking and apoptosis during acute inflammation. *The Journal of Clinical Investigation*. **112**, 598-607.

- McNeela, E.A., Burke, A., Neill, D.R., Baxter, C., Fernandes, V.E., Ferreira, D., Smeaton, S., El-Rachkidy, R., McLoughlin, R.M., Mori, A., Moran, B., Fitzgerald, K.A., Tschopp, J., Petrilli, V., Andrew, P.W., Kadioglu, A., Lavelle, E.C., 2010. Pneumolysin activates the NLRP3 inflammasome and promotes proinflammatory cytokines independently of TLR4. *PLoS Pathogens*. **6**, e1001191.
- McPeck, M.S., 2000. From mouse to human: fine mapping of quantitative trait loci in a model organism. *Proceedings of the National Academy of Sciences of the United States of America*. **97**, 12389-12390.
- Mellor, A.L. & Munn, D.H., 2011. Physiologic control of the functional status of Foxp3<sup>+</sup> regulatory T cells. *Journal of Immunology (Baltimore, Md.: 1950)*. **186**, 4535-4540.
- Mertens, J., Fabri, M., Zingarelli, A., Kubacki, T., Meemboor, S., Groneck, L., Seeger, J., Bessler, M., Hafke, H., Odenthal, M., Bieler, J.G., Kalka, C., Schneck, J.P., Kashkar, H., Kalka-Moll, W.M., 2009. Streptococcus pneumoniae serotype 1 capsular polysaccharide induces CD8CD28 regulatory T lymphocytes by TCR crosslinking. *PLoS Pathogens*. **5**, e1000596.
- Mills, K.H., 2004. Regulatory T cells: friend or foe in immunity to infection? *Nature Reviews.Immunology*. **4**, 841-855.
- Miossec, P., Korn, T., Kuchroo, V.K., 2009. Interleukin-17 and type 17 helper T cells. *The New England Journal of Medicine*. **361**, 888-898.
- Mitchell, T.J., Andrew, P.W., Saunders, F.K., Smith, A.N., Boulnois, G.J., 1991. Complement activation and antibody binding by pneumolysin via a region of the toxin homologous to a human acute-phase protein. *Molecular Microbiology*. **5**, 1883-1888.
- Mogensen, T.H., 2009. Pathogen recognition and inflammatory signaling in innate immune defenses. *Clinical Microbiology Reviews*. **22**, 240-73, Table of Contents.
- Mombo, L.E., Lu, C.Y., Ossari, S., Bedjabaga, I., Sica, L., Krishnamoorthy, R., Lapoumeroulie, C., 2003. Mannose-binding lectin alleles in sub-Saharan Africans and relation with susceptibility to infections. *Genes and Immunity*. **4**, 362-367.
- Morampudi, V., De Craeye, S., Le Moine, A., Detienne, S., Braun, M.Y., D'Souza, S., 2011. Partial depletion of CD4(+)CD25(+)Foxp3(+) T regulatory cells significantly increases morbidity during acute phase Toxoplasma gondii infection in resistant BALB/c mice. *Microbes and Infection / Institut Pasteur*. **13**, 394-404.
- Moreira, A.L., Tsenova, L., Aman, M.H., Bekker, L.G., Freeman, S., Mangaliso, B., Schroder, U., Jagirdar, J., Rom, W.N., Tovey, M.G., Freedman, V.H., Kaplan, G., 2002. Mycobacterial antigens exacerbate disease manifestations in Mycobacterium tuberculosis-infected mice. *Infection and Immunity*. **70**, 2100-2107.
- Morton, D.B. & Griffiths, P.H., 1985. Guidelines on the recognition of pain, distress and discomfort in experimental animals and an hypothesis for assessment. *The Veterinary Record*. **116**, 431-436.

Musher, D.M., 1992. Infections caused by *Streptococcus pneumoniae*: clinical spectrum, pathogenesis, immunity, and treatment. *Clinical Infectious Diseases : An Official Publication of the Infectious Diseases Society of America*. **14**, 801-807.

Nagaraj, S., Collazo, M., Corzo, C.A., Youn, J.I., Ortiz, M., Quiceno, D., Gabrilovich, D.I., 2009. Regulatory myeloid suppressor cells in health and disease. *Cancer Research*. **69**, 7503-7506.

Nath, D., van der Merwe, P.A., Kelm, S., Bradfield, P., Crocker, P.R., 1995. The amino-terminal immunoglobulin-like domain of sialoadhesin contains the sialic acid binding site. Comparison with CD22. *The Journal of Biological Chemistry*. **270**, 26184-26191.

Neill, D.R., Fernandes, V.E., Wisby, L., Haynes, A.R., Ferreira, D.M., Laher, A., Strickland, N., Gordon, S.B., Denny, P., Kadioglu, A., Andrew, P.W., 2012. T regulatory cells control susceptibility to invasive pneumococcal pneumonia in mice. *PLoS Pathogens*. **8**, e1002660.

Nelson, A.L., Roche, A.M., Gould, J.M., Chim, K., Ratner, A.J., Weiser, J.N., 2007. Capsule enhances pneumococcal colonization by limiting mucus-mediated clearance. *Infection and Immunity*. **75**, 83-90.

Ng, M.C., Shriner, D., Chen, B.H., Li, J., Chen, W.M., Guo, X., Liu, J., Bielinski, S.J., Yanek, L.R., Nalls, M.A., Comeau, M.E., Rasmussen-Torvik, L.J., Jensen, R.A., Evans, D.S., Sun, Y.V., An, P., Patel, S.R., Lu, Y., Long, J., Armstrong, L.L., Wagenknecht, L., Yang, L., Snively, B.M., Palmer, N.D., Mudgal, P., Langefeld, C.D., Keene, K.L., Freedman, B.I., Mychaleckyj, J.C., Nayak, U., Raffel, L.J., Goodarzi, M.O., Chen, Y.D., Taylor, H.A., Jr, Correa, A., Sims, M., Couper, D., Pankow, J.S., Boerwinkle, E., Adeyemo, A., Doumatey, A., Chen, G., Mathias, R.A., Vaidya, D., Singleton, A.B., Zonderman, A.B., Igo, R.P., Jr, Sedor, J.R., FIND Consortium, Kabagambe, E.K., Siscovick, D.S., McKnight, B., Rice, K., Liu, Y., Hsueh, W.C., Zhao, W., Bielak, L.F., Kraja, A., Province, M.A., Bottinger, E.P., Gottesman, O., Cai, Q., Zheng, W., Blot, W.J., Lowe, W.L., Pacheco, J.A., Crawford, D.C., eMERGE Consortium, DIAGRAM Consortium, Grundberg, E., MuTHER Consortium, Rich, S.S., Hayes, M.G., Shu, X.O., Loos, R.J., Borecki, I.B., Peyser, P.A., Cummings, S.R., Psaty, B.M., Fornage, M., Iyengar, S.K., Evans, M.K., Becker, D.M., Kao, W.H., Wilson, J.G., Rotter, J.I., Sale, M.M., Liu, S., Rotimi, C.N., Bowden, D.W., MEta-analysis of type 2 Diabetes in African Americans Consortium, 2014. Meta-analysis of genome-wide association studies in African Americans provides insights into the genetic architecture of type 2 diabetes. *PLoS Genetics*. **10**, e1004517.

NIAID, 2012. *Pneumococcal pneumonia: treatment*. [online]. Available at: <http://www.niaid.nih.gov/topics/pneumonia/pages/treatment.aspx>2012].

Niederman, M.S., Mandell, L.A., Anzueto, A., Bass, J.B., Broughton, W.A., Campbell, G.D., Dean, N., File, T., Fine, M.J., Gross, P.A., Martinez, F., Marrie, T.J., Plouffe, J.F., Ramirez, J., Sarosi, G.A., Torres, A., Wilson, R., Yu, V.L., American Thoracic Society, 2001. Guidelines for the management of adults with community-acquired pneumonia. Diagnosis, assessment of severity, antimicrobial therapy, and prevention. *American Journal of Respiratory and Critical Care Medicine*. **163**, 1730-1754.

- Nitschke, L., Carsetti, R., Ocker, B., Kohler, G., Lamers, M.C., 1997. CD22 is a negative regulator of B-cell receptor signalling. *Current Biology : CB*. **7**, 133-143.
- Noh, J., Choi, W.S., Noh, G., Lee, J.H., 2010. Presence of Foxp3-expressing CD19(+)CD5(+) B Cells in Human Peripheral Blood Mononuclear Cells: Human CD19(+)CD5(+)Foxp3(+) Regulatory B Cell (Breg). *Immune Network*. **10**, 247-249.
- Nollmann, M., Gilbert, R., Mitchell, T., Sferrazza, M., Byron, O., 2004. The role of cholesterol in the activity of pneumolysin, a bacterial protein toxin. *Biophysical Journal*. **86**, 3141-3151.
- Nordqvist, C., 2012. *All About Pneumococcal Disease*. [online]. Available at: <http://www.medicalnewstoday.com/info/pneumococcal-disease/pneumococcal-vaccine.php>2012].
- O'Brien, K.L., Millar, E.V., Zell, E.R., Bronsdon, M., Weatherholtz, R., Reid, R., Becenti, J., Kvamme, S., Whitney, C.G., Santosham, M., 2007. Effect of pneumococcal conjugate vaccine on nasopharyngeal colonization among immunized and unimmunized children in a community-randomized trial. *The Journal of Infectious Diseases*. **196**, 1211-1220.
- Orihuela, C.J., Gao, G., Francis, K.P., Yu, J., Tuomanen, E.I., 2004. Tissue-specific contributions of pneumococcal virulence factors to pathogenesis. *The Journal of Infectious Diseases*. **190**, 1661-1669.
- Osterholm, M.T., 2005. Preparing for the next pandemic. *The New England Journal of Medicine*. **352**, 1839-1842.
- Paterson, G.K. & Orihuela, C.J., 2010. Pneumococci: immunology of the innate host response. *Respirology (Carlton, Vic.)*. **15**, 1057-1063.
- Paton, J.C., Lock, R.A., Hansman, D.J., 1983. Effect of immunization with pneumolysin on survival time of mice challenged with *Streptococcus pneumoniae*. *Infection and Immunity*. **40**, 548-552.
- Perlino, C.A., 1984. Laboratory diagnosis of pneumonia due to *Streptococcus pneumoniae*. *The Journal of Infectious Diseases*. **150**, 139-144.
- Pettigrew, M.M., Fennie, K.P., York, M.P., Daniels, J., Ghaffar, F., 2006. Variation in the presence of neuraminidase genes among *Streptococcus pneumoniae* isolates with identical sequence types. *Infection and Immunity*. **74**, 3360-3365.
- Pham, C.T., 2006. Neutrophil serine proteases: specific regulators of inflammation. *Nature Reviews.Immunology*. **6**, 541-550.
- Plant, J. & Glynn, A.A., 1976. Genetics of resistance to infection with *Salmonella typhimurium* in mice. *The Journal of Infectious Diseases*. **133**, 72-78.

- Plotkowski, M.C., Puchelle, E., Beck, G., Jacquot, J., Hannoun, C., 1986. Adherence of type I Streptococcus pneumoniae to tracheal epithelium of mice infected with influenza A/PR8 virus. *The American Review of Respiratory Disease*. **134**, 1040-1044.
- Preston, J.A., Thorburn, A.N., Starkey, M.R., Beckett, E.L., Horvat, J.C., Wade, M.A., O'Sullivan, B.J., Thomas, R., Beagley, K.W., Gibson, P.G., Foster, P.S., Hansbro, P.M., 2011. Streptococcus pneumoniae infection suppresses allergic airways disease by inducing regulatory T-cells. *The European Respiratory Journal : Official Journal of the European Society for Clinical Respiratory Physiology*. **37**, 53-64.
- Price, K.E. & Camilli, A., 2009. Pneumolysin localizes to the cell wall of Streptococcus pneumoniae. *Journal of Bacteriology*. **191**, 2163-2168.
- Pyrosequencing AB, 2012. *Single Stranded Templates for Pyrosequencing*. [online]. Available at: <http://www.invitrogen.com/site/us/en/home/Products-and-Services/Applications/DNA-RNA-Purification-Analysis/napamisc/Capture-of-Biotinylated-Targets/Single-Stranded-Templates-for-Pyrosequencing.html>.
- Qureshi, S.T., Lariviere, L., Leveque, G., Clermont, S., Moore, K.J., Gros, P., Malo, D., 1999. Endotoxin-tolerant mice have mutations in Toll-like receptor 4 (Tlr4). *The Journal of Experimental Medicine*. **189**, 615-625.
- Rabinovich, G.A., Baum, L.G., Tinari, N., Paganelli, R., Natoli, C., Liu, F.T., Iacobelli, S., 2002. Galectins and their ligands: amplifiers, silencers or tuners of the inflammatory response? *Trends in Immunology*. **23**, 313-320.
- Rajam, G., Anderton, J.M., Carlone, G.M., Sampson, J.S., Ades, E.W., 2008. Pneumococcal surface adhesin A (PsaA): a review. *Critical Reviews in Microbiology*. **34**, 163-173.
- Ram, S., Lewis, L.A., Rice, P.A., 2010. Infections of people with complement deficiencies and patients who have undergone splenectomy. *Clinical Microbiology Reviews*. **23**, 740-780.
- Reinert, R.R., 2009. The antimicrobial resistance profile of Streptococcus pneumoniae. *Clinical Microbiology and Infection : The Official Publication of the European Society of Clinical Microbiology and Infectious Diseases*. **15 Suppl 3**, 7-11.
- Reinert, R.R., Al-Lahham, A., Lemperle, M., Tenholte, C., Briefs, C., Haupts, S., Gerards, H.H., Luttkick, R., 2002. Emergence of macrolide and penicillin resistance among invasive pneumococcal isolates in Germany. *The Journal of Antimicrobial Chemotherapy*. **49**, 61-68.
- Renaudineau, Y., Pers, J.O., Bendaoud, B., Jamin, C., Youinou, P., 2004. Dysfunctional B cells in systemic lupus erythematosus. *Autoimmunity Reviews*. **3**, 516-523.
- Rincon, M., 2012. Interleukin-6: from an inflammatory marker to a target for inflammatory diseases. *Trends in Immunology*. **33**, 571-577.

Ring, A., Weiser, J.N., Tuomanen, E.I., 1998. Pneumococcal trafficking across the blood-brain barrier. Molecular analysis of a novel bidirectional pathway. *The Journal of Clinical Investigation*. **102**, 347-360.

Robbins, J.B., Austrian, R., Lee, C.J., Rastogi, S.C., Schiffman, G., Henrichsen, J., Makela, P.H., Broome, C.V., Facklam, R.R., Tiesjema, R.H., 1983. Considerations for formulating the second-generation pneumococcal capsular polysaccharide vaccine with emphasis on the cross-reactive types within groups. *The Journal of Infectious Diseases*. **148**, 1136-1159.

Robinson, K.A., Baughman, W., Rothrock, G., Barrett, N.L., Pass, M., Lexau, C., Damaske, B., Stefonek, K., Barnes, B., Patterson, J., Zell, E.R., Schuchat, A., Whitney, C.G., Active Bacterial Core Surveillance (ABCs)/Emerging Infections Program Network, 2001. Epidemiology of invasive *Streptococcus pneumoniae* infections in the United States, 1995-1998: Opportunities for prevention in the conjugate vaccine era. *JAMA : The Journal of the American Medical Association*. **285**, 1729-1735.

Rochman, B., 2012. Want to know my future? *Time*.

Romagnani, S., 2004. The increased prevalence of allergy and the hygiene hypothesis: missing immune deviation, reduced immune suppression, or both? *Immunology*. **112**, 352-363.

Rose, L., Shivshankar, P., Hinojosa, E., Rodriguez, A., Sanchez, C.J., Orihuela, C.J., 2008. Antibodies against PsrP, a novel *Streptococcus pneumoniae* adhesin, block adhesion and protect mice against pneumococcal challenge. *The Journal of Infectious Diseases*. **198**, 375-383.

Rosenow, C., Ryan, P., Weiser, J.N., Johnson, S., Fontan, P., Ortqvist, A., Masure, H.R., 1997. Contribution of novel choline-binding proteins to adherence, colonization and immunogenicity of *Streptococcus pneumoniae*. *Molecular Microbiology*. **25**, 819-829.

Ross, M.E. & Caligiuri, M.A., 1997. Cytokine-induced apoptosis of human natural killer cells identifies a novel mechanism to regulate the innate immune response. *Blood*. **89**, 910-918.

Rowe, J.H., Ertelt, J.M., Aguilera, M.N., Farrar, M.A., Way, S.S., 2011. Foxp3(+) regulatory T cell expansion required for sustaining pregnancy compromises host defense against prenatal bacterial pathogens. *Cell Host & Microbe*. **10**, 54-64.

Roy, S., Hill, A.V., Knox, K., Griffiths, D., Crook, D., 2002. Research pointers: Association of common genetic variant with susceptibility to invasive pneumococcal disease. *BMJ (Clinical Research Ed.)*. **324**, 1369.

Roy, S., Knox, K., Segal, S., Griffiths, D., Moore, C.E., Welsh, K.I., Smarason, A., Day, N.P., McPheat, W.L., Crook, D.W., Hill, A.V., Oxford Pneumococcal Surveillance Group, 2002. MBL genotype and risk of invasive pneumococcal disease: a case-control study. *Lancet*. **359**, 1569-1573.

- Rubtsov, Y.P., Rasmussen, J.P., Chi, E.Y., Fontenot, J., Castelli, L., Ye, X., Treuting, P., Siewe, L., Roers, A., Henderson, W.R., Jr, Muller, W., Rudensky, A.Y., 2008. Regulatory T cell-derived interleukin-10 limits inflammation at environmental interfaces. *Immunity*. **28**, 546-558.
- Sakaguchi, S., 2003. The origin of FOXP3-expressing CD4+ regulatory T cells: thymus or periphery. *The Journal of Clinical Investigation*. **112**, 1310-1312.
- Sakaguchi, S., Miyara, M., Costantino, C.M., Hafler, D.A., 2010. FOXP3+ regulatory T cells in the human immune system. *Nature Reviews.Immunology*. **10**, 490-500.
- Salehen, N. & Stover, C., 2008. The role of complement in the success of vaccination with conjugated vs. unconjugated polysaccharide antigen. *Vaccine*. **26**, 451-459.
- Sampson, J.S., O'Connor, S.P., Stinson, A.R., Tharpe, J.A., Russell, H., 1994. Cloning and nucleotide sequence analysis of psaA, the Streptococcus pneumoniae gene encoding a 37-kilodalton protein homologous to previously reported Streptococcus sp. adhesins. *Infection and Immunity*. **62**, 319-324.
- Sanders, M.S., van Well, G.T., Ouburg, S., Lundberg, P.S., van Furth, A.M., Morre, S.A., 2011. Single nucleotide polymorphisms in TLR9 are highly associated with susceptibility to bacterial meningitis in children. *Clinical Infectious Diseases : An Official Publication of the Infectious Diseases Society of America*. **52**, 475-480.
- Sandgren, A., Albiger, B., Orihuela, C.J., Tuomanen, E., Normark, S., Henriques-Normark, B., 2005. Virulence in mice of pneumococcal clonal types with known invasive disease potential in humans. *The Journal of Infectious Diseases*. **192**, 791-800.
- Sapru, A. & Quasney, M.W., 2011. Host genetics and pediatric sepsis. *The Open Inflammation Journal*. **4**, 82-100.
- Sathish, J.G., Walters, J., Luo, J.C., Johnson, K.G., Leroy, F.G., Brennan, P., Kim, K.P., Gygi, S.P., Neel, B.G., Matthews, R.J., 2004. CD22 is a functional ligand for SH2 domain-containing protein-tyrosine phosphatase-1 in primary T cells. *The Journal of Biological Chemistry*. **279**, 47783-47791.
- Scanlon, K.L., Diven, W.F., Glew, R.H., 1989. Purification and properties of Streptococcus pneumoniae neuraminidase. *Enzyme*. **41**, 143-150.
- Schauer, R., 2000. Achievements and challenges of sialic acid research. *Glycoconjugate Journal*. **17**, 485-499.
- Schoenborn, J.R. & Wilson, C.B., 2007. Regulation of interferon-gamma during innate and adaptive immune responses. *Advances in Immunology*. **96**, 41-101.
- Schrag, S., Bealle, B. and Dowell, S., 2001. Resistant Pneumococcal Infections: the Burden of Disease and Challenges in Monitoring and Controlling Antimicrobial Resistance. WHO/CDS/CSR/DRS, ed. In: 2001 2001, World Health Organization.

Scott, J.R., Millar, E.V., Lipsitch, M., Moulton, L.H., Weatherholtz, R., Perilla, M.J., Jackson, D.M., Beall, B., Craig, M.J., Reid, R., Santosham, M., O'Brien, K.L., 2012. Impact of more than a decade of pneumococcal conjugate vaccine use on carriage and invasive potential in Native American communities. *The Journal of Infectious Diseases*. **205**, 280-288.

Sepulveda, R.L., Heiba, I.M., Navarrete, C., Elston, R.C., Gonzalez, B., Sorensen, R.U., 1994. Tuberculin reactivity after newborn BCG immunization in mono- and dizygotic twins. *Tubercle and Lung Disease : The Official Journal of the International Union Against Tuberculosis and Lung Disease*. **75**, 138-143.

Shaper, M., Hollingshead, S.K., Benjamin, W.H., Jr, Briles, D.E., 2004. PspA protects *Streptococcus pneumoniae* from killing by apolactoferrin, and antibody to PspA enhances killing of pneumococci by apolactoferrin [corrected]. *Infection and Immunity*. **72**, 5031-5040.

Shapiro, E.D., Berg, A.T., Austrian, R., Schroeder, D., Parcells, V., Margolis, A., Adair, R.K., Clemens, J.D., 1991. The protective efficacy of polyvalent pneumococcal polysaccharide vaccine. *The New England Journal of Medicine*. **325**, 1453-1460.

Shen, S., Shin, J.J., Strle, K., McHugh, G., Li, X., Glickstein, L.J., Drouin, E.E., Steere, A.C., 2010. Treg cell numbers and function in patients with antibiotic-refractory or antibiotic-responsive Lyme arthritis. *Arthritis and Rheumatism*. **62**, 2127-2137.

Siber, G.R., 2012. Novel pneumococcal vaccines and their regulatory pathways. March, 2012 2012, ISPPD-8.

Siber, G.R., Klugman, K.P. and Makela, P.H., 2008. *Pneumococcal Vaccines: The Impact of Conjugate Vaccine*. American Society for Microbiology.

Sjostrom, K., Spindler, C., Ortqvist, A., Kalin, M., Sandgren, A., Kuhlmann-Berenzon, S., Henriques-Normark, B., 2006. Clonal and capsular types decide whether pneumococci will act as a primary or opportunistic pathogen. *Clinical Infectious Diseases : An Official Publication of the Infectious Diseases Society of America*. **42**, 451-459.

Soehnlein, O., Kenne, E., Rotzius, P., Eriksson, E.E., Lindbom, L., 2008. Neutrophil secretion products regulate anti-bacterial activity in monocytes and macrophages. *Clinical and Experimental Immunology*. **151**, 139-145.

Sorensen, T.I., Nielsen, G.G., Andersen, P.K., Teasdale, T.W., 1988. Genetic and environmental influences on premature death in adult adoptees. *The New England Journal of Medicine*. **318**, 727-732.

Stahl, P.D. & Ezekowitz, R.A., 1998. The mannose receptor is a pattern recognition receptor involved in host defense. *Current Opinion in Immunology*. **10**, 50-55.

Standish, A.J. & Weiser, J.N., 2009. Human neutrophils kill *Streptococcus pneumoniae* via serine proteases. *Journal of Immunology (Baltimore, Md.: 1950)*. **183**, 2602-2609.

- Stanic, B., van de Veen, W., Wirz, O.F., Ruckert, B., Morita, H., Sollner, S., Akdis, C.A., Akdis, M., 2014. IL-10-overexpressing B cells regulate innate and adaptive immune responses. *The Journal of Allergy and Clinical Immunology*.
- Steiniger, B., Timphus, E.M., Barth, P.J., 2006. The splenic marginal zone in humans and rodents: an enigmatic compartment and its inhabitants. *Histochemistry and Cell Biology*. **126**, 641-648.
- Sutton, C.E., Mielke, L.A., Mills, K.H., 2012. IL-17-producing gammadelta T cells and innate lymphoid cells. *European Journal of Immunology*. **42**, 2221-2231.
- Suzuki, Y., Orellana, M.A., Wong, S.Y., Conley, F.K., Remington, J.S., 1993. Susceptibility to chronic infection with *Toxoplasma gondii* does not correlate with susceptibility to acute infection in mice. *Infection and Immunity*. **61**, 2284-2288.
- Swiatlo, E. & Ware, D., 2003. Novel vaccine strategies with protein antigens of *Streptococcus pneumoniae*. *FEMS Immunology and Medical Microbiology*. **38**, 1-7.
- Taams, L.S., Vukmanovic-Stejic, M., Smith, J., Dunne, P.J., Fletcher, J.M., Plunkett, F.J., Ebeling, S.B., Lombardi, G., Rustin, M.H., Bijlsma, J.W., Lafeber, F.P., Salmon, M., Akbar, A.N., 2002. Antigen-specific T cell suppression by human CD4+CD25+ regulatory T cells. *European Journal of Immunology*. **32**, 1621-1630.
- Talbot, U.M., Paton, A.W., Paton, J.C., 1996. Uptake of *Streptococcus pneumoniae* by respiratory epithelial cells. *Infection and Immunity*. **64**, 3772-3777.
- Tedder, T.F., Tuscano, J., Sato, S., Kehrl, J.H., 1997. CD22, a B lymphocyte-specific adhesion molecule that regulates antigen receptor signaling. *Annual Review of Immunology*. **15**, 481-504.
- Thornton, A.M., Korty, P.E., Tran, D.Q., Wohlfert, E.A., Murray, P.E., Belkaid, Y., Shevach, E.M., 2010. Expression of Helios, an Ikaros transcription factor family member, differentiates thymic-derived from peripherally induced Foxp3+ T regulatory cells. *Journal of Immunology (Baltimore, Md.: 1950)*. **184**, 3433-3441.
- Thornton, C.A. & Morgan, G., 2009. Innate and adaptive immune pathways to tolerance. *Nestle Nutrition Workshop Series.Paediatric Programme*. **64**, 45-57; discussion 57-61, 251-7.
- Tilley, S.J., Orlova, E.V., Gilbert, R.J., Andrew, P.W., Saibil, H.R., 2005. Structural basis of pore formation by the bacterial toxin pneumolysin. *Cell*. **121**, 247-256.
- Todar, K., 2003. *Streptococcus Pneumoniae: Pneumococcal pneumonia*. *Todar's online textbook of bacteriology*. [online].2011].
- Torzillo, P.J., Hanna, J.N., Morey, F., Gratten, M., Dixon, J., Erlich, J., 1995. Invasive pneumococcal disease in central Australia. *The Medical Journal of Australia*. **162**, 182-186.

- Trappetti, C., Kadioglu, A., Carter, M., Hayre, J., Iannelli, F., Pozzi, G., Andrew, P.W., Oggioni, M.R., 2009. Sialic Acid: A Preventable Signal for Pneumococcal Biofilm Formation, Colonization, and Invasion of the Host. *The Journal of Infectious Diseases*. **199**, 1497-1505.
- Tse, W.T., Tang, J., Jin, O., Korsgren, C., John, K.M., Kung, A.L., Gwynn, B., Peters, L.L., Lux, S.E., 2001. A new spectrin, beta IV, has a major truncated isoform that associates with promyelocytic leukemia protein nuclear bodies and the nuclear matrix. *The Journal of Biological Chemistry*. **276**, 23974-23985.
- Tuomanen, E.I., Austrian, R., Masure, H.R., 1995. Pathogenesis of pneumococcal infection. *The New England Journal of Medicine*. **332**, 1280-1284.
- Tuomanen, E.I., Mitchell, T.J., Morrison, D.A. and Spratt, B.G., eds, 2004. *The Pneumococcus*. Washington, D.C.: American Society for Microbiology.
- Tweten, R.K., 2005. Cholesterol-dependent cytolysins, a family of versatile pore-forming toxins. *Infection and Immunity*. **73**, 6199-6209.
- van der Merwe, P.A., Crocker, P.R., Vinson, M., Barclay, A.N., Schauer, R., Kelm, S., 1996. Localization of the putative sialic acid-binding site on the immunoglobulin superfamily cell-surface molecule CD22. *The Journal of Biological Chemistry*. **271**, 9273-9280.
- van der Sluijs, K.F., van Elden, L.J., Nijhuis, M., Schuurman, R., Pater, J.M., Florquin, S., Goldman, M., Jansen, H.M., Lutter, R., van der Poll, T., 2004. IL-10 is an important mediator of the enhanced susceptibility to pneumococcal pneumonia after influenza infection. *Journal of Immunology (Baltimore, Md.: 1950)*. **172**, 7603-7609.
- van Oss, C.J., 1978. Phagocytosis as a surface phenomenon. *Annual Review of Microbiology*. **32**, 19-39.
- van Rossum, A.M., Lysenko, E.S., Weiser, J.N., 2005. Host and bacterial factors contributing to the clearance of colonization by *Streptococcus pneumoniae* in a murine model. *Infection and Immunity*. **73**, 7718-7726.
- Vidal, S.M., Malo, D., Vogan, K., Skamene, E., Gros, P., 1993. Natural resistance to infection with intracellular parasites: isolation of a candidate for Bcg. *Cell*. **73**, 469-485.
- Visscher, P.M. & Montgomery, G.W., 2009. Genome-wide association studies and human disease: from trickle to flood. *JAMA : The Journal of the American Medical Association*. **302**, 2028-2029.
- Vivier, E., Raulet, D.H., Moretta, A., Caligiuri, M.A., Zitvogel, L., Lanier, L.L., Yokoyama, W.M., Ugolini, S., 2011. Innate or adaptive immunity? The example of natural killer cells. *Science (New York, N.Y.)*. **331**, 44-49.
- Wadwa, R.P. & Feigin, R.D., 1999. Pneumococcal vaccine: an update. *Pediatrics*. **103**, 1035-1037.

Waheed, A.A., Shimada, Y., Heijnen, H.F., Nakamura, M., Inomata, M., Hayashi, M., Iwashita, S., Slot, J.W., Ohno-Iwashita, Y., 2001. Selective binding of perfringolysin O derivative to cholesterol-rich membrane microdomains (rafts). *Proceedings of the National Academy of Sciences of the United States of America*. **98**, 4926-4931.

Walker, J.A., Allen, R.L., Falmagne, P., Johnson, M.K., Boulnois, G.J., 1987. Molecular cloning, characterization, and complete nucleotide sequence of the gene for pneumolysin, the sulfhydryl-activated toxin of *Streptococcus pneumoniae*. *Infection and Immunity*. **55**, 1184-1189.

Walker, J.A. & Smith, K.G., 2008. CD22: an inhibitory enigma. *Immunology*. **123**, 314-325.

Walsh, F.M. & Amyes, S.G., 2004. Microbiology and drug resistance mechanisms of fully resistant pathogens. *Current Opinion in Microbiology*. **7**, 439-444.

Wang, B., Dileepan, T., Briscoe, S., Hyland, K.A., Kang, J., Khoruts, A., Cleary, P.P., 2010. Induction of TGF-beta1 and TGF-beta1-dependent predominant Th17 differentiation by group A streptococcal infection. *Proceedings of the National Academy of Sciences of the United States of America*. **107**, 5937-5942.

Watson, D.A., Musher, D.M., Jacobson, J.W., Verhoef, J., 1993. A brief history of the pneumococcus in biomedical research: a panoply of scientific discovery. *Clinical Infectious Diseases : An Official Publication of the Infectious Diseases Society of America*. **17**, 913-924.

Weber, G.F., Chousterman, B.G., Hilgendorf, I., Robbins, C.S., Theurl, I., Gerhardt, L.M., Iwamoto, Y., Quach, T.D., Ali, M., Chen, J.W., Rothstein, T.L., Nahrendorf, M., Weissleder, R., Swirski, F.K., 2014. Pleural innate response activator B cells protect against pneumonia via a GM-CSF-IgM axis. *The Journal of Experimental Medicine*. **211**, 1243-1256.

Weber, S.E., Tian, H., Pirofski, L.A., 2011. CD8+ cells enhance resistance to pulmonary serotype 3 *Streptococcus pneumoniae* infection in mice. *Journal of Immunology (Baltimore, Md.: 1950)*. **186**, 432-442.

Wellek, B., Hahn, H., Opferkuch, W., 1976. Opsonizing activities of IgG, IgM antibodies and the C3b inactivator-cleaved third component of complement in macrophage phagocytosis. *Agents and Actions*. **6**, 260-262.

Wen, L.P., Madani, K., Fahrni, J.A., Duncan, S.R., Rosen, G.D., 1997. Dexamethasone inhibits lung epithelial cell apoptosis induced by IFN-gamma and Fas. *The American Journal of Physiology*. **273**, L921-9.

WHO, 2014. *Pneumonia*. [online]. Available at: <http://www.who.int/mediacentre/factsheets/fs331/en/2014>].

WHO, 2009. *Acute Respiratory Infections*. [online]. Available at: [http://www.who.int/vaccine\\_research/diseases/ari/en/index3.html](http://www.who.int/vaccine_research/diseases/ari/en/index3.html)2012].

- WHO, 2008. *Weekly epidemiological record: No.42*. [online]. Available at: <http://www.who.int/wer/2008/wer8342.pdf> [2012].
- WHO, 2007. *Weekly epidemiological record: No.12*. [online]. Available at: <http://www.who.int/wer/2007/wer8212.pdf> [2012].
- WHO, 2001. *Resistant pneumococcal infections: the burden of disease and challenges in monitoring and controlling antimicrobial resistance*. [online]. Available at: [www.who.int/entity/drugresistance/technicalguidance/en/resistantinfection.pdf](http://www.who.int/entity/drugresistance/technicalguidance/en/resistantinfection.pdf) [2012].
- Wiertsema, S.P., Khoo, S.K., Baynam, G., Veenhoven, R.H., Laing, I.A., Zielhuis, G.A., Rijkers, G.T., Goldblatt, J., LeSouf, P.N., Sanders, E.A.M., 2006. Association of CD14 Promoter Polymorphism with Otitis Media and Pneumococcal Vaccine Responses. *Clinical and Vaccine Immunology*. **13**, 892-897.
- Williams, M.A. & Bevan, M.J., 2006. Immunology: exhausted T cells perk up. *Nature*. **439**, 669-670.
- Wing, K., Onishi, Y., Prieto-Martin, P., Yamaguchi, T., Miyara, M., Fehervari, Z., Nomura, T., Sakaguchi, S., 2008. CTLA-4 control over Foxp3+ regulatory T cell function. *Science (New York, N.Y.)*. **322**, 271-275.
- Winter, C., Herbold, W., Maus, R., Langer, F., Briles, D.E., Paton, J.C., Welte, T., Maus, U.A., 2009. Important role for CC chemokine ligand 2-dependent lung mononuclear phagocyte recruitment to inhibit sepsis in mice infected with *Streptococcus pneumoniae*. *Journal of Immunology (Baltimore, Md.: 1950)*. **182**, 4931-4937.
- Wisby, L., Fernandes, V.E., Neill, D.R., Kadioglu, A., Andrew, P.W., Denny, P., 2013. Spir2; a novel QTL on chromosome 4 contributes to susceptibility to pneumococcal infection in mice. *BMC Genomics*. **14**, 242-2164-14-242.
- Witko-Sarsat, V., Rieu, P., Descamps-Latscha, B., Lesavre, P., Halbwachs-Mecarelli, L., 2000. Neutrophils: molecules, functions and pathophysiological aspects. *Laboratory Investigation; a Journal of Technical Methods and Pathology*. **80**, 617-653.
- Wu, Z., Sofronic-Milosavljevic, L., Nagano, I., Takahashi, Y., 2008. *Trichinella spiralis*: nurse cell formation with emphasis on analogy to muscle cell repair. *Parasites & Vectors*. **1**, 27-3305-1-27.
- Xu, G., Kiefel, M.J., Wilson, J.C., Andrew, P.W., Oggioni, M.R., Taylor, G.L., 2011. Three *Streptococcus pneumoniae* Sialidases: Three Different Products. *Journal of the American Chemical Society*.
- Yang, X.O., Nurieva, R., Martinez, G.J., Kang, H.S., Chung, Y., Pappu, B.P., Shah, B., Chang, S.H., Schluns, K.S., Watowich, S.S., Feng, X.H., Jetten, A.M., Dong, C., 2008. Molecular antagonism and plasticity of regulatory and inflammatory T cell programs. *Immunity*. **29**, 44-56.

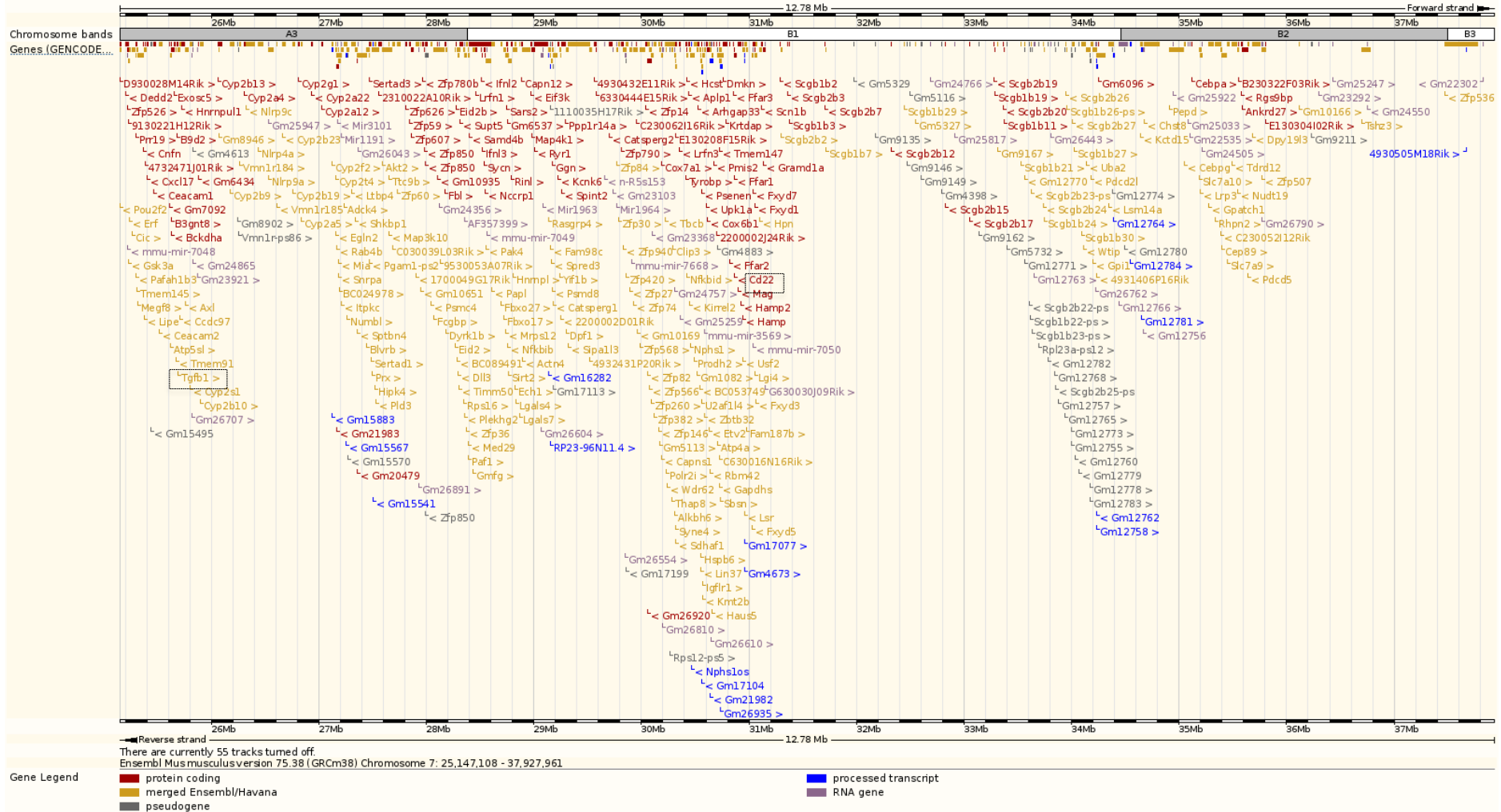
Yoneyama, M. & Fujita, T., 2004. RIG-I: critical regulator for virus-induced innate immunity. *Tanpakushitsu Kakusan Koso. Protein, Nucleic Acid, Enzyme*. **49**, 2571-2578.

Zhang, J.R., Mostov, K.E., Lamm, M.E., Nanno, M., Shimida, S., Ohwaki, M., Tuomanen, E., 2000. The polymeric immunoglobulin receptor translocates pneumococci across human nasopharyngeal epithelial cells. *Cell*. **102**, 827-837.

Zhang, Q., Leong, S.C., McNamara, P.S., Mubarak, A., Malley, R., Finn, A., 2011. Characterisation of regulatory T cells in nasal associated lymphoid tissue in children: relationships with pneumococcal colonization. *PLoS Pathogens*. **7**, e1002175.

Zysk, G., Schneider-Wald, B.K., Hwang, J.H., Bejo, L., Kim, K.S., Mitchell, T.J., Hakenbeck, R., Heinz, H.P., 2001. Pneumolysin is the main inducer of cytotoxicity to brain microvascular endothelial cells caused by *Streptococcus pneumoniae*. *Infection and Immunity*. **69**, 845-852.

# Appendix 1: genes in the *Spir1* region



Supplementary Figure 1 - Genes in the *Spir1* region. Figure represents the chromosome 7 genes located between 24Mb (*D7Mit341*) and 37Mb (*D7Mit247*). Image was exported from Emsembl (version 75). The genes investigated in this work, *tgfb1* (Chapter 5) and *cd22* (Chapter 6), were highlighted in the figure (dashed box).

## Appendix 2: Primer list

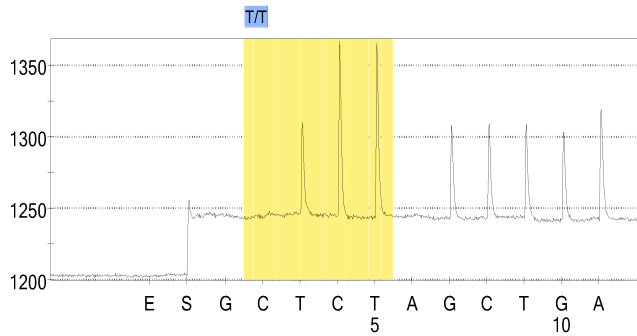
Code	Chr7 Location	SNP Position (Mb)	Ref. SNP	Observed (BALB/c vs CBA/Ca)	Forward Primer	Reverse Primer	Sequencing Primer
7_04	7:4734349	4 Mb	rs32128868	T/C	TATCCTGTCAGGTCCCGGATG	AGAGGTGGGTGGGCATTG (Biotin)	GCTTCTCTTGTCTCTT
7_09	7:11029385	11 Mb	rs3673010	GG, CC/ AA, TT	NNNTGTGTATGACTTATTTCCCTTGTTG	TGCACAACGTCCTGTGTTCC (Biotin)	CTTGTTGATCATACTCTAA
7_17	7:17634197	17 Mb	rs36950082	T/C	GGAGTGGGAGGTCATAGAAGACAA	CCCTGAACCCCAAATACTAAGGC (Biotin)	GGGAGGTCATAGAAGACAA
7_20	7:20527060	20 Mb	rs3655750	T/C	TATAAAGATCTGGGGTGGC (Biotin)	GTCTCATTGAGCCGTAAGTGT	TGTACCCACATGGGTC
7_26	7:26479896	26 Mb	rs32393147	T/C	GGTAGTTGAAGGAGGAGTTGAC	CTTGCCTTTATTCATCTCAGAG (Biotin)	TGGAGGAGAGGGCAT
7_27	7:27375676	27 Mb	rs6168040	G/A	GCTTTCAACCGATGTTAGAGATGC (Biotin)	NNNTGACTGGTGACATTTACAAAGTGCAG	GGTGTCTAACAGCACCC
7_31	7:31662605	31 Mb	N/A	G/A	AACCCAGATTCCCCTGTCA (Biotin)	AACGCCACAAAGACTGAGAAGGAC	TCTGAGCTGTACCTTCTA
7_35	7:35011176	35 Mb	rs32488598	A/G	TCCCAGGAAGTCCTATATACAGGT	GCCAGGAGCCATTCTAGATC (Biotin)	AGTCCTATATACAGGTGTCG
7_46	7:46553347	46 Mb	rs3089205	C/T	CTCAGTGGAGGCTGTTTCT (Biotin)	GTCAGGAAACTGAGAGTCCA	CAGCAGTGGTGCCAT
7_51	7:51783768	51 Mb	rs3024058	C/T	GGCACGGGGCTCTATCACTG (Biotin)	NNNTGCAACTACTCCAGAGGCTGAGG	CCAGAGGCTGAGGAA
7_63	7:63025252	63 Mb	rs32961897	G/C	CTCCGATTCACTAGCTACCC	CTGCCAGAGAATAGAAGCTGTCC (Biotin)	CCCATGACTCTGGTACA
7_54	7:73234304	73 Mb	rs4226656	A/C	NNNCCATCTGCTACCAGCCATGAGA	TCTTTGTGAGCTTGACTTTGTCAGA (Biotin)	GCCATGAGAAATAAGAAAA
7_123	7:141852931	141 Mb	rs4228417	G/A	NNNCCGTGCTCCCAAAGGTCTCA	TGGACATTCAATTGGGCCATA (Biotin)	CTTTCACAATGGGCA

Table A1 - List of SNP primers between BALB/c and CBA/Ca located in chromosome 7. Primers were used to amplify BALB/c and CBA/Ca DNA fragments used for pyrosequencing. “(Biotin)” = biotinylated primer.

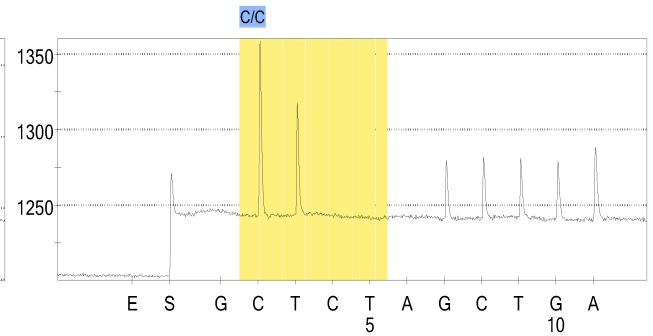
### Appendix 3: Pyrosequencing - Pyrogram outputs

#### 7\_04 SNP:

Homozygous BALB/c (T/T)

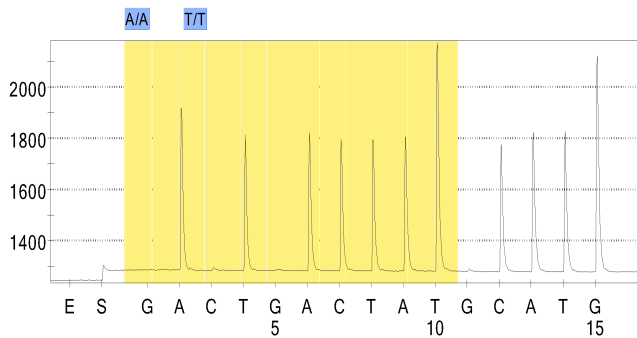


Homozygous CBA/Ca (C/C)

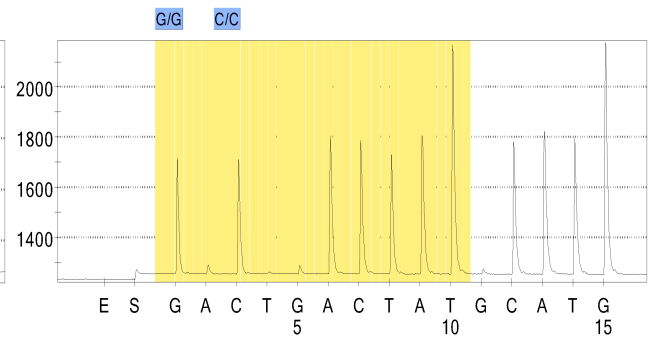


#### 7\_09 SNP:

Homozygous BALB/c (G/G, C/C)

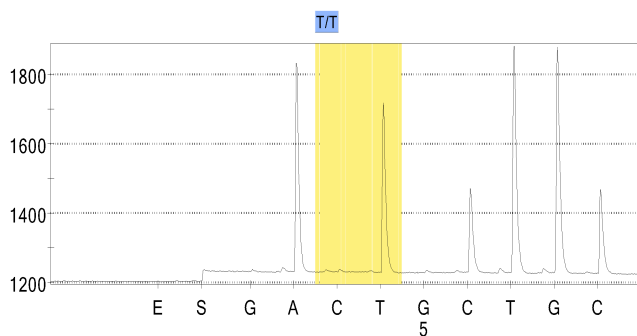


Homozygous CBA/Ca (A/A, T/T)

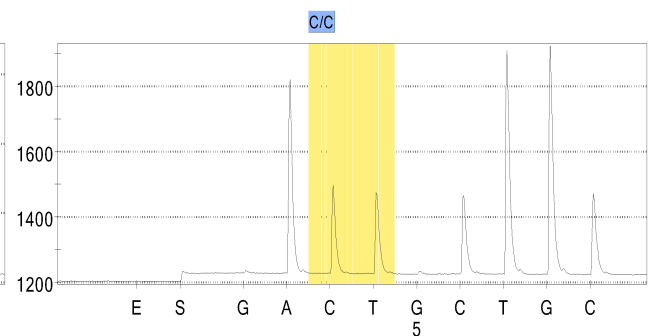


#### 7\_17 SNP:

Homozygous BALB/c (T/T)

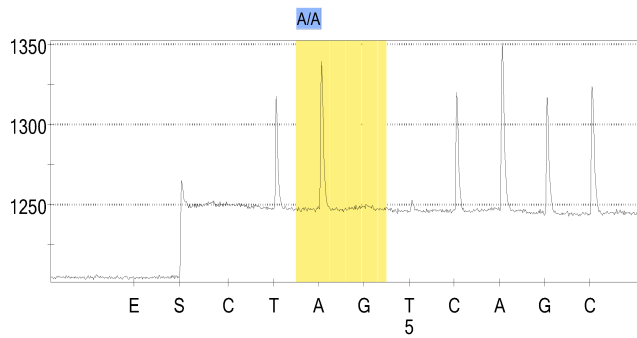


Homozygous CBA/Ca (C/C)

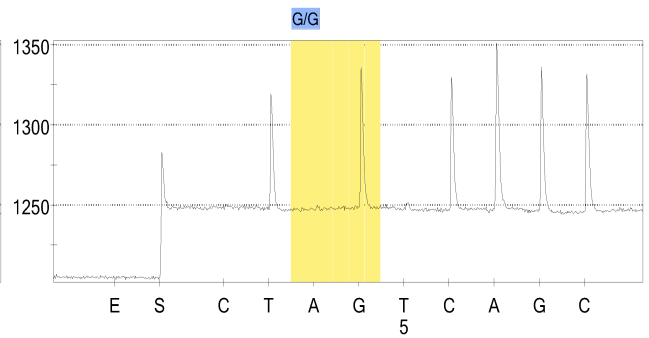


**7\_20 SNP:**

Homozygous BALB/c (A/A)

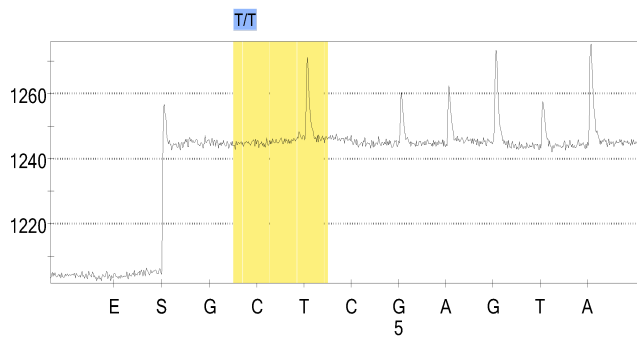


Homozygous CBA/Ca (G/G)

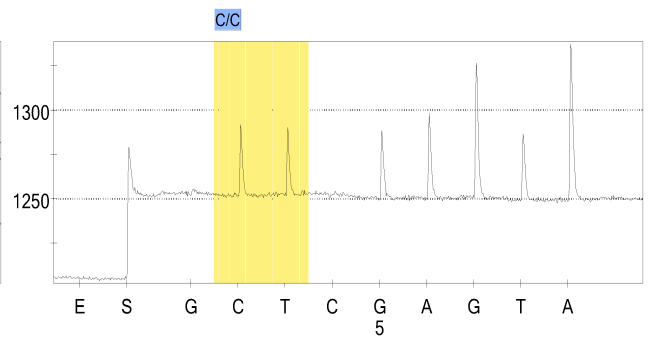


**7\_26 SNP:**

Homozygous BALB/c (T/T)

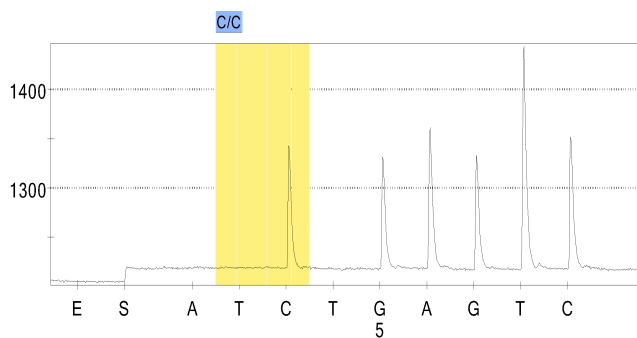


Homozygous CBA/Ca (C/C)

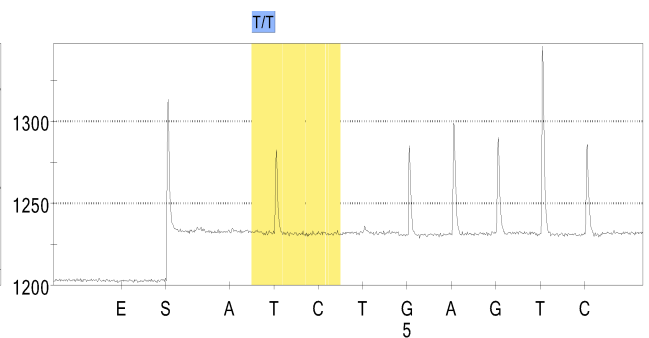


**7\_27 SNP:**

Homozygous BALB/c (C/C)

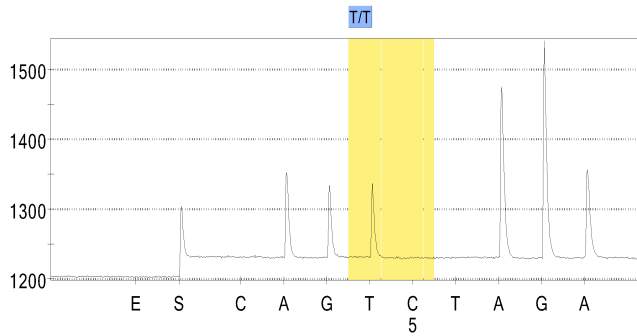


Homozygous CBA/Ca (T/T)

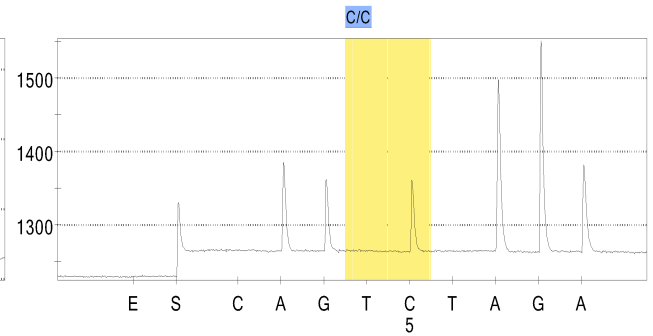


**7\_31 SNP:**

Homozygous BALB/c (C/C)

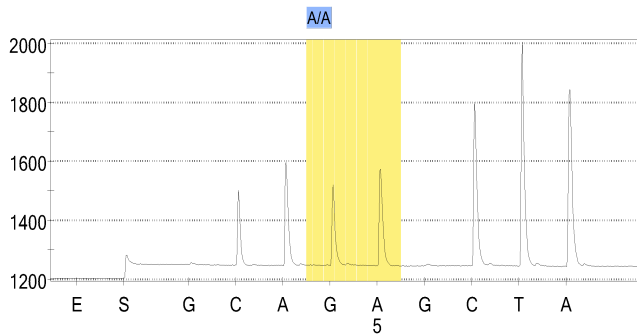


Homozygous CBA/Ca (T/T)

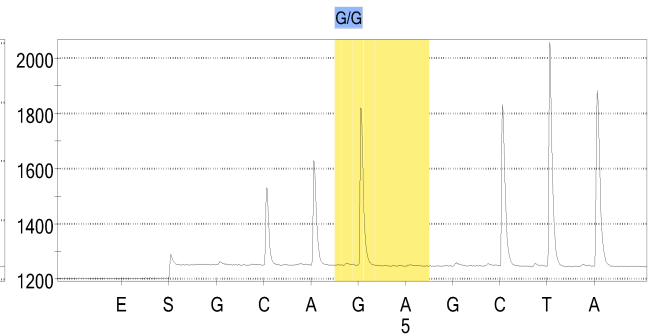


**7\_35 SNP:**

Homozygous BALB/c (A/A)

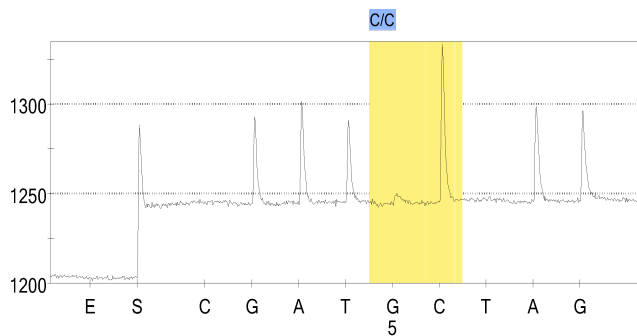


Homozygous CBA/Ca (G/G)

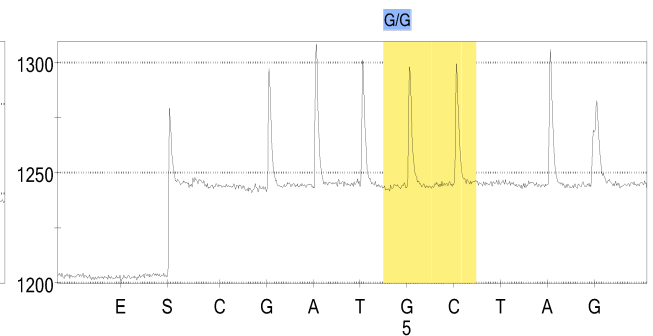


**7\_46 SNP:**

Homozygous BALB/c (C/C)

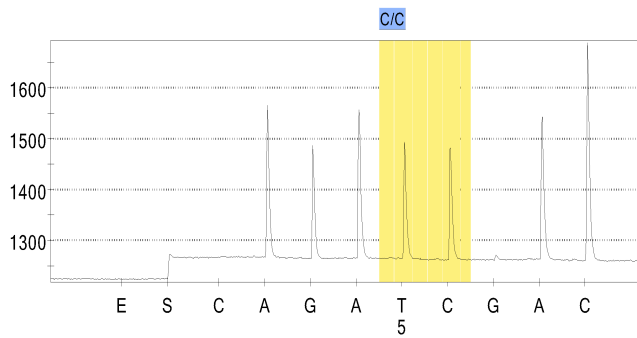


Homozygous CBA/Ca (G/G)

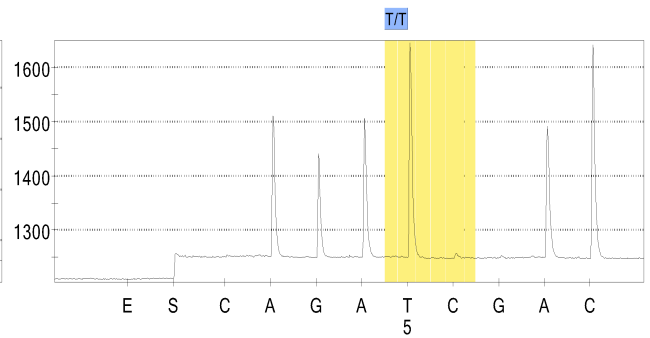


**7\_51 SNP:**

Homozygous BALB/c (C/C)

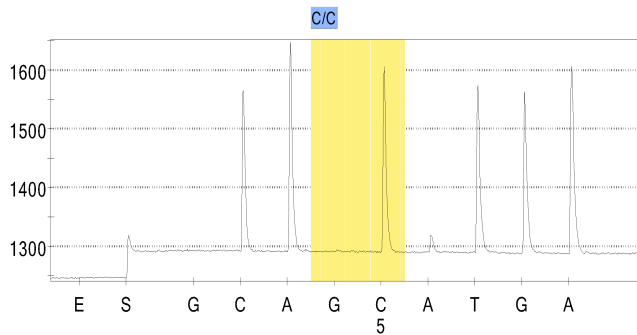


Homozygous CBA/Ca (T/T)

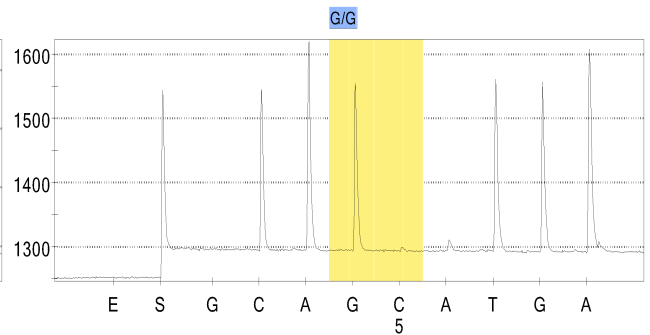


**7\_63 SNP:**

Homozygous BALB/c (G/G)

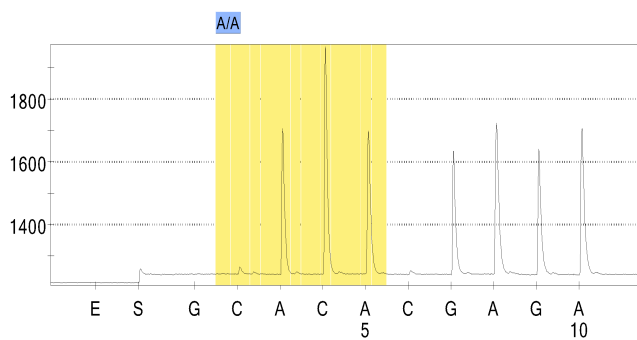


Homozygous CBA/Ca (C/C)

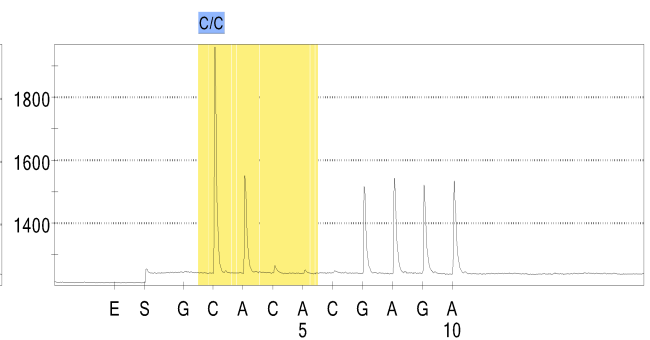


**7\_54 SNP:**

Homozygous BALB/c (G/G)

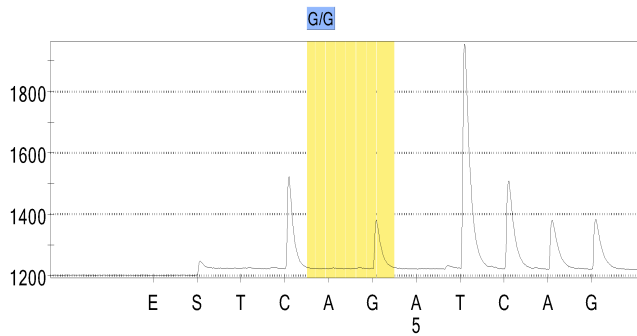


Homozygous CBA/Ca (A/A)

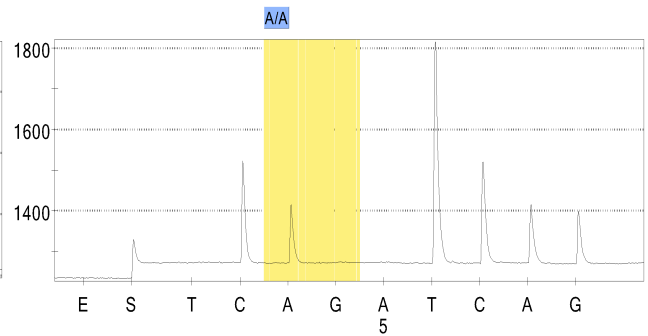


### 7\_123 SNP:

Homozygous BALB/c (G/G)



Homozygous CBA/Ca (A/A)



Supplementary Figure 2 - Pyrosequencing analysis of all the SNPs used in the marker-assisted congenic program. Figures represent pyrosequencing program output (pyrogram) for each of the SNPs used (7\_04, 7\_09, 7\_17, 7\_20, 7\_26, 7\_27, 7\_31, 7\_35, 7\_46, 7\_51, 7\_63, 7\_54 and 7\_123 marker), showing an example of the results with the controls in the congenic program (section 4.1.1) – homozygous BALB/c (left pyrogram) and homozygous CBA/Ca (right pyrogram) mice.

## Appendix 4: Genotyping and Phenotyping data of the N<sub>10</sub> congenic lines

BBB line

No.	Sex	UID	Log <sub>10</sub> CFU/ml	Survival Time (hrs)	Chromosome 7 SNP markers													
					7_04	7_09	7_17	7_20	7_26	7_27	7_31	7_35	7_46	7_51	7_63	7_54	7_123	
1	Female	3431	0.00	168	FAIL	B	B	B	FAIL	B	B	B	B	B	B	B	B	
2	Female	3399	0.00	168	B	B	B	B	B	B	B	B	B	B	B	B	B	
3	Female	3588	0.00	168	FAIL	B	B	B	FAIL	B	B	B	B	B	B	B	B	
4	Male	3439	0.00	168	FAIL	B	B	B	FAIL	B	B	B	B	B	B	B	B	
5	Male	3448	0.00	168	FAIL	B	B	B	FAIL	B	B	B	B	B	B	B	B	
6	Male	3449	0.00	168	FAIL	B	B	B	FAIL	B	B	B	B	B	B	B	B	
7	Male	3424	0.00	168	B	B	B	B	B	B	B	B	B	B	B	B	B	
8	Male	3590	0.00	168	FAIL	B	B	B	FAIL	B	B	B	B	B	B	B	B	
9	Male	3591	0.00	168	FAIL	B	B	B	FAIL	B	B	B	B	B	B	B	B	
10	Female	3592	0.00	168	FAIL	B	B	B	FAIL	B	B	B	B	B	B	B	B	
11	Female	3593	0.00	168	FAIL	B	B	B	FAIL	B	B	B	B	B	B	B	B	
12	Female	3594	0.00	168	B	B	B	B	B	B	B	B	B	B	B	B	B	
13	Female	3595	0.00	168	FAIL	B	B	B	FAIL	B	B	B	B	B	B	B	B	
14	Female	3408	0.00	75	B	B	B	B	B	B	B	B	B	B	B	B	B	
15	Female	3406	0.00	168	FAIL	B	B	B	B	B	B	B	B	B	B	B	B	
16	Male	3386	0.00	168	FAIL	B	B	B	FAIL	B	B	B	B	B	B	B	B	
17	Female	3390	0.00	168	FAIL	B	B	B	FAIL	B	B	B	B	B	B	B	B	
18	Female	3391	0.00	168	FAIL	B	B	B	FAIL	B	B	B	B	B	B	B	B	
19	Female	3452	4.21	48	FAIL	B	B	B	FAIL	B	B	B	B	B	B	B	B	
20	Female	3432	0.00	168	FAIL	B	B	B	FAIL	B	B	B	B	B	B	B	B	
21	Female	3443	0.00	168	FAIL	B	B	B	FAIL	B	B	B	B	B	B	B	B	
22	Male	3604	0.00	168	FAIL	B	B	B	FAIL	B	B	B	B	B	B	B	B	
23	Male	3605	0.00	168	FAIL	B	B	B	FAIL	B	B	B	B	B	B	B	B	
24	Male	3613	0.00	168	FAIL	B	B	B	FAIL	B	B	B	B	B	B	B	B	
25	Male	3628	0.00	75	FAIL	B	B	B	B	B	FAIL	B	B	FAIL	FAIL	B	B	
26	Female	3630	0.00	168	FAIL	B	B	B	B	B	FAIL	B	B	B	B	B	B	
27	Female	3631	0.00	168	FAIL	B	B	B	FAIL	B	B	B	B	B	B	B	B	
28	Male	4657	6.81	49	FAIL	B	B	B	FAIL	B	FAIL	B	B	B	FAIL	B	B	
29	Male	4658	2.70	168	FAIL	B	B	B	FAIL	FAIL	FAIL	FAIL	B	FAIL	FAIL	FAIL	B	B
30	Male	4659	0.00	168	FAIL	B	B	B	FAIL	B	FAIL	B	HET	B	FAIL	B	B	
31	Female	4660	2.52	168	FAIL	B	B	B	FAIL	B	FAIL	HET	B	B	FAIL	B	B	
32	Female	4661	0.00	168	FAIL	B	B	B	FAIL	B	FAIL	FAIL	FAIL	FAIL	FAIL	B	B	
33	Female	4662	2.82	168	FAIL	B	B	FAIL	FAIL	B	FAIL	B	FAIL	FAIL	FAIL	B	B	
34	Female	4217	0.00	168	n.a.	B	n.a.	B	B									
35	Female	4219	0.00	168	n.a.	B	n.a.	B	B									
36	Female	4337	0.00	168	n.a.	B	n.a.	B	B									
37	Male	4214	0.00	168	n.a.	B	n.a.	B	B									
38	Male	4212	2.52	48	n.a.	B	n.a.	B	B									
39	Female	4545	0.00	168	n.a.	B	n.a.	B	B									
40	Female	4546	3.34	168	n.a.	B	n.a.	B	B									
41	Female	4547	2.22	168	n.a.	B	n.a.	B	B									
42	Male	4544	0.00	168	n.a.	B	n.a.	B	B									
43	Male	4543	5.94	48	n.a.	B	n.a.	B	B									
44	Male	4542	0.00	168	n.a.	B	n.a.	B	B									
45	Female	4553	0.00	168	n.a.	B	n.a.	B	B									
46	Female	4554	0.00	168	n.a.	B	n.a.	B	B									
47	Male	4590	2.70	72	n.a.	B	n.a.	B	B									
48	Male	4591	0.00	168	n.a.	B	n.a.	B	B									
49	Male	4592	0.00	168	n.a.	B	n.a.	B	B									
50	Female	4548	0.00	168	n.a.	B	n.a.	B	B									
51	Male	4549	1.71	30	n.a.	B	n.a.	B	B									
52	Male	4550	0.00	168	n.a.	B	n.a.	B	B									
53	Male	4551	0.00	168	n.a.	B	n.a.	B	B									
54	Male	4552	0.00	168	n.a.	B	n.a.	B	B									

BBC line

					Chromosome 7 SNP markers												
No.	Sex	UID	Log10 CFU/ml	Survival Time (hrs)	7_04	7_09	7_17	7_20	7_26	7_27	7_31	7_35	7_46	7_51	7_63	7_54	7_123
1	Male	3649	0.00	168	FAIL	B	B	B	FAIL	B	B	B	B	B	B	B	C
2	Male	3650	0.00	168	FAIL	B	B	B	FAIL	B	B	B	B	B	B	B	C
3	Male	3651	0.00	168	FAIL	B	B	B	FAIL	B	B	B	B	B	B	B	C
4	Male	3652	0.00	168	FAIL	B	B	B	FAIL	B	B	B	B	B	B	B	C
5	Male	3700	0.00	168	FAIL	B	B	B	FAIL	B	B	B	B	B	B	B	C
6	Female	3702	4.36	57	FAIL	B	B	B	FAIL	B	B	B	B	B	B	B	C
7	Female	3703	0.00	168	FAIL	B	B	B	FAIL	B	B	B	B	B	B	B	C
8	Male	3706	3.26	168	FAIL	B	B	B	B	B	B	B	B	B	B	B	C
9	Male	3707	0.00	168	FAIL	B	B	B	FAIL	B	B	B	B	B	B	B	C
10	Male	3708	2.52	168	B	B	B	B	B	B	B	B	B	B	B	B	C
11	Male	3710	4.52	168	FAIL	B	B	B	FAIL	B	B	B	B	B	B	B	C
12	Male	3711	0.00	168	FAIL	B	B	B	FAIL	B	B	B	B	B	B	B	C
13	Male	3712	2.52	168	B	B	B	B	B	B	B	B	B	B	B	B	C
14	Male	3713	5.10	168	FAIL	B	B	B	FAIL	B	B	B	B	B	B	B	C
15	Female	3714	0.00	168	FAIL	B	B	B	FAIL	B	B	B	B	B	B	B	C
16	Female	3715	0.00	120	B	B	B	B	B	B	B	B	B	B	B	B	C
17	Female	3716	3.75	168	B	B	B	B	B	B	B	B	B	B	B	B	C
18	Female	3717	5.88	57	FAIL	B	B	B	FAIL	B	FAIL	B	B	C	B	B	C
19	Male	3722	2.22	168	FAIL	B	B	B	FAIL	B	FAIL	B	B	B	B	B	C
20	Male	3723	0.00	168	FAIL	B	B	B	FAIL	B	B	B	B	B	B	B	C
21	Male	3724	6.09	32	B	B	B	B	B	B	B	B	B	B	B	B	C
22	Male	3725	0.00	168	B	B	B	B	B	B	B	B	B	B	B	B	C
23	Male	3726	0.00	168	FAIL	B	B	B	FAIL	B	B	B	B	B	B	B	C
24	Female	3727	0.00	168	B	B	B	B	B	B	B	B	B	B	B	B	C
25	Female	3728	0.00	168	FAIL	B	B	B	FAIL	B	B	B	B	B	B	B	C
26	Female	3729	0.00	168	FAIL	B	B	B	B	B	B	B	B	B	B	B	C
27	Female	3730	0.00	168	FAIL	B	B	B	FAIL	B	FAIL	B	B	FAIL	FAIL	B	C
28	Female	3731	0.00	168	FAIL	B	B	B	FAIL	B	B	B	B	B	B	B	C
29	Male	3772	0.00	168	FAIL	B	B	B	FAIL	B	B	B	B	B	B	B	C
30	Male	3773	0.00	168	FAIL	B	B	B	FAIL	B	B	B	B	B	FAIL	B	C
31	Male	3774	0.00	168	FAIL	B	B	B	FAIL	B	B	B	B	B	B	B	C
32	Female	3775	0.00	168	FAIL	B	B	B	B	B	B	B	B	B	B	B	C
33	Male	3776	0.00	168	FAIL	B	B	B	FAIL	B	B	B	B	B	B	B	C
34	Male	3777	0.00	168	FAIL	B	B	B	FAIL	B	B	B	B	FAIL	B	B	C
35	Female	3778	2.70	168	FAIL	B	B	B	FAIL	B	B	B	B	B	B	B	C
36	Female	3779	0.00	168	B	B	B	B	B	B	B	B	B	B	B	B	C
37	Female	3780	0.00	168	FAIL	B	B	B	B	B	B	B	B	B	B	B	C
38	Female	3781	0.00	168	B	B	B	B	B	B	B	B	B	B	B	B	C
39	Male	3787	0.00	168	FAIL	B	B	B	FAIL	B	B	B	HET	B	B	B	C
40	Female	3787a	0.00	168	FAIL	B	B	B	FAIL	B	B	B	B	B	B	B	C
41	Female	3787b	0.00	168	FAIL	B	B	B	FAIL	B	B	B	B	B	B	B	C
42	Male	3855	0.00	168	B	B	B	B	B	B	B	B	B	B	B	B	C
43	Male	3856	0.00	168	FAIL	B	B	B	FAIL	B	B	B	B	B	B	B	C
44	Male	3857	0.00	168	FAIL	B	B	B	FAIL	B	B	B	B	B	B	B	C
45	Male	3858	0.00	168	FAIL	B	B	B	FAIL	B	B	B	B	B	B	B	C
46	Female	3859	0.00	168	FAIL	B	B	B	FAIL	B	B	B	B	B	B	B	C
47	Female	3860	2.82	168	FAIL	B	B	B	FAIL	B	B	B	B	B	FAIL	B	C
48	Female	3861	0.00	168	FAIL	B	B	B	FAIL	B	B	B	B	B	B	B	C
49	Female	3862	0.00	168	FAIL	B	B	B	FAIL	B	B	B	B	B	B	B	C
50	Female	3863	0.00	168	B	B	B	B	B	B	B	B	B	B	B	B	C
51	Male	4117	6.30	30	FAIL	B	B	B	FAIL	B	B	B	B	B	B	B	C
52	Male	4128	4.11	168	FAIL	B	B	B	FAIL	B	B	B	B	B	B	B	C
53	Male	4129	0.00	168	FAIL	B	B	B	FAIL	B	FAIL	B	B	B	B	B	C
54	Male	4130	4.22	48	FAIL	B	B	B	FAIL	B	HET	B	B	B	B	B	C
55	Male	4131	0.00	168	FAIL	B	B	B	FAIL	B	B	B	B	B	FAIL	B	C
56	Male	4262	4.48	48	FAIL	B	B	B	FAIL	B	B	B	B	B	B	B	C
57	Male	4252	0.00	168	FAIL	B	B	B	FAIL	B	B	B	B	B	B	B	C
58	Male	4247	0.00	168	FAIL	B	B	B	FAIL	B	B	B	B	B	B	B	C
59	Male	4248	4.73	72	FAIL	B	B	B	FAIL	B	B	B	B	B	B	B	C
60	Male	4176	5.06	72	FAIL	B	B	B	FAIL	B	B	B	B	B	B	B	C
61	Male	4167	4.50	30	FAIL	B	B	B	FAIL	B	B	B	B	B	B	B	C
62	Male	4117	6.30	30	FAIL	B	B	FAIL	FAIL	FAIL	FAIL	FAIL	B	FAIL	B	FAIL	C
63	Male	4128	4.11	168	FAIL	B	FAIL	FAIL	FAIL	FAIL	FAIL	B	FAIL	FAIL	FAIL	B	C

BCC line

					Chromosome 7 SNP markers													
No.	Sex	UID	Log10 CFU/ml	Survival Time (hrs)	7_04	7_09	7_17	7_20	7_26	7_27	7_31	7_35	7_46	7_51	7_63	7_54	7_123	
1	Male	4014	0.00	168	FAIL	B	B	B	FAIL	B	B	B	B	C	C	C	C	
2	Male	4015	0.00	168	FAIL	B	B	B	FAIL	B	B	B	B	B	B	C	C	
3	Male	4016	0.00	168	FAIL	B	B	B	FAIL	B	B	B	B	HET	B	C	C	
4	Male	4036	0.00	168	FAIL	B	B	B	FAIL	B	B	B	B	HET	C	C	C	
5	Male	4037	3.37	94	B	B	B	B	B	B	B	B	B	B	HET	C	C	
6	Female	4038	0.00	168	B	B	B	B	B	B	B	B	B	B	HET	C	C	
7	Female	4039	0.00	168	FAIL	B	B	B	FAIL	B	B	B	B	HET	C	C	C	
8	Female	4040	0.00	168	FAIL	B	B	B	FAIL	B	B	B	B	C	C	C	C	
9	Female	4041	0.00	168	FAIL	B	B	B	FAIL	B	B	B	HET	HET	HET	C	C	
10	Male	4060	3.50	168	FAIL	B	B	B	FAIL	B	FAIL	B	HET	HET	C	C	C	
11	Male	4061	3.07	168	B	B	B	B	B	B	B	B	B	B	B	HET	C	C
12	Male	4101	0.00	168	B	B	B	B	B	B	B	B	B	B	B	C	C	
13	Male	4102	0.00	168	FAIL	B	B	B	FAIL	B	B	B	B	HET	B	C	C	
14	Male	4103	0.00	168	FAIL	B	B	B	FAIL	B	B	B	B	C	HET	C	C	
15	Male	4104	5.87	29	FAIL	B	B	B	FAIL	B	FAIL	B	B	C	HET	C	C	
16	Male	4105	0.00	168	FAIL	B	B	B	FAIL	B	B	B	B	B	C	C	C	
17	Female	4106	0.00	168	FAIL	B	B	B	FAIL	B	B	B	B	HET	B	C	C	
18	Female	4107	4.64	120	FAIL	B	B	B	FAIL	B	B	B	B	HET	HET	C	C	
19	Female	4108	0.00	168	B	B	B	B	B	B	B	B	B	B	B	C	C	
20	Female	4109	3.71	72	FAIL	B	B	B	FAIL	B	B	B	B	HET	HET	C	C	
21	Male	4159	6.19	29	FAIL	B	B	B	FAIL	B	B	B	HET	C	C	C	C	
22	Male	4160	0.00	168	B	B	B	B	B	B	B	B	B	B	HET	C	C	
23	Male	4161	0.00	168	FAIL	B	B	B	B	B	B	B	B	C	C	C	C	
24	Male	4162	0.00	168	FAIL	B	B	B	FAIL	B	B	B	B	HET	C	C	C	
25	Female	4163	0.00	168	FAIL	B	B	B	FAIL	B	B	B	B	C	HET	HET	C	C
26	Female	4164	0.00	168	FAIL	B	B	B	FAIL	B	B	B	HET	HET	HET	C	C	
27	Female	4165	0.00	168	FAIL	B	B	B	FAIL	B	B	B	C	HET	C	C	C	
28	Female	4166	0.00	168	FAIL	B	B	B	FAIL	B	B	B	B	B	HET	C	C	
29	Female	4230	0.00	168	FAIL	B	B	B	FAIL	B	B	B	B	B	B	C	C	
30	Female	4231	0.00	168	B	B	B	B	B	B	B	B	B	B	B	C	C	
31	Female	4232	4.43	30	FAIL	B	B	B	FAIL	B	B	B	HET	HET	HET	C	C	
32	Female	4233	3.60	84	FAIL	B	B	B	FAIL	B	B	B	B	B	FAIL	C	C	
33	Female	4234	0.00	168	FAIL	B	B	B	B	B	B	B	B	B	B	HET	C	C
34	Female	4235	4.37	71	FAIL	B	B	B	FAIL	B	B	B	HET	HET	B	C	C	
35	Male	4266	0.00	168	FAIL	B	B	B	FAIL	B	B	B	B	C	C	C	C	
36	Male	4267	0.00	168	FAIL	B	B	B	FAIL	B	B	B	B	HET	HET	C	C	
37	Male	4268	0.00	168	FAIL	B	B	B	FAIL	B	B	B	B	HET	HET	C	C	
38	Male	4269	0.00	168	FAIL	B	B	B	FAIL	B	B	B	B	C	C	C	C	
39	Male	4270	4.26	27	B	B	B	B	B	B	B	B	B	B	B	C	C	C
40	Female	4271	0.00	168	FAIL	B	B	B	FAIL	B	B	B	B	HET	C	C	C	
41	Female	4272	0.00	168	FAIL	B	B	B	FAIL	B	B	B	B	C	C	C	C	
42	Female	4273	0.00	168	FAIL	B	B	B	FAIL	B	B	B	B	C	C	C	C	
43	Male	4282	2.70	168	FAIL	B	B	B	FAIL	B	B	B	B	HET	C	C	C	
44	Male	4283	0.00	168	B	B	B	B	B	B	B	B	B	B	HET	C	C	
45	Male	4284	3.12	168	FAIL	B	B	B	FAIL	B	B	B	B	HET	HET	C	C	
46	Male	4285	4.87	152	FAIL	B	B	B	FAIL	B	B	B	B	HET	C	C	C	
47	Male	4286	0.00	168	FAIL	B	B	B	B	B	B	B	B	B	HET	C	C	
48	Male	4287	0.00	168	FAIL	B	B	B	FAIL	B	B	B	B	B	HET	C	C	

CCC line

No.	Sex	UID	Log10 CFU/ml	Survival Time (hrs)	Chromosome 7 SNP markers												
					7_04	7_09	7_17	7_20	7_26	7_27	7_31	7_35	7_46	7_51	7_63	7_54	7_123
1	Male	3640	6.19	27	FAIL	C	C	C	FAIL	C	C	C	C	C	HET	C	C
2	Male	3670	6.53	27	C	C	C	C	C	C	C	C	C	C	C	C	C
3	Male	3671	6.15	27	FAIL	C	C	C	FAIL	C	C	C	C	C	HET	C	C
4	Male	3673	5.04	75	FAIL	C	C	C	FAIL	C	C	C	C	C	C	C	C
5	Male	3674	5.27	27	FAIL	C	C	C	FAIL	C	C	C	C	C	C	C	C
6	Female	3684	3.37	168	C	C	C	C	C	C	C	C	C	C	C	C	C
7	Male	3732	7.68	24	FAIL	C	C	C	FAIL	C	C	C	C	C	C	C	C
8	Female	3736	3.52	77	FAIL	C	C	C	FAIL	C	C	C	C	C	C	C	C
9	Male	3741	3.54	32	C	C	C	C	C	C	C	C	C	C	C	C	C
10	Male	3743	7.11	28	FAIL	C	C	C	FAIL	C	C	C	C	C	C	C	C
11	Male	3744	7.02	24	C	C	C	C	C	C	C	C	C	C	C	C	C
12	Female	3749	0.00	168	FAIL	C	C	C	FAIL	C	C	C	C	C	C	C	C
13	Female	3751	5.83	28	FAIL	C	C	C	FAIL	C	C	C	C	C	C	C	C
14	Male	3813	0.00	168	FAIL	C	C	C	FAIL	C	C	C	FAIL	B	C	C	C
15	Male	3814	0.00	168	FAIL	C	C	C	FAIL	C	C	C	C	C	C	C	C
16	Male	3816	3.67	168	FAIL	C	C	C	FAIL	C	C	C	C	C	HET	C	C
17	Female	3817	4.82	29	FAIL	C	C	C	FAIL	C	C	C	C	C	C	C	C
18	Female	3818	3.12	168	FAIL	C	C	C	FAIL	C	C	C	C	C	C	C	C
19	Male	3819	0.00	168	FAIL	C	C	C	FAIL	C	C	C	C	C	C	C	C
20	Male	3820	0.00	168	FAIL	C	C	C	FAIL	C	C	C	C	C	C	C	C
21	Male	3821	0.00	168	FAIL	C	C	C	FAIL	C	C	C	C	C	C	C	C
22	Male	3822	2.22	168	FAIL	C	C	C	FAIL	C	C	C	C	C	C	C	C
23	Male	3823	0.00	168	FAIL	C	C	C	FAIL	C	C	C	C	C	C	C	C
24	Female	3824	5.41	27	C	C	C	C	C	C	C	C	C	C	C	C	C
25	Female	3825	4.74	27	C	C	C	C	C	C	C	C	C	C	C	C	C
26	Male	3903	3.52	48	FAIL	C	C	C	FAIL	C	C	C	C	C	C	C	C
27	Male	3904	8.52	24	FAIL	C	C	C	FAIL	C	HET	C	C	C	HET	C	C
28	Male	3905	3.00	48	FAIL	C	C	C	FAIL	C	C	C	C	C	C	C	C
29	Female	3907	6.61	24	C	C	C	C	C	C	C	C	C	C	C	C	C
30	Female	3908	0.00	168	C	C	C	C	C	C	C	C	C	C	C	C	C
31	Female	3909	7.52	24	C	C	C	C	C	C	C	C	C	C	C	C	C
32	Female	3910	6.55	24	FAIL	C	C	C	FAIL	C	C	C	C	C	HET	C	C
33	Female	3911	3.73	24	C	C	C	C	C	C	C	C	C	C	C	C	C
34	Male	3903	3.52	48	FAIL	C	C	FAIL	FAIL	C	FAIL	C	C	FAIL	FAIL	C	C
35	Male	3904	8.52	24	FAIL	C	FAIL	C	C								
36	Male	3905	3.00	48	FAIL	C	FAIL	C	C								
37	Female	3907	6.61	24	FAIL	C	FAIL	C	C								
38	Female	3908	0.00	72	FAIL	C	FAIL	C	C								
39	Female	3909	7.52	24	FAIL	C	FAIL	FAIL	FAIL	FAIL	FAIL	C	FAIL	FAIL	FAIL	C	C
40	Female	3910	6.55	24	FAIL	C	FAIL	C	C								
41	Female	3911	3.73	24	FAIL	C	FAIL	C	C								
42	Male	3952	5.37	28	FAIL	C	FAIL	FAIL	FAIL	FAIL	FAIL	C	FAIL	FAIL	FAIL	C	C
43	Male	3970	4.03	48	FAIL	C	C	FAIL	FAIL	FAIL	FAIL	C	FAIL	FAIL	FAIL	C	C
44	Male	4124	0.00	144	FAIL	C	C	FAIL	C	C							
45	Male	4125	0.00	48	FAIL	C	FAIL	C	C								
46	Male	4126	6.48	28	FAIL	C	FAIL	C	C								
47	Male	4127	0.00	168	FAIL	C	C	FAIL	FAIL	C	FAIL	C	C	C	FAIL	C	C
48	Male	4135	0.00	168	FAIL	C	C	FAIL	FAIL	FAIL	FAIL	C	FAIL	FAIL	FAIL	C	C
49	Male	4172	6.00	28	FAIL	C	C	FAIL	FAIL	FAIL	FAIL	C	FAIL	FAIL	FAIL	C	C
50	Male	4181	5.07	36	FAIL	C	C	FAIL	FAIL	C	FAIL	C	FAIL	FAIL	FAIL	C	C
51	Male	4182	6.78	28	FAIL	C	FAIL	FAIL	FAIL	FAIL	FAIL	C	FAIL	FAIL	FAIL	C	C
52	Male	4183	7.52	28	FAIL	C	C	FAIL	FAIL	FAIL	FAIL	C	FAIL	FAIL	FAIL	C	C
53	Male	4299	5.87	28	FAIL	C	C	FAIL	FAIL	FAIL	FAIL	C	FAIL	FAIL	FAIL	C	C
54	Male	4300	5.90	28	C	C	C	C	C	C	FAIL	C	C	C	FAIL	C	C
55	Male	4449	4.58	168	FAIL	C	C	FAIL	FAIL	FAIL	FAIL	C	FAIL	FAIL	FAIL	C	C
56	Male	4450	5.50	48	FAIL	C	FAIL	FAIL	FAIL	FAIL	FAIL	C	FAIL	FAIL	FAIL	C	C
57	Male	4451	4.78	168	FAIL	C	FAIL	C	FAIL	FAIL	FAIL	C	FAIL	FAIL	FAIL	C	C
58	Male	4452	3.96	168	FAIL	C	FAIL	FAIL	FAIL	FAIL	FAIL	C	FAIL	FAIL	FAIL	C	C
59	Male	4459	5.40	28	FAIL	C	C	FAIL	FAIL	FAIL	FAIL	C	C	FAIL	FAIL	C	C
60	Male	4460	0.00	168	FAIL	C	FAIL	FAIL	FAIL	FAIL	FAIL	C	FAIL	FAIL	FAIL	C	C
61	Male	4461	5.45	28	FAIL	C	C	C	FAIL	C	C						

CCB line

No.	Sex	UID	Log10 CFU/ml	Survival Time (hrs)	Chromosome 7 SNP markers													
					7_04	7_09	7_17	7_20	7_26	7_27	7_31	7_35	7_46	7_51	7_63	7_54	7_123	
1	Male	3662	0.00	168	FAIL	C	C	C	FAIL	C	C	C	C	C	C	C	C	B
2	Female	3663	6.60	27	FAIL	C	C	C	FAIL	C	C	C	C	C	C	C	C	B
3	Female	3664	0.00	168	FAIL	C	C	C	FAIL	C	C	C	C	C	C	C	C	B
4	Female	3680	4.38	69	FAIL	C	C	C	FAIL	C	C	C	C	C	C	C	C	B
5	Female	3682	4.02	168	FAIL	C	C	C	FAIL	C	C	C	C	C	C	C	C	B
6	Female	3637	0.00	168	FAIL	C	C	C	FAIL	C	C	C	C	C	C	C	C	B
7	Male	3685	4.56	168	FAIL	C	C	C	FAIL	C	C	FAIL	C	C	C	C	C	B
8	Male	3686	0.00	168	B	C	C	C	C	C	C	C	C	C	C	C	C	B
9	Male	3687	0.00	168	B	C	C	C	C	C	FAIL	C	C	C	C	C	C	B
10	Male	3688	0.00	168	B	C	C	C	C	C	FAIL	C	C	C	C	FAIL	C	B
11	Female	3689	6.11	28	FAIL	C	C	C	FAIL	C	FAIL	C	C	C	C	C	C	B
12	Female	3690	0.00	168	B	C	C	C	FAIL	C	FAIL	C	C	C	C	C	C	B
13	Male	3752	0.00	168	B	C	HET	C	C	C	FAIL	C	C	C	FAIL	C	C	B
14	Male	3753	5.09	28	B	C	C	C	FAIL	C	C	C	C	C	FAIL	C	C	B
15	Male	3754	4.54	32	FAIL	C	C	C	FAIL	C	C	C	C	C	FAIL	C	C	B
16	Female	3755	4.89	168	B	C	C	C	C	C	FAIL	C	C	C	C	C	C	B
17	Female	3756	5.07	28	FAIL	C	C	C	FAIL	C	FAIL	C	C	C	C	C	C	B
18	Female	3757	6.99	28	FAIL	C	C	C	FAIL	C	C	C	C	C	C	C	C	B
19	Male	3801	6.59	29	B	C	C	C	C	C	C	C	C	C	C	C	C	B
20	Male	3802	6.26	27	B	C	C	C	C	C	C	C	C	C	C	C	C	B
21	Male	3803	0.00	168	B	C	C	C	C	C	C	C	C	C	C	C	C	B
22	Female	3804	3.18	168	B	C	C	C	FAIL	C	FAIL	C	C	C	C	C	C	B
23	Female	3805	0.00	168	B	C	C	C	C	C	C	C	C	C	C	C	C	B
24	Female	3806	0.00	29	FAIL	C	C	C	C	C	FAIL	C	C	C	FAIL	C	C	B
25	Male	4054	4.12	27	FAIL	C	C	C	FAIL	C	C	C	C	C	C	C	C	B
26	Female	4032	0.00	168	B	C	C	C	FAIL	C	FAIL	C	C	C	C	C	C	B
27	Female	3887	4.68	31	B	C	C	C	FAIL	C	C	C	C	C	FAIL	C	C	B
28	Female	3889	5.60	31	FAIL	C	C	C	FAIL	C	C	C	C	C	C	C	C	B
29	Male	4031	3.85	30	FAIL	C	C	FAIL	FAIL	FAIL	FAIL	C	C	C	FAIL	C	C	B
30	Male	4055	5.48	48	FAIL	C	C	C	FAIL	FAIL	C	FAIL	C	C	C	FAIL	C	B
31	Male	4056	3.12	48	FAIL	C	C	FAIL	FAIL	FAIL	FAIL	C	FAIL	FAIL	FAIL	FAIL	C	B
32	Male	4079	6.23	30	FAIL	C	C	C	FAIL	FAIL	C	FAIL	C	C	C	FAIL	C	B
33	Male	4080	5.14	48	FAIL	C	C	FAIL	FAIL	C	FAIL	C	C	C	FAIL	C	C	B
34	Male	4081	4.03	96	FAIL	C	C	FAIL	FAIL	FAIL	FAIL	C	FAIL	FAIL	FAIL	C	C	B
35	Male	4082	0.00	168	B	C	C	C	FAIL	C	FAIL	C	C	C	FAIL	C	C	B
36	Male	4083	2.22	48	FAIL	C	C	FAIL	FAIL	C	FAIL	C	C	C	FAIL	C	C	B
37	Male	4154	0.00	55	FAIL	C	C	FAIL	FAIL	C	FAIL	C	C	FAIL	FAIL	FAIL	C	B
38	Female	4391	6.06	48	FAIL	C	FAIL	FAIL	FAIL	FAIL	FAIL	C	FAIL	FAIL	FAIL	C	C	B
39	Female	4392	0.00	168	FAIL	C	C	FAIL	FAIL	FAIL	FAIL	C	FAIL	FAIL	FAIL	C	C	B
40	Female	4393	7.81	30	FAIL	C	C	FAIL	FAIL	C	FAIL	C	FAIL	FAIL	FAIL	C	C	B
41	Male	4274	0.00	168	FAIL	C	C	FAIL	FAIL	FAIL	FAIL	C	C	C	FAIL	C	C	B
42	Male	4275	5.92	30	FAIL	C	C	FAIL	FAIL	FAIL	FAIL	C	FAIL	FAIL	FAIL	C	C	B
43	Male	4276	0.00	168	FAIL	C	C	FAIL	FAIL	C	FAIL	C	FAIL	FAIL	FAIL	C	C	B
44	Male	4277	4.81	168	FAIL	C	C	FAIL	FAIL	C	FAIL	C	C	C	FAIL	C	C	B
45	Male	4280	3.45	48	FAIL	C	C	C	FAIL	C	FAIL	C	C	C	FAIL	C	C	B
46	Male	4311	5.91	30	FAIL	C	C	FAIL	FAIL	FAIL	FAIL	C	FAIL	FAIL	FAIL	C	C	B
47	Male	4312	6.58	30	FAIL	C	C	FAIL	FAIL	C	FAIL	C	FAIL	FAIL	FAIL	C	C	B
48	Male	4313	0.00	168	FAIL	C	C	FAIL	FAIL	C	FAIL	C	FAIL	C	FAIL	C	C	B
49	Female	4244	6.03	29	n.a.	C	n.a.	C	B									
50	Female	4245	5.39	29	n.a.	C	n.a.	C	B									
51	Male	4241	2.52	168	n.a.	C	n.a.	C	B									
52	Male	4242	0.00	168	n.a.	C	n.a.	C	B									

CBB line

No.	Sex	UID	Log <sub>10</sub> CFU/ml	Survival Time (hrs)	Chromosome 7 SNP markers													
					7_04	7_09	7_17	7_20	7_26	7_27	7_31	7_35	7_46	7_51	7_63	7_54	7_123	
1	Female	4335	3.62	144	FAIL	C	FAIL	B	B									
2	Male	4215	5.54	29	FAIL	C	FAIL	B	B									
3	Female	4203	0.00	168	C	C	C	C	FAIL	HET	HET	HET	HET	B	B	B	B	B
4	Male	4498	6.16	29	C	C	C	FAIL	FAIL	FAIL	FAIL	C	C	FAIL	B	B	B	B
5	Male	4496	4.50	29	FAIL	C	FAIL	C	FAIL	HET	FAIL	HET	FAIL	FAIL	B	B	B	B
6	Female	4445	0.00	168	HET	C	C	C	C	HET	FAIL	HET	B	B	B	B	B	B
7	Female	4446	3.86	72	FAIL	C	FAIL	B	B									
8	Female	4447	4.50	48	HET	C	C	C	C	HET	HET	HET	B	B	B	B	B	B
9	Female	4448	0.00	168	HET	C	C	C	FAIL	HET	FAIL	HET	B	B	B	B	B	B
10	Male	4668	0.00	168	C	C	C	C	FAIL	HET	HET	HET	C	B	B	B	B	B
11	Male	4669	3.43	30	C	C	C	C	C	HET	HET	HET	HET	B	B	B	B	B
12	Male	4670	2.82	48	C	C	C	C	FAIL	HET	FAIL	HET	C	FAIL	FAIL	B	B	B
13	Male	4671	4.98	48	FAIL	C	FAIL	B	B	B	B	B						
14	Female	4673	0.00	168	C	C	HET	C	FAIL	HET	HET	HET	C	B	B	B	B	B
15	Female	4674	0.00	168	C	C	HET	C	FAIL	FAIL	FAIL	HET	HET	B	FAIL	B	B	B
16	Female	4675	5.62	24	C	C	HET	C	FAIL	FAIL	FAIL	HET	C	FAIL	FAIL	FAIL	B	B
17	Male	4676	4.26	30	FAIL	C	FAIL	B	B									
18	Female	4678	5.86	30	FAIL	C	FAIL	FAIL	FAIL	FAIL	FAIL	C	FAIL	FAIL	B	B	B	B
19	Female	4679	5.43	48	FAIL	C	C	C	FAIL	C	C	C	C	B	B	B	B	B
20	Female	4680	5.97	30	FAIL	C	C	FAIL	FAIL	C	C	C	C	B	B	B	B	B
21	Female	4681	4.34	72	C	C	HET	C	C	C	C	C	C	B	B	B	B	B
22	Female	4682	0.00	168	C	C	HET	C	FAIL	C	C	C	C	B	B	B	B	B
23	Male	4706	5.56	72	FAIL	C	FAIL	FAIL	FAIL	FAIL	FAIL	C	FAIL	HET	HET	B	B	B
24	Male	4707	3.00	72	FAIL	C	FAIL	B	B									
25	Male	4596	1.40	30	HET	C	C	C	C	C	C	C	HET	B	B	B	B	B
26	Male	4597	1.41	30	FAIL	C	FAIL	FAIL	FAIL	FAIL	FAIL	B	FAIL	FAIL	FAIL	FAIL	B	B
27	Male	4598	1.43	30	FAIL	C	FAIL	FAIL	FAIL	FAIL	FAIL	C	B	FAIL	FAIL	FAIL	B	B
28	Male	4599	0.00	168	C	C	HET	C	C	HET	HET	HET	HET	B	B	B	B	B
29	Male	4600	0.00	168	C	C	C	C	C	C	C	C	C	B	B	B	B	B
30	Male	4698	1.48	30	C	C	HET	C	C	HET	HET	HET	HET	B	B	B	B	B
31	Male	4699	0.00	168	C	C	C	C	FAIL	B	B	B	B	B	B	B	B	B
32	Male	4700	0.00	168	HET	C	C	C	C	B	B	B	B	B	B	B	B	B
33	Male	4701	0.00	168	FAIL	C	C	C	C	HET	HET	HET	HET	B	B	B	B	B
34	Female	4702	0.00	168	C	C	C	C	C	C	C	C	HET	B	B	B	B	B
35	Female	4703	1.54	168	FAIL	C	FAIL	B	B									
36	Female	4704	0.00	168	C	C	C	C	C	HET	HET	HET	HET	B	B	B	B	B
37	Female	4705	0.00	168	C	C	HET	C	C	HET	HET	HET	HET	B	B	B	B	B
38	Female	4711	0.00	168	C	C	C	C	FAIL	C	C	C	C	B	B	B	B	B
39	Female	4712	1.59	168	FAIL	C	FAIL	B	B									
40	Female	4713	0.00	168	C	C	C	C	C	C	C	C	C	B	B	B	B	B
41	Female	4714	1.61	30	C	C	C	C	C	C	C	C	C	B	B	B	B	B
42	Male	4761	1.62	30	C	C	C	C	C	C	C	C	C	B	B	B	B	B
43	Female	4762	0.00	168	C	C	C	C	C	HET	HET	HET	HET	B	B	B	B	B
44	Female	4763	0.00	168	C	C	C	C	C	HET	HET	HET	HET	C	B	B	B	B
45	Female	4764	0.00	168	C	C	C	C	C	C	C	C	C	B	B	B	B	B
46	Female	4765	1.66	47	FAIL	C	C	C	FAIL	HET	HET	HET	HET	B	B	B	B	B
47	Female	4766	0.00	168	C	C	C	C	C	HET	HET	HET	HET	B	B	B	B	B
48	Male	4484	1.68	30	FAIL	C	FAIL	FAIL	FAIL	HET	FAIL	C	FAIL	FAIL	B	B	B	B
49	Female	4830	1.69	30	C	C	C	C	FAIL	C	C	C	C	B	B	B	B	B
50	Female	4485	1.70	47	C	C	C	C	FAIL	C	C	C	HET	B	B	B	B	B
51	Female	4201	1.71	47	HET	C	HET	HET	FAIL	HET	HET	HET	HET	B	B	B	B	B

Supplementary Figure 3 - Genotyping of the six N<sub>10</sub> congenic lines with all SNP markers and the mouse phenotyping to *S. pneumoniae*. Six detailed lists (one list for each line: BBB, BBC, BCC, CCC, CCB and CBB) containing information about gender, unique identification number for each mouse, bacteraemia (log<sub>10</sub> CFU/ml) at 24 hrs p.i., survival time (hrs) (black highlight: lethargic animal; white highlight: survived animal) and the genotyping result (B: homozygous BALB/c; C: homozygous CBA/Ca; HET: heterozygous; **FAIL**: undetectable/unreadable SNP; n.a.: not analysed) for each of the thirteen SNP markers tested (the three main markers: 7\_09, 7\_54 and 7\_123; and the ten additional markers: 7\_04, 7\_17, 7\_20, 7\_26, 7\_27, 7\_31, 7\_35, 7\_46, 7\_51 and 7\_63).

**Appendix 5: List of SNPs in *tgfb1* gene between BALB/c and CBA/Ca mice**

*Detailed list of SNPs between BALB/c and CBA/Ca found in tgfb1 gene sequences:*

Location	CBA Allele	BALB Allele	Gene	Ensembl Transcript ID	Functional class	Feature type	Transcript SNP reference	Transcript SNP reads	Ensembl Protein ID	UniProt ID	Reference SNP
7:26479896	C	T	ENSMUSG0000002603	ENSMUST0000002678	INTRONIC	Transcript	C	T	ENSMUSP0000002678	TGFB1_MOUSE	rs32393147
7:26493006	G	A	ENSMUSG0000002603	ENSMUST0000002678	DOWNSTREAM	Transcript	A	G	ENSMUSP0000002678	TGFB1_MOUSE	rs32519556

Supplementary Figure 4 - List of SNPs between BALB/c and CBA/Ca inbred mouse strains in *tgfb1* gene. List contains predictions of functional consequences of variants generated from available tools on Ensembl website.

## Appendix 6: List of SNPs in *cd22* gene between BALB/c and CBA/Ca mice

Detailed list of SNPs between BALB/c and CBA/Ca found in *cd22* gene sequences:

Uploaded Variation	Location	CBA Allele	BALB Allele	Gene	Feature	Feature type	Consequence	Position in cDNA	Position in CDS	Position in protein	Amino acid change	Codon change	Co-located Variation
7_31649919_-/A	7:31649918-31649919	-	A	ENSMUSG00000044453	ENSMUST00000052700	Transcript	UPSTREAM	-	-	-	-	-	-
7_31649919_-/A	7:31649918-31649919	-	A	ENSMUSG00000030577	ENSMUST00000019248	Transcript	DOWNSTREAM	-	-	-	-	-	-
7_31649919_-/A	7:31649918-31649919	-	A	ENSMUSG00000030577	ENSMUST00000108123	Transcript	DOWNSTREAM	-	-	-	-	-	-
7_31649919_-/A	7:31649918-31649919	-	A	ENSMUSG00000030577	ENSMUST00000108125	Transcript	DOWNSTREAM	-	-	-	-	-	-
7_31650263_G/C	7:31650263	G	C	ENSMUSG00000030577	ENSMUST00000108125	Transcript	DOWNSTREAM	-	-	-	-	-	-
7_31650263_G/C	7:31650263	G	C	ENSMUSG00000030577	ENSMUST00000019248	Transcript	DOWNSTREAM	-	-	-	-	-	-
7_31650263_G/C	7:31650263	G	C	ENSMUSG00000030577	ENSMUST00000108123	Transcript	DOWNSTREAM	-	-	-	-	-	-
7_31650263_G/C	7:31650263	G	C	ENSMUSG00000044453	ENSMUST00000052700	Transcript	UPSTREAM	-	-	-	-	-	-
7_31650309_C/T	7:31650309	C	T	ENSMUSG00000030577	ENSMUST00000108123	Transcript	DOWNSTREAM	-	-	-	-	-	rs49180946
7_31650309_C/T	7:31650309	C	T	ENSMUSG00000044453	ENSMUST00000052700	Transcript	UPSTREAM	-	-	-	-	-	rs49180946
7_31650309_C/T	7:31650309	C	T	ENSMUSG00000030577	ENSMUST00000108125	Transcript	DOWNSTREAM	-	-	-	-	-	rs49180946
7_31650309_C/T	7:31650309	C	T	ENSMUSG00000030577	ENSMUST00000019248	Transcript	DOWNSTREAM	-	-	-	-	-	rs49180946
7_31650324_T/C	7:31650324	T	C	ENSMUSG00000030577	ENSMUST00000108125	Transcript	DOWNSTREAM	-	-	-	-	-	rs50694357
7_31650324_T/C	7:31650324	T	C	ENSMUSG00000030577	ENSMUST00000108123	Transcript	DOWNSTREAM	-	-	-	-	-	rs50694357
7_31650324_T/C	7:31650324	T	C	ENSMUSG00000044453	ENSMUST00000052700	Transcript	UPSTREAM	-	-	-	-	-	rs50694357
7_31650324_T/C	7:31650324	T	C	ENSMUSG00000030577	ENSMUST00000019248	Transcript	DOWNSTREAM	-	-	-	-	-	rs50694357
7_31650423_G/A	7:31650423	G	A	ENSMUSG00000044453	ENSMUST00000052700	Transcript	UPSTREAM	-	-	-	-	-	rs51904377
7_31650423_G/A	7:31650423	G	A	ENSMUSG00000030577	ENSMUST00000108125	Transcript	3PRIME_UTR	4097	-	-	-	-	rs51904377
7_31650423_G/A	7:31650423	G	A	ENSMUSG00000030577	ENSMUST00000019248	Transcript	3PRIME_UTR	3972	-	-	-	-	rs51904377

Figure: part 1 of 7

Uploaded Variation	Location	CBA Allele	BALB Allele	Gene	Feature	Feature type	Consequence	Position in cDNA	Position in CDS	Position in protein	Amino acid change	Codon change	Co-located Variation
7_31650731_T/C	7:31650731	T	C	ENSMUSG00000030577	ENSMUST00000108125	Transcript	3PRIME_UTR	3789	-	-	-	-	rs46507452
7_31650731_T/C	7:31650731	T	C	ENSMUSG00000030577	ENSMUST00000108123	Transcript	3PRIME_UTR	3687	-	-	-	-	rs46507452
7_31650731_T/C	7:31650731	T	C	ENSMUSG00000030577	ENSMUST00000019248	Transcript	3PRIME_UTR	3664	-	-	-	-	rs46507452
7_31650731_T/C	7:31650731	T	C	ENSMUSG00000044453	ENSMUST00000052700	Transcript	UPSTREAM	-	-	-	-	-	rs46507452
7_31651103_-/AGA	7:31651102-31651103	-	AGA	ENSMUSG00000030577	ENSMUST00000108123	Transcript	3PRIME_UTR	3315-3316	-	-	-	-	-
7_31651103_-/AGA	7:31651102-31651103	-	AGA	ENSMUSG00000044453	ENSMUST00000052700	Transcript	UPSTREAM	-	-	-	-	-	-
7_31651103_-/AGA	7:31651102-31651103	-	AGA	ENSMUSG00000030577	ENSMUST00000019248	Transcript	3PRIME_UTR	3292-3293	-	-	-	-	-
7_31651103_-/AGA	7:31651102-31651103	-	AGA	ENSMUSG00000030577	ENSMUST00000108125	Transcript	3PRIME_UTR	3417-3418	-	-	-	-	-
7_31651150_-/TGAC	7:31651149-31651150	-	TGAC	ENSMUSG00000030577	ENSMUST00000108125	Transcript	3PRIME_UTR	3370-3371	-	-	-	-	-
7_31651150_-/TGAC	7:31651149-31651150	-	TGAC	ENSMUSG00000030577	ENSMUST00000108123	Transcript	3PRIME_UTR	3268-3269	-	-	-	-	-
7_31651150_-/TGAC	7:31651149-31651150	-	TGAC	ENSMUSG00000030577	ENSMUST00000019248	Transcript	3PRIME_UTR	3245-3246	-	-	-	-	-
7_31651150_-/TGAC	7:31651149-31651150	-	TGAC	ENSMUSG00000044453	ENSMUST00000052700	Transcript	UPSTREAM	-	-	-	-	-	-
7_31651283_G/T	7:31651283	G	T	ENSMUSG00000030577	ENSMUST00000108123	Transcript	3PRIME_UTR	3135	-	-	-	-	rs50862211
7_31651283_G/T	7:31651283	G	T	ENSMUSG00000030577	ENSMUST00000019248	Transcript	3PRIME_UTR	3112	-	-	-	-	rs50862211
7_31651283_G/T	7:31651283	G	T	ENSMUSG00000030577	ENSMUST00000108125	Transcript	3PRIME_UTR	3237	-	-	-	-	rs50862211
7_31651283_G/T	7:31651283	G	T	ENSMUSG00000044453	ENSMUST00000052700	Transcript	UPSTREAM	-	-	-	-	-	rs50862211
7_31651287_G/T	7:31651287	G	T	ENSMUSG00000030577	ENSMUST00000019248	Transcript	3PRIME_UTR	3108	-	-	-	-	rs8240993
7_31651287_G/T	7:31651287	G	T	ENSMUSG00000030577	ENSMUST00000108123	Transcript	3PRIME_UTR	3131	-	-	-	-	rs8240993
7_31651287_G/T	7:31651287	G	T	ENSMUSG00000030577	ENSMUST00000108125	Transcript	3PRIME_UTR	3233	-	-	-	-	rs8240993
7_31651287_G/T	7:31651287	G	T	ENSMUSG00000044453	ENSMUST00000052700	Transcript	UPSTREAM	-	-	-	-	-	rs8240993
7_31651415_C/T	7:31651415	C	T	ENSMUSG00000030577	ENSMUST00000108125	Transcript	3PRIME_UTR	3105	-	-	-	-	rs51937698

Figure: part 2 of 7

Uploaded Variation	Location	CBA Allele	BALB Allele	Gene	Feature	Feature type	Consequence	Position in cDNA	Position in CDS	Position in protein	Amino acid change	Codon change	Co-located Variation
7_31651415_C/T	7:31651415	C	T	ENSMUSG00000030577	ENSMUST00000108123	Transcript	3PRIME_UTR	3003	-	-	-	-	rs51937698
7_31651415_C/T	7:31651415	C	T	ENSMUSG00000030577	ENSMUST00000019248	Transcript	3PRIME_UTR	2980	-	-	-	-	rs51937698
7_31651415_C/T	7:31651415	C	T	ENSMUSG00000044453	ENSMUST00000052700	Transcript	UPSTREAM	-	-	-	-	-	rs51937698
7_31651856_A/G	7:31651856	A	G	ENSMUSG00000030577	ENSMUST00000108125	Transcript	INTRONIC	-	-	-	-	-	rs8240978
7_31651856_A/G	7:31651856	A	G	ENSMUSG00000030577	ENSMUST00000019248	Transcript	INTRONIC	-	-	-	-	-	rs8240978
7_31651856_A/G	7:31651856	A	G	ENSMUSG00000030577	ENSMUST00000108123	Transcript	INTRONIC	-	-	-	-	-	rs8240978
7_31651938_A/T	7:31651938	A	T	ENSMUSG00000030577	ENSMUST00000108123	Transcript	INTRONIC	-	-	-	-	-	rs8240980
7_31651938_A/T	7:31651938	A	T	ENSMUSG00000030577	ENSMUST00000019248	Transcript	INTRONIC	-	-	-	-	-	rs8240980
7_31651938_A/T	7:31651938	A	T	ENSMUSG00000030577	ENSMUST00000108125	Transcript	INTRONIC	-	-	-	-	-	rs8240980
7_31651992_A/G	7:31651992	A	G	ENSMUSG00000030577	ENSMUST00000108123	Transcript	INTRONIC	-	-	-	-	-	rs51839349
7_31651992_A/G	7:31651992	A	G	ENSMUSG00000030577	ENSMUST00000108125	Transcript	INTRONIC	-	-	-	-	-	rs51839349
7_31651992_A/G	7:31651992	A	G	ENSMUSG00000030577	ENSMUST00000019248	Transcript	INTRONIC	-	-	-	-	-	rs51839349
7_31652072_A/T	7:31652072	A	T	ENSMUSG00000030577	ENSMUST00000108123	Transcript	NON_SYNONYMOUS_CODING	2701	2338	780	S/T	Tcg/Acg	-
7_31652072_A/T	7:31652072	A	T	ENSMUSG00000030577	ENSMUST00000108125	Transcript	NON_SYNONYMOUS_CODING	2803	2440	814	S/T	Tcg/Acg	-
7_31652072_A/T	7:31652072	A	T	ENSMUSG00000030577	ENSMUST00000019248	Transcript	NON_SYNONYMOUS_CODING	2678	2440	814	S/T	Tcg/Acg	-
7_31652212_G/C	7:31652212	G	C	ENSMUSG00000030577	ENSMUST00000019248	Transcript	INTRONIC	-	-	-	-	-	rs47178166
7_31652212_G/C	7:31652212	G	C	ENSMUSG00000030577	ENSMUST00000108123	Transcript	INTRONIC	-	-	-	-	-	rs47178166
7_31652212_G/C	7:31652212	G	C	ENSMUSG00000030577	ENSMUST00000108125	Transcript	INTRONIC	-	-	-	-	-	rs47178166
7_31652264_T/C	7:31652264	T	C	ENSMUSG00000030577	ENSMUST00000019248	Transcript	INTRONIC	-	-	-	-	-	rs46899359
7_31652264_T/C	7:31652264	T	C	ENSMUSG00000030577	ENSMUST00000108125	Transcript	INTRONIC	-	-	-	-	-	rs46899359
7_31652264_T/C	7:31652264	T	C	ENSMUSG00000030577	ENSMUST00000108123	Transcript	INTRONIC	-	-	-	-	-	rs46899359

Figure: part 3 of 7

Uploaded Variation	Location	CBA Allele	BALB Allele	Gene	Feature	Feature type	Consequence	Position in cDNA	Position in CDS	Position in protein	Amino acid change	Codon change	Co-located Variation
7_31652374_G/A	7:31652374	G	A	ENSMUSG00000030577	ENSMUST00000108125	Transcript	INTRONIC	-	-	-	-	-	rs46095146
7_31652374_G/A	7:31652374	G	A	ENSMUSG00000030577	ENSMUST00000019248	Transcript	INTRONIC	-	-	-	-	-	rs46095146
7_31652374_G/A	7:31652374	G	A	ENSMUSG00000030577	ENSMUST00000108123	Transcript	INTRONIC	-	-	-	-	-	rs46095146
7_31652381_C/T	7:31652381	C	T	ENSMUSG00000030577	ENSMUST00000108123	Transcript	INTRONIC	-	-	-	-	-	rs51856952
7_31652381_C/T	7:31652381	C	T	ENSMUSG00000030577	ENSMUST00000019248	Transcript	INTRONIC	-	-	-	-	-	rs51856952
7_31652381_C/T	7:31652381	C	T	ENSMUSG00000030577	ENSMUST00000108125	Transcript	INTRONIC	-	-	-	-	-	rs51856952
7_31652384_T/G	7:31652384	T	G	ENSMUSG00000030577	ENSMUST00000108125	Transcript	INTRONIC	-	-	-	-	-	rs47899568
7_31652384_T/G	7:31652384	T	G	ENSMUSG00000030577	ENSMUST00000019248	Transcript	INTRONIC	-	-	-	-	-	rs47899568
7_31652384_T/G	7:31652384	T	G	ENSMUSG00000030577	ENSMUST00000108123	Transcript	INTRONIC	-	-	-	-	-	rs47899568
7_31652485_T/C	7:31652485	T	C	ENSMUSG00000030577	ENSMUST00000108123	Transcript	NON_SYNONYMOUS_CODING	2647	2284	762	T/A	Act/Gct	rs48887107
7_31652485_T/C	7:31652485	T	C	ENSMUSG00000030577	ENSMUST00000019248	Transcript	NON_SYNONYMOUS_CODING	2624	2386	796	T/A	Act/Gct	rs48887107
7_31652485_T/C	7:31652485	T	C	ENSMUSG00000030577	ENSMUST00000108125	Transcript	NON_SYNONYMOUS_CODING	2749	2386	796	T/A	Act/Gct	rs48887107
7_31652486_G/A	7:31652486	G	A	ENSMUSG00000030577	ENSMUST00000108123	Transcript	SYNONYMOUS_CODING	2646	2283	761	N	aaC/aaT	rs48455985
7_31652486_G/A	7:31652486	G	A	ENSMUSG00000030577	ENSMUST00000108125	Transcript	SYNONYMOUS_CODING	2748	2385	795	N	aaC/aaT	rs48455985
7_31652486_G/A	7:31652486	G	A	ENSMUSG00000030577	ENSMUST00000019248	Transcript	SYNONYMOUS_CODING	2623	2385	795	N	aaC/aaT	rs48455985
7_31652531_G/A	7:31652531	G	A	ENSMUSG00000030577	ENSMUST00000019248	Transcript	SYNONYMOUS_CODING	2578	2340	780	T	acC/acT	rs51826772
7_31652531_G/A	7:31652531	G	A	ENSMUSG00000030577	ENSMUST00000108123	Transcript	SYNONYMOUS_CODING	2601	2238	746	T	acC/acT	rs51826772
7_31652531_G/A	7:31652531	G	A	ENSMUSG00000030577	ENSMUST00000108125	Transcript	SYNONYMOUS_CODING	2703	2340	780	T	acC/acT	rs51826772
7_31652760_C/A	7:31652760	C	A	ENSMUSG00000030577	ENSMUST00000019248	Transcript	INTRONIC	-	-	-	-	-	rs49674170
7_31652760_C/A	7:31652760	C	A	ENSMUSG00000030577	ENSMUST00000108123	Transcript	INTRONIC	-	-	-	-	-	rs49674170
7_31652760_C/A	7:31652760	C	A	ENSMUSG00000030577	ENSMUST00000108125	Transcript	INTRONIC	-	-	-	-	-	rs49674170

Figure: part 4 of 7

Uploaded Variation	Location	CBA Allele	BALB Allele	Gene	Feature	Feature type	Consequence	Position in cDNA	Position in CDS	Position in protein	Amino acid change	Codon change	Co-located Variation
7_31653018_C/A	7:31653018	C	A	ENSMUSG00000030577	ENSMUST00000019248	Transcript	NON_SYNONYMOUS_CODING	2397	2159	720	C/F	tGc/tTc	rs46349251
7_31653018_C/A	7:31653018	C	A	ENSMUSG00000030577	ENSMUST00000108125	Transcript	NON_SYNONYMOUS_CODING	2522	2159	720	C/F	tGc/tTc	rs46349251
7_31653018_C/A	7:31653018	C	A	ENSMUSG00000030577	ENSMUST00000108123	Transcript	NON_SYNONYMOUS_CODING	2420	2057	686	C/F	tGc/tTc	rs46349251
7_31653259_A/G	7:31653259	A	G	ENSMUSG00000030577	ENSMUST00000108125	Transcript	INTRONIC	-	-	-	-	-	rs32085852
7_31653259_A/G	7:31653259	A	G	ENSMUSG00000030577	ENSMUST00000019248	Transcript	INTRONIC	-	-	-	-	-	rs32085852
7_31653259_A/G	7:31653259	A	G	ENSMUSG00000030577	ENSMUST00000108123	Transcript	INTRONIC	-	-	-	-	-	rs32085852
7_31655923_-/ TTCCCTTGTTG	7:31655922-3 1655923	-	TTCCCT TGTTG	ENSMUSG00000030577	ENSMUST00000019248	Transcript	INTRONIC	-	-	-	-	-	-
7_31655923_-/ TTCCCTTGTTG	7:31655922-3 1655923	-	TTCCCT TGTTG	ENSMUSG00000030577	ENSMUST00000108125	Transcript	INTRONIC	-	-	-	-	-	-
7_31655923_-/ TTCCCTTGTTG	7:31655922-3 1655923	-	TTCCCT TGTTG	ENSMUSG00000030577	ENSMUST00000108123	Transcript	INTRONIC	-	-	-	-	-	-
7_31656609_G/C	7:31656609	G	C	ENSMUSG00000030577	ENSMUST00000108123	Transcript	INTRONIC	-	-	-	-	-	rs32076841
7_31656609_G/C	7:31656609	G	C	-	ENSMUSR00000170819	Regulatory Feature	REGULATORY_REGION	-	-	-	-	-	rs32076841
7_31656609_G/C	7:31656609	G	C	ENSMUSG00000030577	ENSMUST00000108125	Transcript	INTRONIC	-	-	-	-	-	rs32076841
7_31656609_G/C	7:31656609	G	C	ENSMUSG00000030577	ENSMUST00000019248	Transcript	INTRONIC	-	-	-	-	-	rs32076841
7_31657217_G/C	7:31657217	G	C	ENSMUSG00000030577	ENSMUST00000108123	Transcript	INTRONIC	-	-	-	-	-	rs51633032
7_31657217_G/C	7:31657217	G	C	ENSMUSG00000030577	ENSMUST00000108125	Transcript	INTRONIC	-	-	-	-	-	rs51633032
7_31657217_G/C	7:31657217	G	C	ENSMUSG00000030577	ENSMUST00000019248	Transcript	INTRONIC	-	-	-	-	-	rs51633032
7_31657422_-/ ATTCATTC	7:31657421-3 1657422	-	ATTCATT C	ENSMUSG00000030577	ENSMUST00000108125	Transcript	INTRONIC	-	-	-	-	-	-
7_31657422_-/ ATTCATTC	7:31657421-3 1657422	-	ATTCATT C	ENSMUSG00000030577	ENSMUST00000108123	Transcript	INTRONIC	-	-	-	-	-	-
7_31657422_-/ ATTCATTC	7:31657421-3 1657422	-	ATTCATT C	ENSMUSG00000030577	ENSMUST00000019248	Transcript	INTRONIC	-	-	-	-	-	-
7_31660886_C/T	7:31660886	C	T	ENSMUSG00000030577	ENSMUST00000108123	Transcript	NON_SYNONYMOUS_CODING	1010	647	216	R/H	cGt/cAt	rs45991074
7_31660886_C/T	7:31660886	C	T	ENSMUSG00000030577	ENSMUST00000019248	Transcript	NON_SYNONYMOUS_CODING	987	749	250	R/H	cGt/cAt	rs45991074

Figure: part 5 of 7

Uploaded Variation	Location	CBA Allele	BALB Allele	Gene	Feature	Feature type	Consequence	Position in cDNA	Position in CDS	Position in protein	Amino acid change	Codon change	Co-located Variation
7_31660886_C/T	7:31660886	C	T	ENSMUSG00000030577	ENSMUST00000108125	Transcript	NON_SYNONYMOUS_CODING	1112	749	250	R/H	cGt/cAt	rs45991074
7_31660896_G/A	7:31660896	G	A	ENSMUSG00000030577	ENSMUST0000019248	Transcript	NON_SYNONYMOUS_CODING	977	739	247	R/C	Cgc/Tgc	rs49806898
7_31660896_G/A	7:31660896	G	A	ENSMUSG00000030577	ENSMUST00000108125	Transcript	NON_SYNONYMOUS_CODING	1102	739	247	R/C	Cgc/Tgc	rs49806898
7_31660896_G/A	7:31660896	G	A	ENSMUSG00000030577	ENSMUST00000108123	Transcript	NON_SYNONYMOUS_CODING	1000	637	213	R/C	Cgc/Tgc	rs49806898
7_31661480_A/G	7:31661480	A	G	ENSMUSG00000030577	ENSMUST0000019248	Transcript	INTRONIC	-	-	-	-	-	rs50328233
7_31661480_A/G	7:31661480	A	G	ENSMUSG00000030577	ENSMUST00000108123	Transcript	INTRONIC	-	-	-	-	-	rs50328233
7_31661480_A/G	7:31661480	A	G	ENSMUSG00000030577	ENSMUST00000108125	Transcript	INTRONIC	-	-	-	-	-	rs50328233
7_31661644_G/A	7:31661644	G	A	ENSMUSG00000030577	ENSMUST00000108125	Transcript	INTRONIC	-	-	-	-	-	rs45776325
7_31661644_G/A	7:31661644	G	A	ENSMUSG00000030577	ENSMUST0000019248	Transcript	INTRONIC	-	-	-	-	-	rs45776325
7_31661644_G/A	7:31661644	G	A	ENSMUSG00000030577	ENSMUST00000108123	Transcript	INTRONIC	-	-	-	-	-	rs45776325
7_31662605_G/A	7:31662605	A	G	ENSMUSG00000030577	ENSMUST0000019248	Transcript	STOP_GAINED	533	295	99	Q/*	Caa/Taa	-
7_31662605_G/A	7:31662605	A	G	ENSMUSG00000030577	ENSMUST00000108125	Transcript	STOP_GAINED	658	295	99	Q/*	Caa/Taa	-
7_31662605_G/A	7:31662605	A	G	ENSMUSG00000030577	ENSMUST00000108123	Transcript	STOP_GAINED	658	295	99	Q/*	Caa/Taa	-
7_31662858_G/A	7:31662858	G	A	ENSMUSG00000030577	ENSMUST00000108125	Transcript	SYNONYMOUS_CODING	405	42	14	H	caC/caT	rs3698643
7_31662858_G/A	7:31662858	G	A	ENSMUSG00000030577	ENSMUST0000019248	Transcript	SYNONYMOUS_CODING	280	42	14	H	caC/caT	rs3698643
7_31662858_G/A	7:31662858	G	A	ENSMUSG00000030577	ENSMUST00000108123	Transcript	SYNONYMOUS_CODING	405	42	14	H	caC/caT	rs3698643
7_31664352_G/A	7:31664352	G	A	ENSMUSG00000030577	ENSMUST0000019248	Transcript	UPSTREAM	-	-	-	-	-	rs50804830
7_31664352_G/A	7:31664352	G	A	ENSMUSG00000030577	ENSMUST00000108123	Transcript	5PRIME_UTR	204	-	-	-	-	rs50804830
7_31664352_G/A	7:31664352	G	A	ENSMUSG00000030577	ENSMUST00000108125	Transcript	5PRIME_UTR	204	-	-	-	-	rs50804830
7_31664416_-/ GCTT	7:31664415-3 1664416	-	GCTT	ENSMUSG00000030577	ENSMUST0000019248	Transcript	UPSTREAM	-	-	-	-	-	-
7_31664416_-/ GCTT	7:31664415-3 1664416	-	GCTT	ENSMUSG00000030577	ENSMUST00000108125	Transcript	INTRONIC	-	-	-	-	-	-

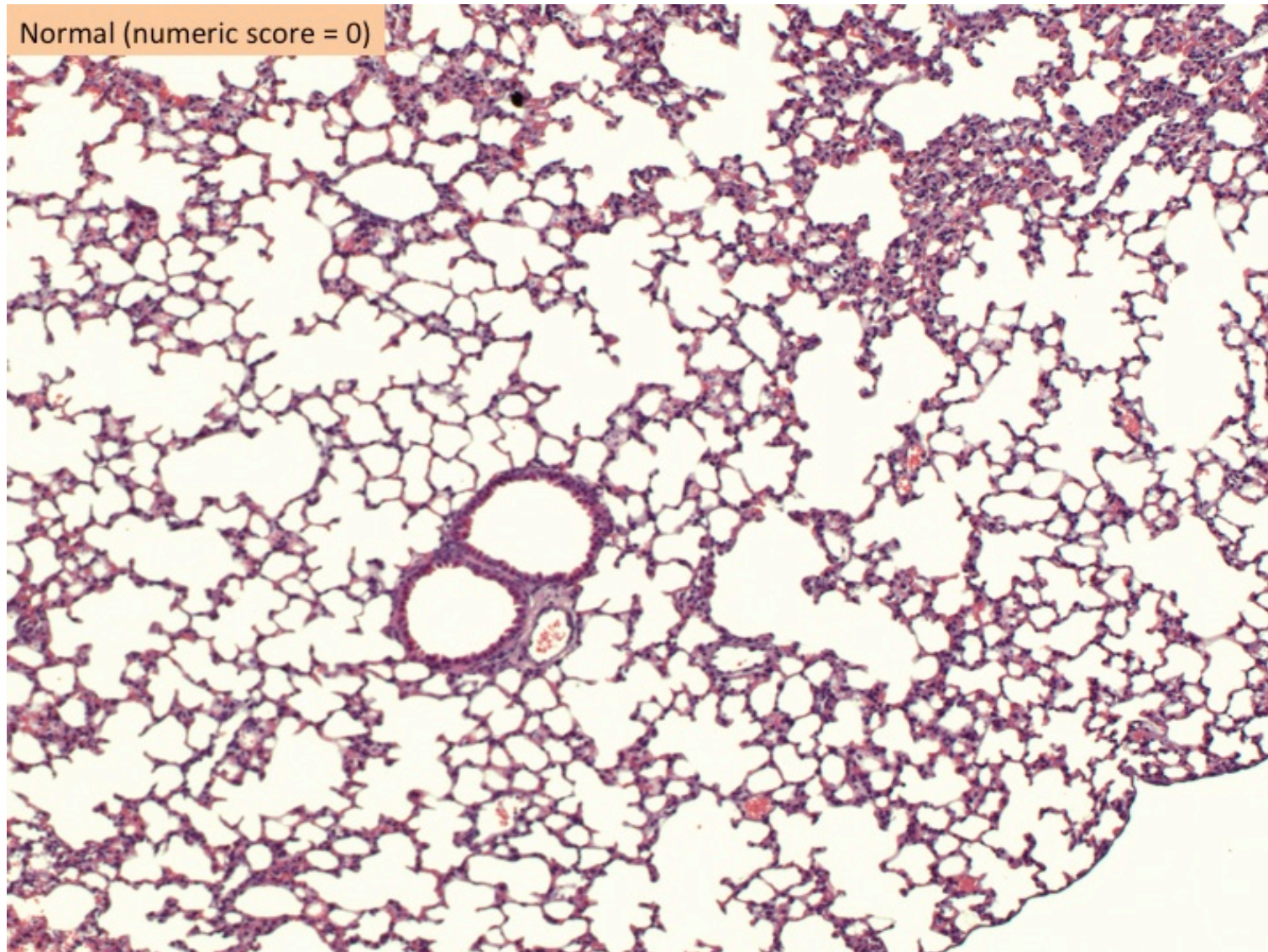
Figure: part 6 of 7

Uploaded Variation	Location	CBA Allele	BALB Allele	Gene	Feature	Feature type	Consequence	Position in cDNA	Position in CDS	Position in protein	Amino acid change	Codon change	Co-located Variation
7_31664416_-/ GCTT	7:31664415-3 1664416	-	GCTT	ENSMUSG000 00030577	ENSMUST0000 0108123	Transcript	INTRONIC	-	-	-	-	-	-
7_31665751_A/C	7:31665751	A	C	ENSMUSG000 00030577	ENSMUST0000 0108123	Transcript	UPSTREAM	-	-	-	-	-	rs45641602
7_31665751_A/C	7:31665751	A	C	ENSMUSG000 00030577	ENSMUST0000 0019248	Transcript	UPSTREAM	-	-	-	-	-	rs45641602
7_31665751_A/C	7:31665751	A	C	ENSMUSG000 00030577	ENSMUST0000 0108125	Transcript	UPSTREAM	-	-	-	-	-	rs45641602
7_31665860_C/G	7:31665860	C	G	ENSMUSG000 00030577	ENSMUST0000 0019248	Transcript	UPSTREAM	-	-	-	-	-	rs46328252
7_31665860_C/G	7:31665860	C	G	ENSMUSG000 00030577	ENSMUST0000 0108125	Transcript	UPSTREAM	-	-	-	-	-	rs46328252
7_31665860_C/G	7:31665860	C	G	ENSMUSG000 00030577	ENSMUST0000 0108123	Transcript	UPSTREAM	-	-	-	-	-	rs46328252

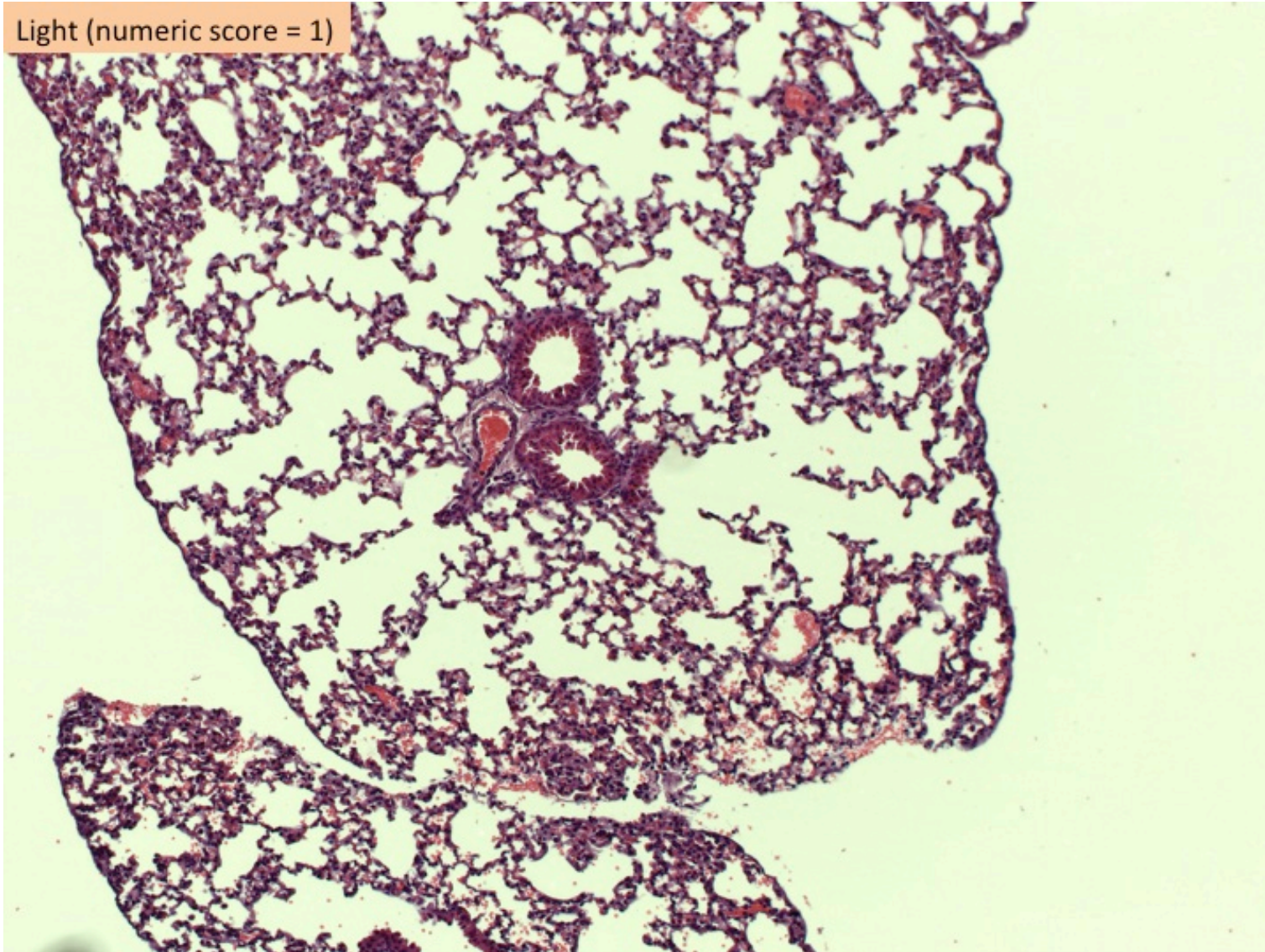
Figure: part 7 of 7

Supplementary Figure 5 - List of SNPs between BALB/c and CBA/Ca inbred mouse strains in *cd22* gene. List contains predictions of functional consequences of variants generated from available tools on Ensembl website. 40 SNPs were found in the gene and in red-colour font (part 6 of 7) was highlighted the mutation introducing a stop codon in the CBA/Ca background.

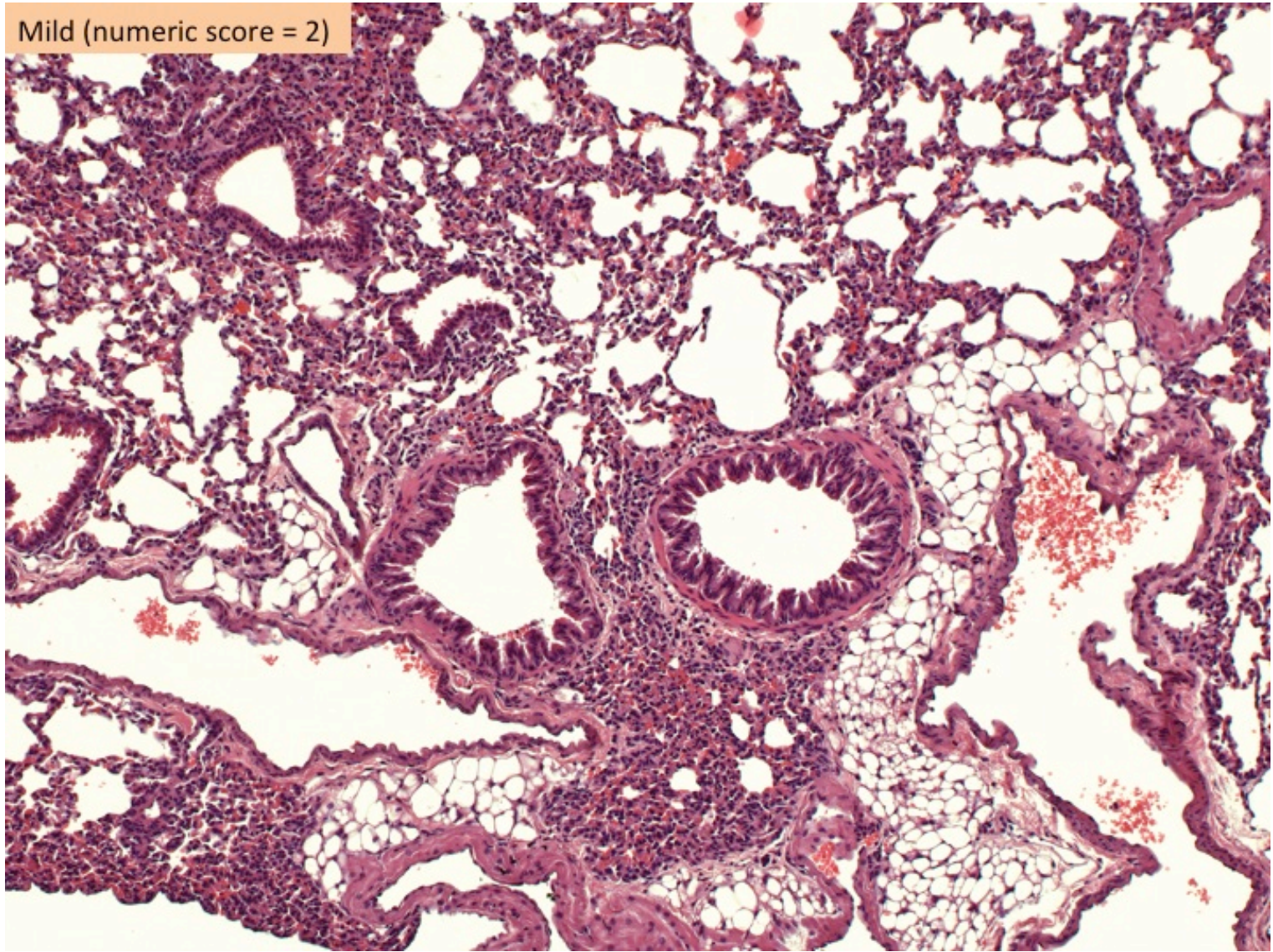
**Appendix 7: Representation of the different level of cellular infiltration in lung tissue sections.**



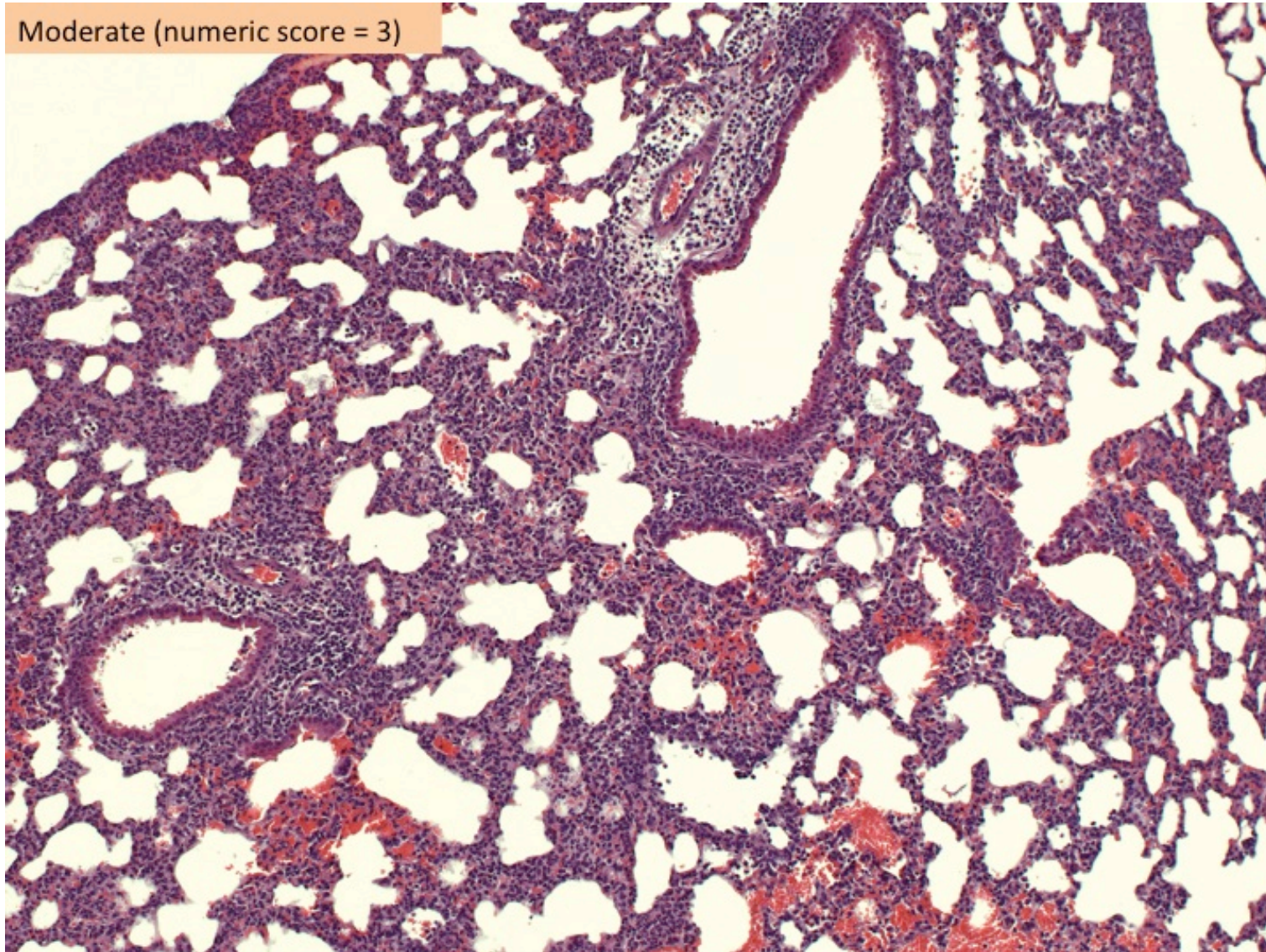
Light (numeric score = 1)



Mild (numeric score = 2)



Moderate (numeric score = 3)





Supplementary Figure 6 - Example images characterising each level of tissue inflammation (see section 2.9.5).

**Appendix 8: BALB/c and CBA/Ca lung and spleen weights  
(quantification of the number of cells per mg of lung tissue)**

Staining of CD45<sup>+</sup> cells (hematopoietic cells), Gr-1<sup>+</sup> cells (neutrophil cells), F4/80<sup>+</sup> cells (macrophage cells) and FcεRI<sup>+</sup> cells (mast cells), CD4<sup>+</sup> cells (T<sub>helper</sub> cells), CD8<sup>+</sup> cells (cytotoxic T cells) and CD19<sup>+</sup> cells (B cells):

Strain	Sex	Time point (hrs)	Mouse Identifier	Tissue Type	Tissue Weight (mg)
BALB/cOlaHsd	Female	0	B1	Lung	189
BALB/cOlaHsd	Female		B2	Lung	191
BALB/cOlaHsd	Female		B3	Lung	167
BALB/cOlaHsd	Female		B4	Lung	158
CBA/CaOlaHsd	Female	0	C1	Lung	181
CBA/CaOlaHsd	Female		C2	Lung	197
CBA/CaOlaHsd	Female		C3	Lung	188
CBA/CaOlaHsd	Female		C4	Lung	164
BALB/cOlaHsd	Female	6	B5	Lung	179
BALB/cOlaHsd	Female		B6	Lung	181
BALB/cOlaHsd	Female		B7	Lung	188
BALB/cOlaHsd	Female		B8	Lung	168
CBA/CaOlaHsd	Female	6	C5	Lung	151
CBA/CaOlaHsd	Female		C6	Lung	150
CBA/CaOlaHsd	Female		C7	Lung	176
CBA/CaOlaHsd	Female		C8	Lung	178
BALB/cOlaHsd	Female	12	B9	Lung	174
BALB/cOlaHsd	Female		B10	Lung	187
BALB/cOlaHsd	Female		B11	Lung	195
BALB/cOlaHsd	Female		B12	Lung	204
CBA/CaOlaHsd	Female	12	C9	Lung	155
CBA/CaOlaHsd	Female		C10	Lung	170
CBA/CaOlaHsd	Female		C11	Lung	177
CBA/CaOlaHsd	Female		C12	Lung	172
BALB/cOlaHsd	Female	24	B13	Lung	206
BALB/cOlaHsd	Female		B14	Lung	188
BALB/cOlaHsd	Female		B15	Lung	212
BALB/cOlaHsd	Female		B16	Lung	197
CBA/CaOlaHsd	Female	24	C13	Lung	164
CBA/CaOlaHsd	Female		C14	Lung	205
CBA/CaOlaHsd	Female		C15	Lung	160
CBA/CaOlaHsd	Female		C16	Lung	199

Staining of NKp46<sup>+</sup> cells (NK cells):

Strain	Sex	Time point (hrs)	Mouse Identifier	Tissue Type	Tissue Weight (mg)
BALB/cOlaHsd	Female	PBS	B1	Lung	159
BALB/cOlaHsd	Female		B2	Lung	149
BALB/cOlaHsd	Female		B3	Lung	124
BALB/cOlaHsd	Female		B4	Lung	142
BALB/cOlaHsd	Female		B5	Lung	173
CBA/CaOlaHsd	Female	24	C1	Lung	187
CBA/CaOlaHsd	Female		C2	Lung	189
CBA/CaOlaHsd	Female		C3	Lung	180
CBA/CaOlaHsd	Female		C4	Lung	182
CBA/CaOlaHsd	Female		C5	Lung	188
BALB/cOlaHsd	Female	24	B6	Lung	189
BALB/cOlaHsd	Female		B7	Lung	191
BALB/cOlaHsd	Female		B8	Lung	167
BALB/cOlaHsd	Female		B9	Lung	158
BALB/cOlaHsd	Female		B10	Lung	181

Staining of  $\gamma\delta$  TCR<sup>+</sup> cells ( $\gamma\delta$  T cells):

Strain	Sex	Time point (hrs)	Mouse Identifier	Tissue Type	Tissue Weight (mg)
BALB/cOlaHsd	Female	PBS	B1	Lung	139
BALB/cOlaHsd	Female		B2	Lung	149
BALB/cOlaHsd	Female		B3	Lung	124
BALB/cOlaHsd	Female		B4	Lung	142
BALB/cOlaHsd	Female		B5	Lung	173
CBA/CaOlaHsd	Female	PBS	C1	Lung	128
CBA/CaOlaHsd	Female		C2	Lung	133
CBA/CaOlaHsd	Female		C3	Lung	129
CBA/CaOlaHsd	Female		C4	Lung	145
CBA/CaOlaHsd	Female		C5	Lung	136
BALB/cOlaHsd	Female	24	B6	Lung	260
BALB/cOlaHsd	Female		B7	Lung	249
BALB/cOlaHsd	Female		B8	Lung	259
BALB/cOlaHsd	Female		B9	Lung	223
BALB/cOlaHsd	Female		B10	Lung	196
CBA/CaOlaHsd	Female	24	C6	Lung	187
CBA/CaOlaHsd	Female		C7	Lung	189
CBA/CaOlaHsd	Female		C8	Lung	168
CBA/CaOlaHsd	Female		C9	Lung	153
CBA/CaOlaHsd	Female		C10	Lung	188

Staining of CD22<sup>+</sup> CD19<sup>+</sup> cells (CD22<sup>+</sup> B cells):

Strain	Sex	Time point (hrs)	Mouse Identifier	Tissue Type	Tissue Weight (mg)	Tissue Type	Tissue Weight (mg)
BALB/cOlaHsd	Female	0	B1	Lung	122	Spleen	174
BALB/cOlaHsd	Female		B2	Lung	173	Spleen	178
BALB/cOlaHsd	Female		B3	Lung	123	Spleen	171
BALB/cOlaHsd	Female		B4	Lung	201	Spleen	175
CBA/CaOlaHsd	Female	0	C1	Lung	174	Spleen	72
CBA/CaOlaHsd	Female		C2	Lung	179	Spleen	62
CBA/CaOlaHsd	Female		C3	Lung	153	Spleen	76
CBA/CaOlaHsd	Female		C4	Lung	131	Spleen	82
BALB/cOlaHsd	Female	6	B5	Lung	121	Spleen	133
BALB/cOlaHsd	Female		B6	Lung	142	Spleen	116
BALB/cOlaHsd	Female		B7	Lung	127	Spleen	132
BALB/cOlaHsd	Female		B8	Lung	130	Spleen	127
CBA/CaOlaHsd	Female	6	C5	Lung	135	Spleen	73
CBA/CaOlaHsd	Female		C6	Lung	123	Spleen	71
CBA/CaOlaHsd	Female		C7	Lung	121	Spleen	77
CBA/CaOlaHsd	Female		C8	Lung	126	Spleen	73
BALB/cOlaHsd	Female	12	B9	Lung	149	Spleen	103
BALB/cOlaHsd	Female		B10	Lung	151	Spleen	145
BALB/cOlaHsd	Female		B11	Lung	145	Spleen	109
BALB/cOlaHsd	Female		B12	Lung	148	Spleen	119
CBA/CaOlaHsd	Female	12	C9	Lung	157	Spleen	75
CBA/CaOlaHsd	Female		C10	Lung	131	Spleen	80
CBA/CaOlaHsd	Female		C11	Lung	131	Spleen	72
CBA/CaOlaHsd	Female		C12	Lung	139	Spleen	75
BALB/cOlaHsd	Female	24	B13	Lung	154	Spleen	176
BALB/cOlaHsd	Female		B14	Lung	155	Spleen	133
BALB/cOlaHsd	Female		B15	Lung	137	Spleen	180
BALB/cOlaHsd	Female		B16	Lung	191	Spleen	142
CBA/CaOlaHsd	Female	24	C13	Lung	165	Spleen	75
CBA/CaOlaHsd	Female		C14	Lung	199	Spleen	76
CBA/CaOlaHsd	Female		C15	Lung	126	Spleen	77
CBA/CaOlaHsd	Female		C16	Lung	167	Spleen	73

Table A2 - BALB/c and CBA/Ca lung and spleen tissue weight used for the calculation of the number of cells per mg of tissue. The equation is stated in section 2.7.6.

## Appendix 9: Author's publications

Glenn Cruse, **Vitor E. Fernandes**, Jose de Salort, Depesh Pankhania, Marta S. Marinas, Hannah Brewin, Peter W Andrew, Peter Bradding and Aras Kadioglu. 2010. Human lung mast cells mediate pneumococcal cell death in response to activation by pneumolysin. *Journal of Immunology*. 184, 7108-7115.

Ananth Tellabati, **Vitor E. Fernandes**, Friederike Teichert, Rajinder Singh, Jamie Rylance, Stephen Gordon, Peter W Andrew, Jonathan Grigg. 2010. Acute exposure of mice to high-dose ultrafine carbon black decreases susceptibility to pneumococcal pneumonia. *Particle and Fibre Toxicology*. 19, 7:30.

Edel A. McNeela, Áine Burke, Daniel R. Neill, Cathy Baxter, **Vitor E. Fernandes**, Daniela Ferreira, Sarah Smeaton, Rana El-Rachkidy, Rachel M. McLoughlin, Andres Mori, Barry Moran, Katherine A. Fitzgerald, Jurg Tschopp, Virginie Pétrilli, Peter W. Andrew, Aras Kadioglu, Ed C. Lavelle. 2010. Pneumolysin activates the NLRP3 inflammasome and promotes proinflammatory cytokines independently of TLR4. *PLoS Pathogens*. 6, e1001191.

Aras Kadioglu, Katia De Filippo, Mathieu Bangert, **Vitor E. Fernandes**, Luke Richards, Kristian Jones, Peter W. Andrew and Nancy Hogg. 2011. The integrins Mac-1 and alpha4beta1 perform crucial roles in neutrophil and T cell recruitment to lungs during *Streptococcus pneumoniae* infection. *Journal of Immunology*. 186, 5907-5915.

Daniel R. Neill, **Vitor E. Fernandes**, Laura Wisby, Andrew R. Haynes, Daniela M. Ferreira, Ameera Laher, Natalie Strickland, Stephen B. Gordon, Paul Denny, Aras Kadioglu, Peter W. Andrew. 2012. T regulatory cells control susceptibility to invasive pneumococcal pneumonia in mice. *Plos Pathogens* 8 (4): e1002660.

Laura Wisby, **Vitor E. Fernandes**, Daniel R. Neill, Aras Kadioglu, Peter W. Andrew and Paul Denny. 2013. Spir2; a novel QTL on chromosome 4 contributes to susceptibility to pneumococcal infection in mice. *BMC Genomics*. 10.1186/1471-2164-14-242.

Magda S. Jonczyk, Michelle Simon, Saumya Kumar, **Vitor E. Fernandes**, Nicolas Sylvius, Ann-Marie Mallon, Paul Denny, Peter W. Andrew. 2014. Genetic factors regulating lung vasculature and immune cell functions associate with resistance to pneumococcal infection. *Plos One*. 9(3): e89831.

Morten Kjos, Rieza Aprianto, **Vitor E. Fernandes**, Peter W. Andrew, Jos A. G. van Strijp, Reindert Nijland and Jan-Willem Veening. 2014. Bright fluorescent *Streptococcus pneumoniae* for live cell imaging of host-pathogen interactions. *Journal of Bacteriology*. 10.1128/JB.02221-14.

Laura Paixão, Joana Oliveira, André Veríssimo, Susana Vinga, Eva C. Lourenço, M. Rita Ventura, Morten Kjos, Jan-Willem Veening, **Vitor E. Fernandes**, Peter W. Andrew, Hasan Yesilkaya, Ana Rute Neves. Host Glycan Sugar-Specific Pathways in *Streptococcus pneumoniae*: Galactose as a Key Sugar in Colonisation and Infection. *Plos One*. 10.1371/journal.pone.0121042.